Current Topics in Developmental Biology

Edited by

Roger A. Pedersen

Volume 29

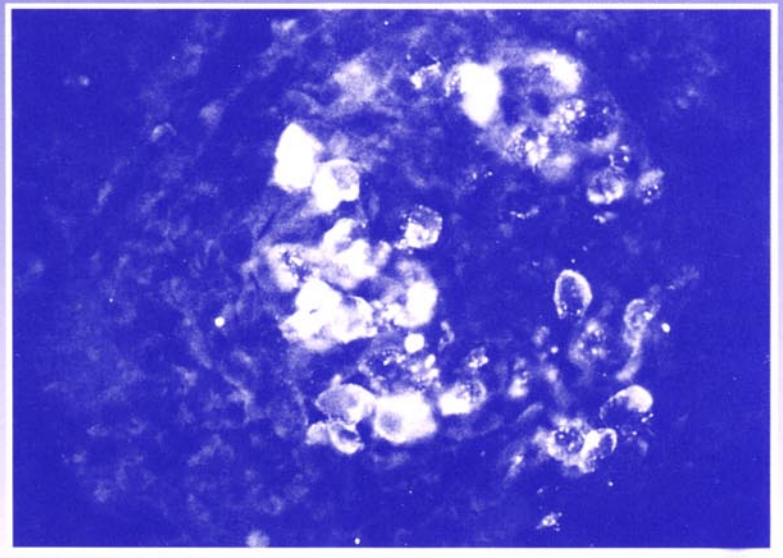

Current Topics in Developmental Biology

Volume 29

Current Topics in Developmental Biology

Volume 29

Edited by

Roger A. Pedersen
Laboratory of Radiobiology and Environmental Health
University of California
San Francisco, California

Academic Press
San Diego New York Boston London Sydney Tokyo Toronto

Front cover photograph: Identification of PGCs by alkaline phosphatase histochemistry and reactivity with an anti-SSEA-1 antibody. Photo courtesy of Peter J. Donovan. (For more details see Chapter 6, Figure 2).

This book is printed on acid-free paper. ♾

Academic Press, Inc.
A Division of Harcourt Brace & Company
525 B Street, Suite 1900, San Diego, California 92101-4495

United Kingdom Edition published by
Academic Press Limited
24-28 Oval Road, London NW1 7DX

International Standard Serial Number: 0070-2153

International Standard Book Number: 0-12-153129-5

PRINTED IN THE UNITED STATES OF AMERICA
94 95 96 97 98 99 BC 9 8 7 6 5 4 3 2 1

Contents

3

Evolution of Developmental Mechanisms: Spatial and Temporal Modes of Rostrocaudal Patterning

David A. Weisblat, Cathy J. Wedeen, and Richard G. Kostriken

4

Axonal Guidance from Retina to Tectum in Embryonic *Xenopus*

Chi-Bin Chien and William A. Harris

5

6

7

8

9

Contributors

Numbers in parentheses indicate the pages on which the authors' contributions begin.

Richard R. Behringer Department of Molecular Genetics, The University of Texas, M.D. Anderson Cancer Center, Houston, Texas 77030 (171)

Chi-Bin Chien Department of Biology, University of California, San Diego, La Jolla, California 92093 (135)

Wilson Crone Department of Botany and Plant Sciences, University of California, Riverside, California 92521 (325)

Peter J. Donovan Mammalian Genetics Laboratory, ABL-Basic Research Program, NCI-Frederick Cancer Research and Development Center, Frederick, Maryland 21702 (189)

Ursula Eichenlaub-Ritter Universität Bielefeld, Gentechnologie/Mikrobiologie, 33501 Bielefeld, Germany (281)

Anders Fjose Department of Biochemistry and Molecular Biology, University of Bergen, N-5009 Bergen, Norway (65)

Joseph D. Gold Laboratory of Radiobiology and Environmental Health, University of California, San Francisco, San Francisco, California 94143 (227)

William A. Harris Department of Biology and Center for Molecular Genetics, University of California, San Diego, La Jolla, California 92093 (135)

Jeffrey P. Hill Department of Botany and Plant Sciences, University of California, Riverside, Riverside, California 92521 (325)

Richard G. Kostriken Department of Molecular and Cell Biology, University of California, Berkeley, Berkeley California 94720 (101)

Elizabeth M. Lord Department of Botany and Plant Sciences, University of California, Riverside, California 92521 (325)

Roger A. Pedersen Laboratory of Radiobiology and Environmental Health, University of California, San Francisco, San Francisco, California 94143 (227)

Luis Puelles Department of Morphological Sciences, Faculty of Medicine, University of Murcia, Murcia 30100, Spain (1)

John L. R. Rubenstein Nina Ireland Laboratory for Developmental Biology, Department of Psychiatry and Programs in Neuroscience and Developmental Biology, University of California, San Francisco, San Francisco, California 94143 (1)

Cathy J. Wedeen Department of Molecular and Cell Biology, University of California, Berkeley, Berkeley, California 94720 (101)

David A. Weisblat Department of Molecular and Cell Biology, University of California, Berkeley, Berkeley, California 94720 (101)

Preface

This volume continues the recent tradition of this Serial in addressing developmental mechanisms in a variety of experimental systems. However, in soliciting chapters for this volume, I have emphasized my own current interests more than in previous volumes. Consequently, there is a strong contingent of chapters on the early development of the neuroectoderm cell lineage into an axially organized nervous system, and there is a bolus of chapters devoted to development of the mammalian reproductive system, its pluripotent germ cells and embryos, as well as a chapter on development of the plant reproductive system, or flower. While previous volumes have begun with plants, this volume turns that order on its head, and begins instead with the vertebrate brain.

The chapter by Rubenstein and Puelles synthesizes recent observations on segmental patterns of homeobox gene expression in the mammalian forebrain into a hypothesis of "prosomeric" organization of the forebrain (similar to the rhombomeres of the hindbrain), then goes on to evaluate the evidence that homeobox genes are involved in regulating many brain morphogenetic processes. In his chapter, Fjose extends this analysis of homeobox gene expression to the zebrafish, a uniquely valuable system for studies of embryonic development, and shows how the functions of these genes reveal strong conservation of fundamental mechanisms of vertebrate nervous system development, from fish to mammals. In their chapter, Weisblat, Wedeen, and Kostriken compare the roles of segmentation and regionalization in the development of an annelid, the leech, and an arthropod, *Drosophila,* to gain insight into the mechanisms of rostrocaudal axis formation. The fourth chapter dealing with the nervous system, by Chien and Harris, addresses the mechanisms of pathfinding by retinal axons growing toward the optic tectum in the amphibian embryo, using *Xenopus laevis* as a model system, and examining current evidence for the molecular nature and distribution of axonal guidance cues.

Turning to reproduction and development, we have the chapter by Behringer, who reviews both classical evidence and his new studies on the role of the gonadal hormone, Müllerian-inhibiting substance, during mammalian sexual differentiation and germ cell development. Then, the chapter by Donovan addresses the regulation of primordial germ cell differentiation, proliferation, and migration, focusing on *in vitro* ap-

proaches that have been used to define the roles of specific growth factors and to obtain long-term cultures of primordial germ cells. In their review, Gold and Pedersen discuss the molecular mechanisms of genomic imprinting, the parental-allele-specific expression of certain genes that occurs during gametogenesis and early embryogenesis of eutherian mammals. In her chapter, Eichenlaub-Ritter provides an overview of the meiotic origin of aneuploidy in mammals and evaluates potential mechanisms underlying chromosomal nondisjunction in both oogenesis and spermatogenesis. In the final chapter, Lord, Crone, and Hill describe genes effecting heterochrony (developmental timing) or homeosis (flower organ identity) during flower organogenesis in the model system, *Arabidopsis thaliana*, culminating with a revised model for flower development.

Together with other volumes in this Serial, this volume provides a comprehensive survey of the major issues at the forefront of modern developmental biology. These chapters should be valuable to researchers in the fields of animal and plant development, as well as to students and professionals who want an introduction to current topics in cellular and molecular approaches to developmental biology. This volume in particular will be essential reading for anyone interested in the development of the nervous system and reproductive system and in the role of homeobox-related transcription factors and growth factors in axis and organ development.

This volume has benefited from the ongoing cooperation of a team of participants who are jointly responsible for the content and quality of its material. The authors deserve the full credit for their success in covering their subjects in depth yet with clarity, and for challenging the reader to think about these topics in new ways. I thank the members of the Editorial Board, John Gerhart, Peter Grüss, Philip Ingham, Story Landis, David McClay, Gerald Schatten, Virginia Walbot, and Mitsuki Yoneda for their suggestions of topics and authors. I thank Liana Hartanto for her exemplary administrative support, and the Laboratory of Radiobiology and Environmental Health for accomodating the editorial office for the Serial. I am grateful to Ms. Barbara Poetter for her excellent editorial assistance. And I thank my family members, including my wife, Carmen Arbona, and our daughters, Ramona and Anita Pedersen y Arbona, for their unwavering encouragement and support. Together, we would like to dedicate this volume to the memory of our friend, Mrs. Aïda Ducato Miller, who regaled us with accounts of her experiences during the San Francisco earthquake of 1906, the Panama–Pacific Exposition of 1915, and more contemporary events; she loved pastels and flowers of any color, especially violet; and she would have been delighted to see this volume.

Finally, I am pleased to announce that effective with the next volume, Dr. Gerald Schatten of the University of Wisconsin-Madison will

join me as co-editor, continuing a tradition of partnership begun when the Serial was launched in 1966 by A. A. Moscona and Alberto Monroy. The forthcoming publication of Volume 30 will mark a major milestone in the life of *Current Topics in Developmental Biology*, the longest-running public forum for contemporary issues in developmental biology.

Roger A. Pedersen
San Francisco, California

This Page Intentionally Left Blank

1

Homeobox Gene Expression during Development of the Vertebrate Brain

John L. R. Rubenstein
Nina Ireland Laboratory for Developmental Biology
Department of Psychiatry and Programs in Neuroscience and Developmental Biology
University of California, San Francisco, California 94143

Luis Puelles
Department of Morphological Sciences
Faculty of Medicine
University of Murcia
Murcia 30100, Spain

Current Topics in Developmental Biology, Vol. 29

I. Introduction

Progress in molecular biology and experimental embryology now permits investigations into the genetic mechanisms that control regional specification and differentiation of the vertebrate brain. These processes begin at the onset of gastrulation, when patterning along the anterior–posterior (A–P) axis is initiated (Doniach,1992; Doniach *et al.*, 1992). Signals apparently are transmitted from the organizer region along the plane of the ectoderm that induces the primitive ectoderm to differentiate into neural ectoderm. Furthermore, these signals induce spatially restricted patterns of expression of regulatory genes. These conclusions are based on *in vitro* experiments using planar explants of *Xenopus* embryos. To date, four homeobox genes (*engrailed, XlHbox1, XlHbox6,* and *distal-less*) and one zinc finger gene (*Krox20*) are expressed in transverse domains in this *in vitro* system (Doniach, 1992; Doniach *et al.*, 1992; Papalopulu and Kintner, 1993). Longitudinal patterning also appears to occur in these explants, as demonstrated by the expression of the *Xash-3* basic helix-loop-helix gene (Zimmerman *et al.*, 1993). These results suggest that signals, possibly in the form of morphogenetic gradients, lead to spatially restricted expression of regulatory genes that begin the process of regional specification.

During gastrulation, mesoderm migrates under the presumptive neural ectoderm. Mesoderm also has the capacity to induce overlying ectoderm to become specific neural tissues; this is called vertical induction (Slack, 1991). Thus, both planar and vertical mechanisms may play a role in neural induction and in A–P patterning.

While ectodermal organizer tissue and paraxial mesoderm specify neural tissue along the A–P axis, specialized midline (axial) mesodermal structures have a role in patterning along the dorso–ventral (D–V) axis (Yamada *et al.*, 1993). The axial mesodermal structures, such as the notochord and the prechordal plate, underlie the midline of the neural plate. The notochord induces the floor plate of the neural tube, which forms the ventral midline of most of the central nervous system (CNS). The floor plate produces diffusible factors that regulate differentiation of basal plate cells, including motor neurons (Yamada *et al.*, 1993). Thus, the underlying mesoderm has a role in patterning along the medio–lateral axis of the neural plate. Note that once the neural plate folds into the neural tube, the lateral edges fuse to form the dorsal midline (roof plate); this converts the mediolateral axis of the neural plate into the D–V axis of the neural tube. Therefore, the notochord regulates differentiation along the D–V axis to generate longitudinal domains that span much of the neural tube.

Before the formation of the cephalic flexure, the anterior end of the notochord ends just caudal to the primordium of the mammillary pouch

(Morris-Kay, 1981; Jacobson and Tam, 1982). The diencephalon, as defined by us (Puelles *et al.*, 1987; Puelles and Rubenstein, 1993), is thereby initially epichordal. This relationship changes as development of the cephalic flexure proceeds (Goodrum and Jacobson, 1981); the rostral tip of the notochord moves progressively caudal to lie approximately at the midbrain–diencephalic boundary. Rostral to the notochord is the prechordal plate. This midline mesoderm underlies the secondary prosencephalon (the prosencephalon rostral to the diencephalon). It is thought that the prechordal plate has inducing properties involved in the D–V patterning of the secondary prosencephalon (Muller and O'Rahilly, 1989; Cohn and Sulik, 1992).

Thus, evidence supports the hypothesis that the neural ectoderm is subdivided into a checkerboard of developmental compartments by the intersection of transverse and longitudinal domains. A further tenet of this hypothesis is that differentiation of each of these domains is controlled by a specific set of transcriptional regulators that specify its developmental program. Over the last 9 years, candidates for these genes have been identified. This chapter describes one class of transcriptional regulators, the homeobox genes. Due to space constraints, other classes of transcriptional regulators, such as basic-helix-loop-helix, fork head, HMG, leucine zipper, MAD, and zinc finger proteins, that may have equally important roles, will not be described in detail. Available evidence suggests that homeobox genes have a central role in regional specification in all animals (McGinnis and Krumlauf, 1992). Thus, it is probable that these genes also have an important role in the regulation of vertebrate brain development. This chapter also restricts its scope to the expression of homeobox genes in the brain, and thus will not describe their interesting role in the development of the spinal cord, peripheral nervous system, and nonneural tissues.

A. Definition and Structure of the Homeodomain

Homeobox genes encode proteins that have a homeodomain which is a 60–61 amino acid motif that was initially found in several *Drosophila melanogaster* homeotic genes. Since then, the homeobox has been found in all of the known homeotic genes in *Drosophila,* as well as in many other genes that regulate other aspects of development. In general, the homeodomain is the major conserved amino acid motif found in these proteins, although other motifs are found in some of these proteins (Fig. 1; also described later). These include the Paired, *POU,* and LIM domains. Furthermore, zinc finger (Fortini *et al.*, 1991) and leucine zipper (Schena and Davis, 1992) motifs have been found on homeodomain pro-

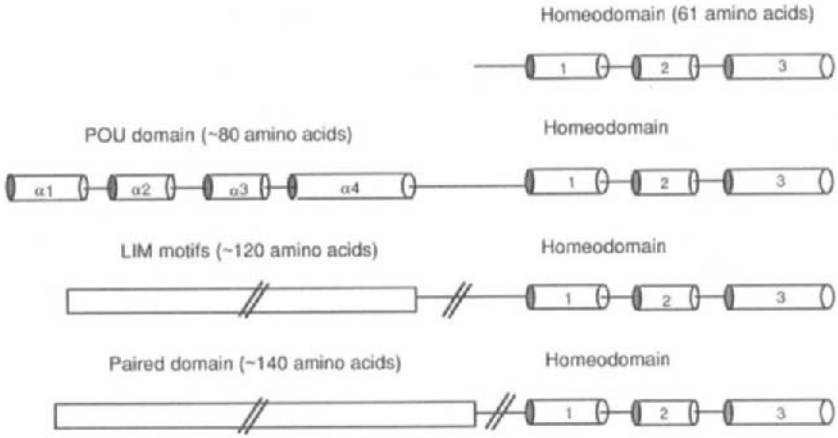

Fig. 1 The homeodomain and other functional motifs found in homeodomain proteins expressed in the brain. The top line shows that the homeodomain consists of a 61 amino acid polypeptide that has three α-helices (illustrated as cylinders) separated by nonhelical domains that allow the helices to bend with respect to each other. DNA sequence recognition is mediated by the third helix and an N-terminal nonhelical domain. The next line shows the bipartite structure found in POU proteins, which have the ~80 amino acid POU domain (four helices), a spacer, and the homeodomain. LIM/homeodomain proteins have a ~120 amino acid cysteine and histidine-rich LIM motif followed by the homeodomain. Some LIM proteins do not have a homeodomain. Finally, some of the *Pax* genes have both the ~140 amino acid *Paired* domain followed by the homeodomain, others only have the *Paired* domain.

teins, although expression of these classes of homeodomain proteins has not yet been identified in the vertebrate brain.

The homeodomain forms a helix-turn-helix structure that binds DNA in a sequence-specific manner. The three-dimensional structure of the homeodomain bound to DNA has been solved for two homeodomains (*engrailed* from *Drosophila* and *MAT*α*2* from yeast) (Kissinger *et al.*, 1990; Wolberger *et al.*, 1991). Although the amino acid sequence of these peptides is quite divergent, their structures are nearly identical. These homeodomains have three α-helices and a flexible N-terminal arm. The structure of the second and the third helices are similar to the helix-turn-helix of bacterial repressor proteins. DNA sequence specificity is conferred by three residues in helix 3 and one to two residues in the N-terminal arm. The helix 3 side chains make base contacts to the major groove in DNA and the N-terminal arm side chain(s) interacts with the minor groove. Contacts with the deoxyribose-phosphate backbone are made by eight amino acid side chains; these residues are identical between *engrailed* and *MAT*α*2*, and are postulated to be responsible for proper positioning

of the homeodomain on the DNA. The rules that govern the DNA binding specificity of homeodomain proteins are just beginning to be elucidated and early results suggest that the situation may be complex. For instance, in yeast, accessory proteins MATa1 and MCM1 can alter the binding specificity of the MATα2 protein [see Herskowitz (1989) for a review].

B. Function of Homeobox Genes

Homeodomain proteins are transcriptional regulators. They belong to a large family of helix-turn-helix proteins that are found in all organisms. In bacteria these proteins include the lambda, *trp*, and *lac* repressors. In yeast, homeodomain proteins MATa1 and MATα2 have pivotal roles in determining the dimorphic mating type phenotypes, whereas the PHO 2 protein is involved in phosphate metabolism. In all eukaryotes, these proteins take part in a wide range of functions; studied in greatest detail in *Drosophila melanogaster* (Lawrence, 1992). During embryogenesis of the fruit fly, homeodomain proteins play integral roles in setting up the embryonic axes, in establishing segmentation (gap, pair rule, and segment polarity genes), and in determining the identity of the segments (homeotic genes). Once the basic body plan has been determined, homeodomain proteins then have roles in controlling morphogenesis of body parts and in regulating cellular differentiation.

As noted earlier, all of the homeotic genes in *Drosophila* have a homeobox. The homeotic genes that specify the identity of the abdomen, thorax, and posterior part of the head are assembled in two clusters, called the *antennapedia-bithorax* cluster. The regulatory genes that specify the anterior part of the head (e.g., *empty spiracle* and *orthodenticle*) are not organized as a cluster. Null mutants of the *antennapedia-bithorax* genes lead to two general types of phenotypes [see McGinnis and Krumlauf (1992) for a review]: the deletion of a segment such as in null mutants of the labial and the deformed genes, and the transformation of a segment to a more posterior phenotype (a homeotic transformation) as exemplified by null mutants of the *sex combs reduced, antennapedia, ultrabithorax,* and *abdominal A* and *B* genes. In each case, the region that is affected is the body segment that is the anterior-most domain where the gene is expressed. Ectopic expression of homeotic genes can cause transformations of body parts (McGinnis and Krumlauf, 1992). For instance, expression of the antennapedia gene in the head causes a partial homeotic transformation of the head epidermis into thoracic epidermis.

In the last several years, homologues of the genes in the *antennapedia-bithorax* clusters have been identified in all metazoans (McGinnis and Krumlauf, 1992). In most metazoans, these genes are organized as a single

cluster. Evidence suggests that these genes subserve a central function in the development of all animals—the identity of cells along the anterior–posterior axis. Mutational analysis of these genes in nematodes, flies, and mice supports this hypothesis.

Vertebrates have four copies of the *antennapedia-bithorax* cluster (McGinnis and Krumlauf, 1992). In mice, these genes are called the *Hox* genes, and the clusters are called *Hox A, B, C,* and *D* (the nomenclature used to be *Hox-1, 2, 3,* and *4*) (Fig. 2). These genes are expressed along most of the longitudinal axis of vertebrate embryos into the posterior part of the head, analogous to their expression patterns in *Drosophila* (Fig. 3). Genes at the 3′ end of the cluster are expressed earliest and in

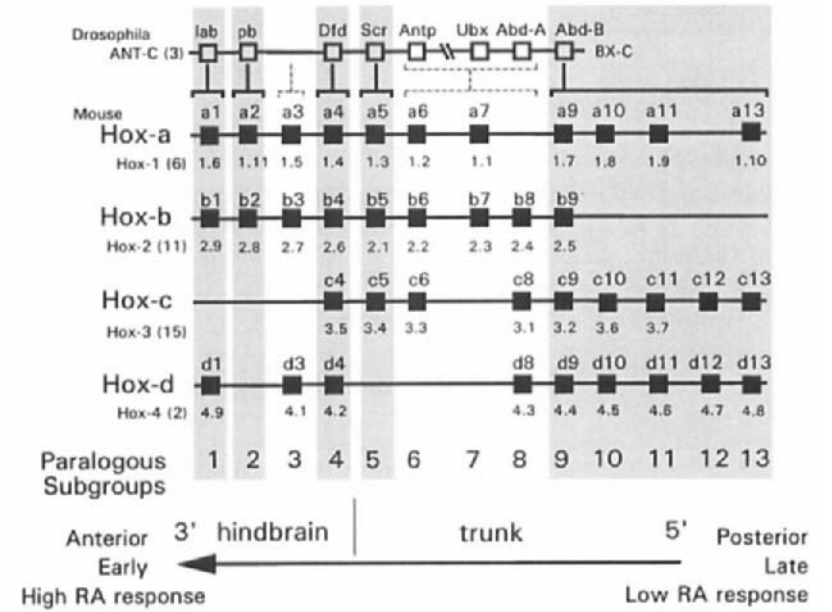

Fig. 2 Organization and alignment of the *HOM-C* and *Hox* complexes. The top line shows the genomic organization of the *Drosophila melanogaster antennapedia-bithorax* (*ANT-BX-C*) complex homeotic selector genes. Genes at the left are 3′ to genes at the right. Below the *HOM-C* genes are the four mouse *Hox* clusters (a,b,c, and d). The names for each gene are written above the genes (black boxes). Previous nomenclature referred to these gene clusters as *Hox-1, -2, -3,* and *-4* (the old names for each gene are written below each of the boxes). The murine chromosomal assignments for each gene complex are listed in parentheses in the left-hand column. There are 13 vertebrate *Hox* paralogue groups that are hypothesized to represent homologues of specific *HOM-C* genes. None of the *Hox* clusters have genes in all paralogue groups. Genes at the 3′ end of the clusters are expressed the earliest during development, in the most rostral domains, and are the most sensitive to induction by retinoic acid (RA). [From Krumlauf (1993) with permission.]

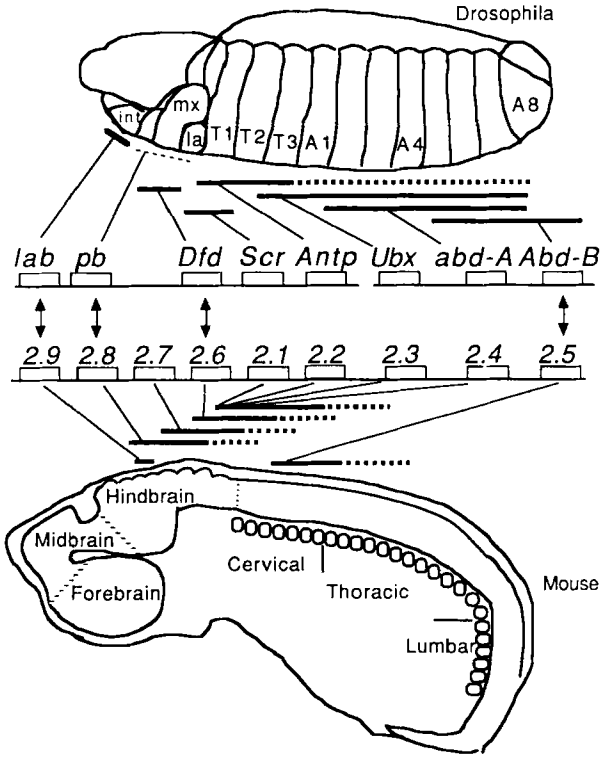

Fig. 3 The expression domains of the *HOM-C* and *Hox*-b (*Hox*-2) genes. (Top) *HOM-C* gene expression in the epidermis and CNS of a 10-hr *Drosophila* embryo. (Bottom) *Hox*-b gene expression in the CNS of a 12-day mouse embryo. [From McGinnis and Krumlauf (1992) with permission.]

the most anterior positions, whereas genes at the 5′ end of the cluster are expressed later and in the most posterior position. There are 13 *Hox* paralogue groups (Fig. 2) that are believed to be evolutionarily related to a primordial *Hox* cluster. The mouse *Hox* clusters have between 9 and 12 *Hox* genes; thus, not all of the paralogue groups are represented in each cluster. In the central nervous system, these genes are expressed in the spinal cord and into the hindbrain, but do not reach the midbrain/hindbrain junction. Thus, as in *Drosophila*, a different set of genes is used to control regional specification of the anterior part of the central nervous system. This chapter describes the homeobox genes that are expressed during development of the mammalian brain. These include the *Hox* genes that are expressed in the hindbrain, as well as several other families of homeobox genes, most of which have homologues in *Drosophila*. These

include the *Dbx, Dlx, Emx, En, Gbx, Gtx, LIM/homeobox, Msx, Nkx, Otx, Pax,* and *POU* genes. The amino acid sequence of the homeodomain from an example of each of these classes is shown in Table I. In the following sections, the structural information, expression patterns, and data regarding the function of these genes are reviewed, when available. At this point, descriptive data far outweigh functional insights. The expression patterns of many of these genes have provided unique insight into structural domains within the embryonic brain. These insights have played an important part in supporting the present model of hindbrain segmentation (Lumsden and Keynes, 1989; Keynes and Lumsden, 1990), and have provided a similar foundation for our model of forebrain organization (Bulfone *et al.*, 1993b; Puelles and Rubenstein, 1993). To understand the expression patterns that are described in the subsequent sections, it is necessary to understand the anatomy of the embryonic brain; the next section provides a brief overview of brain morphogenesis.

C. Overview of Brain Morphogenesis

During gastrulation the neural plate is formed along the dorsal side of the entire longitudinal axis of the embryo. The lateral edges of the neural plate, which give rise to the neural crest, fold toward the dorsal midline to form the neural tube. The cells lining the ventricular surface of the neural tube form a pseudostratified epithelium called the ventricular zone. This cell layer contains the neural stem cells. When stem cells leave the cell cycle, they migrate away from the ventricular zone and begin to differentiate in the mantle zone of the neural tube. At specified positions along the longitudinal axis, constrictions form in the wall of the neural tube. These constrictions are the morphological correlates of boundaries that separate the principal structures of the central nervous system, i.e., the spinal cord, and the primary brain vesicles: the hindbrain (rhombencephalon), the midbrain (mesencephalon) and the forebrain (prosencephalon) (Fig. 4). Further morphogenetic events then modify each of the brain vesicles. This includes additional constrictions in the hindbrain and forebrain. In the hindbrain, these constrictions subdivide the rhombencephalon into the large isthmo-cerebellar region rostrally and seven (or eight) transverse segments (rhombomeres) caudally (Vaage, 1969) The midbrain and isthmus, which are not clearly separated morphologically at early stages, appear to be subdivided into several transverse regions that contribute to the mature midbrain and isthmic and cerebellar structures (Vaage, 1973; Puelles and Martinez-de-la-Torre, 1987; Martinez and Alvarado-Mallart, 1989; Hallonet *et al.*, 1990; Marin and Puelles, 1994). Finally, the forebrain is also subdivided by transverse constrictions that

Table I Homeodomain Sequences of Selected Homeobox Genes Expressed in the Mouse Brain

Dlx-2	VRKPRTIYSSFQLAALQRRFQKTQYLALPERAELAASLGLTQTQVKIWFQNRRSKFKKMWK	61/61
Msx-1	N--P--PFTTA--L--E-K-RQK---SIA----FSSS-S--E----------A-A-RLQE	34/61
Gbx-2	N-RR--AFT-E--LE-EKE-HCKK--S-T--SQI-HA-K-SEV----------A-W-RVKA	28/61
Gtx	KKHS-PTF-GQ-IF--EKT-EQ-K---G----R--Y---MTES---V------TKWR-RHA	28/61
Hox-B1	PGGL--NFTTR--TE-EKE-HFNK--SRAR-V-I--T-E-NE----------M-Q--RER	28/61
Nkx-2.1	R--R-VLF-QA-VYE-E---KQQK--SA---EH--SMI H--P---------H-Y-M-RQA	27/60
Dbx	GMLR-AVF-DV-RK--EKT---QK-ISK-D-KK--SK---KDS----------M-WRNSKE	27/61
En-1	DKR---AFTAE--QR-KAE--ANR-ITEQR-QT--QE-S-NES-I------K-A-I--ATG	25/61
Emx-1	PKRI--AF-PS-LLR-E-A-E-NH-VVGA--KQ--G--SLSE----VN-Q---TKYKRQKL	25/61
Otx-1	Q-RE--TFTRS--DV-EAL-A--R-PDIFM-E-V-LKI N-PESR-QV--K---A-CRQQQQ	21/61
Pit 1	K--R--TI-IAAKD--E-H-GEHSKPSSQ-IMRM-EE-N-EKEV-RV--C---QRE-RVK	20/60
Isl-1	TTRV--VLNEK--HT-RTCYAANPRPDALMKEQ-VEMT--SPRVI RV----K-C-D--RS	16/60
Pax-6	LQRN--SFTQE-IE--EKE-ER-H-PDVFA-ER---KI D-PEARI QV--S---AKWRREE-	18/61
LH-2	TKRM--SFKHH--RTMKSY-AI NHNPDAKDLKQ--QKT---KRVLQV----A-A--RRNLL	17/61

Note. An attempt was made to choose one member of each class of homeodomain gene family. All of the amino acid sequences are compared relative to the *Dix-2* homeodomain, and the amino acid identities are listed to the right. See the text for the references for each gene.

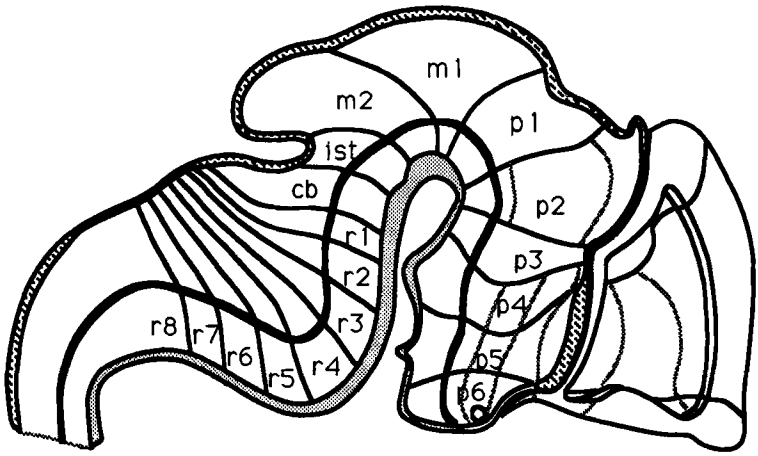
m1
m2
p1
ist
cb
p2
r1
p3
r2
p4
r8
r7
r3
r6
r5
r4
p5
p6

Fig. 4

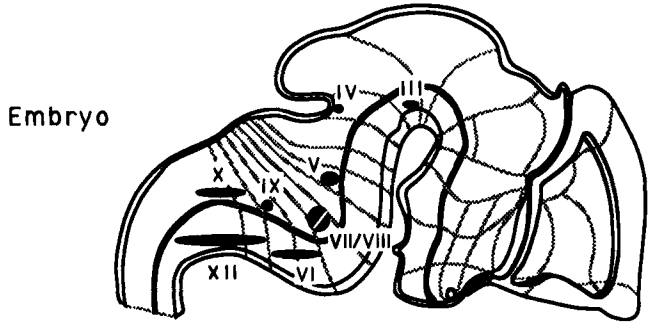
Embryo
IV
III
V
X
IX
VII/VIII
XII
VI

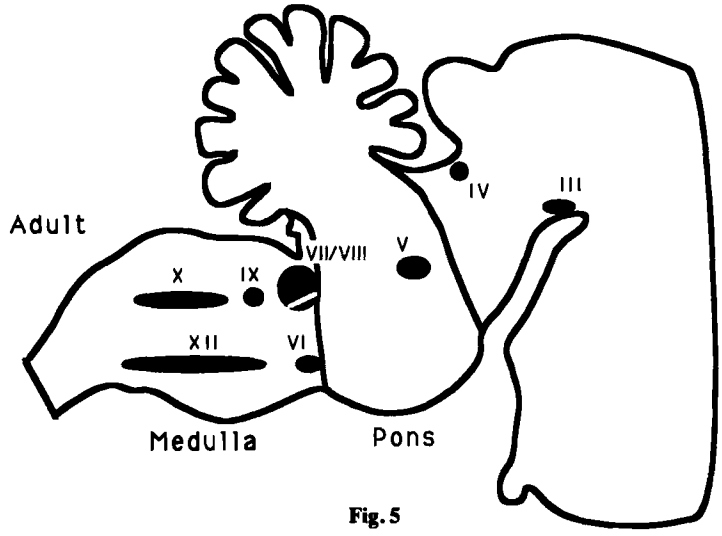
Adult
IV
III
VII/VIII
V
X
IX
XII
VI
Medulla
Pons

Fig. 5

may represent the boundaries between six forebrain segments called prosomeres (Bulfone *et al.*, 1993b; Puelles and Rubenstein, 1993).

Within the entire neuraxis, there are four principal zones that are stacked ventrodorsally in parallel to the longitudinal axis. The floor plate and roof plate are found at the ventral and dorsal midlines, respectively, and generally do not give rise to neurons. Between them are the major neurogenic plates, the basal (ventral) plate and the alar (dorsal) plate (His, 1893). The longitudinal axis of the neural tube changes direction at three places. These bends occur at the junction of the spinal cord with the hindbrain (cervical flexure, ~90° flexion), in the middle of the hindbrain (pontine flexure, ~90° extension), and in the middle of the midbrain (cephalic flexure, ~180° flexion). It is critical to appreciate these changes in the direction of the longitudinal axis in order to understand neuromeric (segmentation) models of the brain. Available evidence suggests that differential rates of mitosis in basal and alar plates regulate, in part, the changes in curvature of the neural tube. Furthermore, the end of the rigid notochord near the junction of the midbrain with the forebrain may also contribute to the hairpin flexure at the midbrain–forebrain junction.

Additional morphogenetic changes further modify the brain. These are particularly complex in the prosencephalon. Upon closure of the rostral neuropore, the prosencephalon is a single vesicle called the primary prosencephalon. As noted earlier, the primary prosencephalon is subsequently subdivided by constrictions into transverse domains that may represent

Fig. 4 A medial view of the brain of an E12.5 mouse. The transverse (neuromeric) subdivisions are delineated by solid thin black lines that are perpendicular to the principal longitudinal subdivision (thick black line) that divides the alar and basal zones, and defines the longitudinal axis of the brain. Four longitudinal zones are shown in the spinal cord (from dorsal to ventral): roof plate (dotted), alar plate, basal plate, and floor plate (stippled). These four zones extend to the rostral limit of the prosencephalon. The rhombomeric (r1–r7) and the theoretic cerebellar (cb), isthmic (ist), mesencephalic (m1 and m2), and prosencephalic (p1–p6) segments are identified. The optic stalk is shown as a circle in p6. See Fig. 4 in Puelles and Rubenstein (1993) for a more extensive description.

Fig. 5 The relationship of the pons (metencephalon) in the adult brain to various morphological features and cranial nerve exist points in the embryonic and adult hindbrain and midbrain. This figure shows that various structures in the adult pons come from different embryological locations, and therefore it can be misleading to draw conclusions about embryological relationships based on morphological analyses of the adult brain. (Top) A neuromeric model of the brain (see Fig. 4), including the exit points for cranial nerves III–XII. (Bottom) A medial view of the adult hindbrain, midbrain, and part of the forebrain, indicating the major morphological features and the location of the cranial nerve exit points. The pons, which includes the cerebellum and the fifth nerve, is outlined. Note that according to the neuromeric conception, the cerebellum originates rostral to the rhombomeres that are the pontine primordia (r1–r3). See text for a more complete discussion.

the forebrain neuromeres (Puelles *et al.*, 1987; Bulfone *et al.*, 1993b; Puelles and Rubenstein, 1993). From caudal to rostral, the first three constitute the diencephalon, and the last three form the secondary prosencephalon. Additionally, a series of evaginations occur in the prosencephalon. These form the paired telencephalic vesicles, optic vesicles, and the preoptic and mammillary recesses, as well as the midline infundibulum and epiphysis. Regions in the telencephalon where there is rapid inward growth form prominent collections of mitotic cells that are called the lateral, medial, and caudal ganglionic eminences.

As specification and morphogenesis take place, cellular differentiation and migration begin to generate the region-specific tissues of the forebrain. Mitotic zones are largely restricted to the periventricular layers of cells: the ventricular and subventricular zones. Cells that are programmed to leave the proliferative zones, migrate superficially and settle in the mantle layer where they undergo region-specific differentiation programs to produce particular cell types and intercellular connections. In the following sections, evidence shows that homeobox genes are expressed at most of these stages and regions in brain development, and therefore are candidates for regulating many of these morphogenetic processes.

II. Homeobox Genes Expressed in the Rhombencephalon

A. Expression of *Hox* Genes Respect Segmental Boundaries

The hindbrain in adult vertebrates consists of the medulla, pons, and isthmus, structures that contain cranial nerves IV–II, as well as other important nuclei (Figs. 5 and 7). Apart from the rostral isthmocerebellar region, the embryonic hindbrain (rhombencephalon) of all vertebrates displays seven neural segments called rhombomeres. An eighth rhombomere has been postulated as well (Keynes and Lumsden, 1990). Each segment contains a floor plate, a basal plate (where the motor neurons are located), an alar plate (where the commisural and relay neurons are located), and a roof plate. Hindbrain neural crest is derived from the dorsal edges of the alar plate. Neural crest begins to migrate away from the neural plate before it has completely closed and contributes to a wide range of tissues including the cranial ganglia, mesenchymal tissues in the branchial arches, the meninges, and the skull. During periods when regional specification is taking place, differential adhesive properties at the boundaries restrict the mixing of neuroepithelial cell clones between rhombomeres (Fraser *et al.*, 1990). Furthermore, there are discontinuities of intercellular communication at the rhombomeric boundaries (Martinez *et al.*, 1992). Cells within a rhombomere are electrically coupled and allow

diffusion of small dye molecules from one cell to another, whereas at rhombomeric boundaries there are cells that restrict the diffusion of small molecules. At this embryonic stage, it is hypothesized that specific patterns of gene expression specify the identity of each rhombomere (Krumlauf, 1993; Krumlauf *et al.*, 1993). In particular, homeobox genes are expressed in the hindbrain in patterns that respect inter-rhombomeric boundaries (Krumlauf, 1993; Krumlauf *et al.*, 1993). To date, most of the work has focused on the *Hox* homeobox genes, but other classes of homeobox genes are also expressed in the embryonic hindbrain (see later). As will be discussed later, mutational analysis of several *Hox* genes demonstrates that they have important functions in the patterning of the hindbrain as well as the cranial neural crest.

The expression patterns of the *Hox* genes follow some general rules, but exceptions add complexity to this subject [see Krumlauf (1993) and Krumlauf *et al.* (1993) for a more complete discussion]. The *Hox* genes are expressed in longitudinal domains extending through varying extents of the spinal cord. Genes from paralog groups 5–13 have their rostral expression boundaries in the spinal cord, whereas genes from paralogue groups 1–4 end in the hindbrain (Fig. 2). The rostral expression boundaries of these *Hox* genes end at inter-rhombomeric boundaries (Figs. 6 and 7). Genes at the 3′ end of the *Hox* clusters are usually expressed in the most anterior positions. An exception to this rule is the *Hox-A2* gene; it is expressed up to the r1/r/2 (r, rhombomere) boundary, rostral to the *Hox-A1* gene that is expressed up to the r2/r3 limit (Joseph Grippo, Hoffman LaRoche, personal communication). This is illustrated in Figs. 6 and 7 and in Table II which describe the expression patterns of the *Hox* genes in the hindbrain. Paralogue groups 3 and 4 from the *Hox A*, *B*, and *D* clusters have identical rhombomeric boundaries at r4/r5 and r6/r7, respectively, whereas paralogue groups 1 and 2 do not always share common boundaries. For instance, at E8 both *Hox-A1* and *Hox-B1* are expressed in a continuous domain up to the r3/r4 boundary; however, by E9.5 their patterns diverge. At this age, the caudal boundary of *Hox-B1* is modified so that its expression is restricted to r4, whereas the anterior boundary of *Hox-A1* moves rostrally to r2/r3. Therefore, *Hox-A1* expression extends one rhombomere rostral to *Hox-B1*. Likewise, *Hox-A2* is expressed up to r1/r2, whereas *Hox-B2* is expressed up to r2/r3. The latter gene becomes restricted to the r3–r5 segments later in development.

The expression patterns also show additional temporal and spatial complexities. At E8.0–E9.25, the level of expression of all the *Hox* genes is relatively uniform along the longitudinal axis. By E9.5, variations in the levels of expression are observed, as different rhombomeres have different levels of expression, and typically, the rostral-most domain has the highest level of expression. For example, *Hox-A3* and *Hox-B3* have the

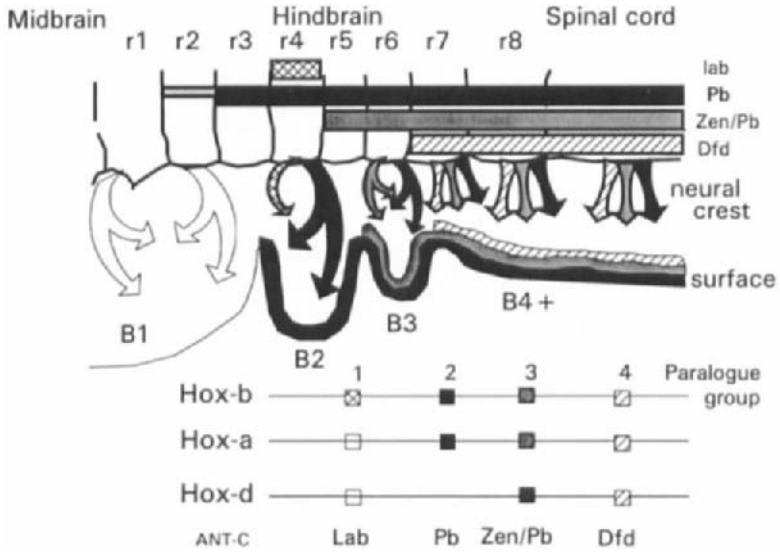

Fig. 6 The relationship among hindbrain position, *Hox* gene expression, and hindbrain neural crest migration into the branchial arches. (Top) *Hox* expression in the hindbrain; the rostral boundaries of *Hox* gene expression respect rhombomere boundaries. The arrows below the rhombomeres show the migration pathways of the cranial neural crest into the mesenchyme of the branchial arches (B1, B2, B3, and B4), thereby showing how *Hox* gene expression in the hindbrain could contribute to patterning of the branchial arches. (Bottom) Paralogue groups 1–4 of the *Hox-A*, *Hox-B*, and *Hox-D* clusters are shown, as well as their relationship to four *HOM-C* genes from the antennapedia complex (*ANT-C: Lab, Pb, Zen/Pb, Dfd*). [From Krumlauf (1993) with permission.]

strongest expression in r5. On the other hand, the *Hox-A2* gene, which is expressed up to the r1/r2 boundary, has its highest levels of expression in r3 and r5.

The expression patterns of the *Hox* genes are also spatially restricted along the dorsoventral axis; furthermore, these variations are dependent on the stage of development. For instance, up to E9.5 the *Hox-B* genes are uniformly expressed, but then many show a restriction to the dorsal spinal cord. Krumlauf (1993) points out that this transition in expression occurs concomitantly with the appearance of specific cell types (commissural and sensory neurons), and suggests that these genes may specify distinct cell types. On the other hand, *Hox-A2*, which is expressed up to r1/r2, does so only in the ventral part of r2; thus, because it is not expressed dorsally in r2, cranial neural crest cells derived from r2 are probably not exposed to the *Hox-A2* protein.

As noted earlier, the *Hox* genes are also expressed in the cranial neural crest that contribute to parts of the cranial ganglia and branchial arches.

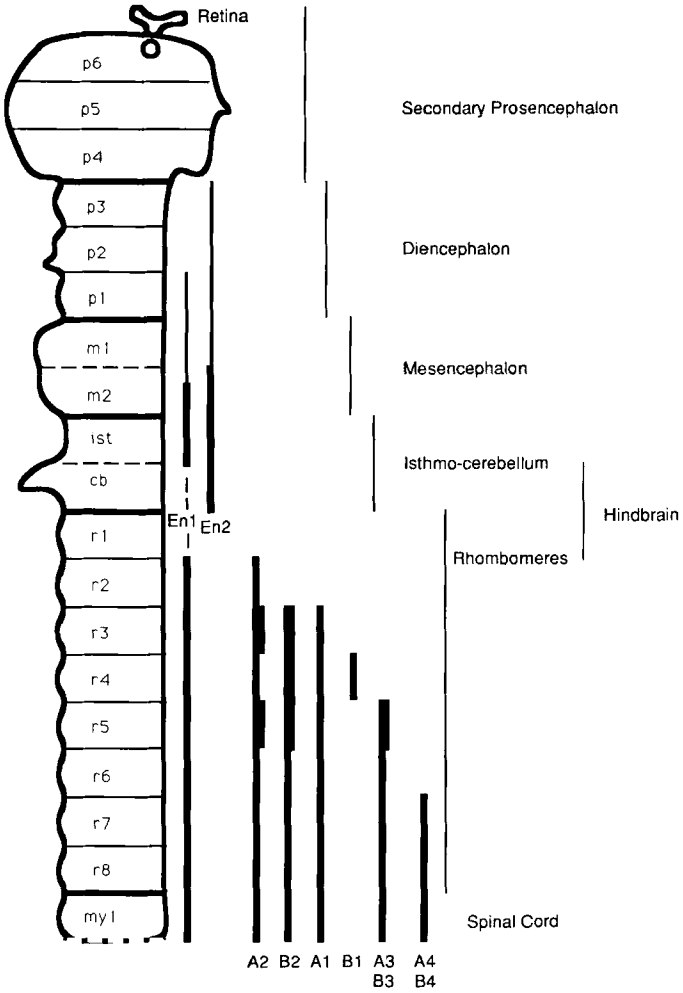

Fig. 7 Schematic representation of the longitudinal patterns of gene expression relative to the rhombomeres and hypothesized neural segments in the isthmocerebellum, mesencephalon, and prosencephalon. Eight rhombomeres (r1–r8) and six prosomeres (p1–p6) are indicated. Subdivisions of the isthmocerebellum (ist and cb) and mesencephalon (m1 and m2) are indicated by dotted lines. The optic stalk (circle) and retina are shown as part of prosomere 6 (p6). The locations of the major brain regions [secondary prosencephalon, diencephalon, mesencephalon, isthmo-cerebellum, rhombomeres, and spinal cord (my)] are shown to the far right of the figure. The longitudinal expression patterns of the *En-1* and *En-2* (at ~E12.5) and selected *Hox-A* and *Hox-B* genes (at E9.5) are shown, with boundaries at specific interneuromeric limits. The width of the lines relates to the amplitude of gene expression within these tissues; dotted lines signify no expression.

Table II Expression Patterns and Chromosomal Localization of Homeobox Genes Expressed in Mouse Brain

Gene	Chr: mouse	Chr: human	Spinal cord	Hindbrain	Midbrain	Forebrain	Pituitary/ eye
Hox A	IV	VII	Yes	r2–r7	No	No	No
Hox B	XI	XVII	Yes	r3–r7	No	No	No
Hox C	XV	XII	Yes	No	No	No	No
Hox D	II	II	Yes	r5–r7	No	No	No
En-1,2	I, V		Yes	r1	Yes	?	No
Dix-1,2	II	II	No	No	No	Yes	Eye
Nkx-2.1,2.2	XII, II	XIV	No	No	No,Yes	Yes	No
Otx-1			No	No	Yes	Yes	Eye
Otx-2			No	Yes	Yes	Yes	Eye and pit
Emx-1			No	No	No	Yes	No
Emx-2			No	No	Yes	Yes	No
Gbx-1	I		Yes	~r1–r2	No	Yes	No
Dbx			Yes	Yes	Yes	Yes	No
Gtx			Yes	Yes	Yes	Yes	Eye
Msx-1		IV	Yes	Yes	Yes	Yes	Eye
Msx-2		V	No	No	No	No	Eye
Pax-3	I	II	Yes	Yes	Yes	Yes	No
Pax-7			Yes	Yes	Yes	Yes	No
POU							
Brn-1	I	I	Yes	Yes	Yes	Yes	No
Brn-2	IV		Yes	Yes	Yes	Yes	No
Brn-3.0	XIV	XIII	Yes	Yes	Yes	Yes	Eye and pit
Brn-3.1	XVIII		?	?	?	?	No
Brn-3.2			Yes	Yes	Yes	?	Eye
Brn-4(RHS2)	I	I	Yes	?	Yes	Yes	No
Brn-5 (Emb)	XV		ND	ND	ND	ND	No
Oct-1(OTF-1)	I	I	?	?	?	?	?
Oct-2(OTF-2)	VII	XIX	Yes	Yes	Yes	Yes	No
Oct-6(Tst 1)	IV		?	Yes	Yes	Yes	No
Pit-1(GHF-1)	XVI		No	No	No	No	Pit
LIM							
LH-2			Yes	Yes	?	Yes	Eye
lsl-1	VII		Yes	Yes	Yes	Yes	Eye

Note. The names for all of the homeobox genes (that the authors are aware of) that are expressed in the brain are listed in the left hand column, followed by the chromosomal localization (when available) of these genes in the mouse and in humans. The expression domains of each gene are crudely described in terms of whether they are expressed in the spinal cord, hindbrain (r, rhombomere), midbrain, forebrain, pituitary, and the eye. Yes/no indicates whether the gene is expressed in the indicated domain; ? indicates uncertainty; ND indicates that data were not found by the authors. This chart does not indicate when the gene is expressed. References and more detailed descriptions of the expression for each gene (in some cases figures showing the expression) can be found in the text.

Crest cells from a given rhombomere migrate ventrally to populate the branchial arch mesenchyme that is at the same relative position along the longitudinal axis (Fig. 6). Thus, crest cells from r1 and r2 fill branchial arch 1 (B1), those from r4 fill B2, crest cells from r6 fill B3, and those from r7 and r8 fill B4. *Hox* genes are expressed in the crest cells emanating from r4, r6, r7, and r8 [there is some debate about whether rhombomeres 3 and 5 produce crest cells, although evidence suggests that they make some and that they have distinct migration pathways (Sechrist *et al.*, 1993)]. Thus, potentially, *Hox* gene expression in the hindbrain can contribute to the development of cranial ganglia and branchial arch-derived structures. Mutations of *Hox-A1* and *Hox-A3* bear out this hypothesis (see the following section). No *Hox* genes are expressed in the crest cells that populate B1 (see the earlier discussion for *Hox-B2* restriction to the noncrest cells in r2); thus other regulatory genes must be involved in the development of B1. Expression of the *Dlx-1* and *Dlx-2* genes has been observed in neural crest derivatives in B1 (and in cranial ganglia) as well as in B2, B3, and probably B4 (Dollé *et al.*, 1992; Bulfone *et al.*, 1993a). It is interesting that available data suggest that the *Dlx* genes are not expressed in the hindbrain, implying that these genes are turned on only after the crest cells have left the neural tube.

B. Regulation of *Hox* Expression in the Rhombencephalon

The regulation of *Hox* gene expression has just begun to be studied. As noted earlier, most of these genes are expressed in complex temporal and spatial patterns. Thus, it is likely that the regulatory pathways that control *Hox* gene expression are intricate. Several laboratories have initiated studies into this problem by identifying regulatory elements using transgenic mouse assays. These are done by making a transgenic mouse that expresses a chimeric gene consisting of a fusion of a putative regulatory genomic fragment of a *Hox* gene to the *LacZ* coding region. Several transgenic mouse strains have been constructed that express *LacZ* in a pattern that is similar or identical to the endogenous *Hox* genes; these include strains expressing *LacZ* under the control of *Hox-A5* (Zakany *et al.*, 1988), *Hox-A7* (Puschel *et al.*, 1991), *Hox-B1* (Marshall *et al.*, 1992), *Hox-B2* (Marshall *et al.*, 1992), *Hox-B4* (Whiting *et al.*, 1991), *Hox-B6* (Schughart *et al.*, 1991), and *Hox-C8* (Bieberich *et al.*, 1990). Systematic analysis of smaller parts of these regulatory domains allows the identification of the DNA sequences responsible for controlling various aspects of the expression patterns. Analysis of the *Hox-B2* gene has already led to the identification of DNA fragments that control expression in rhombomeres 3 and 5 (Sham *et al.*, 1993) and rhombomere 4 (Marshall *et al.*, 1992).

Once putative enhancer and silencer elements are functionally identified, their DNA sequences can be studied. For instance, DNA footprinting analysis of the *Hox-B2* fragment that confers expression in rhombomeres 3 and 5 revealed a motif that is recognized by the *Krox20* protein (Sham *et al.*, 1993). This was interesting because the *Krox20* protein is also expressed in rhombomeres 3 and 5. This finding was further studied using transgenic mice that express two transgenes. One transgene consisted of *LacZ* under the control of the *Hox-B2* fragment. The other transgene consisted of the *Krox20* coding sequence under the transcriptional control of the *Hox-B4* gene (*Hox-B4* is expressed in r7 and r8). Thus, this transgene ectopically expressed *Krox20* in the caudal hindbrain (with a boundary at r6/r7). Therefore, in these mouse embryos, there were three domains of *Krox20* expression, the normal rhombomere 3 and 5 domains, as well as the ectopic domain in the caudal hindbrain. When the *Hox-B2–LacZ* expression was studied, β-galactosidase activity was found in rhombomeres 3 and 5, and in the caudal hindbrain. These studies strongly support the idea that the *Krox20* gene regulates the expression of *Hox-B2* in rhombomeres 3 and 5. Mice homozygous for a loss-of-function allele of the *Krox20* gene have been constructed (Swiatek and Gridley, 1993). Using molecular markers, it was concluded that rhombomeres 3 and 5 were missing in *Krox20* mutant embryos. Therefore, in this experiment it was not possible to test whether *Hox-B2* expression was affected by the lack of *Krox20*.

Thus, while this approach is making inroads into understanding how other transcriptional regulators can control expression of *Hox* genes, they do not address how spatial information can regulate these genes. For instance, what is the substance(s) that is produced by Spemann's organizer that travels along the plane of the ectoderm and induces neural tissue and transverse bands of homeobox and *Krox20* gene expression? How is this signal(s) transduced to alter gene expression? There are many other examples of inductive and morphogenetic processes in neural development for which there are few data regarding their molecular mechanisms. However, retinoic acid is a candidate for having a role in several of these processes. Furthermore, retinoic acid can effect the expression of the *Hox* genes.

Retinoic acid and/or chemical relatives of this molecule have been implicated in a wide variety of embryological processes including limb development (Tabin, 1991), gastrulation (Hogan *et al.*, 1992), and olfactory bulb induction (LaMantia *et al.*, 1993). The initial evidence that retinoic acid can regulate homeobox gene expression came from experiments with embryonal carcinoma cells [for a review see Boncinelli *et al.* (1991)]. Treatment of these cells with retinoic acid leads to stereotypic responses in the expression of the *Hox* genes. Genes at the 3′ end of the clusters

are induced first and reach maximal levels of expression within about 24 hr. Genes at the 5′ end of the clusters are either induced late or weakly; expression of some of the 5′ genes also show inhibition by the retinoic acid. For instance, genes in the middle of the clusters reach maximal levels of expression around 60–80 hr after exposure to retinoic acid, and some genes at the 5′ end of the clusters do not reach maximal expression even after 180 hr.

These cell culture experiments have been extended by studying the expression of *Hox* genes in retinoic acid-treated embryos. Retinoic acid is a potent teratogen; its effects are complex because they are dependent on the dose and stage of the treated embryo. Retinoic acid exposure of all vertebrate species results in morphological abnormalities of the hindbrain. These abnormalities appear to be due in part to a posteriorization of the hindbrain (Maden and Holder, 1992). Furthermore, the expression of the *Hox* genes in retinoic acid-treated embryos is abnormal; the rostral boundaries of the genes are more anterior than normal (Marshall *et al.*, 1992; Kessel, 1993). Analysis of the effect of retinoic acid on homeobox gene expression has been aided by the use of several transgenic mouse strains that express the *LacZ* reporter gene under the control of different regulatory sequences: *Hox-B1, Hox-B2, Krox20* (Marshall *et al.*, 1992), and *Hox-A7* (Kessel, 1993). For instance, retinoic acid treatment of mouse embryos harboring the *Hox-B1–LacZ* gene at ~E7.5 causes an anterior shift in the expression domain extending through the entire rostral hindbrain at E8.5 (the expression in the hindbrain at E8.5 of untreated embryos is restricted to rhombomere 4). Examination of the retinoic acid-treated embryos at E9.5 revealed a refinement of the pattern such that *LacZ* was found in rhombomeres 2 and 4; again untreated embryos at this age expressed *LacZ* only in rhombomere 4. This showed that retinoic acid caused a duplication of the rhombomere 4 *Hox-B1* domain in rhombomere 2, implying that the ectopic expression of *Hox-B1* and perhaps other genes leads to the respecification of rhombomere 2 as rhombomere 4. This was substantiated by the analysis of expression patterns of the *Hox-B2* transgenes (Marshall *et al.*, 1992). Furthermore, examination of the expression pattern of the *Krox20* transgene suggested that rhombomere 3 had been respecified as rhombomere 5. Analysis of the patterning of motor neurons and axon pathways in these rhombomeres also supports these conclusions (Marshall *et al.*, 1992; Kessel, 1993). These studies clearly demonstrate that retinoic acid changes the phenotype of rhombomeres 2 and 3 into structures that have the same gene expression patterns, motor neuron organization, and axon trajectories as those seen in rhombomeres 4 and 5. They suggest, but do not prove, that the changes in *Hox* gene expression have a role in respecifying the hindbrain neuroepi-

thelium. Direct evidence for the role of the *Hox* genes in hindbrain development has come from a mutational analysis of these genes, which is described later.

At this juncture, it is important to mention that there are many other homeobox genes that are expressed in the embryonic hindbrain. Most of the known genes appear to be expressed continuously along the longitudinal axis, including several *POU* and *Pax* genes (see the following section). There are additional homeobox genes that are expressed in spatially restricted domains, including *Gbx-2*, roughly in rhombomeres 6-7 and 1-2 (Bulfone *et al.*, 1993b) and *En-1*, in the rostral rhombencephalon (Davidson *et al.*, 1988).

C. Analysis of *Hox* Gene Function in Rhombencephalon Development

Loss of function mutations of four murine *Hox* genes (*Hox-A1*, *Hox-A3*, *Hox-B4*, and *Hox-C8*), produced using gene targeting methods, have been published (Table III). Two of these mutations (*Hox-A1* and *Hox-A3*) affect genes that are expressed in the hindbrain. In each case, the region of the embryo affected by these homozygous mutations (heterozygotes appear

Table III Homeobox Mutations

Gene	Species	Genetics	Principal abnormalities
Hox-A1	Mouse	Recessive	Abnormal development of brain stem and ear
Hox-A3	Mouse	Recessive	Abnormal development of cranial neural crest
Hox-B4	Mouse	Recessive	Abnormal development of cervical vertebrae and sternum
Hox-C8	Mouse	Recessive	Abnormal development of axial skeleton
Pit-1	Mouse	Recessive	Loss of specific cell types in anterior pituitary
Pit-1	Human	Recessive	Loss of specific cell types in anterior pituitary
Pax-3	Mouse	Semidominant	sp/+: pigmentation and neural crest defects sp/sp: spina bifida, exencephaly
Pax-3	Human	Semidominant	Pigmentation and hearing defects
Pax-6	Mouse	Semidominant	sey/+: small eyes sey/sey: absence of eyes and nasal primordia
Pax-6	Human	Semidominant	Abnormal development of iris, lens, cornea, and retina
En-2	Mouse	Recessive	Abnormal cerebellar folia
Msx-2	Human	Dominant	Craniosynostosis

Note: Homeobox genes that have known mutations, the species where the mutation has been observed, the genetics of the mutation, and the principal phenotype of the mutant animal/human. References describing these mutations can be found in the text. sp, splotched mice; sey, small eye mice.

normal) correspond to the anterior part of the gene expression domain; for the *Hox-A3* mutation, structures anterior to its expression domain were also disrupted. The *Hox-A1* and *Hox-A3* mutations did not produce homeotic transformations; they generated malformations and perhaps deletions of certain structures.

Mutation of *Hox-A1* has been studied by two laboratories (Lufkin *et al.*, 1991; Chisaka *et al.*, 1992; Dolle *et al.*, 1993; Carpenter *et al.*, 1993). Their major findings were similar while there were some minor differences in the phenotypes. This may be due to differences in the deletions that they made in the *Hox-A1* gene, which produces two transcripts, one of which appears not to encode the homeodomain. The mutation generated by Lufkin *et al.* (1991) should eliminate both transcripts, whereas the mutation made by Chisaka *et al.* (1992) eliminates only the transcript encoding the homeodomain. In both mutations, heterozygotes were normal whereas homozygotes died at birth and had a range of defects in the part of the hindbrain derived from rhombomeres 4–7 (r4–r7), as well as defects in the derivatives of the neurogenic neural crest, the inner and middle ear, and the occipital bones of the skull. The defects included absence of the motor nucleus of the 7th nerve, part of the acoustic ganglia of the 8th nerve, the roots of the 9th and 10th nerves, and the superior olivary complex. Chisaka *et al.* (1992) observed that the morphology of the rhombomeres was disrupted, and Lufkin *et al.* (1991) found that the mutation caused delayed closure of the rostral neural tube. Both laboratories have reported more detailed analyses of the anatomy and gene expression patterns of mutant embryos (Carpenter *et al.*, 1993; Dolle *et al.*, 1993). Again, there were similarities and differences in the phenotype of the mutants. Analysis of the gene expression patterns of certain *Hox* genes, *Int-2* (*FGF-3*) and the *Krox20* genes, at E8.5–E9.5 in the rhombencephalon of *Hox-A1* mutant embryos clearly shows abnormalities in rhombomeres 4 and 5. Both groups found that rhombomere 5 was largely or completely deleted. Carpenter *et al.* (1993) interpreted their results as a total deletion of rhombomere 5 and a decrease in the size and a reduced level of *Hox-B1* expression in rhombomere 4. Dolle *et al.* (1993) interpreted their findings as a deletion of most of rhombomeres 4 and 5, although vestiges of each could be detected. For instance, they found that expression of *Hox-B1*, which is limited to rhombomere 4 at E9.5, is reduced to a small cluster of cells at the dorsal r3/r4 border. Likewise, the r5 expression domain of *Krox20* is reduced to a thin dorsal cluster of cells at the rostral boundary of r6. Associated with this size reduction of r4 and r5 are morphological alterations including the absence of two rhombomeres, the rostral displacement of the otic vesicle, disruption of the facial acoustic ganglion (which is formed in part by neural crest cells derived from r4), and the

lack of the neural crest-free area flanking r5. Dolle *et al.* (1993) suggest that r4 and r5 are deleted in the *Hox-A1* mutant, and propose that the absence of *Hox-A1* causes either apoptosis or alterations in growth control of cells in r4 and r5. Because there are thin strips of cells expressing r4 and r5 markers between r3 and r6, they point out that specification of these rhombomeres has not been entirely disrupted. It is interesting that mutations in the *Pit-1* homeobox gene also lead to decreases in the number of cells that are believed to be specified by expression of this gene. In the section on the *Pit-1* gene, we describe a potential mechanism that links this gene with growth control mechanisms.

Finally, Carpenter *et al.* (1993) found that the wiring of the mutant hindbrains was abnormal. For instance, they discovered that in mutant embryos, cranial nerves VII and VIII receive efferent axons from rhombomeres 6–8; these nerves normally contain efferents only from cell bodies in rhombomeres 4 and 5. Therefore, while the main embryonic field disrupted by the *Hox-A1* mutation is rhombomeres 4 and 5, more posterior parts of the hindbrain are also affected indirectly by this genetic defect.

Mutation of the *Hox-A3* gene produced a surprising phenotype because, although it is expressed in the embryonic hindbrain, abnormalities were restricted to cranial neural crest derivatives (Chisaka and Capecchi, 1991). Furthermore, the cranial neural crest defects did not disrupt the peripheral nervous system, as had the *Hox-A1* mutation. Instead, the mutation affected mesenchymal and endocrine development, including disruption of the thymus, parathyroid, thyroid, heart, and great vessels.

Mutations of the *Hox-B4* gene, which is expressed along the spinal cord into the hindbrain in rhombomere 7 and in the nodose ganglia, does not have a readily detectable phenotype in any neural structure (Ramirez-Solis *et al.*, 1993). Although the nervous system is not apparently affected, this mutation does cause a morphological change in the cervical vertebrae that is consistent with a homeotic transformation.

In sum, mutational analysis of the *Hox-A1*, *Hox-A3*, and *Hox-B4* mutations leads to several conclusions: (1) *Hox-A1* is implicated in regional specification and growth control and/or cell survival in the rhombencephalon; (2) homeobox gene expression in the hindbrain does not mean that it has a necessary function in the hindbrain proper as exemplified by the *Hox-A3* and *B4* mutations; (3) specific subsets of cranial neural crest derived from the region where the mutated homeobox gene is expressed are affected by the mutation; thus, while the *Hox-A1* mutation disrupts neurogenic cranial neural crest structures, the *Hox-A3* mutation causes abnormalities in nonneural cranial neural crest cells; and (4) patterning of cranial neural crest by the *Hox-A1* probably occurs while the crest precursor is still in the hindbrain because expression of this gene is not detected in the migrating cells.

III. Homeobox Genes Expressed in the Midbrain, Isthmus, and Cerebellum

In the adult, the midbrain, isthmus, and cerebellum consist of alar structures, such as the superior (tectum) and inferior colliculi, the parabigeminal and parabrachial nuclei, and the cerebellum, as well as basal structures, such as the red nucleus, substantia nigra, and the motor nuclei for cranial nerves III and IV. In the embryo, this brain region is intercalated between the rhombomeres and prosomeres. At early stages, it does not have distinct morphological features that clearly subdivide it into distinct segments. This has led to controversy and confusion regarding the organization of this region. However, cytoarchitectural patterns, fate maps, and gene expression patterns distinguish several parts that are disposed serially along the longitudinal axis. Based on these, a provisional model is shown in Figs. 5 and 7 that distinguishes the mesencephalon (m) and an isthmocerebellar complex as two main transverse domains. It also indicates by dotted lines that each of these units may be subdivided into two parts (m into m1 and m2; cb into cb and isthmus) [See also Gribnau and Geijsberts (1985) for a similar schema in the Rhesus monkey.]

In order to clarify the relationship of this model to standard anatomical nomenclature, it is useful to point out how the pons can be understood within the context of the model in Fig. 5. The mature pons, or metencephalon, is a region that is characterized by ventrally prominent structures, including the middle cerebellar peduncle and pontine nuclei. It also includes the trigeminal main motor and sensory nuclei which are derived from rhombomeres 1–3. Classic definitions of the pons generally include the cerebellum as its dorsal structure. However, there are inconsistencies with this definition. For instance, the cerebellum largely originates rostral to r1 (Fig. 5) (Martinez and Alvarado-Mallart, 1989; Hallonet *et al.*, 1990), from the *En-2* positive domain (see Fig. 7 and below). Also, some definitions of the human pons also include the nuclei of the VI and VII cranial nerves, though these originate in r4–r6. This false impression is due to the topological deformation of the massive pontine region found in the adult human brain. Therefore, there is nonconcordance of the classical concept of the pons (metencephalon) with the modern neuromeric schemata. It is our opinion that the neuromeric conception agrees more completely with experimental observations and suggest that this terminology should be used.

There are two homeobox genes whose expression is largely restricted to this brain region: *En-1* and *En-2* (Figs. 7 and 11) (Joyner and Martin, 1987; Davis and Joyner, 1988; Davis *et al.*, 1988; Davidson *et al.*, 1988; Bally-Cuif *et al.*, 1992). Many other homeobox genes are also expressed in this region (see Table II and Figs. 9–13), but the midbrain, isthmus,

and/or cerebellum do not make up their principal domains. The *En-1* and *En-2* genes (homologues of the *Drosophila engrailed* gene) have been studied in the greatest detail. In *Drosophila*, the *engrailed* gene has a homologue called *invected;* these genes are closely linked (Poole *et al.*, 1985). *En-1* and *En-2* are not linked; *En-1* is on the central part of mouse chromosome 1 and *En-2* is on the proximal part of mouse chromosome 5 (Joyner and Martin, 1987). Like the *engrailed* and invected genes, *En-1* and *En-2* are expressed with similar patterns during embryogenesis.

The expression of these genes has been studied in zebrafish (where there are three *engrailed* genes each, expressed in different overlapping sets of cells; Ekker *et al.* (1992a)], frog (Davis *et al.*, 1991), chicken (Davis *et al.*, 1991; Martinez *et al.*, 1991; Gardner and Barald, 1992), and mouse (Davis *et al.*, 1988, 1991; Davidson *et al.*, 1988; Bally-Cuif *et al.*, 1992). These comparative studies reveal that the expression patterns have been highly conserved between these vertebrate species.

En-1 and *En-2* expression begins at about E8.0 in a transverse band of neuroepithelium that encircles the neural tube at the mesencephalon–rhombencephalon junction (Davis *et al.*, 1988). An interesting aspect of this is that expression of the growth/differentiation factor *Wnt-1* may begin a few hours before *En-1/2* in this same domain (Bailly-Cuif *et al.*, 1992) (*Wnt-1* has additional domains of expression where the *engrailed* homologs are not expressed). There is accumulating evidence that as in *Drosophila*, the *Wnt-1* gene may have a role in the regulation of *En* expression. This point will be amplified later. *En-1* and *En-2* are expressed in a bidirectional gradient, with maximal expression at the isthmus, and decreasing expression rostrally into the mesencephalon (perhaps extending at least to the m/p1 boundary) and caudally into the cerebellar part of the rhombencephalon. From E8 to E11, the *En-1* and *En-2* patterns are largely indistinguishable, but at E12 their expression diverges. *En-1* expression becomes weaker than *En-2*, and *En-1* forms new expression zones both within and outside the nervous system [it is expressed in two longitudinal stripes along the basal plate of the hindbrain and spinal cord; these cells probably represent the primordia of motor nuclei inasmuch as the trigeminal motor nucleus clearly expresses *En-2* at E17.5 (Davis *et al.*, 1988)]. Furthermore, there are differences in their expression in r1 and in the primordia of the cerebellum (see Figs. 7 and 11). Their expression late in gestation and into adulthood further diverges as exemplified by the fact that only *En-2* is expressed throughout development of the cerebellar and isthmic regions. Both *En-1* and *En-2* are also expressed in the periaqueductal grey internal to the inferior colliculus and in the substantia nigra (m2) in the adult mouse.

A. Functional Analysis of the *En* Genes

Information regarding the function of the vertebrate *En* genes has come from the analysis of the *En-2* mutation and experimental embryological manipulations. The gene targeting method was used to create a mouse strain with a null mutation in the *En-2* gene (Joyner *et al.*, 1991). Mice that do not express *En-2* have a subtle alteration in the structure of the adult cerebellum, characterized by abnormal foliation and no clear neurobehavioral phenotype. Thus, it is possible that *En-2* and *En-1* (and perhaps other genes) share redundant functions; the cerebellar phenotype may have arisen because *En-1* is not expressed in the laterocaudal part of this structure late in gestation (Davis and Joyner, 1988).

The function of the *En* genes has also been studied using an indirect approach: through observing the effects of ectopically transplanting *En*-expressing neural tissues. There have been several general approaches utilized in these experiments. Nakamura and colleagues transplanted chick embryo tecta into the caudal diencephalon (Itasaki *et al.*, 1991). They found that the ectopic tecta continued to express *En*, but did so in a gradient opposite to the normal mesencephalic caudal to rostral gradient. They found that the closer the mesencephalic graft was to the mesencephalic/diencephalic junction, the lower the expression of *En*. These results provided evidence for a repressive influence on En expression from the mes/dien boundary; presently there are no candidate molecules for this repressor. Furthermore, the observation that *En-2* expression normally continues into the diencephalon along the basal plate, but not the alar plate, suggests that the postulated repressor only operates in the alar plate. It was also found that the cytoarchitecture of the ectopic tecta resembled the normal tectum. Furthermore, within the normal tectum there is a gradient of development; the higher *En* expression in the caudal tectum correlates with a retarded pattern of histodifferentiation. This phenomenon was also true in the ectopic tecta.

B. Regulation of *En* Expression

Very little is know about the extracellular and intracellular molecules that regulate *En* gene expression. A potential inroad to this area is based on information from *Drosophila*, where the wingless protein plays an important role in the induction and maintenance of *engrailed* expression (DiNardo *et al.*, 1988). Consistent with this, there is indirect evidence that one of the vertebrate wingless homologs, *Wnt-1*, may regulate *En* gene expression. This hypothesis is based on the following reason-

ings: (1) *Wnt-1* is expressed just before *En-1/En-2* at the mesencephalon/rhombencephalon (mes/rhom) junction (Davis and Joyner, 1988; Bailly-Cuif *et al.*, 1992); (2) transplantation of different transverse slices from the mes/rhom junction into the diencephalon induces the adjacent diencephalic tissue to express *En* (Martinez *et al.*, 1991; Gardner and Barald, 1992); the slices that induce the most *En* come from the region where *Wnt-1* is expressed the highest (Bailly-Cuif *et al.*, 1992); (3) *Wnt-1* mutations (two via gene replacement and one spontaneous mutation called swaying) result in phenotypes that range from deletion of the entire *En-1/En-2* expression domain to loss of only the middle of the *En* domain (Thomas and Capecchi, 1990; McMahon and Bradley, 1990; Thomas *et al.*, 1991; McMahon *et al.*, 1992). Additional studies are needed to directly test whether *Wnt-1* can regulate *En-1/En-2* expression.

As noted previously, experimental embryological manipulations involving ectopically transplanted pieces of isthmus into the forebrain identified the isthmus as source of an agent, perhaps *Wnt-1*, that can induce *En* expression. Conversely, when mesencephalic tissue was transplanted into the diencephalon, the level of *En* expression was reduced in the part of the ectopic tissue that was closest to the mesencephalic/diencephalic boundary (Itasaki *et al.*, 1991). Martinez *et al.* (1991) also found that transplantation of such prospective isthmocerebellar tissue into the rostral diencephalon resulted in maintenance of *En* expression in the ectopic tissue as well as induction of *En* expression in the adjacent diencephalic cells. The transplant developed into a cerebellar-like structure. However, when *En*-expressing prospective isthmocerebellar tissue was transplanted into the rostral mesencephalon, near the mesencephalic/diencephalic boundary, the level of *En* was reduced and the tissue developed into a mesencephalic phenotype instead of that of a cerebellum (Itasaki *et al.*, 1991; Martinez *et al.*, 1991; Alvarado-Mallart, 1993), suggesting that the mesencephalic/diencephalic boundary is a source for a repressor of *En* expression. Of note, induction of *En* expression in the diencephalon does not extend across interprosomeric boundaries, as observed for the zona limitans (p2/p3; Martinez *et al.*, 1991) and the pretecto–thalamic boundary (Marin and Puelles, 1994; Alvarado-Mallart *et al.*, 1993, Abstract ENA Meeting, Madrid 1993), and possibly respects the alar/basal boundary (Martinez *et al.*, 1991). This suggests that boundary cell populations may be nonpermissive for the propagation of the signal transduction cascade necessary for diffusion of the *En*-inducing agent. Curiously, only pretectal and dorsal thalamic prospective portions of the diencephalon are susceptible to *En* induction. The rostral-most forebrain, encompassing ventral thalamus and telencephalon, supports the differentiation in cerebellum of the *En-2* positive grafts, but does not express *En-2* nor change its differentiation pattern (Martinez *et al.*, 1991).

Thus, these experiments provide evidence for the existence and the location of factors within the embryonic brain that induce or repress *En* expression. They also provide indirect, yet suggestive evidence that correlates the ectopic expression of *En* with a change in phenotype. Thus, as Martinez *et al.* (1991) point out, ectopic expression of *En* in the diencephalon (adjacent to ectopically transplanted isthmocerebellar tissue) correlated with differentiation into a mesencephalic phenotype. Marin and Puelles (1994) have shown that inversion of a neuroepithelial ring containing the mesencephalon, isthmus, and cerebellar primordia controls correct histogenetic differentiation of all midbrain and isthmic centers in adjacent neuroepithelia that are susceptible to *En-2* induction (Fig. 8). The histogenic patterns are polarized according to the relative position of the isthmocerebellar ring. It is postulated that the polarizing activity underlies the rostrocaudal gradient of maturation in the tectum and other discrete differentiation differences normally found in the midbrain and isthmus (including the oculomotor and trochlear motor nuclei).

Therefore, this line of investigation provides strong evidence for the presence of an organizer-like structure at the midbrain–hindbrain boundary that secretes morphogenetic signals which pattern histodifferentiation in adjacent neuroepithelial domains. It also suggests that patterning in other CNS regions may be orchestrated by additional morphogenetic organizers. These experiments also implicate the *En* homeobox gene in this process and suggest that ectopic expression of this gene in discrete locations within the embryonic brain could be used to test this hypothesis.

While there is some evidence for the existence and possible identity of diffusable factors that induce *En* expression in permissive cells, information regarding surface receptors, signal transducing machinery, and transcription factors that induce or repress *En* expression is lacking. Inroads to this are beginning to be made by identifying the regulatory elements that control the temporal and regional specificity of expression of the *En-2* gene. Two enhancer-containing regions upstream of the *En-2* transcribed sequences have been found to control tissue-specific expression (Logan *et al.*, 1993). A 1.5-kb fragment contains an enhancer that controls expression in the midbrain/hindbrain region, and a 1.0-kb fragment regulates expression in the mandibular myoblasts. As the authors point out, these fragments can be used to identify proteins that bind to the DNA sequences that regulate tissue-specific expression.

IV. Homeobox Genes Expressed in the Forebrain

The forebrain consists of the diencephalon, and secondary prosencephalon. As postulated recently in our forebrain model (see discussion of the

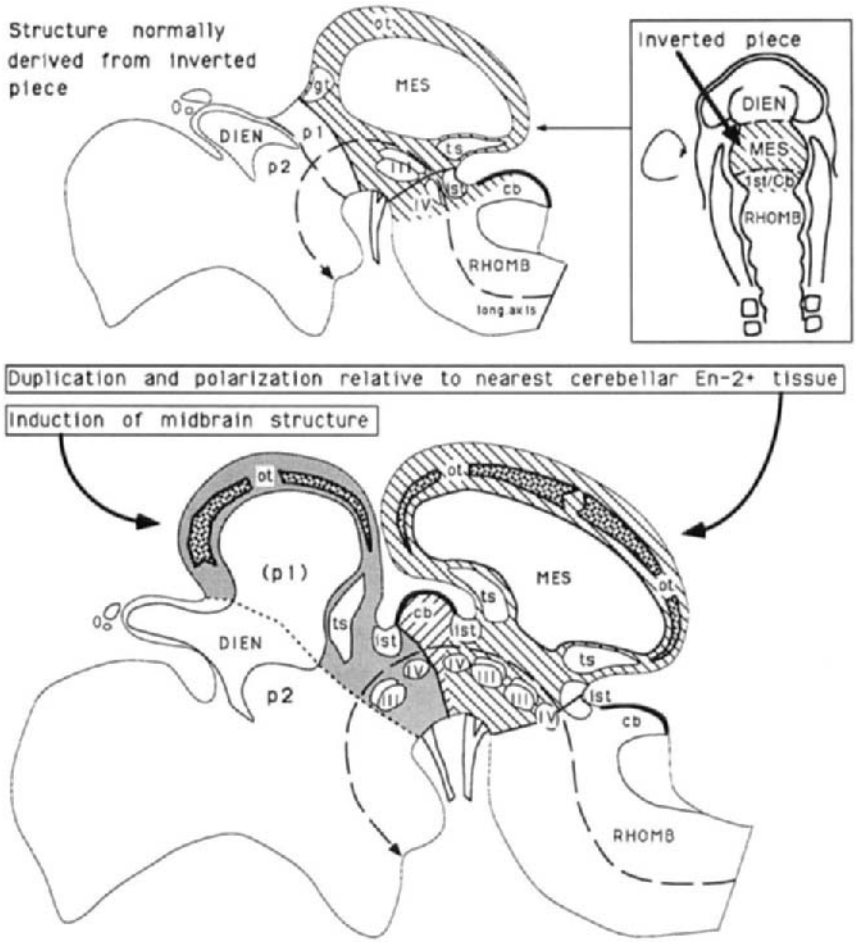

Fig. 8 Histogenic transformations obtained after rostrocaudal inversion of the entire mesencephalic vesicle. As indicated in the inset at the upper right and the drawing at the upper left, the rotated tissue (hatched areas) contains the presumptive midbrain, isthmic, and cerebellar cells groups. Various intersegmental and longitudinal boundaries [longitudinal (long.) axis shown by a broken line with an arrow] are indicated. (Bottom) The morphology of the embryos with the inverted mesencephalon reveals a doubly polarized duplication of the midbrain and isthmic structures within the inverted tissue (hatched area; this was a graft from a quail donor to a chicken host). Note the two inverted maturation gradients in the tectum (illustrated by the two arrows pointing opposite directions in the tectum). The normal maturational gradient is rostrocaudal. The presumptive pretectal (p1) region of the host (fine stippled area) was induced to adopt a midbrain phenotype (including *En-2* expression), polarized relative to the adjoining isthmocerebellar part of the graft. An additional cerebellum (cb) regenerated in the host hindbrain and apparently served to polarize the caudal part of the graft. Note the transformation of both alar and basal centers, with three sets of trochlear (*IV*) and oculomotor nuclei (*III*) and an additional oculomotor nerve originating from the transformed p1 segment. cb, cerebellum; gt, grisium tectale; ist, isthmus; ot, optic tectum; p1, pretectal segment; p2, dorsal thalamic segment; ts, torus semicircularis; III, third nerve; IV, fourth nerve. See text and Marin and Puelles (1994) for additional details.

prosomeric model later in this chapter and Figs. 4 and 14) (Puelles and Rubenstein, 1993; Bulfone *et al.*, 1993b), the secondary prosencephalon includes the whole hypothalamus, the eye stalks and vesicles, the preoptic region and commissural plate, the telencephalic peduncle, and the telencephalic vesicles. The telencephalon is the largest and most complex part of the mammalian brain; it contains the cerebral cortex, basal ganglia, olfactory bulbs, and other structures. Several classes of homeobox genes are expressed in the embryonic forebrain, or prosencephalon. Some of these are only expressed in restricted forebrain domains, whereas others are expressed throughout most of the nervous system. To date, mutations have been identified in only two of these genes (*Pax-3* and *Pax-6*, discussed later); thus most of this section will describe the expression patterns of these genes. Like the expression of the *Hox* genes in the hindbrain, the expression patterns of many of these genes show sharp transverse and longitudinal boundaries that are reminiscent of the *Hox* expression at rhombomeric boundaries. Using these and other data, a neuromeric model of forebrain organization that allows detailed morphological mapping of gene expression patterns, eschewing the difficulties posed by conventional schemata has been proposed (Bulfone *et al.*, 1993b; Puelles and Rubenstein, 1993). As described in greater detail later, this schema proposes that the forebrain is subdivided into transverse domains called prosomeres (p). In the next section, we will provide some of the salient details about many of the genes that are known to be expressed in the forebrain, and relate their expression domains to the hypothesized prosomeres.

A. Genes Expressed Discontinuously but Extensively along the A–P Axis and into the Forebrain: *POU, Pax, Gbx, Dbx, Gtx,* and LIM/Homeodomain

1. *POU* Genes

POU genes (Pit/Oct/Unc) encode proteins with two functional domains: the *POU* domain and a homeodomain (Fig. 1) (Wegner *et al.*, 1993). These motifs are colocalized within a stretch of 150–160 amino acids: the amino-terminal 75–82 amino acids are the *POU*-specific domain; this motif is followed at a conserved linker region that separates the *POU*-specific domain from the 60 amino acid homeodomain. Based on the amino acid sequence of the linker region and the amino-terminal part of the homeodomain, the mammalian POU proteins are categorized into six groups: I (Pit-1); II (Oct-1 and Oct-2); III [Brn-1, Brn-2, Brn-4, and Oct-6 (Tst-1 and SCIP)]; IV (Brn-3.0, Brn-3.1, and Brn-3.2); V (Oct-3/4); and VI (Brn-5) (Wegner *et al.*, 1993). Presently, there are 13 known mammalian *POU* genes, 11 of which are expressed in the developing and adult central

nervous system as well as many other parts of the mouse (Table II). The best characterized mammalian *POU* gene is *Pit-1*. It is expressed in the embryonic pituitary, and will be discussed subsequently.

Most of the other *POU* genes are widely expressed during embryogenesis in the proliferative zone of the CNS. Due to the limited published information on the embryonic expression patterns of most of these genes, it is difficult to make firm conclusions about specific boundaries. Therefore, our interpretations are tentative.

Brn-1, Brn-2, Brn-3, and *Tst-1* are expressed in all of the visible parts of the E13 rat CNS (He *et al.*, 1989). At E16, *Brn-1* is expressed in most of the CNS, although the anterior entopeduncular, preoptic, chiasmatic, and tuberal areas are negative. *Brn-2* expression at E16 is also extensive, although there is a gap caudal to r8 that may include the two most rostral myelomeres (assuming there is not a tissue defect in this section). *Brn-3.0* (He *et al.*, 1989) and *Brn-3.2* (Turner *et al.*, 1994) have a much more restricted expression pattern at E16 (see later discussion). Data on *Tst-1* (*SCIP* or *Oct-6*) show that it is expressed in the embryonic telencephalon at E16 (He *et al.*, 1989; Suzuki *et al.*, 1990), as well as in a caudal-rostral gradient in the alar mesencephalon (Suzuki *et al.*, 1990). *Brn-4* expression maps in the basal plate up to p4/p5 (tuberomammillary boundary). Its rostral alar limit is difficult to discern, but may stop at either p1/p2 or p2/p3.

Postnatally the various *POU* genes continue to show restricted expression in specific neuronal populations. Thus, *Brn-1* and *Brn-2*, which have the most widespread expression patterns, appear in the inferior and superior olives, motor and interpeduncular nuclei as well as the cerebellum and isthmic alar formations of the brainstem (spinal cord, r1-r8, Cb, and Ist) (He *et al.*, 1989). Expression is also found in the alar and basal midbrain (m1, m2), medial habenula (p2), and ventral thalamus (reticular nucleus and zona incerta; p3). Both genes are expressed throughout the cerebral cortex and the olfactory bulb (p4-p6), in various basal telencephalic populations like the nucleus of the lateral olfactory tract, the islands of Calleja, medial septum, diagonal band, substantia innominata, and the bed nucleus of the stria terminalis as well as in the lateral mammillary and tuberomammillary nuclei, other posterior hypothalamic formations, the supraoptic/paraventricular complex (p4), suprachiasmatic nucleus, and medial preoptic area (p6). Their expression is excluded from the amygdala, striatum, and main centers of the pallidum (He *et al.*, 1989).

In contrast to the widespread expression of *Brn-1* and *Brn-2*, *Brn-3.0* and *Brn-3.2* expression is more restricted (He *et al.*, 1989; Turner *et al.*, 1994; Gerrero *et al.*, 1994). These genes are also expressed in both the embryo and the adult brain, and appear to be expressed primarily in postmitotic cells. These *POU* genes have the greatest ho-

mology to the *C. elegans Unc-86* gene. *Unc-86* has a role in differentiation of hermaphrodite-specific motor neurons (Desai *et al.*, 1988) and mechanosensory neurons (Chalfie and Au, 1989). *Brn-3.0* RNA is found in sensory ganglia, inferior olive, and the ambiguous motor nucleus in the caudal brainstem. It is also expressed in a large transverse domain in the isthmus and both inferior and superior colliculi, as well as in a set of cells in the medial and lateral habenular nuclei (p2), in the posterior hypothalamus pituitary and the retina (He *et al.*, 1989; Gerrero *et al.*, 1994). Gerrero *et al.* (1994) present evidence that *Brn-3.0* regulates the expression of the proopiomelanocortin gene. *Brn-3.2* shares similar expression domains with *Brn 3.0;* its RNA is found in the spinal cord, spinal and trigeminal ganglia, inferior olive, superior colliculus, interpeduncular nucleus, and the retina (Turner *et al.*, 1994).

Brn-4 expression becomes restricted in advanced fetuses to the subcommissural organ (p1), the medial habenula (p2), the striatal subependymal layer and supraoptic/paraventricular complex (p5), nucleus accumbens (p6), and possibly the mammillary complex (p4)(Mathis *et al.*, 1992; Le Moine and Young, 1992).

Other *POU* genes show similarly discrete expression in adult animals, including *Oct-6* (*SCIP, Tst-1*) expression in specific cell types in the cerebral cortex (He *et al.*, 1989; Suzuki *et al.*, 1990); *Oct-1* expression in cerebellar granule cells; and *Oct-2* expression in the suprachiasmatic and medial mammillary nuclei (He *et al.*, 1989). Furthermore, *SCIP* (*Oct-6, Tst-1*) is expressed in the oligodendrocyte and Schwann cell lineages. It is induced by cyclic AMP (Monuki *et al.*, 1989) and during periods of rapid cell division. Furthermore, it has been implicated in repressing myelin-specific genes (Monuki *et al.*, 1990).

2. *Pax* Genes

The *Pax* genes have a paired box which is a 128 amino acid motif that is homologous to the DNA-binding domain of the *Drosophila Paired* protein. Presently, there are 10 known *Pax* genes in mammals (8 in mice); most of these genes encode proteins that also contain homeodomains (Fig. 1; only *Pax 1, 2, 5,* and *8* do not have homeodomains)[for a review see Chalepakis *et al.* (1993)]. Unlike the *Hox* genes, the *Pax* genes are not organized into multigene clusters. Several of these genes are known to be expressed in the forebrain, although these also have extensive expression domains in more caudal regions of the central nervous system and in other parts of the embryo. Although *Pax-2, Pax-5,* and *Pax-8* do not have homeodomains, they are included in this discussion. *Pax-1* is not expressed in the CNS and therefore will not be discussed.

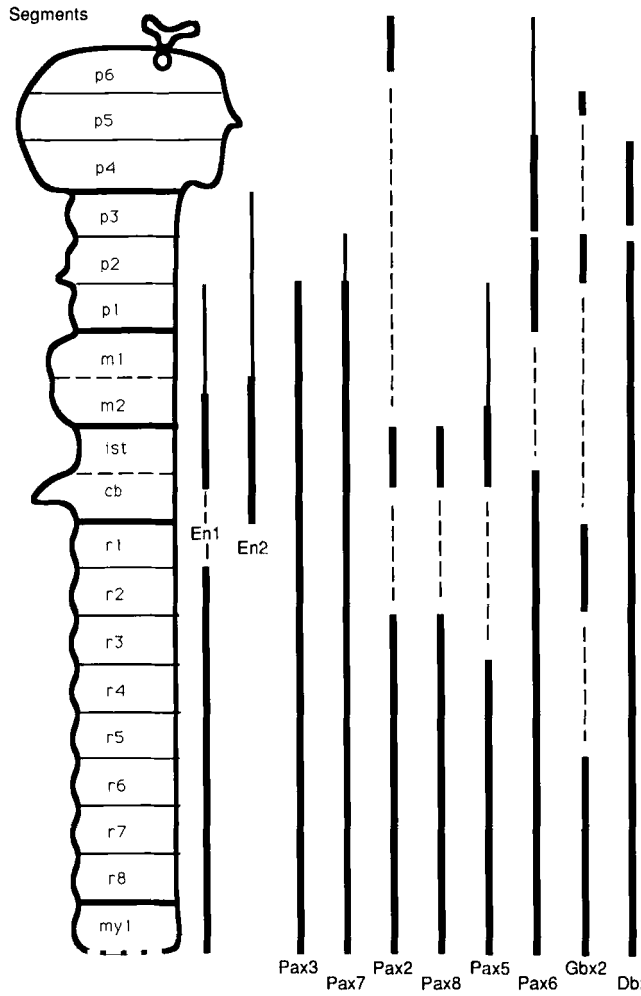

Fig. 9 The longitudinal patterns of expression of the *En*, *Pax*, *Gbx*, and *Dbx* genes relative to the rhombomeres and hypothesized neural segments in the isthmocerebellum, mesencephalon, and prosencephalon. Eight rhombomeres (r1–r8) and six prosomeres (p1–p6) are indicated. Subdivisions of the isthmocerebellum (ist and cb) and mesencephalon (m1 and m2) are indicated by dotted lines. The optic stalk (circle) and retina are shown as part of prosomere 6 (p6). The longitudinal expression domains at E12.5 are shown; boundaries are indicated at specific interneuromeric limits. The width of the lines relates to the amplitude of gene expression; dotted lines signify no expression.

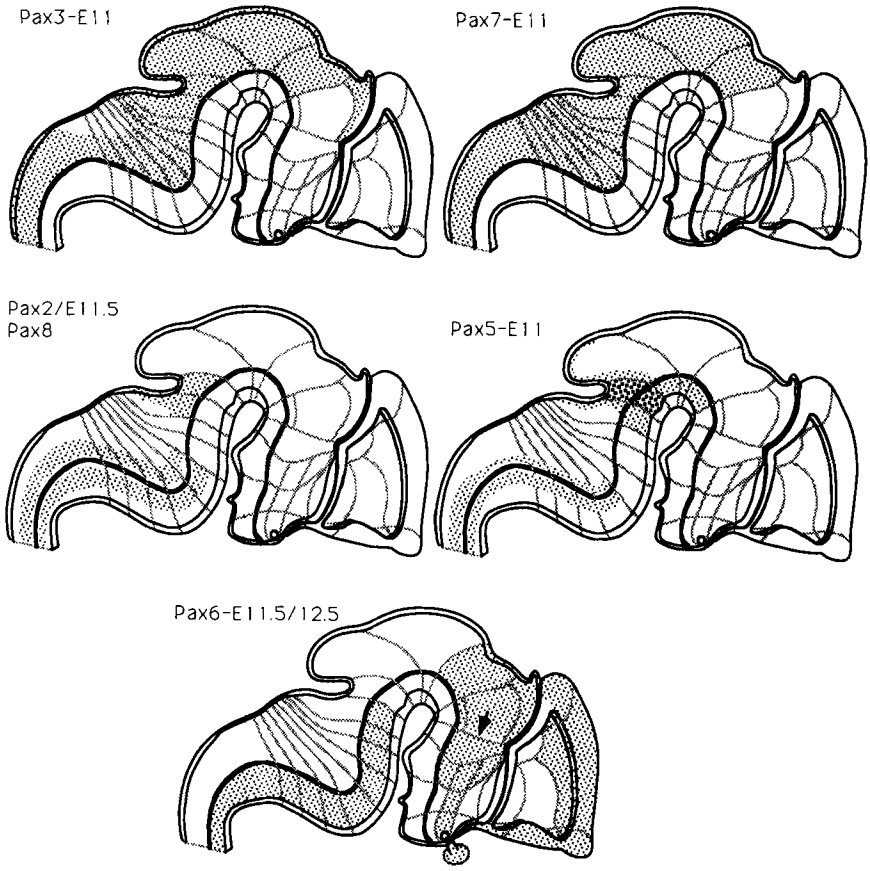

Fig. 10 The expression of *Pax* genes in the embryonic mouse brain. Data were taken from embryonic day 11–12.5 (E11–12.5) embryos and are listed to the right of the names of each gene. See Fig. 4 for details about the neuromeric schema used in this figure and the text for references and details about the expression patterns. The arrow in the *Pax-6* schema points to the gap in expression at the p2/p3 (zona limitans) boundary.

The expression of the *Pax* genes can be used to divide them roughly into three groups (Figs. 9 and 10; Table II). *Pax-3* (Goulding *et al.*, 1991) and *Pax-7* (Jostes *et al.*, 1991) genes begin to be expressed at ~E8–E8.5 in neuroepithelial cells. Their patterns of expression are very similar as they are found in alar territories that extend longitudinally throughout the spinal cord, hindbrain, and midbrain into the caudal diencephalon. Their rostral limits are at the p1/p2 boundary; although *Pax-3* may extend into the epithalamus, a region that we include as the most dorsal alar domain

in p2. Although both genes are expressed in the dorsal neural tube, only *Pax-3* is expressed in the roof plate (the dorsal midline).

The expression of *Pax-2* (Nornes *et al.*, 1990), *Pax-5* (Asano and Gruss, 1992; Adams *et al.*, 1992), and *Pax-8* (Plachov *et al.*, 1990) begins slightly later in development than *Pax-3* and *Pax-7* (at ~E9.5–E10), at a time that coincides with early neurogenesis. Note that these genes have no homeobox. Genes of this second class are expressed in neuroepithelial cells and in neurons. All show expression domains that cover specific alar and basal territories. *Pax-2*, *Pax-5*, and *Pax-8* have rather similar patterns, characterized by a rostral domain that is centered in the isthmic region, and a more extensive caudal domain that extends along the entire spinal cord into the hindbrain up to the pontine region (at E11.5 *Pax-2* and *Pax-8* seem to stop at the r2/r3 boundary, whereas *Pax-5* apparently stops at the r3/r4 boundary). *Pax-2* is also expressed in the ventral retina and ventral eye stalk.

These three genes also exhibit distinct expression patterns within the isthmic domain in patterns that are similar to the *En* genes. *Pax-2* and *Pax-8* transcripts predominate in the dorsolateral alar region of the rostral cerebellar and isthmic "segments" and expression ends abruptly at the 1st/m2 boundary. On the other hand, *Pax-5*, whose expression in the caudal hindbrain and spinal cord is weaker and restricted to fewer neurons, has a more intense and extensive rostral domain, including again the cerebellum and the whole isthmus and the caudal-most part of m2. Moreover, *Pax-5* extends into the ventrobasal isthmic regions. Its domain within the midbrain basal plate may be more extensive rostralward, perhaps reaching p1. Functional analysis of these genes is quite limited, although injection of antibodies against the zebrafish *Pax-2* homologue (*Pax[zf-b]*) into zebrafish embryos has been shown to disrupt expression of the zebrafish homologues of *Wnt-1* and *En-2* as well as development of the isthmic region (Krauss *et al.*, 1992).

The *Pax-6* gene makes up the third *Pax* group. Its transcripts are the most apparent in a rostral domain, within the alar region of the forebrain (at E11.5–12.5)(Walther and Gruss, 1991). This domain has a sharp caudal limit that coincides with the m1/p1 boundary. It extends continuously throughout alar p1 and p2, stopping just short of the boundary that separates p2/p3 (the zona limitans). Expression extends more rostrally within alar p3 and p4 (excluding the caudal ganglionic eminence) and then continues in a thin longitudinal band through p5 and p6 (within the anterior hypothalamic and posterior preoptic domains) into the optic stalk and eye vesicle. Expression within p5 and p6 is also found in the cerebral cortex, olfactory bulb, septum, and diagonal band domains. Note that *Pax-6* is also expressed in a separate caudal domain within the basal plate of the Cb, r1-r8, and the spinal cord.

At later developmental stages, *Pax-6* transcripts diminish in the dorsal thalamus (alar p2) and in p4-p6, but remain high in the ventral thalamus (alar p3). Finally, a novel domain appears between E15.5 and E18.5 in the rhombic lip and its derivatives (external granule layer of the cerebellum and pontine and olivary nuclei).

The expression patterns of the *Pax* genes have been conserved across vertebrate evolution. For instance, the expression of *Pax[zf-a]* (Krauss *et al.*, 1991), which is the *Pax-6* homologue in zebrafish, is very similar to the mouse *Pax-6* gene (Puschel *et al.*, 1992a). Expression is found in the basal plate of the spinal cord and hindbrain, as well as in the alar plate of the forebrain. Within the forebrain, the published data indicate that the interruption of expression within the p2/p3 interprosomeric boundary arises secondarily. Initially, there is a continuous alar domain from the m1/p1 boundary to the optic stalk. There is no expression in the telencephalon, at least at the published embryonic stages. *Pax[zf-b]* (Krauss *et al.*, 1991) expression is similar to *Pax-2* (Puschel *et al.*, 1992b). Both have separate domains in the eye vesicle and stalk, in the isthmomesencephalic boundary, and in the caudal brainstem and spinal cord.

The functions of several *Pax* genes have been studied using naturally occurring mutations (Table III). Mutations have been identified for three *Pax* genes in mice and in two *Pax* genes in humans. *Pax-1* mutations (called *undulated* in mouse) affect the vertebral column (Chalepakis *et al.*, 1991), and will not be discussed because this gene is not expressed in the CNS. On the other hand, homozygous mutations in *Pax-3* (called *splotch* in mouse and Waardenberg's syndrome in humans) cause severe malformations of the central nervous system that have been primarily described as dysraphias, or neural tube closure defects, and abnormalities of tissues that contain neural crest (Epstein *et al.*, 1991, 1993). Heterozygotes have white spotting of their abdomen, tail, and feet ("splotching"), presumably due to an abnormality of melanocytes that are neural crest derivatives. Mutations in the human *Pax-3* gene result in Waardenberg's syndrome, characterized by pigmentation disturbances (e.g., a white forelock) and sensorineural deafness (Tassabehji *et al.*, 1992, 1993). At this point, deficits in hearing have not been identified in the mouse *Pax-3* mutants. This discrepancy may be accounted for by allelic variation of the known mutations, different redundant systems, or truly different functions in these two species.

Mutations of the *Pax-6* gene have also been identified in mice and humans. In mice, heterozygotes for the mutant allele are viable and have small eyes; this is the basis for the name of the mutation: *small eye* or *sey* (Hill *et al.*, 1991). Homozygotes are inviable, probably because they develop no nasal cavities. They also do not develop eyes. The mechanism for these defects is uncertain, but may involve abnormal induction of the

nasal and lens placodes. A defect in the migration of midbrain neural crest has been detected in *Pax-6* mutant rats; these cells normally migrate throughout the face, but in the mutant they did not migrate to the nasal rudiment, suggesting that this gene plays a role in nasal placode induction (Matsuo *et al.*, 1993). Humans lack an iris, when they are heterozygotes for a mutation of *Pax-6*, in a syndrome called aniridia (Ton *et al.*, 1991; Glaser *et al.*, 1992; Jordan *et al.*, 1992). As described earlier, *Pax-6* is widely expressed in the embryonic CNS, yet mutations of this gene apparently only affect development of a small subset of these tissues, although a detailed analysis of the brains of these mutants remains to be published.

3. *Gbx*

The *Gbx-2* gene (gastrulation-brain-homeobox; also known as *MMox-a*) (Murtha *et al.*, 1991) does not have a known *Drosophila* homologue. It is related to another murine gene called *Gbx-1*. *Gbx-1* and *Gbx-2* are located on mouse chromosomes 5 and 1, respectively (Frohman *et al.*, 1994). *Gbx-2* is expressed during neurulation in the neural ectoderm and underlying mesoderm with a rostral boundary in the region of the midbrain–hindbrain junction (M. Frohman and G. Martin, unpublished results). By E12.5 it is expressed in two longitudinal stripes in the spinal cord up to the r6/r5 boundary, and has additional separate domains in rhombomeres r2 and r1, in the dorsal thalamus (alar p2), and in a superficial cell population of the medial ganglionic eminence (MGE) (Bulfone *et al.*, 1993b)(Figs. 9 and 14; Table II). Expression of *Gbx-1* has not been detected in the brain at E12.5 (Bulfone *et al.*, 1993b).

4. *Dbx*

The *Dbx* gene does not have a known *Drosophila* homologue; it is expressed longitudinally in a thin strip of subventricular and mantle cells along a line that may correlate with the alar/basal boundary (Lu *et al.*, 1992; Figs. 9 and 11; Table II). This expression domain extends across the spinal cord, hindbrain, midbrain, and may extend to the p2/p3 boundary in the diencephalon, although the published illustrations do not clearly resolve this latter point. This domain, or perhaps a separate domain, is also present at the alar/basal boundary of p3 and ends rostrally in a wider zone corresponding to the mammillary area (basal p4). Additionally, *Dbx* is expressed less intensely in the alar plate of the m1, m2, p1, and p2 segments, being sharply limited at the m2/Ist and p2/p3 boundaries. A smaller separate domain maps in the telencephalon to mantle cells superficial to the lateral ganglionic eminence (LGE), a region that may become the claustrum.

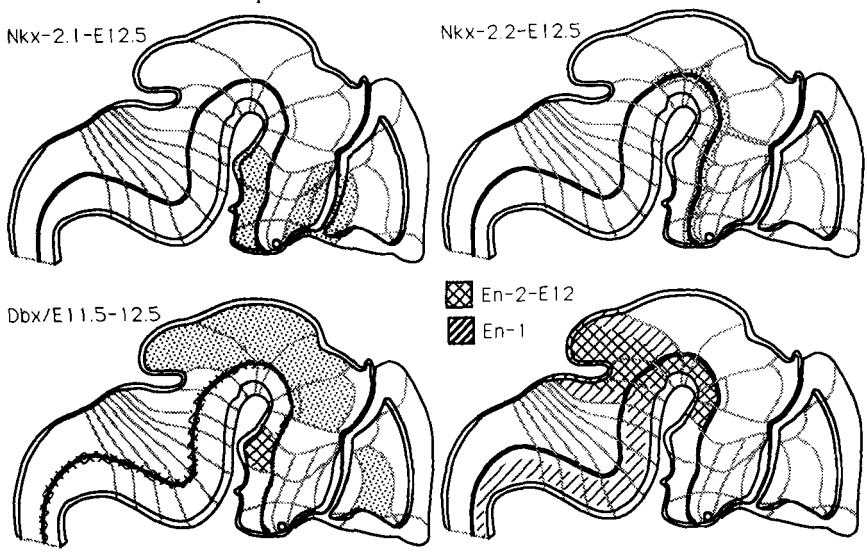

Fig. 11 The expression of the *En*, *Nkx*, and *Dbx* genes in the E12.5 mouse brain. See Fig. 4 for details about the neuromeric schema used in this figure and the text for references and details about the expression patterns.

5. *Gtx*

The *Gtx* gene encodes a highly diverged homeodomain with no known *Drosophila* homologue, which is also unusual because of its DNA-binding specificity (Komuro *et al.*, 1993). Unlike most homeodomain proteins, *Gtx* does not efficiently bind to a variety of standard oligonucleotide sequences such as (TAA)5. Rather, it binds to a consensus binding site named MEF-2, which is found in a variety of enhancers, such as in the muscle creatine kinase gene. *Gtx* shares binding specificity with a family of transcriptional regulators that share a structural motif called the MADS box. *Gtx* is expressed at higher levels in the adult than in the embryonic CNS. At E18, expression is seen in the spinal cord, hindbrain, midbrain, and hypothalamic area (Table II). In the adult brain, *Gtx* is expressed in the white matter in astrocytes and oligodendrocytes.

6. LIM/Homeodomain

The LIM/homeodomain genes encode proteins with two structural motifs: the LIM and homeodomains (Fig. 1). The LIM motif corresponds to a conserved polypeptide domain found in the *Lin-11*, *Isl-1*, and *Mec-3* regulatory proteins that control cell fate determination in *C. elegans* (*Lin-11* and *Mec-3* genes) and bind the insulin I enhancer region (*Isl-1*

gene). The LIM motif encodes metal-binding cysteine and histidine-rich domains of unknown function. LIM domains are also found in a *Drosophila* homeobox gene called *apterous* (Cohen *et al.*, 1992), as well as in the *rhombotin* protein that is expressed in various CNS locations. *Rhombotin* is implicated as a T-cell oncogene (Boehm *et al.*, 1991).

To date, two mammalian LIM/homeodomain genes have been reported to be expressed in the brain (Table II). *LH-2* is expressed in embryonic and adult forebrain and midbrain regions, as well as in developing lymphocytes (Xu *et al.*, 1993). The *Isl-1* gene is expressed in subsets of neurons and endocrine cells in the adult rat (Thor *et al.*, 1991). It is found in peripheral organs, including the sensory ganglia, as well as in the CNS, where it is expressed in subsets of spinal cord and brainstem motor nuclei, and probably in some catecholaminergic neurons. Expression in the forebrain is remarkable because it is found in cells that are derivatives of neuroepithelial domains that express *Dlx-1* and *Dlx-2*. Expression is found in derivatives of the ventral thalamus (alar p3; the reticular nucleus and zona incerta), hypothalamic anlage (alar p4-p6; paraventricular/supraoptic, suprachiasmatic, and arcuate nuclei), and basal telencephalon (alar p5-p6; septum and caudoputamen). Of note, no expression is found in the optoeminential domain where the *Dlx* genes are not expressed. Finally, a *Xenopus* LIM/homeodomain gene has also been reported to be expressed in embryonic and adult CNS structures (Taira *et al.*, 1993).

The LIM/homeodomain proteins are interesting because, like many of the *POU* proteins and some other homeodomain genes, they are expressed in differentiated cells that have left the mitotic cycle (postmitotic cells). Therefore, it is likely that they are downstream targets of homeodomain proteins that are expressed at earlier stages of differentiation.

B. Genes Expressed in Regionally Restricted Domains of the Midbrain and/or the Forebrain: *Otx*, *Emx*, *Nkx*, *Dlx*, and *Msx*

1. *Otx*

There are two genes that are homologues of the *Drosophila orthodenticle* gene: *Otx-1* and *Otx-2* (Simeone *et al.*, 1992a, 1993; Boncinelli *et al.*, 1993). The *orthodenticle* gene regulates development of specific structures in the head of *Drosophila* [for a review see Cohen and Jurgens (1991)]. The homeodomains of the *Otx* class are distinctive because they are similar to the *Drosophila bicoid* protein. The bicoid protein is required for the initial steps of A-P patterning of the *Drosophila* embryo and regulates expression of the *orthodenticle* gene (Finkelstein and Perrimon, 1991); hence there is great interest in whether the *Otx* genes have similar functions to the bicoid and *orthodenticle* genes. *Otx-2* is expressed in embryonal

stem cells and is found at E5.5 in the entire embryonic ectoderm (Simeone *et al.*, 1993). However, during gastrulation, expression disappears posteriorly and becomes restricted to the anterior region of the ectoderm: the primordia of the mid and forebrain. By E8.5, *Otx-1* expression also begins in a large anterior neuroectodermal domain (Simeone *et al.*, 1993). Thus, *Otx-1* and *Otx-2* are expressed in similar overlapping patterns that are largely restricted to the midbrain and forebrain in midgestation (Figs. 12 and 13; Table II). At E10, *Otx-1* is expressed throughout the dorsoventral extent of a domain that comprises the midbrain and much of the forebrain (p1–p4). The caudal mesencephalic boundary is a ring-shaped transverse band that stops abruptly in front of the fovea isthmi. Following this limit at the m2/ist boundary is a thin gap, and then expression continues caudally in only the basal plate of the isthmic and cerebellar segments, ending sharply at the cb/r1 boundary. After E10, expression is also found in the entire cortex (p4–p6) with a ventral boundary at the dorsal limit of *Dlx-1* expression in the lateral ganglionic eminence (see the *Dlx* section). It is also expressed in the optic stalk, eye, and the posterior preoptic area (POP).

At E10, *Otx-2* is also expressed through the dorsoventral extent of m2-p4, and there is some expression in alar p5 (primordia of the cortex) and in p6 (rostal cortex, septum, diagonal band, anterior preoptic area, and optic stalk). Like *Otx-1*, *Otx-2* expression ends abruptly at the m2/isthmic boundary, but unlike *Otx-1*, *Otx-2* is not expressed more caudally. By E12.5, expression decreases in the cortex.

Although *Otx-2* expression is continuous across the alar diencephalon, it has a peculiar pattern at the p3/p4 boundary (the zona limitans). At this boundary, the ventricular zone is positive, whereas the mantle does not express *Otx-2*. Abutting on both sides of the negative mantle zone is the mantle of p2 and p3, both of which express *Otx-2*. Cells in the p3 mantle express *Dlx-1* and *Dlx-2* (Bulfone *et al.*, 1993b); cells in the p2 mantle express *Gbx-2* (Bulfone *et al.*, 1993b) and possibly *Nkx-2.2* (Price *et al.*, 1992).

2. *Emx*

There are two genes that are homologues of the *Drosophila empty spiracle* gene: *Emx-1* and *Emx-2* (Simeone *et al.*, 1992a,b; Boncinelli *et al.*, 1993). The *empty spiracle* gene regulates development of specific structures in the head of *Drosophila* [for a review see Cohen and Jurgens (1991)]. The murine genes are primarily expressed in overlapping patterns in the primordia of the cerebral cortex (Figs. 12 and 13; Table II). Expression of *Emx-2* is also found in a domain that extends from the midbrain into p1, and separately, in the mammillary or tuberomammillary area. Other

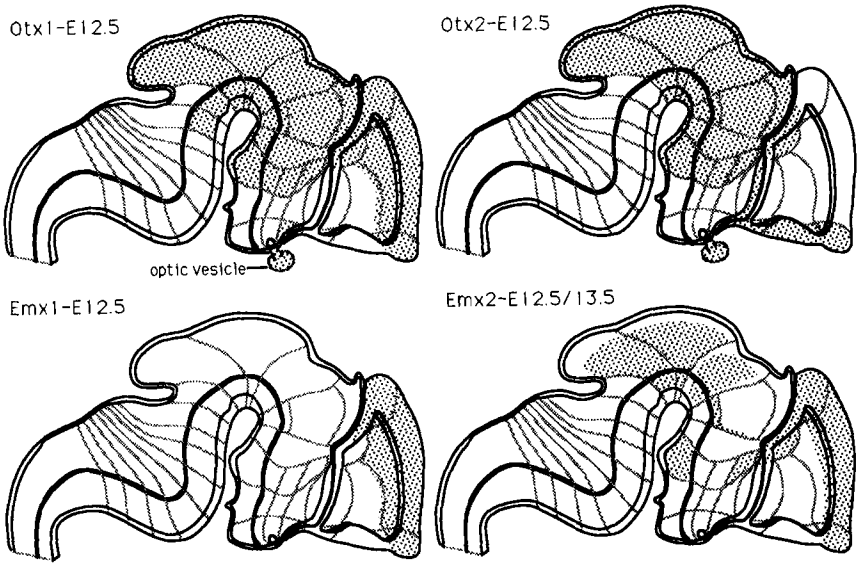

Fig. 12 The expression of the *Otx* and *Emx* genes in the E12.5 mouse brain. See Fig. 4 for details about the neuromeric schema used in this figure and the text for references and details about the expression patterns.

patches of expression in the diencephalic wall appear to be adjacent to the p1/p2 and p2/p3 interprosomeric boundaries. *Emx-1* and *Emx-2* expression in the cortex appears to be restricted at E10 to p4, but extends at E12.5 to the whole cortex (p4–p6). *Emx-1* expression may be stronger and extend more laterally in the cortex then *Emx-2*. *Emx-2* is also expressed in the chorioid plexus of the lateral ventricle and the caudal ganglionic eminence.

3. *Nkx*

There are four reported mouse genes and one reported *Xenopus* gene (*XeNK-2;* Saha *et al.*, 1993) that are homologues of the *Drosophila* NK2 gene (the function of the *NK2* gene is not known). The mouse genes are called *Nkx-2.1*, *Nkx-2.2*, *Nkx-2.3*, and *Nkx-2.4*. *Nkx-2.2* is located on mouse chromosome 2 (Price *et al.*, 1992). The expression patterns of *Nkx-2.1* and *Nkx-2.2* have been reported (Lazzaro *et al.*, 1991; Price *et al.*, 1992; Price, 1993) (Figs. 11 and 13; Table II). *Nkx-2.1* appears along the basal plate and floor region of p4–p6 at ~E10. At E12.5, a separate domain occupies the hemispheric stalk which includes the eminentia thalami, anterior entopeduncular area, and preoptic area, as well as in the cerebral

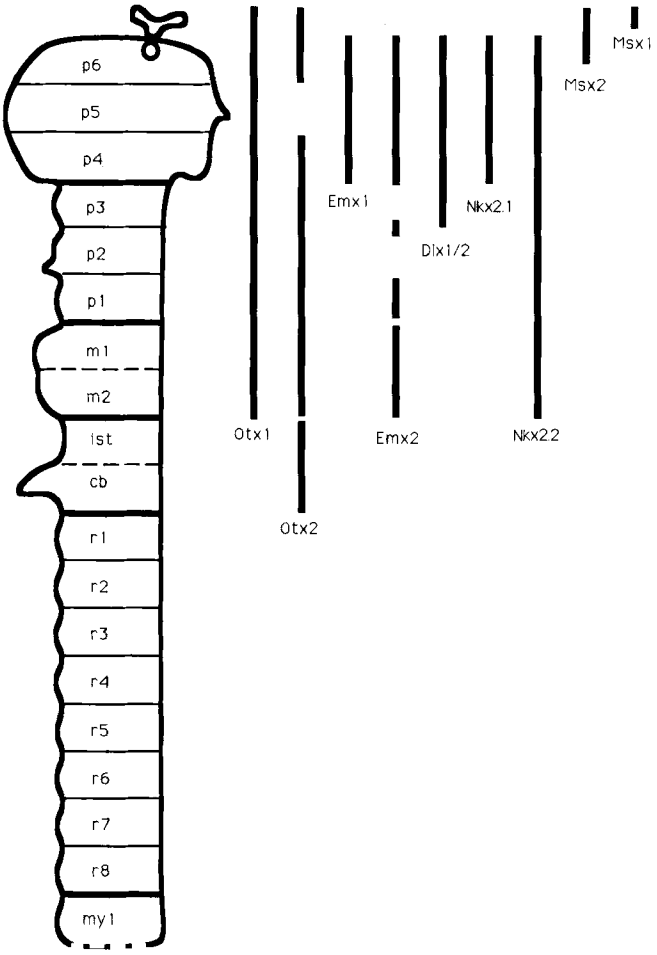

Fig. 13 The longitudinal patterns of expression of the *Otx*, *Emx*, *Dlx*, *Nkx*, and *Msx* genes relative to the rhombomeres and hypothesized neural segments in the isthmocerebellum, mesencephalon, and prosencephalon. Eight rhombomeres (r1–r8), and six prosomeres (p1–p6) are indicated. Subdivisions of the isthmocerebellum (ist and cb) and mesencephalon (m1 and m2) are indicated by dotted lines. The optic stalk (circle) and retina are shown as part of prosomere 6 (p6). The longitudinal expression domains at E12.5 are shown; boundaries at specific interneuromeric limits are indicated. The width of the lines relates to the amplitude of gene expression.

hemispheric (in the medial ganglionic eminence and diagonal band). At E14.5, expression in EMT diminishes or disappears.

Nkx-2.2 is expressed in a longitudinal strip that overlaps the alar/basal boundary of the whole midbrain and forebrain. Its caudal limit is at the isthmus and it extends to the rostral limit of the brain, where it is just ventral to the optic stalk and suprachiasmatic area. Additionally, *Nkx-2.2* is expressed in two alar transverse strips that are immediately caudal to the p2/p3 and p3/p4 boundaries. There is fragmentary evidence that a similar pattern may also be found just caudal to the m/p1, p4/p5, and p5/p6 boundaries.

4. *Dlx*

There are at least four murine *Dlx* genes. The sequence of their homeodomains is homologous to the *Drosophila distal-less* gene (*Dll*) (Vachon *et al.*, 1992). *Distal-less* is expressed in the primordia of the limbs, in ectodermal facial appendages (Cohen, 1990), and in the brain (S. Cohen, personal communication) of fly embryos. Mutations of *distal-less* affect development of the appendages; the effect on brain development has not yet been investigated. *Dlx* genes have been identified in zebrafish (Ekker *et al.*, 1992a), *Xenopus* (Asano *et al.*, 1992; Papalopulu and Kintner, 1993; Dirkson *et al.*, 1993), newt (Beauchemin and Savard, 1992), and chicken (C. A. Keleher and J. L. R. Rubenstein, unpublished results). In the mouse, the expression patterns have only been reported for *Dlx-1* and *Dlx-2* (also known as *Tes-1*) (Price *et al.*, 1991; Porteus *et al.*, 1991; Robinson *et al.*, 1991; Dollé *et al.*, 1992; Salinas and Nusse; 1992; Bulfone *et al.*, 1993a,b; Simeone *et al.*, 1993; Price, 1993) (Figs. 11, 13, and 14; Table II). These genes are expressed in the forebrain, limb ectoderm, and the branchial arches. *Dlx-1* and *Dlx-2* are located within about 10 kb of each other on mouse chromosome 2 (McGuinness *et al.*, 1992). They are also located on human chromosome 2 (Özçelik *et al.*, 1992).

Neural expression of mouse *Dlx-2* begins around E9.5 along an alar longitudinal domain (p3–p6) that spans from the zona limitans, through the primordia of the ventral thalamus to the region just caudal to the optic stalk (Bulfone *et al.*, 1993a). A few hours later, a second zone of expression begins that extends from the preoptic area along most of the basal telencephalon (p5–p6). The neural expression pattern of *Dlx-1* is largely indistinguishable with that of *Dlx-2* (at E12.5), except that *Dlx-2* may initiate expression before *Dlx-1* (available evidence suggests that *Dlx-1* expression begins around E10). The most extensive data come from studies at E12.5 that strongly suggest that these genes are co-expressed in the same cells and that also show that they respect both transverse and longitudinal boundaries in the neuroepithelium (Bulfone *et al.*, 1993b). As described

later, the study of the *Dlx* genes, in conjunction with the expression of the *Gbx-2* and *Wnt-3* genes, stimulated us to propose a neuromeric model of the forebrain (Bulfone *et al.*, 1993b; Puelles and Rubenstein, 1993; Fig. 14). A similar study was performed using *Dlx-1* and *Wnt-3* (Salinas and Nusse, 1992).

Expression of the *Dlx-1* and *Dlx-2* genes largely turns off postnatally, although several additional features are of note. First, although expression is not found in the dorsal telencephalon at E12.5, expression of these genes is found at later stages in this region (Porteus *et al.*, 1991; M. H. Porteus and J. L. R. Rubenstein, unpublished results). In particular, expression is found in the postnatal subventricular zone of the neocortex at a time when gliogenesis is predominantly occurring. Furthermore, *Dlx-1* expression has been noted in the adult olfactory bulb (Salinas and Nusse, 1992).

5. *Msx*

The mouse *Msx-1* and *Msx*-2 were originally *called Hox-7.1* and *Hox-8.1*, and are related to the *Drosophila muscle segment homeobox* (*Msh*) gene (Gehring, 1987). As described in the next section, they are expressed during development of the eye (Monaghan *et al.*, 1991) (Fig. 13; Table II). Furthermore, *Msx-1* is expressed in roof plate cells of the neural tube, as well as the neuroepithelial primordia of the chorioid plexus (MacKenzie *et al.*, 1991). These genes also have widespread expression in a variety of nonneural tissues of the head. For instance, *Msx*-2 is expressed in cephalic neural crest-derived mesenchyme. This is of note because a mutation of the human *Msx*-2 gene is associated with dominant craniosynostosis (Jabs *et al.*, 1993; Table III).

C. Homeobox Genes Expressed in the Pituitary

Although it is debatable whether anterior pituitary is derived from the neuroepithelium, for the purposes of this chapter it is included as part of the forebrain because of its close association with the hypothalamus and because of the illuminating work that has elucidated the role of a *POU* protein (*Pit-1*) in its development. Other homeobox genes that are expressed in the embryonic anterior pituitary include *Pax-6* (Walther and Gruss, 1991) and *Brn-3.0* (Gerrero *et al.*, 1994); *Otx-2* is expressed in the embryonic posterior pituitary (Simeone *et al.*, 1993) (Table II).

The anterior pituitary derives from an invagination of the roof of the oral cavity (Rathke's pouch) that comes into contact with a midline evagination of the hypothalamus (the infundibulum). There are five major cell

Fig. 14 Realistic (top) and topological (bottom) maps of *Dlx-1/2*, *Gbx-2*, and *Wnt-3* expression in the E12.5 mouse brain according to the neuromeric model (Bulfone *et al.*, 1993b; Puelles and Rubenstein, 1993). This schema shows a medial view of the brain of an E12.5 mouse. The transverse (neuromeric) subdivisions are delineated by solid black lines that are perpendicular to the principal longitudinal subdivision that divides the alar and basal zones (shown by a red line), and defines the longitudinal axis of the brain. Four longitudinal zones are shown in the spinal cord (SC) (from dorsal to ventral): roof plate (black), alar plate, basal plate, and floor plate (gray). These four zones extend to the rostral limit of the prosencephalon. The rhombomeres (r1–r7) and theoretical prosomeres (p1–p6) are labeled adjacent to the floor plate domains of their neuromeres. The expression patterns of the genes depicted in this figure are shown in the following colors: *Dlx-1* and *-2*, green; *Gbx-2*, purple fishnet; *Wnt-3*, magenta. The *Wnt-3* expression is shown as a dorsal-to-ventral gradient. The site of the optic stalk is indicated by the black circle in the POP domain. Midline specialized structures are also shown. Roof plate structures include the chorioid plexus (CP, shaded in gray) in the rhombencephalon (RH) and prosencephalon; the epiphysis (EP) is an evagination in p2; and the commissural plate (future site of the hippocampal commissure, corpus callosum, and anterior commissure) is shown as a thick black line in the secondary prosencephalon. The infundibulum (IN) is shown as an evagination from the floor plate region of p5. This figure illustrates several points. The *Dlx-1* and *Dlx-2* genes are coexpressed, apparently in the same cells, in two distinct domains. Domain I extends from the boundary separating the dorsal thalamus (DT) and the ventral thalamus (VT; known as the zona limitans interparencephalica or interthalamica) to just behind the optic stalk. The expression boundary at the zona limitans coincides with a ventricular ridge. Domain II extends from just in front of the optic stalk along most of the basal telencephalon. The *Gbx-2* gene is also expressed in two domains in the forebrain. Domain I is within the dorsal thalamus; its rostral boundary abuts the *Dlx*-positive ventral thalamus at the zona limitans. Caudally it is sharply limited at the thalamopretectal boundary, which is also marked by the course of the retroflex tract. Domain II lies superficially to the *Dlx*-positive zone of the medial ganglionic eminence within the basal telencephalon. Finally, forebrain expression of the putative growth-differentiation factor *Wnt-3* is restricted to the pretectum (PT), epithalamus (ET), and the dorsal thalamus, and also stops abruptly at the zona limitans, where it abuts the expression of the *Dlx* genes. In the topologic map, the longitudinal axis of the brain has been straightened. To flatten the telencephalic vesicle, the roof plate (filled in black) has been cut across the rostral chorioid plexus (CH) and also from its union with the median alar plate (lamina terminalis). The positions of the rhombencephalon, mesencephalon (M), diencephalon (DI), and secondary prosencephalon (which contains the telencephalon in its alar longitudinal tiers beginning with the eminentia thalami (EMT), anterior entopeduncular area (AEP), anterior preoptic area (POA) layer) are indicated above the diagram. The topological relationship of the olfactory bulb (OB) and the septum (SE) with the rostral-most part of the commissural plate (the anterior commissure) is not yet adequately resolved by this model. The course of the p5/p6 boundary inside the telencephalon, which is based on gene mapping data, is tentative and therefore provisional. The horizontal dotted line in TU represents the observed *Dlx* expression in lateral parts of TU; in this region we are not certain whether *Dlx* expression extends into the basal domain. The caudal boundary of the *Gbx-2* expression in p5 is not known with precision. ACX, archicortex; AH, anterior hypothalamus; CB, cerebellum; CGE, caudal ganglionic eminence (l, lateral; m, medial); DB, diagonal band; HCC, hypothalamic cell cord; IS, isthumus of mesencephalon; LGE, lateral ganglionic eminence; MA, mammillary area (basal zone of p4); MGE, medial ganglionic eminence; NCX, neocortex; PEP, posterior entopedunuclar area; RCH, retrochiasmatic area (basal zone of p6); RM, retromammillary area (basal zone of p3); SCH, suprachiasmatic area; SPV, supraoptic/paraventricular area.

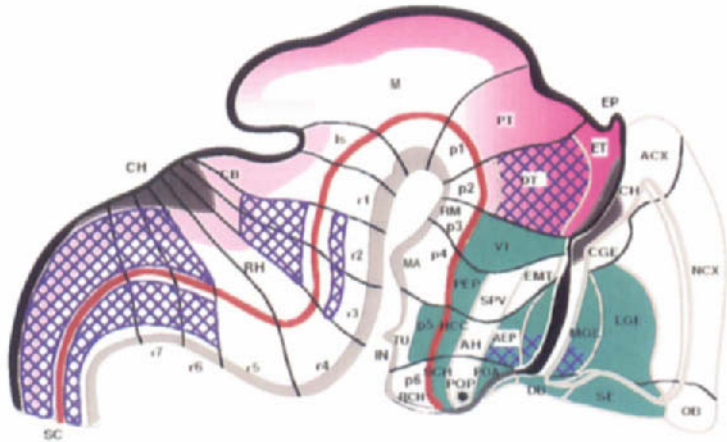
M
PT
EP
Is
p1
ET
ACX
CH
CB
DT
p2
r1
RM
p3
VT
CGE
r2
RH
MA
p4
EMT
NCX
PEP
SPV
r3
p5
HCC
LGE
TU
AH
AEP
MGE
IN
r7
r6
r5
r4
p6
RCH
POP
DB
SE
OB
SC

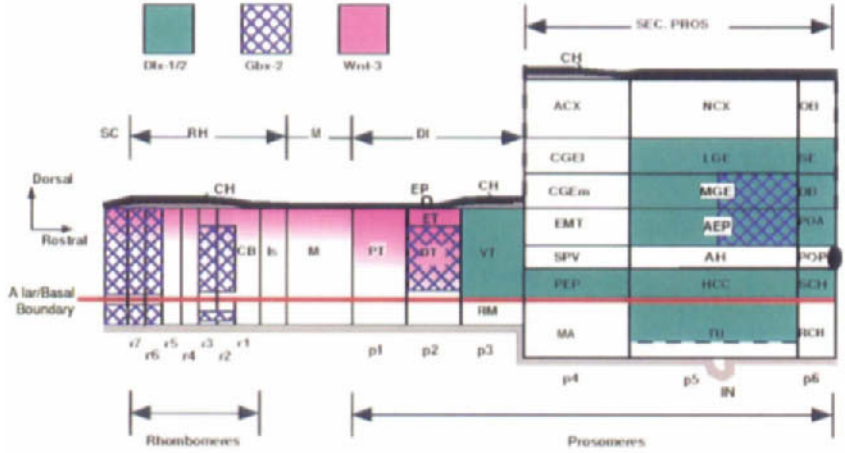
Dlx-1/2
Gbx-2
Wnt-3
SEC. PROS
CH
SC
RH
M
DI
ACX
NCX
OB
CGE3
LGE
SE
Dorsal
CH
EP
CH
CGEm
MGE
OB
Rostral
CB
Is
M
PT
DT
ET
VT
EMT
AEP
POA
SPV
AH
POP
A lar/Basal
Boundary
PEP
HCC
SCH
RM
MA
TU
RCH
r7
r6
r5
r4
r3
r2
r1
p1
p2
p3
p4
p5
IN
p6
Rhombomeres
Prosomeres

This Page Intentionally Left Blank

types in the anterior pituitary that secrete peptide hormones: growth hormone, prolactin, adrenocorticotropin hormone, thyroid-stimulating hormone, and melanotropin-stimulating hormone. In an effort to understand the genetic regulation of the growth hormone gene, Rosenfeld and co-workers identified a protein that bound to an enhancer element of this gene. They then cloned this binding protein and thereby identified one of the first POU proteins, which they named *Pit-1* [Ingraham *et al.* (1988); for a review see Wegner *et al.* (1993)]. *Pit-1* is expressed in a restricted domain of the anterior pituitary during embryogenesis, and the onset of its expression occurs before the appearance of cells expressing growth hormone or prolactin. Mutations in this gene in mice disrupt development of the anterior pituitary, resulting in hypoplasia of the organ [for a review see Wegner *et al.* (1993)]. Hypoplasia is caused by the absence of the cells that produce growth hormone, thyroid-stimulating hormone, and prolactin; other cell types still develop (e.g., corticotrophs and melanotrophs). On the other hand, a *Pit-1* mis-sense mutation in humans results in the absence of somatotrophs and lactotrophs without hypoplasia [see Wegner *et al.* (1993)]. Thus, both the murine and human mutant *Pit-1* proteins result in the inability to form specific differentiated cells, while only the mouse mutant has a deficiency in cell proliferation and/or viability. The explanation for this difference is unclear at present, although a hint has come from the discovery that another gene downstream from *Pit-1* is the growth hormone-releasing factor receptor (*GRFR*) gene (Lin *et al.*, 1992). *GRF* stimulates mitosis in the precursors of growth hormone-producing cells. Thus, a defect in *Pit-1* can cause less expression of *GRFR*, and thereby result in an inability of these cells to proliferate in response to *GRF*. As Rosenfeld and co-workers point out, "the regulation of a trophic factor receptor by *Pit-1* provides a model for the coordination of cell proliferation and the progression of cellular differentiation by POU-domain proteins" (Wegner *et al.*, 1993).

D. Homeobox Genes Expressed in the Eye

The neural retina is derived from an evagination of the forebrain, and a number of homeobox genes have been identified that are expressed in this tissue. These include *Msx-1*, *Msx-2*, *Pax-6*, *Dlx-1*, *Dlx-2*, *Otx-1*, *Otx-2*, *Gtx*, *Brn-3.0*, *Brn-3.2*, *LH-2*, and *Isl-1* (Table II). The *Msx* genes, originally called *Hox-7.1* and *Hox-8.1*, are expressed in distinct compartments within the embryonic eye (Monaghan *et al.*, 1991). *Msx*-2 is expressed in the surface ectoderm and the optic vesicle before invagination occurs. These regions are the primordia of the cornea and retina, respectively. *Msx-1* is expressed after formation of the optic cup in a domain

that becomes the ciliary body. *Pax-6* is expressed in the primordia of the retina, lens, and the cornea (Walther and Gruss, 1991). As noted earlier, mutation of *Pax-6* results in a defect in lens induction in mice and in the absence of the iris in humans (Table III). Analysis of *Dlx-1* and *Dlx-2* expression has shown that these genes are expressed in the primordia of the retina (Dolle *et al.*, 1992; Bulfone *et al.*, 1993b). *Otx-1* and *Otx-2* are expressed in the optic stalks and vesicles at E10, as well as in a variety of optic structures later in development (Simeone *et al.*, 1993). The *POU* gene *Brn-3.0* is transiently expressed in terminally differentiating retinal ganglion cells (Gerrero *et al.*, 1994). Finally, *Isl-1* is expressed in subsets of neurons in the adult retina (Thor *et al.*, 1991).

E. Homeobox Genes Expressed in Peripheral Cranial Sense Organs

The focus of this chapter has been primarily on CNS structures. Thus we will only briefly note that homeobox genes are expressed in the embryonic inner ear, olfactory epithelium, and cranial ganglia. We are not aware of information on the taste organs of the tongue. For instance, the *Dlx* (Ekker *et al.*, 1992a), *Msx* (Ekker *et al.*, 1992a), and *Otx-1*/2 (Simeone *et al.*, 1993) genes are expressed in subsets of tissues in the embryonic inner ear. Expression in the olfactory epithelium has been noted for *Emx-2* (Simeone *et al.*, 1992b), *Otx-1*/2 (Simeone *et al.*, 1993), and potentially *Dlx-2* in subsets of olfactory tissue (Porteus *et al.*, 1991). Finally, cranial ganglia express several *Hox* (Krumlauf *et al.*, 1993), *Dlx-2* (Bulfone *et al.*, 1993a), and *Brn-3.0* and *Brn-3.2* (Turner *et al.*, 1994) genes.

V. Conclusions

A. Expression Patterns of Homeobox and Other Genes in the Forebrain Support a Neuromeric Model of the Forebrain

The study of gene expression patterns in the embryonic forebrain provides insights into the underlying organization of this structure and has led us to question previous morphological models of the forebrain in mammals and other vertebrates. The conventional interpretation of forebrain organization is based on the columnar model developed by His (1893), Herrick (1910), Kuhlenbeck (1973), and several other neuroembryologists. This model has become increasingly discordant with experimental evidence (Puelles and Rubenstein, 1993). This is due in large part because it is based on an obsolete conception of the longitudinal axis in the forebrain (which requires a discontinuity of the forebrain longitudinal axis with

more caudal parts of the neural tube) and because of its dependence on unreliable morphological landmarks (ventricular sulci) for the boundaries of forebrain subdivisions. In contrast, the study of gene expression patterns in the forebrain provide evidence for an alternative model (Figs. 4 and 14) (Bulfone *et al.*, 1993b; Puelles and Rubenstein, 1993). Evidence for an alternative interpretation of the longitudinal axis comes in part from the observation of expression patterns that are continuous across the entire brain, and that follow the contours of the secondary axial bends (flexures) of the neural tube [in this regard, see the expression of *XeNK-2* in Saha *et al.* (1993)]. Furthermore, evidence for alternative limits of forebrain subdivisions come from the observation that the vast majority of expression patterns show sharp boundaries, some of which are perpendicular (transverse) and others parallel to the proposed longitudinal axis. The transverse boundaries do not coincide with the ventricular sulci posited to limit forebrain compartments in the columnar model. Therefore, these experimental observations are not consistent with the predictions of the columnar model.

On the other hand, the expression patterns are compatible with the segmental model of the brain encompassed in the "neuromeric theory" that evolved contemporaneously to the "columnar theory" (His, 1893; von Kupffer, 1906; Palmgren, 1921; Rendahl, 1924; Bergquist and Kallen, 1954; Kallen, 1965; Vaage, 1969; Keyser, 1972; Gribnau and Geijsberts, 1985) [also see Puelles *et al.* (1987, 1991) for a discussion of this subject]. Following the discovery of gene expression patterns that respect hindbrain segment boundaries [reviewed by Krumlauf (1993)], various reports tentatively suggested the possibility of a segmental interpretation of gene expression patterns observed in the forebrain (Price *et al.*, 1991; Lo *et al.*, 1991; Zimmer and Zimmer, 1992; Salinas and Nusse, 1992). In parallel, work with the *Dlx-1*, *Dlx-2*, *Gbx-2*, and *Wnt-3* genes has led to the formulation of the prosomeric model (Porteus *et al.*, 1991; Bulfone *et al.*, 1993a,b; Puelles and Rubenstein, 1993). The study of cell migration within the plane of the chick embryo neuroepithelium has also led Figdor and Stern (1993) to support a neuromeric model of diencephalic organization.

The basic elements of the prosomeric model can be stated as follows: There are three axial reference lines: the floor plate, the alar/basal boundary, and the roof plate. These lines define the longitudinal axis of the neural tube, and as such will be perpendicular to the transverse boundaries that separate brain segments. A brain segment is expected to represent a transverse ring of the neural tube exhibiting metamery of its elements (floor, basal, alar, and roof plates) as well as specific properties that characterize the intersegmental boundaries [see Puelles and Rubenstein (1993) for a more complete discussion of this subject]. Many of the postulated interprosomeric boundaries in fact correspond to previously defined limits of neuronal complexes and to the pathways of various fiber tracts.

The model postulates two main subdivisions of the forebrain: the diencephalon and the secondary prosencephalon. The ventral part of the secondary prosencephalon largely consists of the hypothalamus; the dorsal part includes the telencephalon, the telencephalic peduncle (stalk), the preoptic region, and the optic stalk and vesicle. Both the diencephalon and secondary prosencephalon are subdivided into three prosencephalic neuromeres (prosomeres, p), p1–p3, and p4–p6, respectively. Further transverse and longitudinal boundaries later subdivide the prosomeres into the discrete neuronal populations that make up the forebrain.

Evidence for this model comes in part from the detailed comparison of the expression of *Dlx-1*, *Dlx-2*, *Gbx-2*, and *Wnt-3* (Bulfone *et al.*, 1993b), and the examination of the expression patterns of nearly 50 other published genes [see Puelles and Rubenstein (1993) and this chapter]. The boundaries of these expression patterns consistently agree with those postulated by the prosomeric model (Bulfone *et al.*, 1993b; Puelles and Rubenstein, 1993). Pending further corroboration through additional experimental analysis, this model should provide a useful instrument to aid in the interpretation of gene expression data, as well as in the analysis of experimental manipulations of the embryonic forebrain.

B. Why Are Homeobox Genes Expressed in Complex Patterns in the Brain?

Having reviewed the expression of some 40 genes, it is clear that their patterns are frequently complex both in space and time. Spatial complexity has several different forms. For instance, many genes have multiple discontinuous domains (e.g., *Gbx-2* has four), suggesting that these genes have distinct regulatory cassettes controlling expression in each domain. In some regions, *Gbx-2* is expressed in the proliferative zone of the neural tube, whereas in the basal telencephalon, it is exclusively expressed in the cells that have left the mitotic cycle (Bulfone *et al.*, 1993b). Thus, this suggests that *Gbx-2* may have different functions in different regions. Perhaps it has a role in regional specification when it is expressed in the proliferative zone, and a role in histotype differentiation when it is expressed in postmitotic cells.

Many homeobox genes are expressed in gradients, such as the *En* genes in the tectum (Davis and Joyner, 1988). The gradients appear to be the result of the response to morphogenetic signals emanating from organizer-like sources, such as in the isthmic tissue (see section on cerebellum, isthmus, and mesencephalon)(Itasaki *et al.*, 1991; Martinez *et al.*, 1991). These results suggest that gradients of *En* expression may have a role in patterning development, perhaps by controlling the rate of differentiation

or by regulating the level of expression of downstream genes involved in processes such as synaptic recognition.

Some of the genes are expressed in thin strips of tissue apparently at boundaries separating histogenic domains, such as the *Nkx-2.2* gene at the p2/p3 boundary (Price *et al.*, 1992). Expression of other genes shows a converse property, such as *Pax-6*, which exhibits a thin gap of expression also at the p2/p3 boundary (Walther and Gruss, 1991). Again, the significance behind these observations is unclear, but may relate to the specialized role of boundary zones for patterning axon pathways, for serving as a barrier to prevent cell mixing between neuroepithelial compartments, or for serving as the source of morphogenetic signals.

In sum, the logic behind the complexity of the expression patterns of homeobox genes in the vertebrate brain is just beginning to be uncovered. The complexity may in part be the result of structural distortions that occur during morphogenesis of the brain; thus the expression patterns may simplify once they are related topologically to a fate map of the neural plate. At this point, the expression patterns do not appear to relate to specific neurological systems; this is consistent with the idea that functional systems are established, at least in part, by the interconnection of neuronal populations that arise from distinct developmental compartments.

As alluded to previously, it is possible that the expression of some genes marks the route used by axon pathways and cell migrations. For instance, one of the earliest axon tracts in the forebrain, the tract of the posterior optic commissure (Easter *et al.*, 1993), runs a course parallel to *Dlx-1/2* expression in the hypothalamus and ventral thalamus (Bulfone *et al.*, 1993b). Furthermore, the expression at distinct transverse or longitudinal landmarks, perhaps in specialized boundary cells, also correlates with the trajectories of many fiber tracts. Thus, these boundary cells may form the blueprint that directs the trajectories of the principal axonal and migratory pathways.

It is clear from the functional analyses of a few of these genes (Table III) that expression does not necessarily mean that the gene has an important function. Thus, mutational studies of these genes will elucidate where their expression is important, and this information will replace the "expression maps" with "function maps" which may provide inroads toward understanding the logic behind the complex temporal and spatial regulation of these genes. Finally, it is likely that no one gene functions alone to regulate patterning and differentiation of any given region of the brain, and therefore it will be necessary to understand the genetic network that controls the development of each compartment. Thus, the "function maps" of individual genes may yield only partial information, whereas the intersection of "function maps" of many genes (perhaps through genetic analyses) may provide the key to understanding why the genes are expressed in these patterns.

C. Homeobox Genes Are Generally Expressed in Multiple Tissues during Embryogenesis

The expression of the homeobox genes outside of the CNS have not yet been described. In general, each of these genes is expressed in a variety of nonneuronal embryonic structures. For instance, the *Hox* and *Dlx* genes are expressed in the limbs, genital eminence, branchial arches, and other tissues. Thus, mutations in these genes can potentially simultaneously alter development of a variety of structures. In mice and humans, there are birth defect syndromes that are characterized by specific combinations of dysmorphic structures. For instance, in humans a single genetic locus can result in defects in the face and limbs (e.g., ectrodactyly-ectodermal dysplasia-clefting, Miller, Mohr, and Nager syndromes), some of which also cause mental deficiencies (e.g., oral-facial-digital, Shprintzen, Ruval-caba syndromes)(Smith, 1982). To date, mutations in four homeobox-containing genes have been linked to human and mouse developmental disorders (Table III), and it is likely that additional homeobox-containing genes will be implicated in other birth defect syndromes.

It is tempting to speculate that whereas some mutations seriously disrupt development, others may lead to adaptive phenotypes in one or more of the structures where the gene is expressed. This hypothesis predicts that certain structures may coevolve. Thus, a mutation in the *Dlx-2* gene may cause subtle alterations in the brain, face, and limbs, which if adaptive, could lead to a strain difference manifested in phenotypes in all three developmental fields. More restricted phenotypes would be caused by mutations in specific regulatory elements.

The effect of mutations in vertebrate homeobox genes may be complicated because many of these genes exist within multigene families. For instance there are four homologous clusters of the *Hox* genes (although there are not always four paralogues of each gene), at least four *Dlx* and *Nkx* genes, and two *En, Msx, Gbx, Otx,* and *Emx* genes. Are the functions of these genes redundant or do they each have unique and important regulatory roles? The answers are just beginning to come in. So far, there are no reported mutations of homeobox genes without phenotypes. It is interesting to note that mutations of the *Pax* genes are semidominant, while mutations of the *Hox* genes are recessive (Table III). The reason for this is not known, but may relate to genetic redundancy within the *Hox* clusters.

Homeobox genes that are in clusters, or that have structural homologues within the same genome, are not fully redundant, as illustrated by the fact that mutations of the *Hox-A1, Hox-A3, Hox-B4, Hox-C8, En-2,* and *Msx*-2 genes each disrupt development (Table III). However, only a subset of the cells expressing these genes are affected. In zebrafish, there are

three known *En* genes, and each is expressed in a distinct set of cells in the region of the midbrain/hindbrain junction (Ekker *et al.*, 1992b). Likewise, functional analysis of *Hox-A1* and *Hox-A3* provides evidence that these genes regulate development in different subsets of cranial neural crest cells. Therefore, while it is premature to make any firm generalizations, it appears that multigene families of homeobox genes may provide additional genetic information that is utilized to regulate development of subsets of cells within a developmental field. This genetic complexity may also facilitate evolutionary changes.

D. Do Homeobox Genes Define a Central Blueprint for Head Development in All Animals?

Evidence is rapidly accumulating showing that many homeobox genes are expressed in analogous patterns in most or all animals (McGinnis and Krumlauf, 1992; Slack *et al.*, 1993). This is particularly the case for genes that define the identity of body and head segments in *Drosophila*. For instance, the *Hox* genes (homologues of the *Drosophila* genes that specify body segment identity) are expressed along the A–P axis in a similar pattern in mice, frogs (*Xenopus*), fish (zebrafish), fruit flies (*Drosophila*), and worms (*C. elegans*) (Fig. 15). Similarly, homologues of the genes involved in development of the fly head (*orthodenticle*, *empty spiracle*, and *distal-less*) are expressed in the head of mouse embryos. In addition, the *distal-less* gene of *Drosophila* is expressed in the primordia of the limbs, facial appendages, and brain (Cohen, 1990); in vertebrates *Dlx-1* and *Dlx-2* are expressed in limb buds, the anlage of facial structures and the forebrain [see Dolle *et al.* (1992) and Bulfone *et al.* (1993a)].

This relationship is not general for all homeobox genes, as many are not expressed in analogous patterns in vertebrates and invertebrates. For instance, genes involved in setting up segmentation in *Drosophila*, such as the *engrailed*, *paired*, and *even-skipped* genes, are not expressed in striped patterns during segmentation in vertebrates. This disparity may be due to the fact that the morphogenetic mechanisms that control segmentation are very different in *Drosophila* and vertebrates.

The similarities of the expression patterns of homeobox genes that are implicated in defining the identity of parts of the embryo along the A–P axis have stimulated the hypothesis that these genes have a central, and highly conserved, role in defining positional information within all animal embryos (McGinnis and Krumlauf, 1992; Slack *et al.*, 1993). Furthermore, there is evidence that these genes use similar regulatory mechanisms in

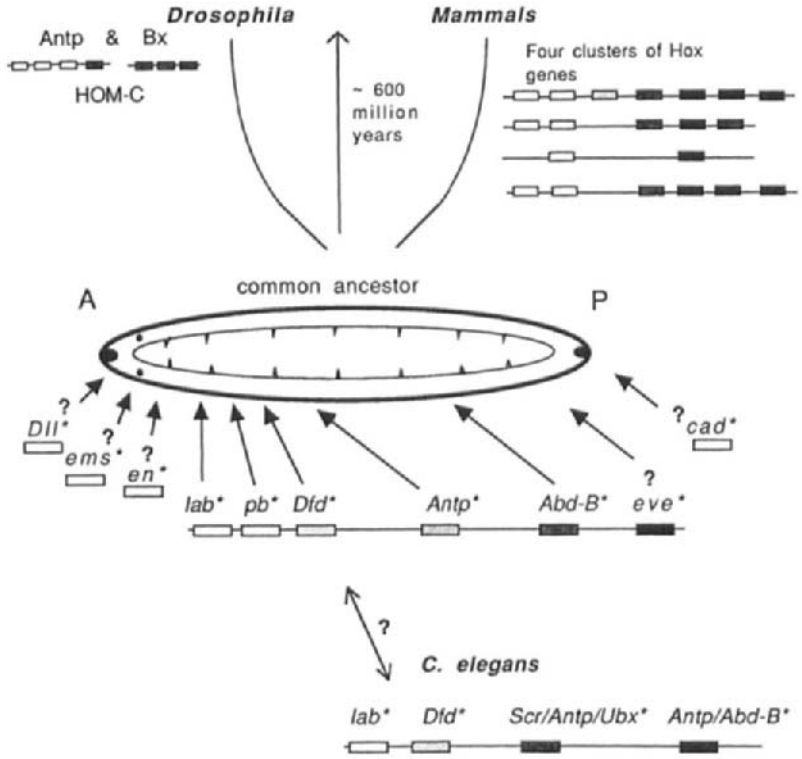

Fig. 15 The hypothesis that *Hox* and other homeobox genes may have a conserved role in specifying positional information in all animals. It is suggested (McGinnis and Krumlauf, 1992) that a common ancestor to insects and vertebrates had a precursor of the *Hox* (*HOM-C*) complex that controlled regional specification along most of the A–P axis. Furthermore, additional homeobox genes were involved in controlling development of the head [*distal-less* (*Dll*), *empty-spiracle* (*ems*), *engrailed* (*en*) *orthodenticle* (*otd*; not shown in this figure)] and of the tail [*caudal* (*cad*)]. The nematode, *C. elegans*, also has a cluster of homeobox genes that may correspond to a form of the *Hox* (*HOM-C*) complex present in the simpler organisms that were the ancestors to insects and vertebrates (Wang *et al.*, 1993). *C. elegans* also has a homeobox gene called ceh-23, whose homeodomain is 52% homologous to the *empty-spiracle* and 50% to *distal-less*, that maps ~30 kb from the other homeotic genes (Wang *et al.*, 1993). [From McGinnis and Krumlauf (1992) with permission.]

various species. For instance, enhancer elements from mammalian genes express genes in analogous regions of the fly embryo (Malicki *et al.*, 1992). This suggests that the genetic hierarchies in diverse species may be very similar. Thus information regarding upstream regulatory genes and downstream target genes from one animal system may be applicable in other distantly related species.

E. Future

A few years ago, there were no candidates for genes that encode regulators of vertebrate brain morphogenesis, regional specification and differentiation. Now there is no shortage of putative regulatory genes. This chapter has attempted to summarize information about homeobox genes but has omitted important results concerning many other types of molecules, including other transcription factors, secreted signals, their receptors, and intracellular signaling pathways.

Several fundamental questions remain regarding development of the vertebrate brain that are now amenable to study at the molecular level. These include how early patterning of the neural plate and neural tube are accomplished; how morphogenetic signals are interpreted into specific patterns of gene expression of regulatory molecules; and how the hierarchy of transcriptional regulators result in the expression of tissue-specific genes.

The answers to these complex problems will undoubtedly involve a variety of approaches. First, additional candidate regulatory genes will need to be identified using a number of methods, including hybridization and PCR screens for homology to known genes; genetic screens in worms, flies, fish, and mice; subtractive hybridization followed by screens of the expression patterns of the subtracted clones (Porteus *et al.*, 1992); and functional screens using methods such as the two hybrid system in yeast (Chien *et al.*, 1991).

With putative regulatory molecules in hand, their functions can be tested. Loss of function analyses have been revolutionized by the ability to make mutations in specific genes in mice [for reviews see Capecchi (1989) and Joyner (1993)]. Since the discovery of this method, hundreds of genes have been mutated, and it seems likely that this approach will lead to the functional analysis of a significant fraction of the known candidate regulatory molecules in the next few years. Furthermore, additional loss-of-function approaches, including tissue-specific gene inactivation using recombinases, dominant negative molecules, and antisense and ribozyme methods, should provide additional avenues to study gene function.

Gain of function studies, such as ectopic expression of regulatory genes in transgenic animals, are also extremely effective experiments to assess the role of a gene. The isolation of regulatory elements that confer highly specific temporal and regional expression has already been used to study the effect of ectopic expression of several *Hox* genes [e.g., Sham *et al.* (1993)]. As more of these regulatory elements become available, increasingly sophisticated experiments will be possible. Furthermore, the use of recombinant viral vectors, and possibly DNA transfection methods, will enable one to study the effect of ectopic expression in small sets of cells.

Experimental embryology and cell biology will be important approaches to study many types of developmental processes. Transplantation experiments will provide assays for the presence of, and response to, morphogenetic signals (see section on midbrain development). Furthermore, a variety of experimental approaches will be needed to study the role of patterning molecules in organizing developmental compartments, in setting up compartment boundaries, and in establishing the molecular blueprint that directs the trajectories of axons and cell migrations.

Transgenic studies of gene function will provide information about the role of these genes in regulating development at the morphological and cellular level. Likewise, transplantation and cellular approaches can correlate gene activity with complex developmental phenomena. However, none of these approaches address the underlying biochemical mechanisms that in fact control these processes. Because it is likely that there is an immensely complex hierarchy of transcription factors that operate as a network to regulate development, a combination of genetic and biochemical approaches will be necessary to elucidate this subject. Inroads in this area are perhaps best exemplified by the studies of sex determination in yeast (Herskowitz, 1989). This work provides insights into how the binding specificity and affinity of homeodomain proteins (MAT-a1 and MAT-α2) are effected by their interaction with each other and with other protein cofactors (e.g., MCM-1) (Keleher *et al.*, 1988; Wolberger *et al.*, 1991). Thus it is likely that protein–protein interactions between various classes of transcription factors and accessory proteins have general roles in regulating the function of homeobox genes. This is further illustrated by the interaction of the herpes simplex virus VP16 protein with the *Oct-1* homeodomain, an interaction that alters the activity of *Oct-1*(Stern and Herr, 1991).

Progress in discovering the genes that regulate expression of the homeobox genes described in this chapter is also beginning [e.g., *Krox20* regulation of *Hox-B2,* Sham *et al.* (1993)]. However, work in *Drosophila* may again provide shortcuts for solving this problem in vertebrates. For instance, the *orthodenticle* gene is regulated by the *bicoid* and *torso* genes (Finkelstein and Perrimon, 1991), the *distal-less* gene is regulated by the *deformed* gene (O'Hara *et al.*, 1993) and the *bithorax* complex genes (Vachon *et al.*, 1992), and the homeotic selector genes are regulated by the *extradenticle* gene (Rauskolb *et al.*, 1993) and *polycomb* genes (Epstein, 1992). Furthermore, advances in finding the targets of the homeobox genes are accelerating (Gould *et al.*, 1990; Andrew and Scott, 1992; Tomotsune *et al.*, 1993). Thus, we are at the beginning of deciphering the "wiring diagram" of the transcriptional hierarchy that controls brain development.

The development of the vertebrate brain is perhaps the most complex frontier in developmental biology. Reagents and methods are now avail-

able to study this important subject, and the results of these investigations will have an impact beyond developmental neurobiology that ranges from gaining insights into evolution of the nervous system to elucidating the molecular basis of some human neurodevelopmental disorders.

Acknowledgments

The authors thank Tabitha Doniach for her helpful comments, and the members of their respective laboratories. Support for this work comes from grants to L.P. from the Spanish Government (DGICYT PB90/0296-C01) and to J.L.R.R. from the Pfizer Scholars, John Merck Scholars, NARSAD Young Investigator and Basil O'Connor-March of Dimes programs, and the NIMH (RO1 MH49428-01; K02 MH01046-01).

References

Adams, B., Dorfler, P., Aguzzi, A., Kozmik, Z., Urbanek, P., Maurer-Fogy, I., and Busslinger, M. (1992). *Pax-5* encodes the transcription factor BSAP and is expressed in B lymphocytes, the developing CNS and adult testis. *Genes Dev.* **6,** 1589–1607.

Alvarado-Mallart, R. M. (1993). Fate and potentialities of the avian mesencephalic/metencephalic neuroepithelium. *J. Neurobiol.* **24,** 1341–1355.

Andrew, D. J., and Scott, M. P. (1992). Downstream of the homeotic genes. *New Biologist* **4,** 5–15.

Asano, M., and Gruss, P. (1992). *Pax-5* is expressed at the midbrain-hindbrain boundary during mouse development. *Mech. Dev.* **39,** 29–39.

Asano, M., Emori, Y., Saigo, K., and Shiokawa, K. (1992). Isolation and characterization of a *Xenopus* cDNA which encodes a homeodomain highly homologous to *Drosophila distal-less*. *J. Biol. Chem.* **267,** 5044–5047.

Bally-Cuif, L., Alvarado-Mallart, R. M., Darnell, D. K., and Wassef, M. (1992). Relationship between *Wnt-1* and *En-2* expression domains during early development of normal and ectopic met-mesencephalon. *Development* **115,** 999–1009.

Beauchemin, M., and Savard, P. (1992). Two *distal-less* related homeobox-containing genes expressed in regeneration blastemas of the newt. *Dev. Biol.* **154,** 55–65.

Bergquist, H., and Kallen, B. (1954). Notes on the early histogenesis and morphogenesis of the central nervous system in vertebrates. *J. Comp. Neurol.* **100,** 627–660.

Bieberich, C. J., Utset, M. F., Awgulewitsch, A., and Ruddle, F. H. (1990). Evidence for positive and negative regulation of the *Hox-3.1* gene. *Proc. Natl. Acad. Sci. USA* **87,** 8462–8466.

Boehm, T., Foroni, L., Kaneko, Y., Perutz, M. F., and Rabbitts, T. H. (1991). The rhombotin family of cysteine-rich LIM-domain oncogenes: Distinct members are involved in T-cell translocations to human chromosomes 11p15 and 11p13. *Proc. Natl. Acad. Sci. USA* **88,** 4367–4371.

Boncinelli, E., Gulisano, M., and Broccoli, V. (1993). *Emx* and *Otx* homeobox gene in the developing mouse brain. *J. Neurobiol.* **24,** 1356–366.

Boncinelli, E., Simeone, A., Acampora, D., and Mavilio, F. (1991). *HOX* gene activation by retinoic acid. *Trends Genetics* **7,** 330–334.

Bulfone, A., Kim, H. J., Puelles, L., Porteus, M. H., Grippo, J., and Rubenstein,

J. L. R. (1993a). The mouse *Dlx-2* (Tes-1) gene is expressed in spatially restricted domains of the forebrain, face and limbs in midgestation mouse embryos. *Mech. Dev.* **40,** 129–140.

Bulfone, A., Puelles, L., Porteus, M. H., Frohman, M. A., Martin, G. R., and Rubenstein, J. L. R. (1993b). Spatially restricted expression of *Dlx-1*, *Dlx-2* (Tes-1), *Gbx-2* and *Wnt-3* in the embryonic day 12.5 mouse forebrain defines potential transverse and longitudinal segmental boundaries. *J. Neurosci.* **13**(7), 3155–3172.

Capecchi, M. (1989). Altering the genome by homologous recombination. *Science* **244,** 1288–1292.

Carpenter, E. M., Goddard, J. M., Chisaka, O., Manley, N. R., and Capecchi, M. R. (1993). Loss of *Hox-A1 (Hox 1.6)* function results in the reorganization of the murine hindrbrain. *Development* **118,** 1063–1075.

Chalepakis, G., Fritsch, R., Fickenscher, H., Deutsch, U., Goulding, M., and Gruss, P. (1991). The molecular basis of the undulated/*Pax-1* mutation. *Cell* **66,** 873–884.

Chalepakis, P., Stoykova, A., Wijnholds, J., Tremblay, P., and Gruss, P. (1993). *Pax*: gene regulators in the developing nervous system. *J. Neurobiol.* **24**(10), 1367–1384.

Chalfie, M., and Au, M. (1989). Genetic control of differentiation of the *Caenorhabditis elegans* touch receptor neurons. *Science* **243,** 1027–1033.

Chien, C. T., Bartel, P. L., Sternglanz, R., and Fields, S., (1991). The two-hybrid system: a method to identify and clone genes for proteins that interact with a protein of interest. *Proc. Natl. Acad. Sci. USA* **88,** 9578–9582.

Chisaka, O., and Capecchi, M. R. (1991). Regionally restricted developmental defects resulting from targeted disruption of the mouse homeobox gene *Hox-1.5*. *Nature* **350,** 473–479.

Chisaka, O., Musci, T. S., and Capecchi, M. R. (1992). Developmental defects of the ear, cranial nerves and hindbrain resulting from targeted disruption of the mouse homeobox gene *Hox-1.6*. *Nature* **355,** 516–520.

Cohen, B., McGuffin, M. E., Pfeifle, C., Segal, D., and Cohen, S. M. (1992). *Apterous*, a gene requried for imaginal disc development in *Drosophila*, encodes a member of the LIM family of developmental regulatory proteins. *Genes Dev.* **6,** 715–729.

Cohen, S., and Jurgens, G. (1991). *Drosophila* headlines. *TIG* **7**(8), 267–272.

Cohen, S. M. (1990). Specification of limb development in the *Drosophila* embryo by positional cues from segmentation genes. *Nature* **343,** 173–177.

Cohn, M. M., Jr., and Sulik, K. K. (1992). Perspectives on holoprosencephaly. II. Central nervous system, craniofacial anatomy, syndrome commentary, diagnostic approach and experimental studies. *J. Cranio. Facial Gen. Dev. Biol.* **12,** 196–244.

Davidson, D., Graham, E., Sime, C., and Hill, R. (1988). A gene with sequence similarity to *Drosophila engrailed* is expressed during the development of the neural tube and vertebrae in the mouse. *Development* **104,** 305–316.

Davis, C. A., Holmyard, D. P., Millen, K. J., and Joyner, A. L. (1991). Examining pattern formation in mouse, chicken and frog embryos with an *En*-specific antiserum. *Development* **111,** 287–298.

Davis, C. A., and Joyner, A. L. (1988). Expression patterns of the homeo box-containing genes *En-1* and *En-2* and the proto-oncogene *int-1* diverge during mouse development. *Genes Dev.* **2,** 1736–1744.

Davis, C. A., Noble-Topham, S. E., Rossant, J., and Joyner, A. L. (1988). Expression of the homeo box-containing gene *En-2* delineates a specific region of the developing mouse brain. *Genes Dev.* **2,** 361–371.

Desai, C., Garriga, G., McIntire, S. L., and Horvitz, H. R. (1988). A genetic pathway for the development of the *Caneorhabditis elegans* HSN motor neurons. *Nature* **336,** 638–646.

DiNardo, S., Sher, E., Heemskerk-Jongens, J., Kassis, J. A., and O'Farrell, P. H.

(1988). Two-tiered regulation of spatially patterned *engrailed* gene expression during *Drosophila* embryogenesis. *Nature* **332,** 604–609.

Dirkson, M. L., Mathers, P., and Jamrich, M. (1993). Expression of a *Xenopus distal-less* homeobox gene involved in forebrain and cranio-facial development. *Mech. Dev.* **41,** 121–128.

Dolle, P., Lufkin, T., Krumlauf, R., Mark, M., Duboule, D., and Chambon, P. (1993). Local alterations of *Krox-20* and *Hox* gene expression in the hindbrain suggest lack of rhombomeres 4 and 5 in homozygote null *Hoxa-1 (Hox-1.6)* mutant embryos. *Proc. Natl. Acad. Sci. USA* **90,** 7666–7670.

Dollé, P., Price, M., and Duboule, D. (1992). Expression of the murine *Dlx-1* homeobox gene during facial, ocular and limb development. *Differentiation* **49,** 93–99.

Doniach, T. (1992). Induction of anteroposterior neural pattern in *Xenopus* by planar signals. *Development*(Supp.) 183–193.

Doniach, T., Phillips, C. R., and Gerhart, J. C. (1992). Planar induction of anteroposterior pattern in the developing central nervous system of *Xenopus laevis*. *Science* **257,** 542–545.

Easter, S. S., Jr., Ross, L. S., and Frankfurter, A. (1993). Initial tract formation in the mouse brain. *J. Neurosci.* **13,** 285–299.

Ekker, M., Akimenko, M. A., Bremiller, R., and Westerfield, M. (1992a). Regional expression of three homeobox transcripts in the inner ear of zebrafish embryos. *Neuron* **9,** 27–35.

Ekker, M., Wegner, J., Akimenko, M. A., and Westerfield, M. (1992b). Coordinate embryonic expression of three zebrafish *engrailed* genes. *Development* **116,** 1001–1010.

Epstein, D. J., Vekemans, M., and Gros, P. (1991). Splotch (Sp^{2H}), a mutation affecting development of the mouse neural tube, shows a deletion within the paired homeodomain of *Pax-3*. *Cell* **67,** 767–774.

Epstein, D. J., Vogan, K. J., Trasler, D. G., and Gros, P. (1993). A mutation within intron 3 of the *Pax-3* gene produces aberrantly spliced mRNA transcripts in the splotch (*Sp*) mouse mutant. *Proc. Natl. Acad. Sci. USA* **90,** 532–536.

Epstein, H. (1992). Polycomb and friends. *Bioessays* **14,** 411–413.

Figdor, M. C., and Stern, C. D. (1993). Segmental organization of embryonic diencephalon. *Nature* **363,** 630–634.

Finkelstein, R., and Perrimon, N. (1991). The molecular genetics of head development in *Drosophila melangaster*. *Development* **112,** 899–912.

Fortini, M. E., Lai, Z., and Rubin, G. M. (1991). The *Drosophila zfh-1* and *zfh-2* genes encode novel proteins containing both zinc-finger and homeodomain motifs. *Mech. Dev.* **34,** 113–122.

Fraser, S., Keynes, R., and Lumsden, A. (1990). Segmentation in the chick embryo hindbrain is defined by cell lineage restrictions. *Nature* **344,** 431–435.

Frohman, M. A., Dickinson, M. E., Hogan, B. L. M., and Martin, G. R. (1994). Mapping of *Gbx-1* to mouse chromosome 5 and *Gbx-2* to mouse chromosome 1. *Mouse NewLett.* **91,** 323–325.

Gardner, C. A., and Barald, K. F. (1992). Expression patterns of *engrailed*-like proteins in the chick embryo. *Dev. Dyn.* **193,** 370–388.

Gehring, W. J. (1987). The homeobox: structural and evoultionary aspects. *In* "Molecular Approaches to Developmental Biology," pp. 115–129. A. R. Liss, New York.

Gerrero, M. R., McEvilly, R. J., Turner, E., Lin, C. R., O'Connell, S., Jenne, K. J., Hobbs, M. V., and Rosenfeld, M. G. (1994). *Brn-3.0*: a *POU* domain protein expressed in the sensory, immune and endocrine systems that selectively functions on non-octamer motifs. *Proc. Natl. Acad. Sci. USA* (in press).

Glaser, T., Walton, D. S., and Maas, R. L. (1992). Genomic structure, evolutionary conservation and aniridia mutations in the human *PAX6* gene. *Nature Gen.* **2,** 232–238.

Goodrum, G. R., and Jacobson, A. G. (1981). Cephalic flexure formation in the chick embryo. *J. Exp. Zool.* **216,** 399–408.

Gould, A. P., Brookman, J. J., Strutt, D. I., and White, R. A. H. (1990). Targets of homeotic gene control in *Drosophila*. *Nature* **348,** 308–312.

Goulding, M. D., Chalepakis, G., Deutsch, U., Erselius, J. R., and Gruss, P. (1991). *Pax-3,* a novel murine DNA binding protein expressed during early neurogenesis. *EMBO J.* **10,** 1135–1147.

Gribnau, A. A. M., and Geijberts, L. M. G. (1985). Morphogenesis of the brain in staged Rhesus monkey embryos. *Adv. Anat. Embryol. Cell Biol.* **91,** 1–69.

Hallonet, M. E., Teillet, M. A., and Le Douarin, N. M. (1990). A new approach to the development of the cerebellum provided by the quail-chick marker system. *Development* **108,** 19–31.

He, X., Treacy, M. N., Simmons, D. M., Ingraham, H. A., Swanson, L. W., and Rosenfeld, M. G. (1989). Expression of a large family of *POU*-domain regulatory genes in mammalian brain development. *Nature* **340,** 35–41.

Herrick, C. J. (1910). The morphology of the forebrain in amphibia and reptilia. *J. Comp. Neurol.* **20,** 413–547.

Herskowitz, I. (1989). A regulatory hierarchy for cell specialization in yeast. *Nature* **342,** 749–757.

Hill, R. E., Favor, J., Hogan, B. L. M., Ton, C. C. T., Saunders, G. F., Hanson, I. M., Prosser, J., Jordan, T., Hastie, N. D., and van Heyningen, V. (1991). Mouse *Small Eye* results from mutations in a paired-like homeobox-containing gene. *Nature* **354,** 522–525.

His, W. (1893). Uber die frontale ende des gehirurohes. *Arch Anat Entwicklungsgesch.* (Leipzig), 157–171.

Hogan, B. L. M., Thaller, C., and Eichele, G. (1992). Evidence that Hensen's node is a site of retinoic acid synthesis. *Nature* **359,** 237–241.

Ingraham, H. A., Chen, R., Mangalam, H. J., Elsholtz, H. P., Flynn, S. E., Lin, C. R., Simmons, D. M., Swanson, L., and Rosenfeld, M. G. (1988). A tissue-specific transcription factor containing a homeodomain specifies a pituitary phenotype. *Cell* **55,** 519–529.

Itasaki, N., Ichijo, H., Hama, C., Matsuno, T., and Nakamura, H. (1991). Establishment of rostrocaudal polarity in tectal primordium: *engrailed* expression and subsequent tectal polarity. *Development* **113,** 1133–1144.

Jabs, E. W., Muller, U., Li, X., Ma, L., Luo, W., Haworth, I. S., Klisak, I., Sparkes, R., Warman, M. L., Mulliken, J. B., Snead, M. L., and Maxon, R. (1993). A mutation in the homeodomain of the human *MSX2* gene in a family affected with autosomal dominant craniosynostosis. *Cell* **75,** 443–450.

Jacobson, A. G., and Tam, P. P. (1982). Cephalic neurulation in the mouse embryo analyzed by SEM and morphometry. *Anat. Rec.* **203,** 375–396.

Jordan, T., Hanson, I., Zaletayev, D., Hodgson, S., Prosser, J., Seawright, A., Hastie, N., and van Heyningen, V. (1992). The human *PAX6* gene is mutated in two patients with aniridia. *Nature Gen.* **1,** 328–332.

Jostes, B., Walther, C., and Gruss, P. (1991). The murine paired box gene, *Pax-7,* is expressed specifically during the development of the nervous and muscular system. *Mech. Dev.* **33,** 27–38.

Joyner, A. L. (1993). "Gene Targeting: A Practical Approach." Oxford University Press, Oxford.

Joyner, A. L., Herrup, K., Auerbach, B. A., Davis, C. A., and Rossant, J. (1991). Subtle cerebellar phenotype in mice homozygous for a targeted deletion of the *En-2* homeobox. *Science* **251,** 1239–1243.

Joyner, A. L., and Martin, G. R. (1987). *En*-1 and *En*-2, two mouse genes with sequence homology to the *Drosophila engrailed* gene: expression during embryogenesis. *Genes Dev.* **1,** 29–38.

Kallen, B. (1965). Early morphogenesis and pattern formation in the central nervous system. *In* "Organogenesis," pp. 107–128. Holt, Rhinehart & Wilson, New York.

Keleher, C. A., Goutte, C., and Johnson, A. D. (1988). The yeast cell-type-specific repressor $\alpha 2$ acts cooperatively with a non-cell-type-specific protein. *Cell* **53,** 927–936.

Kessel, M. (1993). Reversal of axonal pathways from rhombomere 3 correlates with extra *Hox* expression domains. *Neuron* **10,** 379–393.

Keynes, R., and Lumsden, A. (1990). Segmentation and the origin of regional diversity in the vertebrate central nervous system. *Neuron* **2,** 1–9.

Keyser, A. (1972). The development of the diencephalon of the chinese hamster. *Acta Anat.***83** (Suppl. 59), 1–181.

Kissinger, C. R., Liu, B., Martin-Blanco, E., Kornberg, T. B., and Pabo, C. O. (1990). Crystal structure of an *engrailed* homeodomain-DNA complex at 2.8 A resolution: a framework for understanding homeodomain-DNA interactions. *Cell* **63,** 579–590.

Komuro, I., Schalling, M., Jahn, L., Bodmer, R., Jenkins, N. A., Copeland, N. G., and Izumo, S. (1993). *Gtx*: a novel murine homeobox-containing gene, expressed specifically in glial cells of the brain and germ cells of testis, has a transcriptional repressor activity *in vitro* for a serum-inducible promoter. *EMBO J.* **12,** 1387–1401.

Krauss, S., Johansen, T., Korzh, V., and Fjose, A. (1991). Expression pattern of zebrafish *Pax* genes suggests a role in early brain regionalization. *Nature* **353,** 267–270.

Krauss, S., Maden, M., Holder, N., and Wilson, S.W. (1992). Zebrafish *Pax*[b] is involved in the formation of the midbrain-hindbrain boundary. *Nature* **360,** 87–89.

Krumlauf, R. (1993). *Hox* genes and pattern formation in the branchial region of the vertebrate head. *Trends Genetics* **9,** 106–112.

Krumlauf, R., Marshall, H., Studer, M., Nonchev, S., Sham, M. H., and Lumsden, A. (1993). *Hox* homeobox genes and regionalization of the nervous system. *J. Neurobiol.* **24,** 1328–1340.

Kuhlenbeck, H. (1973). "The Central Nervous System of Vertebrates." Karger, Basel.

LaMantia, A. S., Colbert, M. C., and Linney, E. (1993). Retinoic acid induction and regional differentiation prefigure olfactory pathway formation in the mammalian forebrain. *Neuron* **10,** 1035–1048.

Lawrence, P. A. (1992). "The Making of a Fly: The Genetics of Animal Design." Blackwell Scientific Publications, London.

Lazzaro, D., Price, M., De Felice, M., and Di Lauro, R. (1991). The transcription factor TTF-1 is expressed at the onset of thyroid and lung morphogenesis in restricted regions of the foetal brain. *Development* **113,** 1093–1104.

Le Moine, C., and Young, S. W., III. (1992). *RHS2*, a *POU* domain-containing gene, and its expression in developing and adult rat. *Proc. Natl. Acad. Sci. USA* **89,** 3285–3289.

Lin, C., Lin, S.-C., Chang, C.-P., and Rosenfeld, M. G. (1992). *Pit-1* dependent expression of the receptor for growth factor releasing hormone factor mediates pituitary cell growth. *Nature* **360,** 765–768.

Lo, L.-C., Johnson, J. E., Wuenschell, C. W., Saito, T., and Anderson, D. J. (1991). Mammalian *achaete-scute* homolog 1 is transiently expressed by spatially restricted subsets of early neuroepithelial and neural crest cells. *Genes Dev.* **5,** 1524–1537.

Logan, C., Khoo, W. K., Cado, D., and Joyner, A. L. (1993). Two enhancer regions in

the mouse *En-2* locus direct expression to the mid/hindbrain region and mandibular myoblasts. *Development* **117,** 905–916.

Lu, S., Bogarad, L. D., Murtha, M. T., and Ruddle, F. H. (1992). Expression pattern of a murine homeobox gene, *Dbx,* displays extreme spatial restriction in embryonic forebrain and spinal cord. *Proc. Natl. Acad. Sci. USA* **89,** 8053–8057.

Lufkin, T., Dierich, A., LeMeur, M., Mark, M., and Chambon, P. (1991). Disruption of the *Hox-1.6* homeobox gene results in defects in a region corresponding to its rostral domain of expression. *Cell* **66,** 1105–1119.

Lumsden, A., and Keynes, R. (1989). Segmental patterns of neuronal development in the chick hindbrain. *Nature* **33,** 424–428.

Lumsden, A., Sprawson, N., and Graham, A. (1991). Segmental origin and migration of neural crest cells in the hindbrain region of the chick embryo. *Development* **113,** 1281–1291.

Mackenzie, A., Ferguson, M. W. J., and Sharpe, P. T. (1991). *Hox-7* expression during murine craniofacial development. *Development* **113,** 601–611.

Maden, M., and Holder, N. (1992). Retinoic acid and development of the central nervous system. *BioEssays* **14**(7), 431–438.

Malicki, J., Cianetti, L. C., Peschle, C., and McGinnis, W. (1992). A human *HOX4B* regulatory element provides head-specific expression in *Drosophila* embryos. *Nature* **358,** 345–347.

Marin, F., and Puelles, L. (1994). Patterning of the embryonic avian midbrain after experimental inversions: a polarizing activity from the isthmus. *Dev. Biol.* (in press).

Marshall, H., Nonchev, S., Sham, M. H., Muchamore, I., Lumsden, A., and Krumlauf, R. (1992). Retinoic acid alters hindbrain *Hox* code and induces transformation of rhombomeres 2/3 into a 4/5 identity. *Nature* **360,** 737–741.

Martinez, S., and Alvarado-Mallart, R. M. (1989). Rostral cerebellum originates from the caudal portion of the so-called "mesencephalic" vesicle: a study using chick-quail chimeras. *Eur. J. Neurosci.* **1,** 549–560.

Martinez, S., Geijo, E., Sanchez-Vives, M. V., Puelles, L., and Gallego, R. (1992). Reduced junctional permeability at interrhombomeric boundaries. *Development* **116,** 1069–1076.

Martinez, S., Wassef, M., and Alvarado-Mallart, R. M. (1991). Induction of a mesencephalic phenotype in the 2-day-old chick prosencenphalon is preceded by the early expression of the homeobox gene *en. Neuron* **6,** 971–981.

Mathis, J. M., Simmons, D., He, X., Swanson, L. W., and Rosenfeld, M. G. (1992). *Brain 4:* a novel mammalian *POU* domain transcription factor exhibiting restricted brain-specific expression. *EMBO J.* **11,** 2551–2561.

Matsuo, T., Osumi-Yamashita, N., Noji, S., Ohuchi, H., Koyama, E., Myokai, F., Matsuo, N., Taniguchi, S., Doi, H., Iseki, S., Ninomiya, Y., Fujiwara, M., Watanabe, T., and Eto, K. (1993). A mutation in the *Pax-6* gene in rat *small eye* is associated with impaired migration of midbrain crest cells. *Nature Genetics* **3,** 299–304.

McGinnis, W., and Krumlauf, R. (1992). Homeobox genes and axial patterning. *Cell* **68,** 283–302.

McGuinness, T. L., MacDonald, G. P., Koch, T. K., and Rubenstein, J. L. R. (1992). Evidence for linkage of Tes-1 and *Dlx-1,* two homeobox genes expressed in the developing mammalian forebrain. *Soc. Neurosci.* [Abstract 404.5]

McMahon, A. P., and Bradley, A. (1990). The *Wnt-1* (*int-1*) proto-oncogene is required for development of a large region of the mouse brain. *Cell* **62,** 1073–1085.

McMahon, A. P., Joyner, A., Bradley, A., and McMahon, J. A. (1992). The midbrain-hindbrain phenotype of *Wnt-1*$^{-}$/*Wnt-1*$^{-}$ mice results from stepwise deletion of *engrailed*-expressing cells by 9.5 days postcoitum. *Cell* **69,** 581–595.

Monaghan, A. P., Davidson, D. R., Sime, C., Graham, E., Baldock, R., Bhattacharya, S. S., and Hill, R. E. (1991). The *Msh*-like homeobox genes define domains in the developing vertebrate eye. *Development* **112,** 1053–1061.

Monuki, E. S., Kuhn, R., Weinmaster, G., Trapp, B. D., and Lemke, G. (1990). Expression and activity of the *POU* transcription factor SCIP. *Science* **249,** 1300–1303.

Monuki, E. S., Weinmaster, G., Kuhn, R., and Lemke, G. (1989). SCIP: a glial *POU* domain gene regulated by cyclic AMP. *Neuron* **3,** 783–793.

Morris-Kay, G. M. (1981). Growth and development of pattern in the cranial neural epithelium of rat embryos during neurulation. *J. Embryol. Exp. Morphol.* **65** (Suppl.), 225–241.

Muller, F., and O'Rahilly, R. (1989). Mediobasal prosencephalic defects, including holoprosencephaly and cyclopia, in relation to the development of the human forebrain. *Amer. J. Anat.* **185,** 391–414.

Murtha, M. T., Leckman, J .F., and Ruddle, F. H. (1991). Detection of homeobox genes in development and evolution. *Proc. Natl. Acad. Sci. USA* **88,** 10711–10715.

Nornes, H. O., Dressler, G. R, Knapik, E. W., Deutsch, U., and Gruss, P. (1990). Spatially and temporally restricted expression *Pax-2* during murine neurogenesis. *Development* **109,** 797–809.

O'Hara, E., Cohen, B., Cohen, S. M., and McGinnis, W. (1993). *Distal-less* is a downstream gene of *deformed* required for ventral maxillary identity. *Development* **117,** 847–856.

Özçelik, T., Porteus, M. H., Rubenstein, J. L. R., and Francke, U. (1992). *DLX2* (*TES1*), a homeobox gene of the *Distal-less* family, assigned to conserved regions on human and mouse chromosomes 2. *Genomics* **13,** 1157–1161.

Palmgren, A. (1921). Embryological and morphological studies on the midbrain and cerebellum of vertebrates. *Acta Zool. (Stockholm)* **2,** 1–94.

Papalopulu, N., and Kintner, C. (1993). *Xenopus Distal-less* related homeobox genes are expressed in the developing forebrain and are induced by planar signals. *Development* **117,** 961–975.

Plachov, D., Chowdhury, K., Walther, C., Simon, D., Guenet, J. L., and Gruss, P. (1990). *Pax8,* a murine paired box gene expressed in the developing excretory system and thyroid gland. *Development* **110,** 643–651.

Poole, S. J., Kauvar, L. M., Drees, B., and Kornberg, T. (1985). The *engrailed* locus of *Drosophila:* structural analysis of an embryonic transcript. *Cell* **40,** 37–43.

Porteus, M. H., Brice, A. E. J., Bulfone, A., Usdin, T. B., Ciaranello, R. D., and Rubenstein, J. L. R. (1992). Isolation and characterization of a library of cDNA clones that are preferentially expressed in the embryonic telencephalon. *Mol. Brain Res.* **12,** 7–22.

Porteus, M. H., Bulfone, A., Ciaranello, R. D., and Rubenstein, J. L. R. (1991). Isolation and characterization of a novel cDNA clone encoding a homeodomain that is developmentally regulated in the ventral forebrain. *Neuron* **7,** 221–229.

Price, M. (1993). Members of the *Dlx*- and *Nkx*2- gene families are regionally expressed in the developing forebrain. *J. Neurobiol.* **24**(10), 1385–1399.

Price, M., Lazzaro, D., Pohl, T., Mattei, M.-G., Rüther, U., Olivo, J.-C., Duboule, D., and Di Lauro, R. (1992). Regional expression of the homeobox gene *Nkx-2.2* in the developing mammalian forebrain. *Neuron* **8,** 241–255.

Price M., Lemaistre, M., Pischetola, M., Di Lauro, R., and Duboule, D. (1991). A mouse gene related to *Distal-less* shows a restricted expression in the developing forebrain. *Nature* **351,** 748–751.

Puelles, L., Amat, J. A., and Martinez-de-la-Torre, M. (1987). Segment-related, mosaic

neurogenetic pattern in the forebrain and mesencephalon of early chick embryos. I. Topography of AChE-positive neuroblasts up to stage HH18. *J. Comp. Neurol.* **266,** 247–268.

Puelles, L., Guillen, M., and Martinez-de-la-Torre, M. (1991). Observations on the fate of the nucleus superficialis magnocellularis of Rendahl in the avian diencephalon, bearing on the organization and nomeclature of neighboring retinorecipient nuclei. *Anat. Embryol.* **183,** 221–233.

Puelles, L., and Martinez-de-la-Torre, M. (1987). Autoradiographic and golgi study on the early development of n. isthmi principalis and adjacent grisea in the chick embryo: A tridimensional viewpoint. *Anat. Embryol.***176,** 19–34.

Puelles, L., and Rubenstein, J. L. R. (1993). Expression patterns of homeobox and other putative regulatory genes in the embryonic mouse forebrain suggest a neuromeric organization *Trends Neurosci.* **16**(11), 472–479.

Puschel, A. W., Balling, R., and Gruss, P. (1991). Separate elements cause lineage restriction and specify boundaries of *Hox-1.1* expression. *Development* **112,** 279–287.

Puschel, A. W., Gruss, P., and Westerfield, M. (1992a). Sequence and expression of *Pax-6* are highly conserved between zebrafish and mice. *Development* **114,** 643–651.

Puschel, A. W., Westerfiled, M., and Dressler, G. R. (1992b). Comparative analysis of *Pax-2* protein distributions during neurulation in mice and zebrafish. *Mech. Dev.* **38,** 197–208.

Ramirez-Solis, R., Zheng, H., Whiting, J., Krumlauf, R., and Bradley, A. (1993). *Hox*b-4 (*Hox*-2.6) mutant mice show homeotic transformation of a cervical vertebra and defects in the closure of the sternal rudiments. *Cell* **73,** 279-294.

Rauskolb, C., Peifer, M., and Wieschaus, E. (1993). *extradenticle*, a regulator of homeotic gene activity, is a homolog of the homeobox-containing human proto-oncogene *pbx-1*. *Cell* **74,** 1101–1112.

Rendahl, H. (1924). Embryologische und morphologische Studien über das Zwischenhirn beim Huhn. *Acta. Zool.* **5,** 241–344.

Robinson, G. W., Wray, S., and Mahon, K. A. (1991). Spatially restricted expression of a member of a new family of murine *Distal-less* homeobox genes in the developing forebrain. *New Biologist* **3,** 1183–1194.

Saha, M. S., Michel, R. B., Gulding, K. M., and Grainger, R. M. (1993). A *Xenopus* homeobox gene defines dorsal-ventral domains in the developing brain. *Development* **118,** 193–202.

Salinas, P. C., and Nusse, R. (1992). Regional expression of the *Wnt-3* gene in the developing mouse forebrain in relationship to diencephalic neuromeres. *Mech. Dev.* **39,** 151–160.

Schena, M., and Davis, R. W. (1992). HD-Zip proteins: members of an *Arabidopsis* homeodomain protein superfamily. *Proc. Natl. Acad. Sci. USA* **89,** 3894–3898.

Schughart, K., Bieberich, C. J., Eid, R., and Ruddle, F. H. (1991). A regulatory region from the mouse *Hox-2.2* promoter directs gene expression into developing limbs. *Development* **112,** 807–811.

Sechrist, J., Serbedzija, G. N., Scherson, T., Fraser, S. E., and Bronner-Fraser, M. (1993). Segmental migration of the hindbrain neural crest does not arise from its segmental generation. *Development* **118,** 691–703.

Sham, M. H., Vesque, C., Nonchev, S., Marshall, H., Frain, M., Gupta, R. D., Whiting, J., Wilkinson, D., Charnay, P., and Krumlauf, R. (1993). The zinc finger gene *Krox20* regulates *HoxB2* (*Hox2.8*) during hindbrain segmentation. *Cell* **72,** 183–196.

Simeone, A., Acampora, D., Gulisano, M., Stornaiuolo, A., and Boncinelli, E. (1992a). Nested expression domains of four homeobox genes in developing rostral brain. *Nature* **358,** 687–690.

Simeone, A., Acampora, D., Mallamaci, A., Stornaiuolo, A., D'Aprice, M. R., Nigro, V., and Boncinelli, E. (1993). A vertebrate gene related to *orthodenticle* contains a homeodomain of the bicoid class and demarcates anterior neuroectoderm in the gastrulating mouse embryo. *EMBO J.* **12**(7), 2735–2747.

Simeone, A., Gulisano, M., Acampora, D., Stornaiuolo, A., Rambaldi, M., and Boncinelli, E.(1992b). Two vertebrate homeobox genes related to the *Drosophila empty spiracles* gene are expressed in the embryonic cerebral cortex. *EMBO J.* **11,** 2541–2550.

Slack, J. M. W. (1991). "From Egg to Embryo: Regional Specification in Early Development." Cambridge University Press, London/New York.

Slack, J. M. W., Holland, P. W. H., and Graham, C. F. (1993). The zootype and the phylotypic stage. *Nature* **361,** 490–492.

Smith, D. W. (1982). "Recognizable Patterns of Human Malformation." Saunders, Philadelphia.

Stern, S., and Herr, W. (1991). The herpes simplex virus trans-activator VP16 recongnizes the Oct-1 homeodomain: evidence for a homeo domain recognition subdomain. *Genes Dev.* **5,** 2555–2566.

Suzuki, N., Rohdewohld, H., Neuman, T., Gruss, P., and Scholer, H. R. (1990). *Oct-6*: a *POU* transcription factor expressed in embryonal stem cells and in the developing brain. *EMBO J.* **9,** 3723–3732.

Swiatek, P. J., and Gridley, T. (1993). Perinatal lethality and defects in hindbrain development in mice homozygous for a targeted mutation of the zinc finger gene *Krox20*. *Genes Dev.***7,** 2071–2084.

Tabin, C. J. (1991). Retinoids, homeoboxes and growth factors: towards molecular models for limb development. *Cell* **66,** 199–217.

Taira, M., Hayes, W. P., Otani, H., and Dawid, I. B. (1993). Expression of LIM class homeobox gene *Xlim-3* in *Xenopus* development is limited to neural and neuroendocrine tissues. *Dev. Biol.* **159,** 245–256.

Tassabehji, M., Read, A. P., Newton, V. E., Harris, R., Balling, R., Gruss, P., and Strachan, T. (1992). Waardenburg's syndrome patients have mutations in the human homologue of the *Pax-3* paired box gene. *Nature* **355,** 635–638.

Tassabehji, M., Read, A. P., Newton, V. E., Patton, M., Gruss, P., Harris, R., and Strachan, T. (1993). Mutations in the *PAX3* gene causing Waardenburg syndrome type 1 and type 2. *Nature Gen.* **3,** 26.

Thomas, K. R., and Capecchi, M. R. (1990). Targeted disruption of the murine *int-1* proto-oncogene resulting in severe abnormalities in midbrain and cerebellar development. *Nature* **346,** 847–850.

Thomas, K. R., Musci, T. S., Neumann, P. E., and Capecchi, M. R. (1991). *Swaying* is a mutant allele of the proto-oncogene *Wnt-1*. *Cell* **67,** 969–976.

Thor, S., Ericson, J., Brannstrom, T., and Edlund, T. (1991). The homeodomain LIM protein *Isl-1* is expressed in subsets of neurons and endocrine cells in the adult rat. *Neuron* **7,** 881–889.

Tomotsune, D., Shojl, H., Wakamatsu, Y., Knodoh, H., and Takahashi, N. (1993). A mouse homologue of the *Drosophila* tumor-suppressor gene *I(2)gl* controlled by *Hox-C8 in vivo*. *Nature* **365,** 69–72.

Ton, C. C. T., Hirvonen, H., Miwa, H., Weil, M. M., Monaghan, P., Jordan, T., van Heyningen, V., Drechsler, M., Royer-Pokora, B., Collins, F., Swaroop, A., Strong, L. C., and Saunders, G. F. (1991). Positional cloning and characterization of a paired box- and homeobox-containing gene from the aniridia region. *Cell* **67,** 1059–1074.

Turner, E. R., Jenne, K. J., and Rosenfeld, M. G. (1994). Brn-3.2: a Brn-3 related transcription factor with distinctive central nervous system expression and regulation by retinoic acid. *Neuron* (in press).

This Page Intentionally Left Blank

2

Homeobox and *pax* Genes in Zebrafish Development

Anders Fjose
Department of Biochemistry and Molecular Biology
University of Bergen
N-5009 Bergen, Norway

I. Introduction

Inspired by the idea that the zebrafish (*Brachydanio rerio*) is an ideal vertebrate for the genetic analysis of development (Marcey and Nüsslein-Volhard, 1986), investigators in several laboratories have begun studying the putative developmental regulatory genes in this organism. However, the progress in identifying developmental mutants in zebrafish has been very slow, perhaps because of limited resources. Since only a few interesting mutations have been described, one might argue that the potential of the zebrafish as a genetic model remains largely unexploited. Fortunately, the relatively simple features of the translucent zebrafish embryo offer

Current Topics in Developmental Biology, Vol. 29

special opportunities for analyzing and manipulating the development of single identifiable cells in the central nervous system (CNS) and other tissues. As a consequence, in several cases it has been possible to analyze embryonic gene expression at higher resolution than has been achieved in other vertebrates. In addition, the evolutionary distance of more than 400 million years between fish and mammals may allow the most essential functions to be identified on the basis of the degree of conservation of gene structure and expression. Thus, despite the recent initiation of molecular analysis of zebrafish (Eiken *et al.*, 1987), studies of homeobox and *pax* genes in this species have made significant contributions to the field of vertebrate molecular embryology.

II. Sequence Conservation between Zebrafish and Mammalian Homologs

Most of the putative developmental regulatory genes characterized so far for zebrafish are members of the subfamilies of homeobox genes that have previously been analyzed in mammals and *Drosophila*. In many cases, it has been possible to unambiguously identify the fish homologs of specific mammalian genes. Interestingly, the degree of amino acid (aa) sequence conservation between the homologs varies considerably (from 50 to nearly 100%). This relationship has been most extensively analyzed for the zebrafish *hox* genes.

A. *Hox* Genes

Zebrafish counterparts of mammalian homeobox (*hox*)-containing genes located in both the Hox-B (Hox-2) and Hox-C (Hox-3) clusters have been isolated, but it is still unclear whether the fish genome also contains a Hox-A or a Hox-D complex. The identification of the two closely linked zebrafish genes *hox-B5* (*hox-2.1*) and *hox-B6* (*hox-2.2*), which correspond directly to a similar related pair of genes in the mammalian Hox-B complex (Fig. 1), confirmed the existence of the Hox-B cluster in the zebrafish genome Njølstad *et al.*, 1988b, 1990). Comparison of *hox-B5* with its murine homolog revealed several highly conserved features (Njølstad *et al.*, 1988b). The putative protein products are of similar length (about 275 residues), and the 96 aa C-terminal, including the 60 aa homeodomain and the pentapeptide, are identical (Fig. 2). Within the N-terminal region, the first 25 residues are identical, but the remaining parts show less homology. These features are reflected in a total level of protein sequence conservation of 81%. A significantly lower level (70%) of sequence identity between homologs was observed for the protein derived from the adjacent gene,

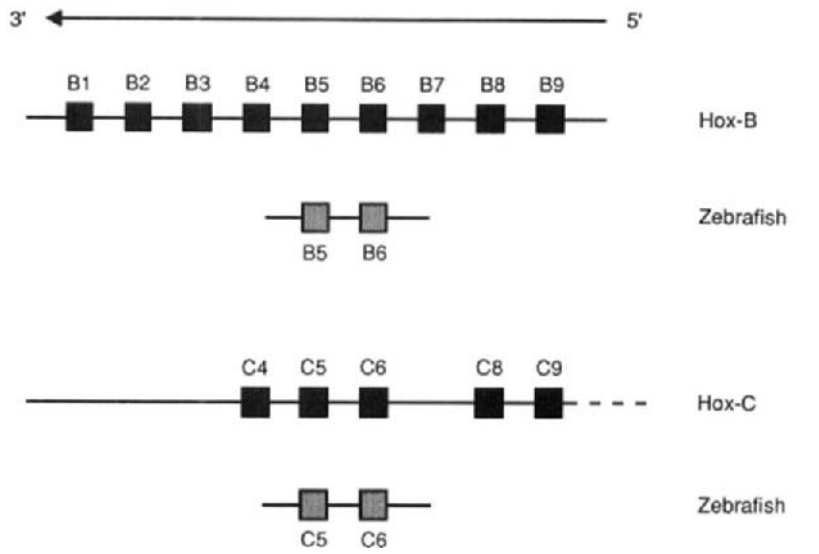

Fig. 1 The organization of murine *Hox* genes and homologous genes in zebrafish. The entire *Hox-B* complex of mouse is shown, together with the identified zebrafish homologs (shaded). For the murine *Hox-C* cluster, only the 3′ part is shown. The zebrafish homologs *hox-C5* and *hox-C6* are indicated below (shaded). The arrow on top of the figure indicates the direction of transcription in the *Hox* complexes. [Based on information from Njølstad *et al.* (1990) and Molven *et al.* (1993).]

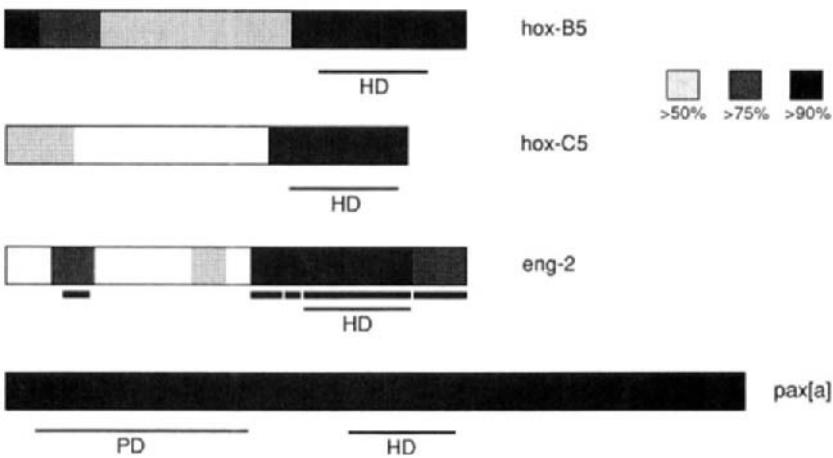

Fig. 2 The distribution of amino acid sequence homology in zebrafish homologs of the murine Hox-B5, Hox-C5, En-2 (eng-2), and Pax-6 (pax-[a]) proteins, respectively. The positions of the homeodomain (HD) and paired domain (PD) are shown. In the case of eng-2, the locations of the *engrailed* homology regions (EH 1-5; see text) are indicated by thick bars. The shading indicates the degree of sequence identity. [Based on information from Njølstad *et al.* (1988b), Krauss *et al.* (1991c), Püschel *et al.* (1992a), Fjose *et al.* (1992), and Ericson *et al.* (1993).]

hox-B6 (Njølstad *et al.*, 1990). The conservation for this gene is also very high in the homeodomain-containing region and at the N terminus. A similar distribution of homology is present in the *hox-C5* (*hox-3.4*) protein (Fig. 1; Ericson *et al.*, 1993). The homeodomain predicted from the zebrafish *hox-C5* gene is identical to the corresponding sequences of the murine *hox-C5* and human *HOXC5* cognates (Fig. 2). Further comparison to the human HOXC5 protein showed that the corresponding zebrafish and human proteins are quite diverged (56% sequence identity). This divergence reflects a smaller amount of conservation in the regions flanking the homeodomain and a particularly low level of sequence identity (18%) in the middle part of the protein (Fig. 2).

The differences in divergence of *hox-B5*, *hox-B6*, and *hox-C5* show that the conservation of the individual genes in the vertebrate *Hox* clusters is quite variable. Moreover, the data suggest a faster divergence rate for the *Hox-C* genes. Supporting this interpretation, the C-terminal region encoded by the zebrafish *hox-C6* (*hox[zf-61]*) gene is also quite diverged relative to its murine counterpart (Njølstad *et al.*, 1990).

Zebrafish and mammalian homologs located in the Hox-B and Hox-C clusters show very similar embryonic expression patterns (see Section III) in addition to structural conservation. Therefore, the most essential elements of the regulatory network involving these Hox genes have probably been maintained during evolution. To identify candidate control regions, noncoding sequences of the zebrafish and mammalian cognates have been compared. Surprisingly, the zebrafish and murine genomic regions, including the *Hox-B5* and *Hox-B6* homologs, contain very few conserved sequences outside the open reading frames (Molven *et al.*, 1993). For both homologous pairs, the most significant conservation is present in stretches extending about 0.3 kb upstream from the initiation codons. In the case of *Hox-B6*, these zebrafish and mouse upstream sequences are 67% identical, whereas the corresponding conservation of the *Hox-B5* homologs is 92%. Although these strong homologies in the upstream regions probably reflect a functional significance in transcriptional and/or translational control, the sequences appear to contain very few recognition elements for known transcription factors. In contrast, comparison among the noncoding sequences of the zebrafish, murine, and human *Hox-C6* homologs revealed conserved elements that seem to be more directly linked to transcriptional control (Arcioni *et al.*, 1992; Ericson *et al.*, 1993). Within a 180-bp TATA box-containing region, the zebrafish gene has about 60% sequence identity with its murine and human cognates. The two homeodomain binding sites identified within this promoter region of the human *Hox-C6* gene (Arcioni *et al.*, 1992) are also present in the zebrafish sequence. In addition, the promoter of the human gene contains a sequence recognized by an unknown protein in response to retinoic acid treatment, and this sequence is partially conserved in the zebrafish

cognate. Multiple stretches (15–140 bp) of homology (60–90%) are also scattered throughout the zebrafish and human *Hox-C6* genes (Ericson *et al.*, 1993). However, no common binding sites for known transcription factors were identified in these elements, which in most cases have different locations within the two cognates.

It is not yet clear whether the structural organization of the zebrafish *hox* clusters correlates closely with the arrangements reported for the four mammalian complexes. The best evidence for such a correlation concerns the Hox-B cluster. In addition to *hox-B5* and *hox-B6*, a homeobox sequence with striking similarity to *Hox-B4* has been identified (Njølstad *et al.*, 1988a). Using the murine *Hox-B1*, *Hox-B2* and *Hox-B3* genes as probes, several cross-hybridizing zebrafish cDNA clones have also been isolated (J. U. Ericson, personal communication). Despite these correlations, several observations suggest that the zebrafish and mammalian Hox complexes may differ somewhat in structural organization. In agreement with this idea, a zebrafish sequence (*hox[zf-54]*) closely related to *Hox-B6* has been identified, which seems not to be a cognate of either of the two other mammalian genes of the same subgroup (Njølstad *et al.*, 1988b). Therefore, this zebrafish gene seems to be the result of a unique *Hox-B5* duplication in fish. To clarify this issue, it will be necessary to sequence the remaining part of the *hox[zf-54]* gene and to determine whether or where it is located within the zebrafish *hox* clusters.

In the case of the *hox[zf-114]* gene, the correspondence to the mammalian *Hox* genes is even more complicated (Molven *et al.*, 1992). Although the entire coding sequence of this gene is known, significant homologies have only been identified for the homeodomain and the pentapeptide. Among the known mammalian *Hox* sequences, the homeodomain of *hox[zf-114]* is most similar to that of *Hox-B3* (79%), but these two genes are definitely not true homologs (Molven *et al.*, 1992). There are also differences (e.g., in the pentapeptide and in the expression pattern) indicating that *hox[zf-114]* does not belong to the third group of paralogous *Hox* genes at all, but rather should be placed in group 5. Alternatively, *hox[zf-114]* could have evolved as a consequence of a separate duplication event after the divergence of fishes and tetrapods, thus being a fish-specific gene. Although the major features of the *Hox* clusters in fish and mammals are likely to be very similar, further analysis of the zebrafish *hox* genes could provide additional examples of divergence that may help to elucidate the evolution of this vertebrate gene family.

B. *engrailed*-Related Genes

Similar to the studies of *hox* genes, analyses of zebrafish *engrailed* (*en*)-related genes have revealed several features that diverge from those of

other vertebrates. Apart from zebrafish, only two genes of the *engrailed* type have been identified in the vertebrate species analyzed so far (Joyner and Martin, 1987; Joyner and Hanks, 1991). A potential zebrafish homolog of the mammalian *En-2* gene was reported by Fjose and colleagues (1988), but this study suggested, based on Southern analysis, that the zebrafish genome might contain more than two *engrailed* sequences. This proposal has been confirmed by Ekker and colleagues (1992b), who have identified and characterized three distinct *engrailed* genes (*eng-1*, *eng-2*, and *eng-3*). Whether the zebrafish has additional *engrailed*-like sequences is still unclear, but the cross-hybridization analysis indicates the existence of at least four members of this gene family (Fjose *et al.*, 1988). Multiple *engrailed*-related genes may not be a unique feature of fish. The finding of a third, and highly diverged, *engrailed*-like gene in *Drosophila* (U. Weber and M. Mlodzik, personal communication) provides some support for this assumption.

Differences between zebrafish and mammalian *engrailed* genes are also clearly evident at the level of protein sequence homology. Although the putative cognates contain several highly conserved domains, the total level of sequence identity between the zebrafish and murine proteins is quite low (65–69%). Among the three known zebrafish *engrailed* sequences, *eng-1* is the most closely related to the murine *En-1* gene. The conservation of the putative Eng-1 protein, which shares 65% sequence identity with En-1, is mainly located within the five *engrailed* homology regions (EH1–5) that are common to all known *engrailed* genes (Fig. 2; Logan *et al.*, 1992). Thus, apart from the EH1 region, no significant sequence conservation is present between the N-terminal domains of Eng-1 and the murine En-1 protein.

Several characteristics indicate that *eng-2* and *eng-3* are products of a duplication of an ancestral *En-2* gene. The putative protein products of *eng-2* and *eng-3* share 65 and 69% sequence identity, respectively, with the murine En-2 protein (Ekker *et al.*, 1992b). The predicted zebrafish proteins have extended homologies in the EH1 and EH5 regions relative to En-2. An additional serine-rich peptide sequence, which was initially found to be conserved in the N-terminal part of Eng-2 and *Xenopus* XEn-2 (Fjose *et al.*, 1992), is also present in the proteins derived from zebrafish *eng-3* and the mouse *En-2* gene (Fig. 2). Moreover, these four genes have conserved sequences in the 3′ untranslated region (Ekker *et al.*, 1992b; Logan *et al.*, 1992).

C. Other Homeobox-Containing Genes

In addition to the *engrailed* genes, more than 15 distinct subgroups of vertebrate homeobox genes have been defined on the basis of differences

among their derived homeodomain sequences, and many of these groups are related to specific *Drosophila* genes (Scott *et al.*, 1989; Laughon, 1991). Zebrafish genes that belong to at least six of these subgroups have so far been isolated. When the zebrafish members of each of these groups are compared to the corresponding mammalian genes, the degree of sequence identity is quite variable, perhaps because of differences in functional conservation.

Although four zebrafish genes containing *muscle segment homeobox* (*msh*) type sequences have been characterized, their evolutionary relationship to the two known murine members of this subgroup, *Msx-1* (*Hox-7*) and *Msx-2* (*Hox-8*), remains to be determined (Holland, 1991; Ekker *et al.*, 1992a). Comparison of the putative Msx-1/Msx-2 proteins with the aa sequences derived from the zebrafish *msh-C* and *msh-D* genes revealed a high degree of sequence identity (>90%) within an 88 amino acid region containing the homeodomain (Ekker *et al.*, 1992a). However, outside this conserved region, there is very little sequence similarity among any of the four proteins. Thus, it is not possible to identify true homologs from sequence comparison alone, and the current information about the expression patterns is not sufficient to resolve this issue. For the zebrafish *msh-A* and *msh-B* genes, where only the homeobox sequences have been determined (Holland, 1991), further sequencing is required to see how they relate to the two murine *Msx* genes. However, it also remains to be determined whether the zebrafish and mouse genomes contain the same number of *msh*-like genes. Since more genes of this subgroup have been identified for zebrafish, it could be that independent duplications have occurred in mammals and fish.

For the zebrafish gene *cdx[Zf-cad1]*, which belongs to the *caudal* group (Mlodzik *et al.*, 1985), the extent of homology relative to the known members in mouse, chicken and *Xenopus* is quite limited (Joly *et al.*, 1992). The degree of sequence identity between the different homeodomains is moderate (80–86%), and only a few short stretches of conserved amino acids are present in the N-terminal region. Thus, for none of these vertebrate species have true homologs been identified. Further research is clearly required to determine how many *caudal*-like genes are present in these different vertebrate genomes and how these sequences are related.

The putative protein products of the zebrafish, *Xenopus*, and murine cognates of the *goosecoid* gene are very similar to the Hox proteins with respect to the distribution of conserved sequences. While a C-terminal region of about 100 amino acids that includes the homeodomain is highly conserved (>93%), a moderate level of sequence identity (<65%) is present in the N-terminal parts (Stachel *et al.*, 1993). As a consequence, these homologous proteins have an overall identity of about 75%. Whether the genes also share a significant degree of sequence identity in noncoding regions has not been determined.

Other subgroups of homeobox genes for which zebrafish members have been identified include *Distal-less* homeobox (*dlx*), H2.0-like homeobox (*hlx*), and *Pit/Oct/Unc* (POU) type sequences. Since only limited sequence data have been obtained for the zebrafish genes (Ekker *et al.*, 1992a; Fjose *et al.*, 1994; Johansen *et al.*, 1993; Matsuzaki *et al.*, 1992), it is premature to draw any conclusions regarding their conservation. It should also be mentioned that zebrafish homologs of several other categories of vertebrate developmental genes, including the *wingless* homolog *int-1* (*Wnt-1*) proto-oncogene, *Krüppel*-related zinc finger (*Krox-20*), chicken ovalbumine upstream promoter (COUP) transcription factor, and the *Brachyury* (*T*) gene, have been reported (Molven *et al.*, 1991; Oxtoby and Jowett, 1993; Fjose *et al.*, 1993; Schulte-Merker *et al.*, 1992). The fish and mammalian proteins derived from these genes have a level of sequence identity (69–76%) comparable to that of the *Hox* and *eng* cognates. The exception is the zebrafish COUP homolog, *sup[44]*, which displays the same profound evolutionary conservation as *pax[zf-a]* (see Section II,D; Fjose *et al.*, 1993).

D. *Pax* Genes

Of the eight *paired* box-containing genes (*Pax*) that are known for the mouse, four also encode *paired* type homeodomains (Gruss and Walther, 1992). For one of these genes, *Pax-6*, a true homolog (*pax[a]*) has been identified in zebrafish (Krauss *et al.*, 1991a,c; Püschel *et al.*, 1992a). In contrast to the known *hox* and *eng* cognates in zebrafish, where only the homeoboxes and other discrete elements show a high degree of sequence similarity, the entire protein-coding regions of the two *Pax-6* homologs are highly conserved (97%; Fig. 2). Both species also have a variant form of *Pax-6* transcript that includes an identical insert of 14 amino acids in the paired domain (Püschel *et al.*, 1992a). The functional importance of the insert is presently unclear. However, its location within the paired domain is likely to affect DNA binding and/or protein–protein interactions and thereby provide an additional mode for developmental regulation. Another zebrafish *pax* gene, *pax[b]*, is highly conserved relative to three murine genes (*Pax-2, Pax-5, Pax-8*) that form a subgroup of *Pax* genes (Krauss *et al.*, 1991a,b; Gruss and Walther, 1992). The putative protein products of *Pax-2, Pax-5,* and *Pax-8* have a total similarity of 87, 71, and 65%, respectively, to the predicted amino acid sequence of Pax[b] (Krauss *et al.*, 1991b; Adams *et al.*, 1992). Thus, *pax[b]* and *Pax-2* seem to be true homologs. Potential zebrafish homologs of *Pax-1, Pax-3,* and *Pax-7* have also been identified (S. Krauss, H. G. Elken, S. Nornes, and A. Fjose, unpublished results), but the entire coding sequences have not yet

been determined. At present it is unclear whether the zebrafish genome contains additional members of the *Pax-2/Pax-5/Pax-8* subgroup.

Computer analysis of the putative Pax[b] protein sequence revealed the presence of a region homologous to the N-terminal half of the paired-type homeodomain (Krauss *et al.*, 1991b). This conserved sequence, which is located roughly at the same relative position as the homeobox in other *Pax* genes, was discovered simultaneously in *Pax-2* and *Pax-8* (Krauss *et al.*, 1991b; Walther and Gruss, 1991). A possible explanation for the existence of this partial homeodomain is that the C-terminal half was lost in a process of exon shuffling. However, the subsequent conservation of the remaining N-terminal part is also likely to reflect functional constraints imposed by an involvement of this subdomain in DNA binding and/or protein–protein interactions.

III. Patterning of the Hindbrain and Spinal Cord

The spinal cord and hindbrain regions of the embryonic CNS have several features in common, indicating that the underlying developmental regulatory mechanisms are similar. Because these are general properties of all vertebrates, any species could in principle be used as a model to investigate these mechanisms. However, in this context, the relatively simple organization of the zebrafish hindbrain and spinal cord provide several advantages in analyzing the genetic networks controlling neural patterning.

A. Segmentation and Anteroposterior Specification

As in chicken and mice, the hindbrain of zebrafish embryos becomes transiently subdivided into a series of rhombomere segments that are morphologically visible (Hanneman *et al.*, 1988; Kimmel, 1993; Trevarrow *et al.*, 1990). Moreover, the seven most-anterior rhombomeres seem to be directly homologous in the different vertebrate species. In chicken, the morphologically visible rhombomeres are defined as segmental units on the basis of several criteria, including lineage restriction, mitotic patterning, arrangement of somatic motor nuclei, and the localization of transverse axons at the boundaries (Keynes and Lumsden, 1990). Some of these criteria have been confirmed for the zebrafish rhombomeres, and a segmental arrangement is observed at the level of single identified neurons (Metcalfe *et al.*, 1986; Hannemann *et al.*, 1988; Kimmel, 1993). Thus, the reticulospinal interneurons can be assigned to different families of segmental homologs on the basis of morphological similarities (Metcalfe *et al.*, 1986).

Consistent with the idea that rhombomeres are of developmental significance, several categories of regulatory genes have rhombomere-restricted expression (Wilkinson *et al.*, 1988,1989a; Ruberte *et al.*, 1991; McGinnis and Krumlauf, 1992). The various genes within the individual *Hox* clusters have overlapping expression domains, and the anterior expression limit of each gene correlates closely with the position of the gene in the complex. In the hindbrain, the 3′ members of a particular complex are expressed in segment-specific patterns, with successive genes having borders at two-segment intervals (Wilkinson *et al.*, 1989b; McGinnis and Krumlauf, 1992). This pattern suggests an involvement in segment formation or specification of segment identities, and similar correlations would be expected for the neural expression of zebrafish *Hox* genes.

In agreement with this prediction, analysis of the zebrafish *Hox-B5–6* and *Hox-C5* cognates revealed that the anterior limits of expression are located in the region of junction between the hindbrain and spinal cord (Njølstad and Fjose, 1988; Njølstad *et al.*, 1990; Molven *et al.*, 1990; Ericson *et al.*, 1993). However, the limited resolution achieved in these experiments, together with the lack of distinct segmental boundaries in the posterior hindbrain, prevented direct comparison of these homologs in mouse and zebrafish. Thus, it has not yet been directly demonstrated that the 3′ *Hox* genes of zebrafish follow the same rules of collinearity and rhombomere-restricted expression as their murine counterparts. Nevertheless, indirect evidence for such a relationship has been obtained from studies on the zebrafish homolog (*krx-20*) of the murine *Krox-20* gene, which encodes a protein with three C_2H_2-type zinc fingers (Chavrier *et al.*, 1988; Oxtoby and Jowett, 1993). In mouse embryos, *Krox-20* is expressed at a high level in rhombomeres 3 and 5 (r3 and r5), both before and after they become visible (Wilkinson *et al.*, 1989a). Accordingly, it has been postulated to be a segmentation gene regulating *Hox* expression (Wilkinson *et al.*, 1989b; Wilkinson and Krumlauf, 1990), and direct evidence for this hypothesis was obtained for the expression of *Hox-B2* (Sham *et al.*, 1993). In zebrafish, *krx-20* transcripts are first detected in the primordia of r3 and r5 at 100% epiboly (9–10 hr), suggesting that segmentation in the zebrafish hindbrain, at the molecular level, occurs at this stage (Oxtoby and Jowett, 1993). This is several hours before the morphological manifestation of rhombomeres in 15- to 16-hr embryos, and it could therefore regulate the segment-restricted expression of zebrafish *hox* genes.

Another example of segmental expression in the zebrafish hindbrain is the *hlx-1* gene (Fjose *et al.*, 1994), which belongs to the same group of homeobox genes as H2.0 in *Drosophila* (Barad *et al.*, 1988). In this case, a transverse stripe of expression was first observed in the r5 primordium of 12-hr embryos (Fjose *et al.*, 1994). At a later developmental stage

(15–16 hr), different levels of *hlx-1* transcripts were also detected within rhombomeres 1–3 (Fig. 3). Because the expression domains are dorsoventrally restricted, *hlx-1* is probably not involved in segmentation. Moreover, the level of expression varies for the individual rhombomeres and could be regulated by factors such as Hox proteins, which are likely to specify segmental identities.

Studies of the embryonic expression of *pax[b]* and the zebrafish *eng* genes have revealed aspects of segmentation and AP specification at the level of single cells. In both cases, the expression patterns have been investigated by *in situ* hybridization and immunohistochemical methods. However, for the *eng* genes, the results obtained with the two different methods are somewhat contradictory. In the hindbrain, the 4D9 antibody (Patel *et al.*, 1989), which cross-reacts with all of the three known zebrafish Eng proteins (Ekker *et al.*, 1992b), labels clusters of cells only in the three most-anterior rhombomeres (Hatta *et al.*, 1991a). The other antibody,

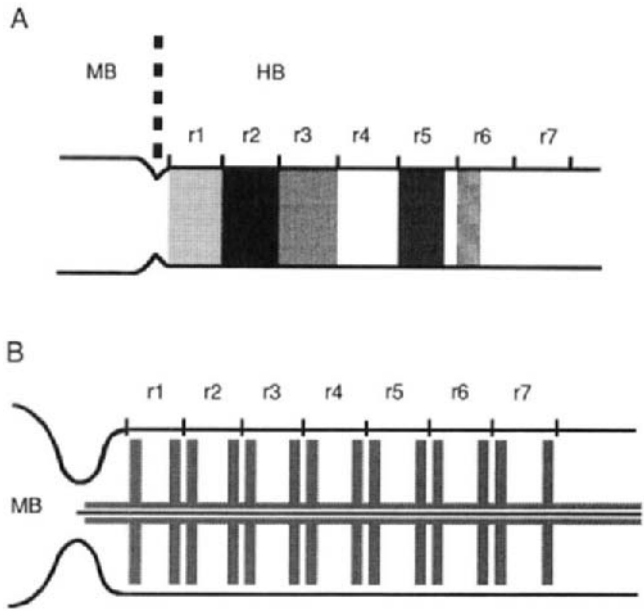

Fig. 3 The hindbrain expression of the *hlx-1* gene in 15-hr embryos (A) and at 30 hr (B). The rhombomeres (r1–r7) and the boundary (stippled line) between midbrain (MB) and hindbrain (HB) are indicated. The different expression levels of the individual rhombomeres of the 15-hr embryo are illustrated by different shading. In 30-hr embryos (B) paired stripes of expression, which are connected by a column of expressing cells at the ventricular side, are located in the boundary regions of the rhombomeres. [Based on information from Fjose et al. (1994).]

originally generated against the mouse EN-2 homeodomain, αEnhb-1 (Davis *et al.*, 1991), revealed a more complex expression pattern in which clusters of stained cells were detected in all of the rhombomeres and the spinal cord (Hatta *et al.*, 1991a). In comparison with observations in the mouse, where only the *En-1* gene is expressed throughout the hindbrain and spinal cord (Davidson *et al.*, 1988; Davis and Joyner, 1988), these observations are confusing, because Western blot analysis has revealed that αEnhb-1 only detects the Eng-2 and Eng-3 proteins (Ekker *et al.*, 1992b). Unfortunately, *in situ* hybridization analyses with specific probes from the three *eng* genes did not resolve this issue (Ekker *et al.*, 1992b).

Despite the problem of identifying which of the *eng* genes are expressed in the hindbrain and spinal cord cells, several interesting conclusions can be derived from these studies. The location of the expressing cells suggests that they consist of at least two different types of interneurons (Hatta *et al.*, 1991). Cells labeled with αEnhb-1 are detected earlier by (18 hr) than the 4D9-positive cells (24 hr) and are not restricted to a specific AP level. The segmentally repeating αEnhb-1 pattern also appears transiently in the spinal cord, where expression extends posteriorly over time. While the younger hemisegments have one or two labeled cells, the older segments (more anterior) show expression in additional cells that fill in the row until the periodicity is lost (Hatta *et al.*, 1991a). This observation indicates that *engrailed*-expressing cells in the hindbrain and spinal cord are partially regulated by the same segmentally repeating information, even though most of the spinal cord neurons are not segmentally organized (Bernhardt *et al.*, 1990; Kuwada and Bernhardt, 1990).

It has been proposed by Kimmel (1982) and by Metcalfe and colleagues (1986) that the hindbrain rhombomeres exhibit unique segmental identities, with each segment containing a specific set of identifiable reticulospinal neurons. Results obtained from studies on the *pax[b]* gene are compatible with this model and demonstrate the advantage of using the zebrafish for analyzing these aspects at the molecular level (Krauss *et al.*, 1991b; Mikkola *et al.*, 1992). A polyclonal antibody raised against the C-terminal end of the Pax[b] protein (which does not include the conserved paired domain) was used to investigate expression in zebrafish embryos (Mikkola *et al.*, 1992). At the 13-hr stage, Pax[b] staining was first detectable in a distinct set of 12–15 nuclei on either side of the neural keel in the region including the posterior hindbrain and anterior spinal cord. The Pax[b]-positive cells in the hindbrain of 21-hr embryos were identified by their location and by axonal trajectories made visible by double labeling with acetylated α-tubulin antibodies. According to this analysis, the *pax[b]* gene is expressed in the MiD2c primary commissural interneuron in r5 and in a pair of similar interneurons (MiD3c) in r6 (Fig. 4). In addition, a previously unclassified set of interneurons that was termed commissural caudal-rhombomere as-

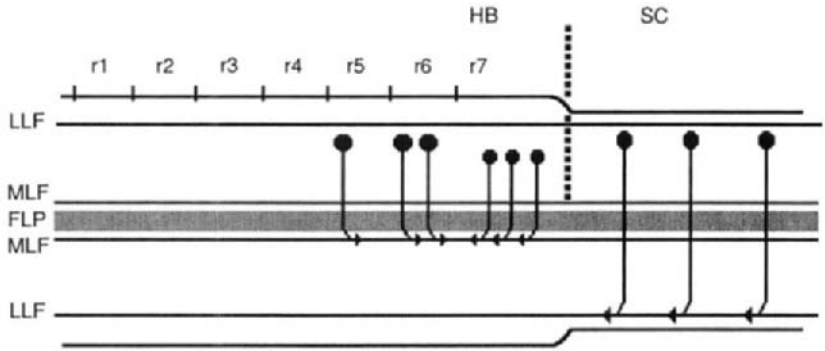

Fig. 4 The location of *pax[b]*-expressing commissural neurons in the hindbrain (HB) and spinal cord (SC). Only the neurons (on one side of the midline) that have projected axons at the 21-hr stage are shown. The locations of the floor plate (FLP; shaded), lateral longitudinal fascicle (LLF), medial longitudinal fascicle (MLF), and boundary between hindbrain and spinal cord (stippled line) are shown. Arrowheads indicate the direction of the axons of the various commissural neurons. [Based on information from Mikkola *et al.* (1992).]

cending (CoCaA) was shown to be Pax[b] positive in the caudal hindbrain. In the spinal cord, where the *pax[b]* expression pattern does not have segmental features, the Pax[b]-positive neurons have also been identified (see Section III,B).

These observations suggest that *pax[b]* is in some way involved in determining the specific fates of particular neurons or their subsequent differentiation. In the case of the MiD2c and MiD3c cells, Pax[b] proteins are detectable 3 hr before these neurons start to project their axons. This timing of *pax[b]* expression is consistent with a role in determining cell fate, since some neurons in zebrafish embryos are unalterably specified as late as 1 hr before they project their growth cones (Eisen, 1991).

Studies on zebrafish have also revealed neuron-specific distribution of Hox proteins. Using an antibody raised against the *Xenopus* homeodomain protein X1Hbox1, which probably is the homolog of *Hox-C6*, expression (commencing at the 16-hr stage) was detected in the anterior spinal cord (Molven *et al.*, 1990). Within this region, a dorsal row of X1Hbox1-positive cells were identified as Rohon-Beard (RB) sensory neurons (Fig. 5). Interestingly, at 25 hr these neurons exhibit a graded decrease in staining intensity from anterior to posterior over the domain of expression. The spatiotemporal expression pattern indicates that the zebrafish *Hox-C6* homolog is involved in AP specification of these neurons. However, the gene probably does not play a role in specifying the RB cell type, since expression is first detected after these neurons start to differentiate (Bernhardt *et al.*, 1990).

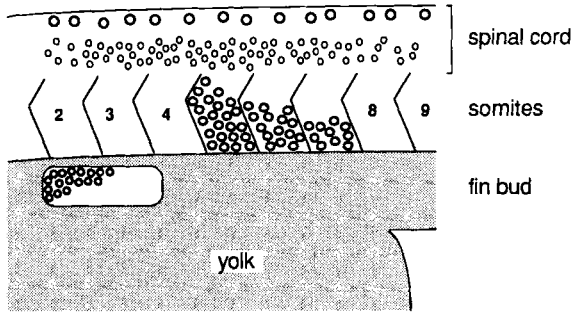

Fig. 5 The trunk region of a 22-hr embryo with cells stained by the X1Hbox1 antibody indicated. There is a graded decrease in staining from anterior (left) to posterior (right). The large circles at the top represent the Rohon-Beard cells. [From Molven (1991).]

B. Dorsoventral Patterning

The spinal cord of vertebrates exhibits a characteristic dorsoventral (DV) pattern, with specific classes of neurons differentiating according to their DV position (Lumsden, 1991). Moreover, surgical manipulations of chicken embryos have shown that the notochord plays a crucial role in ventralizing the neural tube by inducing cells at the ventral midline to become floor plate cells (Yamada *et al.*, 1991). Studies indicate that the *Pax* genes are of particular importance in controlling the embryonic DV patterning. The murine *Pax-3* and *Pax-7* genes are expressed in partially overlapping areas in the dorsal region of the ventricular zone (Gruss and Walther, 1992). *Pax-7* is expressed in the alar plate region, excluding the roof plate and neural crest cells, while *Pax-3* expression is detected in all three of these subregions (Jostes *et al.*, 1991; Goulding *et al.*, 1991). Similarly, the murine *Pax-6* gene is active in the entire basal plate, excluding the floor plate and cells directly adjacent to it (Walther and Gruss, 1991).

Analyses of the embryonic expression of the zebrafish *Pax-6* homolog, *pax[a]*, have revealed the same kind of DV restriction (Krauss *et al.*, 1991c; Püschel *et al.*, 1992a). In addition, preliminary data from *in situ* hybridization analyses of the potential zebrafish homologs of *Pax-3* and *Pax-7* were consistent with the observations for the two murine genes (S. Krauss and A. Fjose, unpublished results). These results indicate an involvement of *Pax* genes in specifying DV identities of different populations of mitotic cells in the ventricular zone.

In chicken embryos, removal of the notochord or implantation of an additional notochord dramatically alters the DV expression patterns of the *Pax-3* and *Pax-6* homologues (Goulding *et al.*, 1993). The changes in the expression of both genes also show a close correlation with the changes

in cell phenotype (Yamada *et al.*, 1991; Goulding *et al.*, 1993). This correlation suggests that the effects of the notochord on the expression of genes such as *Pax-3* and *Pax-6* in neural progenitor cells may influence their subsequent pathways of differentiation.

Pax genes may also be involved at later stages of neuronal differentiation. Consistent with this idea, the *Pax-2, Pax-5,* and *Pax-8* genes are expressed in postmitotic cells located at specific levels in the intermediate zone in the spinal cord of mouse embryos (Nornes *et al.*, 1990; Gruss and Walther, 1992). Although these cells are probably precursors of different types of interneurons, it has not been possible to determine their exact identities. In contrast, the relatively simple organization of the zebrafish spinal cord at early embryonic stages makes it a convenient model for analyzing neuron-specific expression patterns. A small number of identifiable classes of neurons, including sensory RB cells, motor neurons, and several classes of interneurons, are present in 18- to 20-hr embryos (Bernhardt *et al.*, 1990; Kuwada and Bernhardt, 1990). By exploiting this knowledge, it was possible to determine the identity of spinal cord neurons expressing the zebrafish *Pax-2* homolog, *pax[b]* (Mikkola *et al.*, 1992). This identification, which in part relied on double labeling with antibodies recognizing specific neural antigens, showed that the *pax[b]* gene is expressed in commissural secondary ascending (CoSA) interneurons. These cells are present at variable densities (one to five per spinal hemisegment) along the entire spinal cord (Bernhardt *et al.*, 1990). As observed for the *pax[b]*-expressing reticulospinal neurons in the hindbrain (see Section III,A), the CoSA neurons project their axons several hours after the Pax[b] protein is detected. Accordingly, the differentiation of these neurons could also in part be determined by the *pax[b]* gene.

Dorsoventrally restricted expression in the embryonic hindbrain and spinal cord has been observed for the murine *Dbx* and chicken *ChoxE* genes, which belong to the same group of homeobox sequences as the zebrafish *hlx-1* gene (see Sections II,C and III,A; Rangini *et al.*, 1991; Lu *et al.*, 1992). In both cases, bilateral columns of expression, restricted to the proliferating zone in the dorsal basal plate, extend throughout the hindbrain and spinal cord. For *hlx-1,* a similar expression pattern was observed (Fjose *et al.*, 1994), but in this case more detailed information was obtained by whole-mount *in situ* hybridization analysis. After a segmental *hlx-1* pattern appears in the hindbrain of 12- to 15-hr embryos (see Section III,A), expression extends as a contiguous column throughout the hindbrain and spinal cord. This dorsoventrally restricted column, which is located near the dorsal boundary of the basal plate, may include both mitotic and postmitotic precursors of particular types of neurons. Alternatively, the highly restricted *hlx-1* expression domain could play a role in defining a boundary between the basal and alar plates.

C. Subdivisions within Rhombomeres

Analyses of the neural pattern of rhombomeres indicate that the individual segmental units can be subdivided along the AP axis. In the hindbrain of the chick, motor nuclei are in the segment centers, and early commissures are near the borders (Lumsden and Keynes, 1989). Also, the centers of rhombomeres have a higher mitotic density and shorter cell-cycle time than the boundaries (Keynes and Lumsden, 1990). Moreover, studies at the molecular level have revealed that expression of the neural-cell adhesion molecule N-CAM is localized to the central regions of the rhombomeres, whereas Ng-CAM/L1 is restricted to the boundaries (Lumsden and Keynes, 1989). Despite this patterning of individual rhombomeres, none of the developmental regulatory genes analyzed so far is expressed selectively within particular subregions.

In zebrafish, these aspects have been investigated in further detail with various monoclonal antibodies that stain different subpopulations of cells within the hindbrain (Trevarrow *et al.*, 1990). This revealed an arrangement of neurons, commissural tracts, neuropil areas, and radial glial fibers that reflects an alternating pattern along a series of seven segments. In the model proposed from this pattern (Trevarrow *et al.*, 1990), the rhombomere centers contain the first basal-plate neurons to develop and the first neuropil. The other region, surrounding the segment boundaries, contains the first alar-plate neurons.

Studies of the embryonic expression of the *hlx-1* gene revealed spatiotemporal changes in the hindbrain of 1-day-old embryos that seem to be consistent with this model (Fjose *et al.*, 1994). Each longitudinal column of expressing cells transforms into series of transverse stripes, and by the 30-hr stage a repeated pattern of paired stripes is clearly visible along both sides of the midline. The spacing between each pair of *hlx-1* stripes correlates well with the width of hindbrain rhombomeres (Fig. 3). Interestingly, the pattern is very similar to the staining detected with the zn-5 antibody, which labels clusters of commissural interneurons at the segment boundaries (Trevarrow *et al.*, 1990). This indicates a possible involvement of *hlx-1* in the subdivision of rhombomeres, in particular in the specification or differentiation of the zn-5-positive neurons.

IV. Patterning of the Rostral Brain

Expression studies of various types of vertebrate developmental genes in the hindbrain and spinal cord have revealed clear correlations with the neural patterning observed along the AP and DV axes. Because of the great complexity of the rostral brain in mouse embryos, a relationship between the expression domains of regulatory genes and morphological

subdivisions appears to be harder to elucidate. Studies on *pax* and *eng* genes have shown that the relatively simple organization of the zebrafish brain at early embryonic stages may facilitate analysis of the genetic mechanisms responsible for its morphogenesis.

A. Expression during Early Stages of Regionalization

Whole-mount, *in situ* hybridization analysis of the zebrafish *pax[b]* gene revealed the earliest signs of regionalization in the rostral neurectoderm of 9-hr embryos (Krauss *et al.*, 1991b). At this late gastrula stage, *pax[b]* transcripts are detectable within two transverse bands of cells separated by a nonexpressing area at the dorsal midline (Fig. 6). Both the width

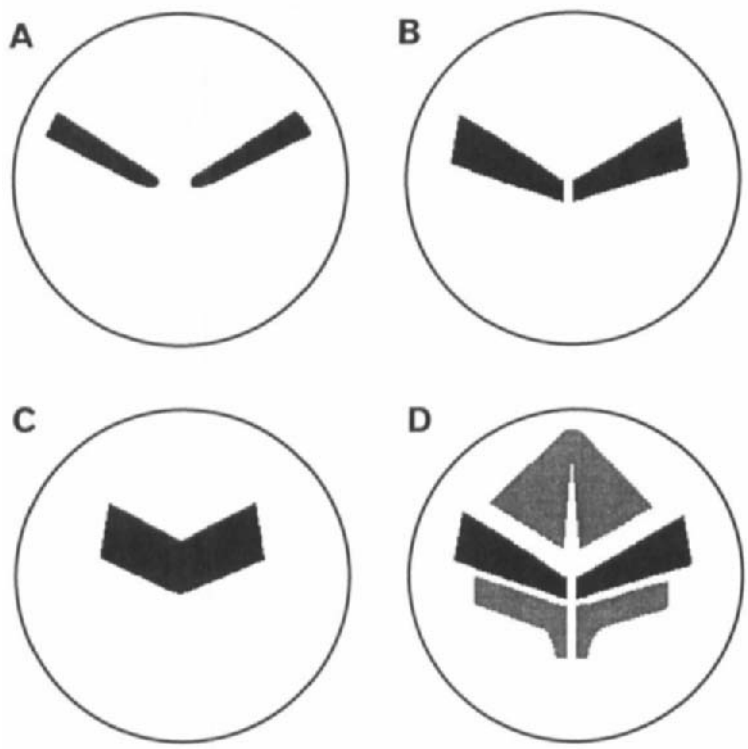

Fig. 6 The early regional expression of *pax[a]* and *pax[b]*. (A–C) Dorsal view of the expression of *pax[b]* in the region of the presumptive midbrain–hindbrain boundary in 9- to 10-hr embryos (rostral end at the top). (D) Relationship between the expression domains of *pax[b]* (dark shading) and *pax[a]* (gray shading) at the 10-hr stage. [Based on information from Krauss *et al.* (1991b) and E. Salaneck and A. Fjose (unpublished observations).]

and the length of these stripes, which point somewhat posteriorly at an angle of about 60° relative to the midline, increase simultaneously with the expression level during the subsequent hour of development. Probably as a result of convergence of cells that generate the neural keel, the two stripes start to fuse at the dorsal midline in 10-hr embryos. Thus, by the 12-hr stage, the *pax[b]* expression domain is a solid transverse band in the neural keel. Analysis of later developmental stages showed that this area corresponds to a region including the midbrain–hindbrain boundary (see Sections IV,B,C). Pax[b] proteins were detected in 9-hr embryos using the *pax[b]* antibody (Section III,A), and the spatiotemporal pattern in subsequent stages appeared to be the same as for the transcripts (Mikkola *et al.*, 1992). In the case of *eng-2* and *pax[a]*, the observed spatiotemporal expression patterns are similar to those for *pax[b]*. However, while the transverse stripes of *eng-2* expression are present at the same AP level as *pax[b]* (Fjose *et al.*, 1992), the *pax[a]* gene is active in two separate domains, located in the forebrain and the hindbrain regions (Püschel *et al.*, 1992a; E. Salaneck and A. Fjose, unpublished results). In the anterior hindbrain, *pax[a]* is initially expressed within two transverse stripes that later are extended posteriorly throughout the hindbrain and the spinal cord (Fig. 6D; E. Salaneck and A. Fjose, unpublished results). The rostral domain of *pax[a]* expression first appears as two triangular areas that fuse at the midline (Fig. 6D). For both of the *pax[a]* domains, the transverse expression boundaries are almost parallel to the *pax[b]* and *eng-2* stripes. This pattern is reminiscent of the segmental expression domains of their *Drosophila* homologs *paired* and *engrailed* (Kilchherr *et al.*, 1986; Fjose *et al.*, 1985; Ingham, 1988) and suggests the involvement of related subdividing mechanisms in the midbrain region. It is interesting to note that the *pax[b]*/*eng-2* stripes are located within the gap between the two *pax[a]* domains. The expression of *eng-1* and *eng-3*, which has not yet been analyzed at this early stage (Ekker *et al.*, 1992b), is likely to be restricted to transverse stripes within this gap. Whether these relationships reflect repressor functions for *pax[b]* and the three *engrailed* genes in the regulation of *pax[a]* transcription remains to be demonstrated.

B. Regional Expression Patterns and Neuromere Organization

A periodic array of swellings, called neuromeres, is present in the neural tube during early embryonic stages of zebrafish and other vertebrates. Rostral to the seven segment-like hindbrain neuromeres (rhombomeres), three distinct neuromeres have been identified in zebrafish embryos (Kimmel, 1993; Ross *et al.*, 1992). These neuromeres, which become visible in 16-hr embryos, correspond to the definitive midbrain and the two divi-

sions of the forebrain, the diencephalon and telencephalon. Although the rostral brain neuromeres are about three times as long as the hindbrain rhombomeres, they have some related features of organization.

Similar to the bilateral clusters of early differentiating neurons which appear in the basal plate of individual rhombomeres, two clusters positive for acetylcholinesterase (AChE) have been identified in the basal plate of the midbrain and diencephalon (Wilson *et al.*, 1990; Chitnis and Kuwada, 1990; Ross *et al.*, 1992). However, reflecting their larger size, the initial clusters in the rostral neuromeres contain more cells. Like the rhombomeres, the midbrain and diencephalon are separated by a commissure (Wilson *et al.*, 1990; Chitnis and Kuwada, 1990). This prominent posterior commissure (PC) crosses dorsally, whereas the intersegmental commissures in the hindbrain are located ventrally. In contrast to the diencephalon, midbrain, and hindbrain neuromeres, the first neural cluster of the telencephalon appears in the alar plate (Ross *et al.*, 1992). Thus, on the basis of morphological criteria, it remains unclear whether the rostral neuromeres are segmental units. Analysis of the expression patterns of the genes that are regionally expressed in the rostral brain may help to resolve this issue.

Several characteristics of the *pax[a]* expression pattern appear to link this gene to regionalization in the rostral brain. A restricted domain of expression is first detected at the 9- to 10-hr stage (see Section IV,A), more than 5 hr before the neuromeres are formed. Also, as expected for a regionalizing gene, the transcripts are uniformly distributed in all cells within the area of expression (Krauss *et al.*, 1991a,c; Püschel *et al.*, 1992a). In addition, the posterior expression border coincides well with the boundary between the diencephalon and midbrain neuromeres that has become visible at the 17-hr stage (Krauss *et al.*, 1991a,c). Moreover, the area of expression remains almost unaltered during the period when the first morphological subdivisions and neuronal differentiation occur. Within the forebrain, the *pax[a]* expression domain is restricted to the presumptive thalamic part of the diencephalon (Fig. 7). Therefore, the gene is likely to play a role in specifying this subdivision of the diencephalon. Surprisingly, preliminary studies of the phenotype of mice carrying mutant alleles of the homologous *Pax-6* gene revealed no defects in the forebrain (Hill *et al.*, 1991). One possible explanation for this finding is that subtle alterations were not detected, due to a lack of appropriate markers. Alternatively, the normal phenotype could reflect functional redundancy of *Pax* genes with overlapping expression domains.

It is tempting to speculate that the stripes of *pax[b]* and *eng-2* expression observed at early embryonic stages (see Section IV,A) correlate with segment-like units. A double labeling experiment with *pax[b]* and the HNK-1 antibody, which labels the hindbrain rhombomeres r2 and r4, has

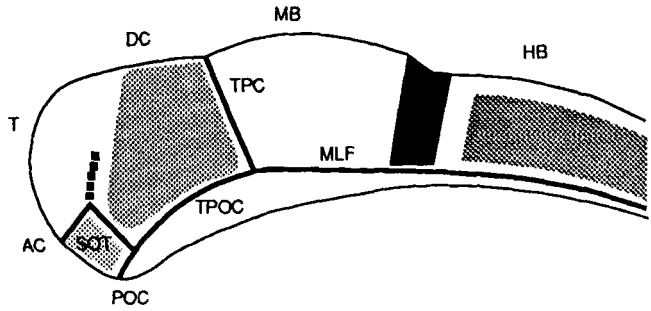

Fig. 7 The relationship between the location of the earliest axon tracts (in 21-hr embryos) and the regional expression of *pax[a]* and *pax[b]*. Expression of *pax[b]* at the midbrain–hindbrain boundary (black band) and in the optic stalk region (gray shading) among the anterior commissure (AC), postoptic commissure (POC), and supraoptic tract (SOT) is indicated. The areas of *pax[a]* expression in the diencephalon (DC) and hindbrain (HB) are indicated by dark shading. Apart from the diencephalic tract (not shown), the various tracts (thick lines) that are present at this embryonic stage are indicated. MLF, medial longitudinal fascicle; MB, midbrain; T, telencephalon; TPC, tract of posterior commissure. [Based on information from Krauss *et al.* (1991a,b,c).)

revealed some evidence in support of this proposal (Mikkola *et al.*, 1992). In 14-hr embryos, a periodic pattern was observed, in which a transverse stripe of *pax[b]* expression with a width similar to that of a rhombomere was located approximately one segmental unit anterior to the HNK-1 labeling in r2. However, no morphological subdivisions seem to correspond to this *pax[b]*-positive, rhombomere-like unit at later developmental stages. Instead, the expression of *pax[b]* and several other genes related to *Drosophila* segmentation genes can be correlated with the formation of a deep furrow at the midbrain–hindbrain boundary in 20-hr embryos.

C. Determination of the Midbrain–Hindbrain Boundary

Results obtained from grafting experiments in chickens and targeted disruption of the *En-2* and *Wnt-1* genes in mice have provided strong evidence that these two vertebrate homologs of the segmentation genes *engrailed* and *wingless* in *Drosophila* are required for normal development of the regions flanking the midbrain–hindbrain boundary (McMahon and Bradley, 1990; Itasaki *et al.*, 1991; Joyner *et al.*, 1991; McMahon *et al.*, 1992).

Studies of the corresponding genes in zebrafish have provided more detailed information about the exact relation between the expression domains and the morphological boundary separating the midbrain and hindbrain (Hatta *et al.*, 1991a; Molven *et al.*, 1991; Ekker *et al.*, 1992b; Fjose *et al.*, 1992). Moreover, the segment-like expression of *pax[b]* in the same region (see earlier) indicates an involvement in the formation of this boundary. It is interesting in light of this observation that the related *Drosophila* paired box genes, *paired* and *gooseberry*, are required for proper expression of *engrailed* and *wingless* during segmentation (DiNardo and O'Farrell, 1987; Ingham, 1988; Hidalgo and Ingham, 1990). A similar situation could exist in zebrafish, where *pax[b]* expression is initiated earlier than the *eng-2* and *wnt-1* domains and partially overlaps them (Krauss *et al.*, 1991a,b; Fjose *et al.*, 1992; A. Fjose and A. Molven, unpublished results).

Further evidence for regulatory interactions among these three genes has been obtained from intracellular microinjection experiments with a Pax[b]-specific antibody (Krauss *et al.*, 1992). Embryos injected with this antibody shortly after fertilization did not form the furrow at the midbrain–hindbrain boundary. This abnormality occurred even though the development of other tissues where *pax[b]* is expressed appeared to be normal. To investigate the molecular mechanisms underlying these observations, Krauss and colleagues (1992) analyzed the expression of *pax[b]*, *eng-2*, and *wnt-1* by *in situ* hybridization. The expression of all three genes was greatly reduced within the transverse midbrain–hindbrain stripes, while other domains were unaffected. These alterations suggest an autoregulatory function for the Pax[b] protein in regulating transcription of the *pax[b]* gene. Moreover, the downregulation of *eng-2* and *wnt-1* provides experimental support for a regulatory network involving these three genes in the vertebrate embryo.

Although these results indicate a key role for *pax[b]* in regulating the formation of the midbrain–hindbrain boundary, it remains unclear how the position of the furrow is determined. In this connection, it is of interest to consider the exact location of the expression borders of the individual genes found to be active in this region of the neural tube. As judged from the expression pattern of the *eng-1* gene (Ekker *et al.*, 1992b), this gene may be of particular importance in defining the location of the furrow. The anterior border of *eng-1* expression has not been defined at high resolution, but it seems to coincide with the center of this morphological boundary (Ekker *et al.*, 1992b).

Similarly, recent analyses of *wnt-1* expression by whole-mount *in situ* hybridization showed that the posterior border of the transverse *wnt-1* stripe is located close to the center of this furrow as well (A. Fjose and A. Molven, unpublished results). Thus, the *eng-1* and *wnt-1* domains may

be directly juxtaposed in the same way as the stripes of *wingless* and *engrailed* expression observed at the parasegmental boundaries in *Drosophila* (Ingham, 1988). This resemblance suggests important roles for *eng-1* and *wnt-1* in specifying the exact location of the midbrain–hindbrain furrow. Alternatively, the combinatory expression of several genes, including *wnt-1*, *pax[b]*, and the three *eng* genes, could determine this position.

D. Eye Development

The eye primordia of zebrafish are first detected as lateral swellings in the diencephalon of 11- to 12-hr embryos. The generation of these primordia is therefore one of the first morphological consequences of the underlying molecular regionalization of the neural tube. Studies of the embryonic expression patterns of *pax[a]* and *pax[b]* have provided evidence that regionalization within the eye primordium also occurs very early. Transcripts of *pax[b]* are first seen at the 12-hr stage, and expression is restricted to the region where the optic stalk appears (Krauss *et al.*, 1991b). In 18-hr embryos, the expression level is higher, and the area of expression includes the optic stalk and the ventral part of the optic vesicle. This spatial pattern is also maintained in later developmental stages. A similar spatiotemporal expression pattern was observed for the murine homolog *Pax-2* (Nornes *et al.*, 1990; Püschel *et al.*, 1992b), suggesting that the gene performs a role in eye development.

Stronger evidence for a function in the specification of the vertebrate eye has been obtained for *pax[a]* and its highly conserved murine homolog *Pax-6*. In the case of *pax[a]*, transcripts are first detected in the optic vesicles of 12-hr embryos (Krauss *et al.*, 1991c). The initial expression is restricted to the portion of the eye primordium that faces the diencephalon, excluding most of the optic stalk region. This expression domain expands, and in 24-hr embryos a uniform transcript level is observed throughout the optic cup.

At this stage, *pax[a]* transcripts are also detected in the ectoderm overlying the retina (Krauss *et al.*, 1991c; Püschel *et al.*, 1992a), indicating an involvement in inducing the lens and/or the cornea. An interesting feature in this context is that *pax[a]* is expressed in both the inducing (optic vesicle) and the responding tissue. The samé results have been obtained for the murine *Pax-6* gene (Walther and Gruss, 1991), and mutant alleles (*Small eye; Sey*) of this gene have been identified that cause abnormal eye development (Hill *et al.*, 1991). In homozygotes, eyes do not develop, whereas in individuals carrying a single *Sey* allele, eyes are smaller than normal and have vacuolated lenses. These semidominant features proba-

bly reflect a threshold requirement for the Pax-6 protein during the inductive interactions between the lens placode and the optic cup.

Analyses of the embryonic expression of *pax[b]* and several homeobox genes of the *msh* and *dlx* type also provide circumstantial evidence for an involvement in ear development (Krauss *et al.*, 1991b; Ekker *et al.*, 1992a; Mikkola *et al.*, 1992). Similar to the eye, several inductive interactions are essential for morphogenesis of the ear (Represa *et al.*, 1991). The expression patterns of these zebrafish genes indicate that they could be involved in early steps of regionalization and during development of specific cell types at later stages (Ekker *et al.*, 1992a).

E. Expression Domains and Axonogenesis

A prominent feature of the first neuronal clusters of the rostral neuromeres in zebrafish embryos is that they project axons in a stereotyped pattern and thereby establish an early invariant scaffold of tracts. Axonogenesis occurs in a specific temporal sequence during the 16- to 24-hr stages of embryonic development (Wilson *et al.*, 1990; Chitnis and Kuwada, 1990; Ross *et al.*, 1992) and therefore correlates with the period when *pax[a]* and *pax[b]* are expressed within sharply defined areas in the rostral brain (Krauss *et al.*, 1991a,b,c). A comparison of the axonal scaffold and the expression pattern (Fig. 7) suggests that several of the early tracts follow pathways along the expression borders of the two *pax* genes (Krauss *et al.*, 1991a). The reported positions of the tracts of the postoptic commissure (TPOC) and the PC appear to be at the ventral and caudal expression borders of *pax[a]*, respectively. Anteriorly, the TPOC lies near the border between the *pax[b]*-expressing optic stalk and the forebrain. In addition, the anterior commissure axons and supraoptic tract seem to follow pathways in the forebrain that are closely juxtaposed to *pax[b]*-expressing cells in the optic stalk. In the posterior midbrain, the medial longitudinal fascicle, which is pioneered by neurons in the ventral midbrain cluster, also has a pathway near the ventral border of *pax[b]* expression.

Although the correlations between *pax* gene expression and the formation of early axonal tracts are intriguing, it remains to be demonstrated by double-labeling experiments that the tracts and expression borders coincide exactly. If this proves true, it will be of considerable interest to elucidate its molecular basis. The most simple explanation would be that the pax[a] and pax[b] proteins directly regulate the expression of genes encoding cell-surface molecules and have inhibitory effects on the pioneering growth cones. This idea is consistent with the proposed function of homeodomain proteins in regulating the expression of molecules with important cell-adhesion functions (Jones *et al.*, 1992a,b).

V. Expression Patterns in Mesodermal Tissues

As discussed earlier, the neural expression patterns of many different homeobox and *pax* genes have been extensively analyzed in zebrafish embryos. Considerably less is known about the genes' mesodermal expression. In the case of *hox* genes, this is due to limitations in the sensitivity of the *in situ* hybridization method and the fact that the mesodermal transcript levels of these genes appear to be lower than in the CNS. However, recent improvements of the *in situ* hybridization techniques used for zebrafish and the application of immunohistochemical methods will undoubtedly facilitate future investigations of mesodermal patterning and differentiation in this species.

A. Patterning of Somitic Mesoderm

For the zebrafish *hox-C6* gene, the limited sensitivity of the *in situ* hybridization method was avoided by applying a cross-reacting antibody raised against the protein product of the *Xenopus* homolog XlHbox1 (Oliver *et al.*, 1988a; Molven *et al.*, 1990). With this antibody, weak staining was first detected in anterior somites of 14-hr zebrafish embryos (Molven *et al.*, 1990). By the 16-hr stage, more prominent staining was observed in the somitic mesoderm and expression was restricted to the lateral surfaces of somites 5 to 7. The anterior border of expression coincided exactly with the boundary between somite 4 and 5, while in a posterior direction the expression decreased in a graded fashion over somites 6 and 7 (Fig. 5). The XlHbox1 staining detected in *Xenopus* and mouse embryos was similar, but the correlations between the expression border and somite boundary were defined less precisely (Oliver *et al.*, 1988a). These results suggest a conserved role of *hox-C6* in specifying the AP position of somites.

Studies on the zebrafish *eng* genes have provided evidence for an involvement in patterning of the individual somites (Hatta *et al.*, 1991a; Ekker *et al.*, 1992b; Fjose *et al.*, 1992). Using the 4D9 antibody (see Section III), Eng proteins were observed in clusters of cells located at the medial surface of the somites, facing the notochord (Hatta *et al.*, 1991a). This expression was detected after the 13-hr stage and followed a spatiotemporal sequence that directly correlated with the posteriorly directed wave of somite formation. Thus, for a particular somite, Eng staining appeared 1 to 2 hr after its formation. The Eng-labeled cells were identified as muscle pioneers, which are the first cells to differentiate within the myotome that develops from each somite (Felsenfeld *et al.*, 1991; Hatta *et al.*, 1991a). The muscle pioneers undergo extensive morpho-

genetic changes, and a furrow appears where the horizontal myoseptum eventually forms and separates the dorsal and ventral muscles (Felsenfeld *et al.*, 1991). On the basis of the correlation between *eng* expression and the generation of furrows both at the midbrain–hindbrain boundary (see Section IV) and in the myotome, it was proposed that one or more of the *eng* genes are critical in specifying the positions of these morphological boundaries (Hatta *et al.*, 1991).

The roles of the individual *eng* genes in the myotomes have been further investigated by *in situ* hybridization analyses with gene-specific probes. Expression of both *eng-1* and *eng-2*, but not *eng-3*, was observed in the muscle pioneers (Ekker *et al.*, 1992b; Fjose *et al.*, 1992). Since *eng-2* is only transiently expressed, the *eng-1* gene is probably more essential in subdividing the myotomes. Reflecting the divergence of the *eng* genes, the murine and chicken homologs have somewhat different somitic expression patterns (Davis *et al.*, 1991). However, the *En-1* gene is expressed in a lateral stripe in the middle of the dermatomes of both chicken and mouse embryos, indicating a similar role in subdividing the somitic mesoderm.

B. Expression in Nonsomitic Mesoderm

Both whole-mount *in situ* hybridization and immunohistochemical staining have shown that the embryonic kidney is a major site of *pax[b]* expression (Krauss *et al.*, 1991b; Mikkola *et al.*, 1992; Püschel *et al.*, 1992b). Posterior to the position of the second somite, a continuous column of two to three cells expressing *pax[b]* forms a half circle at the edge of the constricting embryonic shield in 13-hr embryos (Mikkola *et al.*, 1992). These mesodermal cells, which include the nephritic primordium and the Wolffian duct, still express the *pax[b]* gene at the 24-hr stage (Krauss *et al.*, 1991b). This spatiotemporal pattern suggests an early involvement in specification and/or differentiation of the cells generating the kidney. Consistent with this assumption, the murine homolog *Pax-2* has a very similar expression pattern (Dressler *et al.*, 1990; Püschel *et al.*, 1992b), and deregulation of this gene in transgenic mice causes severe kidney abnormalities (Dressler *et al.*, 1993).

Studies of the embryonic expression of zebrafish *hox* genes have also revealed evidence for functional conservation in nonsomitic mesoderm. Using the XlHbox1 antibody to investigate expression of the zebrafish *hox-C6* gene, Molven and colleagues (1990) observed labeling of the pectoral fin bud. Expression was first detected in the fin-forming region, about 10 hr before the fin bud itself becomes visible in 29-hr embryos as a condensation of lateral mesodermal cells at the level of somites 2 and 3. During this

period, the expression becomes gradually restricted to the anterior part, and at 48 hr staining is maximal in the anterior and proximal region of the fin mesoderm. Interestingly, immunohistochemical analyses with the XlHbox1 antibody on *Xenopus* and mouse embryos revealed very similar expression patterns in the forelimb bud (Oliver *et al.*, 1988b). Thus, these studies have provided some molecular evidence supporting the assumption that the tetrapod forelimb and pectoral fin of early bony fishes have a common evolutionary origin.

Additional evidence for conservation of the genetic mechanisms underlying patterning of the forelimb has been gained from analyses of the *eng* genes. Engrailed proteins were detected with the 4D9 antibody in the epidermal cells of the pectoral fin bud of 26-hr embryos (Hatta *et al.*, 1991a). This uniform labeling was limited to the ventral-anterior half of the fin bud, and the boundary of expression at later stages followed the ridge of the flattened fin, which is the equivalent of the apical ectodermal ridge (AER) of other vertebrates (Wood, 1982). Using gene-specific probes, Ekker and colleagues (1992b) have shown by *in situ* hybridization that only the *eng-1* gene is expressed in the pectoral fin bud. Similarly, *En-1* expression was observed in the ventral ectoderm of the forelimb bud in mouse embryos (Davis *et al.*, 1991). Also in this case the expression boundary coincided with the AER. These observations indicate a conserved role for the *eng-1*/*En-1* genes in defining differences between the dorsal and ventral regions of the bud and perhaps in specifying the position where the AER forms. In relation to these questions, it will be of interest to investigate whether cell lineage restrictions correlate with the compartment-like boundary.

In addition to the muscle pioneers, *eng* expression has been detected in mesenchymal cells that develop to form two specific jaw muscles in the zebrafish (Hatta *et al.*, 1990). Expression was initially observed in scattered mesenchymal cells, caudal to the eyes and lateral to the hindbrain in 24-hr embryos. In later developmental stages, the labeled cells moved rostrally and aggregated to form a single cluster in the mandibular arch, which eventually differentiated as two specific jaw muscles. Only transcripts of the *eng-2* and *eng-3* genes were detected in the muscle precursor cells by *in situ* hybridization (Ekker *et al.*, 1992b). Interestingly, the growth cones of trigeminal motoneurons were associated with the *eng*-positive mesenchymal cells a few hours after onset of expression (Hatta *et al.*, 1990). These observations suggested that the *eng* genes play a role in specifying a particular subset of muscles from the pharyngeal arch mesoderm and that they indirectly contribute to neuromuscular target recognition. These functions may be conserved, since the murine *En* genes are expressed in mandibular myoblasts (Logan *et al.*, 1993).

VI. Signals Responsible for Establishing the Expression Patterns

The close similarities between the observed expression patterns of homologous *pax* and homeobox genes in zebrafish and other vertebrates suggest that the essential mechanisms responsible for regulating embryonic expression are highly conserved. These signaling pathways have been most extensively studied in *Xenopus*, chicken, and mouse embryos, and have provided preliminary evidence for the involvement of retinoids and several types of secreted proteins and their receptors. In the few cases where these aspects have also been investigated in zebrafish, the results are consistent with the findings in higher vertebrates.

Two zebrafish homologs of *Xenopus* and mouse genes that are known to be involved in axial patterning during gastrulation have been analyzed in considerable detail. One of these, Zf-T, is directly homologous to the mouse *Brachyury* (*T*) gene, which is required for normal AP patterning of the mesoderm and the generation of a notochord (Wilson, 1990). As in mice, the *T* gene in zebrafish is expressed in the notochord and early mesoderm (Schulte-Merker *et al.*, 1992). Both in *Xenopus* and zebrafish, transcription of the *T* gene can be activated by the mesodermal-inducing growth factor activin A (Smith *et al.*, 1991; Schulte-Merker *et al.*, 1992). This observation suggests that the fundamental inductive events have been conserved.

The *Xenopus* homeobox gene *goosecoid* can also be induced by activin in the Spemann's organizer region, and the gene probably plays a central role in both DV and AP patterning (Cho *et al.*, 1991). Results obtained from analyses of the embryonic expression of the zebrafish *goosecoid* homolog are in agreement with this proposal (Stachel *et al.*, 1993). Zygotic expression of the zebrafish gene is first detected at the midblastula stage in the presumptive dorsal lip region. In gastrulating embryos, expression is localized within the anterior axial hypoblast, suggesting that *goosecoid* might be specifically associated with the head organizer, as has been proposed for the *Xenopus* homolog (Cho *et al.*, 1991). One of the immediate consequences of this expression in the anterior hypoblast could be the induction of genes involved in head patterning. Consistent with this assumption, a requirement for vertical signals from underlying axial mesoderm in patterning of the forebrain has been demonstrated in *Xenopus* (Ruiz i Altaba, 1992).

Studies on the early expression of the zebrafish *hlx-1* gene have shown that this gene could be located downstream of *goosecoid* in a regulatory cascade (Fjose *et al.*, 1994). At the 8-hr stage, *hlx-1* is induced within a circular area in the rostral region, and following dynamic alterations

of the expression domain, the transcripts become restricted within prechordal plate cells underlying the midbrain and forebrain. Further studies are required to determine whether this spatiotemporal pattern reflects an involvement of the *hlx-1* gene in development of the rostral brain.

VII. Mutational and Transgenic Analyses

Many properties of the zebrafish, including small size, large number of embryos, speed of development, and transparency of embryos, are favorable for genetic analysis. In addition, the ability to generate haploids with almost normal embryonic development allows the detection of recessive, early acting mutations without breeding homozygotes (Kimmel and Warga, 1988). Taken together, these properties should facilitate saturation screening for developmental mutants in the zebrafish. Until recently, such screens have not been performed, and as a result few zebrafish mutations have been described (Grunwald *et al.*, 1988; Kimmel *et al.*, 1989; Hatta *et al.*, 1991b).

Despite this problem, the information obtained from the characterization of the *cyclops* (*cyc-1*) and *spadetail* (*spt-1*) mutations has clearly shown that genetic analysis of zebrafish is a fruitful approach for investigating vertebrate development (Hatta *et al.*, 1991b; Ho *et al.*, 1990). One of these mutations, *spt-1*, which acts autonomously in prospective mesodermal cells to misdirect their gastrulation movements (Ho *et al.*, 1990), has also been used to investigate the regulation of homeobox genes. Despite the severe somitic abnormalities in the trunk region of *spt-1* embryos, staining with the XlHbox1 antibody indicated that the *hox-C6* gene was expressed within the appropriate AP domains in both the CNS and the mesoderm (Molven *et al.*, 1990). Consequently, the positional information responsible for regulating *hox-C6* seemed unaffected by the abnormal somitic segmentation caused by the mutation. In contrast, the expression of *eng* genes in muscle pioneers was affected in *spt-1* embryos (Hatta *et al.*, 1991a). In the trunk region of mutant embryos, the myotomes were poorly patterned and lacked horizontal myosepta, as well as *eng*-expressing muscle pioneers. This observation supported the interpretation that cells expressing *eng* in the somite play an important role in the dorsoventral subdivision of the myotome (see Section V,A).

To elucidate the functions of the various homeobox and *pax* genes identified in zebrafish, it is necessary to apply transgenic methods. Although transgenic zebrafish have been reported for several types of promoter–reporter constructions (Stuart *et al.*, 1988, 1990; Culp *et al.*, 1991;

Bayer and Campos-Ortega, 1992), further technical advances are clearly required before such methods can be efficiently exploited for functional studies of the developmental genes. Using *lacZ* as a reporter gene, various promoter–*lacZ* fusions have been used for transgenic analysis of the cis-acting elements involved in regulating the embryonic expression of the murine *Hox* and *En* genes (Sham *et al.*, 1993; Logan *et al.*, 1993). Permanent germ-line transformants of promoter–*lacZ* constructs have not been reported for any of the zebrafish homeobox or *pax* genes, but mammalian *Hox* promoters have been successfully analyzed in mosaically transgenic zebrafish (Westerfield *et al.*, 1992). Using the *lacZ* reporter gene, the activity of any promoter can in principle be assayed directly in microinjected embryos. Using this approach, Westerfield and colleagues (1992) have shown that the promoters of the murine *Hox-A7* (*Hox-1.1*) and human *HOX-C6* can specify expression within the same spatial domains in the CNS and paraxial mesoderm of zebrafish embryos as in mice, suggesting conservation of the promoter functions. In these experiments, the expression domains were defined on the basis of the mosaic expression observed in many embryos. Unfortunately, the resolution obtained by this strategy seems to be rather low and therefore will probably not allow detailed analysis of the spatial regulatory mechanisms. However, an advantage of generating transgenic lines with the *lacZ* reporter is that these can be used as sources of specific types of labeled cells in transplantation experiments.

A stable transgenic line of zebrafish expressing *lacZ* with enhancer-trap features was reported by Bayer and Campos-Ortega (1992). This line was generated by the injection of a construct containing a truncated mouse heat-shock promoter fused to *lacZ*. It is hoped that further technical advances will improve the efficiency of generating such enhancer- or gene-trap lines in zebrafish. Such studies will also help to establish DNA insertional mutagenesis as an alternative method for the identification and cloning of developmental genes.

The studies reviewed here have confirmed that the fundamental mechanisms of development are strongly conserved among vertebrates from fish to mammals. This is an important argument for further use of the zebrafish model. By exploiting the simple features of zebrafish embryos, it has also been possible to analyze the development of cells and morphological subdivisions at a higher resolution than in other vertebrates. Thus, even without a large number of developmental mutants, the zebrafish provides opportunities for analyzing aspects that may not be accessible for investigation in mammals. Still, its success as a developmental model will strongly depend on the advances made in mutant screening and transgene technology during the next few years.

Acknowledgments

I thank J. U. Ericson, M. Mlodzik, and U. Weber for sharing unpublished observations. I am also very grateful to A. Molven for his helpful comments on the manuscript. Original work from my laboratory was supported by the Norwegian Cancer Society, Nansen Foundation, and Norwegian Research Council NAVF.

References

Adams, B., Doerfler, P., Aguzzi, A., Kozmik, Z., Urbanek, P., Maurer-Fogy, I., and Busslinger, M. (1992). *Pax-5* encodes the transcription factor BSAP and is expressed in B lymphocytes, the developing CNS and adult testis. *Gene Dev.* **6,** 1589–1607.

Arcioni, L., Simeone, A., Guazzi, S., Zappavigna, V., Boncinelli, E., and Mavioli, F. (1992). The upstream region of the human homeobox gene *HOX3D* is a target for regulation by retinoic acid and HOX homeoproteins. *EMBO J.* **11,** 265–277.

Barad, M., Jack, T., Chadwick, R., and McGinnis, W. (1988). A novel, tissue-specific, *Drosophila* homeobox gene. *EMBO J.* **7,** 2151–2161.

Bayer, T. A., and Campos-Ortega, J. (1992). A transgene containing *lacZ* in primary sensory neurons in zebrafish. *Development* **115,** 421–426.

Bernhardt, R. R., Chitnis, A. B., Lindamer, L., and Kuwada, J. Y. (1990). Identification of spinal neurons in embryonic and larval zebrafish. *J. Comp. Neurobiol.* **302,** 603–616.

Chavrier, P., Zerial, M., Lemaire, P., Almendral, J., Bravo, R., and Charnay, P. (1988). A gene encoding a protein with zinc fingers is activated during G_0/G_1 transition in cultured cells. *EMBO J.* **7,** 29–35.

Chitnis, A. B., and Kuwada, J. Y. (1990). Axonogenesis in the brain of zebrafish embryos. *J. Neurosci.* **10,** 1892–1905.

Cho, K. W. Y., Blumberg, B., Steinbeisser, H., and De Robertis, E. M. (1991). Molecular nature of the Spemann's organizer: the role of the *Xenopus* homeobox gene *goosecoid*. *Cell* **67,** 1111–1120.

Culp, P., Nüsslein-Volhard, C., and Hopkins, N. (1991). High-frequency germ-line transmission of plasmid DNA sequences injected into fertilized zebrafish eggs. *Proc. Natl. Acad. Sci. USA* **88,** 7953–7957.

Davidson, G., Graham, E., Sime, C., and Hill, R. (1988). A gene with sequence similarity to *Drosophila engrailed* is expressed during the development of the neural tube and vertebrae in the mouse. *Development* **104,** 305–316.

Davis, C. A., and Joyner, A. L. (1988). Expression patterns of the homeo box-containing genes *En-1* and *En-2* and the proto-oncogene *int-1* diverge during mouse development. *Genes Dev.* **2,** 1736–1744.

Davis, C. A., Holmyard, D. P., Millen, K. J., and Joyner, A. L. (1991). Examining pattern formation in mouse, chicken, and frog embryos with an *En*-specific antiserum. *Development* **111,** 287–298.

DiNardo, S., and O'Farrell, P. H. (1987). Establishment and refinement of segmental pattern in the *Drosophila* embryo: spatial control of *engrailed* expression by pair-rule genes. *Genes Dev.* **1,** 1212–1225.

Dressler, G. R., Deutsch, U., Chowdhury, K., Nornes, H. O., and Gruss, P. (1990). *Pax-2*, a new murine paired-box-containing gene and its expression in the developing excretory system. *Development* **109,** 787–795.

Dressler, G. R., Wilkinson, J. E., Rothenpieler, U. W., Patterson, L. T., Williams-

Simons, L., and Westphal, H. (1993). Deregulation of *Pax-2* expression in transgenic mice generates severe kidney abnormalities. *Nature* **362,** 65–67.

Eiken, H. G., Njølstad, P. R., Molven, A., and Fjose, A. (1987). A zebrafish homeobox-containing gene with embryonic transcription. *Biochem. Biophys. Res. Commun.* **149,** 1165–1171.

Eisen, J. S. (1991). Determination of primary motoneuron identity in developing zebrafish embryos. *Science* **252,** 569–572.

Ekker, M., Akimenko, M. A., Bremiller, R., and Westerfield, M. (1992a). Regional expression of three homeobox transcripts in the inner ear of zebrafish embryos. *Neuron* **9,** 27–35.

Ekker, M., Wegner, J., Akimenko, M. A., and Westerfiled, M. (1992b). Coordinate embryonic expression of three zebrafish *engrailed* genes. *Development* **116,** 1001–1010.

Ericson, J. U., Krauss, S., and Fjose, A. (1993). Genomic sequence and embryonic expression of the zebrafish homeobox gene *hox-3.4*. *Int. J. Dev. Biol.* **37,** 263–272.

Felsenfeld, A. L., Curry, M., and Kimmel, C. B. (1991). The *fub-1* mutation blocks initial myofibril formation in zebrafish muscle pioneer cells. *Dev. Biol.* **148,** 23–30.

Fjose, A., Eiken, H. G., Njølstad, P. R., Molven, A., and Hordvik, I. (1988). A zebrafish *engrailed*-like sequence expressed during embryogenesis. *FEBS Lett.* **231,** 355–360.

Fjose, A., Izpisua-Belmonte, J. C., Fromental-Ramain, C., and Duboule, D. (1994). Expression of the zebrafish gene *hlx-1* in the prechordal plate and during CNS development. *Development* **120,** 71–81.

Fjose, A., McGinnis, W., and Gehring, W. J. (1985). Isolation of a homeobox-containing gene from the *engrailed* region of *Drosophila* and the spatial distribution of its transcripts. *Nature* **313,** 284–289.

Fjose, A., Njølstad, P. R., Nornes, S., Molven, A., and Krauss, S. (1992). Structure and early embryonic expression of the zebrafish *engrailed-2* gene. *Mech. Dev.* **39,** 51–62.

Fjose, A., Nornes, S., Weber, U., and Mlodzik, M. (1993). Functional conservation of *seven-up* related genes in neurogenesis and eye development. *EMBO J.* **12,** 1403–1414.

Goulding, M. D., Chalepakis, G., Deutsch, U., Erselius, J. R., and Gruss, P. (1991). Pax-3, a novel murine DNA binding protein expressed during early neurogenesis. *EMBO J.* **10,** 1135–1147.

Goulding, M. D., Lumsden, A., and Gruss, P. (1993). Signals from the notochord and floor plate regulate the region-specific expression of two Pax genes in the developing spinal cord. *Development* **117,** 1001–1016.

Grunwald, D., Kimmel, C. B., Westerfield, M., Walker, C., and Streisinger, G. (1988). A neural degeneration mutation that spares primary neurons in the zebrafish. *Dev. Biol.* **126,** 115–128.

Gruss, P., and Walther, C. (1992). Pax genes in development. *Cell* **69,** 719–722.

Hanneman, E., Trevarrow, B., Metcalfe, W. K., Kimmel, C. B., and Westerfield, M. (1988). Segmental pattern of development of the spinal cord and hindbrain of the zebrafish embryo. *Development* **103,** 49–58.

Hatta, K., Bremiller, R., Westerfield, M., and Kimmel, C. B. (1991a). Diversity of expression of *engrailed*-like antigens in zebrafish. *Development* **112,** 821–832.

Hatta, K., Kimmel, C. B., Ho, R. K., and Walker, C. (1991b). The cyclops mutation blocks specification of the floor plate of the zebrafish central nervous system. *Nature*, **350,** 339–341.

Hatta, K., Schilling, T. F., Bremiller, R. A., and Kimmel, C. B. (1990). Specification of jaw muscle in zebrafish: correlation with *engrailed*-homeoprotein expression. *Science* **250,** 802–805.

Hidalgo, A., and Ingham, P. W. (1990). Cell patterning in the *Drosophila* segment: spatial regulation of the segment polarity gene *patched*. *Development* **110,** 291–301.

Hill, R. E., Favor, J., Hogan, B. L. M., Ton, C. C. T., Saunders, G. F., Hanson, I. M., Prosser, J., Jordan, T., Hastie, N. D., and van Heyningen, V. (1991). Mouse *Small eye* results from mutations in a paired-like homeobox-containing gene. *Nature* **354,** 522–525.

Ho, R. K., and Kane, D. A. (1990). Cell-autonomous action of zebrafish *spt-1* mutation in specific mesodermal precursors. *Nature* **348,** 728–730.

Holland, P. W. H. (1991). Cloning and evolutionary analysis of *msh*-like homeobox genes from mouse, zebrafish and ascidian. *Gene* **98,** 253–257.

Ingham, P. W. (1988). The molecular genetics of embryonic pattern formation in *Drosophila*. *Nature* **335,** 25–34.

Ingham, P. W., Baker, N. E., and Martinez-Arias, A. (1988). Regulation of segment polarity genes in the *Drosophila* blastoderm by *fushi tarazu* and *even skipped*. *Nature* **331,** 73–75.

Itasaki, N., Ichijo, H., Hama, C., Matsuno, T., and Nakamura, H. (1991). Establishment of rostrocaudal polarity in tectal primordium: *engrailed* expression and subsequent tectal polarity. *Development* **113,** 1133–1144.

Johansen, T., Moens, U., Holm, T., Fjose, A., and Krauss, S. (1993). Zebrafish *pou[c]:* a divergent POU family gene ubiquitously expressed during embryogenesis. *Nucleic Acids Res.* **21,** 475–483.

Joly, J. S., Maury, M., Joly, C., Duprey, P., Boulekbache, H., and Condamine, H. (1992). Expression of a zebrafish *caudal* homeobox gene correlates with the establishment of posterior cell lineages at gastrulation. *Differentiation* **50,** 75–87.

Jones, F. S., Chalepakis, G., Gruss, P., and Edelman, G. M. (1992a). Activation of the cytotactin promoter by the homeobox-containing gene *Evx-1*. *Proc Natl. Acad. Sci. USA* **89,** 2091–2095.

Jones, F. S., Prediger, E. A., Bittner, D. A., De Robertis, E. M., and Edelman, G. M. (1992b). Cell adhesion molecules as targets for *Hox* genes: neural cell adhesion molecule promoter activity is modulated by cotransfection with *Hox-2.5* and *-2.4*. *Proc. Natl. Acad. Sci. USA* **89,** 2086–2090.

Jostes, B., Walther, C., and Gruss, P. (1991). The murine paired box gene, *Pax7*, is expressed specifically during the development of the nervous and muscular system. *Mech. Dev.* **33,** 27–38.

Joyner, A. L., and Hanks, M. (1991). The *engrailed* genes: evolution of function. *Sem. Dev. Biol.* **2,** 435–445.

Joyner, A. L., Herrup, K., Auerbach, B. A., Davis, C. A., and Rossant, J. (1991). Subtle cerebellar phenotype in mice homozygous for a targeted deletion of the *En-2* homeobox. *Science* **251,** 1239–1243.

Joyner, A. L., and Martin, G. M. (1987). *En-1* and *En-2*, two mouse genes with sequence homology to the *Drosophila engrailed* gene: expression during embryogenesis. *Genes Dev.* **1,** 29–38.

Keynes, R., and Lumsden, A. (1990). Segmentation and the origin of regional diversity in the vertebrate central nervous system. *Neuron* **4,** 1–9.

Kilchherr, F., Baumgartner, S., Bopp, D., Frei, E., and Noll, M. (1986). Isolation of the *paired* gene of *Drosophila* and its spatial expression during early embryogenesis. *Nature* **321,** 493–499.

Kimmel, C. B. (1982). Reticulospinal and vestibulospinal neurons in the young larva of a teleost fish, *Brachydanio rerio*. *Prog. Brain Res.* **57,** 1–23.

Kimmel, C. B. (1993). Patterning the brain of the zebrafish embryo. *Annu. Rev. Neurosci.* **16,** 707–732.

Kimmel, C. B., Kane, D. A., Walker, C., Warga, R. M., and Rothman, M. B. (1989). A mutation that changes cell movement and cell fate in the zebrafish embryo. *Nature* **337,** 358–362.

Kimmel, C. B., and Warga, R. M. (1988). Cell lineage and developmental potential of cells in the zebrafish embryo. *Trends Genet.* **4,** 68–74.

Krauss, S., Johansen, T., Korzh, V., and Fjose, A. (1991a). Expression pattern of zebrafish *pax* genes suggests a role in early brain regionalization. *Nature* **353,** 267–270.

Krauss, S., Johansen, T., Korzh, V., and Fjose, A. (1991b). Expression of the zebrafish paired box gene *pax[zf-b]* during early neurogenesis. *Development* **113,** 1193–1206.

Krauss, S., Johansen, T., Korzh, V., Moens, U., Ericson, J. U., and Fjose, A. (1991c). Zebrafish *pax[zf-a]:* a paired box-containing gene expressed in the neural tube. *EMBO J.* **10,** 3609–3619.

Krauss, S., Maden, M., Holder, N., and Wilson, S. W. (1992). Zebrafish *pax[b]* is involved in the formation of the midbrain–hindbrain boundary. *Nature* **360,** 87–90.

Kuwada, J. Y., and Bernhardt, R. (1990). Axonal outgrowth by identified neurons in the spinal cord of zebrafish embryos. *Exp. Neurobiol.* **109,** 29–34.

Laughon, A. (1991). DNA binding specificity of homeodomains. *Biochemistry* **30,** 11,357–11367.

Logan, C., Hanks, M. C., Noble-Topham, S., Nallainathan, D., Provart, N. J., and Joyner, A. L. (1992). Cloning and sequence comparison of the mouse, human, and chicken *engrailed* genes reveal potential functional domains and regulatory regions. *Dev. Gen.* **13,** 345–358.

Logan, C., Khoo, W. K., Cado, D., and Joyner, A. L. (1993). Two enhancer regions in the mouse *En-2* locus direct expression to the mid/hindbrain region and mandibular myoblasts. *Development* **117,** 905–916.

Lu, S., Bogarad, L. D., Murtha, M. T., and Ruddle, F. H. (1992). Expression pattern of a murine homeobox gene, *Dbx,* displays extreme spatial restriction in embryonic forebrain and spinal cord. *Proc. Natl. Acad. Sci. USA* **89,** 8053–8057.

Lumsden, A. (1991). Motorizing the spinal cord. *Cell* **64,** 471–473.

Lumsden, A., and Keynes, R. (1989). Segmental patterns of neuronal development in the chick brain. *Nature* **337,** 424–428.

Marcey, D., and Nüsslein-Volhard, C. (1986). News and views: embryology goes fishing. *Nature* **321,** 380–381.

Matsuzaki, T., Amanuma, H., and Takeda, H. (1992). A POU-domain gene of zebrafish, ZFPOU1, specifically expressed in the developing neural tissues. *Biohem. Biophys. Res. Commun.* **187,** 1446–1453.

Mavilio, F. (1993). Regulation of vertebrate homeobox-containing genes by morphogens. *Eur. J. Biochem.* **212,** 273–288.

McGinnis, W., and Krumlauf, R. (1992). Homeobox genes and axial patterning. *Cell* **68,** 283–302.

McMahon, A. P., and Bradley, A. (1990). The *Wnt-1* (*int-1*) proto-oncogene is required for development of a large region of the mouse brain. *Cell* **62,** 1073–1085.

McMahon, A. P., Joyner, A. L., Bradley, A., and McMahon, J. A. (1992). The midbrain-hindbrain phenotype of *Wnt-1*$^-$/*Wnt-1*$^-$ mice results from stepwise deletion of engrailed-expressing cells by 9.5 days postcoitum. *Cell* **69,** 581–595.

Metcalfe, W. K., Mendelson, B., and Kimmel, C. B. (1986). Segmental homologies among reticulospinal neurons in the hindbrain of the zebrafish larva. *J. Comp. Neurol.* **251,** 147–159.

Mikkola, I., Fjose, A., Kuwada, J. Y., Wilson, S. W., Guddal, P. H., and Krauss, S. (1992). The paired domain-containing nuclear factor pax[b] is expressed in specific commissural interneurons in zebrafish embryos. *J. Neurobiol.* **23,** 933–936.

Mlodzik, M., Fjose, A., and Gehring, W. J. (1985). Isolation of *caudal*, a *Drosophila* homeobox-containing gene with maternal expression, whose transcripts form a concentration gradient at the preblastoderm stage. *EMBO J.* **4,** 2961–2969.

Molven, A. (1991). "Pattern Formation and Neurogenesis in a Vertebrate Embryo: Study of Developmentally Regulated Genes in the Zebrafish. PhD thesis, University of Bergen.

Molven, A., Hordvik, I., and Njølstad, P. R. (1993). Sequence analysis of the zebrafish *hox*-B5/B6 region. *Biochim. Biophys. Acta* **1173,** 102–106.

Molven, A., Hordvik, I., Njølstad, P. R., Van Ghelue, M., and Fjose, A. (1992). The zebrafish homeobox gene *hox[zf-114]:* primary structure, expression pattern and evolutionary aspects. *Int. J. Dev. Biol.* **36,** 229–237.

Molven, A., Njølstad, P. R., and Fjose, A. (1991). Genomic structure and restricted neural expression of the zebrafish *wnt-1* (*int-1*) gene. *EMBO J.* **10,** 799–807.

Molven, A., Wright, C. V. E., Bremiller, R., de Robertis, E. M., and Kimmel, C. B. (1990). Expression of a homeobox gene product in normal and mutant zebrafish embryos: evolution of the tetrapod body plan. *Development* **109,** 279–288.

Njølstad, P. R., and Fjose, A. (1988). *In situ* hybridization patterns of zebrafish homeobox genes homologous to *Hox-2.1* and *Eng-2* of mouse. *Biochem. Biophys. Res. Commun.* **157,** 426–432.

Njølstad, P. R., Molven, A., Apold, J., and Fjose, A. (1990). The zebrafish homeobox gene *hox-2.2:* transcription unit, potential regulatory regions and *in situ* localization of transcripts. *EMBO J.* **9,** 515–524.

Njølstad, P. R., Molven, A., Eiken, H. G., and Fjose, A. (1988a). Structure and neural expression of a zebrafish homeobox sequence, *Gene* **73,** 33–46.

Njølstad, P. R., Molven, A., Hordvik, I., Apold, J., and Fjose, A. (1988b). Primary structure, developmentally regulated expression and potential duplication of the zebrafish homeobox gene ZF-21. *Nucleic Acids Res.* **16,** 9097–9111.

Nornes, H. O., Dressler, G. R., Knapik, E. W., Deutsch, U., and Gruss, P. (1990). Saptially and temporally restricted expression of *Pax2* during murine neurogenesis. *Development* **109,** 797–809.

Oliver, G., Wright, C. V. E., Hardwicke, J., and De Robertis, E. M. (1988a). Differential antero-posterior expression of two proteins encoded by a homeobox gene in *Xenopus* and mouse embryos. *EMBO J.* **7,** 3199–3209.

Oliver, G., Wright, C. V. E., Hardwicke, J., and De Robertis, E. M. (1988b). A gradient of homeodomain protein in developing forelimbs of *Xenopus* and mouse embryos. *Cell* **55,** 1017–1024.

Oxtoby, E., and Jowett, T. (1993). Cloning of the zebrafish *krox-20* gene (*krx-20*) and its expression during hindbrain development. *Nucleic Acids Res.* **21,** 1087–1095.

Patel, N. H., Martin-Blanco, E., Coleman, K. G., Poole, S. J., Ellis, M. C., Kornberg, T. B., and Goodman, C. (1989). Expression of engrailed proteins in arthropods, annelids, and chordates. *Cell* **58,** 955–968.

Püschel, A. W., Gruss, P., and Westerfield, M. (1992a). Sequence and expression pattern of *pax-6* are highly conserved between zebrafish and mice. *Development* **114,** 643–651.

Püschel, A. W., Westerfield, M., and Dressler, G. R. (1992b). Comparative analysis of Pax-2 protein distributions during neurulation in mice and zebrafish. *Mech. Dev.* **38,** 197–208.

Rangini, Z., Ben-Yehuda, A., Shapira, E., Gruenbaum, Y., and Fainsod, A. (1991). CHoxE, a chicken homeogene of the H2.0 type, exhibits dorsoventral restriction in the proliferating region of the spinal cord. *Mech. Dev.* **35,** 13–24.

Represa, J., Leon, Y., Miner, C., and Giraldez, F. (1991). The *int-2* proto-oncogene is responsible for induction of the inner ear. *Nature* **353,** 561–563.

Ross, L. S., Parrett, T., and Easter, S. S. (1992). Axonogenesis and morphogenesis in the embryonic zebrafish brain. *J. Neurosci.* **12,** 467–482.

Ruberte, E., Dolle, P., Chambon, P., and Moriss-Kay, G. (1991). Retinoic acid receptors and cellular retinoid binding proteins. II. Their differential pattern of transcription during early morphogenesis in mouse embryos. *Development* **111,** 45–60.

Ruiz i Altaba, A. (1992). Planar and vertical signals in the induction and patterning of the *Xenopus* nervous system. *Development* **116,** 67–80.

Schulte-Merker, S., Ho, R. K., Herrmann, B. G., and Nüsslein-Volhard, C. (1992). The protein product of the zebrafish homologue of the mouse T gene is expressed in nuclei of the germ ring and the notochord of the early embryo. *Development* **116,** 1021–1032.

Scott, M. P., Tamkun, J. W., and Hartzell, G. W. (1989). The structure and function of the homeodomain. *Biochim. Biophys. Acta* **989,** 25–48.

Sham, M. H., Vesque, C., Nonchev, S., Marshall, H., Frain, M., Das Gupta, R., Whiting, J., Wilkinson, D., Charnay, P., and Krumlauf, R. (1993). The zinc finger gene *Krox20* regulates *HoxB2* (*Hox2.8*) during hindbrain segmentation. *Cell* **72,** 183–196.

Smith, J. C., Price, B. M. J., Green, J. B. A., Weigel, D., and Herrmann, B. G. (1991). Expression of a *Xenopus* homolog of *Brachyury* (*T*) is an immediate-early response to mesoderm induction. *Cell* **67,** 79–87.

Stachel, S. E., Grunwald, D. J., and Myers, P. Z. (1993). Lithium perturbation and *goosecoid* expression identify a dorsal specification pathway in the pregastrula zebrafish. *Development* **117,** 1261–1274.

Stuart, G. W., McMurray, J. V., and Westerfield, M. (1988). Replication, integration and stable germ-line tansmission of foreign sequences injected into early zebrafish embryos. *Development* **103,** 403–412.

Stuart, G. W., Vielkind, J. R., McMurray, J. V., and Westerfield, M. (1990). Stable lines of transgenic zebrafish exhibit reproducible patterns of transgene expression. *Development* **109,** 577–584.

Trevarrow, B., Marks, D. L., and Kimmel, C. B. (1990). Organization of hindbrain segments in the zebrafish embryo. *Neuron* **4,** 669–679.

Walther, C., and Gruss, P. (1991). *Pax-6*, a murine paired box gene, is expressed in the developing CNS. *Development* **113,** 1435–1449.

Westerfield, M., Wegner, J., Jegalian, B., De Robertis, E. M., and Püschel, A. (1992). Specific activation of mammalian *Hox* promoters in mosaic transgenic zebrafish. *Genes Dev.* **6,** 591–598.

Wilkinson, D., Bhatt, S., Chavrier, P., Bravo, R., and Charnay, P. (1989a). Segment-specific expression of a zinc finger gene in the developing nervous system of the mouse. *Nature* **337,** 461–464.

Wilkinson, D., Bhatt, S., Cook, M., Boncinelli, E., and Krumlauf, R. (1989b). Segmental expression of Hox-2 homeobox-containing genes in the developing mouse hindbrain. *Nature* **341,** 405–409.

Wilkinson, D., and Krumlauf, R. (1990). Molecular approaches to the segmentation of the hindbrain. *Trends Neurosci.* **13,** 335–339.

Wilkinson, D., Peters, G., Dickson, C., and McMahon, A. (1988). Expression of the FGF-related proto-oncogene *int-2* during gastrulation and neurulation in the mouse. *EMBO J.* **7,** 691–695.

Wilson, K. (1990). The mouse *Brachyury* gene and mesoderm formation. *Trends Genet.* **6,** 104–105.

Wilson, S. W., Ross, L. S., Parrett, T., and Ester, S. S. (1990). The development of a simple scaffold of axon tracts in the brain of the embryonic zebrafish, *Brachydanio rerio*. *Development* **108,** 121–145.

Wood, A. (1982). Early pectoral fin development and morphogenesis of the apical ectodermal ridge in the killifish, *Ahyosemion scheeli*. *Anat. Rec.* **204,** 349–356.

Yamada, T., Placzek, M., Tanaka, H., Dodd, J., and Jessel, T. M. (1991). Control of cell pattern in the developing nervous system: polarizing activity of the floor plate and notochord. *Cell* **64,** 635–647.

3

Evolution of Developmental Mechanisms: Spatial and Temporal Modes of Rostrocaudal Patterning

David A. Weisblat
*Cathy J. Wedeen**
*Richard G. Kostriken**
Department of Molecular and Cell Biology
University of California
Berkeley, California 94720

I. Introduction: Evolution and Developmental Change

Scientists have sought to understand the basis of the evolutionary changes that generate species diversity ever since the theory of evolution was accepted. The connection between phyletic change and ontogenetic

* Present Address: Department of Cell Biology and Anatomy, New York Medical College, Valhalla, New York 10595.

Current Topics in Developmental Biology, Vol. 29

change was already apparent to Darwin and his contemporaries [for a full discussion, see Gould (1977)]. Much of the work in this area has been restricted to descriptive comparisons of morphological development in different species. This approach has produced a bewildering array of abstractions (ranging from allomorphosis, anaboly, and archallaxis, through heterochrony, heterotopy, and hypermorphosis, to progenesis, proterogenesis, and terminal addition) that describe possible mechanisms of phylogenetic change. Simply put, the conclusions drawn from all this work seem to be that phyletic change can result from the addition or deletion of structures or processes at any point between the beginning and the end of development, and also from changes in the relative timing of one or more developmental processes.

These conclusions, while valid, are unsatisfying because they exclude so few possibilities and also because the abstractions yield few insights into the cellular and molecular basis of either development or phyletic change. Nonetheless, it remains undisputed that changes in developmental processes underlie evolution and that the burden of elucidating the basis of evolutionary changes therefore falls largely on developmental biologists. Dramatic advances in understanding development in a few experimentally favorable species have been made in recent years. Therefore, using these data as a standard against which to measure evolutionary change in developmental processes, we could in principle observe and analyze evolutionary changes as they occur over time among wild populations of the animals we have studied. Using this approach, direct observations of evolutionary change and mechanistic explanations of the underlying developmental changes should be forthcoming within a few hundred thousand years, assuming that the various species involved (including our own) do not become extinct first. In the meantime, the only way to glean some understanding of evolutionary change is to persist in the historical approach of interpreting comparative studies of development in light of phylogenetic relationships of the species being compared. From this work, it might be possible to draw inferences about the developmental processes of the ancestral species, and hence about the developmental changes that have occurred during evolution.

II. The Contribution of Molecular Phylogeny

In using comparative development to understand evolutionary change, it is important to consider how we arrive at the phylogenetic tree on which the comparisons are based. Obviously, the conclusions drawn from comparative studies hinge on our assumptions about the phylogenetic relation-

ships of the species being compared. Unfortunately, to the extent that embryological characteristics have been used in constructing phylogenetic trees, the use of these same phylogenetic trees as a framework for comparative developmental studies can lead to circular reasoning. Fortunately, although DNA sequence comparisons per se are of little help in understanding the evolution of development (see later discussion), they do provide a way of constructing phylogenetic trees independent of data from comparative morphology or comparative embryology. This means that, for the first time, the problem of constructing phylogenetic trees can be divorced from the problem of understanding the developmental changes by which the trees have arisen.

III. Evolution as a Historical Process

What sort of results can be expected from such comparative studies? One result will certainly be the identification of developmental processes that are widely seen in modern species and are therefore apt to have been inherited more or less intact from the ancestral species. The identification of such "universal" aspects of development is certainly exciting, but may be overemphasized in this age of the "central dogma." It will be equally significant in understanding evolutionary change to characterize the *differences* in developmental processes between species that account for the diversity of living forms. As a consequence, it should be appreciated that any attempt at explaining development on the basis of any one "model" system would be incomplete, because that explanation would fail to distinguish between the general and the specific.

Another approach to this issue is to realize that evolution is truly a historical process. Each step in evolutionary history reflects a "tinkering" (Jacob, 1982) with previously existing forms. Moreover, the course of evolution is highly contingent upon chance occurrences (e.g., genetic mutations, weather patterns, geological and cosmological events) whose timing and consequences are unpredictable. Thus, even apart from the slow time scale involved, evolution is not deterministic in the way that colliding billiard balls are. This does not mean it is not worthwhile or interesting to try to understand what happened during evolution; other perfectly respectable areas of scientific inquiry, such as cosmology and geology, also have major historical components. But it does mean that not all of the interesting results will be universal truths, and it also means that conclusions having to do with the historical aspects of the inquiry will be based on plausibility rather than on the results of carefully controlled experiments.

IV. Evolution and Genetic Change

Since genetic mutations are a fundamental component of evolutionary change, one might propose to study phyletic change simply by comparing DNA sequences from the species of interest. But this approach is unworkable because knowledge of genomic sequences is insufficient to explain developmental processes. This failure might simply reflect our present, rudimentary understanding of the cellular and molecular basis of embryogenesis or it might reflect a theoretical barrier to predicting the properties of complex systems from the properties of their simple components [see also Stent (1981)].

Thus, at least for the time being, a satisfactory understanding of developmental processes and the changes they undergo during evolution requires the correlation of genetic change with developmental change at the cellular level. With this in mind, we study the development of glossiphoniid leeches and compare our results with observations in other kinds of animals.

V. Distinguishing between Segmentation and Regionalization

One aspect of leech development that we seek to understand is how the rostrocaudal patterning of the body plan is generated. In addressing this issue, it is important to distinguish between "segmentation" and "regionalization" as two distinct features of rostrocaudal patterning. Segmentation refers to the organization of the body into a series of similar units, or segments, along the rostrocaudal axis. Regionalization refers to the division of the animal into dissimilar regions (e.g., head, trunk, and thorax) along its length. In segmented animals, regionalization is reflected in the fact that the segments are similar, but not identical, to one another along the rostrocaudal axis.

The importance of distinguishing between segmentation and regionalization comes from the fact that these processes probably arose independently during evolution and therefore might operate independently during development. Regionalization in animal body plans had clearly evolved long before the separation of the lineages leading to protostomes and deuterostomes (Fig. 1): regionalization is obvious in various pseudocoelomate phyla that give no indication of segmentation. In contrast, segmentation is usually regarded as having arisen independently in the chordate sublineage of the deuterostomes and in the protostomes, although the foundations of this process may already have been laid in flatworms (Ghysen, 1992).

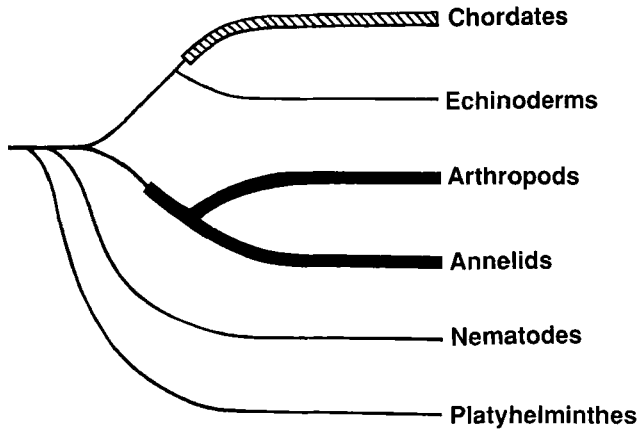

Fig. 1 Appearance of regionalization and segmentation during evolution. A simplified phylogenetic tree showing the postulated evolutionary relatedness of six different phyla, all of which have regionalized body plans, i.e, that exhibit distinct anterior–posterior polarity. Groups such as nematodes and platyhelminthes have regionalized body plans but are not overtly segmented; they are believed to have arisen by divergence from animals that were common ancestors of protostomes (arthropods and annelids) and deuterostomes (chordates and echinoderms). Thus it seems that segmentation arose long after regionalization and occurred independently within the protostome and deuterstome lineages (heavy black lines and hatched lines, respectively).

The molecular–genetic basis of both regionalization and segmentation is relatively well understood in *Drosophila* [Fig. 2; for a concise review, see Tautz (1992)]. Moreover, the hierarchy of developmental regulatory genes controlling these processes in *Drosophila* is consistent with their evolutionary histories. Both processes depend on the establishment of longitudinal concentration gradients of maternal gene products, such as *bicoid* in the zygote and on the differential expression of "gap genes" such as *hunchback, kruppel,* and *knirps* in response to different values of the *bicoid* gradient. From there, quasi-separate genetic pathways exist for regionalization (via the homeotic genes) and segmentation (via the pair-rule and segment polarity genes).

VI. Temporal and Spatial Modes of Segmentation in Annelids and Arthropods

Comparing the segmentation processes in annelids and other segmented protostomes is particularly interesting because these groups are generally considered as having a common ancestor that was already segmented. Thus, it is expected that they share a common molecular-genetic basis

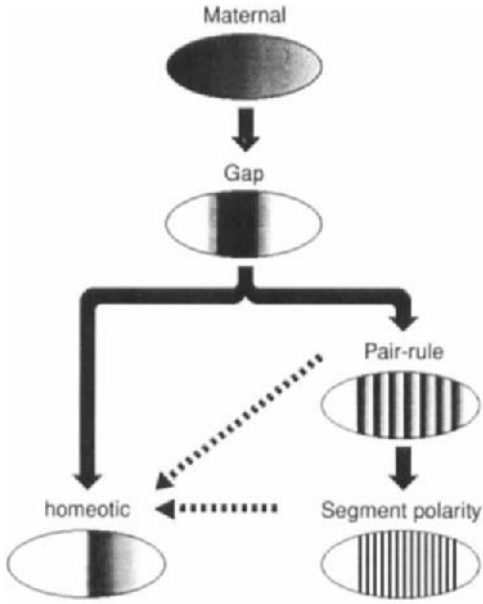

Fig. 2 Genetic regulation of regionalization and segmentation in *Drosophila:* a schematic overview. Rostrocaudal gradients of maternally deposited gene products, such as *bicoid*, regulate the expression of gap genes in broad regions along the length of the body. Further refinements of the regionalization process, leading to the establishment of specific segmental identities, entails the expression of specific homeotic genes, under the control of maternal and gap gene products. Evolutionary evidence suggests that this regionalization process (left side) is a modified version of one inherited from a regionalized, but unsegmented, ancestor of the arthropods. Segmentation (right side) involves the expression of pair-rule and segment polarity genes, also under the control of the maternal and gap genes, but acting relatively independently of the homeotic genes. Interactions between the two pathways (indicated by dotted lines) serve to coordinate regionalization and segmentation, for the production of the final rostrocaudal pattern. Anterior is to the left.

for segmentation, as well as for regionalization. And yet the cellular processes of rostrocaudal pattern formation in protostomes vary dramatically, with long germ band insects and leeches at two extremes.

A priori, one can imagine segments arising either simultaneously throughout the length of the embryo from a preexisting field of cells, or one by one in a strict progression starting at one end of the embryo (Fig. 3). For convenience, these two logical extremes will be referred to as the "spatial" and "temporal" modes of segmentation, respectively. Most readers will probably recognize immediately that the spatial mode of segmentation is a good approximation of the course of events in the *Drosophila* embryo and other long germ band insects. Less widely appreciated, however, is the fact that the temporal mode, commonly associated with chordate development, is also observed in protostomes. Leech develop-

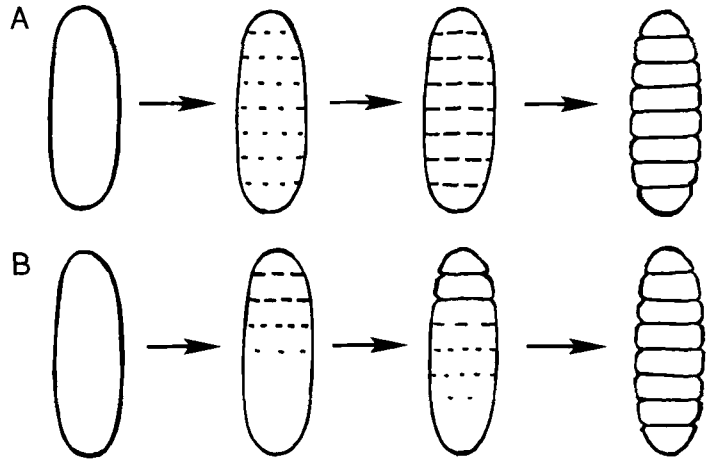

Fig. 3 Representations of spatial and temporal modes of segmentation. In the spatial mode (A), segment primordia form simultaneously along the length of the anterior–posterior body axis. In the temporal mode (B), segmental primordia arise sequentially from anterior to posterior. Anterior is up in this and all subsequent figures.

ment, as summarized later, is a paradigm of this latter mode of segmentation. Moreover, in most other protostomes, including short germ band insects, crustaceans, and other arthropods, the segmentation processes are a mixture of the spatial and temporal modes (Anderson, 1973; Dohle and Scholtz, 1988). Thus, one might hope that an understanding of segmentation in fly and leech would aid in understanding protostome segmentation in general.

VII. Three Levels of Molecular-Genetic Homology

A reasonable (though not inviolate) starting assumption for comparative developmental studies is that homologous developmental processes should exhibit homologies at the molecular biological and genetic levels. Thus, the extensive molecular-genetic studies of segmentation in *Drosophila* should provide a solid foundation for analyzing the process in leech, for which no genetic techniques are presently available. We are pursuing the now common procedure of identifying and characterizing homologs in leech of genes that have been identified as developmentally important in other organisms, especially *Drosophila*. One question that needs answering is how to account for the dramatic differences between the cellular processes of temporal and spatial segmentation. To what extent do these two different processes involve completely different developmental regu-

latory genes rather than changes in the function or regulation of genes involved in the segmentation of the common ancestor?

In describing this work, however, it is important to note that "homology" can exist on several different levels. Three distinct levels of molecular–genetic homology have been defined (Weisblat *et al.*, 1993). Similarities between two or more nucleic acid coding sequences constitute sequence homology; analyzing the divergence between sequence homologs allows the construction of phylogenetic trees independent of morphological or embryological considerations [e.g., see Lake (1990)]. At a slightly higher level, biochemical homology denotes the conservation of biophysical properties between the polypeptides encoded and, as a result, the most proximal biological function of two or more sequence homologs. Neither sequence homology nor biochemical homology is particularly noteworthy from the standpoint of comparative development because neither one addresses the issue of how the gene(s) in question operates in creating the shape and pattern of the animal.

The third and highest level of molecular-genetic homology takes into account how genes function at the operational level. Garcia-Bellido (1985) proposed that two categories of genes can play a role in development: realizator (i.e., structural and "house-keeping") genes and selector (i.e., regulatory) genes. Selector genes are capable of regulating realizator gene expression as well as their own and other selector gene expression. Therefore, while a mutation in a realizator gene *may* affect developmental pattern, mutations in selector genes that lead to their misexpression can result in a cascade of gene misexpression and might therefore be expected to have a much greater impact on developmental pattern.

Identified sets of interacting selector genes have been shown to play roles in specific aspects of early development of the *Drosophila* embryo. Moreover, the groups of selector genes involved in one aspect of development may operate quite independently of those involved in other aspects. For example, the groups of genes involved in establishing the dorsoventral patterning of the *Drosophila* embryo operate independently of those involved in rostrocaudal patterning. And among the genes involved in rostrocaudal patterning, as described earlier, those late-acting genes involved in regionalization operate quasi-independently of late-acting genes involved in segmentation.

Such sets of cross-regulating selector genes (and their target loci) have been called syntagmata (Garcia-Bellido, 1985). Just which genes should be included in a particular syntagma in a given species is difficult to establish because the strengths of interactions between genes vary and cannot be experimentally determined with precision (or at *all* in most species!). But a corollary of Garcia-Bellido's definition of the syntagma is that such interacting genes and their operational role in development should be transmitted and modified collectively rather than individually

during evolution. Accordingly, the term syntagmal homology will be used to refer to the conservation of developmentally significant gene function between species in addressing the question of what is preserved as developmental processes change during evolution.

Sequence homologs of many of the developmental regulatory genes from *Drosophila* have been identified outside of the arthropods. Insofar as different sequence homologs have been demonstrated to encode transcription factors, they can be classified as biochemical homologs as well. In addition, the homologs can be compared at the level of spatial and temporal expression patterns. For example, one can ask whether they are expressed in homologous tissues and at comparable times in development.

In keeping with the evolutionary antiquity of the regionalization process, homologs of the homeotic gene complexes, designated as the HOM/Hox complex, appear to be involved in the regionalization of animals ranging from nematodes to vertebrates (McGinnis and Krumlauf, 1992). In light of this, it is not at all surprising that HOM/Hox genes appear to be conserved in annelids as well, and it seems likely that these genes are involved in the regionalization process of leeches. Thus, we are now in a position to ask whether syntagmal homologies also exist for the segmentation processes in leeches and flies, and if so, how homologous genes function in temporal and spatial modes of segmentation.

VIII. Cellular Basis of Segmentation in Leech Development

In all but the most primitive leeches, the tubular body is organized into 32 segments (Fig. 4). Most of its length is occupied by 21 midbody segments, numbered M1–M21. In addition, there are four fused rostral segments (R1–R4) and seven fused caudal segments (C1–C7). Segments are strikingly similar to one another, especially within the midbody; for instance, each segmental ganglion consists of stereotyped numbers (Macagno, 1980) of individually identified neurons (Muller *et al.*, 1981), most of which have obvious homologs in other ganglia along the length of the animal. Despite this similarity between segments, segment-specific differences in both neural and nonneural tissues provide evidence of regionalization of the leech body plan (Muller *et al.*, 1981; Shankland *et al.*, 1991; Stent *et al.*, 1992). This, plus the fact that the number of segments is invariant, makes it clear that individual segments are assigned specific identities at some point in the development of leeches as in arthropods. In addition to the segmental tissues, the anterior end of the adult leech has nonsegmental tissues, such as a pharynx and a supraesophageal ganglion; collectively, these tissues are referred to as the prostomium. The gut and reproductive tissues are also generally regarded as nonsegmental tissues (Sawyer, 1986) [see Nardelli-Haefliger and Shankland (1993)].

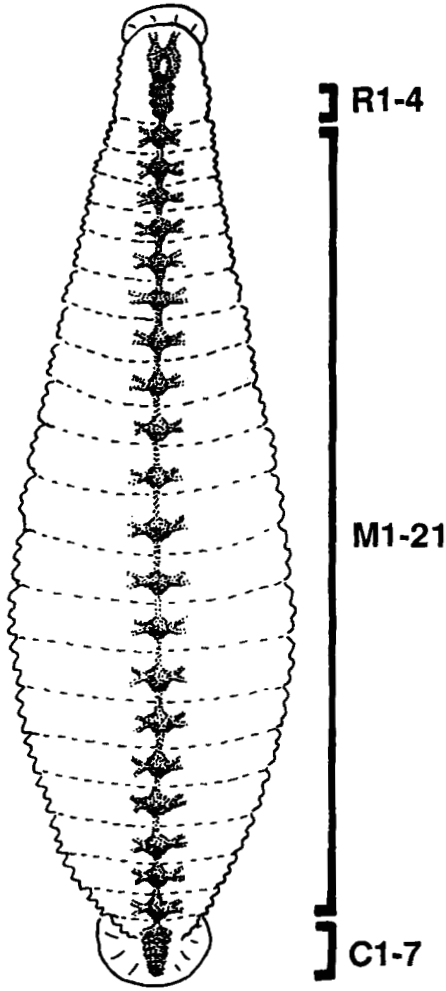

Fig. 4 Designation of segments in the body plan of a leech. Segmental ganglia are shown as viewed through the dorsal body wall. Segmental borders are designated by dotted lines. Brackets indicate the 4 fused rostral segments (R1–R4), the 21 midbody segments (M1–M21), and the 7 fused caudal segments (C1–C7).

The embryonic development of glossiphoniid leeches is divided into 11 stages (Stent *et al.*, 1992). The overt cellular processes leading to morphologically recognizable segments occur during stages 6 to 9. In the species used in our research (primarily *Helobdella triserialis*, *H. robusta*, and *H. stagnalis*), eggs (each about 0.5 mm in diameter) are fertilized internally, but arrest in first meiosis until deposited in transparent cocoons attached to the ventral surface of the parent; zygotes and embryos can

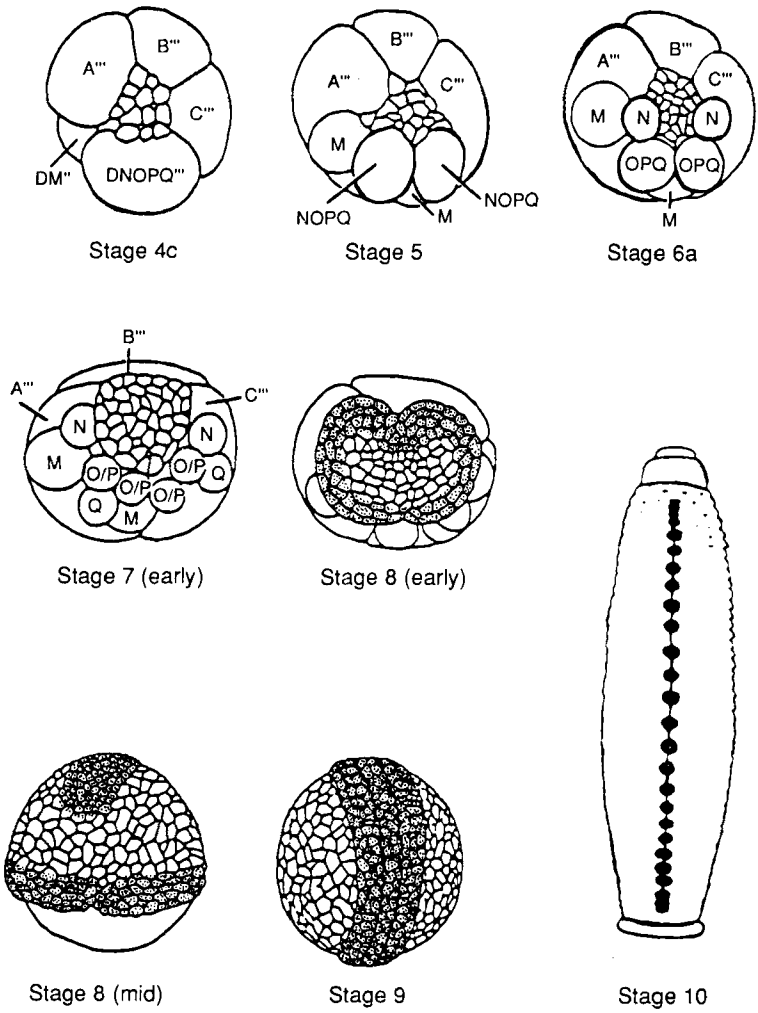

Fig. 5 Selected stages in the development of glossiphoniid leech embryos. Representations of embryos as viewed looking down at the animal pole (stages 4c through midstage 8) or ventral midline (stages 9 and 10). At stage 4c, the embryo consists of three macromeres, designated A'''-C''', two teloblast precursors, designated DM'' and DNOPQ''', plus a group of micromeres clustered at the animal pole. By stage 7, the teloblast precursors have cleaved further to generate five bilateral pairs of teloblasts, and the teloblasts have begun producing columns of blast cells called germinal bandlets (not visible here; see Fig. 7) beneath a provisional epithelium derived from the micromeres. By early stage 8, the bandlets are organized into parallel arrays called germinal bands (stippling) that lie under the margins of the micromere-derived epithelium. During the rest of stage 8, the germinal bands move over the surface of the embryo, accompanied by an expansion of the provisional epithelium. During stage 9, the completed germinal plate expands, gradually displacing the provisional epithelium. By stage 10, the edges of the germinal plate have coalesced along the dorsal midline, completing the body tube of the leech, and organogenesis is well underway. The segmental body plan is manifest; the chain of ganglia in the ventral nerve cord is indicated in black. Nonsegmental, prostomial tissues are present at the anterior end of the animal.

be easily removed for experimental manipulation at any time during development. Stages 1 to 6 consist of a series of highly stereotyped, holoblastic cleavages, giving rise to three distinct classes of individually identifiable blastomeres: macromeres, micromeres, and teloblasts (Fig. 5).

Cell lineage studies begun by C. O. Whitman (1878, 1887, 1892) and refined extensively since the mid 1970s [summarized in Stent *et al.* (1992)] indicate that the three macromeres contribute to the gut [see also Nardelli-Haefliger and Shankland (1993)] and provide nutrition for the embryo. The 25 micromeres (3 arise from each of the A, B, and C quadrants of the embryo, and 16 arise from the D quadrant) contribute epithelical cells to a transient larval integument, as well as neurons, muscle cells, and epidermis to the prostomial tissues of the leech, whereas the 10 teloblasts generate the segmental tissues (Fig. 5).

Teloblasts are five bilateral pairs of embryonic stem cells that also arise from the D quadrant of the embryo (macromere D'; stage 4a). One pair of teloblasts, designated M, gives rise to the mesoderm; and four pairs of teloblasts, designated N, O/P, O/P, and Q, together give rise to the ectoderm, immediately overlying the mesoderm. Segmental organization of the ectoderm and mesoderm is first manifested in the direct descendants of the teloblasts (stages 6 and 7). Beginning an hour after its birth (i.e., stage 5 for the M cells and stage 7 for the O/P cells), each teloblast repeatedly divides (about once per hour and several dozen times in all) from a single anterior budding site, giving rise to much smaller primary blast cells. Each blast cell remains in contact with the one born immediately before it and with the one born immediately after it. Consequently, the blast cells are organized into coherent columns (bandlets) in the order of their individual birth rank. Ultimately, the first-born blast cells contribute their definitive progeny to anterior segments, and later-born cells contribute to the posterior segments.

The five bandlets on each side of the embryo join together to form structures called germinal bands (stage 7) which lengthen as blast cells are produced at the posterior end of the bandlets. The germinal bands on each side of the embryo meet at the site of the future head and coalesce progressively from anterior to posterior along the future ventral midline, forming a structure called germinal plate (stage 8).

In normal development, each teloblast contributes a distinct, segmentally iterated set of definitive progeny to the leech via its primary blast cell progeny. The composition of these segmentally iterated sets of cells, called M, N, O, P, or Q kinship groups, can be predicted from the identity of the parent teloblast, except in the case of the O/P teloblasts; ipsilateral O/P teloblasts arise from an equal cleavage as indistinguishable sister cells. In fact, each O/P teloblast and its immediate progeny are developmentally plastic, capable of generating either O or P kinship groups. In any given

Helobdella embryo, the particular fate of the O/P teloblasts can be determined retrospectively, at which point they can be designated as "generative O" and "generative P" teloblasts (Weisblat and Blair, 1984) [for an update, see Lans *et al.* (1994)].

During stage 9, segments become apparent in the germinal plate in an anterior-to-posterior progression, first through the delineation of mesodermal hemisomites and later through the appearance of segmental ganglia along the ventral midline. During stage 10, the edges of the expanding germinal plate meet along the dorsal midline, thereby closing the body tube. By the end of stage 11, the segmental tissues have differentiated to a state approximating their mature form.

IX. Possible Points of Homology between Annelids and Arthropods

One attractive but short-lived proposal for homology between leech and fly development held that each teloblast underwent five (or more) rounds of syncytial nuclear divisions to generate multiples of 32 nuclei, which were then parceled out by the subsequent blast cell divisions (G. S. Stent and D. A. Weisblat, unpublished). This proposal had the advantage of providing a point of homology between annelids and arthropods, as well as a mechanism for counting out the correct number of segmental founder cells. However, it was quickly shown that the teloblasts undergo one round of mitosis per blast cell produced (Zackson, 1982). Moreover, teloblasts generate supernumerary blast cells, which fail to generate segmental primordia (Weisblat *et al.*, 1984; Zackson, 1984). The mechanism by which segments are counted out remains a mystery.

Cell lineage analyses of segmentation suggest other possible points of homology. One important set of observations concerns the relationship between primary blast cells and the final segments. In three of the segmental lineages (M, O, and P), a single primary blast cell makes one segment's worth of progeny, whereas two primary blast cells are required in the N and Q lineages (Weisblat *et al.*, 1984; Zackson, 1984; Weisblat and Shankland, 1985). As discussed in greater detail in the next section, the two n and two q blast cells that contribute to a segment can be assigned distinct identities on the basis of various differences. The first to be observed was a difference in the timing of their first mitoses (Zackson, 1984); thus, they are referred to as nf (first-to-divide) and ns (second-to-divide) and qf and qs blast cells, respectively.

A prominent feature of metamerism in *Drosophila* is the establishment of subdivisions called compartments within the ectoderm of the embryo. Compartments were originally defined by the property that the cells in a

compartment would mingle readily among themselves, but not with cells in adjacent compartments (Garcia-Bellido *et al.*, 1973; Garcia-Bellido, 1975). Like the alternating nf and ns blast cells in the leech embryo, compartments arise along the length of the fly embryo at exactly twice the spatial frequency of the segments. Each metameric repeat therefore contains two compartments, which can therefore be defined as "anterior" and "posterior" compartments on the basis of their position within the traditionally defined segments. In fact, a variety of experiments indicate that the "parasegments" generated by pairing each "posterior" compartment with the *caudally* located "anterior" compartment are of greater

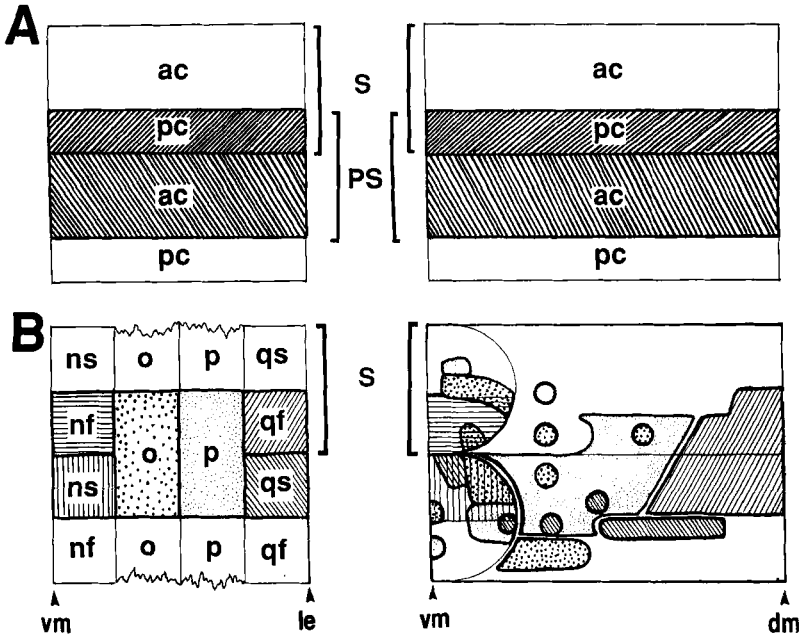

Fig. 6 Comparison of compartments, segments, and parasegments in *Drosophila* ectoderm with the clonal contributions of the six classes of ectodermal blast cells in leech. (A) *Drosophila*. Both the blastoderm (left) and the adult epidermis (right) are divided into anterior and posterior compartments (ac and pc) consisting of polyclones of indeterminate lineage (not shown). Adjacent pairs of compartments define segments (S) or parasegments (PS). The final distribution of clones arising from individual cells within a compartment in normal development has not been determined, but they are believed to be variable in size and shape. (B) Leech. In each half of the early germinal plate (left), clones arising from single primary ectodermal blast cells (nf, ns, o, p, qf, qs) are aligned more or less according to the boundaries anticipated from a parasegmental organization. Whether these early clones experience compartment-like restrictions on cell mingling is unknown, but the final distribution of the primary blast cell clones (right) crosses even segment boundaries, both in the central nervous system (hemicircles along ventral midline denote segmental ganglia) and in the body wall. vm, ventral midline; le, lateral edge of germinal plate; dm, dorsal midline.

embryological significance (Fig. 6A; Martinez-Arias and Lawrence, 1985). Each compartment is a polyclone [i.e., the sum of all the cells descended from each of a set of founder cells; Crick and Lawrence (1975)] and extends across the entire epidermis.

The similarity at the cellular level between the alternating nf and ns blast cells in leech and the alternation of compartments in fly is obvious, but whether this represents homology is less clear-cut. For example, leech segments are *not* polyclones founded by seven bilateral pairs of primary blast cells, because there is extensive interdigitation of adjacent clones, especially within the M, O, and P lineages (Fig. 6B; Weisblat and Shankland, 1985). This extensive interdigitation of blast cell clones also means that leech segments cannot be subdivided into compartments per se.

These complications notwithstanding, the observation that two primary blast cells in each N (and Q) cell line are required to make one segment's worth of definitive progeny had led, at least indirectly, to more promising comparisons between leech and fly at both the cellular and the molecular levels. Early lineage-tracing experiments showed that in normal development, the two n blast cells contributing to a given segment make distinct sets of definitive progeny, mainly neurons of the segmental ganglion (Weisblat *et al.*, 1984; Kramer and Weisblat, 1985; Weisblat and Shankland, 1985). The blast cell clones that arise from alternate n blast cells can also be easily distinguished by their morphology in the germinal plate during stages 8 and 9 (i.e., one clone extends farther laterally than the other). Similar observations hold for the q blast cells, which mainly contribute dorsal epidermal progeny to the segment (Weisblat and Shankland, 1985; Torrence, 1991). Thus, the N and Q teloblasts constitute an intriguing variant of the stem cell division mode termed the "grandparental iteration" (Chalfie *et al.*, 1981) [for a discussion, see Stent and Weisblat (1985)].

Obvious questions regarding this pattern exactly alternating cell fates are: when and by what mechanisms do the alternate primary blast cells in the n bandlet become determined to assume distinct fates? Do they start out as equipotent cells and then assume distinct fates through a rostrocaudal version of the mediolateral interactions regulating cell fate in the O–P equivalence group? Or are they assigned distinct fates at birth? The distinction between these alternatives is important for guiding our thinking about the expression and function of segmentation genes in the leech embryo.

X. Blast Cell Identity May Be Determined at Birth: nf/ns Differences

Various ablation experiments failed to reveal the plasticity in the fates of n blast cells that would be expected if their fates were determined by cell

interactions within the germinal bands (Bissen and Weisblat, 1987). While such negative evidence can never be convincing, several different sets of observations, summarized here, lend support to the alternative idea that primary blast cells have distinct identities from birth.

Stereotyped differences in the timing and symmetry of early mitoses of the primary blast cells provide evidence that these cells are different from one another, at least by the time they enter their first mitoses. For example, the class of primary n blast cells designated nf has a cell cycle of 20 hr duration and then divides unequally to generate larger anterior and smaller posterior secondary blast cells (Zackson, 1984); nf contributes progeny mostly to the posterior portion of the segmental ganglion (Bissen and Weisblat, 1987). Alternate primary n blast cells, of the class designated ns, have a cell cycle of about 28 hr, divide equally, and contribute mostly to the anterior portion of the ganglion.

To look for earlier differences among primary blast cells, the composition of their cell cycles was examined in detail using BrdUTP incorporation to label S-phase nuclei (Bissen and Weisblat, 1989). However, since all the primary ectodermal blast cells lack G1 phase and have S phases of about the same length (about 4 hr), this analysis provided no earlier time point by which the cells were obviously different. For technical reasons, it is impossible to learn the precise composition of the cell cycles by which the parent teloblast generates nf and ns blast cells using the BrdUTP labeling technique. However, some intriguing observations with microinjected lineage tracers provide evidence for a subtle difference between alternate cell cycles of N teloblasts (Bissen and Weisblat, 1987).

If N teloblasts in a group of embryos are injected with lineage tracer at random times during stage 7, after they have begun producing primary blast cells, the most anterior-labeled primary blast cell (i.e., the first primary blast cell produced after the microinjection) is equally as likely to be of the nf class as of the ns class. This observation indicates that the cell cycles by which nf and ns blast cells are produced are equal in overall length. Moreover, microinjected cell lineage tracers diffuse throughout the injected teloblast in minutes; and because the relatively large volume of the teloblast acts as a reservoir of lineage tracer, the primary blast cells to which the teloblast subsequently gives rise are usually labeled with equal intensity. However, in a significant proportion of embryos, the first blast cell produced after the injection is labeled with markedly less intensity than all the subsequent cells. For brevity, these faintly labeled cells are called "faint first blast cells" (Fig. 7). The exact cause of this phenomenon is unknown; one possibility is that it results when the tracer is injected near the end of cytokinesis, before the membranes have completely sealed, but when the presence of the midbody prevents ready diffusion between the two compartments. A priori, one would expect that these faint first

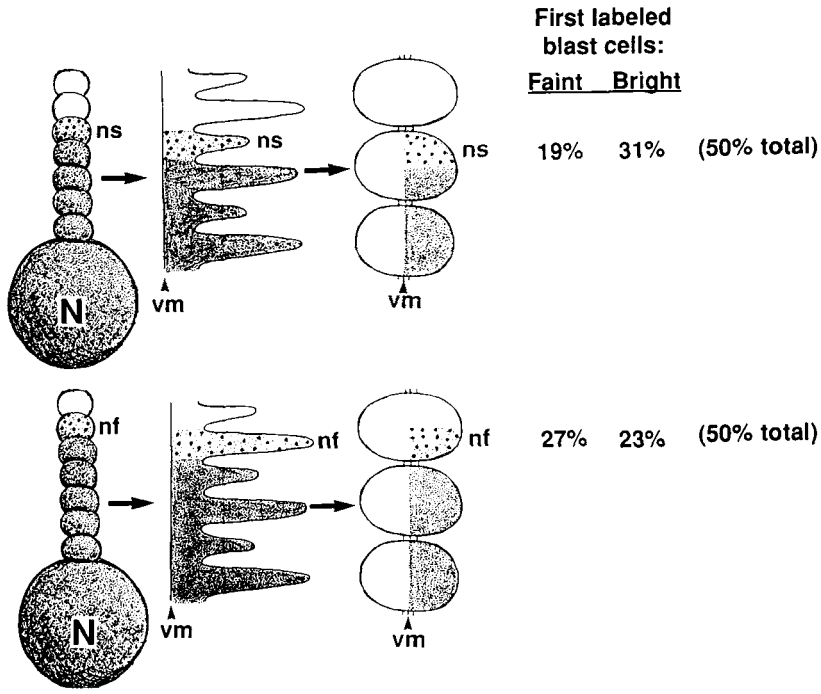

Fig. 7 Evidence that nf/ns blast cell identity is determined at birth. When an N teloblast is injected with lineage tracer (stippling) during stage 7, after blast cell production is already underway, the first blast cell in the resulting chain of tracer-labeled blast cells is equally likely to be of the ns (top) or nf (bottom) class. The nf and ns classes can be distinguished by the timing and symmetry of the first division (not shown), the shape of the clone in the germinal plate (center), or the location of the definitive progeny within the segment (right). Typically, all the blast cells born after the injection are labeled with equal intensity. But occasionally, as illustrated in both the bandlets here, the first cell born after the injection is less intensely labeled (light stippling) than all the subsequent cells (dark stippling). Such "faint first" blast cells are in fact more commonly found when the first labeled blast cell is of the nf class, indicating that teloblast cell cycles producing nf and ns blast cells differ in composition, despite being equal in overall length.

blast cells would be equally likely to be of the nf and ns classes. But faint first blast cells are in fact more common when the first labeled blast cell is of the nf class than when it is of the ns class (Fig. 7). This result could reflect a longer telophase in cell cycles generating nf blast cells than in cell cycles generating ns blast cells. In any case, the difference in the distribution of faint first blast cells appears to reflect some inherent difference in the cell cycles by which nf and ns blast cells are produced, and suggests that the two classes are different at birth.

XI. Blast Cell Identity May Be Determined at Birth: Regional Differences

Another set of observations regarding the acquisition of specific identities by individual blast cells concerns regionalization, i.e., the generation of segment-specific differences in blast cell fates. Immunostaining with commercially prepared antibodies revealed segment-specific differences in the distribution of some of the neurons that exhibit small cardioactive peptide (SCP)-like immunoreactivity; double labeling with lineage tracer and antibody showed that these neurons arise from the N teloblast in anterior ganglia R4 and M1–M3 (Shankland and Martindale, 1989). These neurons have no homologs in midbody ganglia M4–M17. (Curiously, posterior homologs of these neurons in ganglia M18–M21 and C1–C4 arise from the M teloblast!) Using a photolesioning technique (Shankland, 1984) that causes blast cells in individual bandlets to be shifted several segments posterior to the segments to which they would normally contribute, Martindale and Shankland (1990) showed that n blast cells still give rise to SCP-like immunoreactive neurons when shifted to segments that normally lack such neurons (Fig. 8).

The n blast cells whose fates are assayed in these experiments are not shifted until several hours before their first mitosis, i.e., more than 12 hr after their birth; therefore, it cannot be concluded that they inherit a segment-specific identity at birth. However, when the photolesioning technique was applied to the M lineage (Gleizer and Stent, 1993), and m blast cells were shifted either anterior or posterior to their normal location as soon as 2–3 hr after their birth, they still gave rise to ectopically situated progeny (in this case nephridia and gonadal tissues).

Thus, it seems appropriate to look for molecular-genetic explanations of teloblast function that account for the generation of segment-specific identities in blast cells as they are produced. In the N and Q lineages, this process needs to be overlaid with a separate process in which alternate blast cells are simultaneously assigned anterior and posterior identities within the segment. Within this framework of knowledge regarding the cellular processes of regionalization and segmentation, we can now address the issues of molecular-genetic homology in rostrocaudal patterning between leech and fly.

XII. Molecular-Genetic Basis of Rostrocaudal Patterning in *Drosophila*

The process of regionalization and segmentation in *Drosophila* can be divided into five semidistinct steps, as defined by the action of different genetic syntagmata [for a review, see Tautz (1992)]. First, maternal regula-

tory gene products such as *bicoid* are deposited asymmetrically along the anterior–posterior (A–P) axis in the egg. These products determine where the second set of genes, that define broad regions along the A–P axis, the gap genes, are expressed in the syncytial blastoderm. Before cellularization, interactions between the gap genes and the maternal regulatory gene products allow the third set of genes, that control segment number, the pair-rule genes, to be expressed in metamerically repeated stripes along the A–P axis, separated by a single segment's width. The members of a fourth set of genes, called the segment polarity genes, operate at various times, each within a specific portion of a given segment, to establish A–P polarity. After cellularization of the blastoderm, further interactions between the pair-rule and gap gene products determine where along the A–P axis each of the fifth set of genes, the homeotic genes, is expressed. These genes affect regionalization, i.e., individual segment identity, by interacting with target realizator genes. With this wealth of molecular–genetic illumination available from the study of rostrocaudal patterning in *Drosophila*, where should we start to look for syntagmal homologs?

XIII. Putative Regionalization Genes in Leech: Expression of Homeotic Gene Homologs

A frequent (though not universal) characteristic of homeotic genes in *Drosophila* is that the domain of action (Lewis, 1978) and expression (Harding *et al.*, 1985) lies posterior to some rostrocaudal boundary, the exact position of which varies from one homeotic gene to another. One of the most dramatic, and yet to be understood, aspects of the homeotic genes is that they are physically arrayed along the chromosome within a single complex in the order reflecting the rostrocaudal progression of the boundaries defined by their expression. Moreover, not only are homologs of these genes found in other phyla, including chordates (McGinnis and Krumlauf, 1992), but this same correlation between expression pattern and chromosomal arrangement holds true (Graham *et al.*, 1989; Duboule and Dolle, 1989).

In light of the foregoing considerations, it is hardly surprising that several candidates for homologs of homeotic genes have been identified in leeches [summarized in Shankland *et al.* (1991)]. To date, the expression of only one of these genes, *Lox-2*, has been published (Wysocka-Diller *et al.*, 1989; Nardelli-Haefliger and Shankland, 1992). This gene bears equally close sequence homology to two *Drosophila* homeotic genes, *Ultrabithorax* (*Ubx*) and *abdominal-A* (*abdA*). In *Drosophila* embryos, transcripts of the homeotic genes begin to accumulate at approximately the same time as do those of *en* (Harding *et al.*, 1985), but *Lox-2* transcripts accumulate in late stage 8 and stage 9, around the time when germinal

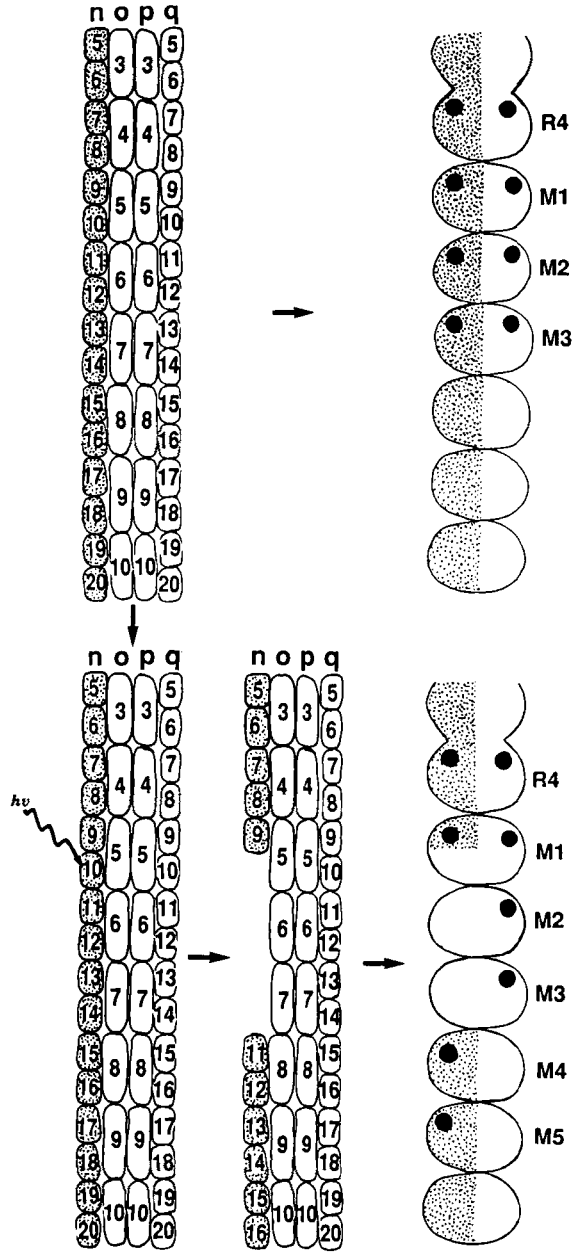

Fig. 8 Evidence that segmental identities of blast cells are determined early in development. A schematic representation of part of a germinal band (upper left) shows the normal relationships of blast cell clones in the ectodermal bandlets. Anterior is up; numbers indicate the birth rank ordering of the blast cells and their descendant clones. In normal development,

plate formation is completed and markedly later than the early expression of *ht-en* protein. Nonetheless, the pattern of accumulation shows striking parallels to that of homeotic genes in *Drosophila*. *Lox-2* is expressed in all five bandlets, except possibly the p bandlet, beginning in segment M6 or M7 and extending throughout all (or most, depending on the species of leech examined) of the more posterior segments.

XIV. Putative Segmentation Genes in Leech: Expression of an *engrailed* Homolog

Given the analogy between the subdivisions of the N (and Q) lineage in leech embryos and the anterior/posterior compartments in *Drosophila*, one obvious place to look for homology in their segmentation processes was with the *Drosophila* segment polarity gene called *engrailed* (*en*). At about the same time that compartment boundaries of established in *Drosophila*, a circumferential band of cells corresponding to the posterior compartment of each segment begins expressing the gene *en* (Kornberg *et al.*, 1985; DiNardo, 1985). As one would expect when dealing with interacting regulatory genes, the assumption of anterior and posterior compartment fates does not reduce to simply whether the cells express *en*. But *Drosophila* embryos mutant for *en* do show signs that the identity of the posterior compartment has been perturbed; restrictions on cell mingling across presumptive compartment boundaries are lost and cuticular structures appropriate for the anterior compartment are seen in the presumptive posterior compartment (Lawrence and Morata, 1976; Nusslein-Volhard and Weischaus, 1980; Kornberg, 1981a,b; Lawrence and Struhl, 1982). The *en* gene is also expressed during neurogenesis in *Drosophila*, in a subset of segmentally iterated neurons, where it presumably participates in the specification of particular neuronal phenotypes (Patel *et al.*, 1989). The question of whether this neural expression in later development is confined to cells of one compartment remains unanswered.

Because *en* homologs had been cloned from a number of animal groups, including even vertebrates, it seemed likely that a homolog should be

---

this section of germinal band contributes to the ipsilateral half of the portion of the ventral nerve cord indicated at top left, including RAS neurons (black circles) which normally occur only in ganglia R4-M3 and are progeny of n blast cells numbered 7, 9, 11, and 13, respectively. If the n bandlet contains a photosensitizing lineage tracer (stippling), a laser beam directed through the microscope objective can be used to kill a single blast cell in the n bandlet (bottom left). Cells posterior to the lesion in the n bandlet then slip caudally with respect to the other bandlets (bottom center). As a result, these blast cells contribute their progeny ectopically and RAS neurons appear in segments M4 and M5, where they are not normally found (bottom right).

present in leech, and this proved to be the case. (That this point was even in question in the 1980s illustrates the dramatic progress made since then in the comparative aspects of our field at the molecular level.) The expression of this *engrailed*-class gene (*ht-en*) was studied with the expectation or, more accurately, the hope that it might be a marker for the early differentiation of the two classes of blast cells produced in the n (and/or q) bandlets, e.g., nf and ns primary blast cells. Since it had been shown that primary blast cells initiate transcription immediately upon their birth (Bissen and Weisblat, 1991), it was hoped that *ht-en* would be expressed by alternate blast cells and their descendant clones in the n and q bandlets from the time of their birth, or even by the parent teloblast during every other cell cycle. Although the actual results are not that simple, they nonetheless strongly suggest syntagmal homology between the *engrailed*-class genes in annelids and arthropods.

The expression pattern of *ht-en* was initially misinterpreted (Patel *et al.*, 1989; Weisblat *et al.*, 1988) through the use of a monoclonal antibody that cross-reacts with *engrailed* homologs in many, but not all, species (Patel *et al.*, 1989). Leeches are among the exceptions (Wedeen and Weisblat, 1991). Using a polyclonal antibody raised against a translation product of the leech gene, investigators have described in some detail the true expression pattern of *ht-en* (Wedeen and Weisblat, 1991; Lans *et al.*, 1993). The main features of this expression pattern are summarized in Fig. 9. *ht-en* is expressed in a highly stereotyped, segmentally iterated pattern, both in early development before gangliogenesis and later during neurogenesis. The early expression of *ht-en* is transient; the protein eventually disappears from almost all of the cells that initially express it. Later expression arises *de novo* in cells of the nervous system and body wall. In *Helobdella*, it is clear that many of these cells expressing *ht-en* later are not clonal descendants of cells that initially express *ht-en* (a point that remains unresolved for cells expressing *engrailed* in later *Drosophila* development). The later expression is predominantly, if not exclusively, in segmentally iterated neurons and appears to persist into adulthood.

Before gangliogenesis, *ht-en* is expressed in a specific subset of cells in each of the bandlets, including the mesodermal (m) bandlet and the two ectodermal bandlets (o and p), in which each primary blast cell makes one segment's worth of progeny. The timing of *ht-en* expression varies among the five types of bandlets; within each bandlet, the timing of expression is invariant with respect to age of the individual blast cell clones and therefore occurs in a rostrocaudal progression that mirrors the birth order of the blast cells. *ht-en* is not expressed by any of the primary blast cells or teloblasts. The earliest expression (e.g., in the p bandlet) is in blast cell clones comprising at least five cells. When cells expressing *ht-en* divide, *ht-en* may be expressed by one, both, or neither of the daughter cells.

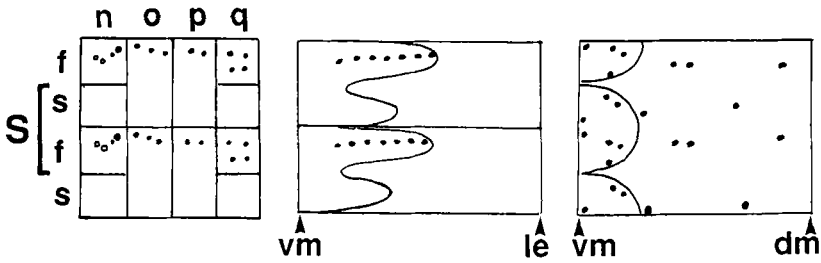

Fig. 9 *ht-en* expression in *Helobdella*. Each panel respresents one hemisegment (large S) and parts of the hemisegments just anterior and posterior to it. In the germinal band and early germinal plate (left), ectodermal blast cell clones (squares and rectangles) are arrayed as shown in Fig. 6B (f and small s denote the two classes of n and q blast cells). *ht-en* expression in ectodermal nuclei (black circles) and underlying mesodermal nuclei (white circles) occurs asynchronously in different bandlets, but cells that express *ht-en* during this early period lie in a narrow rostrocaudal domain in the caudal portion of the prospective segment. During gangliogenesis (center) the nf and ns clones extend laterally (longer and shorter contours, respectively); *ht-en* is expressed by a transverse row of cells (black circles) that are a subset of the nf clone. Later still, *ht-en* expression (black circles) is observed in a specific subset of neurons in segmental ganglia (denoted by hemicircular contour) and in peripheral cells. Some cells expressing *ht-en* at this time are descendants of those that expressed it earlier; other are not. vm, ventral midline; le, lateral edge of germinal plate; dm, dorsal midline.

The early expression of *ht-en* occurs in a transverse stripe of cells that defines the boundary between prospective ganglia. This stripe is most obvious in the cells that express *ht-en* in the N lineage, but all the cells that express *ht-en* during this early period line up within a narrow rostrocaudal domain of the prospective segment.

In the n and q bandlets, the early expression of *ht-en* is confined to just one of the two types of blast cells. In the n bandlet, the transverse stripe of cells that express *ht-en* are members of the nf clone. In the q bandlet, the entire qf clone expresses *ht-en* during the period when the clone consists of four or five cells.

XV. Comparison with Arthropods

By comparing the expression patterns of *engrailed*-class genes in various organisms, we can try to infer the common features that would have been present in their common ancestor. Until techniques are devised for manipulating the expression of *ht-en* in leech embryos, these comparisons can also guide speculation about the function of *ht-en* in leech development.

The features of *engrailed*-class gene expression that appear to be common to leeches and flies include expression both before gangliogenesis and during neurogenesis in unrelated sets of cells. Early expression is known to play a role in segmentation in fly and is at least correlated with the formation of interganglionic boundaries in leech. Although the definitive segments in the leech body do not constitute polyclones and cannot be divided into compartments as in *Drosophila,* the alignment between bandlets of the cells that express *ht-en* suggests the possibility of a transient grouping of clones in the germinal plate during stages 8 and 9 that is homologous to the *Drosophila* parasegment (Figs. 6 and 9).

It was once assumed that the expression of *en* defined the posterior compartment throughout the lifetime of *Drosophila* and that the compartment boundaries were maintained by the clonal inheritance of *en* expression from en^+ cells in early embryogenesis. However, studies show that cells expressing *en* can divide and give rise to en^- cells (Vincent and O'Farrell, 1992), and that in later development *en* cells are found within the boundaries of the posterior compartment (Blair, 1992). Therefore, in *Drosophila,* early *en* expression is not clonally transmitted, and *en* expression is not required in the entire compartment throughout the lifetime of the animal. A similar transient and nonclonally transmitted expression of *ht-en* was initially observed in leech. These features may be general features of the expression of *engrailed*-class genes in protostomes since other arthropods (crustaceans) do not show strict clonal transmission of *en* expression. Scholtz *et al.* (1993) found that a subset of *en*-expressing cells in a clone loses *en* expression, but that a partial subset of the nonexpressing cells later regains expression. The finding that *ht-en* is expressed in the mesoderm of *Helobdella* contrasts with the findings in *Drosophila.* But mesodermal expression of *engrailed*-class genes is seen in other distantly related groups, including chordates (Hatta *et al.,* 1991; Davis *et al.,* 1991) and onychophorans (Wedeen and Whitington, unpublished observations). Thus, it seems likely that *engrailed* was expressed in both mesoderm and ectoderm of the common ancestor of these groups (if the common ancestor had mesoderm) and that it was lost from the mesoderm of arthropods after the annelid and arthropod lines separated in evolution.

XVI. Expanding the Syntagmata

Given the similarity of expression patterns for *engrailed*-class genes in annelids and arthropods, the syntagma concept can be investigated by looking for annelid homologs of genes that interact with *en* in *Drosophila* and characterizing their expression patterns. Two genes that interact with

en in *Drosophila* are *wingless* (*wg*) and *cubitus interruptus Dominant* (*ci-D*): in the cellular blastoderm of *Drosophila, wg* is expressed in the band of cells just anterior to those expressing *en* in each segment (van den Heuvel *et al.*, 1989), and *ci-D* is eventually expressed in all the cells except those expressing en (Orenic *et al.*, 1990). These genes are also segment polarity genes and (with others) can be considered as belonging to the same syntagma as *en*. This syntagma appears to function also in the development of the wing imaginal disc, presumably by operating on a different set of realizator genes (Blair, 1992). Both of these genes have homologs in other species, including vertebrates. *wg*, in particular, is part of the *Wnt* family, which has at least three members in *Drosophila* (Eisenberg *et al.*, 1992; Russell *et al.*, 1992) and more in vertebrates (Sidow, 1992) (*wg* and its direct homologs in other species are now assigned to the *wnt-1* subfamily).

In leech, a clear sequence homolog to *ci-D* (designated *Htr-ci-1*) has been identified by PCR (Weisblat *et al.*, 1993), and a sequence homologue to *wnt-1* may have been found (R. Kostriken, unpublished observations). Given the detailed knowledge of the expression patterns of *ht-en*, clear predictions as to how these genes would be expressed if their syntagmal relationships were conserved can now be made (Fig. 10).

Other possible leech homologs of *Drosophila* homeotic genes have also been isolated, and their expression patterns are being analyzed; these include *Lox5*, an *Antennapedia*-like gene; *Lox6*, a *Deformed*-like gene; and *Lox7*, a *labial*-like gene [reviewed in Shankland *et al.* (1991); M. Shankland, personal communication]. Obvious questions are how many

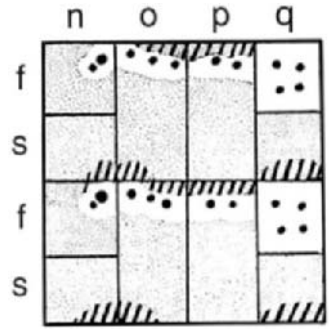

Fig. 10 Expected expression patterns for *htr-ci* and *htr-wnt-1* in the germinal band and early germinal plate; compare with left panel in Fig. 9. If syntagmal interactions are conserved for the leech homologs of the *Drosophila* segment polarity genes, we expect that *ci-D* expression (stippling) will be seen in all the ectodermal cells that do not express *ht-en* (black circles) and that *htr-wnt-1* (hatching) will occur in a narrow domain of cells just anterior to the cells that express *ht-en*.

and what other homologs of what is now termed the HOM/Hox complex (Akam, 1989; Graham *et al.*, 1989) will be present in leech and whether their organization along the chromosome(s) will also be conserved.

XVII. Speculation on Temporal Mechanisms of Patterning

As described earlier, embryological evidence suggests that blast cells' fates are specified one by one as they arise from the parent teloblast. Thus, understanding how this cell cycle-dependent specification of cell fate proceeds, presumably with the involvement of homologs of the same genes that control regionalization in *Drosophila*, becomes the crux of the distinction between the spatial and temporal modes of regionalization and segmentation.

For the rostrocaudal patterning gene homologs that have been described to date in leech, expression occurs only after proliferation of secondary blast cells is well advanced, and thus gives no definitive information about processes in the teloblasts. [*Lox5*, the *Antp* homolog may be the first exception (M. Shankland, personal communication).] As yet, no leech homologs to *Drosophila* genes in the maternal, gap, or pair-rule classes of developmental regulatory genes have been identified. But assuming these classes of genes do exist in leech, can the results already obtained with the homologs of segment polarity and homeotic genes guide our thinking about what to anticipate for their occurrence and function?

One means by which a cell cycle-dependent specification of blast cell fates might be achieved would be for the teloblast to undergo a heritable change with each cell cycle. Thus, each blast cells would receive an inheritance reflecting the state of the teloblast during the cell cycle of its birth. The results obtained so far suggest that the state of the teloblast might be dictated by the qualitative and quantitative mix of factors that regulate segment polarity and homeotic genes (Fig. 11). For example, a *bicoid* homolog translated from a maternally inherited mRNA (if such exists) could be present at high levels in the newborn teloblast, and then decline continuously during blast cell production as the *bicoid*-homolog mRNA and protein are either degraded and/or partitioned into blast cell progeny. Thus, the *bicoid* homolog would exhibit a temporal concentration gradient within the teloblast, in contrast with its spatial concentration gradient in the *Drosophila* zygote.

If homologs of gap genes were also present in leech and functioning in an evolutionarily conserved syntagma with the postulated *bicoid* homolog, we could further predict that a young teloblast would also contain high levels of *hunchback* homolog, whose expression would fall as *bicoid* levels dropped, permitting the expression of *Kruppel* and *Knirps* homologs to

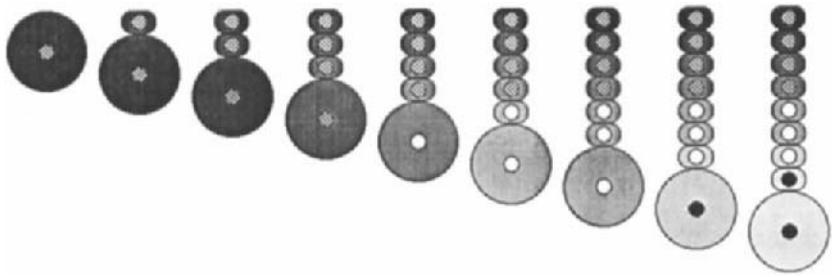

Fig. 11 Speculation on a temporal mechanism for regionalization. A maternally inherited gene (analogous to *bicoid* in *Drosophila*) that is active at high levels (dark shading, left) in young teloblasts (large circles) and declines gradually (progressively lighter shading, center and right) during production of blast cells (small circles) would effect a temporal gradient of gene activity within the teloblast. This temporal gradient could affect the transciptional activity of blast cells born at different times both directly and by affecting the phasic transcription of one or more zygotic gap-like genes (checkered, white and black circles) within the teloblast and blast cells that are turned on and off as the declining activity of the maternal gene product passes through different threshold values.

rise and fall sequentially within the teloblast and their descendant blast cells (Fig. 11). Each chain of blast cells would be thereby subdivided into transcriptionally distinct groups of cells. These transcriptional subdivisions would then in turn differentially express genes such as the homologs of the HOM/Hox genes to specify segment identity. Thus a series of segment identity genes would be activated sequentially along the chains of blast cells descended from each teloblast.

XVIII. Speculation on Temporal Mechanisms of Segmentation

The temporal control of segmentation is relatively straightforward in the case of the O, P, and M lineages. Since individual blast cells produced by M and O/P teloblasts give rise to one segmental complement of progeny, the simple reiteration of (approximately) the same developmental program by each blast cell produces a segmentally repeated pattern of tissues along the anterior–posterior body axis.

The behavior of the N and Q lineages is more complex and appears to require an additional level of regulation, however. Each n and q bandlet consists of alternating cell types (nf and ns; qf and qs), so that for these bandlets, one segmental complement is descended from a pair of blast cells. As described here, it appears that the f and s blast cells differ at birth; moreover, since *ht-en* (the leech homolog of *engrailed*) is not

expressed until the s and f blast cell clones are well along their separate developmental pathways, it seems unlikely that a putative syntagma of segment polarity gene homologs in leech is involved in the initial specification of different fates for f and s blast cells. Another possibility is that "upstream" regulators of the segment polarity genes are involved in distinguishing the s from f cells; if we persist in seeking homology with *Drosophila,* homologs of the pair-rule genes (again, assuming that there are homologs of these genes in leech) would be logical candidates for such upstream regulators.

In *Drosophila,* it is believed that the expression of "primary" pair-rule genes, such as *runt, even skipped,* and *hairy,* is regulated directly by levels of bicoid and gap genes (Small and Levine, 1991; Tautz, 1992). The large promoters of these genes contain many, relatively independent regulatory sites, each of which is capable of initiating expression in response to a particular concentration of *bicoid* and gap gene products. Thus, these promoters "read" the position of the nucleus along the length of the embryo. Other secondary pair-rule genes, such as *fushi tarazu,* are regulated by the primary genes.

In leech, the production of f and s class cells could result from a further refinement of the heritable states through which the teloblast progresses, due to cyclic changes in the concentration (or activity) of one or more pair-rule gene products. Any such scheme requires that the pair-rule gene products be relatively short lived and also that the effects of pair-rule gene expression be reversible in some sense, so that the state of the teloblast can be "reset" from the state in which one pair-rule gene is on to the one in which it is off and vice versa. The cyclic changes in activity of the pair-rule genes would result from interactions among the products of the pair-rule genes themselves and with other genes, including presumably the gap genes, and one or more of the genes involved in controlling the cell cycle of the teloblast. Interaction with the cell cycle control mechanism is postulated to account for the fact that f and s blast cells arise in strict alternation during successive cell cycles of the N and Q teloblasts.

The postulated network of interacting genes would constitute a biochemical oscillator. Activities of the components of such oscillators (in this case, presumably the various gene products) rise and fall in defined phase relationships. Here, one or more of these cycling gene products would also serve to determine the different states of successive blast cell progeny. In the simplest form of this model (Fig. 12A), a single pair-rule gene product would be expressed, during alternate cell cycles in the N and Q teloblasts. Alternatively, two or more pair-rule genes functioning within the teloblast, each with fewer but longer periods of overlapping expression, which define distinct states of the teloblast in a combinatorial manner (Fig. 12B). This latter model is appealing because it more closely resembles

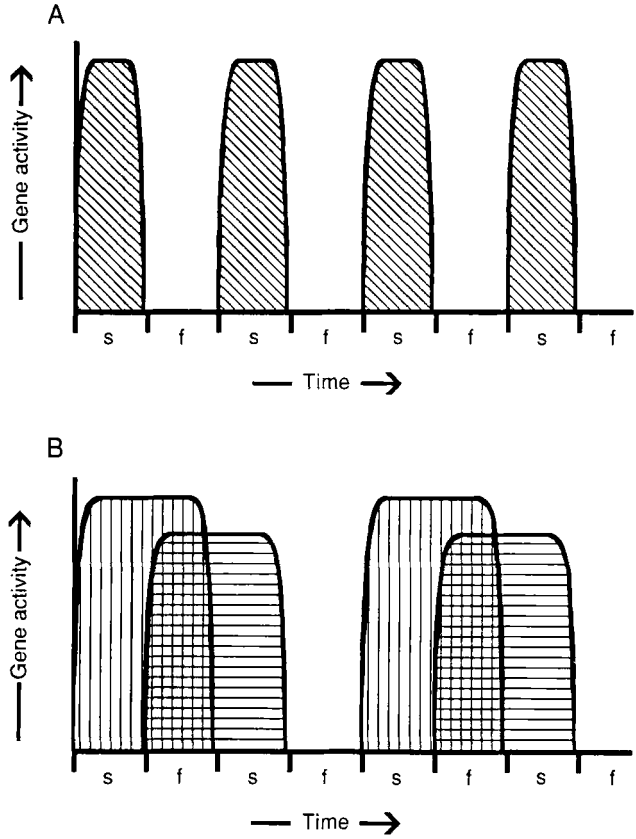

Fig. 12 Two models for temporal control of segmentation by pair-rule homologs. Successive teloblast cell cycles, leading to the production of alternating f and s blast cells, are separated by vertical ticks on the time axis. A single pair-rule gene would suffice to determine distinct f and s types if the activity of its gene product (diagonal hatching) turns on and off in alternate cycles of the teloblast (A). Alternatively (B), two or more genes expressed for longer, but overlapping periods could be used in a combinatorial manner to determine distinct f and s cell types. In this case, expression of either of two pair-rule genes (vertical and horizontal hatching) alone determines the s state, while expression of both or neither determines the f state.

the current proposals for the role of pair-rule genes in specifying cell fates in the *Drosophila* blastoderm (Baumgartner and Noll, 1990). But evolutionary arguments notwithstanding, we must also bear in mind that this aspect of leech development may be controlled by a genetic mechanism that is unrelated to those involved in *Drosophila* (such as that used in yeast mating type switching) (Haber, 1992; Klar, 1992) or by a mechanism that is not directly related to gene expression at all.

XIX. Conclusions

Descriptive comparisons of morphology and development in different species indicate that developmental changes during evolution can occur either as "terminal variations" appended to highly conserved early processes or as modification of the intermediate steps leading to relatively well-conserved endpoints. Here, we have considered the paradox posed by the fact that the segmented body plans of leeches and flies, while surely homologous, arise by dramatically different "temporal" and "spatial" modes of segmentation, respectively.

We have heightened this paradox by focusing on these two extremes in the continuum of possible modes of segment formation. But it is important to bear in mind that many or most of the other arthropods (short germ band insects and crustaceans) are intermediate between the long germ band insects and the annelids in that they utilize aspects of both the spatial and temporal modes of segment formation, often in different regions of the embryo [e.g., see Dohle and Scholtz (1988)]. We suggest that the experimental analysis of segmentation can be simplified by focusing first on the two extremes exemplified by fly and leech. Nonetheless, despite the common notion that arthropods and other segmented protostomes arose from annelid-like ancestors, we cannot rule out the possibility that the spatial and temporal modes of segmentation may *both* be highly derived versions of an ancestral process. Further studies in comparative development, along with refinement of the underlying phylogenetic relationships by independent methods, should help to solve this puzzle.

Acknowledgments

This work was supported by NIH Grant RO1 HD23328 and NSF Grant IBN-9105713 to D. A. W.; C. J. W. was also supported by the Cancer Fund of the Damon Runyon-Walter Winchell Foundation. C.J.W. and R.K. have both received support from NIH Training Grant HD-07299. We thank Marty Shankland for helpful discussions.

References

Akam, M. (1989). Hox and HOM: homologous gene clusters in insects and vertebrates. *Cell* **57**, 347–349.

Anderson, D. T. (1973). "Embryology and Phylogeny in Annelids and Arthropods." Pergamon Press, Oxford.

Bastian, H., and Gruss, P. (1990). A *murine even-skipped* homologue, *EVX 1*, is expressed during early embryogenesis and neurogenesis in a biphasic manner. *EMBO J.* **9**, 1839–1852.

Baumgartner, S., and Noll, M. (1990). Network of interactions among pair-rule genes regulating *paired* expression during primordial segmentation of *Drosophila*. *Mech. Dev.* **33,** 1–18.

Bissen, S. T., and Weisblat D. A. (1987). Early differences between alternate n blast cells in leech embryos. *J. Neurobiol.* **18,** 251–269.

Bissen, S. T., and Weisblat, D. A. (1989). The durations and compositions of cell cycles in embryos of the leech, *Helobdella triserialis*. *Development* **106,** 105–118.

Bissen, S. T., and Weisblat, D. A. (1991). Transcription in leech: mRNA synthesis is required for early cleavages in *Helobdella* embryos. *Dev. Biol.* **146,** 12–23.

Blair, S. S. (1992). *engrailed* expression in the anterior lineage compartment of the developing wing blade of *Drosophila*. *Development* **115,** 21–33.

Chalfie, M., Horvitz, H. R., and Sulston, J. E. (1981). Mutations that lead to reiterations in the cell lineages of *C. elegans*. *Cell* **24,** 59–69.

Crick, F. H. C., and Lawrence, P. A. (1975). Compartments and polyclones in insect development. *Science* **189,** 340–347.

Davis, C. A., Holmyard, D. P., Miller, K. J., and Joyner A. L. (1991). Examining pattern formation in the mouse, chicken and frog embryos with an *en*-specific antiserum. *Development* **111,** 287–298.

DiNardo, S., Kuner, J. M., Theis, J., and O'Farrell, P. H. (1985). Development of embryonic pattern in *D. melanogaster* as revealed by accumulation of the nuclear *engrailed* protein. *Cell* **43,** 59–69.

Dohle, W., and Scholtz, G. (1988). Clonal analysis of the crustacean segment: The discordance between genealogical and segmental borders. *Development* **104** (Suppl.), 147–160.

Duboule, D., and Dolle, P. (1989). The structural and functional organization of the murine HOX gene family resembles that of *Drosophila* homeotic genes. *EMBO J.* **8,** 1497–1505.

Eisenberg, L. M., and Ingham, P. W., and Brown, A. M. (1992). Cloning and characterization of a novel *Drosophila Wnt* gene, *Dwnt-5* a putative downstream target of the homeobox gene *distal-less*. *Dev. Biol.* **154,** 73–83.

Garcia-Bellido, A. (1975). *In* "Cell Patterning" R. Porter and J. Rivers, eds.). CIBA Foundation Symposium 29, Associated Sci. Publishers, Amsterdam.

Garcia-Bellido, A. (1985). Cell lineages and genes. *Phil. Trans. R. Soc. Lond. B* **312,** 101–128.

Garcia-Bellido, A., Ripoll, P., and Morata, G. (1973). Developmental compartmentalization of the wing disk of *Drosophila*. *Nature New Biol.* **245,** 251–253.

Ghysen, A. (1992). The developmental biology of neural connectivity. *Int. J. Dev. Biol.* **36,** 47–58.

Gleizer, L., and Stent, G. S. (1993). Developmental origin of segmental identity in the leech mesoderm. *Development* **117,** 177–189.

Gould, S. J. (1977). "Ontogeny and Phylogeny." Harvard University Press, Cambridge.

Graham, A., Papalopulu, N., and Krumlauf, R. (1989). The murine and *Drosophila* homeobox gene complexes have common features of organization and expression. *Cell* **57,** 367–378.

Haber, J. E. (1992). Mating-type gene switching in *Saccharomyces cerevisiae*. *Trends Genetics* **8,** 446–452.

Harding, K., Wedeen, C., McGinnis, W., and Levine, M. (1985). Spatially regulated expression of homeotic genes in *Drosophila*. *Science* **229,** 1236–1242.

Hatta, K., Bremiller, R., Weterfield, M., and Kimmel, C. B. (1991). Diversity of expression of *engrailed*-like antigens in zebrafish. *Development* **112,** 821–832.

Jacob, F. (1982). "The Possible and the Actual." University of Washington Press, Seattle/London.

Klar, A. J. S. (1992). Developmental choices in mating-type interconversion in fission yeast. *Trends Genetics* **8,** 208–213.

Kornberg, T. (1981a). Compartments in the abdomen of *Drosophila* and the role of the *engrailed* locus. *Dev. Biol.* **86,** 363–381.

Kornberg, T. (1981b). *engrailed:* a gene controlling compartment and segment formation in *Drosophila. Proc. Natl. Acad. Sci. USA* **78,** 1095–1099.

Kornberg, T., Siden, I., O'Farrell, P., and Simon, M. (1985). The *engrailed* locus of *Drosophila:* in situ localization of transcripts reveals compartment-specific expression. *Cell* **40,** 45–53.

Kramer, A. P., and Weisblat, D. A. (1985). Developmental neural kinship groups in the leech. *J. Neurosci.* **5,** 388–407.

Lake, J. A. (1990). Origin of the metazoa. *Proc. Natl. Acad. Sci. USA* **87,** 763–766.

Lans, D., Ho, R. K., and Weisblat, D. A. (1994). Cell fates in leech embryos with duplicated lineages. *Proc. Natl. Acad. Sci. USA* **91,** (in press).

Lans, D., Wedeen, C. J., and Weisblat, D. A. (1993). Cell lineage analysis of the expression of an *engrailed* homolog in leech embryos. *Development* **117,** 857–871.

Lawrence, P., and Struhl, G. (1982). Further studies of the *engrailed* phenotype in *Drosophila. EMBO J.* **1,** 827–833.

Lawrence, P. A., and Morata, G. (1976). Compartments in the wing of *Drosophila:* A study of the *engrailed* gene. *Dev. Biol.* **50,** 321–337.

Lewis, E. B. (1978). A gene complex controlling segmentation in *Drosophila. Nature* **276,** 565–570.

Macagno, E. R. (1980). Number and distribution of neurons in leech segmental ganglia. *J. Comp. Neurol.* **190,** 283–302.

Martindale, M. Q., and Shankland, M. (1990). Intrinsic segmental identity of segmental founder cells of the leech embryo. *Nature* **347,** 672–674.

Martinez-Arias, A., and Lawrence, P. A. (1985). Parasegment and compartment in the *Drosophila* embryo. *Nature* **313,** 639–642.

McGinnis, W., and Krumlauf, R. (1992). Homeobox genes and axial patterning. *Cell* **68,** 283–302.

Muller, K. J., Nicholls, J. G., and Stent, G. S. (eds.) (1981). "Neurobiology of the Leech." Cold Spring Harbor Laboratory, New York.

Nardelli-Haefliger, D., and Shankland, M. (1992). *Lox2,* a putative leech segment identy gene, is expressed in the same segmental domain in different stem cell lineages. *Development* **116,** 697–710.

Nardelli-Haefliger, D., and Shankland, M. (1993). *Lox 10,* a member of the *NK-2* homeobox gene class, is expressed in a segmental pattern in the endoderm and in the cephalic nervous system of the leech *Helobdella. Development* **118,** 877–892.

Nusslein-Volhard, C., Frohnhofer, H. G., and Lehmann, R. (1987). Determination of anteriorposterior polarity in *Drosophila. Science* **238,** 1675–1681.

Nusslein-Volhard, C., and Wieschaus, E. (1980). Mutations affecting segment number and polarity in *Drosophila. Nature* **287,** 795–801.

Orenic, T. V., Slusarski, D. C., Kroll, K. L., and Holmgren, R. A. (1990). Cloning and characterization of the segment polarity gene *cubitus interruptus Dominant* of *Drosophila. Genes Dev.* **4,** 1053–1067.

Patel, N. H., Ball, E. E., and Goodman C. S. (1992). Changing role of *even-skipped* during the evolution of insect pattern formation. *Nature* **357,** 339–342.

Patel, N. H., Martin-Blanco, E., Coleman, K., Poole, S. J., Ellis, M. C., Kornberg, T. B., and Goodman, C. (1989). Expression of *engrailed* proteins in arthropods, annelids, and chordates. *Cell* **58,** 955–968.

Russell, J., Gennissen, A., and Nusse, R. (1992). Isolation and expression of two novel *Wnt/wingless* gene homologs in *Drosophila. Development* **115,** 475–485.

Sawyer, R. T. (1986). "Leech Biology and Behavior" Clarendon Press, Oxford.

Scholtz, G., Dohle, W., Sandemae, R. E., and Richter, S. (1993). Expression of *engrailed* can be lost and regained in cells of one clone in crustacean embryos. *Int. J. Dev. Biol.* **37,** 299–304.

Shankland, M. (1984). Positional control of supernumerary blast cell death in the leech embryo. *Nature* **307,** 541–543.

Shankland, M., and Martindale, M. Q. (1989). Segmental specificity and lateral asymmetry in the differentiation of develomentally homologous neurons during leech embryogenesis. *Dev. Biol.* **135,** 431–448.

Shankland, M., Martindale, M. Q., Nardelli-Haefliger, D., Baxter, E., and Price, D. J. (1991). Origin of segmental identity in the development o the leech nervous system. *Development* (Suppl.) **2,** 29–83.

Shankland, M., and Weisblat, D. A. (1984). Stepwise commitment of blast cell fates during the positional specification of the O and P cell fates during serial blast cell divisions in the leech embryo. *Dev. Biol.* **106,** 326–342.

Sidow, A. (1992). Diversification of the *Wnt* gene family on the ancestral lineage of vertebrates. *Proc. Natl. Acad. Sci. USA* **89,** 5098–5102.

Small, S., and Levine, M. (1991). The initiation of pair-rule stripes in the *Drosophila* blastoderm. *Curr. Opin. Genetics Dev.* **1,** 255–260.

Stent, G. S. (1981). Strength and weakness of the genetic approach to the development of the nervous system. *Annu. Rev. Neurosci.* **4,** 163–194.

Stent, G. S., Kristan, W. B., Jr., Torrence, S. A., French, K. A., and Weisblat, D. A. (1992). Development of the leech nervous system. *Int. Rev. Neurobiol.* **33,** 109–193.

Stent, G. S., and Weisblat, D. A. (1985). Cell lineage in the development of invertebrate nervous systems. *Annu. Rev. Neurosci.* **8,** 45–70.

Tautz, D. (1992). Genetic and molecular analysis of early pattern formation in *Drosophila*. *In* "Development: The Molecular Genetic Approach" (V. E. A. Russo, S. Brody, D. Cove, and S. Ottolenghi, eds.), pp. 308–327. Springer-Verlag, Berlin.

Torrence, S. A. (1991). Positional cues governing cell migration in leech neurogenesis. *Development* **111,** 993–1005.

van den Heuvel, M., Nusse, R., Johnston, P., and Lawrence, P. A. (1989). Distribution of the *wingless* gene product in *Drosophila* embryos: a protein involved in cell-cell communication. *Cell* **59,** 739–749.

Vincent, J. P., and O'Farrell, P. H. (1992). The state of *engrailed* expression is not clonally transmitted during early *Drosophila* development. *Cell* **68,** 923–931.

Wedeen, C. J., and Weisblat, D. A. (1991). Segmental expression of *engrailed*-class gene during early development and neurogenesis in an annelid. *Development* **113,** 805–814.

Weisblat, D. A., and Blair, S. S. (1984). Developmental indeterminacy in embryos of the leech *Helobdella triserialis*. *Dev. Biol.* **101,** 326–335.

Weisblat, D. A., Kim, S. Y., and Stent, G. S. (1984). Embryonic origins of cells in the leech *Helobdella triserialis*. *Dev. Biol.* **104,** 65–85.

Weisblat, D. A., and Shankland, M. (1985). Cell lineage and segmentation in the leech. *Phil. Trans. R. Soc. Lond.* **313,** 39–56.

Weisblat, D. A., Price, D. J., and Wedeen, C. J. (1988). Segmentation in leech development. *Development* **104**(Suppl.), 161–168.

Weisblat, D. A., Wedeen, C. J., and Kostriken, R. G. (1993). Evolutionary conservation of developmental mechanisms: comparisons of annelids and arthropods. *In* "Evolutionary Conservation of Developmental Mechanisms" (A. Spradling, ed.), pp. 125–140. Wiley-Liss, New York.

Whitman, C. O. (1878). The embryology of *Clepsine*. *Quart. J. Microscop. Sci.* **18,** 215–315.

Whitman, C. O. (1887). A contribution to the history of the germ layers in *Clepsine*. *J. Morphol.* **1,** 105–182.

Whitman, C. O. (1892). "The Metamerism of *Clepsine*," pp. 385–395. Festschrift zum 70, Geburtstage R. Leuckarts.

Wysocka-Diller, J. W., Aisemberg, G. O., Baumgarten, M., Levine, M., and Macagno, E. R. (1989). Characterization of a homologue of bithorax-complex genes in the leech *Hirudo medicinalis*. *Nature* **341,** 760–763.

Zackson, S. L. (1982). Cell clones and segmentation in leech development. *Cell* **31,** 761–770.

Zackson, S. L. (1984). Cell lineage, cell-cell interaction, and segment formation in the ectoderm of a glossiphoniid leech embryo. *Dev. Biol.* **104,** 143–160.

4

Axonal Guidance from Retina to Tectum in Embryonic *Xenopus*

Chi-Bin Chien
*William A. Harris**
Department of Biology
* and Center for Molecular Genetics
University of California, San Diego
La Jolla, California 92093

I. Introduction

The retinotectal system of lower vertebrates has been studied extensively in the three decades since Sperry proposed his chemoaffinity hypothesis (Sperry, 1963). The straightforward orderliness of the topographic map from retina to tectum, the accessibility of the pathway for anatomical and electrophysiological tracing techniques, and the relative simplicity of transplants, rotations, and other perturbations have combined to make these studies especially fruitful ones. This chapter describes what is known

Current Topics in Developmental Biology, Vol. 29

about the early development of the retinotectal system of the African clawed frog *Xenopus laevis*. Early work on the *Xenopus* retinotectal projection was done by manipulating the embryo and assaying the effects after metamorphosis, but over the last decade attention has shifted to embryonic assays. Not only do embryonic experiments have the practical advantage of taking days instead of months, but they also have a great conceptual advantage. Postmetamorphic studies only show the distant shadows of initial development, twisted and confused by a long period of brain growth and elaboration. Embryonic experiments, on the other hand, allow direct observation of the processes of initial development.

The task of the retinal growth cone finding its way to the tectum can be split into two parts: pathfinding and topography. Imagine the growth cone to be like a traveler on a long automobile journey to visit a friend. First she finds her way across the road map of the brain, stopping when she recognizes the right city (pathfinding); then, she remembers where her friend lives and find the right house within the city (topography). The development of topographically appropriate connections is a rich subject with an extensive and sometimes contradictory experimental history, which has been extensively reviewed [for discussions of topography in *Xenopus* and other species, see Cowan and Hunt (1985), Udin and Fawcett (1988), Fraser (1992), and Holt and Harris (1993)]. This chapter touches only briefly on topography, focusing instead on pathfinding. It concerns itself with the signs and landmarks the driver uses, how she reads the signs, and how she uses this information to steer her car.

II. *Xenopus* as an Experimental System

A. Experimental Tools

Amphibians have long been favored for embryological studies (e.g., Holtfreter, 1943; Spemann and Mangold, 1924) because their external fertilization and development make them easy to observe and manipulate. *Xenopus* are especially useful because they are easily raised in captivity, can be induced to breed by hormonal injection, produce hundreds of embryos per mating, and develop very quickly during embryonic stages. Studies of the development of the retinotectal projection require methods for mapping the projection and for perturbing its development. The retinotectal projection was first mapped using light stimulation and electrophysiological recording (Jacobson, 1968), and physiological mapping remains the only way to make a global retinotopic map from a single animal. However, visualizing the paths of individual axons requires anatomical

tracing methods. The use of anterogradely transported markers has improved greatly, progressing from tritiated proline (Scalia, 1973; Holt and Harris, 1983), to horseradish peroxidase (HRP; Fujisawa *et al.*, 1981; Harris *et al.*, 1985), fluorescent dextrans (O'Rourke and Fraser, 1986), Lucifer Yellow (Holt, 1989), and lipophilic dyes such as DiI and DiA (Harris *et al.*, 1987; Easter and Taylor, 1989). The axon scaffold of the early brain can now be seen by staining with antibodies against acetylated tubulin (anti-AT; Easter and Taylor, 1989), and the location of the optic tract within the scaffold can be seen by HRP filling the eye, then double-labeling with anti-HRP and anti-AT (Cornel and Holt, 1992). At present there are few specific antibodies that work in *Xenopus*, apparently because *Xenopus* antigens rarely cross-react with antibodies made against birds, fish, or mammals, but this shortage is being relieved as antibodies are made specifically against *Xenopus* antigens. *In situ* hybridization has made it possible to see patterns of gene expression (Harland, 1991). The development of whole mount techniques has made fiber tracing, antibody staining, and *in situ* hybridization studies especially convenient. The advent of fluorescent vital stains and low-light time-lapse imaging techniques has made it possible to follow particular retinal fibers as they grow over time (Harris *et al.*, 1987; O'Rourke and Fraser, 1989).

Perturbational methods have improved as well. *Xenopus* is an excellent preparation for classical embryological manipulations such as transplanting or rotating specific tissues, and early studies took advantage of this by using eye rotations and transplantation of eye fragments (Jacobson, 1967). Modern techniques make it possible to perform specific molecular manipulations *in vivo*, using blocking antibodies (Fraser *et al.*, 1984, 1988), bath application of drugs to an exposed-brain preparation (Chien *et al.*, 1993), DNA transfection (Holt *et al.*, 1990), and RNA injection (Harvey and Melton, 1988; Amaya *et al.*, 1991). The ease and speed of RNA injection and DNA transfection largely make up for the lack of genetic techniques, which are impractical because of the long generation time and pseudotetraploid genome of *Xenopus*. Experiments *in vitro* are of course possible: retinal and tectal cells are easily maintained both as explants (Harris *et al.*, 1985; Gooday, 1990) and as dissociated cells (Harris and Messersmith, 1992; Johnston and Gooday, 1991). It will be especially useful to combine RNA and DNA perturbations with other techniques; for instance, transplanting an eye expressing an exogenous RNA into an untreated host and observing the behavior of "mutant" axons in a wild-type environment.

Over the next few years, the combination of sophisticated anatomical techniques with molecular perturbations *in vivo* and *in vitro* should be extremely powerful for studying the cellular and molecular basis of retinal axon pathfinding.

B. Natural History and Ontogeny of *Xenopus*

Before discussing the early development of the retinotectal projection of *Xenopus*, it is useful to describe its behavioral and ontogenetic context. Table I is a timetable of the early development of the *Xenopus* embryo, with particular attention given to the retinotectal system. Stages are given according to the revised normal table of Nieuwkoop and Faber (1967), with developmental times given for room temperature (about 24°C). Some stages are double-numbered (e.g., stage 33/34, 35/36), which has led some authors to use unconventional numbers such as 33 or 34/35 to indicate intermediate stages. For clarity, we eschew these and stick to the stages given explicitly by Nieuwkoop and Faber.

Initial development is extremely rapid. Half a day after fertilization, gastrulation is complete; within another half day, the neural tube has closed. During the third day after fertilization, the embryo hatches from its jelly coat, can swim a little, and responds to visual stimuli in a rudimentary fashion: turning the light off causes a brief bout of swimming. At 4 days, feeding begins. After this extraordinary initial burst, development slows to a more leisurely pace: the tadpole begins metamorphosis at 1 month, becomes a fully metamorphosed froglet at 2 months, and matures sexually at about 18 months.

In the laboratory, pairs of *Xenopus* can be induced to breed by injection of human chorionic gonadotropin; they produce hundreds of embryos per mating. *In vitro* fertilization is also simple since the eggs are laid and fertilized externally. A female is primed by hormonal injection and squeezed to obtain mature eggs, which are then fertilized with sperm from minced testes. The eggs are large (1 mm in diameter) and take several hours to undergo their first two cleavages, so this is an excellent time to inject RNA (Harvey and Melton, 1988) or fluorescent dextrans (O'Rourke and Fraser, 1986). When using small molecules such as dextrans, one can label the entire embryo evenly by injecting both blastomeres at the two-cell stage or all four blastomeres at the four-cell stage. Since the embryo's volume is constant over the first 2 days of development, the injected molecule is partitioned among its cells without dilution.

The need to survive unpredictable external conditions presumably explains the hardiness of *Xenopus* embryos. They can survive between 14 and 27°C, and indeed developmental speed can be changed roughly three-fold by adjusting the incubation temperature. They recover well from tissue transplants and rotations: holding the transplant in place for half an hour with a shard of coverslip is usually sufficient for healing. Embryos use maternally derived yolk stores for 4 days before beginning to feed. Yolk granules are inconvenient for experiments because they are opaque and autofluorescent, but they enable different parts of the embryo to

develop quite autonomously. For instance, retinotectal axons grow for many hours in a decapitated head without any special need for oxygenation (Harris *et al.*, 1987; Chien *et al.*, 1993).

By the third day after fertilization, at about stage 35/36, the embryos hatch and swim freely. Visual responses have been detected in the retina at stage 39 (Witkovsky *et al.*, 1976) and in the tectum at stage 37/38 (Holt and Harris, 1983), and behavioral responses to visual cues can be detected at stage 37/38 (G. Recanzone and W. Harris, unpublished observations). Over the course of evolution, the need to respond to the environment soon after hatching must have applied selective pressure for rapid visual development, because the retina and the tectum both develop very quickly. At stage 24, 1 day after fertilization, the eye vesicle begins to evaginate and the first retinal cells become postmitotic (Holt *et al.*, 1988); by stage 41, 3 days after fertilization, the lens and pigment epithelium have formed, and the central retina is completely postmitotic (Holt *et al.*, 1988) and has separated into three layers. The tectum develops slightly later: the first tectal cells become postmitotic at stage 41 (Gaze and Grant, 1992a).

As in other amphibians and fish, both the eye and the brain of *Xenopus* keep growing throughout life. The retina and tectum have different modes of growth: new cells are born around the entire periphery of the retina, but only at the caudal border of the tectum. Therefore retinal terminals must slowly shift across the tectum in order to stay topographically registered (Gaze *et al.*, 1979). The retina grows symmetrically until the beginning of metamorphosis (stage 54), when the ventral periphery starts growing faster than the dorsal periphery. In early larvae, the eyes point laterally and have nonoverlapping visual fields, so it is not surprising that the retinal projection is largely uncrossed at larval stages. Once metamorphosis begins, the head flattens and the eyes rotate medially (Grobstein and Comer, 1977); correspondingly, binocular responses develop in late larval life. The change from symmetric to asymmetric retinal growth correlates nicely with the transition to binocularity: extra ventral retina is needed in order to enlarge the binocular field. In fact, the metamorphosis-associated hormone thyroxine triggers both asymmetric retinal growth (Beach and Jacobson, 1979a) and the development of ipsilateral retinothalamic projections (Hoskins and Grobstein, 1985b).

III. Normal Pathfinding

The normal pathfinding that retinotectal axons use to get from the retina to the tectum will be discussed first (Fig. 1). This figure and the following description are based on studies using intracellular injection of Lucifer

Table I Timetable of Early *Xenopus* Development

Stage	Age	Overall	Eye	Tectum	Leading retinal axons
10	9 hr	Early gastrula			
13	15 hr	Early neural plate			
28	32 hr	Early tail bud	Optic vesicle well formed (Holt, 1980)		Beginning of axonogenesis (Sakaguchi and Murphey, 1985; Holt, 1989)
31	38 hr		Beginning of ganglion cell dendritogenesis (Sakaguchi and Murphey, 1985; Holt, 1989)		
32	40 hr		Migration from optic stalk complete (Holt, 1980)		At chiasm (Holt, 1984)
33/34	44 hr		Beginning of pigmentation		At ventral optic tract (Holt, 1984)
35/36	50 hr	Embryos hatch			At midoptic tract (Holt, 1984)
37/38	54 hr				Dorsal fibers reach ventral tectum (Holt, 1984)
39	57 hr			Beginning of lateral expansion	Ventral fibers reach dorsal tectum (Holt, 1984)
41	76 hr		Central retina completely postmitotic, well-laminated (Holt *et al.*, 1988)	First postmitotic tectal cells (Gaze and Grant, 1992a)	Arborization under way (Holt, 1984; Sakaguchi and Murphey, 1985; Holt, 1989)
45	4 days	Feeding begins			
54	26 days	Onset of metamorphosis	Ventral retina starts growing faster than dorsal retina (Beach and Jacobson, 1979b)		Major ipsilateral projections start (Hoskins and Grobstein, 1985a)
66	58 days	Metamorphosis complete			

Note. The stages and times of various events in the development of the overall embryo, the eye, and the tectum, and the progress of the leading retinotectal axons. Stages, times, and some events are taken from the normal table of Nieuwkoop and Faber (1967).

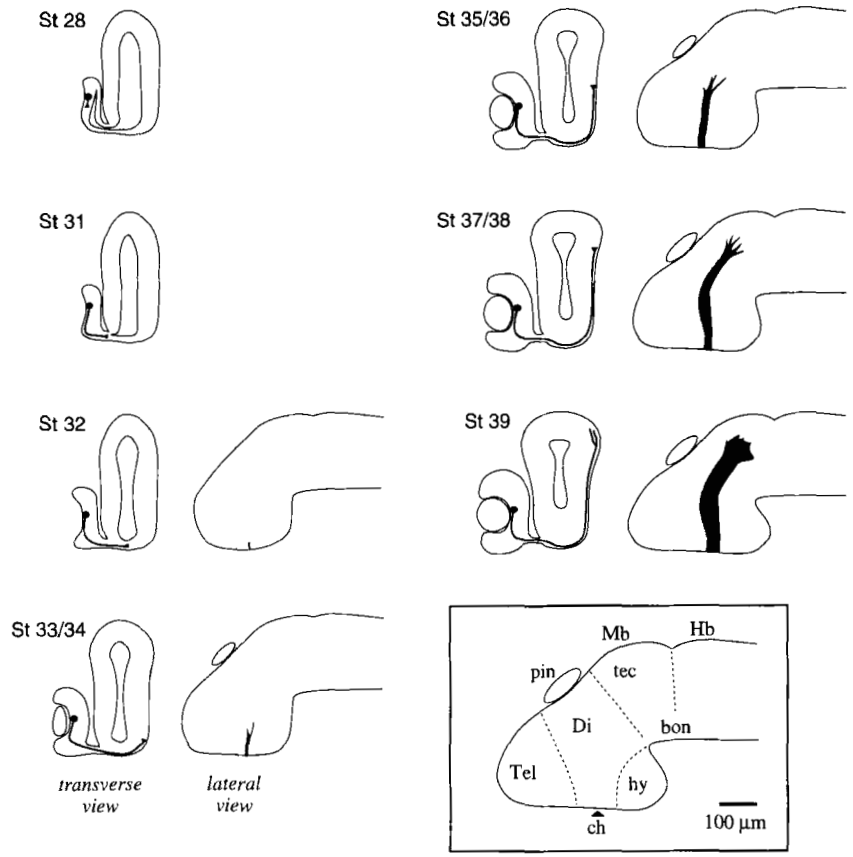

Fig. 1 Development of the retinotectal projection from the right eye, stages 28 to 39. Transverse views show the position of a typical leading growth cone relative to the right eye and brain (the left eye is omitted for clarity). Lateral views show the retinotectal projection on the contralateral (left) side of the brain. Projections to the basal optic nucleus are not shown. Based on Holt (1989) and Easter and Taylor (1989). (Inset) Approximate scale and different regions of the embryonic brain: Tel, telencephalon; Di, diencephalon; Mb, midbrain; Hb, hindbrain; pin, pineal (epiphysis); hy, hypothalamus; tec, tectum; bon, basal optic nucleus; ch, optic chiasm. Note the pistol shape of the embryonic brain.

Yellow and HRP (Holt, 1989) and extracellular application of HRP and DiI (Easter and Taylor, 1989), which agree with earlier studies that used radioactive tracers (Holt and Harris, 1983; Holt, 1984).

A. Normal Retinotectal Projection

The central retina contains approximately 200 retinal ganglion cells, which are postmitotic by stage 31. Their births are asynchronous: birthdating

studies at stages 28–31 show postmitotic cells mixed in with mitotic cells (Straznicky *et al.*, 1971; Holt *et al.*, 1988). There is a slight dorsal-to-ventral gradient, so that dorsocentral cells develop a few hours before ventrocentral cells (Holt, 1984; Holt *et al.*, 1988). After the central retina is formed, newborn cells are added in orderly rings at the retinal periphery. The number of retinal ganglion cells increases by about 860 cells per day until stage 51, then by about 660 cells per day thereafter (Gaze and Grant, 1992b). The first retinal ganglion cells put out axons at stage 28, and put out dendrites by stage 31 (Holt, 1989; Sakaguchi *et al.*, 1984).

The development of the optic tract is quite reproducible, as retinal axons follow a stereotyped path (Fig. 1). Though the time course described here is typical, the development of the optic tract is occasionally found to be one stage earlier or later than the external development of the embryo would indicate. The axons proceed across the surface of the retina to the optic nerve head by stage 29/30, reach the optic nerve at stage 31, reach the chiasm at stage 32, and cross into the contralateral ventral optic tract at stage 33/34. By early stage 35/36, the axons have reached the middle of the optic tract and have started to execute a caudal turn to reorient toward the tectum; they round this turn by late stage 35/36. By stage 37/38, the first fibers have reached the ventral optic tectum, and by stage 39 these fibers have begun to arborize. The trip from chiasm to tectum (stage 32 to 37/38) covers about 430 μm in 13 hr at 22°C (Harris *et al.*, 1985). Later-born axons are continually adding to the optic tract.

The retinal axons are tipped by standard vertebrate growth cones whose average dimensions are about 3 μm wide by 10 μm long, with an average of three or four filopodia (Harris *et al.*, 1985; Holt, 1989). Growth cones are typically rather simple and club-like on the retinal surface, become more complex with backward-branching filopodia at the optic nerve head, and then maintain a relatively constant level of complexity from the optic nerve through the chiasm and optic tract (Holt, 1989). In the optic tract, the growth cones travel within a few microns of the pial surface, passing among the neuroepithelial cells and rarely contacting the basement membrane (Harris *et al.*, 1985; Holt, 1989).

At early larval stages, the great majority of retinal ganglion axons project to the contralateral tectum, but a few fibers project elsewhere. A small projection to the contralateral basal optic nucleus develops at the same time as the retinotectal projection (Sakaguchi and Murphey, 1985; Easter and Taylor, 1989). By stage 44, a few fibers project to contralateral and ipsilateral diencephalon, with an occasional fiber that arborizes in the diencephalon, then continues on and arborizes again in the tectum (Sakaguchi and Murphey, 1985). A very small number of fibers (<1%) seem to project to the ipsilateral tectum (Sakaguchi and Murphey, 1985), and indeed a small ipsilateral retinotectal projection has been reported to persist in the adult (Levine, 1980). Most of the ganglion cells that project

to the contralateral tectum have a single unbranched axon. However, between 5 and 10% have two or even three axons (Holt, 1989), and a small number have axons that branch within the optic tract (Sakaguchi and Murphey, 1985). It is not known whether occasional multiple axons persist into adulthood.

By adult stages, the brain has grown both in size and in its number of retinal projections; these are discussed only briefly. The embryonic brain has what Easter and Taylor (1989) call a "pistol" shape , with the forebrain being the handle and the hindbrain the barrel (Fig. 1). In the adult, the ventral flexure has straightened so that the handle of the pistol is in line with the barrel. The brain has grown greatly, with the tecta bulging out dorsolaterally and the forebrain enlarged relative to the rest of the brain. The contralateral retinal projections have continued to grow and have been joined by substantial ipsilateral projections that begin developing at about stage 54, when the eyes start to move into position for binocular vision. The retina projects to both the contralateral and ipsilateral diencephalon, with terminal fields falling into three groups: anterior (nucleus of Bellonci, corpus geniculatum thalamicum, rostral visual nucleus), posterior (uncinate field, thalamopretectal field, pretectum), and the basal optic nucleus (Levine, 1980). Projections to ipsilateral diencephalon originate from the ventrotemporal retina (Hoskins and Grobstein, 1985a). Binocular vision is mediated by an interaction between the direct contralateral tectal projection and a polysynaptic ipsilateral projection that goes from the retina to the contralateral tectum to the contralateral nucleus isthmi, and then via a crossed isthmotectal projection to the ipsilateral tectum (Glasser and Ingle, 1978; Gruberg and Udin, 1978). How fibers decide to project to the diencephalon instead of the tectum is a very interesting, but unanswered, question.

B. Time-lapse Studies of Normal Pathfinding

It is possible to use fluorescent vital stains and low-light fluorescence microscopy techniques to make time-lapse movies of individual living axons *in vivo* (Harris *et al.*, 1987; O'Rourke and Fraser, 1990; Kaethner and Stuermer, 1992; Sretavan and Reichardt, 1993; Chien *et al.*, 1993). Since time-lapse studies are labor- and equipment-intensive, fewer axons can be observed than in fixed tissue, but detailed observation of individual living axons shows dynamic behaviors that can only be guessed at from fixed samples. Live and fixed studies are complementary: a few movies of living axons can make sense of hundreds of snapshots of fixed ones, but conversely the snapshots are needed to tell whether the behavior of particular axons seen in time-lapse is typical or idiosyncratic.

The growth of retinal axons in the optic tract has been observed in two sets of experiments (Harris *et al.*, 1987; Chien *et al.*, 1993). The first studied the normal growth of axons in the tract and the effects of removing the soma (Harris *et al.*, 1987). The axons were labeled with the fluorescent membrane dye DiI and time-lapse movies were taken using a silicon-intensified-target (SIT) camera, a computer-controlled shutter, and a time-lapse videotape recorder. Figure 2 shows the development of a typical axon. Growth cones grew steadily while in the tract (average speed 54 μm/hr at 20–24°C), and slowed down after passing the presumptive border of the tectum (average speed 16 μm/hr). Axons did not branch while in the optic tract. The filopodia and lamellipodia of the growth cones were very active, changing shape over tens of seconds. Once in the tectum, the axons began to branch and form arbors, not by bifurcation of the growth cone, as had been previously assumed, but by the formation of backbranches along the shaft of the axon. If the labeled eye was removed to break off the axon's soma, the axon grew normally for up to 3 hr before suddenly dying. It apparently took some time for the growth cone to learn of the soma's disappearance.

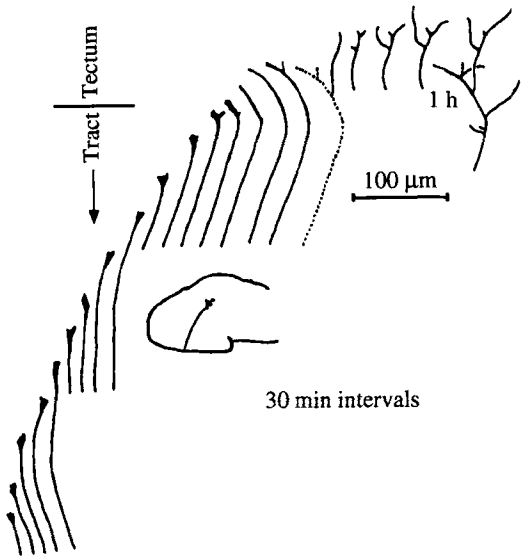

Fig. 2 An example of a single axon growing in the optic tract and arborizing in the tectum. Four phases are apparent: (1) steady growth in the tract, (2) deceleration near the target, followed by (3) loss of normal growth cone morphology, and (4) backbranching in the tectum. At the dotted line, the focus was switched onto a more superficial branch. On the right is a focus-through reconstruction of the terminal arbor. [From Harris *et al.* (1987). Copyright Company of Biologists Ltd.]

The second study looked at the effects of using the drug cytochalasin to remove growth cone filopodia (Chien *et al.*, 1993). Figure 3 is a diagram of the experimental preparation, modified from that used earlier in order to allow perfusion of drugs. Time-lapse movies, taken digitally to allow better time resolution and more accurate quantitation of growth, gave rise to several new observations about control axons. Growth was saltatory over short periods (minutes), but was steady over longer periods (30 min), in agreement with the earlier observations. Occasionally, a growth cone in the optic tract would bifurcate for a few minutes, then choose one of the two branches and follow it, leaving the other branch to be resorbed into the axon (C.-B. Chien, unpublished data). If the axon should sometimes follow *both* branches, such bifurcations could give rise to the branched axons seen by Sakaguchi and Murphey (1985). An axon that began arborizing in the diencephalon was also seen (C.-B. Chien, unpublished data); this was presumably part of the normal retinodiencephalic projection.

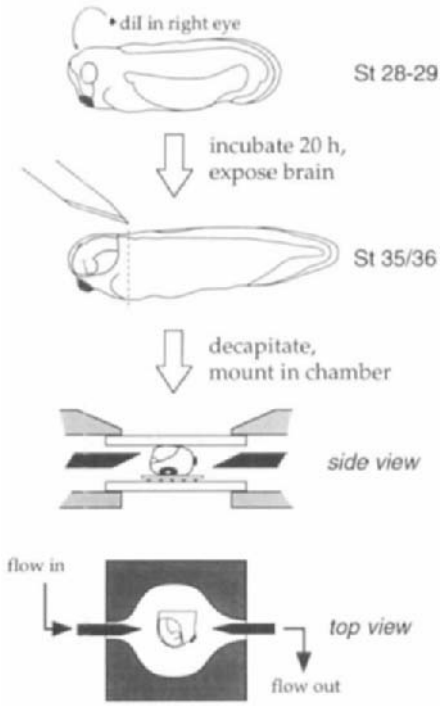

Fig. 3 Mounting in perfusion chamber for time-lapse video experiments.Several brains are exposed, a specimen is chosen with one or a few axons that are brightly labeled with dil, and its head is mounted in a coverslip chamber for viewing and perfusion. [Adapted from Chien *et al.* (1993).]

C. Normal Topography

As shown in Fig. 4, the normal projection to the contralateral tectum is a retinotopic map with both axes reversed: dorsal (D) retina projects to ventral (V) tectum, V retina to D tectum, anterior (A) retina to posterior (P) tectum, and P retina to A tectum. The image has previously been reversed by the lens, so that anterodorsal retina sees the posteroventral visual field. In the early embryo, when the eyes face laterally and the tectum is still flush with the rest of the midbrain, the topographic axes are dorsoventral (D–V) and anteroposterior (A–P). As the eyes move and the tecta expand during development, these directions no longer make sense, and so in the adult it is conventional to call the axes of the retina dorsoventral and nasotemporal, and those of the tectum mediolateral and rostrocaudal. The topography of the projection can be assayed electrophysiologically by sequentially placing a metal recording electrode in different positions in the tectum and moving a spot of light to find the

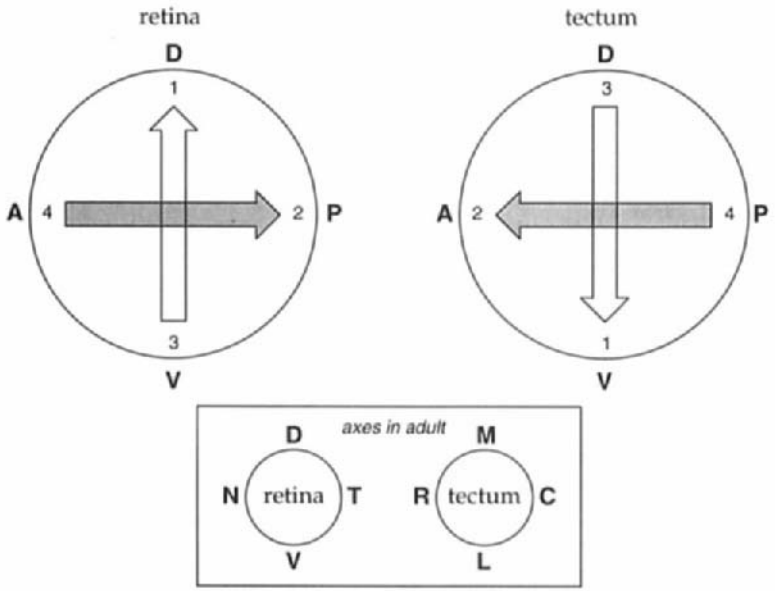

Fig. 4 The orientation of the normal retinotopic map. The retina and contralateral tectum of the embryo are shown schematically as circles, with the poles labeled: A, anterior; P, posterior; D, dorsal; V, ventral. Numbers and arrows are retinotopically equivalent positions and axes: for instance, a ganglion cell at position 1 on the retina would project to position 1 on the tectum, etc. (Inset) Labeling of the axes in the adult: N, nasal; T, temporal; M, medial; L, lateral; R, rostral; C, caudal.

visual receptive field that best stimulates each position (Jacobson, 1968). Anatomically, it can be assayed by placing HRP or another anterograde marker on a small area of the retina and looking at the corresponding tectal projection.

The retinotectal projection is topographically ordered very early on, with D–V order being evident earlier than A–P order. Holt and Harris (1983) found order in both axes at stage 39, using tritiated proline as an anterograde label to assay D–V order and using electrophysiology to assay A–P order. Using cobalt fills to visualize individual arbors, Sakaguchi and Murphey (1985) found that both axes are well ordered at stages 40–45. The cobalt-filled retinal arbors tended to be narrow in the D–V axis and elongated along the A–P axis.

O'Rourke and Fraser (1986) have studied early topography in greater detail. They first used fluorescent dextrans to vitally stain populations of fibers, finding that D–V order was present from stage 47, the earliest stage studied, but that A–P order developed between stages 47 and 49. They then followed the development of A–P topography by using confocal microscopy of DiI-stained arbors to watch individual arbors developing over time (O'Rourke and Fraser, 1990). At stage 45, arbors of nasal and temporal fibers covered most of the A–P extent of the tectal neuropil, overlapping completely. The only difference seen was in anterior tectum, where temporal arbors branched slightly more than nasal arbors. As the tectum grew over time, nasal arbors selectively lost anterior branches and elaborated posterior branches, giving rise to clear A–P separation by stage 49. The lack of A–P order at stage 45 is at odds with the results of Holt and Harris (1983), who found A–P order earlier, at stage 39. This discrepancy is presumably due to a difference in technique: the electrophysiological assay used by Holt and Harris averages over the responses of many arbors and thus may be able to detect a slight difference in branching patterns between nasal and temporal arbors, even though they overlap in rostrocaudal extent.

IV. Nature of Guidance Cues

A. Autonomous Pathfinding by Growth Cones

As the retinal growth cones navigate through the brain and recognize the tectum, they respond to signals of some kind. The first question is whether these signals come from within the cell. An internal timing mechanism seems unlikely since retinal axons can find the tectum and terminate there after starting from ectopic positions (Harris, 1986), which should

drastically disrupt the normal timing. The cell body is not required since axons can pathfind and arborize normally for several hours after the soma has been broken off (Harris *et al.*, 1987). Sodium-based action potentials in the axon are also probably not required, since normal retinotectal projections form in axolotls in the presence of blocking levels of tetrodotoxin (TTX) (Harris, 1980, 1984), and similar observations have been made in *Xenopus* (Ferguson, 1983) and zebrafish (Stuermer *et al.*, 1990). A role for calcium action potentials remains a formal possibility, although no such spikes were detected electrophysiologically in TTX-blocked axolotls (Harris, 1980). Microtubules in the axon may bias it toward straight growth: axons in culture seem to have an inherent tendency to grow straight (Katz, 1985), and *in vivo*, retinal axons that have been disoriented by cytochalasin miss a normal turn and instead grow straight (Chien *et al.*, 1993). In general, though, the growth cone seems to act autonomously of the cell body and axon, making pathfinding decisions based on the external signals that it encounters.

What is the nature of these external guidance signals? This question is discussed in three parts: first the distribution of the cues in the brain, then their cellular location, and finally what is known about their molecular nature.

B. Distribution of Positional Guidance Cues

How are pathfinding cues distributed in the brain? Several groups have studied this question using embryological manipulations that Taylor (1991) likens to a game of hide and seek. Either the eye or the tectum is transplanted to an ectopic position, and retinal axons are then assayed to see if they can overcome this challenge and find the tectum.

One might expect pathfinding cues to be narrowly restricted to the optic pathway, but this does not seem to be the case. When eyes are transplanted to ectopic positions in the brain, retinal axons still find their way to the tectum (Harris, 1986; Fig. 5A), although in some eyes transplanted to the hindbrain, a subset of axons went the wrong way and headed down the spinal cord. Furthermore, this ectopic pathfinding is not a random search: the axons orient correctly as soon as they enter the brain. Thus there are globally distributed positional cues that allow a growth cone to set its compass toward the tectum.

What is the range of influence of the positional cues? If a small (100 μm) patch of neuroepithelium in the optic tract is rotated by 90° at stages 26–28, axons that later enter the rotated tissue are deflected in the direction of rotation (Fig. 5B; Harris, 1989; Taylor, 1991). When the tectum is excised, retinal axons grow right up to its normal position before

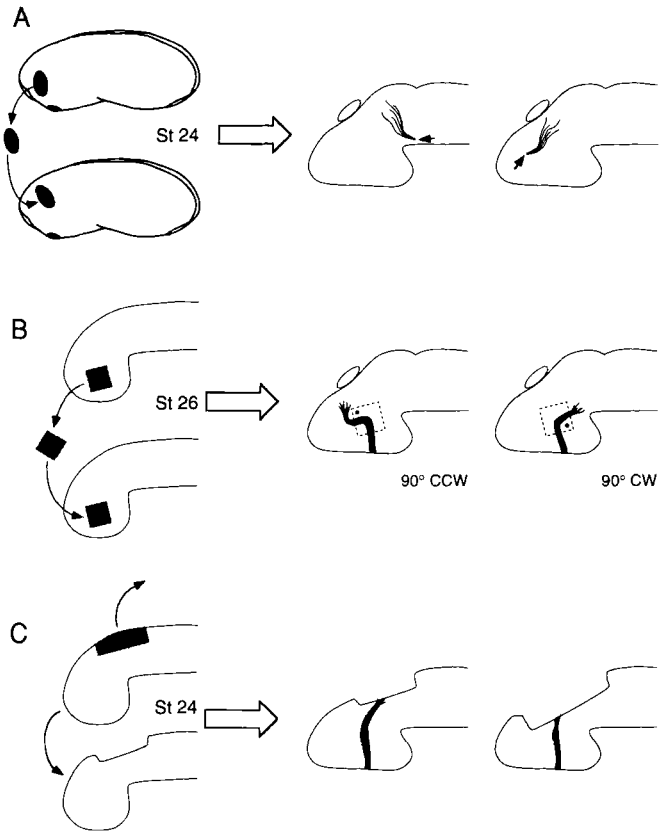

Fig. 5 Hide and seek with the tectum: embryonic manipulations and their effect on the retinal projection. (A) Ectopic eye transplants. When the eye is transplanted to an ectopic location, retinal fibers not only find the tectum in most cases, but orient toward the tectum as soon as they enter the brain (arrows indicate entry point). [Adapted from Harris (1986).] (B) Tract rotations. When a small patch of presumptive optic tract is rotated by 90°, retinal fibers that later enter the patch follow a path that is rotated similarly. The small black dot indicates the direction of rotation. [Adapted from Harris (1989).] (C) Tectal deletions. When the presumptive tectum is deleted, retinal fibers grow right up to the edge of the deletion before turning in an aberrant direction (aberrant projections not shown). [Adapted from Taylor (1990).]

growing across the midline into the contralateral optic tract or heading down the spinal cord (Fig. 5C; Taylor, 1990). Thus the positional cues have short-range effects and seem to be finely distributed and tightly associated with the developing neuroepithelium. Furthermore, the positional fate of the neuroepithelial cells seems to be determined early, by stage 24, since the cues do not become respecified after rotation or tectal

deletion. When are the positional cues first expressed? Using heterochronic transplants, Cornel and Holt (1992) showed that retinal axons forced to grow into a young brain can pathfind to the tectum and reach it at stage 32, 8 hr before they would normally arrive. Thus, cues are present quite early. The authors point out that most neuroepithelial cells are mitotically active at this stage, so positional cues are apparently expressed before the neuroepithelium has undergone terminal mitosis.

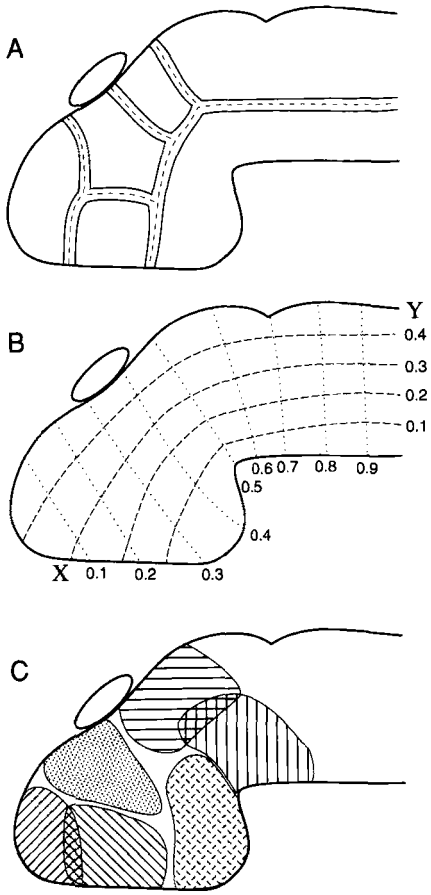

Fig. 6 Models of positional cues. (A) Highways. Early growing axons act as highways for later-growing axons. (B) X–Y coordinates. Two molecules, X and Y, are distributed in gradients over the brain; lines indicate contours of constant X or Y. The growth cone senses these gradients and navigates to a particular coordinate position. (C) Patchwork cues. Shaded patches indicate the distribution of different cue molecules; patches sometimes overlap. Growth cones follow the edges of these patches.

C. Models for Positional Guidance Cues

Figure 6 schematizes three possible models for the pattern of positional cues: highways, X–Y coordinates, and patchwork cues. As in other aspects of axonal guidance, the different mechanisms are not mutually exclusive: axons could use a combination of all three.

1. Highways

In this model, the retinal growth cone grows along preexisting axons, switching at certain points in order to reach the tectum. This method is much like driving on highways, where a route to a destination can be specified as a sequence of turns onto the next highway. Axons from ectopically transplanted eyes would presumably follow an alternate highway that also reached the tectum. Easter and Taylor (1989) described the pattern of early axonal tracts that form in the *Xenopus* brain, and by analogy with the "labeled pathways" hypothesis proposed for grasshopper and *Drosophila* (Raper *et al.*, 1983), proposed that later-growing axons selectively fasciculate with early tracts. In particular, they found that ingrowing optic fibers form a tight bundle along the rostrodorsal border of the tract of the postoptic commissure (TPOC), and therefore proposed that fasciculation with the TPOC is an important factor in guidance. One weakness of this hypothesis was that electron microscopic (EM) observation showed only occasional contacts between retinal axons and axons of the TPOC (Easter and Taylor, 1989; Holt, 1989). This lack of fasciculation was later confirmed by EM observations in developing zebrafish (Burrill and Easter, 1991) and double-label confocal microscopy in *Xenopus* (Cornel and Holt, 1992). The most definitive evidence against a highway model is from the heterochronic transplant experiments of Cornel and Holt (1992), who showed that retinal axons could find the tectum in brains that were young enough that no other axonal tracts were present. Though preexisting tracts may contribute to normal guidance, they are clearly not *necessary* for retinotectal pathfinding.

2. X–Y Coordinates

The second and third models are much more theoretical, as there is little direct evidence either for or against them. In an X–Y coordinate model, two positional molecules are distributed over the surface of the brain, and the growth cone reads out their local concentration in order to find its map coordinates. This is the strategy of a driver in a city where the streets are numbered sequentially in one direction and lettered in the other. Gierer (1987) discusses very nicely how a retinal growth cone could find its way

using global positional gradients. Chemical gradients are often used in modeling of Sperry's chemoaffinity theory (Sperry, 1963; Fraser and Perkel, 1990), and indeed Trisler, Bonhoeffer, and their respective collaborators have found molecules that are distributed in gradients across the retina and tectum (discussed later). However, there is at present no experimental evidence for global gradients distributed across the whole brain, and unfortunately there is no obvious way to find them except to screen monoclonal antibodies. An unattractive feature of this model is that it requires the signal molecules to be set up in a smooth gradient across the whole brain. Such gradients would require exquisite developmental control. Moreover, reconciling this model with the results of tract-rotation experiments would require that growth cones could navigate based on very small differences in gradient concentration.

3. Patchwork Cues

In the third model, the surface of the brain is a patchwork quilt made up of patches of neuroepithelium that express different cell-surface or extracellular matrix molecules. Retinal axons navigate along the seams between neighboring patches, skirting around several different patches until they reach the tectum. If the growth cone was a car in the countryside, its driver might follow these instructions: "go between the woods and the meadow, then follow the edge of the cornfield until you reach some haystacks." Several mechanisms could constrain axons to patch boundaries: for instance, two neighboring patches of outgrowth-promoting activity might overlap slightly, so that the axons grew best along the border. Alternately, if the patches were inhibitory, the axons might prefer to stay in a narrow gap between patches. There is some evidence for such guidance patches in grasshopper limb bud, where adjacent bands of cells express the cell-surface proteins fasciclin IV (fas IV) and alkaline phosphatase, and the intracellular protein annulin (Kolodkin *et al.*, 1992; Singer *et al.*, 1992). Not only is fas IV expressed in a narrow band along the trochanter–coxa boundary, but it also seems to function in the guidance of Til pioneer axons, since antibodies to fas IV disrupt the path taken by Til axons at this boundary (Kolodkin *et al.*, 1992). An attractive feature of a patchwork model is the ease with which the patches could be set up: the signal molecules could be controlled by the same genes (as yet undetermined) that determine regional fate in the brain. This would fit with the early expression of guidance cues (Cornel and Holt, 1992) and the fact that small pieces of neuroepithelium retain their guidance cues when rotated (Harris, 1989). In fact, some homeobox genes are known to be expressed in patches in the zebrafish brain (Krauss *et al.*, 1991; see Holt and Harris

(1993) and Figdor and Stern (1993) for related discussions). The molecules sensed by the growth cones could be cell-surface molecules, extracellular matrix (ECM) molecules, growth factors bound to the ECM, or some combination thereof. In the end, proof of a particular model will require molecular characterization of the signals involved.

D. Cellular Localization of Guidance Cues

There are four possible cellular sources for the pathfinding signals in the neuroepithelium: a diffusible molecule, the surfaces of axons, the surfaces of neuroepithelial cells, or the extracellular matrix.

1. Diffusible Signals

Two lines of evidence, one *in vitro* and one *in vivo*, make a diffusible chemotropic factor unlikely in the retinotectal system. In other systems, the definitive experiment showing that a chemotropic factor exists has been to coculture explants, using a three-dimensional gel to stabilize diffusional gradients, and show that axons from one explant are attracted to another explant (Lumsden and Davies, 1983). When *Xenopus* retinal and tectal explants are cultured together in a collagen gel (Harris *et al.*, 1985), retinal axons show no propensity to grow toward the tectal tissue; in fact, retinal axons sometimes pass very close to tectal tissue without deflection. Thus, at least under these culture conditions, tectal tissue does not appear to make a chemotropic factor.

As mentioned earlier, *in vivo* experiments with tract rotation (Harris, 1989) and tectal deletion (Taylor, 1990) show that the guidance cues are tightly associated with the neuroepithelium: they are carried along when the neuroepithelium is rotated, and remain if the tectum is removed. This rules out a freely diffusible factor. It is conceivable that a molecule diffuses out of the presumptive tectum at a very early stage and then binds tightly to the extracellular matrix or cell surfaces, thus setting up a fixed gradient. However, the evidence weighs against a diffusible factor that attracts axons toward the tectum.

2. Axonal Cell-Surface Molecules

As discussed earlier for the highway model, interactions with nonretinal axons do not seem to be necessary for pathfinding in the optic tract. Retinal axons do interact with each other, although it is not clear that this

is important for guidance. Retinal axons bundle tightly to each other and show specialized membrane contacts at the EM level (Easter and Taylor, 1989). In time-lapse video experiments in which more than one axon is labeled, a growth cone will occasionally make filopodial contact with another axon or grow along another axon for a short distance, but there is no tendency for growth cones to follow along preceding axons (C.-B. Chien, unpublished observations); however, this evidence is far from compelling because only a small fraction of axons were labeled in these experiments. In the mammalian optic chiasm, time-lapse video experiments show that axons sometimes turn and project ipsilaterally after contact with axons from the other eye (Sretavan and Reichardt, 1993). Interactions between axons may be important for the retinotectal topographic map, and several models of the development of topography have incorporated interactions between fibers (Fraser and Perkel, 1990).

The first retinal axons to grow out in *Xenopus* are from dorsocentral retina. Do these temporal pioneers guide later axons? Holt (1984) tested this idea by transplanting young dorsal retina into older embryos, thus delaying the dorsal fibers so that ventral fibers grew in to the brain first. This reversal of the normal temporal order had no effect on pathfinding. Therefore the dorsal pioneers have no special function that cannot be performed by ventral fibers. In summary, there is little evidence that retinal axons need each other to find the tectum.

3. Neuroepithelial Cell Surfaces and Extracellular Matrix

Since evidence is either lacking or negative for chemotropic factors and signals from other axons, it seems likely that guidance signals come from the cells and ECM of the optic tract neuroepithelium. In some invertebrate systems, growing axons form gap junctions with guidepost cells, as demonstrated by dye coupling (Bentley and Keshishian, 1982); however, Lucifer Yellow-filled retinal axons show no evidence of dye coupling to cells in the optic tract (Holt, 1989). Therefore the pathfinding signals must reside on the surfaces of the neuroepithelial cells or in the ECM that is presumably made by them. Although specialized membrane contacts have not been described, the growing retinal axons are closely apposed to the surfaces of these cells and sometimes plunge filopodia into them (Holt, 1989). One way to test for positional cues is to culture cells from different parts of the brain and see whether they affect axons differently. Indeed, temporal retinal axons can distinguish between diencephalic and tectal glia cultured from stage 54 embryos, fasciculating more on the tectal cells (Gooday, 1990). The fasciculation is especially marked on cells from the caudal third of the tectum (Jack *et al.*, 1991); in time-lapse video re-

cordings, individual retinal growth cones collapse upon contacting caudal tectal glia (Johnston and Gooday, 1991).

Thus, the results of embryological manipulations encourage us to search for guidance signals in neuroepithelial cells and the ECM. However, embryological manipulations can only go so far: there is no obvious way to specifically transplant or delete the ECM. What remains, then, is to start the molecular characterization of guidance cues.

V. Molecules Involved in Guidance

In the last part of this chapter, the molecular nature of guidance cues in the *Xenopus* retinotectal system is discussed, concentrating especially on the molecular studies that have already begun in the Harris and Holt laboratories.

A. Molecular Perturbations

Figure 7 illustrates two main experimental tools. The first is an exposed-tract preparation in which the skin, dura, and eye are dissected off one side of the brain in order to expose the optic tract. The growth cones from the contralateral eye can then be easily observed and exposed to bath-applied reagents. This is essentially the same preparation that was first used for time-lapse video experiments (Harris *et al.*, 1987); indeed, by mounting the head in a perfusion chamber, time-lapse movies can be made of growth cones as drugs are washed on and off (Chien *et al.*, 1993). Effects of a particular reagent on pathfinding can be studied by exposing the tract to the reagent overnight, then filling the retinal fibers with HRP and viewing them in whole mount (Fig. 7A). The second tool is *in vivo* lipofection (Holt *et al.*, 1990), which allows the introduction of a specific gene construct into retinal cells. The DNA is lipofected into the eye at an early stage, along with a marker construct. Since the frequency of cotransfection is very high (Holt *et al.*, 1990), the transfected cells can be identified using antibodies to the marker. Thick sections (50 μm) cut on a vibratome make it easy to find the transfected cells and see if their morphology has been affected by expression of the construct.

B. Criteria for Guidance Molecules

How does retinotectal guidance work on a molecular level? As in other parts of the nervous system, only rudimentary knowledge of the molecules

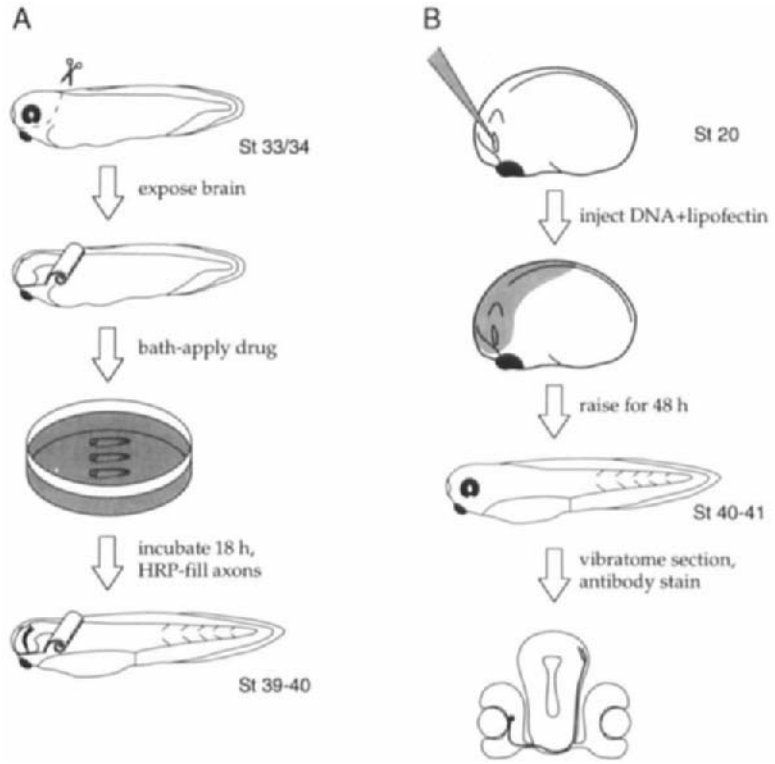

Fig. 7 (A) Exposed-brain preparation. At stage 33/34, the embryo is partially dissected to expose the left optic tract to bath-applied agents, and allowed to develop overnight. At stage 39, the right eye is filled with HRP to reveal the course of the retinal fibers. [Adapted from Chien *et al.* (1993).] (B) *In vivo* lipofection of DNA. A DNA construct of interest, mixed with lipofection agent and a luciferase construct as a cotransfected marker, is injected into the eye at stage 20, and the embryo is allowed to develop for 2 days. At stage 40, the embryo is fixed and sectioned, and the morphology of the transfected cells is observed using an antibody against luciferase. [Adapted from Holt *et al.* (1990).]

involved exists. Particular molecules might be specifically involved in axon outgrowth, in axon steering, or in target recognition. Too little is known about growth-cone cell biology to say whether growth, steering, and target recognition are separate cellular functions, so some molecules might be involved in all three. Candidate molecules must satisfy three criteria: the molecule must be distributed appropriately in the brain; it must show appropriate biochemical function in cell extracts or in culture; and, most critically, its function must be demonstrated by disruption *in vivo*. At present, no molecules are known to satisfy all three criteria, and only a few satisfy two.

C. Adhesion Molecules

The most abundant and best characterized neural-cell adhesion molecules are NCAM and N-cadherin [reviewed by Jessell (1988)]. *In vitro*, these transmembrane proteins mediate cell binding via homophilic adhesion mechanisms, calcium-independent in the case of NCAM and calcium-dependent in the case of N-cadherin. The best characterized substrate adhesion molecules are the integrins, a class of heterodimeric transmembrane proteins that mediate binding to various molecules in the ECM (Jessell, 1988). In culture, the outgrowth of chick retinal axons on astrocytes depends on NCAM, N-cadherin, and integrins, since blocking antibodies to all three have additive outgrowth-blocking effects (Neugebauer *et al.*, 1988). These three molecules are not the only ones used by neurons since there was some residual adhesion to astrocytes even in the presence of all three blocking antibodies. As in other species, antibody staining in *Xenopus* shows that NCAM, N-cadherin, and integrins are present on retinal axons and widely distributed throughout the rest of the brain (Gawantka *et al.*, 1992; R. Riehl, A. Walz, and C. Holt, unpublished data).

There have been several studies *in vivo* using blocking antibodies to NCAM. When Fraser and collaborators (1984, 1988) implanted antibody-laden agarose spikes into the tectum of adult frog, they found that retinal axons avoided the area around the spike and that the retinotopic map became less precise. The observation that Fab fragments of monoclonal antibodies produced these effects, but control antibodies did not, suggested that they were caused by inhibition of homophilic binding. In chicks, intraocular injection of NCAM antibodies caused minor disruption of retinotopic order in the optic nerve and optic tract, but did not prevent axons from finding the tectum and establishing a topographic map there (Thanos *et al.*, 1984; Silver and Rutishauser, 1984). These results suggest that NCAM function could be important for pathfinding in the optic tract. To test this idea, Walz applied blocking NCAM antibodies to the exposed-tract preparation and found that intact polyclonal antibodies reduced the length of the optic tract but did not appear to affect its course (A. Walz and C. Holt, unpublished observations). Together with the global distribution of NCAM, this observation suggests that NCAM is important for the elongation, but not the guidance, of retinal axons.

The roles of cadherins and integrins in pathfinding *in vivo* have been studied only recently. Sakaguchi and co-workers injected blocking antibodies to both N-cadherin and the $\beta 1$ subunit of integrin into the optic tract, and found that each antibody alone has only subtle effects, but that both applied together cause some retinal fibers to take aberrant paths (Sakaguchi and Radke, 1992; E. Stone and D. Sakaguchi, personal commu-

nication). Riehl and Lilienbaum used lipofection *in vivo* to express DNA constructs that encode putative dominant negative mutant forms of N-cadherin or β1 integrin (Lilienbaum *et al.*, 1993). The results for both molecules are similar: of the retinal ganglion cells (RGCs) that express either mutant N-cadherin or mutant β1 integrin, most lack axons. This is in marked contrast to RGCs that were untransfected or only transfected with the luciferase marker, which nearly all have axons. The few axons that are seen on mutant-transfected RGCs seem to project properly to the tectum. Thus, N-cadherin and β1 integrin seem to be necessary for axon elongation and may play a cooperative role in guidance.

D. Other Cell-Surface Molecules

MAb-A5 is a monoclonal antibody that seems to specifically label retinal targets: the optic tectum, basal optic nucleus, and several diencephalic nuclei, but not the optic nerve or optic tract (Takagi *et al.*, 1987). Staining in the tectum is first detectable at stage 39, at the same time that retinal fibers first arrive. Intriguingly, A5 also labels the general somatosensory tract in the spinal cord, which is a pathway sometimes taken by retinal axons making aberrant projections from ectopically transplanted eyes (Fujisawa *et al.*, 1989). The A5 antigen appears to be a cell-surface protein of approximately 140 kDa; however, a functional role for this antigen has yet to be demonstrated.

E. ECM Molecules

NOB1 (neurite-outgrowth-blocking-1) is a polyclonal antiserum that inhibits the outgrowth of retinal neurites on ECM made by cultured XR1 cells (Sakaguchi *et al.*, 1989). XR1 is an astroglial cell line derived from embryonic *Xenopus* retina that serves as an excellent substrate for retinal neurite outgrowth. When XR1 cultures are osmotically lysed and extracted to remove cellular components, the ECM that is left behind retains outgrowth-promoting activity. This activity is sensitive to protease and does not seem to be associated with laminin or fibronectin. The NOB1 antigen is generally distributed throughout the eye and brain (D. Sakaguchi, personal communication). Thus, the NOB1 antigen seems to be a general outgrowth-promoting factor laid down in the ECM by glial cells. No function has yet been shown *in vivo*.

Recent work has shown that growth factors can bind to the ECM and that regulation of their concentration may be one of its important functions. Antibodies to basic FGF and to heparan sulfate label the developing *Xenopus* diencephalon (A. Walz, S. McFarlane, and C. Holt, unpublished

results). Walz has found that 100 μg/ml heparin applied to the exposed-tract preparation appears to have a dramatic effect on target recognition, causing the retinal axons to skirt around the tectum rather than entering it (McFarlane *et al.*, 1993). Heparin is a heparan-related carbohydrate that affects the binding of growth factors to heparan sulfate proteoglycans (Kan *et al.*, 1993), which are a major component of the ECM. Though heparin has several other known actions, it is plausible that it affects some growth factor involved in target recognition by preventing the growth factor from binding to the ECM.

F. Topography Molecules

Although implicated in topographic specificity rather than pathfinding, the TOP proteins described by Trisler and collaborators (Trisler, 1990) and the 33-kDa repulsive molecule identified by Bonhoeffer and collaborators (Stahl *et al.*, 1990) deserve mention here. TOP_{DV} and TOP_{AP} are cell-surface proteins in chick, identified as antigens to particular monoclonal antibodies. They are distributed in steep dorsal-to-ventral and posterior-to-anterior gradients in the retina and are also present in tectum, distributed in retinotopically corresponding (i.e., inverted) gradients. The TOP proteins are obviously candidates for chemoaffinity molecules à la Sperry, though as yet the only evidence as to their function is that synaptogenesis in the retina is delayed by injection of antibody to TOP_{DV} (Trisler, 1990).

Bonhoeffer and collaborators found that chick temporal retinal axons grown in culture can choose between lanes of anterior and posterior tectal membranes, preferring to grow on the topographically appropriate anterior membranes (Walter *et al.*, 1987). This preference is due not to an attractive anterior molecule, but rather to a repulsive posterior molecule. This molecule has an apparent molecular weight of 33 kDa and is anchored in the membrane by a phosphatidylinositol linkage. In cross-species assays between mouse and chick (Godement and Bonhoeffer, 1989) and fish and chick (Vielmetter *et al.*, 1991), temporal retinal axons from one species grown on tectal membrane stripes from another species always showed a preference for the anterior stripes. Since the repulsive activity is functionally conserved across a wide evolutionary range, it seems certain that the *Xenopus* homologue of this molecule plays a role in topographic specificity.

G. Transduction Machinery

After receiving external guidance signals, the growth cone must transduce these into intracellular effects: cytoskeletal movements for steering, cy-

toskeletal rearrangements to form an arbor, and changes in gene expression upon beginning synaptogenesis. Presumably this signal transduction uses the same second messenger systems as other cells (Strittmatter and Fishman, 1991). The *src* family of nonreceptor tyrosine kinases is expressed in growth cones (Sobue, 1990; Matten *et al.*, 1990), making tyrosine phosphorylation a candidate step in the signaling cascade. On the cell biological level, it is commonly assumed that growth cone filopodia, which continually undergo a striking cycle of extension and retraction, play a role either in detecting signals by sampling the environment or in steering the growth cone by pulling it in particular directions. In culture, there is evidence for both sensory (Davenport *et al.*, 1993) and motile (Wessells and Nuttall, 1978) roles for filopodia.

Using the exposed-brain preparation, a series of second-messenger drugs were screemed for their effects on pathfinding (Chien *et al.*, 1992, and unpublished results). The strategy is to apply a range of concentrations of a membrane-permeant drug for an 18-hr exposure, then fill the retinal fibers with HRP. The lowest concentrations have no effects at all, while the highest are usually toxic to the embryo. The goal is to find an agent to which growth cones are especially sensitive, so that pathfinding or growth-cone morphology is disturbed at some intermediate concentration. High levels of permeant cyclic nucleotide analogs (8-bromo- and dibutyryl-cAMP and cGMP), calcium ionophore (A23187 and ionomycin) and the protein kinase C activator TPA have not yielded detectable effects. It has been found that low levels of external calcium (100–200 μM) seem to perturb pathfinding, resulting in shortened tracts that travel anterior of their normal path. Further experiments will be needed to see if these effects are due to reduced calcium influx or to some other cause. Experiments indicate that mastoporan, a peptide that activates G-proteins and has been shown to cause collapse of chick growth cones in culture (Igarashi *et al.*, 1993), causes collapse of *Xenopus* retinal growth cones *in vivo*. Experiments are underway to see if this collapse can be prevented by pretreatment with pertussis toxin. Though it seems likely that growth cones use one or more of the classical second messenger systems, it remains to be seen whether this *in vivo* screen will successfully reveal them.

To study the role of tyrosine kinases in retinal axon growth *in vivo*, Worley applied tyrosine kinase inhibitors to the exposed-tract preparation (Worley and Holt, 1992; T. Worley and C. Holt, in preparation). Herbimycin A and lavendustin A reduce the length of the retinal tract *in vivo* and cause greatly reduced staining of the exposed tracts with a phosphotyrosine-specific antibody. When applied to dissociated retinal ganglion cells in culture, herbimycin A causes axons to be shorter and growth cones to be larger. Together with the finding that basal levels of cell death and

protein synthesis are not affected in exposed tracts, these observations suggest that herbimycin inhibits the growth of retinal axons *in vivo* directly, rather than through some toxic effect on the neuroepithelium.

To test whether filopodia are necessary for pathfinding *in vivo*, cytochalasin B (CB), a microfilament-disrupting drug, was used to remove filopodia (Chien *et al.*, 1993). Cytochalasin experiments in the grasshopper limb bud had previously shown that loss of filopodia correlated with disrupted pathfinding by the Til pioneer axon (Bentley and Toroian-Raymond, 1986). The effects of cytochalasins on retinal axons were similar. At a concentration of 0.15 μg/ml CB, retinal growth cones were largely devoid of filopodia, and retinal tracts missed their normal caudad turn in the diencephalon and instead continued straight toward the pineal (Fig. 8). The action of CB on filopodia was rapid and reversible: viewed in time-lapse, growth cones *in vivo* lost their filopodia within about 30 min after CB was applied, and regenerated them after CB was removed. The dose dependences of aberrant pathfinding and of filopodial loss both *in vivo* and *in vitro* all roughly agree: at 0.15 μg/ml CB, retinal fibers took an aberrant route and filopodia were absent, while at 0.05 μg/ml CB, retinal fibers took their usual route to the tectum and filopodial numbers were normal. From this agreement, it is concluded that filopodia are required for normal pathfinding.

VI. Conclusions

The great advantages of the *Xenopus* visual system for studying axonal pathfinding have been its accessibility and amenability to embryonic manipulations. The results from transplant and deletion experiments give the following picture: The retinal growth cone acts autonomously, without instruction from the cell body. It does not require the presence of other axons (though it may use them if they are present), but instead follows cues on the surfaces of neuroepithelial cells or in the extracellular matrix. These cues are distributed globally across the brain.

The next step is clearly to dissect the molecular mechanisms that underlie pathfinding. This has already begun, using new methods that allow addition and deletion of specific molecules. As gravity holds the car to the road and permits it to travel forward, a combination of NCAM, N-cadherin, and integrin binding seems to attach the growth cone to the neuroepithelium and allow it to elongate. Tyrosine kinases are at work somewhere in the transmission, and are required for elongation. Target recognition at the tectum seems to be a distinct event, blockable by heparin. The growth cone seems to require filopodia to navigate properly; whether they are radio antennae or wheels used for turning is not yet

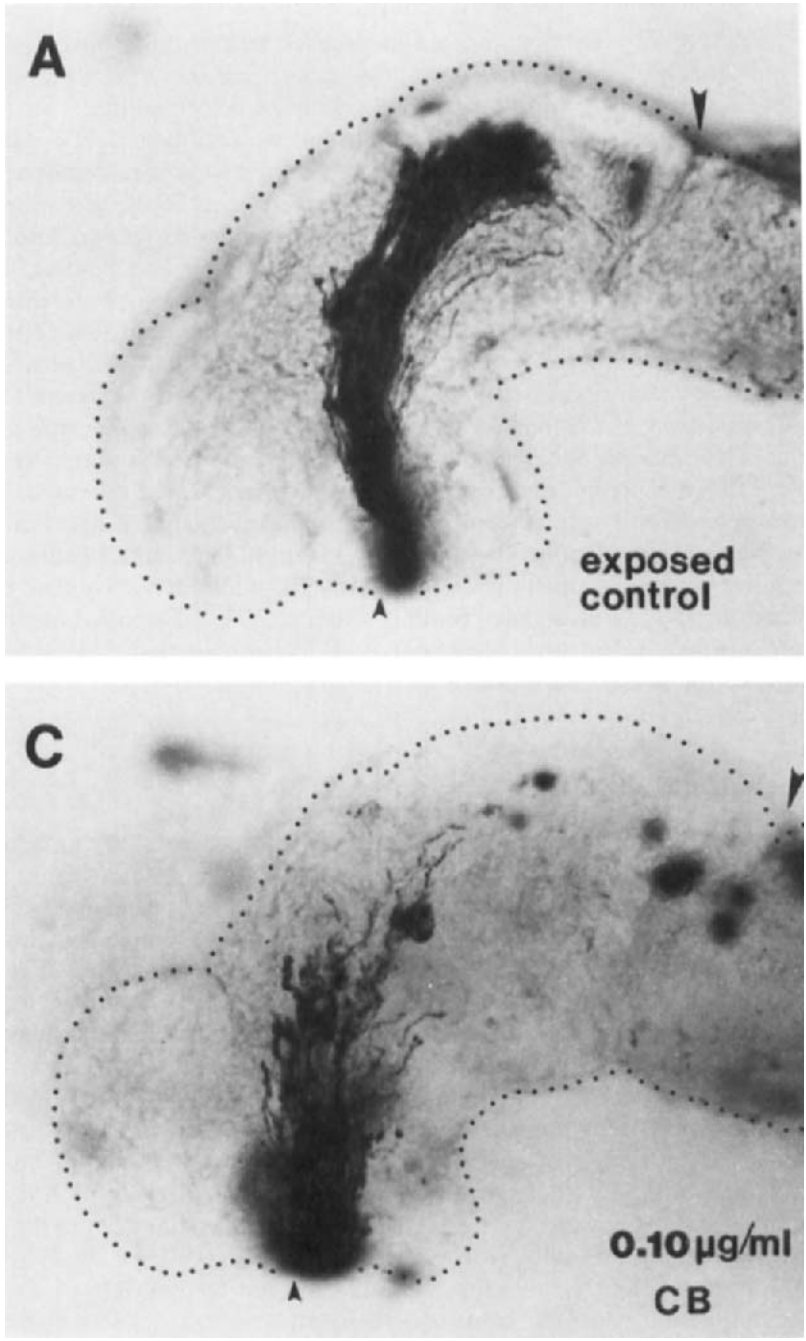

Fig. 8 Dose-dependent effect of cytochalasin B on pathfinding. Retinal fibers have been filled with HRP. Arrowheads indicate the optic chiasm and posterior edge of the tectum. (A) 0.15% DMSO control, St 39. Fibers have turned and arborized normally. (B) 0.05 µg/ml cytochalasin B (CB), St 40. Fibers have reached tectum, tract appears essentially normal.

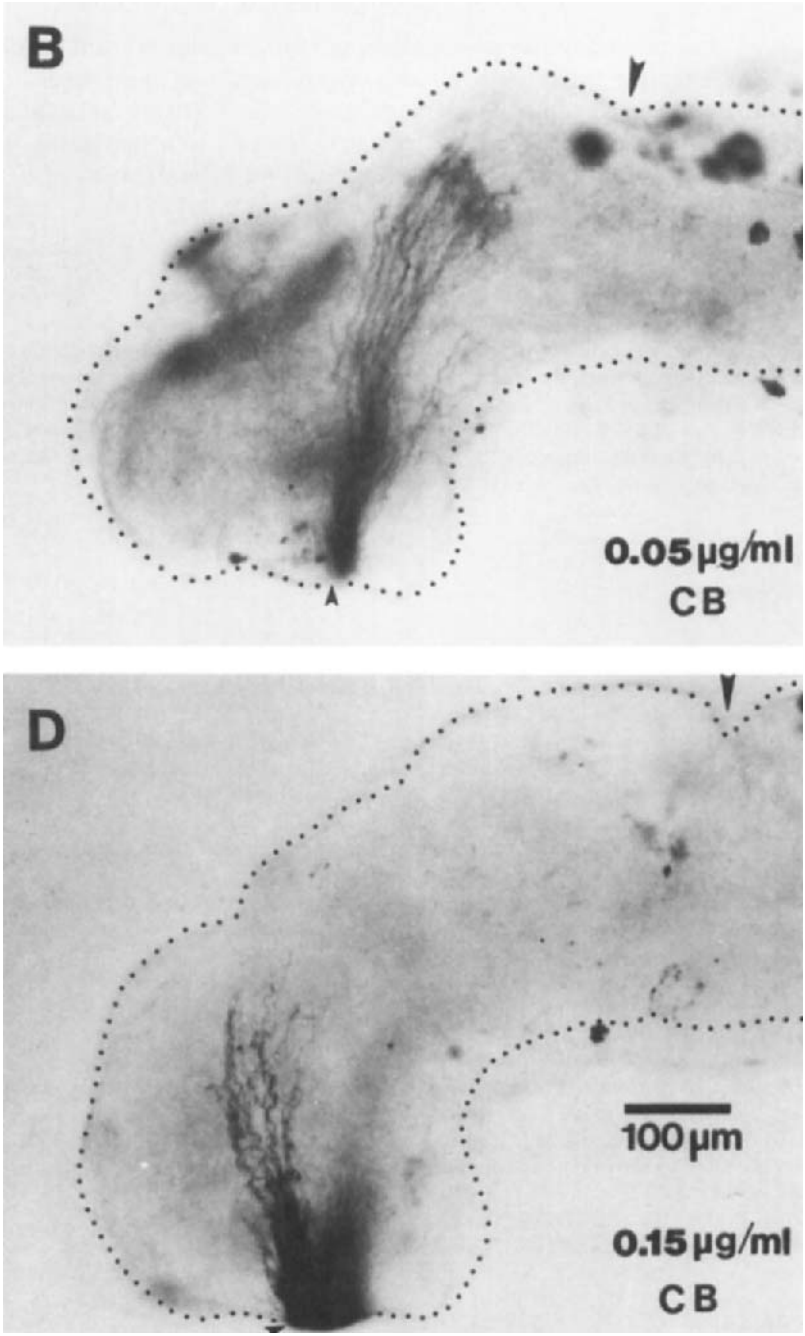

The HRP fill in this sample was unusually light. (C) 0.10 μg/ml CB, St 39. Intermediate effect: some fibers have reached the tectum, but most are going straight. (D) 0.15 μg/ml CB, St 39. Tract has taken an anterior path and failed to reorient; the leading fibers extend nearly to the dorsal midline. [From Chien *et al.* (1993). Copyright Cell Press.]

known. The guidance molecules used by the growth cone are still mysterious. The eventual goal is a complete understanding of the process that leads from the genes controlling the guidance cues, through the guidance molecules themselves, through the signal transduction apparatus, and finally to the end effects on the cytoskeleton and gene expression.

Acknowledgments

We thank members of the Harris and Holt laboratories for comments on the manuscript, and especially thank Christine Holt for discussions that led to many of the ideas set forth here. We thank Alain Lilienbaum, Sarah McFarlane, Rebecca Riehl, Don Sakaguchi, Andreas Walz, and Terri Worley for permission to quote unpublished results. This work was supported by American Cancer Society Postdoctoral Fellowship PF-3711 to C.B.C. and NIH Grant R01-HD14490 to W.A.H.

References

Amaya, E., Musci, T. J., and Kirschner, M. W. (1991). Expression of a dominant negative mutant of the FGF receptor disrupts mesoderm formation in *Xenopus* embryos. *Cell* **66,** 257–270.

Beach, D. H., and Jacobson, M. (1979a). Influences of thyroxine on cell proliferation in the retina of the clawed frog at different ages. *J. Comp. Neurol.* **183,** 615–623.

Beach, D. H., and Jacobson, M. (1979b). Patterns of cell proliferation in the retina of the clawed frog during development. *J. Comp. Neurol.* **183,** 603–613.

Bentley, D., and Keshishian, H. (1982). Pathfinding by peripheral pioneer neurons in grasshoppers. *Science* **218,** 1082–1088.

Bentley, D., and Toroian-Raymond, A. (1986). Disoriented pathfinding by pioneer neurone growth cones deprived of filopodia by cytochalasin treatment. *Nature* **323,** 712–715.

Burrill, J. D., and Easter, S. S. (1991). The relationship of optic growth cones to the tract of the postoptic commissure in the developing zebrafish brain. *Soc. Neurosci. Abstr.* **17,** 39. [Abstract 22.1]

Chien, C.-B., Rosenthal, D. E., Harris, W. A., and Holt, C. E. (1992). Signal transduction by retinal growth cones navigating in vivo: the role of filopodia and second messengers. *Soc. Neurosci. Abstr.* **18,** 34. [Abstract 22.1]

Chien, C.-B., Rosenthal, D. E., Harris, W. A., and Holt, C. E. (1993). Navigational errors made by growth cones without filopodia in the embryonic *Xenopus* brain. *Neuron* **11,** 237–251.

Cornel, E., and Holt, C. (1992). Precocious pathfinding: retinal axons can navigate in an axonless brain. *Neuron* **9,** 1001–1011.

Cowan, W. M., and Hunt, R. K. (1985). The development of the retinotectal projection: an overview. *In* "Molecular Bases of Neural Development" (G. M. Edelman, W. E. Gall, and W. M. Cowan, eds.), pp. 389–428. Wiley, New York.

Davenport, R. W., Dou, P., Rehder, V., and Kater, S. B. (1993). A sensory role for neuronal growth cone filopodia. *Nature* **361,** 721–724.

Easter, S. S., and Taylor, J. S. (1989). The development of the *Xenopus* retinofugal pathway: optic fibers join a pre-existing tract. *Development* **107,** 553–573.

Ferguson, B. A. (1983). Simultaneous elimination of impulse activity and normal pathways does not prevent developing retinal axons from reaching their normal targets. *Soc. Neurosci. Abstr.* **9,** 759. [Abstract 223.3]

Figdor, M. C., and Stern, C. D. (1993). Segmental organization of embryonic diencephalon. *Nature* **363,** 630–634.

Fraser, S. E. (1992). Patterning of retinotectal connections in the vertebrate visual system. *Curr. Opin. Neurobiol.* **2,** 83–87.

Fraser, S. E., Carhart, M. S., Murray, B. A., Chuong, C. M., and Edelman, G. M. (1988). Alterations in the *Xenopus* retinotectal projection by antibodies to *Xenopus* N-CAM. *Dev. Biol.* **129,** 217–230.

Fraser, S. E., Murray, B. A., Chuong, C. M., and Edelman, G. M. (1984). Alteration of the retinotectal map in *Xenopus* by antibodies to neural cell adhesion molecules. *Proc. Natl. Acad. Sci. USA* **81,** 4222–4226.

Fraser, S. E., and Perkel, D. H. (1990). Competitive and positional cues in the patterning of nerve connections. *J. Neurobiol.* **21,** 51–72.

Fujisawa, H., Ohtsuki, T., Takagi, S., and Tsuji, T. (1989). An aberrant retinal pathway and visual centers in *Xenopus* tadpoles share a common cell surface molecule, A5 antigen. *Dev. Biol.* **135,** 231–240.

Fujisawa, H., Watanabe, K., Tani, N., and Ibata, Y. (1981). Retinotopic analysis of fiber pathways in amphibians. II. The frog *Rana nigromaculata*. *Brain Res* **206,** 21–26.

Gawantka, V., Ellinger, Z. H., and Hausen, P. (1992). Beta 1-integrin is a maternal protein that is inserted into all newly formed plasma membranes during early *Xenopus* embryogenesis. *Development* **115,** 595–605.

Gaze, R. M., and Grant, P. (1992a). Development of the tectum and diencephalon in relation to the time of arrival of the earliest optic fibres in *Xenopus*. *Anat. Embryol. (Berlin)* **185,** 599–612.

Gaze, R. M., and Grant, P. (1992b). Spatio-temporal patterns of retinal ganglion cell death during *Xenopus* development. *J. Comp. Neurol.* **315,** 264–274.

Gaze, R. M., Keating, M. J., Ostberg, A., and Chung, S. H. (1979). The relationship between retinal and tectal growth in larval *Xenopus:* implications for the development of the retino-tectal projection. *J. Embryol. Exp. Morphol.* **53,** 103–143.

Gierer, A. (1987). Directional cues for growing axons forming the retinotectal projection. *Development* **101,** 479–489.

Glasser, S., and Ingle, D. (1978). The nucleus isthmus as a relay station in the ipsilateral visual projection to the frog's optic tectum. *Brain Res.* **159,** 214–218.

Godement, P., and Bonhoeffer, F. (1989). Cross-species recognition of tectal cues by retinal fibers in vitro. *Development* **106,** 313–320.

Gooday, D. J. (1990). Retinal axons in *Xenopus laevis* recognize differences between tectal and diencephalic glial cells in vitro. *Cell Tissue Res.* **259,** 595–598.

Grobstein, P., and Comer, C. (1977). Post-metamorphic eye migration in *Rana* and *Xenopus*. *Nature* **269,** 54–56.

Gruberg, E. R., and Udin, S. B. (1978). Topographic projections between the nucleus isthmi and the tectum of the frog *Rana pipiens*. *J. Comp. Neurol.* **179,** 487–500.

Harland, R. M. (1991). In situ hybridization: an improved whole-mount method for *Xenopus* embryos. *Methods Cell Biol.* **36,** 685–695.

Harris, W. A. (1980). The effects of eliminating impulse activity on the development of the retinotectal projection in salamanders. *J. Comp. Neurol.* **194,** 303–317.

Harris, W. A. (1984). Axonal pathfinding in the absence of normal pathways and impulse activity. *J. Neurosci.* **4,** 1153–1162.

Harris, W. A. (1986). Homing behaviour of axons in the embryonic vertebrate brain. *Nature* **320,** 266–269.

Harris, W. A. (1989). Local positional cues in the neuroepithelium guide retinal axons in embryonic *Xenopus* brain. *Nature* **339,** 218–221.

Harris, W. A., Holt, C. E., and Bonhoeffer, F. (1987). Retinal axons with and without their somata, growing to and arborizing in the tectum of *Xenopus* embryos: a time-lapse video study of single fibres *in vivo*. *Development* **101,** 123–133.

Harris, W. A., Holt, C. E., Smith, T. A., and Gallenson, N. (1985). Growth cones of developing retinal cells in vivo, on culture surfaces, and in collagen matrices. *J. Neurosci. Res.* **13,** 101–122.

Harris, W. A., and Messersmith, S. L. (1992). Two cellular inductions involved in photoreceptor determination in the *Xenopus* retina. *Neuron* **9,** 357–372.

Harvey, R. P., and Melton, D. A. (1988). Microinjection of synthetic Xhox-1A homeobox mRNA disrupts somite formation in developing *Xenopus* embryos. *Cell* **53,** 687–697.

Holt, C. (1980). Cell movements in *Xenopus* eye development. *Nature* **287,** 850–852.

Holt, C. E. (1984). Does timing of axon outgrowth influence initial retinotectal topography in *Xenopus? J. Neurosci.* **4,** 1130–1152.

Holt, C. E. (1989). A single-cell analysis of early retinal ganglion cell differentiation in *Xenopus:* from soma to axon tip. *J. Neurosci.* **9,** 3123–3145.

Holt, C. E., Bertsch, T. W., Ellis, H. M., and Harris, W. A. (1988). Cellular determination in the *Xenopus* retina is independent of lineage and birth date. *Neuron* **1,** 15–26.

Holt, C. E., Garlick, N., and Cornel, E. (1990). Lipofection of cDNAs in the embryonic vertebrate central nervous system. *Neuron* **4,** 203–214.

Holt, C. E., and Harris, W. A. (1983). Order in the initial retinotectal map in *Xenopus:* a new technique for labelling growing nerve fibres. *Nature* **301,** 150–152.

Holt, C. E., and Harris, W. A. (1993). Position, guidance, and mapping in the developing visual system. *J. Neurobiol.* **24,** 1400–1422.

Holtfreter, J. (1943). Properties and functions of the surface coat in amphibian embryos. *J. Exp. Zool.* **93,** 251–323.

Hoskins, S. G., and Grobstein, P. (1985a). Development of the ipsilateral retinothalamic projection in the frog *Xenopus laevis*. I. Retinal distribution of ipsilaterally projecting cells in normal and experimentally manipulated frogs. *J. Neurosci.* **5,** 911–919.

Hoskins, S. G., and Grobstein, P. (1985b). Development of the ipsilateral retinothalamic projection in the frog *Xenopus laevis*. III. The role of thyroxine. *J. Neurosci.* **5,** 930–940.

Igarashi, M., Strittmatter, S. M., Vartanian, T., and Fishman, M. C. (1993). Mediation by G proteins of signals that cause collapse of growth cones. *Science* **259,** 77–79.

Jack, J., Gooday, D., Wilson, M., and Gaze, M. (1991). Retinal axons in *Xenopus* show different behaviour patterns on various glial substrates *in vitro*. *Anat. Embryol. (Berlin)* **183,** 193–203.

Jacobson, M. (1967). Retinal ganglion cells: specification of central connections in larval *Xenopus laevis*. *Science* **155,** 1106–1108.

Jacobson, M. (1968). Development of neuronal specificity in retinal ganglion cells of *Xenopus*. *Dev. Biol.* **17,** 202–218.

Jessell, T. M. (1988). Adhesion molecules and the hierarchy of neural development. *Neuron* **1,** 3–13.

Johnston, A. R., and Gooday, D. J. (1991). *Xenopus* temporal retinal neurites collapse on contact with glial cells from caudal tectum *in vitro*. *Development* **113,** 409–417.

Kaethner, R. J., and Stuermer, C. A. (1992). Dynamics of terminal arbor formation and target approach of retinotectal axons in living zebrafish embryos: a time-lapse study of single axons. *J. Neurosci.* **12,** 3257–3271.

Kan, M., Wang, F., Xu, J., Crabb, J. W., Hou, J., and McKeehan, W. L. (1993). An essential heparin-binding domain in the fibroblast growth factor receptor kinase. *Science* **259,** 1918–1921.

Katz, M. J. (1985). How straight do axons grow? *J. Neurosci.* **5,** 589–595.

Kolodkin, A. L., Matthes, D. J., O'Connor, T. P., Patel, N. H., Admon, A., Bentley, D., and Goodman, C. S. (1992). Fasciclin IV: sequence, expression, and function during growth cone guidance in the grasshopper embryo. *Neuron* **9,** 831–845.

Krauss, S., Johansen, T., Korzh, V., and Fjose, A. (1991). Expression pattern of zebrafish pax genes suggests a role in early brain regionalization. *Nature* **353,** 267–270.

Levine, R. L. (1980). An autoradiographic study of the retinal projection in *Xenopus laevis* with comparisons to *Rana. J. Comp. Neurol.* **189,** 1–29.

Lilienbaum, A., Riehl, R. H., Reszka, A. A., Horwitz, A. F., and Holt, C. E. (1993). Expression of mutant beta-1 integrin and N-cadherin in the developing retina. *Soc. Neurosci. Abstr.* **19,** 1089. [Abstract 451.2]

Lumsden, A. G., and Davies, A. M. (1983). Earliest sensory nerve fibres are guided to peripheral targets by attractants other than nerve growth factor. *Nature* **306,** 786–788.

Matten, W. T., Aubry, M., West, J., and Maness, P. F. (1990). Tubulin is phosphorylated at tyrosine by pp60c-src in nerve growth cone membranes. *J. Cell Biol.* **111,** 1959–1970.

McFarlane, S., Walz, A., and Holt, C. E. (1993). Heparin blocks target recognition in the developing visual system of *Xenopus. Soc. Neurosci. Abstr.* **19,**1087. [Abstract 450.8]

Neugebauer, K. M., Tomaselli, K. J., Lilien, J., and Reichardt, L. F. (1988). N-cadherin, NCAM, and integrins promote retinal neurite outgrowth on astrocytes *in vitro. J. Cell Biol.* **107,** 1177–1187.

Nieuwkoop, P. D., and Faber, J. (1967). "Normal Table of *Xenopus laevis* (Daudin)." North-Holland, Amsterdam.

O'Rourke, N. A., and Fraser, S. E. (1986). Dynamic aspects of retinotectal map formation revealed by a vital-dye fiber-tracing technique. *Dev. Biol.* **114:** 265–76.

O'Rourke, N. A., and Fraser, S. E. (1989). Gradual appearance of a regulated retinotectal projection pattern in *Xenopus laevis. Dev. Biol.* **132,** 251–265.

O'Rourke, N. A., and Fraser, S. E. (1990). Dynamic changes in optic fiber terminal arbors lead to retinotopic map formation: an in vivo confocal microscopic study. *Neuron* **5,** 159–171.

Raper, J. A., Bastiani, M., and Goodman, C. S. (1983). Pathfinding by neuronal growth cones in grasshopper embryos. II. Selective fasciculation onto specific axonal pathways. *J. Neurosci.* **3,** 31–41.

Sakaguchi, D. S., Moeller, J. F., Coffman, C. R., Gallenson, N., and Harris, W. A. (1989). Growth cone interactions with a glial cell line from embryonic *Xenopus* retina. *Dev. Biol.* **134,** 158–174.

Sakaguchi, D. S., and Murphey, R. K. (1985). Map formation in the developing *Xenopus* retinotectal system: an examination of ganglion cell terminal arborizations. *J. Neurosci.* **5,** 3228–3245.

Sakaguchi, D. S., Murphey, R. K., Hunt, R. K., and Tompkins, R. (1984). The development of retinal ganglion cells in a tetraploid strain of *Xenopus laevis:* a morphological study utilizing intracellular dye injection. *J. Comp. Neurol.* **224,** 231–251.

Sakaguchi, D. S., and Radke, K. (1992). Anti-beta 1 integrin antibodies inhibit regenerating retinal ganglion cell axon outgrowth as well as glial cell adhesion and spreading. *Soc. Neurosci. Abstr.* **18,** 606. [Abstract 263.1]

Scalia, F. (1973). Autoradiographic demonstration of optic nerve fibers in the stratum zonale of the frog's tectum. *Brain Res.* **58,** 484–488.

Silver, J., and Rutishauser, U. (1984). Guidance of optic axons in vivo by a preformed adhesive pathway on neuroepithelial endfeet. *Dev. Biol.* **106,** 485–499.

Singer, M. A., Hortsch, M., Goodman, C. S., and Bentley, D. (1992). Annulin, a protein expressed at limb segment boundaries in the grasshopper embryo, is homologous to protein cross-linking transglutaminases. *Dev. Biol.* **154,** 143–159.

Sobue, K. (1990). Involvement of the membrane cytoskeletal proteins and the src gene product in growth cone adhesion and movement. *Neurosci. Res. Suppl.* S80–S91.

Spemann, H., and Mangold, H. (1924). Über induktion von embryonalanlagen durch implantation artfremder organisatoren. *Wilhelm Roux Arch. Entwicklungsmech. Organ.* **100,** 599–638.

Sperry, R. W. (1963). Chemoaffinity in the orderly growth of nerve fiber patterns and connections. *Proc. Natl. Acad. Sci. USA* **50,** 703–710.

Sretavan, D. W., and Reichardt, L. F. (1993). Time-lapse video analysis of retinal ganglion cell axon pathfinding at the mammalian optic chiasm: growth cone guidance using intrinsic chiasm cues. *Neuron* **10,** 761–777.

Stahl, B., Muller, B., von Boxberg, Y., Cox, E. C., and Bonhoeffer, F. (1990). Biochemical characterization of a putative axonal guidance molecule of the chick visual system. *Neuron* **5,** 735–743.

Straznicky, K., Gaze, R. M., and Keating, M. J. (1971). The retinotectal projections after uncrossing the optic chiasma in *Xenopus* with one compound eye. *J. Embryol. Exp. Morphol.* **26,** 523–542.

Strittmatter, S. M., and Fishman, M. C. (1991). The neuronal growth cone as a specialized transduction system. *Bioessays* **13,** 127–134.

Stuermer, C. A., Rohrer, B., and Munz, H. (1990). Development of the retinotectal projection in zebrafish embryos under TTX-induced neural-impulse blockade. *J. Neurosci.* **10,** 3615–3626.

Takagi, S., Tsuji, T., Amagai, T., Takamatsu, T., and Fujisawa, H. (1987). Specific cell surface labels in the visual centers of *Xenopus laevis* tadpole identified using monoclonal antibodies. *Dev. Biol.* **122,** 90–100.

Taylor, J. S. (1990). The directed growth of retinal axons towards surgically transposed tecta in *Xenopus;* an examination of homing behaviour by retinal ganglion cell axons. *Development* **108,** 147–158.

Taylor, J. S. (1991). The early development of the frog retinotectal projection. *Development* (Suppl 2), 95–104.

Thanos, S., Bonhoeffer, F., and Rutishauser, U. (1984). Fiber-fiber interaction and tectal cues influence the development of the chicken retinotectal projection. *Proc. Natl. Acad. Sci. USA* **81,** 1906–1910.

Trisler, D. (1990). Cell recognition and pattern formation in the developing nervous system. *J. Exp. Biol.* **153,** 11–27.

Udin, S. B., and Fawcett, J. W. (1988). Formation of topographic maps. *Annu. Rev. Neurosci.* **11,** 289–327.

Vielmetter, J., Walter, J., and Stuermer, C. A. (1991). Regenerating retinal axons of goldfish respond to a repellent guiding component on caudal tectal membranes of adult fish and embryonic chick. *J. Comp. Neurol.* **311,** 321–329.

Walter, J., Henke-Fahle, S., and Bonhoeffer, F. (1987). Avoidance of posterior tectal membranes by temporal retinal axons. *Development* **101,** 909–913.

Wessells, N. K., and Nuttall, R. P. (1978). Normal branching, induced branching, and steering of cultured parasympathetic motor neurons. *Exp. Cell Res.* **115,** 111–122.

Witkovsky, P., Gallin, E., Hollyfield, J. G., Ripps, H., and Bridges, C. D. (1976). Photoreceptor thresholds and visual pigment levels in normal and vitamin A-deprived *Xenopus* tadpoles. *J. Neurophysiol.* **39,** 1272–1287.

Worley, T. L., and Holt, C. E. (1992). Effects of tyrosine kinase inhibition on growing retinal ganglion cell axons. *Soc. Neurosci. Abstr.* **18,** 35. [Abstract 22.4]

This Page Intentionally Left Blank

5

The *in Vivo* Roles of Müllerian-Inhibiting Substance

Richard R. Behringer
Department of Molecular Genetics
The University of Texas
M. D. Anderson Cancer Center
Houston, Texas 77030

I. Introduction

Normal development of the reproductive organs and germ cells is essential for an organism to transmit its genes to future generations and, moreover, for the continuation of the species. This chapter focuses on the role of the gonadal hormone, Müllerian-inhibiting substance (MIS), during mammalian sexual differentiation and germ cell development. *In vivo* approaches for studying MIS function, especially those utilizing transgenic mice (Palmiter and Brinster, 1986) and gene targeting technologies in mouse embryonic stem (ES) cells, are emphasized (Capecchi, 1989). Readers interested in the biochemical, cellular, and molecular biological aspects

Current Topics in Developmental Biology, Vol. 29

of MIS are directed to reviews by Donahoe *et al.* (1987); Cate *et al.* (1990); Cate and Wilson (1993); and Josso *et al.* (1993).

II. Mammalian Sex Determination and Differentiation

It has become clear in recent years that a gene termed *SRY* in humans and *Sry* in mouse and located on the Y chromosome encodes a transcription factor that presumably regulates the expression of subordinate genes to direct the differentiation of the pair of indifferent fetal gonads (genital ridges) into testes (Sinclair *et al.*, 1990; Gubbay *et al.*, 1990; Koopman *et al.*, 1991). In the absence of this gene, as in the case of XX individuals, the undifferentiated gonads develop into ovaries. Thus, during the process of sex determination in mammals the activity or lack of activity of *Sry* specifies the fate of a single paired primordium to either a male or a female phenotype. Once sex determination is established (i.e., testes form), the production of hormones secreted by the fetal gonads controls the differentiation of the genital duct systems and external genitalia.

During mammalian embryogenesis, both XX and XY individuals develop two pairs of genital ducts associated with the mesonephroi and undifferentiated gonads (Fig. 1). The paramesonephric ducts (also known as the Müllerian ducts) have the potential to differentiate into female reproductive organs including the uterus, oviducts, and upper portion of the vagina. The mesonephric ducts (also known as the Wolffian ducts) are the primordia of male reproductive organs that include the vas deferens, epididymides, and seminal vesicles. Since each individual, regardless of sex chromosome genotype, has the potential to develop both male and female reproductive organs, one genital duct system must differentiate while the other must regress for normal male or female development to occur. Therefore, a mechanism is required to produce individuals that possess only one sexual type of reproductive organs. This is in contrast to the situation for development of the gonads, where there is only a single pair of primordia that can differentiate into either sexual type depending on the *SRY*/*Sry* genotype.

III. Müllerian Inhibiting Substance

A. Alfred Jost and *l'hormone inhibitrice*

In the middle of this century, Alfred Jost at the University of Paris performed pioneering experiments that investigated the influence of fetal hormones during development (Jost, 1947, 1953). He surgically manipu-

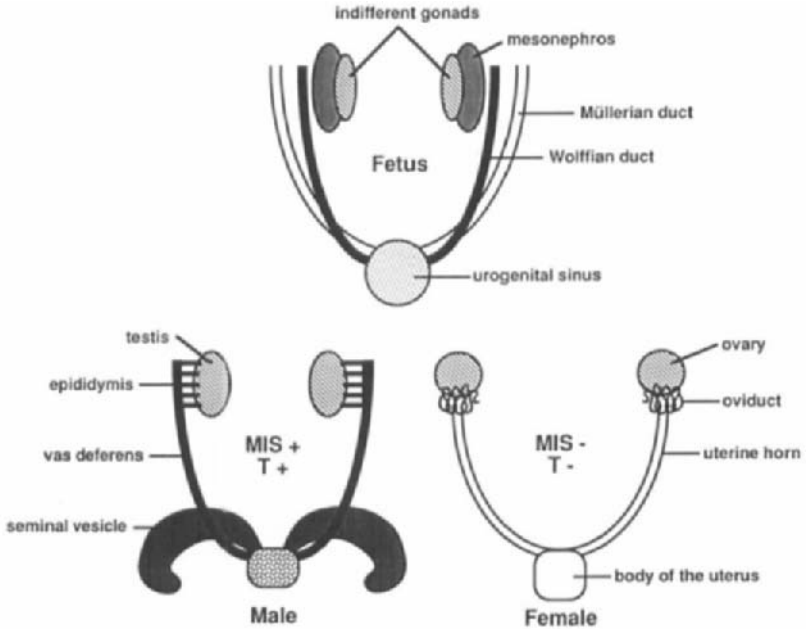

Fig. 1 Mammalian sexual differentiation. The Müllerian ducts (paramesonephric ducts) give rise to the uterus, oviducts, and the upper portion of the vagina. The Wolffian ducts (mesonephric ducts) give rise to the epididymides, vas deferens, and seminal vesicles. MIS produced by the Sertoli cells of the fetal testes causes the regression of the Müllerian ducts, and testosterone (T) produced by Leydig cells induces the differentiation of the Wolffian duct system. The absence of both hormones during female fetal development permits the development of the Müllerian duct system while the Wolffian ducts passively regress.

lated the gonads of fetal rabbits before or at the beginning of, during, and at the later stages of somatic sexual differentiation. Removal of the ovaries from female fetuses at the beginning of somatic sexual differentiation resulted in female development. Castration of male fetuses at this stage also resulted in differentiation to the female phenotype. The Wolffian duct system regressed and the Müllerian ducts persisted and differentiated. Jost noted that development began toward the male phenotype but reversed upon removal of the gonads. These observations led to the hypothesis that the fetal testis secreted two types of hormones: the first hormone possessed stimulatory activity to induce the differentiation of the urogenital sinus and Wolffian duct system while the second hormone possessed inhibitory activity that caused the retrogression of the Müllerian ducts.

Three additional lines of evidence supported the idea of a Müllerian duct regression hormone secreted by the fetal testis. First, unilateral removal of the fetal testis yielded individuals in which the urogenital sinus and exter-

nal genitalia were masculinized. The Wolffian duct on the unoperated side was normal; however, on the operated side, the Wolffian duct was not fully normal and remnants of a uterine horn or a well-developed uterine horn were found. These observations suggested that a Müllerian duct inhibitory factor was normally produced by the testis that was removed and that the factor had a limited distance of action. Second, when a testicular graft was introduced into a female fetus, a local inhibition of the Müllerian duct and stabilization of the Wolffian duct resulted. These findings also supported the idea of a Müllerian duct inhibitory activity produced from the fetal testis. Finally, when a crystal of synthetic androgen was introduced into the abdominal cavity of a castrated male fetus, the development of male structures was stimulated but the Müllerian ducts were not inhibited in their development. These results separated the masculinizing activities of androgens and the Müllerian duct inhibitory activity. These elegant embryological experiments clearly demonstrated the existence of a novel fetal testicular hormone that caused the regression of the Müllerian ducts. Jost initially termed this activity *l'hormone inhibitrice* or, in his English publications, the Müllerian inhibitor (Josso *et al.*, 1993). The hormone is more commonly known as anti-Müllerian hormone (AMH) or Müllerian-inhibiting substance (Josso *et al.*, 1993).

In summary, the pathways of male or female sexual differentiation are controlled by the presence or absence of hormones produced by the fetal gonads (Fig. 1). During male development, XY fetuses usually develop testes that initially produce MIS. MIS in turn actively induces the regression of the Müllerian ducts, thereby preventing the development of female reproductive organs. This regression must occur during a specific window of development because at latter stages the Müllerian ducts become insensitive to MIS (Picon, 1969; Josso *et al.*, 1977). Subsequently, testosterone is produced by the Leydig cells of the testes to induce the differentiation of the Wolffian ducts. During female development, XX fetuses usually develop ovaries that do not express MIS, which creates a permissive environment for the differentiation of the Müllerian ducts. In addition, the lack of testosterone leads to the passive regression of the Wolffian ducts. Thus, MIS and testosterone mediate a switch between the differentiation of the male and female extragonadal reproductive organs.

B. Assays for MIS Activity and Molecular Cloning

In 1969, Picon developed an organ culture system to assay for MIS activity. This assay was instrumental in the purification of the hormone and the subsequent molecular cloning of the gene. In this assay, morphological changes of the Müllerian duct of day 14.5 fetal rat urogenital ridges induced

by MIS are scored histologically. A more quantitative assay for MIS activity has been developed that is based on the ability of MIS to repress aromatase biosynthesis in the fetal ovary (Vigier *et al.*, 1989; di Clemente *et al.*, 1992).

The MIS cDNA was initially cloned by two independent groups (Cate *et al.*, 1986; Picard *et al.*, 1986). One approach sequenced tryptic peptides of bovine MIS and subsequently used degenerate oligonucleotides as probes to screen a newborn bovine testis cDNA library (Cate *et al.*, 1986). The other approach screened a newborn bovine testis cDNA expression library using antisera raised against bovine MIS (Picard *et al.*, 1986). Since then, the MIS gene has been isolated in cow, human, rat, and mouse (Cate *et al.*, 1986; Picard *et al.*, 1986; Haqq *et al.*, 1992; Münsterberg and Lovell-Badge, 1991).

The MIS gene is subdivided into five exons encompassing approximately 2.75 kb. In humans, MIS maps to the short arm of chromosome 19 and in mouse to chromosome 10 between phenylalanine hydroxylase and mast cell growth factor (Cohen-Haguenauer *et al.*, 1987; King *et al.*, 1991). DNA sequencing of MIS revealed a similarity between the C-terminal portion of MIS and members of the transforming growth factor-β (TGF-β) gene superfamily of growth and differentiation factors (Cate *et al.*, 1986). The members of this large gene family include activins, inhibins, and bone morphogenetic factors (Massague, 1990). MIS is a homodimer and, like the other members of the TGF-β gene family, is synthesized as a precursor protein that requires proteolytic cleavage to generate C-terminal bioactive polypeptides (Pepinsky *et al.*, 1988). The N-terminal portion is apparently important for the maintenance of MIS biological activity (Wilson *et al.*, 1993).

C. MIS Expression Pattern

MIS expression is restricted to Sertoli cells of the fetal and adult testis and granulosa cells of the postnatal ovary (Cate *et al.*, 1990). It is initially detected at the time of seminiferous tubule formation (Picon, 1970; Tran *et al.*, 1977; Vigier *et al.*, 1983; Münsterberg and Lovell-Badge, 1991). The highest levels of MIS in males are detected during the period of Müllerian duct regression but remain high until birth, when they precipitously drop during pubertal maturation. In the ovary after birth, MIS is found in granulosa cells of preantral and antral follicles and is not detectable in primary and growing follicles or corpus lutea (Takahashi *et al.*, 1986; Bézard *et al.*, 1987; Ueno *et al.*, 1989; Münsterberg and Lovell-Badge, 1991). MIS protein is detected most abundantly in granulosa cells that contact the oocyte and line the antrum. The levels of MIS in the

ovary after birth are 0.1% of the levels produced by the fetal testes (Josso, 1986). The expression pattern observed in male and female gonads suggests that, in addition to its Müllerian duct inhibitory activity, MIS may regulate gonadal function and gametogenesis.

IV. Gain of Function

A. The Freemartin

In certain species, such as the bovine, exposure of a female fetus to a male twin's blood by chorioallantoic anastomosis results in regression of the Müllerian ducts, a condition known as freemartinism (Jost *et al.*, 1972). In addition, freemartin ovaries cease to grow, become depleted of germ cells, and may develop seminiferous tubules containing Sertoli cells. Some aspects of the freemartin effect, including inhibition of germ cell proliferation and the development of seminiferous cord-like structures, can be reproduced *in vitro* when fetal rat ovaries are exposed to purified MIS (Vigier *et al.*, 1987). Therefore, as Jost first suspected, a proportion of the abnormal phenotypes associated with the freemartin are likely to be due to the ectopic exposure of a female fetus to MIS (Jost *et al.*, 1972).

B. Transgenic Mice That Chronically Express Human MIS

To investigate the potential functions of MIS during mouse development, the human MIS gene was ectopically expressed in transgenic mice by means of the mouse metallothionein (MT) promoter (Behringer *et al.*, 1990). The MT promoter was chosen because it can direct the expression of heterologous genes to a variety of fetal and adult tissues in transgenic mice (Palmiter and Brinster, 1986). As a result, lines of transgenic mice were established that possessed circulating levels of human MIS in plasma ranging on average from 40 to 4400 ng/ml. As one might predict, female transgenic mice expressing the human MIS gene lacked a uterus and oviducts. Surprisingly, in nearly all cases ovaries were also absent in adult transgenic females. However, some transgenic females, predominantly those in the lower-expressing lines, lacked a uterus but retained one or both ovaries. Apparently, the effects of ectopic MIS exposure were titratable, with the Müllerian ducts being the most sensitive to MIS action. When the absence of ovaries in the adult transgenic females was investigated in the highest-expressing line, it was determined that ovaries were present in newborn transgenic females but that germ cells were subsequently lost and the somatic components of the ovary reorganized into

structures reminiscent of the seminiferous tubules of the male gonad (Fig. 2). These virilized ovaries subsequently degenerated since they were never found in adult female transgenic mice.

Interestingly, abnormal phenotypes were also observed in a proportion of the males (5/21) from the highest-expressing lines. Externally, these transgenic males were feminized, exhibiting mammary gland development, internally, Wolffian duct differentiation was arrested, and the testes were undescended (Fig. 3). It was postulated that this feminization phenotype was most likely due to a defect in androgen biosynthesis, suggesting that high levels of MIS could influence the function of Leydig cells.

A number of conclusions can be drawn from the results of these transgenic mouse studies. First, MIS can act *in vivo* as the Müllerian inhibitor. Second, the virilization of the postnatal ovaries and the alteration in Leydig cell function suggest a role for MIS in testicular differentiation. Finally, the observation that altered levels of MIS resulted in abnormal testicular descent is consistent with the idea that regulated levels of MIS are required for proper descent of the testes (Hutson and Donahoe, 1986).

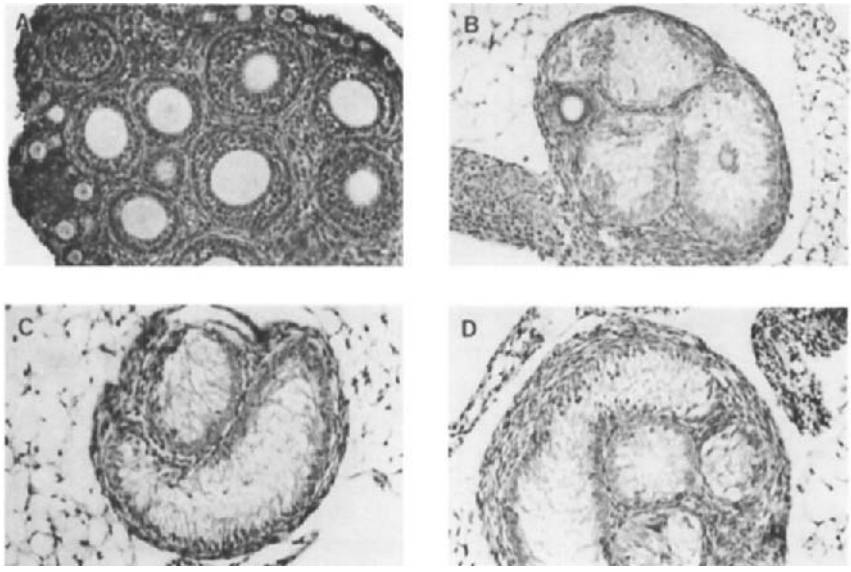

Fig. 2 Histological sections of virilized ovaries from 16-day-old female transgenic mice that chronically express high levels of human MIS. (A) Nontransgenic littermate; (B–D) transgenic. Note that the transgenic ovaries have become depleted of germ cells and the somatic components of the gonad have been reorganized into structures similar in appearance to the seminiferous tubules of the male testis.

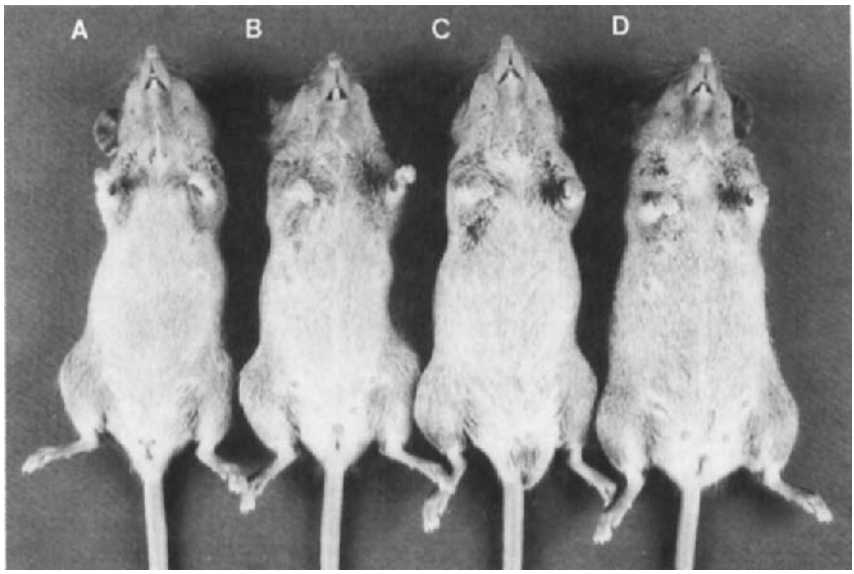

Fig. 3 External appearance of transgenic mice that chronically express human MIS. (A, B) Females; (C, D) males. (A, C) Nontransgenic; (B, D) transgenic. Note that the females are similar in appearance while the transgenic male is feminized. The feminization of transgenic males occurred in the highest MIS-expressing lines in about a quarter of the transgenic males.

V. Loss of Function

A. A Dominant Negative Approach in Transgenic Mice

While the gain-of-function studies discussed earlier demonstrated the potential roles that MIS can play during development, they did not reveal the required functions of this hormone. Answers to those questions require animals lacking MIS function. Therefore, to create mice that lacked MIS function, a dominant negative strategy was employed using transgenic mice.

A mutant human MIS protein in which Arg 427 is converted to Thr cannot be cleaved and is not active in the *in vitro* regression assay (Cate *et al.*, 1990). Therefore, an MT-MIS gene construct in which Arg 427 was mutated to Thr was produced and used to generate transgenic mice (Behringer and Cate, 1994). The expectation was that the mutant human MIS (hMIS) polypeptides would heterodimerize with the endogenous mouse MIS polypeptides and that the resulting heterodimers would not be processed into biologically active C-terminal molecules. Three transgenic

mouse lines were established that expressed 100–3500 ng/ml mutant hMIS in plasma. However, all males and females from the three lines developed normally and were fertile. Perhaps the levels of mutant MIS or cell specificity and timing were not appropriately regulated in Sertoli and granulosa cells by the MT promoter. Nevertheless, these experiments supported *in vivo* the requirement of proteolytic processing for MIS biological activity (Pepinsky *et al.*, 1988, Wilson *et al.*, 1993).

B. Spontaneously Occurring Loss of Function: The Persistent Müllerian Duct Syndrome

In humans, persistent Müllerian duct syndrome (PMDS) is a rare form of male pseudohermaphroditism characterized by the presence of a uterus and Fallopian tubes in XY individuals that are overtly male in phenotype (Guerrier *et al.*, 1989). PMDS is usually detected during surgery for corrections of cryptorchidism or inguinal hernia. Thus, testicular tissue develops but abnormalities in testicular descent are associated with this syndrome. Mutations in the MIS gene have been found in a proportion of the PMDS cases with undetectable or low levels of serum MIS (Knebelmann *et al.*, 1991; Carré-Eusebe *et al.*, 1992; Imbeaud *et al.*, 1994). Interestingly, the first three exons appear to be especially prone to mutation (Imbeaud *et al.*, 1994). Presumably, the PMDS cases in which normal levels of serum MIS are detected are due to the insensitivity of target tissues to the hormone. One dog model for PMDS exists that produces functional MIS and may carry a mutation in the receptor for MIS (Meyers-Wallen *et al.*, 1989).

Thus, mutations in the MIS gene of humans can result in PMDS and confirm the requirement of this fetal hormone for the regression of the Müllerian ducts during male development. However, to fully examine the requirements of this hormone during development and fertility, an experimental animal model for MIS deficiency is required.

C. MIS Mutant Mice

Gene targeting in mouse ES cells makes it possible to generate mice carrying mutations in specific genes (Capecchi, 1989). Therefore, to understand the required functions of MIS during embryogenesis and germ cell development, the MIS gene was mutated by homologous recombination in ES cells to generate MIS mutant mice (Behringer *et al.*, 1994). The mutation was engineered to simultaneously delete a portion of the first exon, the first intron, and the second exon and insert a neomycin resistance

expression cassette in reverse orientation relative to the direction of MIS transcription. Correctly targeted ES clones were obtained and injected into blastocysts to produce mouse chimeras to regenerate mice heterozygous for the MIS mutation.

Males and females homozygous for the MIS mutations were recovered from heterozygous intercrosses at the predicted Mendelian frequencies and were externally indistinguishable from their heterozygous or wild-type littermates. Since a loss of MIS function could possibly alter overt sexual phenotypes, male and female homozygous mutants were genotyped for the presence of the Y chromosome. All phenotypic males were Y chromosome positive, and all phenotypic females were Y chromosome negative.

All of the female homozygous mutants possessed a uterus with oviducts and ovaries that were morphologically normal. In addition, all of the females were fertile. Therefore, although MIS is expressed in a regulated manner in the ovary after birth, there is apparently no requirement for MIS expression for normal ovarian function. Perhaps related molecules that are also expressed in granulosa cells might provide redundant or compensatory functions in the absence of MIS. Candidates for such related molecules include activins and inhibins (see the subsequent discussion).

Morphological abnormalities of the reproductive tract were limited to male homozygous mutants. These animals possessed morphologically normal testes that were completely descended and a fully differentiated Wolffian duct system. But, they also had a uterus. The uterine horns were physically attached to the vas deferens by connective tissue. While no coiled oviducts were found in these animals, oviductal tissue was detected histologically at the distal regions of the uterine horns.

Nearly all (90%) of the MIS-deficient males were infertile. These males were able to mate with females, but sperm were rarely detected in the uteri of the recipient females. Normal numbers of motile sperm were detected in the vas deferens and epididymides of the mutant males, and these were capable of fertilizing oocytes *in vitro*. Restoration of the fertility defect in MIS homozygous mutant mice occurred when the MT-hMIS transgene was bred onto the MIS mutant background (i.e., males that were homozygous for the MIS mutation and carried the MT-hMIS transgene were fertile). The conclusions from these observations were that MIS-deficient males produced functional germ cells but that the simultaneous development of the Müllerian and Wolffian duct systems structurally interfered with the transfer of the sperm into the reproductive tract of females.

Histological examination of the testes of the MIS-deficient mice revealed Leydig cell hyperplasia and, at a low frequency, testicular tumors. The development of tumors in MIS-deficient mice is intriguing because a tar-

geted deletion of the related α-inhibin gene in mice leads to the development of testicular and ovarian tumours (Matzuk *et al.*, 1993). Thus, like inhibin, MIS also appears to function as a gonadal tumor suppressor.

Together, these loss of function studies demonstrate that MIS is the Müllerian inhibitor/*l'hormone inhibitrice* and that regression of the Müllerian duct system during fetal male development is important for male fertility. In addition, MIS is not required for male or female gametogenesis. Furthermore, the Leydig cell hyperplasia and development of tumors suggest that MIS functions in the male gonad to influence Leydig cell proliferation. The effect on Leydig cells is particularly interesting because in the MIS gain-of-function experiments Leydig cell function was apparently also altered in a subset of transgenic males from the highest-expressing lines (Behringer *et al.*, 1990). Finally, the viability of the MIS-deficient mice and the fertility of the homozygous mutant females facilitate subsequent crosses with other relevant mouse mutations.

VI. Mice Mutant for MIS and Other Gene Products

A. MIS/Inhibin Double Mutant Mice

Matzuk *et al.* (1993) generated mice lacking the TGF-β-related hormone inhibin. Surprisingly, both male and female homozygous mutant mice were viable and developed gonadal tumors of stromal cell origin. These findings suggested that inhibin was a negative regulator of gonadal stromal cell proliferation and identified this secreted hormone as having tumor suppressor activity. Like MIS, inhibin expression in the gonads is most abundant in Sertoli and granulosa cells. Prior to tumor formation in the inhibin mice, germ cell development was normal, indicating that inhibin was also not required for male or female germ cell development. Since MIS and inhibin are related hormones and are produced by the same gonadal cell types, and since both loss-of-function mutants develop gonadal tumors, it seems reasonable that MIS and inhibin might share functions in the gonad. Therefore, genetic crosses were initiated to generate double mutant mice lacking both MIS and inhibin (Matzuk *et al.*, 1994).

Both male and female MIS/inhibin double mutant mice were generated at the expected Mendelian ratios. To date, the analysis has primarily focused on the development of testicular tumors in the MIS/inhibin double mutant males. The most prominent phenotype observed upon sacrifice was a fluid-filled uterus and testicular tumors that had retracted from their scrotal position into the abdomen. Fluid secretion into the lumen of the uterus is a typical response of this organ to estrogens (Aitken, 1979). Injections of these double mutant males with an estrogen antagonist elimi-

nated the fluid-filled uterine phenotype. These observations suggested that the gonadal tumors were producing estrogen, and this was confirmed by examining serum estrogen levels. Histologically, the double mutant testicular tumors were similar in character to the inhibin tumors. In addition, the double mutant tumors developed at a significantly faster rate than the tumors that arose in mice mutant for inhibin alone. These observations suggested that MIS can influence the development of testicular tumors initiated by the absence of inhibin. In addition, the production of estrogens from the testicular tumors suggested that their biochemical characteristics had been modified. Further experiments are necessary to determine the nature of these biochemical differences.

Female MIS/inhibin double mutants also developed ovarian tumors but these have not been characterized in detail yet (unpublished observations). It will also be of interest to analyze the testes and ovaries from the MIS/inhibin double mutant mice prior to tumor formation to determine if germ cell development is altered when these two hormones are absent.

B. MIS/*Tfm* Double Mutant Mice

After formation of the testis, male sexual differentiation is primarily controlled by two hormones, testosterone and MIS. With the availability of MIS mutant mice, it became possible to generate mice through genetic crosses that lack both MIS and androgen function (Behringer *et al.*, 1994). This was accomplished by exploiting the classic mouse mutation known as *testicular feminization* (*Tfm*) (Green, 1990), an X chromosome-linked mutation that results in feminization of XY mutant individuals. The mutation is located in the gene encoding the androgen receptor and causes mutant males to become androgen insensitive (He *et al.*, 1991; Charest *et al.*, 1991). Thus, *Tfm*/Y males are overtly feminized, lack Wolffian duct differentiation, and have undescended testes in which spermatogenesis is arrested at meiotic prophase. *Tfm*/Y males do, however, produce MIS as evidenced by the regression of the Müllerian duct system.

Tfm/Y MIS-deficient mice were generated by interbreeding the *Tfm* and MIS mutants. These animals were overtly feminized with improperly descended testes. Also, Wolffian duct differentiation was eliminated and a uterus had developed. Interestingly, coiled oviducts were present, whereas no coiled oviducts were found in the MIS-deficient male pseudohermaphrodites. These results suggest that the elimination of the Wolffian duct during female development may be required for oviductal morphogenesis.

VII. Summary

The fetal testis functions as the sex differentiator by imposing a masculine pattern of development upon a genetic program that is inherently female. Two hormones produced by the fetal testis mediate the differentiation of the Müllerian and Wolffian ducts (Figs. 1 and 4). MIS actively inhibits the development of the Müllerian ducts, and testosterone induces the differentiation of the Wolffian ducts. The absence of these two hormones during fetal development in the female (the hormonal equivalent of no testes) permits Müllerian duct differentiation and does not induce Wolffian duct development. The *in vivo* outcomes of ectopic MIS exposure or MIS

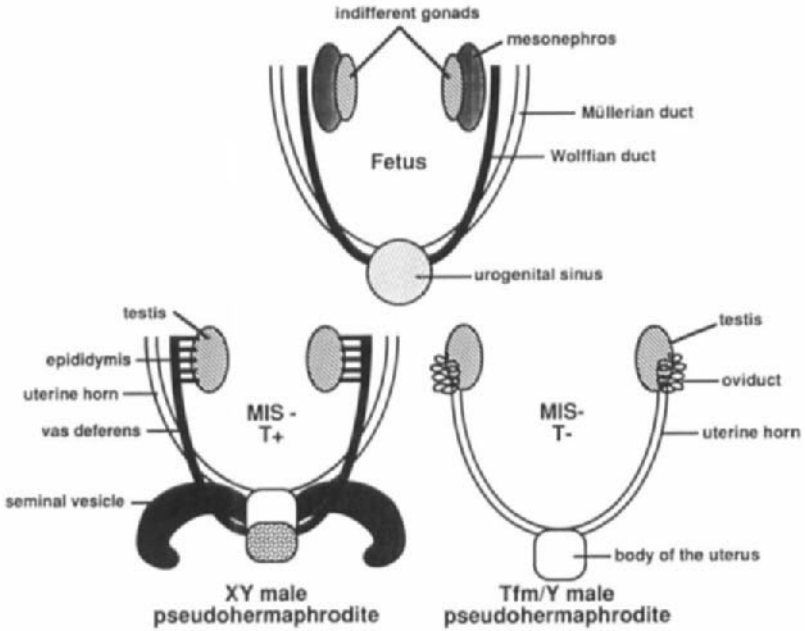

Fig. 4 Male pseudohermaphroditism in XY individuals that lack MIS. XY individuals that only lack MIS differentiate both the Müllerian and Wolffian duct systems and are male in appearance. The presence of both types of reproductive organs severely hinders fertility. The physical association of the resulting oviductal tissue with the Wolffian duct derivatives blocks oviduct coiling. XY individuals that lack MIS and are insensitive to androgens because of the *Tfm* mutation differentiate the Müllerian duct system but the insensitivity to androgens also results in the passive regression of the Wolffian duct system. While these mice have testes, they are female in appearance. Since the Wolffian duct system has been eliminated in these mice the oviductal tissue assumes its normal coiled morphology.

deficiency illustrate the balance required to coordinately differentiate and cause regression of the respective male and female genital ducts. The observations made in the MIS-deficient mice demonstrate that codevelopment of both genital duct systems interferes with normal development of both systems and ultimately interferes with reproduction and fertility. Thus, reproduction and fertility in mammals appear to be most efficient if only one type of genital duct system develops.

The phenotypes of the MIS-overexpressing transgenic mice and the MIS-deficient mice are similar yet different. Some of the explanations that might reconcile these differences probably lie with the receptor for MIS. Since the MIS-overexpressing transgenic mice are exposed to pharmacological levels of MIS during development, it seems possible that this may lead to productive interactions with other related receptors. Candidate genes have been isolated for the MIS receptor that are membrane-bound serine/threonine kinases (Baarends *et al.*, 1994; di Clemente *et al.*, 1994) similar to those cloned for the TGF-β (Lin *et al.*, 1992) and activin (Mathews and Vale, 1991) type II receptors. Interestingly, expression of these putative MIS receptor genes is localized by *in situ* hybridization to the mesenchymal cells adjacent to the Müllerian ducts, suggesting that MIS most likely alters the surrounding mesenchyme to elicit Müllerian duct regression. Experiments are underway to isolate the mouse MIS receptor gene to thereby generate MIS receptor-deficient mice and to compare the phenotype with the MIS gain-of-function and loss-of-function animals.

Isolation of the human MIS receptor gene will facilitate the identification of human PMDS patients with normal levels of MIS that have mutations in the MIS receptor gene. Finally, studies of the MIS receptor gene will open up avenues for the molecular characterization of signal transduction pathways that mediate Müllerian duct regression and Leydig cell proliferation control.

Acknowledgments

The author thanks Dr. Martin Matzuk for his critical reading of the manuscript. This work was aided by a grant from the National Institutes of Health HD30284.

References

Aitken, R. J. (1979). Uterine proteins. *In* "Oxford Review in Reproductive Biology" (C. A. Finn, ed.), Vol. 1, p. 351. Clarendon Press, Oxford.

Baarends, W. M., van Helmond, M. J. L., Post, M., van der Schoot, J. C. M., Hoogerbrugghe, J. W., de Winter, J. P., Uilenbroek, J. T. J., Karels, B., Wilming,

L. G., Meijers, J. H. C., Themmen, A. P. N., and Grootegoed, J. A. (1994). A novel member of the transmembrane serine/threonine kinase receptor family is specifically expressed in the gonads and in mesenchymal cells adjacent to the Müllerian duct. *Development* **120,** 189–197.

Behringer, R. R., and Cate, R. L. (1994). Müllerian inhibiting substance function during mammalian reproductive development. *In* "Cell and Molecular Biology of the Testes" (A. Fabbri, ed.). Ares-Serono Symposium, Majorca (in press).

Behringer, R. R., Cate, R. L., Froelick, G. J., Palmiter, R. D., and Brinster, R. L. (1990). Abnormal sexual development in transgenic mice chronically expressing Müllerian inhibiting substance. *Nature* **345,** 167–170.

Behringer, R. R., Finegold, M. J., and Cate, R. L. (1994). Müllerian-inhibiting substance function during mammalian sexual development. Submitted for publication.

Bézard, J., Vigier, B., Tran, D., Mauléon, P., and Josso, N. (1987). Immunocytochemical study of anti-Müllerian hormone in sheep ovarian follicles during fetal and post-natal development. *J. Reprod. Fertil.* **80,** 509–516.

Capecchi, M. R. (1989). The new mouse genetics: altering the genome by gene targeting. *Trends Genet.* **5,** 70–76.

Carré-Eusebe, D., Imbeaud, S., Harbison, M., New, M. I., Josso, N., and Picard, J.-Y. (1992). Variants of the anti-Müllerian hormone gene in a compound heterozygotes with the persistent Müllerian duct syndrome and his family. *Hum. Genet.* **90,** 389–394.

Cate, R. L., Donahoe, P. K., and MacLaughlin, D. T. (1990). Müllerian inhibiting substance. *In* "Peptide Growth Factors and Their Receptors II" (M. B. Sporn and A. B. Roberts, eds.), pp. 179–210. Springer-Verlag, Berlin.

Cate, R. L., Mattaliano, R. J., Hession, C., Tizard, R., Farber, N. M., Cheung, A., Ninfa, E. G., Frey, A. Z., Gash, D. J., Chow, E. P., Fisher, R. A., Bertonis, J. M., Torres, G., Wallner, B. P., Ramachandran, K. L., Ragin, R. C., Manganaro, T. F., MacLaughlin, D. T., and Donahoe, P. K. (1986). Isolation of the bovine and human genes for Müllerian inhibiting substance and expression of the human gene in animal cells. *Cell* **45,** 685–698.

Cate, R. L., and Wilson, C. A. (1993). Müllerian-inhibiting substance. *In* "Genes in Mammalian Reproduction" (R. B. L. Gwatkin, ed.), pp. 185–205. Wiley-Liss, New York.

Charest, N. J., Zhou, Z.-X., Lubahn, D. B., Olsen, K. L., Wilson, E. M., and French, F. S. (1991). A frameshift mutation destabilizes androgen receptor messenger RNA in the Tfm mouse. *Mol. Endocrinol.* **5,** 573—581.

Cohen-Haguenauer, O., Picard, J.-Y., Mattei, M. G., Serero, S., Nguyen, V. C., de Tand, M. F., Guerrier, D., Hors-Cayla, M. C., Josso, N., and Frézal, J. (1987). Mapping of the gene for anti-Müllerian hormone to the short arm of human chromosome 19. *Cytogenet. Cell. Genet.* **44,** 2–4.

di Clemente, N., Cate, R. L., and Josso, N. (1994). Isolation and expression pattern of the receptor for Müllerian-inhibitor substance. Submitted for publication.

di Clemente, N., Ghaffari, S., Pepinsky, R. B., Pieau, C., Josso, N., Cate, R. L., and Vigier, B. (1992). A quantitative and interspecific test for biological activity of anti-Müllerian hormone: the fetal ovary aromatase assay. *Development* **114,** 721–727.

Donahoe, P. K., Cate, R. L., MacLaughlin, D. T., Epstein, J., Fuller, A. F., Takahashi, M., Coughlin, J. P., Ninfa, E. G., and Taylor, L. A. (1987). Müllerian inhibiting substance: gene structure and mechanism of action of a fetal regressor. *Recent Prog. Horm. Res.* **43,** 431–467.

Green, M. C. (1990). Catalog of mutant genes and polymorhic loci. *In* "Genetic Variants and Strains of the Laboratory Mouse" (M. F. Lyon and A. G. Searle, eds.), pp. 362–363. Oxford University Press, London.

Gubbay, J., Collignon, J., Koopman, P., Capel, B., Economou, A., Münsterberg, A., Vivian, N., Goodfellow, P. N., and Lovell-Badge, R. (1990). A gene mapping to the sex-determining region of the mouse Y chromosome is a member of a novel family of embryonically expressed genes. *Nature* **346,** 245–250.

Guerrier, D., Tran, D., Vanderwinden, J. M., Hideux, S., Van Outryve, L., Legeai, L., Bouchard, M., Van, V. G., Picard, J. Y., Kahn, A., and Josso, N. (1989). The persistent Müllerian duct syndrome: a molecular approach. *J. Clin. Endocrinol. Metab.* **68,** 46–52.

Haqq, C., Lee, M. M., Tizard, R., Wysk, M., DeMarinis, J., Donahoe, P. K., and Cate, R. L. (1992). Isolation of the rat gene for Müllerian inhibiting substance. *Genomics* **12,** 665–669.

He, W. W., Kumar, M. V., and Tindall, D. J. (1991). A frame-shift mutation in the androgen receptor gene causes complete androgen insensitivity in the testicular-feminized mouse. *Nucleic Acids Res.* **19,** 2373–2378.

Hutson, J. M., and Donahoe, P. K. (1986). The hormonal control of testicular descent. *Endocr. Rev.* **7,** 270–283.

Imbeaud, S., Carré-Eusebe, D., Rey, R., Belville, C., Josso, N., and Picard, J.-Y. (1994). Molecular genetics of the persistent Müllerian duct syndrome: a study of 19 families. *Hum. Mol. Genet.* **3,** 125–131.

Josso, N. (1986). Anti-Müllerian hormone: new perspectives for a sexist molecule. *Endocr. Rev.* **7,** 421–433.

Josso, N., Cate, R. L., Picard, J.-Y., Vigier, B., di Clemente, N., Wilson, C., Imbeaud, S., Pepinsky, R. B., Guerrier, D., Boussin, L., Legeai, L., and Carré-Eusebe, D. (1993). Anti-Müllerian hormone: the Jost factor. *Recent Prog. Horm. Res.* **48,** 1–59.

Josso, N., Picard, J. Y., and Tran, D. (1977). The anti-Müllerian hormone. *Recent Prog. Horm. Res.* **33,** 117–160.

Jost, A. (1947). Recherches sur la differnciation sexuelle de l'embryon de lapin. *Arch. Anat. Microsc. Morphol. Exp.* **36,** 271–315.

Jost, A. (1953). Problems of fetal endocrinology: the gonadal and hypophyseal hormones. *Recent Prog. Horm. Res.* **8,** 379–418.

Jost, A., Vigier, B., and Prepin, J. (1972). Freemartins in cattle: the first steps of sexual organogenesis. *J. Reprod. Fertil.* **29,** 349–379.

King, T. R., Lee, B. K., Behringer, R. R., and Eicher, E. M. (1991). Mapping anti-Müllerian hormone (Amh) and related sequences in the mouse: identification of a new region of homology between MMU10 and HSA19p. *Genomics* **11,** 273–283.

Koopman, P., Gubbay, J., Vivian, N., Goodfellow, P., and Lovell-Badge, R. (1991). Male development of chromosomally female mice transgenic for *Sry*. *Nature* **351,** 117–121.

Knebelmann, B., Boussin, L., Guerrier, D., Legeai, L., Kahn, A., Josso, N., and Picard, J.-Y. (1991). Anti-Müllerian hormone Bruxelles: a non-sense mutation in the last exon of the anti-Müllerian hormone gene associated with the persistent Müllerian duct syndrome in three brothers. *Proc. Natl. Acad. Sci. USA* **88,** 3767–3771.

Lin, H. Y., Wang, X., Ng-Eaton, E., Weinberg, R. A., and Lodish, H. F. (1992). Expression cloning of the TGF-β type II receptor, a functional transmembrane serine/threonine kinase. *Cell* **68,** 775–785.

Massagué, J. (1990). The transforming growth factor-β family. *Annu. Rev. Cell Biol.* **6,** 597–641.

Mathews, L., and Vale, W. W. (1991). Expression cloning of an activin receptor, a predicted transmembrane serine kinase. *Cell* **65,** 973–982.

Matzuk, M., Finegold, M. J., Cate, R. L., Bradley, A., and Behringer, R. R. (1994).

Müllerian-inhibiting substance modifies the phenotype of testicular tumors in α-inhibin-deficienc mice. Submitted for publication.

Matzuk, M., Finegold, M. J., Su, J.-G. J., Hseueh., A. J. W., and Bradley, A. (1993). α-Inhibin is a tumour-suppressor gene with gonadal specificity in mice. *Nature* **360,** 313–319.

Meyers-Wallen, V. N., Donahoe, P. K., Ueno, S., Manganaro, T. F., and Patterson, D. F. (1989). Müllerian inhibiting substance is present in testes of dogs with persistent Müllerian duct syndrome. *Biol. Reprod.* **41,** 881–888.

Münsterberg, A., and Lovell-Badge, R. (1991). Expression of the mouse anti-Müllerian hormone gene suggests a role in both male and female sexual differentiation. *Development* **113,** 613–624.

Palmiter, R. D., and Brinster, R. L. (1986). Germ-line transformation of mice. *Annu. Rev. Genet.* **20,** 465–499.

Pepinsky, R. B., Sinclair, L. K., Chow, E. P., Mattaliano, R. J., Manganaro, T. F., Donahoe, P. K., and Cate, R. L. (1988). Proteolytic processing of Müllerian inhibiting substance produces a transforming growth factor-β-like fragment. *J. Biol. Chem.* **263,** 18,961–18,964.

Picard, J.-Y., Benarous, R., Guerrier, D., Josso, N., and Kahn, A. (1986). Cloning and expression of cDNA for anti-Müllerian hormone. *Proc. Natl. Acad. Sci. USA* **83,** 5464–5468.

Picon, R. (1969). Action du testicule foetal sur le developpement *in vitro* des canaux de Müller chez le rat. *Arch. Anat. Microsc. Morphol. Exp.* **58,** 1–19.

Picon, R. (1970). Modification, chez le rat, au cours du développement du testicule, de son action inhibitrice sur les canaux de Müller in vitro. *C.R. Acad. Sci. Sér. D. Paris* **271,** 2370–2372.

Sinclair, A. H., Berta, P., Palmer, M. S., Hawkins, J. R., Griffiths, B. L., Smith, M. J., Foster, J. W., Frischauf, A.-M., Lovell-Badge, R., and Goodfellow, P. N. (1990). A gene from the human sex-determining region encodes a protein with homology to a conserved DNA-binding motif. *Nature* **346,** 240–244.

Takahashi, M., Koide, S. S., and Donahoe, P. K. (1986). Müllerian inhibiting substance as oocyte meiosis inhibitor. *Mol. Cell. Endorinol.* **47,** 225–234.

Tran, R., Meusy-Dessole, N., and Josso, N. (1977). Anti-Müllerian hormone is a functional marker of foetal Sertoli cells. *Nature (London)* **269,** 411–412.

Ueno, S., Takahashi, M., Manganaro, T. F., Ragin, R. C., and Donahoe, P. K. (1989). Cellular localization of Müllerian inhibiting substance in the developing rat ovary. *Endocrinology* **125,** 1060–1066.

Vigier, B., Forest, M. G., Eychenne, B., Bézard, J., Garrigou, O., Robel, P., and Josso, N. (1989). Anti-Müllerian hormone produces endocrine sex-reversal of fetal ovaries. *Proc. Natl. Acad. Sci. USA* **86,** 3684–3688.

Vigier, B., Tran, D., du Mesnil du Buisson, F., Heyman, Y., and Josso, N. (1983). Use of monoclonal antibody techniques to study the ontogeny of bovine anti-Müllerian hormone. *J. Reprod. Fertil.* **69,** 207–214.

Vigier, B., Watrin, F., Magre, S., Tran, D., and Josso, N. (1987). Purified bovine AMH induces a characteristic freemartin effect in fetal rat prospective ovaries exposed to it *in vitro*. *Development* **100,** 43–55.

Wilson, C. A., di Clemente, N., Ehrenfels, C., Pepinsky, R. B., Josso, N., Vigier, B., and Cate, R. L. (1993). Müllerian inhibiting substance requires its N-terminal domain for maintenance of biological activity, a novel finding within the transforming growth factor-β superfamily. *Mol. Endocrinol.* **7,** 247–257.

This Page Intentionally Left Blank

6

Growth Factor Regulation of Mouse Primordial Germ Cell Development

Peter J. Donovan
Mammalian Genetics Laboratory
ABL-Basic Research Program
NCI-Frederick Cancer Research and Development Center
Frederick, Maryland 21702

I. Introduction

A. Scope

The development of the germ line in the mouse embryo involves a number of distinct processes or phases leading to the establishment of the meiotic population (Fig. 1). Primordial germ cells (PGCs), the embryonic precursors of the sperm and ova of the adult animal, arise as a small population of cells in the early postimplantation embryo at about 7 days postcoitus (dpc) (Ginsburg *et al.*, 1990). These PGCs are classically identified as cells expressing alkaline phosphatase (EC 3.1.3.1) and are thought to represent a subpopulation of the total number of PGCs present in the embryo at that time (Ginsburg *et al.*, 1990). During the subsequent 5 or 6 days of embryonic development, PGC numbers increase dramatically and they migrate to the gonad anlagen (Chiquoine, 1954; Mintz and Russell, 1957; Ozdzenski, 1967; Tam and Snow, 1981). Once in the gonad, male germ

Current Topics in Developmental Biology, Vol. 29

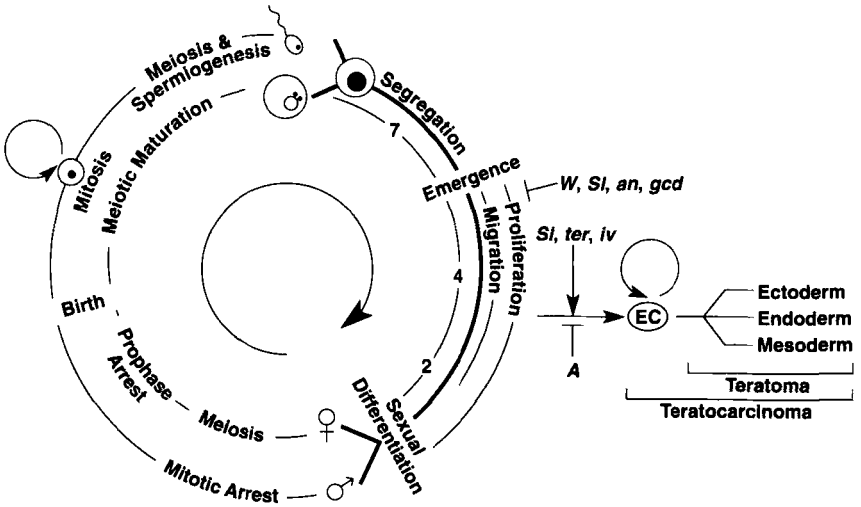

Fig. 1 Life cycle of a germ cell in the mouse. Following fertilization emergence of PGCs takes 7 days of embryonic development. PGCs migrate to the gonad anlagen over the next 4–5 days of development. During this time, and for about two days after they reach the gonad, they proliferate to establish the meiotic population. Mutations at the *W, Sl, an* and *gcd* loci affect PGC development and can cause sterility. Once in the gonad female PGCs enter directly into meiosis, arrest at meiotic prophase and reenter meiosis after birth. Male PGCs enter a mitotic arrest in the embryonic gonad and do not reenter mitosis until after birth. At puberty, male germ cells (spermatogonia) give rise to meiotic derivatives. Teratocarinogenesis represents an alteration of the normal pathway of PGC development and a number of genes (*Sl, iv, ter* and *A*) are known to affect this process also.

cells enter mitotic arrest while female germ cells enter directly into meiosis (McLaren, 1981). Thus the establishment of the germ line in the embryo involves the segregation of PGCs from the somatic lineages, proliferation of PGCs, migration of PGCs to the gonad anlagen, and finally differentiation in the gonad (Fig. 1). These processes are of interest in their own right but are also used as model systems to study cell proliferation, cell migration, and cell differentiation. Surprisingly, although the survival of the germ line is essential to the survival of animal species, until recently very little was known about the factors regulating these distinct phases of PGC development. This chapter focuses on growth factor regulation of PGC development in the mouse embryo.

B. Embryonic History of the Germ Line

PGCs are classically identified as alkaline phosphatase-positive cells (Fig. 2) and are first identified as a population of approximately eight cells in

the extraembryonic mesoderm of the early 7 dpc embryo (Ginsburg *et al.*, 1990). These alkaline phosphatase-positive PGCs probably represent a fraction of the PGCs present in the embryo at that time and which have differentiated from cells originating in the epiblast (Lawson and Hage, 1994). Expression of alkaline phosphatase, therefore, occurs gradually during this period of germ cell differentiation. By 8.0 dpc, approximately 125 alkaline phosphatase-positive PGCs can be identified at the caudal end of the primitive streak near the allantoic rudiment. By this time it is thought that all PGCs express alkaline phosphatase and thus this number represents the total number of PGCs present in the embryo. During the next 24 hr of development PGCs are incorporated into the hind gut as it invaginates. This movement of PGCs is thought to be a passive process brought about by the morphogenetic movements of the embryo (Spiegelman and Bennett, 1973; Clark and Eddy, 1975).

At this point in their development the PGCs are some distance from the site at which they will undergo their final differentiation into meiotic cells. During the subsequent 4 days of development, PGCs undergo active, directed migration to colonize the gonad anlagen (Chiquoine, 1954; Mintz and Russell, 1957; Ozdzenski, 1967; Tam and Snow, 1981). They migrate out of the hind gut, up the dorsal mesentery of the gut toward two thickened ridges of tissue (the genital ridges or gonad anlage) lying either side of the hind gut mesentery on the dorsal body wall. In the course of migration, and following colonization of the gonad anlage, PGC numbers increase dramatically so that by 13.5 dpc they form a population of about 25,000 cells in the gonad (Chiquoine, 1954; Mintz and Russell, 1957; Ozdzenski, 1967; Tam and Snow, 1981). By this time the somatic cells of the gonad have undergone sexual differentiation, and the testis and ovary are morphologically distinguishable (McLaren, 1981). Also at this time PGCs begin the next phase of their own differentiation. In the male, PGCs undergo mitotic arrest but continue to grow in size. They reenter mitosis about 5 days after birth, forming the mitotic stem cell of the postnatal testis, the spermatogonium. These cells give rise to meiotic derivatives that will undergo spermiogenesis and form the functional sperm of the mature adult animal (for a review see Bellve, 1979). In the female, however, PGCs enter directly into meiosis in the embryo, arrest at meiotic prophase, and reenter meiosis a few days after birth (for a review see Siracusa *et al.*, 1985). Up to the time of birth considerable loss of female PGCs occurs through a process known as atresia. These differentiation events occur gradually in the PGC population as is the case with the acquisition of alkaline phosphatase activity earlier in their development. Thus not all male PGCs enter mitotic arrest as a cohort nor do all female PGCs enter meiosis simultaneously.

Coincident with these differentiation events are changes in PGC surface antigen expression (Donovan *et al.*, 1986) (Fig. 2). Many of these cell

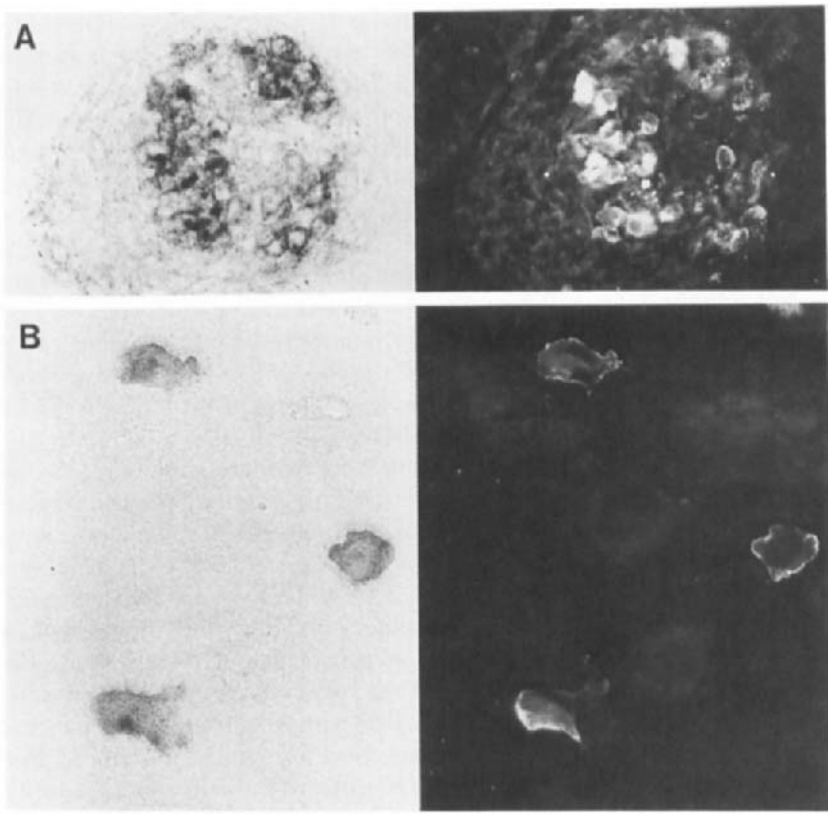

Fig. 2 Identification of PCGs by alkaline phosphatase histochemistry and reactivity with an anti-SSEA-1 antibody. A. PGCs in a 12.5 dpc gonad stained for alkaline phosphatase (left panel) and with an anti-SSEA-1 antibody (right panel). B. Three PGCs identified in culture on STO cell feeder layers by alkaline phosphatase histochemistry (left panel) and anti-SSEA-1 antibody staining (right panel). Not to scale.

surface antigens are carbohydrate differentiation antigens and represent post-translational modifications of glycolipids and glycoproteins (Childs *et al.*, 1983; Ozawa, 1985). Perhaps the best studied of these antigens is the stage-specific embryonic antigen-1 (SSEA-1) (Solter and Knowles, 1978) which represents a fucosylated lactosamine modification of glycoprotein and glycolipid cores (Ozawa *et al.*, 1985). The SSEA-1 antigen is expressed on the PGC surface from 8.5 dpc, through the period of migration, and is lost after PGCs colonize the gonad anlagen (Fox *et al.*, 1981; Donovan *et al.*, 1986). Analysis of the role of the SSEA-1 antigen in

preimplantation development led to the hypothesis that these carbohydrate residues might be involved in compaction and cell adhesion (Bird and Kimber, 1984). Similar studies on the role of the SSEA-1 antigen in PGC development also led to a similar conclusion, namely that the SSEA-1 antigen might be part of a PGC cell adhesion molecule (Donovan *et al.*, 1987). The functional significance of antigenic modulation during the development of PGCs remains unclear but the presence of these antigens on the surface of PGCs represent useful tools for the purification of PGCs from embryonic gonads and their identification in culture (Donovan *et al.*, 1986; McCarrey *et al.*, 1987) (Fig. 2).

This brief sketch describing the embryonic history of the germ line illustrates some of the questions still outstanding about the emergence of the germ line in animal species: (1) When and where is the germ line set aside in the embryo? (2) How is the germ line segregated from the somatic lineages? (3) What triggers PGCs to begin migration to the gonad anlagen? (4) What factor(s) guides PGCs to the gonad anlagen? (5) Upon gonadal colonization, what factor(s) causes cessation of PGC migration? (6) What factor(s) regulates PGC proliferation? (7) What factor(s) regulates PGC differentiation in the gonad? (8) What factors regulate mitotic or meiotic arrest of male and female PGCs?

In vitro analysis has been used to investigate many of these questions. Moreover, like a number of other migratory embryonic cell types (most notably neural crest cells), PGCs have been used as a model system to study the control of cell migration, and much of this analysis has been carried out using *in vitro* systems. PGCs begin and end migration at a specific time in development and migrate to a single site, the gonad anlagen. Their migration is therefore controlled very strictly both temporally and spatially. Like many tumor cells PGCs migrate through solid tissues rather than through pathways of extracellular matrix that form intercellular spaces. Thus PGCs represent a useful model system by which to study the normal control mechanisms that regulate cell migration in tissues and the breakdown of these control mechanisms during tumor metastasis (Wylie *et al.*, 1985; Donovan *et al.*, 1986; Stott and Wylie, 1986). The following sections discuss how *in vitro* systems have been used to analyze growth factor regulation of PGC development and what further developments and advances are likely in the near future.

Two conditions which alter the normal pathway of PGC development identify genes involved in that process. A number of mutations in the mouse cause sterility in the homozygous condition, thereby identifying genes involved in germ cell development (Silvers, 1979). Some of these have been shown to act during the period of PGC development, including *Dominant White Spotting* (*W*), *Steel* (*Sl*), *Hertwigs' macrocytic anemia* (*an*), and *germ cell deficient* (*gcd*) (Bennett, 1956; Mintz and Russell,

1957; McCoshen and McCallion, 1975; Russell *et al.*, 1985; Pellas *et al.*, 1991). The genes encoded at the *W* and *Sl* loci have been characterized at the molecular level and will be described in detail.

A second situation in which PGC development is altered is when PGCs give rise to tumors, benign teratomas, and malignant teratocarcinomas (Stevens, 1967b). In this case the PGC gives rise to a pluripotent stem cell, the embryonal carcinoma (EC) cell, which can differentiate into many cell types representative of all the three primary germ layers. In teratomas, all the EC cells differentiate, thereby forming a benign tumor whereas in teratocarcinomas, some of the EC cells fail to differentiate and continue to proliferate thereby forming a malignant tumor (Stevens, 1967a; Stevens and Pierce, 1975). Some of the genes affecting these processes have been identified by analyzing teratoma and teratocarcinoma incidence in inbred strains of mice and congenic derivatives carrying specific gene mutations. The genes identified that affect teratocarcinogenesis include *Sl*, *situs inversus viscerum* (*iv*), *agouti* (*A*), and *teratocarcinoma* (*ter*) (Stevens, 1983). Understanding the role of these genes in teratocarcinogenesis may provide useful information as to their role in normal PGC development.

II. Growth Regulation of Primordial Germ Cells

A. Primordial Germ Cell Culture

PGCs can be cultured in a variety of conditions, including organ culture, feeder cell-dependent culture, and feeder cell-independent culture (for reviews see Cooke *et al.*, 1993; Buehr and McLaren, 1993). Each technique has its uses and problems. The earliest attempts to culture PGCs were aimed at understanding PGC migration. Blandau and colleagues (1963) derived squash preparations of fetal gonads in order to study the migratory properties of mouse PGCs. These cultures were not aimed at maintaining PGCs in culture for long periods of time. Although PGCs can be cultured on glass, plastic, agar, or gelatin-coated substrata, their survival is poor (DeFelici and McLaren, 1983). Moreover, the number of cells that can be recovered from the embryo onto these substrates makes these experimental conditions unfavorable for most purposes. Extracellular matrix components such as fibronectin, laminin, and type IV collagen can improve recovery of PGCs, but their viability remains low (Alvarez-Buylla and Merchant-Larios, 1986; Wylie *et al.*, 1985; DeFelici and Dolci, 1989; FFrench-Constant *et al.*, 1991). Most long-term cultures of PGCs have therefore involved growing them in conjunction with feeder layers of mitotically inactive somatic cells. Heath (1978) and Evans (1981) both reported that mouse or rat PGCs could be maintained in culture for about

5 days when cultured on top of feeder layers of their own embryonic somatic cells or fibroblast feeder layers. Nevertheless, even in these conditions, PGC numbers declined over the 5-day culture period, and PGCs did not divide or incorporate tritiated thymidine into their DNA (Heath, 1978; Evans, 1981). Although it was not possible at that time to derive long-term cultures of PGCs (or to establish PGC-derived cell lines), various improvements in the culture conditions led to the establishment of cultures in which PGCs could both survive and proliferate for about 7 days. The use of STO cells (a **S**IM mouse embryo-derived, **T**hioguanine- and **O**uabain-resistant fibroblast cell line) (Ware and Axelrad, 1972) or TM4 cells (a mouse Sertoli cell-derived cell line) (Mather, 1980) allows culture of PGCs in conditions in which they both survive and proliferate for up to 7 days (Donovan *et al.*, 1986; DeFelici and Dolci, 1991).

PGCs can be identified in feeder layer culture by alkaline phosphatase histochemistry and by reactivity with antibodies directed against cell surface differentiation antigens such as SSEA-1 (Donovan *et al.*, 1986) (Fig. 2). The major problem with these cultures is their complexity since they contain not only PGCs and feeder cells but also mitotically active embryonic somatic cells. Thus the interpretation of the action of growth factors in these conditions is difficult. Any conclusions about the direct action of a growth factor on PGCs must be supported by a rigorous demonstration that PGCs express a particular growth factor receptor. The use of feeder layer culture for PGCs gradually led to improvements in PGC culture and the identification of conditions for stimulating PGC proliferation. When isolated into culture, PGCs are initially identified as single cells growing on top of the feeder layer. After a few days of culture, small groups of PGCs form either by clonal division or by aggregation. These groups enlarge over the next 3 or 4 days of culture but they eventually disappear. Whether they differentiate into an alkaline phosphatase-negative cell population or simply die is unknown. When isolated from the embryo and placed into culture their mitotic period mirrors that seen *in vivo* as does expression of the carbohydrate differentiation antigen SSEA-1. These two observations suggest that PGCs may differentiate *in vitro* according to their normal schedule *in vivo* (Donovan *et al.*, 1986). The appearance (rather than the disappearance) of differentiation markers would definitively answer this question but no such markers exist at the present time.

Using feeder-dependent culture systems it is possible to investigate factors affecting PGC survival, proliferation, and differentiation. One important observation from *in vitro* assays was that the serum concentration could influence the rate of PGC proliferation—proliferation was greater in medium containing 15% fetal calf serum (FCS) than in 10% FCS (P. J. Donovan, unpublished observations). Another important observation was that cAMP agonists such as forskolin and cholera toxin could greatly

stimulate proliferation (Dolci *et al.*, 1993; P. J. Donovan, unpublished observations). Although these improvements are useful in maintaining PGCs in culture, little was known about the growth factor requirements for PGC survival, proliferation, and differentiation. The major breakthrough in understanding the factors regulating PGC survival and proliferation came from the characterization of the genes encoded at the *Dominant White Spotting* and *Steel* loci.

B. *Dominant White Spotting* and *Steel*

Many mutations at both the *W* and *Sl* loci, in addition to their effects on the hemopoietic system and melanoblasts, cause sterility in the mouse, thereby identifying genes involved in germ cell development. *W* and *Sl* mutations are semidominant and can be identified as heterozygotes by their effect on coat pigmentation (Silvers, 1979). A large number of *W* or *Sl* alleles, when homozygous, cause lethality: *W/W* animals die around the time of birth, while *Sl/Sl* animals begin to die at around day 15 of gestation. Most probably this is because of the dramatic effect of these mutations on the hemopoietic system—both *W/W* and *Sl/Sl* animals are severely anemic. In *W* and *Sl* homozygote mutant embryos, PGCs are formed, but fail to divide, and their numbers remain low (Mintz and Russell, 1957; McCoshen and McCallion, 1975). The few PGCs that reach the gonad do not survive and the animals are generally sterile. Transplantation and grafting studies demonstrated that *W* acts in the affected cells themselves (intrinsically) while *Sl* acts in the cellular environment (extrinsically).

The *W* locus is now known to encode c-*kit*, a receptor tyrosine kinase (RTK) with homology to the receptors for colony-stimulating factor-1 (CSF-1) and platelet-derived growth factor (PDGF) (Chabot *et al.*, 1988; Geissler *et al.*, 1988). These receptors are characterized, in part, by having a unique insert in the tyrosine kinase domain (see Fig. 3). In the embryo, c-*kit* is expressed in cells affected by *W* mutations, that is, hemopoietic stem cells, mast cells, melanoblasts, and PGCs and thus coincides with the cells affected by *W* mutations (Nocka *et al.*, 1989; Motro *et al.*, 1991). A large number of mutations at the *W* locus have been identified, each differing in the severity of their effects on hemopoietic stem cells, germ cells, and melanoblast (Bernstein *et al.*, 1990). Thus some *W* alleles are viable and fertile but lack coat melanocytes, while others impair the hemopoietic system, are severely anemic, and are perinatal lethals. The molecular bases of many *W* mutations have been characterized. Severe *W* mutations (i.e., those causing lethality), such as W^{42}, are characterized by having mutations or deletions in the c-*kit* kinase domain and have impaired

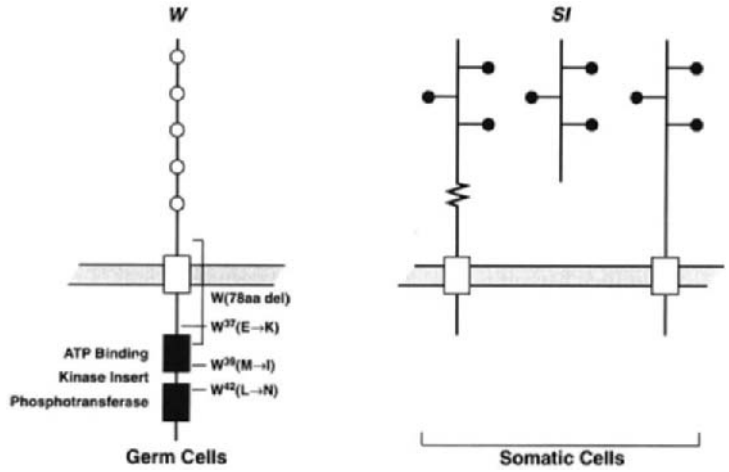

Fig. 3 *W* and *Sl* encode a receptor/ligand pair. The *W* gene (chromosome 5) encodes a receptor tyrosine kinase (c-kit) expressed in PGCs. C-kit is characterized in part by 5 immunoglobulin-like domains in the extracellular domain and a split tyrosine kinase domain. Mutations affecting c-kit activity are shown. The *Sl* gene (chromosome 10) encodes a transmembrane growth factor (SLF) expressed in somatic cells that exists in two forms, generated by alternate splicing. One form (left) has a proteolytic cleavage site in the extracellular domain which can be cleaved to release a soluble factor (middle). The other form (right) lacks the cleavage site and is thought to remain largely as a membrane-bound factor.

or no c-*kit* kinase activity (Nocka *et al.*, 1990; Reith *et al.*, 1990; Tan *et al.*, 1990). Less severe *W* alleles (viable), such as *W-sash* (W^{sh}), are regulatory mutants that affect the level rather than the activity of c-*kit* protein (Duttlinger *et al.*, 1993). Evaluation of many weak, moderate, and severe *W* mutations reveals a correlation between the degree of severity in homozygotes and the level of c-*kit* kinase activity. Thus the simplest explanation for the sterility seen in *W* mutant mice is an impaired c-*kit* signaling pathway in PGCs.

The *Sl* locus is now known to encode the ligand for c-*kit*, known as mast cell growth factor (MGF), kit-ligand (KL), stem cell factor (SCF), and Steel Factor (SLF) (Copeland *et al.*, 1990; Flanagan and Leder, 1990; Zsebo *et al.*, 1990; Williams and Lyman, 1991). For the purposes of this chapter this factor is referred to as Steel Factor. SLF is a transmembrane growth factor that exists in two forms generated by alternate splicing (see Fig. 3) (Flanagan *et al.*, 1991). One of these forms can be efficiently cleaved to release the extracellular domain as a soluble factor while the other form is presumed to remain membrane bound. *In situ* hybridization analysis reveals that SLF mRNA is expressed not in the cells affected by *Sl* mutations (hemopoietic stem cells, germ cells, and melanoblasts)

themselves, but rather in the surrounding tissues (Matsui *et al.*, 1990; Keshet *et al.*, 1991). This is entirely consistent with earlier transplantation and grafting studies demonstrating that the *Sl* gene product acts in the cellular environment. A number of *Sl* mutations have now been characterized. Generally, the most severe *Sl* mutations (lethal), such as *Sl*, Sl^{J}, Sl^{12H}, *Sl-grizzle belly* (Sl^{gbh}), and Sl^{18H}, represent complete deletions of the *Sl* gene (Copeland *et al.*, 1990), while viable *Sl* alleles, such as Sl^{d}, Sl^{17H}, and *Sl-Panda* (Sl^{pan}), involve small deletions or alterations in the *Sl* coding sequence (Sl^{d} and Sl^{17H}) (Brannan *et al.*, 1991, 1992; Flanagan *et al.*, 1991) or in genomic regulatory regions (Sl^{pan}) (Huang *et al.*, 1993; M. A. Bedell, personal communication).

What role does SLF play in PGC development? In principle SLF could have a role in PGC survival, proliferation, migration, or differentiation. Four pieces of evidence suggest that SLF is required for PGC survival. First, the role of SLF expression by somatic cells was examined in *in vitro* assays. In culture, PGCs will survive for up to 7 days when grown on feeder layers of certain fibroblasts. The ability of PGCs to survive and proliferate on fibroblasts is dependent, in part, on the production of SLF by these cells (Dolci *et al.*, 1991). PGCs could not survive for even 24 hr on feeder layers of CV-1 cells that did not produce SLF, although they could adhere to these feeder layers in short-term adhesion assays. When CV-1 cells were reconstituted with SLF by transfection, these reconstituted cells could now support PGCs for up to 3 days. Thus SLF is both necessary and sufficient for PGC survival in culture (Dolci *et al.*, 1991). Second, when a soluble, recombinant form of SLF (rSLF) was added to PGCs grown on STO cells, it increased both the numbers of PGCs and size of PGC colonies in culture. However, in these conditions rSLF did not stimulate PGC proliferation as assessed by bromodeoxyuridine (BrdU) labeling (Godin *et al.*, 1991). Similarly, addition of rSLF was unable to stimulate PGC proliferation on NIH-3T3 feeder layers (Dolci *et al.*, 1991). When rSLF was added to PGCs grown in the absence of feeder cells on gelatin-coated substrata it increased PGC survival (but only for 48 hr) and was unable to stimulate proliferation (Godin *et al.*, 1991). Third, signaling via the c-*kit* receptor was blocked by the addition of an anti-c-*kit* antibody (ACK2) (Matsui *et al.*, 1991). This antibody not only blocks PGC proliferation in culture but also seems to inhibit PGC survival (Matsui *et al.*, 1991; L. Cheng and P. J. Donovan, unpublished observations). These data can be interpreted to show that SLF is not a mitogen by itself but is a PGC survival factor. Fourth, rSLF suppresses apoptosis (programmed cell death) of PGCs in culture consistent with the notion that the c-*kit* signaling pathway is required for PGC survival (Pesce *et al.*, 1993). This is a somewhat controversial issue since rSLF can stimulate PGC proliferation on feeder cells that themselves do not express SLF, although PGC survival

in these conditions is short lived (48 hr) (Matsui *et al.*, 1991). Distinguishing between proliferation and survival in feeder-dependent cultures may be very difficult. An important point to bear in mind, however, is that addition of a survival factor (that itself is not a mitogen) may allow cells to respond more efficiently to available mitogens. Thus addition of rSLF may improve PGC survival sufficiently to allow the cells to respond to other factors. Moreover, factors which can promote cell survival may, in the presence of other factors, act as mitogens. For example, neurotrophin-3 (NT-3) alone can promote short-term survival of oligodendrocytes and their precursors, but in combination with PDGF and ciliary neurotrophic factor (CNTF) (or related factors) it can promote long-term survival and also stimulate proliferation (Barres *et al.*, 1993, 1994).

Evidence for SLF acting in other ways, for example, as a chemoattractant, remains inconclusive. In *in vitro* assays rSLF was unable to act as a chemoattractant (Godin *et al.*, 1991) but these assays were carried out in the presence of STO cells which produce SLF, so interpretation of these data is complicated. Evidence for SLF acting as a PGC adhesion molecule will be presented next. In summary, SLF seems to be required for long-term survival of PGCs in culture and, together with other factors, can stimulate PGC proliferation.

C. Soluble versus Membrane-Bound Steel Factor

As described earlier, SLF exists in two forms generated by alternate splicing (Flanagan *et al.*, 1991). One form is predicted to be a membrane-bound factor whereas the other form can be cleaved to generate a soluble factor. Important questions include why two different forms of SLF exist and whether there are differences in their effect on PGCs? Evidence for the importance of membrane-bound SLF in PGC development comes not only from cell culture analyses but also from the analysis of two *Sl* mutations, Sl^{d} and Sl^{17H}. The Sl^{d} allele has been characterized at the molecular level and results from a discrete 4.0-kb intragenic deletion that removes sequences encoding the SLF cytoplasmic tail and transmembrane region (Brannan *et al.*, 1991; Flanagan *et al.*, 1991). Thus Sl^{d}/Sl^{d} (or Sl/Sl^{d}) animals can produce only a soluble form of SLF (Fig. 4). The sterility seen in Sl/Sl^{d} animals suggests that soluble SLF encoded by the Sl^{d} allele may not be sufficient to support PGC survival. This hypothesis was tested in *in vitro* culture by transfecting CV-1 cells with a gene encoding the Sl^{d} allele. These cells could support limited PGC survival for only 24 hr whereas cells transfected with the wild-type allele could support PGC survival for at least 3 days (Dolci *et al.*, 1991). Similar experiments were carried out using two bone marrow-derived cell lines generated from con-

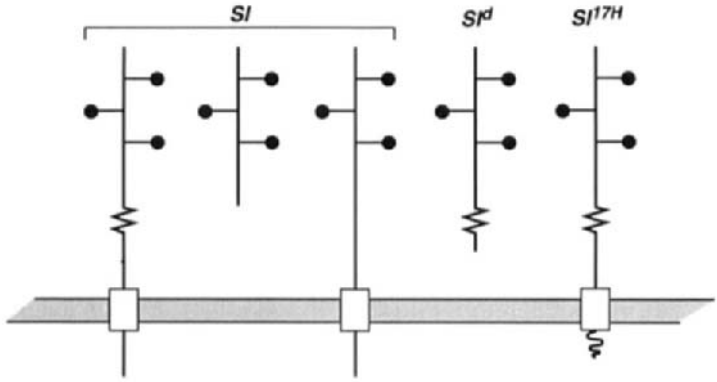

Fig. 4 Structures of wild type and mutant *Steel* gene products. The wildtype gene generates two transmembrane forms of SLF. The Sl^d allele encodes a factor lacking the cytoplasmic tail and transmembrane region and can only generate a soluble protein. The Sl^{17H} allele encodes a factor that is identical with the wildtype factor from the N-terminus to the first amino acid of the cytoplasmic tail. The rest of the cytoplasmic tail is encoded from an alternate reading frame. This mutation removes some juxtamembrane lysine residues as well as a terminal valine residue. These residues may be important for membrane anchorage or ectodomain cleavage of SLF.

genic lines of mice. One cell line (BM-WT) produces membrane-bound factor, while the other cell line (Sl/Sl^d) produces only soluble factor. Once again, PGCs could only survive on the cells expressing the full-length, membrane-bound factor. Addition of further soluble rSLF improved initial survival over 24 hr but was unable to effect long-term survival of PGCs (Dolci *et al.*, 1991). Similarly, Hogan and colleagues have demonstrated that membrane-bound factor is more efficient at supporting PGC proliferation (Matsui *et al.*, 1991). PGC proliferation was assayed in the presence of saturating amounts of soluble, recombinant SLF on a SLF-null cell line (Sl/Sl4) or on a recombinant derivative cell line (Sl-m220) expressing a noncleavable form of SLF. The conclusion drawn from this experiment was that even in the presence of saturating amounts of soluble SLF, PGC proliferation was greater in the presence of membrane-bound SLF and therefore that membrane-bound SLF is required in addition to soluble SLF for optimal effects on PGCs (Matsui *et al.*, 1991). Studies on the effect of SLF on hemopoietic stem cells have also shown that transmembrane forms of the factor enhance stem cell survival and proliferation (Toksoz *et al.*, 1992). Since Sl^d/Sl^d animals lack all coat melanocytes, these data suggest that, like PGCs, melanocytes require full-length transmembrane forms of SLF for their survival and/or proliferation *in vivo*. In culture rSLF is required for the maintenance but not the differentiation of melanoblasts (Steel *et al.*, 1992), while analysis of melanoblast develop-

ment in Sl^d/Sl^d embryos shows that transmembrane forms of SLF are required for melanoblast survival (Steel *et al.*, 1992).

Further evidence for a role for the cytoplasmic tail of SLF (and hence for the role of full-length, transmembrane factor) comes from the analysis of another mutant *Sl* allele, Sl^{17H}. This ethyl nitrosourea (ENU)-induced *Sl* allele is of interest because of its differential effect on the fertility of males and females. Heterozygotes have a lightening of the coat with a pronounced headspot but otherwise are viable and fertile. Homozygotes, on the other hand, are black-eyed but have a white coat. They are fully viable but are fertile only in the female. Molecular analysis of the Sl^{17H} allele revealed the complete absence of exon 8 from Sl^{17H} mRNA. Exon 8 encodes 23 of the 36 amino acids of the SLF cytoplasmic tail and begins 1 amino acid C-terminal to the transmembrane domain. Thus the SLF encoded by the Sl^{17H} allele encodes a protein with identity to the wild-type protein from the N terminus up to the first amino acid of the cytoplasmic tail (Fig. 4). The rest of the Sl^{17H} SLF cytoplasmic tail is produced from an alternate reading frame that encodes 27 amino acids before reaching a stop codon. The cytoplasmic tail of the SLF encoded by the Sl^{17H} allele is, therefore, not only substantially different from the wild-type protein but also shorter (Fig. 4). Two explanations seem possible for this mutation: a point mutation in the 3′ splice acceptor site of intron 7 or a deletion of exon 8. Analysis of Sl^{17H} DNA revealed a T→A transversion in the splice acceptor site of intron 7 by comparison with wild-type DNA and DNA from other strains of mice, confirming the former possibility (Brannan *et al.*, 1992).

Although the protein encoded by the Sl^{17H} allele is altered in its cytoplasmic tail, it is biologically active and can stimulate mast cell proliferation (Brannan *et al.*, 1992). This is perhaps predictable since Sl^{17H}/Sl^{17H} animals are viable and have only mild defects in their hemopoietic system. While the factor encoded by the Sl^{17H} allele has not been tested for its effects on melanoblasts, it can support PGC survival in culture, albeit at a reduced level in comparison to wild-type protein (C. I. Brannan and P. J. Donovan, unpublished observations). In terms of its activity on PGCs it seems to fall somewhere between that of wild-type protein and the protein encoded by the Sl^d allele, or soluble, recombinant protein. How then can the male sterility of Sl^{17H} animals be explained?

Surprisingly, when Sl^{17H} homozygote embryos were examined, it was found that PGC numbers were equally reduced in both males and females even though adult females are fertile. Examination of postnatal and adult gonads of Sl^{17H} homozygotes identified a defect in spermatogenesis but seemingly no effect on oogenesis apart from a reduction in the number of oocytes. This reduction is most likely to be due to the reduction in numbers of PGCs entering and surviving in the embryonic gonad. Over

time all the oocytes and follicular tissue seem to be lost from the ovaries of adult Sl^{17H}/Sl^{17H} animals and the ovary shows invaginations of the surface epithelium and tubular adenoma. This tumor phenotype is also observed in germ cell-deficient W^x/W^v females and is thought to be due to overproduction of pituitary gonadotrophins (Murphy, 1972).

Following colonization of the gonad, germ cell development in male mice is quite distinct from germ cell development in females. While female PGCs enter directly into meiosis in the embryo, male PGCs enter mitotic arrest. In the postnatal animal these mitotically arrested cells, now called gonia, begin to divide mitotically again about 5 days after birth and establish a stem cell population. These spermatogonia give rise to spermatocytes that divide meiotically generating haploid cells. The final stage of male germ cell development, spermiogenesis, involves the complex morphogenetic changes that result in the formation of the spermatozoon. How does the Sl^{17H} mutation affect this process? In wild-type animals at 12 days of age all testis tubules contain spermatogonia and 90% of tubules show all stages of germ cells up to meiotic prophase. In Sl^{17H} homozygotes, on the other hand, 12-day-old postnatal testes lacked spermatogonia in 50% of their testis tubules. While some tubules (27%) contained spermatogonia, in only 23% of tubules had germ cells advanced to the spermatocyte stage. Germ cells in the testes of Sl^{17H} homozygote males continue to develop, such that by 5 weeks of age 52% of the tubules contain germ cells advanced to the elongating or maturing spermatocyte. However, these tubules are severely deficient in spermatocytes, indicating that the next round of spermatogenesis has failed to occur. In 8-week-old animals most of the tubules in mutant homozygotes were completely devoid of germ cells with only a few spermatogonia remaining (Brannan *et al.*, 1992). Spermatogenesis in these animals is therefore late in inception and early in cessation. The conclusion drawn from these studies was that the cytoplasmic tail of transmembrane forms of SLF are required for postnatal germ cell development in the male but not the female.

That membrane-bound forms of SLF are more efficient at supporting PGC survival and/or proliferation is one explanation for the sterility found in Sl/Sl^d animals. Thus it seems likely that the sterility seen in Sl^d mice is due to a specific role for transmembrane forms of SLF. The inability of the soluble form of SLF to support long-term survival of PGCs *in vivo* or *in vitro* could imply (1) a role for membrane-bound SLF in a prolonged receptor–ligand interaction, (2) a requirement for a localized high concentration of SLF, (3) a particular conformation of SLF precluded by soluble factor, or (4) a role for SLF in promoting cell adhesion. A requirement for a transmembrane factor could provide a mechanism for PGC guidance to the gonad anlagen along a haptotactic gradient of SLF. SLF mRNA is expressed in somatic cells along the germ cell migratory route and,

interestingly, Keshet and co-workers (1991) have suggested that a gradient of SLF mRNA may exist along the pathway. However, without knowing precisely where the SLF protein is expressed and localized or how its cleavage is regulated, these data must be interpreted with caution. Interestingly, rSLF can promote PGC adhesion to plastic substrates *in vitro,* supporting the idea that SLF may constitute part of the extracellular substrate required for PGC migration (S. Dolci and P. J. Donovan, unpublished observations). Consistent with this notion, previous studies demonstrated that a transmembrane form of SLF could mediate mast cell adhesion to cellular substrates (Flanagan *et al.*, 1991).

One piece of data that is pertinent to this point is the analysis of PGC migration in Sl/Sl^d animals (McCoshen and McCallion, 1975). Since the *Sl* allele is completely deleted for SLF coding sequences (Copeland *et al.*, 1990), Sl/Sl^d animals can only produce soluble SLF. As adults these animals are sterile, but PGCs are produced in Sl/Sl^d embryos and migrate to the genital ridge. Analysis of PGC migration in these embryos reveals that many PGCs are not on the correct migratory pathway at 11.5 days of development. In wild-type embryos at this stage approximately 70% of PGCs have reached the genital ridge and the remaining 30% are at the coelomic angle (the junction between the mesentery and the dorsal body wall). In the embryos identified as Sl/Sl^d compound heterozygotes, only 24% of PGCs have reached the gonad while 40% are ectopic to the normal pathway of migration (McCoshen and McCallion, 1975) (Table I). While the authors did not present data describing the positions of aberrantly migrating PGCs, it will be interesting to analyze PGC migration in Sl^d animals now that the molecular basis of this locus is understood. Analysis of PGC migration in other *Sl* alleles will also be of interest. Similar studies of PGC proliferation and migration in W^e/W^e embryos also demonstrate that many PGCs are found ectopic to the normal pathway of migration (Buehr *et al.*, 1993). Moreover, these studies demonstrated that many

Table I Analysis of PGC Migration in Sl/Sl^d Embryos[a]

Site-colonized	Wt	Si/Si^d
Genital ridges	70%	23%
Coelomic angle	30%	12%
Gut endoderm	0	21%
Ectopic sites	0	44%

Note. Wt, wild-type; Sl/Sl^d, steel/steel-dickie.

[a] Modified from McCoshen and McCallion (1975).

PGCs in W^e/W^e embryos were clumped together rather than spread out along the migratory route. These data lend support to the idea that the c-*kit*/SLF interaction could play a role in cell adhesion. In W^e/W^e embryos in which this interaction is altered, adhesion between PGCs could predominate over cell–substratum interactions. Thus SLF factor could regulate both PGC survival and migration, providing an exquisite mechanism for controlling the temporal and spatial development of PGCs in the mouse embryo.

The drastic effect of the Sl^{17H} mutation suggests an important role for the SLF cytoplasmic tail not only in PGC development but also in postnatal male germ cell development. The SLF cytoplasmic tail could be important for a number of different functions. Dimerization is required for activation of the c-*kit* RTK, and it is possible that SLF also needs to dimerize to function correctly and that the cytoplasmic tail plays a key role in this process. It is also possible that the SLF tail is involved in signaling inside the cells expressing it. Therefore, when SLF and c-*kit* interact, PGCs would receive a signal via c-*kit* and somatic cells would receive a signal via SLF. Another possibility is that the amino acids comprising the cytoplasmic tail of SLF are important for stabilizing the protein in the cell membrane. In this regard it is important to note the loss of a number of juxtamembrane lysine residues from the SLF encoded by the Sl^{17H} allele (Brannan *et al.*, 1992). These charged residues could be responsible for holding the factor in the membrane. A final possibility is raised by work analyzing the function of the cytoplasmic tail of pro-TGFα. Like SLF, pro-TGFα is a transmembrane growth factor that has an extracellular cleavage site that allows proteolysis and release of the extracellular domain (Pandiella *et al.*, 1992). Studies of the structure of pro-TGFα identified a terminal valine residue to be important for ectodomain cleavage of pro-TGFα (Bosenberg *et al.*, 1992). Mutation of the terminal valine resulted in a pro-TGFα molecule that could not be efficiently cleaved to release a soluble factor. Domain swapping experiments between pro-TGFα and SLF demonstrated that the same regulatory elements exist in the cytoplasmic tail of SLF (Bosenberg *et al.*, 1992). Like pro-TGFα, the C-terminal amino acid of wild-type SLF is a valine residue, and this is altered in the factor encoded by the Sl^{17H} allele. The factor encoded by the Sl^{17H} allele would therefore be expected to show altered regulation of ectodomain cleavage and possibly is not cleaved at all. Thus developmentally regulated cleavage of SLF may play an important role in PGC and postnatal germ cell development.

In conclusion, the differential effects of soluble versus transmembrane SLF *in vitro*, the sterility of Sl/Sl^d (or Sl^d/Sl^d) animals, and the severe effects of the Sl^{17H} mutation on PGC development suggest an important role for transmembrane forms of SLF. Further studies using antibodies

to SLF or mutational analysis of SLF should reveal important new data about the function of soluble and transmembrane forms of this factor. Although the precise action (proliferation versus survival) of SLF on PGCs remains unclear, the analysis of SLF function in *in vitro* systems showed that another factor(s) must be acting on PGCs. One such factor is leukemia inhibitory factor (LIF).

D. Leukemia Inhibitory Factor

Examination of PGC proliferation on different embryonic fibroblast cell lines (STO and NIH-3T3 cells) demonstrated that PGC proliferation does not correlate well with the amount of SLF produced by the feeder layer (Dolci *et al.*, 1991). NIH-3T3 cells produce more SLF mRNA and stimulate greater mast cell proliferation than STO cells. Moreover, addition of recombinant SLF to PGCs cultured on NIH-3T3 cells has no effect on PGC proliferation. The conclusion drawn from these data was either that another factor produced by STO cells could stimulate PGC proliferation or alternatively a factor produced by NIH-3T3 cells could inhibit PGC proliferation (Dolci *et al.*, 1991). Addition of STO cell-conditioned medium (STO-CM) to PGCs cultured on NIH-3T3 cells stimulated PGC proliferation, thus making the former possibility more likely. Similarly, STO-CM stimulates proliferation of PGCs cultured on *Sl*-m220 cells (Matsui *et al.*, 1990). The conclusion drawn from these studies is that STO cells produce, in addition to SLF, another soluble factor that is a PGC mitogen. One of the factors made by STO cells is LIF and indeed LIF stimulates PGC proliferation on *Sl*-m220 cells (Matsui *et al.*, 1990). It seems likely, therefore, that one soluble, mitogenic activity produced by STO cells is LIF.

LIF is a pleiotropic cytokine produced by a variety of different cells that can act in a variety of different ways on a plethora of other cells (Gearing, 1992; Metcalf, 1992; Gough, 1992). The LIF cDNA encodes a protein with a predicted molecular mass of 20,000 kDa but the purified protein is a disulfide-linked monomer with a molecular mass of 50–58 kDa. Known by a variety of different names (including differentiation inhibiting activity, DIA; differentiation retarding factor, DRF; differentiation inducing factor, DIF; cholinergic nerve differentiation factor, CDF; melanoma-derived lipoprotein lipase inhibitor, MLPLI; human interleukin for DA cells, HILDA; and hepatocyte stimulating factor III, HSFIII), LIF can stimulate proliferation, induce or inhibit differentiation, and act as a positive or negative cellular activator (for reviews see Gearing, 1992; Metcalf, 1992; Gough, 1992).

How does LIF act on PGCs? On STO cells and *Sl*-m220 cells LIF clearly stimulates PGC proliferation measured by BrdU incorporation (Matsui *et al.*, 1991; Resnick *et al.*, 1992). On TM4 cells, on the other hand, LIF promotes PGC survival (Dolci *et al.*, 1993). Moreover, like SLF, LIF can suppress apoptosis of PGCs in culture (Pesce *et al.*, 1993). As in the studies on the effects of SLF, analysis of PGC survival/proliferation in different experimental systems seems to lead to different conclusions. It seems likely, however, that multiple factors may be required for the survival of all animal cells except for blastomeres (Raff, 1992). Thus both SLF and LIF could promote PGC survival and, together with other factors, stimulate proliferation.

Another potential mechanism for LIF action, not necessarily excluded by its role as a survival factor, is as a differentiation inhibiting activity. Once in the gonad PGCs cease mitotic proliferation and enter either a mitotic or a meiotic arrest depending on the sex of the embryo (McLaren, 1991). Previous studies, analyzing alkaline phosphatase activity and anti-SSEA-1 reactivity of cultured PGCs, led to the suggestion that PGCs may develop on schedule in culture (Donovan *et al.*, 1986). If LIF were able to inhibit this differentiation step *in vitro* then the observed effect would, presumably, be increased proliferation since PGCs would not progress to a nonmitotic phase. This action of LIF would not be unprecedented since one of its earliest identified activities was as an inhibitor of ES cell differentiation (Smith *et al.*, 1988; Williams *et al.*, 1988). The analysis of the effects of LIF on the expression of PGC stage-specific antigens may allow this question to be addressed.

Whatever the true function of LIF it clearly acts on PGCs and synergizes with SLF to stimulate PGC proliferation *in vitro*. Because of the complex nature of the culture system it is difficult to determine if LIF acts directly on the PGCs or indirectly via STO cells or embryonic somatic cells. A low-affinity, LIF-binding, LIF receptor (LIFR) was cloned and was found to have homology with gp130, the IL-6 signal tranducer (Gearing *et al.*, 1991). This receptor, together with gp130, forms a high-affinity LIF receptor capable of transducing signals in response to LIF (Gearing *et al.*, 1992) (Fig. 5). PGCs isolated from the genital ridge and labeled with an anti-SSEA-1 antibody can also be labeled with an anti-LIFR antiserum, suggesting that PGCs express a LIF receptor (L. Cheng and P. J. Donovan, unpublished observations). These data strongly suggest that PGCs are a direct target of LIF action in culture.

Does LIF play any role in PGC development *in vivo?* In the mouse embryo the greatest expression of LIF transcripts occurs at the time of implantation in the endometrial glands of the mother (Bhatt *et al.*, 1991; Shen and Leder, 1992). LIF mRNA expression declines rapidly after implantation. Consistent with these data, female mice lacking LIF (created

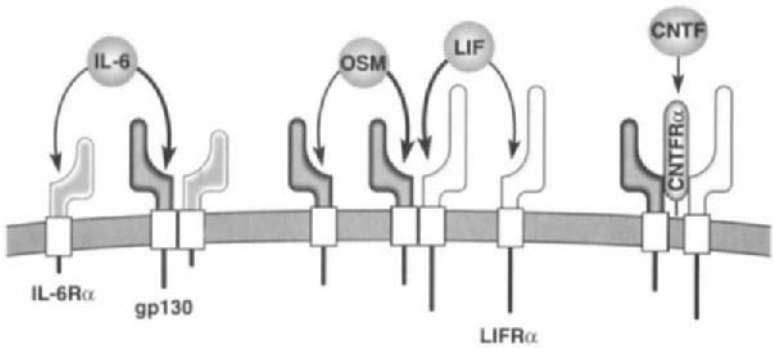

Fig. 5 Comparison of the proposed receptors for LIF, Il-6, OSM and CNTF. The IL-6 receptor comprises an IL-6-binding subunit, IL-6Ra and a signal transducer, gp130. The LIF, OSM and CNTF receptors also contain gp130 as well as a subunit originally identified as a LIF-binding, low affinity receptor, LIFR. The combination of LIFR and gp130 forms a high affinity receptor for LIF and OSM. When combined with the CNTF receptor (CNTFR*a*) this complex is converted into a high affinity LIF receptor. (Modified after Gearing, 1992)

by targeting the LIF gene by homologous recombination in embryonic stem cells) cannot support blastocyst implantation (Stewart *et al.*, 1992). When LIF-/LIF-embryos are transplanted into a pseudopregnant, wild-type female they develop normally and are viable and fertile (Stewart *et al.*, 1992). This suggests that the major role of LIF is to support embryo implantation. Although LIF-deficient mice are fertile in both sexes, it is possible that PGC numbers could be reduced in these animals since mice with severe deficiencies in PGC numbers can still be fully fertile (e.g., female Sl^{17H}/Sl^{17H} animals or male Sl^{pan}/Sl^{pan} animals). It will be important, therefore, to determine if PGC numbers are normal in LIF-deficient animals. If PGC numbers are normal in these animals then this suggests that either LIF is not the natural ligand for PGCs or another closely related cytokine can substitute for LIF in the absence of LIF.

LIF is a member of a family of cytokines that are related by primary amino acid sequence, secondary structure, and genomic organization (Bazan, 1991; Rose and Bruce, 1991). The related cytokines include interleukin-6 (IL-6), ciliary neurotrophic factor (CNTF), oncostatin M (OSM), and granulocyte–colony-stimulating factor (G-CSF). Understanding of the pleiotropic functions of LIF was advanced by the molecular characterization of the cell surface receptor for LIF (Gearing *et al.*, 1991). The LIF receptor comprises a low-affinity, LIF-binding subunit (referred to here as LIFR) and a second signal transducer molecule, gp130 (Gearing *et al.*, 1992) (Fig. 5). Activation of the LIF receptor complex requires heterodimerization of LIFR and gp130 and is accompanied by tyrosine

phosphorylation of both subunits. As members of an emerging cytokine receptor family, LIFR and gp130 serve as components of bi- or tripartite receptors for multiple cytokines. For example, the LIFR/gp130 complex also functions as a high-affinity receptor for the cytokine OSM (Gearing *et al.*, 1992). Addition of a third component, the low-affinity receptor for CNTF (CNTFRα), converts the bipartite LIFR/gp130 complex into a high-affinity receptor for CNTF (Ip *et al.*, 1992, 1993; Davis *et al.*, 1993). Thus both LIFR and gp130 are required for the signal transduction of multiple cytokines, including LIF, OSM, and CNTF (Fig. 5). These data provide some explanation for the overlapping functions of these cytokines as well as suggesting that some of these factors may be functionally redundant. It seems likely, therefore, that in the absence of LIF another cytokine could substitute for its proposed function in PGC development. Of the LIF-related cytokines, OSM is the most closely related to LIF and it is localized next to LIF on human chromosome 22. It is predicted that OSM could perform all the functions of LIF as well as some others of its own (Gearing, 1992). Whether OSM could substitute for LIF in PGC development remains uncertain since the OSM gene has only been identified in humans and simians—a murine homolog has never been cloned. Mice lacking CNTF or IL-6 have been created by gene targeting in ES cells and like LIF-deficient mice these animals are fertile (Masu *et al.*, 1993; Poli *et al.*, 1994). However, in CNTF- or IL-6-deficient animals other members of this cytokine family could potentially substitute for the missing cytokine. Animals deficient in two or more cytokines in this family may allow the roles of these factors in PGC development to be determined. At the present time, therefore, the precise role of LIF in PGC development *in vivo* remains unclear.

Although SLF and LIF can synergize to stimulate PGC proliferation *in vitro* the observed proliferation rate compares poorly with that observed *in vivo*. These observations led to the identification of another factor capable of stimulating PGC proliferation, namely basic fibroblast growth factor (bFGF).

E. Long-Term Proliferation of Primordial Germ Cells

While STO cells can produce LIF, the addition of further recombinant LIF to PGCs cultured on STOs stimulates their proliferation. Even in these conditions PGC proliferation is limited, suggesting that other factors might regulate their growth. Of the numerous factors tested *in vitro*, bFGF showed the greatest stimulation of PGC proliferation both on STO cells and on Sl-m200 cells (Matsui *et al.*, 1992; Resnick *et al.*, 1992). bFGF might stimulate PGC proliferation directly or could act indirectly via stimu-

lation of the feeder layer. At the time of writing no clear picture has emerged. bFGF can stimulate production of LIF (Rathjen *et al.*, 1990) and SLF (J. Resnick and P. J. Donovan, unpublished observations) by feeder cells but could equally act directly on PGCs via a FGF-receptor (FGFR). Until it is known whether PGCs express a FGFR, this question will remain unanswered. Even though bFGF is mitogenic for PGCs, it does not on its own affect the long-term survival of PGCs in culture. The normal pattern of PGC proliferation in culture involves proliferation as single cells; formation of small clones (5–10 cells), either by clonal division or aggregation; and, finally, disappearance of clones between 7 and 10 days after isolation from the embryo. Binary combination of factors (e.g., SLF and LIF or SLF and bFGF) had no effect on this time course of events. However, when PGCs were cultured in the presence of bFGF, LIF, and SLF, long-term proliferation of PGCs was achieved (Matsui *et al.*, 1992; Resnick *et al.*, 1992). On fibroblast feeder layers, and in the presence of these three factors, PGCs form clones (5–10 cells) which initially expand as a cellular monolayer and eventually form multilayered colonies that continue to grow and proliferate (Fig. 6). These multilayered colonies can be isolated, trypsinized, and replated to generate clonal cell lines that continue to proliferate in culture. In the presence of bFGF, therefore, PGC proliferation is maintained indefinitely. The resultant cell lines, which have been termed embryonic germ cells or EG cells, closely resemble feeder-dependent embryonal carcinoma cells, pluripotent cells derived from PGC-derived or embryo-derived tumors, and embryonic stem cells, pluripotent cells derived from the inner cell mass of a preimplantation embryo. EG cells also continue to express alkaline phosphatase activity and to express other PGC markers such as the stage-specific embryonic antigen-1 (Matsui *et al.*, 1992; Resnick *et al.*, 1992). These markers are also shared with EC and ES cells.

Because of the similarity between these EG cells and EC and ES cells they have been tested for their pluripotentiality in a number of assays (see Table II). These assays include teratoma formation in histocompatible adult hosts, embryoid body formation *in vitro*, and, finally, chimera formation when introduced into genetically marked host blastocysts. In these assays both EC and ES cell lines are pluripotent, that is they differentiate into tissues derived from all three primary germ layers (for reviews see Martin, 1980; Robertson, 1991). The major difference between EC cells and ES cells is the efficiency with which they give rise to germ line chimeras when introduced into the blastocyst. ES cells show high levels of contribution to the germ line in chimeras while EC cells rarely do so (Martin, 1980; Robertson, 1991). EG cells (or PGC-derived ES cells) generate teratomas in histocompatible hosts and make embryoid bodies in culture (Matsui *et al.*, 1992; J. L. Resnick, L. S. Bixler, L. Cheng,

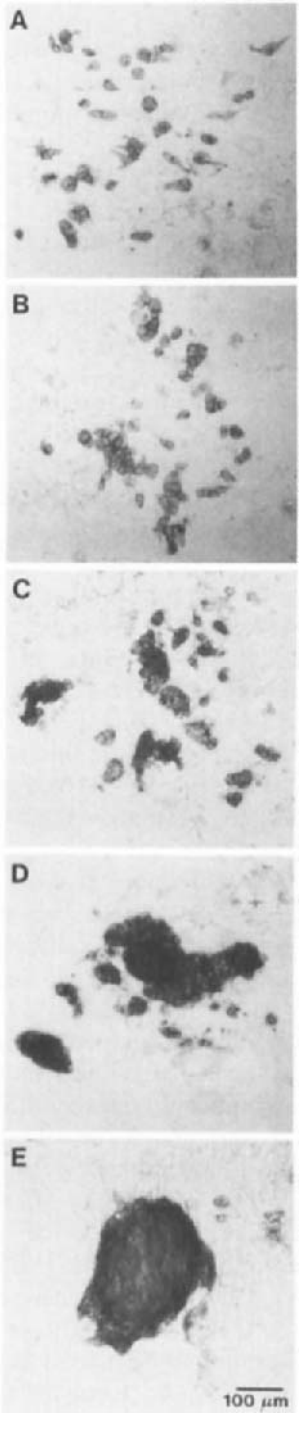
A
B
C
D
E
100 μm

Table II Assays of Developmental Pluripotency

	ICM/ES	PGC	EC	EG
Chimera formation				
Soma	+ + +	−	+ + +	+ + +
Germ line	+ + +	−	−	+/−
Teratoma formation	+ + +	+	+ + +	+ + +
Embryoid body formation	+ + +	−	+ + +	+ + +

Note. ICM, inner cell mass; ES, embryonic stem cells; PGC, primordial germ cells; EC, embryonal carcinoma cells; EG, embryonic germ cells.

and P. J. Donovan, unpublished observations). When introduced into genetically marked blastocysts, EG cells contribute to all the tissues of the embryo and, in a growing number of cases, to the germ line (Matsui *et al.*, 1992; Stewart *et al.*, 1994; Labosky *et al.*, 1994; L. Jackson-Grusby and R. Jaensich, personal communication; U. Klemm, personal communication). These data are in dramatic contrast to the results obtained when PGCs are tested in these assays. Although purified populations of PGCs have not been tested experimentally for their ability to give rise to teratomas or teratocarcinomas, clearly they can do so under certain circumstances since spontaneous teratomas are naturally derived from PGCs (Stevens, 1983). The ability of PGCs to give rise to embryoid bodies in *in vitro* assays has not been tested. However, PGCs have been introduced into blastocysts and have not contributed to any somatic lineage or to the germ line (P. J. Donovan and E. J. Robertson, unpublished observations; V. E. Papaioannou, personal communication; C. L. Stewart, personal communication). Thus mouse PGCs seem to be developmentally restricted and committed to the germ line (see Fig. 8). Clearly, however, developmental totipotency must be restored to the germ line at some point in development since the germ cells, uniquely, carry the genome from generation to generation (Fig. 8). Adding bFGF (together with LIF and SLF)

Fig. 6 Derivation of EG cells in culture. When initially plated into culture PGCs, detected by alkaline phosphatase histochemistry, are identified as single cells growing on the STO cell monolayer (A). Over the next 4–5 days of culture they form small colonies, either by clonal proliferation or by aggregation (B and C). In binary combinations of factors these colonies of PGCs would disappear from the cultures between 7–10 days after their isolation from the embryo. In the presence of SLF, LIF and bFGF, colonies continue to expand (D). Initially expansion occurs by outgrowth of colonies as a cellular mnolayer but eventually the colonies become multilayered and form clumps growing on top of the STO cells (E). Bar = 100μm.

seems, therefore, to alter not only the morphology and proliferative capacity of PGCs, but also broadens their developmental potential. These observations suggest that under certain circumstances PGCs can be made to alter their normal differentiation pathway and regain developmental pluripotency. This observation may have important consequences for the understanding of the mechanism of teratocarcingenesis in mice and humans.

Since SLF, LIF, and bFGF modify the *in vitro* and *in vivo* developmental and proliferative potential of PGCs, a key question is whether PGCs are exposed to LIF or FGF2 (or other fibroblast growth factors) during the course of normal development. Presumably if PGCs were exposed to all three factors *in vivo* they would continue to proliferate and could potentially give rise to teratomas and teratocarcinomas. The expression of these factors must, therefore, be tightly regulated in the embryo. Since SLF is expressed in somatic cells surrounding PGCs (Matsui *et al.*, 1990; Keshet *et al.*, 1991), the factor that "modifies" their developmental and proliferative potential in culture must be either LIF or bFGF or a combination of the two factors. A discussion of whether LIF is expressed in the embryo and whether PGCs express a LIF receptor was presented earlier. The precise role of bFGF is unclear. Two possibilities seem likely: either PGCs never encounter all three factors at once or the combined action of these factors is modified by a negative regulator. To date nine FGFs have been identified: acidic FGF (FGF1), basic FGF (FGF2), FGF3, hst-1/Kaposi FGF (FGF4), FGF5, FGF6, keratinocyte growth factor (KGF) (FGF7), androgen-induced growth factor (FGF8), and glia-acting factor (FGF9) (Basilico and Moscatelli, 1992; Tanaka *et al.*, 1992; Miyamoto *et al.*, 1993). Although the expression pattern of some of these factors has been described, none have been localized to the developing gonad. FGF4 is expressed in the primitive streak and could potentially stimulate proliferation of pregonadal PGCs (Niswander and Martin, 1992; Drucker and Goldfarb, 1993). Despite the fact that bFGF can stimulate PGC proliferation *in vitro,* whether it can do so *in vivo* remains unclear since it lacks a signal sequence and may not be secreted by cells (for a review see Basilico and Moscatelli, 1992). One potential scenario, therefore, is that PGCs never normally encounter bFGF but that tissue damage (or another mechanism) could cause release of bFGF that, together with pre-existing SLF and LIF, would then alter the developmental and proliferative potential of PGCs. In order to clearly understand the potential role of FGFs the most important information will be gained from examining the expression of FGFs or their receptors in somatic and germ cells during development. Since EG cell lines have also been derived from both migratory and gonadal PGCs, this suggests that PGCs of many developmental stages could express a FGF receptor.

A second possibility is that the stimulatory effects of these three factors (SLF, LIF, and bFGF) could be modified *in vivo* by the action of negative regulators such as members of the transforming growth factor (TGF) superfamily. When genital ridges are cultured *in vitro* they produce a factor that has a chemotrophic effect on PGCs and can attract PGCs toward the genital ridge in chemotaxis assays (Godin and Wylie, 1991). A similar effect is seen when TGFβ1 is used in place of genital ridge-conditioned medium, suggesting that the chemotrophic factor is TGFβ1. Moreover, antibodies to TGFβ1 inhibit the chemotrophic effect of genital ridge-conditioned medium. Analysis of TGFβ1 expression in the embryo by indirect immunocytochemistry also reveals the presence of TGFβ1 in the genital ridge. In addition to its chemotrophic properties, TGFβ1 is also a potent inhibitor of PGC proliferation (Godin and Wylie, 1991). Again it is important to note that interpretation of the role of TGFβ1 in culture is complicated by the presence of feeder cells and embryonic somatic cells. Direct action of TGFβ1 on PGCs could be demonstrated if a truly feeder-independent culture of PGCs becomes possible or by demonstration that PGCs express a TGFβ1 receptor. Nevertheless, the mitogenic effects of SLF, LIF, and bFGF on PGCs could be constrained at the appropriate time in development through negative regulation (directly or indirectly) by TGFβ1. Mice lacking TGFβ1 will be an important tool in elucidating the role of this growth factor in PGC development (Shull *et al.*, 1992).

Another candidate negative regulator of PGC development is another member of the TGFβ superfamily, namely Mullerian inhibitory substance (MIS) (reviewed in Chapter 5 of this volume by Richard R. Behringer). MIS is expressed by developing Sertoli cells in embryo and it is possible that MIS induction in Sertoli cells is regulated by the *Sry* gene. Granulosa cells in the ovary also express MIS but expression in this case must be regulated by another mechanism. Female mice overexpressing MIS are sterile, suggesting that MIS might act directly on germ cells, but its direct action on PGCs in culture has not been determined. Whether or not TGFβ or MIS act as negative regulators of PGC growth in the embryo, it seems probable that negative regulation of PGC proliferation plays an important part in PGC development in mice.

How does bFGF act to modify the proliferative and developmental potential of PGCs? One possibility is that bFGF is simply a PGC mitogen and that LIF (or another factor present in the culture system) modifies PGC growth in culture by affecting PGC differentiation (see the earlier discussion of LIF action). The analysis of the role of bFGF in oligodendrocyte precursor proliferation suggests another possibility, namely that bFGF blocks differentiation (Bogler *et al.*, 1990; McKinnon *et al.*, 1990).

Oligodendrocyte Type-2 astrocyte (O-2A) progenitors proliferate in response to PDGF, but after a set number of divisions they differentiate on schedule *in vitro* and lose their ability to respond to PDGF. It has been proposed that PDGF drives the clock that times oligodendrocyte development in culture (Raff *et al.*, 1988). In the presence of bFGF, O-2A progenitors continue to divide and do not differentiate (Bogler *et al.*, 1990; McKinnon *et al.*, 1990). One effect of bFGF is to increase the steady-state level of PDGF receptors on O-2A progenitors and to increase the sensitivity of O-2A progenitors to PDGF (McKinnon *et al.*, 1990). It has been suggested that bFGF (or a related factor) could induce the PDGF receptor in O-2A progenitors *in vivo* and set the clock that times oligodendrocyte development (McKinnon *et al.*, 1990). In culture, therefore, bFGF may block O-2A progenitor differentiation by maintaining responsiveness to PDGF. The parallels between O-2A progenitor development and PGC development are striking. It is intriguing to speculate that exposure of early PGCs (SLF-independent) to FGF4 in the primitive streak might upregulate c-*kit* levels in PGCs initiating a c-*kit*-dependent clock that could regulate the timing of their differentiation. *In vivo* c-*kit* transcripts are downregulated in PGCs once they have reached the gonad anlagen (Manova and Bachvarova, 1991), and in culture PGCs may follow their normal schedule of development (Donovan *et al.*, 1986; Godin *et al.*, 1990; Matsui *et al.*, 1991).

In culture this could involve PGCs downregulating c-*kit* transcripts and differentiating into a nonproliferating cell. bFGF could inhibit this process by maintaining high levels of c-*kit* in PGCs and thus lead to long-term proliferation of PGCs. The fact that EG cells, once established, no longer require addition of bFGF and can be grown in the absence of SLF suggests that autocrine mechanisms of receptor activation may become established in these cells.

Whatever the mechanism of bFGF action, derivation of EG cells directly from PGCs has a number of important consequences. The growth factor requirements for EG cell establishment from PGCs are significantly better understood than those required for ES cell derivation from blastocysts. LIF is still the only factor known to be required for ES cell derivation. Because of this fact it may be possible to extend this technology to other animal species, particularly other mammals. The generation of bovine, porcine, ovine, or equine EG cells could have great commercial potential and value. The generation of human EG lines, while having major ethical consideration, could be of immense medical benefit in, for example, tissue transplantation and repair. Since ES cell technology is so well established in the mouse, EG cell lines may prove to be more useful for studying germ line imprinting and pluripotency (Labosky *et al.*, 1994; Stewart *et al.*, 1994) than for performing gene targeting. The mechanism of EG cells

derivation from PGCs also seems to mimic the process of teratoma formation in mice and it will be interesting to see if bFGF and LIF or their cognate receptors are involved in teratocarcinogenesis in mice or humans.

III. Summary

This chapter focused on three key regulators of PGC survival and proliferation; SLF, LIF, and bFGF. The survival of all animal cells may require multiple polypeptide factors and PGCs seem to be no exception (Fig. 7). A number of lines of evidence suggest that membrane-bound forms of SLF may be required for PGC survival. These data suggest an exquisite mechanism for controlling both PGC survival and migration. Thus PGCs that stray from the normal migratory pathway might be eliminated through programmed cell death. SLF, together with LIF, can stimulate PGC proliferation in culture and it seems likely that LIF or a related cytokine may function *in vivo* to regulate PGC survival and proliferation. Animals doubly deficient in LIF and its relatives may soon allow the roles of these cytokines in PGC development to be determined. Although bFGF is a potent PGC mitogen *in vitro*, whether PGCs ever encounter bFGF *in vivo* remains questionable since in culture it alters both the proliferative and develop-

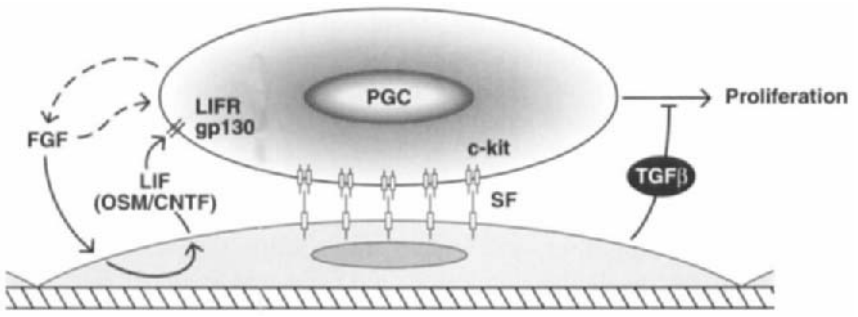

Fig. 7 Factors regulating PGC survival and proliferation. PGC survival *in vitro* (and probably *in vivo*) requires expression in somatic cells of a transmembrane form of SLF which binds to the c-kit receptor expressed in PGCs. LIF may also act as a survival factor but in concert with SLF it can stimulate PGC proliferation. PGCs probably express a high affinity LIF receptor consisting of a low-affinity, LIF-binding subunit (LIFR) and a signal transducer, gp130. A number of related cytokines can bind to this receptor complex, including LIF, OSM and CNTF. Which of these factors is the natural physiological ligand remains to be determined. Whether bFGF is expressed in the embryo or whether PGCs express an FGF receptor also remain to be examined. The actual mode of action of bFGF on PGCs is, therefore, at present unclear. In culture bFGF can upregulate LIF levels in fibroblasts. TGFβ1 is a potent negative regulator of PGC proliferation.

mental potential of PGCs. TGFβ or MIS may be important negative regulators of PGC development, and mice lacking these factors should allow their role in PGC development to be assessed.

IV. Future Prospects

It seems likely that the factors described earlier (SLF, LIF, bFGF, and TGFβ1) are not the only factors that regulate PGC development in the mouse embryo. The proliferation rate of PGCs *in vitro* is low compared with that observed *in vivo*. Although this could be explained by the differences between growth in two- or three-dimensional environments, we have probably only begun to scratch the surface in terms of PGC growth regulators. Since the effects of many *W* and *Sl* mutations are not observed until about 9.5 dpc (Mintz and Russell, 1957; McCoshen and McCallion, 1975; Buehr *et al.*, 1993), PGC development up until this time is most likely independent of the c-*kit* signaling pathway. Thus emergence and proliferation of PGCs up until 9.5 dpc might be regulated by a factor other than SLF. A similar pattern is seen during the embryonic development of the hemopoietic system in which many *Sl* mutations do not have deleterious effects until 13.5 dpc when liver hemopoiesis has commenced (Ikuta and Weissman, 1992). Development of hemopoietic progenitors in the fetal yolk sac is thought to be regulated not by SLF but by another factor. Tumor necrosis factor-α (TNF-α) is a potent mitogen for early PGCs (7.5 dpc) in culture and thus could represent one of the factors required for early PGC development (Kawase *et al.*, 1994). TNF-α was unable to stimulate proliferation of PGCs from 10.5 dpc embryos and thus might act during the c-*kit*/SLF-independent phase of PGC development. As with the other factors identified as PGC mitogens in culture, it will be important to determine if PGCs express receptors for TNF-α. Elucidation of other such factors may be difficult given the small numbers of cells and the problems in isolating them and keeping them alive. One solution to this problem will be to establish immortalized PGC lines. Such cell lines have been produced from postnatal germ cells as well as from PGCs from genital ridges and will undoubtedly be a useful source of both growth factors and growth factor receptors (Hofmann *et al.*, 1992; J.-L. Millan, personal communication). Ultimately, it would be useful to derive permanent cell lines representative of every stage of PGC development. Somatic cell lines of gonadal origin may also be an important source of PGC growth factors (Hofmann *et al.*, 1992; Rassoulzadegan *et al.*, 1993). Such cell lines might provide the appropriate cues to direct normal germ cell development *in vitro*. The recent demonstration of transmeiotic differentiation of spermatogonia on an immortalized Sertoli cell line is an indication of

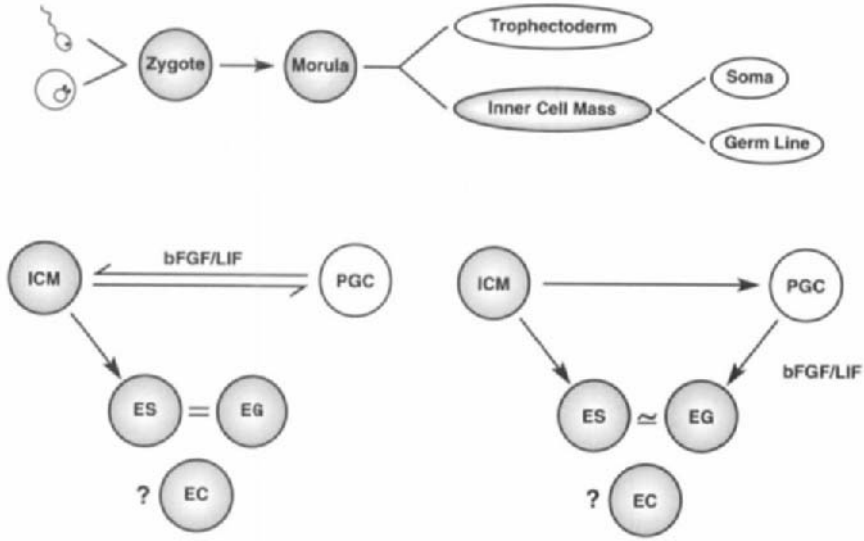

Fig. 8 Alternative pathways of stem cell origin. Fusion of the two gametes produces a single cell (the zygote) that is totipotent and can give rise to all the embryonic and extra-embryonic structures (upper panel). Developmental pluripotency is retained by certain cell lineages (shaded) during development. PGCs are unable to form chimeras when injected into blastocysts and could be considered to have lost developmental pluripotency. However, the germline must retain developmental totipotency since the PGCs give rise to the gametes which give rise to the totipotent zygote. The inner cell mass (ICM) gives rise to the embryo proper including PGCs and somatic cells. PGCs may be considered a differentiated derivative of the ICM or could be set aside as the somatic cells differentiate. The ICM can clearly give rise to pluripotent stem cells (ES cells) in culture. bFGF and/or LIF could cause PGCs to de-differentiate into ICM cells which could then form an ES cell (lower panel, left). Alternatively, bFGF and LIF could turn PGCs into a novel stem cell that is functionally equivalent to, but distinct from, an ES cell (lower panel, right). Either mechanism could represent the mechanism of EC cell generation and hence teratoma formation *in vivo*.

how useful such cells could be for studying embryonic germ cell development (Rassoulzadegan *et al.*, 1993).

Further information about growth factors (or other molecules) involved in PGC development is also likely to come from newly derived "knockout" mice. If such animals survive through any part of the period of PGC development (7.5 to 15.5 dpc), then they can be profitably used to study the role of such factors in PGC development. Two factors that act on PGCs in culture (LIF and TGFβ1) have already been targeted in mice (Shull *et al.*, 1992; Stewart *et al.*, 1992; Escary *et al.*, 1993). These animals, and others like them, will be an important resource for studying germ cell development.

Characterization of other mouse mutants that affect PGC development or teratocarcinogenesis may yield important information about PGC growth regulation. Mutations at the *Hertwigs' macrocytic anemia* (*an*) and *germ cell deficient* (*gcd*) loci affect PGC development, and the timing of action of these mutations suggests that they affect distinct and novel genes. While *an* is a genetic locus unconnected with *W* and *Sl*, the *gcd* mutation has not been mapped on mouse chromosomes. Similarly, the characterization of gene loci known to affect teratocarcinogenesis, such as *ter* (Stevens, 1973), will undoubtedly lead to a better understanding of PGC development.

Although the derivation of EG cells directly from PGCs may represent a mechanism to study some aspects of PGC (or germ line) development such as imprinting and pluripotency, it is not clear at this stage if they will be of great use in studying PGC migration or differentiation. An important question is what do EG cells represent in development terms? Are they a novel cell type, functionally equivalent, but distinct from ES cells or are they simply PGCs that have dedifferentiated to become an ES cell (see Fig. 8)? Answering this question may have important implications in understanding PGC development and teratocarcinogenesis. If PGCs can dedifferentiate into an ES cell then it may be possible to drive ES cell differentiation in culture toward the germ cell lineage. The prospect of deriving PGCs from ES cells (or EG cells) in culture is truly an exciting one!

Acknowledgments

I sincerely thank the members of my laboratory for their patience while I was writing this chapter and for their efforts in generating some of the data quoted herein. In particular I thank Jim Resnick and Linzhao Cheng for help in interpreting their data and for many helpful discussions. Cathy Hahn and Richard Frederickson are thanked for their help in preparing the manuscript and figures, respectively. I am indebted also to Mary Bedell and Leslie Lock for their patient and insightful answers to the many questions I asked them and along with Roger Pederson for reading the manuscript. I am also extremely grateful to Patricia Labosky, Brigid Hogan, Colin Stewart, Chris Wylie, and David Gearing for many thought-provoking dicussions and with Rudi Jaenisch, Frank Costantini, Virginia Papaioannou, Jose-Luis Millan, and Uwe Klemm for communicating unpublished data. This research was supported in part by the National Cancer Institute, DHHS, under contract NO1-CO-74101 with ABL. The contents of this publication do not necessarily reflect the view or policies of the Department of Health and Human Services, nor does mention of trade names, commercial products, or organizations imply endorsement by the US Government.

References

Alvarez-Buylla, A., and Merchant-Larios, H. (1986). Mouse primordial germ cells use fibronectin as a substrate for migration. *Exp. Cell Res.* **165,** 362–368.

Barres, B. A., Raff, M. C., Gaese, F., Bartke, I., Dechant, G., and Barde, Y.-A. (1994). A crucial role for neurotrophin-3 in oligodendrocyte development. *Nature* **367,** 371–375.

Barres, B. A., Schmid, R., Sendnter, M., and Raff, M. C. (1993). Multiple extracellular signals are required for long-term oligodendrocyte survival. *Development* **118,** 283–295.

Basilico, C., and Moscatelli, D. (1992). The FGF family of growth factors and oncogenes. *Adv. Cancer Res.* **59,** 115–165.

Bazan, J. F. (1991). Neuropoietic cytokines in the hematopoietic fold. *Neuron* **7,** 197–208.

Bellve, A. R. (1979). The molecular biology of spermatogenesis. *In* "Oxford Reviews of Reproductive Biology," (C. A. Finn, ed.) pp. 159–261. Clarendon Press, Oxford.

Bennett, D. (1956). Developmental analysis of a mutation with pleiotropic effects in the mouse. *J. Morphol.* **98,** 199–233.

Bernstein, A., Chabot, B., Dubreuil, P., Reith, A., Nocka, K., Majumder, S., Ray, P., and Besmer, P. (1990). The mouse W/c-kit locus. *Ciba Found. Symp.* **148,** 158–166.

Bhatt, H., Brunet, L. J., and Stewart, C. L. (1991). Uterine expression of leukemia inhibitory factor coincides with the onset of blastocyst implantation. *Proc. Natl. Acad. Sci. USA* **88,** 11,408–11,412.

Bird, J. M., and Kimber, S. J. (1984). Oligosaccharides containing fucose linked a(1-3) and a(1-4) to N-acetylglucosamine cause decompaction of mouse morulae. *Dev. Biol.* **104,** 449–460.

Blandau, R. J., White, B. J., and Rummery, R. E. (1963). Observations on the movements of living primordial germ cells in the mouse. *Fertil. Steril.* **14,** 482–489.

Bogler, O., Wren, D., Barnett, S. C., Land, H., and Noble, M. (1990). Cooperation between two growth factors promotes extended self renewal and inhibits differentiation of oligodendrocyte-type-2 astrocyte (O-2A) progenitor cells. *Proc. Natl. Acad. Sci. USA* **87,** 6368–6372.

Bosenberg, M. W., Pandiella, A., and Massague, J. (1992). The cytoplasmic carboxy-terminal amino acid specifies cleavage of membrane TGF alpha into soluble growth factor. *Cell* **71,** 1157–1165.

Brannan, C. I., Bedell, M. A., Resnick, J. L., Eppig, J. J., Handel, M. A., Williams, D. E., Lyman, S. D., Donovan, P. J., Jenkins, N. A., and Copeland, N. G. (1992). Developmental abnormalities in Steel17H mice result from a splicing defect in the steel factor cytoplasmic tail. *Genes Dev.* **6,** 1832–1842.

Brannan, C. I., Lyman, S. D., Williams, D. E., Eisenman, J., Anderson, D. M., Cosman, D., Bedell, M. A., Jenkins, N. A., and Copeland, N. G. (1991). Steel-Dickie mutation encodes a c-kit ligand lacking transmembrane and cytoplasmic domains. *Proc. Natl. Acad. Sci. USA* **88,** 4671–4674.

Buehr, M., and McLaren, A. (1993). Isolation and culture of primordial germ cells. *In* "Methods in Enzymology" (P. M. Wassarman and M. L. DePamphilis, eds.), Vol. 225, pp. 58–77. Academic Press, San Diego.

Buehr, M., McLaren, A., Bartley, A., and Darling, S. (1993). Proliferation and migration of primordial germ cells in We/We mouse embryos. *Dev. Dynam.* **198,** 182–189.

Chabot, B., Stephenson, D. A., Chapman, V. M., Besmer, P., and Bernstein, A. (1988). The proto-oncogene c-kit encoding a transmembrane tyrosine kinase receptor maps to the mouse W locus. *Nature* **335,** 88–89.

Childs, R. A., Pennington, J., Uemura, K., Scudder, P., Goodfellow, P. N., Evans, M. J., and Feizi, T. (1983). High-molecular-weight glycoproteins are the major carriers of the carbohydrate differentiation antigens I, i and SSEA-1 of mouse teratocarcinoma cells. *Biochem. J.* **215,** 491–503.

Chiquoine, A. D. (1954). The identification, origin and migration of primordial germ cells in the mouse embryo. *Anat. Rec.* **118,** 135–146.

Clark, J. M., and Eddy, E. M. (1975). Fine structural observations on the origin and associations of primordial germ cells of the mouse. *Dev. Biol.* **47,** 136–155.

Cooke, J. E., Godin, I., Ffrench-Constant, C., Heasman, J., and Wylie, C. C. (1993). Culture and manipulation of primordial germ cells. *In* "Methods in Enzymology" (P. M. Wassarman and M. L. DePamphilis, eds.), Vol. 225, pp. 37–58. Academic Press, San Diego.

Copeland, N. G., Gilbert, D. J., Cho, B. C., Donovan, P. J., Jenkins, N. A., Cosman, D., Anderson, D., Lyman, S. D., and Williams, D. E. (1990). Mast cell growth factor maps near the steel locus on mouse chromosome 10 and is deleted in a number of steel alleles. *Cell.* **63,** 175–183.

Davis, S., Aldrich, T. H., Stahl, N., Pan. L., Taga, T., Kishimoto, T., Ip, N. Y., and Yancopoulos, G. D. (1993). LIFR beta and gp130 as heterodimerizing signal transducers of the tripartite CNTF receptor. *Science* **260,** 1805–1808.

DeFelici, M., and Dolci, S. (1989). In vitro adhesion of mouse fetal germ cells to extracellular matrix components [published erratum appears in *Cell Differ. Dev.* 1989 Jul;27(2):149]. *Cell Differ. Dev.* **26,** 87–96.

DeFelici, M., and Dolci, S. (1991). Leukemia inhibitory factor sustains the survival of mouse primordial germ cells cultured on TM4 feeder layers. *Dev. Biol.* **147,** 281–284.

DeFelici, M., and McLaren, A. (1983). In vitro culture of mouse primordial germ cells. *Exp. Cell Res.* **144,** 417–427.

Dolci, S., Pesce, M., and DeFelici, M. (1993). Combined action of stem cell factor, leukemia inhibitory factor, and cAMP on in vitro proliferation of mouse primordial germ cells. *Mol. Reprod. Dev.* **35,** 134–139.

Dolci, S., Williams, D. E., Ernst, M. K., Resnick, J. L., Brannan, C. I., Lock, L. F., Lyman, S. D., Boswell, H. S., and Donovan, P. J. (1991). Requirement for mast cell growth factor for primordial germ cell survival in culture. *Nature* **352,** 809–811.

Donovan, P. J., Stott, D., Cairns, L. A., Heasman, J., and Wylie, C. C. (1986). Migratory and postmigratory mouse primordial germ cells behave differently in culture. *Cell* **44,** 831–838.

Donovan, P. J., Stott, D., Godin, I., Heasman, J., and Wylie, C. C. (1987). Studies on the migration of mouse germ cells. *J. Cell Sci. Suppl.* **8,** 359–367.

Drucker, B. J., and Goldfarb, M. (1993). Murine FGF-4 gene expression is spatially restricted within embryonic skeletal muscle and other tissues. *Mech. Dev.* **40,** 155–163.

Duttlinger, R., Manova, K., Chu, T. Y., Gyssler, C., Zelenetz, A. D., Bachvarova, R. F., and Besmer, P. (1993). *W-sash* affects positive and negative elements controlling c-kit expression: Ectopic *c-kit* expression at sites of kit-ligand expression affects melanogenesis. *Development* **118,** 705–717.

Escary, J. L., Perreau, J., Dumenil, D., Ezine, S., and Brulet, P. (1993). Leukaemia inhibitory factor is necessary for maintenance of haematopoietic stem cells and thymocyte stimulation. *Nature* **363,** 361–364.

Evans, M. (1981). Origin of mouse embryonal carcinoma cells and the possibility of their direct isolation into tissue culture. *J. Reprod. Fertil.* **62,** 625–631.

FFrench-Constant, C., Hollingsworth, A., Heasman, J., and Wylie, C. C. (1991). Response to fibronectin of mouse primordial germ cells before, during and after migration. *Development* **113,** 1365–1373.

Flanagan, J. G., Chan, D. C., and Leder, P. (1991). Transmembrane form of the kit ligand growth factor is determined by alternative splicing and is missing in the Sl^d mutant. *Cell* **64,** 1025–1035.

Flanagan, J. G., and Leder, P. (1990). The kit ligand: A cell surface molecule altered in steel mutant fibroblasts. *Cell* **63,** 185–194.

Fox, N. D. I., Martinez-Hernadez, A., Knowles, B. B., and Solter, D. (1981). Immunohistochemical localization of the early embryonic antigen (SSEA-1) in postimplantation mouse embryos and fetal and adult tissues. *Dev. Biol.* **83,** 391–398.

Gearing, D. P. (1992). The leukemia inhibitory factor and its receptor. *Adv. Immunol.* **53,** 31–59.

Gearing, D. P., Comeau, M. R., Friend, D. J., Gimpel, S. D., Thut, C. J., McGourty, J., Brasher, K. K., King, J. A., Gillis, S., Mosley, B., *et al.* (1992). The IL-6 signal transducer, gp130: An oncostatin M receptor and affinity converter for the LIF receptor. *Science* **255,** 1434–1437.

Gearing, D. P., Thut, C. J., VandeBos, T., Gimpel, S. D., Delaney, P. B., King, J., Price, V., Cosman, D., and Beckmann, M. P. (1991). Leukemia inhibitory factor receptor is structurally related to the IL-6 signal transducer, gp130. *EMBO J.* **10,** 2839–2848.

Geissler, E. N., Ryan, M. A., and Housman, D. E. (1988). The dominant-white spotting (*W*) locus of the mouse encodes the *c-kit* proto-oncogene. *Cell* **55,** 185–192.

Ginsburg, M., Snow, M. H. L., and McLaren, A. (1990). Primordial germ cells in the mouse embryo during gastrulation. *Development* **110,** 521–528.

Godin, I., Deed, R., Cooke, J., Zsebo, K., Dexter, M., and Wylie, C. C. (1991). Effects of the Steel gene product on mouse primordial germ cells in culture. *Nature* **352,** 807–809.

Godin, I., Wylie, C., and Heasman, J. (1990). Genital ridges exert long-range effects on mouse primordial germ cell numbers and direction of migration in culture. *Development* **108,** 357–363.

Godin, I., and Wylie, C. C. (1991). TGF beta 1 inhibits proliferation and has a chemotropic effect on mouse primordial germ cells in culture. *Development* **113,** 1451–1457.

Gough, N. (1992). Molecular genetics of leukemia inhibitory factor (LIF) and its receptor. *Growth Factors* **7,** 175–179.

Heath, J. (1978). Mammalian primordial germ cells. *In* "Development in Mammals," Vol. 3, pp. 267–298.

Hofmann, M.-C., Narisawa, S., Hess, R. A., and Millan, J.-L. (1992). Immortalization of germ cells and somatic testicular cells using the SV40 large T antigen. *Exp. Cell. Res.* **201,** 417–435.

Huang, E. J., Manova, K., Packer, A. I., Sanchez, S., Bachvarova, R. F., and Besmer, P. (1993). The murine steel panda mutation affects kit ligand expression and growth of early ovarian follicles. *Dev. Biol.* **157,** 100–109.

Ikuta, K., and Weissman, I. L. (1992). Evidence that hematopoietic stem cells express mouse c-kit but do not depend on steel factor for their generation. *Proc. Natl. Acad. Sci. USA* **89,** 1502–1506.

Ip, N. Y., McClain, J., Barrezueta, N. X., Aldrich, T. H., Pan, L., Li, Y., Wiegand, S. J., Friedman, B., Davis, S., and Yancopoulos, G. D. (1993). The alpha component of the CNTF receptor is required for signaling and defines potential CNTF targets in the adult and during development. *Neuron* **10,** 89–102.

Ip, N. Y., Nye, S. H., Boulton, T. G., Davis, S., Taga, T., Li, Y., Birren, S. J., Yasukawa, K., Kishimoto, T., Anderson, D. J., *et al.* (1992). CNTF and LIF act on neuronal cells via shared signaling pathways that involve the IL-6 signal transducing receptor component gp130. *Cell* **69,** 1121–1132.

Kawase, E., Yamamoto, H. K. H., and Nakatsuji, N. (1994). Tumor necrosis factor-α (TNF-α) stimulates proliferation of mouse primordial germ cells in culture. *Dev. Biol.* **161,** 91–95.

Keshet, E., Lyman, S. D., Williams, D. E., Anderson, D. M., Jenkins, N. A., Copeland, N. G., and Parada, L. F. (1991). Embryonic RNA expression patterns of the c-kit receptor and its cognate ligand suggest multiple functional roles in mouse development. *EMBO J.* **10,** 2425–35.

Labosky, P. A., Barlow, D. P., and Hogan, B. L. M. (1994). Embryonic germ cell lines and their derivation from mouse primordial germ cells. *In* "Germline Development" (Ciba Foundation Symposium 182), pp. 157–178. Wiley, Chichester.

Lawson, K. A., and Hage, W. J. (1994). Clonal analysis of the origin of primordial germ cells in the mouse. *In* "Germline Development" (Ciba Foundation Symposium 182), pp. 68–91. Wiley, Chichester.

Manova, K., and Bachvarova, R. (1991). Expression of *c-kit* encoded at the *W* locus of mice in developing embryonic germ cells and presumptive melanoblasts. *Dev. Biol.* **146,** 312–324.

Martin, G. R. (1980). Teratocarcinomas and mammalian embryogenesis. *Science* **209,** 768–776.

Masu, Y., Wolf, E., Holtmann, B., Sendtner, M., Brem, G., and Thoenen, H. (1993). Disruption of the CNTF gene results in motor neuron degeneration. *Nature* **365,** 27–32.

Mather, J. P. (1980). The establishment and characterization of two distinct mouse testicular epithelial cell lines. *Biol. Reprod.* **23,** 243–252.

Matsui, Y., Toksoz, D., Nishikawa, S., Nishikawa, S., Williams, D., Zsebo, K., and Hogan, B. L. (1991). Effect of Steel factor and leukaemia inhibitory factor on murine primordial germ cells in culture. *Nature* **353,** 750–752.

Matsui, Y., Zsebo, K., and Hogan, B. L. (1992). Derivation of pluripotential embryonic stem cells from murine primordial germ cells in culture. *Cell* **70,** 841–847.

Matsui, Y., Zsebo, K. M., and Hogan, B. L. (1990). Embryonic expression of a haematopoietic growth factor encoded by the *Sl* locus and the ligand for *c-kit*. *Nature* **347,** 667–669.

McCarrey, J. R., Hsu, K. C., Eddy, E. M., Klevecz, R. R., and Bolen, J. L. (1987). Isolation of viable mouse primordial germ cells by antibody-directed flow sorting. *J. Exp. Zool.* **242,** 107–111.

McCoshen, J. A., and McCallion, D. J. (1975). A study of primordial germ cells during their migratory phase in steel mutant mice. *Experientia* **31,** 589–590.

McKinnon, R. D., Matsui, T., Dubois-Dalcq, M., and Aaronson, S. A. (1990). FGF modulates the PDGF driven pathway of oligodendrocyte development. *Neuron* **5,** 603–614.

McLaren, A. (1981). "Germ Cells and Soma: A New Look at an Old Problem." Yale University Press, New Haven, CT.

McLaren, A. (1991). Development of the mammalian gonad: The fate of the supporting cell lineage. *Bioessays* **13,** 151–156.

Metcalf, D. (1992). Leukemia inhibitory factor: A puzzling polyfunctional regulator. *Growth Factors* **7,** 169–173.

Mintz, B., and Russell, E. S. (1957). Gene-induced embryological modifications of primordial germ cells in the mouse. *J. Exp. Zool.* **134,** 207–237.

Miyamoto, M., Naruo, K.-I., Seko, C., Matsumoto, S., Kondo, T., and Kurokawa, T. (1993). Molecular cloning of a novel cytkoine cDNA encoding the ninth member of the fibroblast growth factor family which has a unique secretion property. *Mol. Cell. Biol.* **13,** 4251–4259.

Motro, B., van der Kooy, D.., Rossant, J., Reith, A., and Bernstein, A. (1991). Contiguous patterns of c-kit and steel expression: Analysis of mutations at the *W* and *Sl* loci. *Development* **113,** 1207–1221.

Murphy, E. D. (1972). Hyperplastic and early neoplastic changes in the ovaries of mice after genetic deletion of germ cells. *J. Natl. Cancer Inst.* **48,** 1283–1295.

Murphy, M., Reid, K., Williams, D. E., Lyman, S. D., and Bartlett, P. F. (1992). Steel factor is required for maintenance, but not differentiation, of melanocyte precursors in the neural crest. *Dev. Biol.* **153,** 396–401.

Niswander, L., and Martin, G. R. (1992). *FGF-4* expression during gastrulation, myogenesis, limb and tooth development in the mouse. *Development* **114,** 755–768.

Nocka, K., Majumder, S., Chabot, B., Ray, P., Cervone, M., Bernstein, A., and Besmer, P. (1989). Expression of *c-kit* gene products in known cellular targets of *W* mutations in normal and *W* mutant mice: Evidence for an impaired *c-kit* kinase in mutant mice. *Genes Dev.* **3,** 816–826.

Nocka, K., Tan, J. C., Chiu, E., Chu, T. Y., Ray, P., Traktman, P., and Besmer, P. (1990). Molecular bases of dominant negative and loss of function mutations at the murine c-kit/white spotting locus: W37, Wv, W41 and W. *EMBO J.* **9,** 1805–1813.

Ozawa, M., Muramatsu, T., and Solter, D. (1985). SSEA-1, a stage-specific embryonic antigen of the mouse, is carried by the glycoprotein-bound large carbohydrate in embryonal carcinoma cells. *Cell Differ.* **16,** 169–173.

Ozdzenski, W. (1967). Observations on the origin of primordial germ cells in the mouse. *Zool. Polon.* **17,** 367–379.

Pandiella, A., Bosenberg, M. W., Huang, E. J., Besmer, P., and Massague, J. (1992). Cleavage of membrane-anchored growth factors involves distinct protease activities regulated through common mechanisms. *J. Biol. Chem.* **267,** 24,028–24,033.

Pellas, T. C., Ramachandran, B., Duncan, M., Pan, S. S., Marone, M., and Chada, K. (1991). Germ-cell deficient (gcd), an insertional mutation manifested as infertility in transgenic mice. *Proc. Natl. Acad. Sci. USA* **88,** 8787–8791.

Pesce, M., Farrace, M. G., Piacentini, M., Dolci, S., and DeFelici, M. (1993). Stem cell factor and leukemia inihibitory factor promote primordial germ cell survival by suppressing programmed cell death (apoptosis). *Development* **118,** 1089–1094.

Poli, V., Balena, R., Fattori, E., Markatos, A., Yamamoto, M., Tanaka, H., Ciliberto, G., Rodan, G. A., and Costantini, F. (1994). Interleukin-6 deficient mice are protected from bone loss caused by estrogen depletion. *EMBO J.* **13,** 1189–1196.

Raff, M. C. (1992). Social controls on cell survival and death. *Nature* **356,** 397–400.

Raff, M. C., Lillien, L. E., Richardson, W. D., Burne, J. F., and Noble, M. D. (1988). Platelet-derived growth factor from astrocytes drives the clock that times oligodendrocyte development in culture. *Nature* **333,** 562–565.

Rassoulzadegan, M., Paquis-Flucklinger, V., Bertino, B., Sage, J., Jasin, M., Miyagawa, K., van Heyningen, V., Besmer, P., and Cuzin, F. (1993). Tansmeiotic differentiation of male germ cells in culture. *Cell* **75,** 997–1006.

Rathjen, P. D., Nichols, J., Toth, S., Edwards, D. R., Heath, J. K., and Smith, A. G. (1990). Developmentally programmed induction of differentiation inhibiting activity and the control of stem cell populations. *Genes Dev.* **4,** 2308–2318.

Reith, A. D., Rottapel, R., Giddens, E., Brady, C., Forrester, L., and Bernstein, A. (1990). *W* mutant mice with mild or severe developmental defects contain distinct point mutations in the kinase domain of the *c-kit* receptor. *Genes Dev.* **44,** 390–400.

Resnick, J. L., Bixler, L. S., Cheng, L., and Donovan, P. J. (1992). Long-term proliferation of mouse primordial germ cells in culture. *Nature* **359,** 550–551.

Robertson, E. J. (1991). Using embryonic stem cells to introduce mutations into the mouse germ line. *Biol Reprod.* **44,** 238–245.

Rose, T. M., and Bruce, A. G. (1991). Oncostatin M is a member of a cytokine family

that includes leukemia-inhibitory factor, granulocyte colony-stimulating factor, and interluekin-6. *Proc. Natl. Acad. Sci. USA* **88,** 8641–8645.

Russell, E. S., McFarland, E. C., and Peters, H. (1985). Gametic and pleiotropic defects in mouse fetuses with Hertwig's macrocytic anemia. *Dev. Biol.* **110,** 331–337.

Shen, M. M., and Leder, P. (1992). Leukemia inhibitory factor is expressed by the preimplantation uterus and selectively blocks primitive ectoderm formation in vitro. *Proc. Natl. Acad. Sci. USA* **89,** 8240–8244.

Shull, M. M., Ormsby, I., Kier, A. B., Pawlowski, S., Diebold, R. J., Yin, M., Allen, R., Sidman, C., Proetzel, G., Calvin, D., *et al.* (1992). Targeted disruption of the mouse transforming growth factor-beta 1 gene results in multifocal inflammatory disease. *Nature* **359,** 693–699.

Silvers, W. K. (1979). "The Coat Colors of Mice: A Model for Mammalian Gene Action and Interaction." Springer-Verlag, New York.

Siracusa, G., DeFelici, M., and Salustri, A. (1985). The proliferative and meiotic history of mammalian female germ cells. *Biol. Fertil.* **1,** 253–297.

Smith, A. G., Heath, J. K., Donaldson, D. D., Wong, G. G., Moreau, J., Stahl, M., and Rogers, D. (1988). Inhibition of pluripotential embryonic stem cell differentiation by purified polypeptides. *Nature* **336,** 688–690.

Solter, D., and Knowles, B. B. (1978). Monoclonal antibody defining a stage-specific embryonic antigen (SSEA-1). *Proc. Natl. Acad. Sci. USA* **75,** 5565–5569.

Spiegelman, M., and Bennett, D. (1973). A light- and electron-microscopic study of primordial germ cells in the early mouse embryo. *J. Embryol. Exp. Morphol.* **30,** 97–118.

Steel, K. P., Davidson, D. R., and Jackson, I. J. (1992). TRP-2/DT, a new early melanoblast marker, shows that steel growth factor (c-kit ligand) is a survival factor. *Development* **115,** 1111–1119.

Stevens, L. C. (1967a). The biology of teratomas. *Adv. Morphog.* **6,** 1–31.

Stevens, L. C. (1967b). Origin of testicular teratomas from primordial germ cells in mice. *J. Natl. Cancer Inst.* **38,** 549–552.

Stevens, L. C. (1973). A new inbred subline of mice (129-terSv) with a high incidence of spontaneous congenital testicular teratomas. *J. Natl. Cancer Inst.* **50,** 235–242.

Stevens, L. C. (1983). The origin and development of testicular, ovarian, and embryo-derived teratomas. *In* "Teratocarcinoma Stem Cells" (L. M. Silver, G. R. Martin, and S. Strickland, eds.). Cold Spring Harbor Laboratory.

Stevens, L. C., and Pierce, G. B. (1975). Teratomas: Definitions and terminology. *In* "Teratomas and Differentiation" (M. Sherman and D. Solter, eds.), pp. 13–14. Academic Press, New York.

Stewart, C. L., Gadi, I., and Bhatt, H. (1994). Stem cells from primordial germ cells can reenter the germ line. *Dev. Biol.* **161,** 626–628.

Stewart, C. L., Kaspar, P., Brunet, L. J., Bhatt, H., Gadi, I., Kontgen, F., and Abbondanzo, S. (1992). Blastocyst implantation depends on maternal expression of leukemia inhibitory factor. *Nature* **359,** 76–79.

Stott, D., and Wylie, C. C. (1986). Invasive behaviour of mouse primordial germ cells in vitro. *J. Cell Sci.* **86,** 133–144.

Tam, P. P., and Snow, M. H. (1981). Proliferation and migration of primordial germ cells during compensatory growth in mouse embryos. *J. Embryol. Exp. Morphol.* **64,** 133–147.

Tan, J. C., Nocka, K., Ray, P., Traktman, P., and Besmer, P. (1990). The dominant W^{42} spotting phenotype results from a missense mutation in the *c-kit* receptor kinase. *Science* **247,** 209–212.

Tanaka, A., Miyamoto, K., Minamoto, N., Takeda, M., Sato, B., Matsuo, H., and Matsumoto, K. (1992). Cloning and characterization of an androgen-induced growth factor essential for the androgen-dependent growth of mouse mammary carcinoma cells. *Proc. Natl. Acad. Sci. USA* **89,** 8928–8923.

Toksoz, D., Zsebo, K. M., Smith, K. A., Hu, S., Brankow, D., Suggs, S. V., Martin, F. H., and Williams, D. A. (1992). Support of human hematopoiesis in long-term bone marrow cultures by murine stromal cells selectively expressing the membrane-bound and secreted forms of the human homolog of the steel gene product, stem cell factor. *Proc. Natl. Acad. Sci. USA* **89,** 7350–7354.

Ware, L. M., and Axelrad, A. A. (1972). Inherited resistance to N- and B-tropic murine leukemia viruses in vitro: Evidence that cogenic mouse strains SIM and SIM.R differ at the FV-1 locus. *Virology* **50,** 339–348.

Williams, D. E., and Lyman, S. D. (1991). Characterization of the gene-product of the Steel locus. *Prog. Growth Factor Res.* **3,** 235–242.

Williams, R. L., Hilton, D. J., Pease, S., Willson, T. A., Stewart, C. L., Gearing, D. P., Wagner, E. F., Metcalf, D., Nicola, N. A., and Gough, N. M. (1988). Myeloid leukaemia inhibitory factor maintains the developmental potential of embryonic stem cells. *Nature* **336,** 684–687.

Wylie, C. C., Stott, D., and Donovan, P. J. (1985). Primordial germ cell migration. *In* "Developmental Biology: A Comprehensive Synthesis," Vol. 2, pp. 433–448.

Zsebo, K. M., Williams, D. A., Geissler, E. N., Broudy, V. C., Martin, F. H., Atkins, H. L., Hsu, R. Y., Birkett, N. C., Okino, K. H., Murdock, D. C., *et al.* (1990). Stem cell factor is encoded at the *Sl* locus of the mouse and is the ligand for the *c-kit* tyrosine kinase receptor. *Cell* **63,** 213–224.

This Page Intentionally Left Blank

7

Mechanisms of Genomic Imprinting in Mammals

Joseph D. Gold
Roger A. Pedersen
Laboratory of Radiobiology and Environmental Health
University of California, San Francisco
San Francisco, California 94143

I. Introduction

Recent genetic and embryological studies indicate that normal prenatal development of mammalian embyos requires genetic contributions from both parents. In mice, "isoparental" embryos developing with only maternal or paternal genetic information die at midgestation stages, while in the human, they form ovarian dermoid cysts or hydatidiform moles, respectively. The evident specialization of maternal and paternal genomes in mammals has been defined as genomic imprinting and is thought to arise during gametogenesis. An increasing body of evidence further indicates that genomic imprinting is involved in several human diseases (reviewed by Hall, 1990). Genomic imprinting appears to act by controlling the transcription of a set of genes that are required for normal prenatal

Current Topics in Developmental Biology, Vol. 29

development and cell proliferation. Genes that have been identified as imprinted include the insulin-like growth factor-II gene (*Igf2*), the *Igf2*-mannose-6-phosphate receptor gene (*Igf2r*), *H19* (a gene of unknown function expressed abundantly in the placenta), and the small ribonucleoprotein N gene (*Snrpn*). Each of these is characterized by parental allele-specific gene expression. Because normal, fertilized individuals appear to be functionally hemizygous for these imprinted genes, the phenotypes of isoparental embryos presumably arise from their null or overexpression. Consequently, imprinting identifies a set of developmentally important genes that are particularly interesting from the perspective of both biological consequences and molecular mechanisms. This introduction addresses the experimental genetic and embryological evidence leading to the current understanding of the phenomenon of genomic imprinting and briefly considers the biological significance of imprinting and the unique aspects of its manifestation in mammals. The chapter will then focus on the identity of known imprinted genes and what is known about the molecular basis of their imprinted pattern of expression.

A. Genetic Evidence for Imprinting

The importance of genomic imprinting in mammalian development was first recognized by Lyon and Glenister (1977), who invoked differential expression of the maternal and paternal chromosomes as an explanation for the differential recovery of isoparental duplications and the corresponding deficiencies of specific chromosomes. The combined results of their and others' studies constitute "an imprinting map which has defined regions of autosomes in which one or more genes appear to be modified as they pass through the germ lines of one, or other, or both parents, with the result that the maternal and paternal copies become functionally different in the zygote" (Cattanach and Beechy, 1990). In these studies, Robertsonian translocations (i.e., metacentric chromosomes formed by two conjoined acrocentric chromosomes) were used to generate chromosomally balanced young that had either maternal or paternal duplications with the respective paternal or maternal deficiencies for specific mouse chromosomes (Cattanach and Beechey, 1990; Fig. 1). The studies identified three classes of imprinting effects. In the most severe class, embryos with the noncomplementing duplication died very early in development, as in the case of maternal duplication of proximal chromosome 2, maternal duplication of proximal chromosome 6, and paternal duplication of distal chromosome 7. A class with intermediate severity caused midfetal to early neonatal death, as in maternal duplication for distal chromosome 7 or proximal chromosome 7, and maternal deletion of proximal chromosome 17 (the *Tme* locus). The class of recognized imprinting effects with least

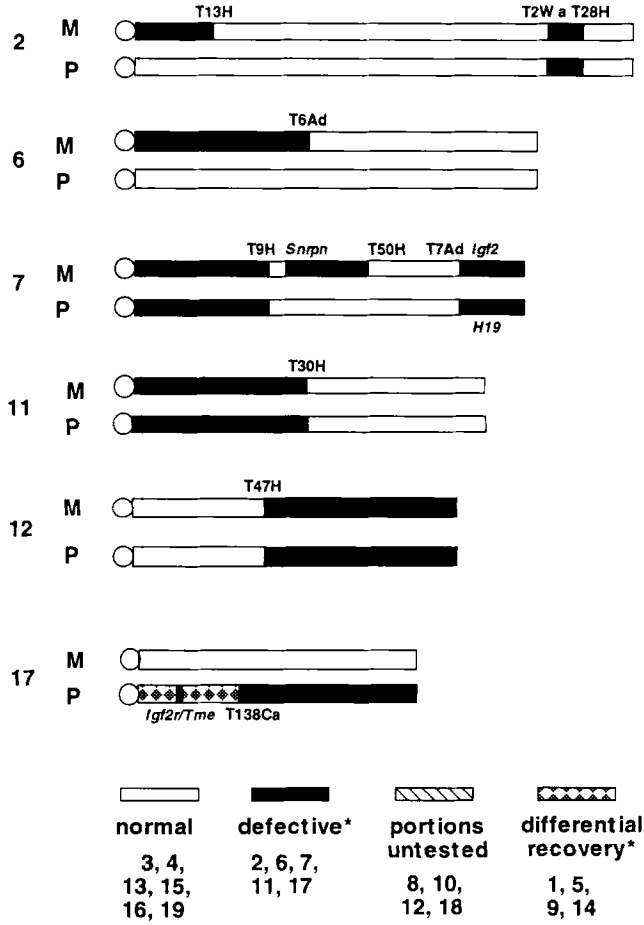

Fig. 1 Mouse imprinting map. Autosomes are diagramed to show regions characterized by defective complementation when both homologs (or segments) are inherited from the same parent. *Defective phenotypes refer to prenatal and neonatal deaths seen when these regions are maternally or paternally duplicated, with the corresponding paternal/maternal deficiency; differential recovery of live young also may occur for certain regions. Also shown are the designations of translocation stocks used to examine autosomal segments (T-) and the approximate location of known imprinted genes, noted as the repressed allele. (Adapted from Pedersen *et al.*, 1993; data from Beechey and Cattanach, 1993.)

severity caused phenotypic or behavioral abnormalities accompanying postnatal lethality/reduced viability, as in maternal or paternal duplication for distal chromosome 2 or proximal chromosome 11, maternal duplication of central chromosome 7, paternal duplication of proximal chromosome 7, or paternal duplication of distal chromosome 17 (Cattanach and Beechey, 1990; Cattanach *et al.*, 1992). It is not clear from the genetic studies whether the imprinting phenomenon is restricted to a few specific genes within these chromosomal regions or if imprinting affects most or all of the genes in each region. Minimally, one gene in each region could account for the imprinting effect (two in those cases where there are both maternal and paternal duplication/deficiency effects), leading to a minimal estimate of 9 to 13 imprinted genes, and a maximal estimate of perhaps 10% of the genome.

In addition to such genetic studies, analysis of the pattern of X chromosome inactivation in extraembryonic tissues of the mouse conceptus has provided additional evidence for genomic imprinting during gametogenesis. In the somatic tissues of female mammals, only one of the two X chromosomes is active, with random inactivation of either the maternal or the paternal homolog in any cell (Lyon, 1961, 1972; Cattanach *et al.*, 1990). Both X chromosomes of normal females are active in the oocyte (Epstein, 1972). In contrast, the X chromosome of spermatogenic cells appears to be expressed at a low level or not at all (Kramer and Erickson, 1981). Thus, X chromosome reactivation occurs during early stages of meiosis in the female, and this activity persists throughout oocyte growth until the time of meiotic maturation. The preimplantation embryo, like the egg, is characterized by activation of both X chromosomes. Cytogenetic observations suggest that X inactivation begins at the blastocyst stage (Takagi, 1974; Mukherjee, 1976). However, evidence from injection chimera experiments using single inner cell mass cells from genetically marked mouse blastocysts [3.5 to 4.5 days gestation (d.g.)] reveals that both X chromosomes are active in the inner cell mass at these donor stages (Gardner and Lyon, 1971). This implies that the cytogenetic results on blastocysts were derived only from the trophectoderm cells. In addition, biochemical evidence indicates that there are two active X chromosomes in the embryonic ectoderm until day 6 of gestation (Monk and Harper, 1978; Kratzer and Gartler, 1978a,b). However, not all inner cell mass derivatives remain active until this time. As evidence for X inactivation, Takagi and associates (1982) showed that by 5.3 d.g. there is an early or late-replicating X chromosome in the visceral endoderm, extraembryonic ectoderm, and ectoplacental cone. Thus, X chromosome inactivation appears to accompany cellular differentiation, occurring first in trophectoderm and its derivatives, then in primitive endoderm and its derivatives, and finally in the primitive ectoderm and its derivatives, including the

germ cells and extraembryonic mesoderm (Monk and Harper, 1979). Significantly, X inactivation in the other extraembryonic tissue lineages is nonrandom, the paternal X chromosome (XP) being preferentially inactivated, and the X^m remaining active in the visceral and parietal endoderm, the ectoplacental cone, and the extraembryonic ectoderm. In marsupials, the paternal X chromosome is preferentially inactivated in somatic tissues (Van de Berg *et al.*, 1983). These parent-specific inactivation phenomena, while affecting many genes on the X chromosome, may nonetheless be a relevant paradigm for imprinting of autosomal genes.

B. Embryological Evidence for Imprinting

Evidence for differential roles of maternal and paternal genomes was obtained in developmental studies of isoparental mouse embryos produced by experimental activation of oocytes (parthenogenesis) or by nuclear transfer at the zygote stage (gynogenesis and androgenesis) (reviewed in Solter, 1988; Surani, 1991). Parthenogenetic embryos (parthenogenones) arise from the diploidization of an oocyte, usually by suppression of second polar body formation, while diploid gynogenones and androgenones are generated from zygotes by nuclear transfer, removing the egg or sperm pronucleus and replacing it with the opposite parental pronucleus from another embryo.

1. Parthenogenesis and Gynogenesis

The maternal genome is incapable of independently supporting development of the mouse conceptus to term, and anecdotal observations of isolated females of many species lead to the conclusion that this is true for mammals in general (for review see Markert and Seidel, 1981; Surani, 1986; Pedersen *et al.*, 1993). Developmental failure of parthenogenetic mouse embryos does not generally occur at preimplantation stages. Rather, diploid parthenogenetic individuals commonly develop until postimplantation stages, with a few developing into small 25 somite embryos by day 10 of gestation (Graham, 1974; Kaufman *et al.*, 1977). Spontaneous parthenogenetic development of ovarian oocytes has also been observed in humans, where it results in disorganized structures, often including teeth, hair, and bone tissues, known as mature teratomas, or dermoid cysts (Stevens, 1984).

Using nuclear transfer in mouse embryos (McGrath and Solter, 1983), it has been posible to define the developmental potential of mouse pronuclei and determine the reasons for developmental arrest of parthenogenones. By transferring a normal pronuclear pair to parthenogenetic egg

cytoplasm and carrying out the reciprocal transfer, it was shown unequivocally that the failure of parthenogenones is determined by their nuclear rather than their cytoplasmic condition (Mann and Lovell-Badge, 1984). Furthermore, gynogenones containing two maternal pronuclei even from different strains of mice manifested a pattern of developmental arrest essentially indistinguishable from that of parthenogenones (McGrath and Solter, 1984; Surani *et al.*, 1984). These embryos never developed to term but arrested at early postimplantation stages, sometimes reaching day 10 as a retarded embryo with sparse extraembryonic tissues (Fig. 2). The consistent phenotype of parthenogenetic and gynogenetic mouse embryos led Surani and co-workers (1984) to hypothesize that paternal genes are uniquely necessary for the proper development of the extraembryonic lineages, particularly for trophoblast proliferation. Further studies of mouse parthenogenones have documented their phenotype in greater de-

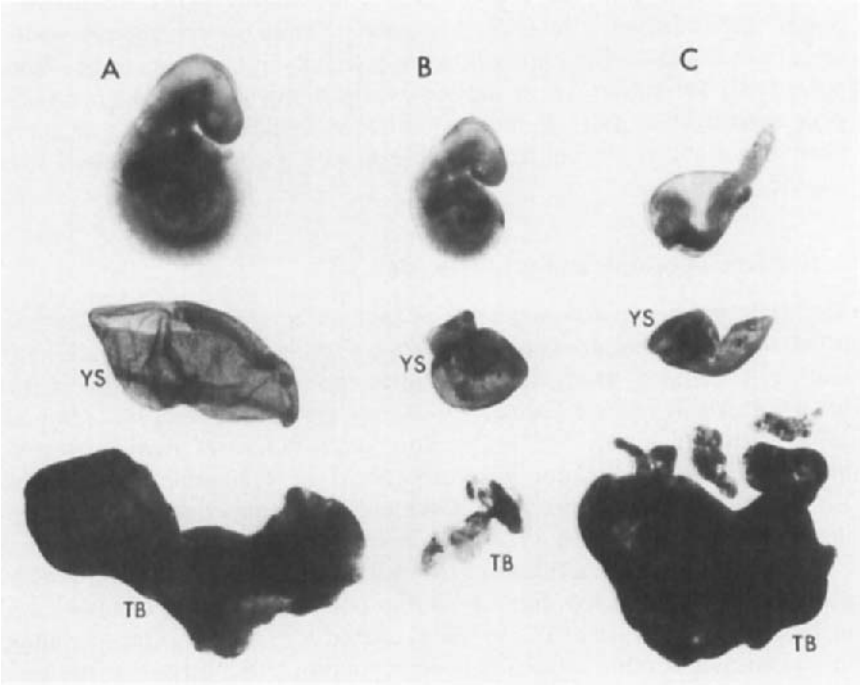

Fig. 2 Comparison of normal conceptus (A) with gynogenetic (B) and androgenetic (C) development. In each case, the conceptus has been dissected into embryo proper (top), yolk sac (YS), or trophoblast (TB) component. Note the reciprocal phenotypes of the gynogenetic conceptus with its vestigal trophoblast and the androgenetic conceptus with its retarded embryo proper. Bar: 1 mm. (From Surani *et al.*, 1986.)

tail and shown their fate in chimeras with normal, fertilized embryos. Parthenogenones that reach postimplantation stages have abnormal differentiation of their trophoblast and primitive endoderm lineages. Their ectoplacental cones consist primarily of trophoblast giant cells (Varmuza *et al.*, 1993; Sturm *et al.* , 1994; reviewed in Pedersen *et al.*, 1993). A similar phenomenon may account for the tendency of parthenogenetically derived ovarian tumors to contain trophoblast cells (Varmuza, 1992).

Studies of chimeras made by aggregating parthenogenetic and normal fertilized embryos, each bearing distinct genetic markers, revealed clear differences in the tissue distribution and fate of normal and parthenogenetic embryonic cells. Despite allocation of parthenogenetic cells to both the trophectoderm and inner cell mass at the blastocyst stage (3.5 d.g.), they were eliminated from the trophoblast lineage by 6.5 d.g. and from primitive endoderm by midgestation stages (9.5 to 11.5 d.g.); however, they persisted in most lineages in the embryo proper (Clarke *et al.*, 1988; Thomson and Solter, 1988, 1989). At later stages of fetal development and after birth, parthenogenetic cells did not contribute to skeletal muscle, and contributions to other tissues gradually declined, as if the parthenogenetic contribution was being selected against. An exception to this negative selection was noted in the germ line of fertile adult females, where the parthenogenetic component persisted throughout fertile life (Nagy *et al.*, 1989; Fundele *et al.*, 1990; Stevens *et al.*, 1977; Surani *et al.*, 1977). Those fetuses and postnatal individuals with extensive parthenogenetic contribution, however, were smaller and grew slower than normal offspring. Embryonic stem cells generated from diploid parthenogenetic blastocysts could also contribute extensively to the embryonic tissues of chimeras, and in contrast to chimeras made from parthenogenetic embryos, they contributed also to skeletal muscle (Evans *et al.*, 1985). Thus, embryonic stem cells provide an additional approach to analyzing genomic imprinting in mice, although their unique developmental history could alter the manifestation of the imprint.

2. Androgenesis

Diandric mouse embryos produced by nuclear transfer developed to early postimplantation stages when transferred to the uteri of foster mothers, but never reached term (McGrath and Solter, 1984; Surani *et al.*, 1984). The postimplantation diandric embryos analyzed on day 10 of gestation had extremely rudimentary embryonic development, but the extent of trophoblast development was near (or in excess of) normal, while yolk sac development was intermediate (Barton *et al.*, 1984; see Fig. 2). The pattern of developmental arrest in experimentally produced diploid diandric embryos is thus strikingly different from that of parthenogenetic and

digynic embryos, which have retarded extraembryonic growth (Barton *et al.*, 1985). The differential phenotypes between parthenogenones and androgenones led Surani and co-workers (1984) to hypothesize a complementary relationship between the two parental genetic contributions, with the maternal component playing a unique role in development of the embryo proper. Subsequent studies have described the phenotypes of late gestation and neonatal chimeras made by aggregating androgenotes with normal, fertilized embryos or injecting androgenetic inner cell mass cells into blastocysts (Barton *et all.*, 1991; Mann and Stewart, 1991). While most of these chimeras died at early postimplantation stages, those surviving into later gestation were larger than normal, stage-matched embryos, and those surviving to birth had pronounced skeletal abnormalities, including hypertrophied rib structures. Interestingly, when ES cells were derived from androgenetic blastocysts and used to generate chimeras, an apparently identical phenotype emerged; moreover, when androgenetic ES cells were injected into mice, they formed teratomas with abundant muscle tissue (Mann *et al.*, 1990). These results underscore the complementary phenotypes of pure parthenogenetic and androgenetic embryos and reaffirm the suggestion (Surani *et al.*, 1988) that the genes affected by imprinting affect embryonic growth and differentiation.

Another case of androgenesis is the development of hydatidiform moles in the human, the result of diploidization of spermatozoa (Jacobs *et al.*, 1980; for a review see Szulman and Surti, 1984). These embryos become androgenetic, due to failure of the maternal genome to participate in development, thus producing a 46 XX conceptus in which all of the chromosomes are from sperm. The trophoblastic hyperplasia and embryonic dysgenesis of moles is strongly reminiscent of the development of diandric mouse embryos. This observation is also consistent with Surani's hypothesis, showing that as a result of imprinting, the paternal genome preferentially supports development of the extraembryonic tissues and fails to support development of the fetus (Surani *et al.*, 1984). In summary, there is now substantial information on the isoparental phenotypes. The central remaining issue is the identity and biological consequence of the imprinted genes.

C. Biological Role of Genomic Imprinting

The evolutionary scope of genomic imprinting, which could provide a clue to its biological role, has not been extensively examined. Evidence for lack of viable parthenogenesis in eutherian mammals (Beatty, 1967) suggests that imprinting may be widespread. Because there is preferential paternal X chromosome inactivation in marsupials, they can also be re-

garded as manifesting imprinting (Cooper, 1993). On the other hand, birds may not have functionally similar imprinting phenomena because parthenogenesis results in viable adults in at least one species, the turkey (Olsen, 1960). Finally, there are examples of viable natural or experimentally induced parthenogenetic strains among reptiles, amphibia, and fish (Beatty, 1967). On the basis of such observations, it would appear that genomic imprinting phenomena such as those seen in mice exist in viviparous mammals, but not in other vertebrate classes.

How can the extent of genomic imprinting among vertebrates be informative about its biological role? Genomic imprinting could confer a generic benefit on animals by precluding parthenogenesis, thereby maintaining heterosis. However, if genomic imprinting had such a generic role, it should be seen generally among vertebrates, including oviparous classes. Alternatively, if genomic imprinting arose as an essential attribute of the eutherian placenta, an invasive organ with a highly developed endocrine function (Hall, 1990), it should be seen in eutherian mammals but not in marsupials. Although marsupials also possess a chorion which mediates exchange between mother and offspring, it is generally noninvasive and has no known endocrine function. In marsupials, greater emphasis is placed on lactation rather than intrauterine nutrition for early growth and development of young, so that the role of the eutherian placenta is in effect replaced by the pouch (Cooper, 1993). Such considerations lead to the expectation that imprinting would not occur in marsupials or would be shown to involve a different set of genes from those in eutherians, while genes imprinted in mice would show a widespread pattern of imprinting among eutherian mammals. Finally, the opposite imprinting of the mouse *Igf2* and *Igf-2r* genes led Haig and Graham (1991) to hypothesize that imprinting arose in mammals as a consequence of conflicting interests between the reproductive strategies of the father and mother. Paternal mutations leading to rapid intrauterine growth would increase the fitness of the father, whereas the mother would instead gain fitness from having larger numbers of (smaller) offspring. In particular, expression of the paternal allele of *Igf2* in the mammalian yolk sac and placenta would increase embryonic growth and confer selective advantage to offspring of a particular father in a polyandric species. This effect could be attenuated by the mother by lowered expression of growth-promoting genes and by high expression of gene products (possibly including *Igf2* receptor) that bind or inactivate growth factors. The expectations of the Haig hypothesis are that genomic imprinting should occur in viviparous taxa, including marsupials, but not in oviparous taxa, where paternal contribution to the genotype of the embryo cannot influence how much nutrition they receive, since yolk is deposited before fertilization.

Molecular evidence for the conservation of the identity of imprinted genes and chromosomal regions could resolve when genomic imprinting arose during evolution and its current extent. Imprinting of *H19* and *Igf2* genes is conserved between domestic and wild mouse species (Bartolomei *et al.*, 1991; A. Villar and R. A. Pedersen, unpublished observations). Also, evidence suggests that there is evolutionary conservation of the imprinting of *H19* and *IGF2* genes between mice and humans (Zhang and Tycko, 1992; Rachmilewitz *et al.*, 1992; Giannoukakis *et al.*, 1993; Ohlsson *et al.*, 1993). Moreover, the human *IGF2* gene is located on chromosome 11p, closely linked to *H19* in an area of synteny with mouse chromosome 7 (Zemel *et al.*, 1992).

Therefore it is important to determine whether these and other genes that are imprinted in mice show parental allele specific expression in other eutherian species and in other vertebrate classes, thereby establishing the extent of genomic imprinting. Further studies that identify and characterize remaining imprinted genes are urgently needed to expand the base of information about molecular mechanisms as well as to resolve the biological role of genomic imprinting. Insight into both the function of genomic imprinting and the mechanisms by which it is accomplished may be gained by examining genes whose expression patterns demonstrate this phenomenon. In the next section, the known examples of imprinted genes will be described in depth.

II. Identities of Imprinted Genes

A. Transgenes

The majority of transgenes which demonstrate imprinted effects do so at the level of differential methylation depending on the sex of the parent from which the transgene was inherited (Swain *et al.*, 1987; Sapienza *et al.*, 1987; Reik *et al.*, 1987, 1990; Hadchouel *et al.*, 1987; McGowan *et al.*, 1989; Sasaki *et al.*, 1991); less frequently the expression of the transgene also follows the imprinted pattern (Swain *et al.*, 1987; Thorey *et al.*, 1992; DeLoia and Solter, 1990; Allen *et al.*, 1990). With one exception (Sapienza *et al.*, 1987), all examined imprinted transgenes show a pattern of hypermethylation after maternal inheritance and hypomethylation after paternal inheritance. Within this broad framework are several noteworthy observations:

Many transgenes only show imprinted behavior on hybrid backgrounds; when introduced into inbred strains, differential effects are lost (Sapi-

enza *et al.*, 1987, 1989; McGowan *et al.*, 1989; Reik *et al.*, 1990; Allen *et al.*, 1990).

The transgene RSV-Ig-mycA, containing the Rous sarcoma virus long terminal repeat and a fusion between the murine Igα heavy chain and c-*myc* genes, shows a correlation between inherited methylation and expression patterns. In this case, expression is restricted to the myocardium (although the differential methylation pattern is seen in all tissues) and is detected only when the transgene is inherited paternally, in both hybrid and inbred backgrounds. This transgene is unique in that multiple lines of transgenic mice carrying Tg.RSVIgmycA in different integration sites demonstrate similar imprinted patterns of methylation and expression, implying that Tg.RSVIgmycA itself contains sequences specifying the imprint (Swain *et al.*, 1987; Chaillet *et al.*, 1991).

Two different transgenes showed methylation imprinting in the embryonic but not extraembryonic lineages (Reik *et al.*, 1987; McGowan *et al.*, 1990).

One line of mice carrying a transgene containing a large genomic fragment of the human keratin18 gene fused to the *lacZ* gene showed a complex pattern of expression in late-stage embryos. While the transgene was expressed equally in some tissues regardless of maternal or paternal inheritance, paternal inheritance resulted in expression in the retina, epicardium, and forebrain but not the liver, while maternal inheritance led to expression in the liver but not retina, epicardium, or forebrain. This pattern was also seen on an inbred background. In all cases, the body of the *lacZ* gene was highly methylated when maternally inherited and unmethylated when paternally inherited (Thorey *et al.*, 1992).

A male mouse was injected at the 1 cell stage with a construct containing a fragment of the hepatitis B virus. Both male and female offspring of this animal produced hepatitis B surface antigen. However, when female offspring carrying the transgene were bred with normal mice, the transgene became both irreversibly methylated and transcriptionally silent. Subsequent passage through the male germ line did not restore expression or cause demethylation of the transgene (Hadchouel *et al.*, 1987).

In one line, a transgene appears to have inserted within a bona fide imprinted gene (DeLoia and Solter, 1990) (see Section IV,C,2).

B. Endogenous Genes

Four genes have been well characterized as endogenous imprinted genes in the mouse: *Igf1l* (DeChiara *et al.*, 1991), *Igf1lr* (Barlow *et al.*, 1991),

H19 (Bartolomei *et al.*, 1991), and *Snrpn* (Leff *et al.*, 1992). *IGFII* and *H19* are also imprinted in humans (Ohlsson *et al.*, 1992; Giannoukakis *et al.*, 1992; Ogawa *et al.*, 1993); the status of *IGFIIr* and *SNRPN* in the human has not been reported. In each case the imprinted genes are adjacent to nonimprinted genes, implying a restricted form of regulation.

The *Xist* gene (Borsani *et al.*, 1991; Brown *et al.*, 1991) also displays a limited pattern of imprinted expression, and two genes of the rat MHC I locus appear to show some level of imprinting (Kanbour-Shakir *et al.*, 1990). In addition, there are several other phenomena in the mouse and human in which imprinting may play a role. These will be considered separately in the following sections.

1. *Igf2*

In the mouse, the *Igf2* gene is located in the distal portion of chromosome 7 (Lalley and Chirgwin, 1984), a region demonstrated to display parental imprinting effects (Searle and Beechey, 1990). The human homologue IGFII maps to 11p15 (Harper *et al.*, 1981; Brissenden *et al.*, 1984). IGFII is mitogenic for numerous cell lines and appears to exert its growth-promoting effects primarily through the IGFI receptor (Czech, 1989). In the rodent embryo, *Igf2* transcripts are detected in preimplantation embryos (Rappolee *et al.*, 1992), then in all trophectoderm derivatives, and in specific embryonic tissues including the kidney. Soon after birth, *Igf2* transcription ceases in all tissues except for the choroid plexus and leptomeninges (Lee *et al.*, 1990; Stylianopoulou *et al.*, 1988a,b).

The imprinted status of this gene was first recognized during the characterization of mice containing a targeted disruption of the *Igf2* gene. Mice heterozygous for the disrupted allele were viable and fertile but small (60% of normal size) when the mutant *Igf2* allele was inherited paternally; heterozygotes inheriting the disrupted allele maternally were phenotypically normal, suggesting that the paternally inherited *Igf2* allele is normally active while the maternal allele is silent (DeChiara *et al.*, 1991). A similar imprinted pattern of expression was also detected in humans (Ohlsson *et al.*, 1992; Giannoukakis *et al.*, 1992). Intriguingly, in the adult murine choroid plexus, expression of both parental alleles of the *Igf2* gene is observed (DeChiara *et al.*, 1991; Sasaki *et al.*, 1992). An examination of the developing mouse brain showed that biallelic expression of *Igf2* is detected as early as embryonic day 13.5, when the choroid plexus is forming (Villar and Pedersen, 1994), suggesting that the imprinting of *Igf2* does not occur in all tissues. Cells derived from androgenetic embryos express the gene at high levels, presumably due to the presence of two paternal alleles, while parthenogenetic embryos express very low levels

of *Igf2* at both preimplantation and fetal stages (Rappolee *et al.*, 1992; Sasaki *et al.*, 1992).

In the human, overproduction of IGF2 due either to loss of the imprinted phenotype (i.e., activation of the maternally derived allele) (Rainier *et al.*, 1993; Ogawa *et al.*, 1993) or uniparental (paternal) disomy of 11p15 (Schroeder *et al.*, 1987; Pal *et al.*, 1990) has been implicated in the development of Wilms' tumor (an embryonal tumor of the kidney) and in Beckwith–Wiedemann syndrome (Henry *et al.*, 1991) (characterized by a predisposition to multiple malignancies and overgrowth of organs).

2. *H19*

H19 was originally identified as a gene under the regulatory control of the same modulators controlling α-fetoprotein (AFP) gene expression in the fetal mouse liver (Pachnis *et al.*, 1984). Like AFP, *H19* is expressed in fetal and neonatal liver, fetal gut, and yolk sac visceral endoderm. Unlike AFP, *H19* is also expressed at high levels in fetal skeletal and cardiac muscle, and at lower levels in all adult muscle (Pachnis *et al.*, 1984). *H19* is expressed during murine embryonic stem cell differentiation *in vitro* and in extraembryonic tissues during implantation; in midgestation embryos *H19* transcripts are detected in many tissues in the midgestation embryo with the exception of blood cells and tissues derived from the neuroectoderm. Like *Igf2*, *H19* is expressed in the developing kidney, and this expression diminishes after birth (Poirier *et al.*, 1991). In the human placenta, H19 is expressed in cytotrophoblasts (Rachmilewitz *et al.*, 1992).

The function of *H19* is unclear. The 2.5-kb transcript does not appear to encode a protein since while both the murine and human genes contain multiple small open reading frames, none is conserved between the two genes. Although spliced, polyadenylated, and located in the cytoplasm, the *H19* transcript is not associated with polyribosomes; it is associated with a ribonuclear protein particle with a sedimentation coefficient of 28S. These observations have led to the suggestion that *H19* may function as a structural RNA (Brannan *et al.*, 1990). Overexpression of *H19* from a transgene led to embryonic lethality at late stages of prenatal development (Brunkow and Tilghman, 1991). Introduction of an *H19* expression construct into two embryonal tumor lines led to the abrogation of both soft agar growth and tumorigenicity in nude mice of the transfected cell lines; no effect was obtained when the construct was introduced into a cervical carcinoma cell line (Hao *et al.*, 1993). Thus, *H19* may function as a tumor-suppressor gene.

In the mouse, *H19* maps to distal chromosome 7 (Pachnis *et al.*, 1984), within 90 kb of the *Igf2* gene (Zemel *et al.*, 1992). This location within

the same imprinted region of chromosome 7 as *Igf2* led Bartolomei *et al.* (1991) to investigate the possibility that *H19* was also an imprinted gene. The surprising finding was that while *H19* is in fact imprinted, its pattern of expression is opposite to that of *Igf2:* the maternally inherited *H19* allele is transcriptionally active, while the paternally inherited allele is silent (Bartolomei *et al.*, 1991). As in the case of *Igf2*, expression of both maternal and paternal *H19* alleles is detected in the brains of embryonic (day 13.5) and newborn mice, presumably in the choroid plexus (Villar and Pedersen, 1994). The human H19 gene maps to 11p15, like the human IGFII gene, and H19 shows the same imprinted pattern of expression in the human (Zhang and Tycko, 1992; Rachmilewitz *et al.*, 1992). Similarly, reactivation of the normally silent (paternal) allele has been reported in some Wilms' tumor samples (Rainier *et al.*, 1993). Complete hydatidiform moles express H19 (Rachmilewitz *et al.*, 1992; Mutter *et al.*, 1993), even though these tissues are androgenetic in origin (i.e., containing only paternally derived chromosomes); either the normal imprint is lost during androgenetic development or imprinting of the H19 gene does not occur in the human placenta. Evidence for the latter suggestion is provided by Zhang and Tycko (1992), who described bialleleic expression of H19 in the human placenta but could not rule out contamination by maternal tissue.

3. *Igf2r*

A third endogenous imprinted gene was identified in a search for a candidate for the T-associated maternal effect (*Tme*) locus, the only known maternal effect mutation in the mouse. Deletions of *Tme* on chromosome 17 (T^{hp} or tl^{lub2}) are lethal when inherited maternally but result in viable, short-tailed offspring when the same deletion is inherited paternally (Johnson, 1974; Winking and Silver, 1984). Analysis of genes mapping to the deleted region demonstrated that one gene, *Igf2r*, was expressed only from the maternally inherited allele (Barlow *et al.*, 1991). Like *Igf2* and *H19*, *Igf2r* appears to be nonimprinted in the embryonic and neonate brain (Villar and Pedersen, 1994).

The IGFIIr protein, which lacks a kinase domain, is identical to the cation-independent mannose-6-phosphate receptor, which transports lysosomal enzymes to their destination by binding their mannose-6-phosphate moieties (Morgan *et al.*, 1987). In the human, mouse, and rat, this protein also binds IGFII, unlike the chicken and *Xenopus* proteins (Clairmont and Czech, 1989). It has been suggested that the IGFIIr protein in mammals serves as a "sink" for IGFII protein, targeting excess growth factor for degradation (Oka *et al.*, 1985; Haig and Graham, 1991). However, there is also evidence that the IGFIIr is coupled to a G protein and that

IgfII can stimulate both DNA synthesis and an increase in cytoplasmic calcium concentration through this receptor (reviewed in Nishimoto, 1993).

There is some controversy over whether the *Igf1Ir* gene is identical to the gene whose maternal allele deletion causes the conditional lethality of T^{hp} and tl^{hp2} (Forejt and Gregorova, 1992; Filson *et al.*, 1993) (see Section IV,C,1).

4. *Snrpn*

The *Snrpn* gene encodes the small nuclear ribonucleoprotein particle-associated peptide SmN (McAllister *et al.*, 1988, 1989). Small nuclear ribonucleoprotein particles (snRNPs) are found in spliceosomes and are involved in mRNA processing (reviewed in Guthrie, 1991; Luhrmann *et al.*, 1990). The expression of *Snrpn* is highest in brain, suggesting it might play a role in the splicing of brain-specific transcripts (Li *et al.*, 1989).

The mouse gene maps to the central region of chromosome 7, which is syntenic with the map location of the human gene at 15q11–q13 (Leff *et al.*, 1992). This region is of great interest to clinical geneticists because the human diseases Prader–Willi syndrome (PWS) and Angelman syndrome (AS) are associated with chromosomal abnormalities within these regions. These syndromes with markedly different symptomologies are both linked to deletions or uniparental disomy of 15q11–q13. However, the source of the chromosomal region is critical. PWS patients may have deletions of the paternal 15q11–q13 region or may have inherited two copies of chromosome 15 from the mother with loss of the paternal chromosome 15. In contrast, AS patients show the reciprocal pattern of chromosome deletion/duplication (reviewed in Nicholls *et al.*, 1992; Nicholls, 1993). These observations suggest the existence of two oppositely imprinted genes within this region; a paternally expressed gene whose loss results in PWS and a maternally expressed gene whose loss results in AS. (The similarity of this pairing of oppositely imprinted genes with the region containing IGFII and H19 may indicate something fundamental about the establishment and maintenance of the imprint as discussed next).

Examination of the expression of the murine *Snrpn* gene revealed that only the paternal copy was transcribed and that the human gene mapped to the smallest deletions associated with PWS (Leff *et al.*, 1992; Ozcelik *et al.*, 1993). The observed imprinting pattern, coupled with the tissue specificity of SnN expression and the profound behavioral effects (including mental retardation, hyperphagia, and learning disabilities) associated with PWS, make *Snrpn* a strong candidate for the PWS gene. In contrast,

the presumptively maternally expressed gene responsible for AS has not yet been identified.

5. *Xist*

Another well-characterized gene that displays parent-of-origin specificity (at least in some tissues) is *Xist* (Borsani *et al.*, 1991; Brown *et al.*, 1991). Both the murine and human homologues of this gene map to the X inactivation center on the X chromosome; oddly, the human and murine *Xist* genes are oriented in opposite directions in an otherwise syntenic region (Brockdorff *et al.*, 1992). *Xist* encodes a large (15 kb) transcript which is expressed only from the *inactive* X chromosome in mice and humans (Borsani *et al.*, 1991; Brown *et al.*, 1991). Like H19, *Xist* does not appear to encode a protein since it lacks a significant open reading frame and is not associated with polysomes. Unlike H19, both polyadenylated and nonpolyadenylated forms of *Xist* have been detected, and the *Xist* transcript is restricted to the nucleus (Brown *et al.*, 1991; Borsani *et al.*, 1991; Brockdorff *et al.*, 1991).

The onset of expression of *Xist* coincides with the inactivation of the single X chromosome in males during meiosis and ceases during the transient reactivation of the inactive X chromosome in females during germ cell development (Richler *et al.*, 1992; Salido *et al.*, 1992, McCarrey and Dilworth, 1992). Its expression at the onset of X chromosome inactivation and its continued expression from the inactive X chromosome have led to the proposal that expression of the *Xist* gene is required for both the establishment and the maintenance of X chromosome inactivation in placental mammals; no *Xist* homologue has yet been detected in marsupials, which also undergo X inactivation (Goldman, 1992).

During the early stages of embryonic development, X chromosome inactivation occurs first in the trophectoderm and primitive endoderm of the early mouse blastocyst; X inactivation in the embryonic lineages occurs approximately 1 day later, at the time of implantation (reviewed in Grant and Chapman, 1988). In the rodent the paternally inherited X chromosome is specifically inactivated in the extraembryonic lineages while the embryo proper and the adult show random X inactivation (Lyon, 1972; Takagi, 1974); in humans, while X inactivation in embryonic and adult tissues appears to be random, there is some conflicting evidence as to whether there is preferential inactivation of the paternal X chromosome in extraembryonic tissues (Harrison, 1989; Mohandas *et al.*, 1989). In the mouse, *Xist* expression is first detected at the 8 cell stage (Kay *et al.*, 1993). Only the paternally inherited *Xist* allele is expressed prior to the time of implantation, at which point random X inactivation occurs in the

embryo and the expression of both alleles is detected (Kay *et al.*, 1993). At least in the extraembryonic tissues of the rodent, *Xist* displays the characteristics of an imprinted gene.

6. MHC Class I Alleles

In the rat, the major histocompatibility complex (MHC) on chromosome 20 contains at least seven genes and spans 0.4 cM. This complex contains genes encoding the classical transplantation antigens and is defined by the *RT1.A* locus at one extreme and by the *RT1.E* locus at the other (reviewed in Cortese-Hasset *et al.*, 1991). The same cluster is located on mouse chromosome 17, which has been shown to contain imprinted regions (Winking and Silver, 1984; Lyon and Glenister, 1977; Cattanach and Beechey, 1990). In the rat placenta, immunohistochemical studies using monoclonal antibodies to class I antigens revealed that only the paternally inherited alleles of the adjacent genes *RT1.A* and *Pa* are expressed in the basal trophoblast (Kanbour-Shakir *et al.*, 1990). These two genes are homologous to the murine *H-2K* and *H-2D* genes and the human HLA-B and HLA-A genes; the imprinted status of these genes in species other than the rat is unknown. Similar studies showed expression of both the maternal and paternal alleles of the *RT1.E* locus, demonstrating the limited size of the putative imprinted region (Kanbour-Shakir *et al.*, 1993). Further work will be required to distinguish between transcriptional and post-transcriptional regulation of expression of these genes. This is the first report of two closely linked genes with identical rather than opposite patterns of imprinted expression.

7. Other Phenomena

In the mouse, the dominant *Fused* (*Fu*) gene is located on chromosome 17 (Reed, 1937; Cattanach, 1986). Penetrance of the fused phenotype is diminished when *Fu* is maternally inherited (Reed, 1937; Belyaev *et al.*, 1981; Ruvinsky *et al.*, 1988; Ruvinsky and Agulnik, 1990). Another example of parent-of-origin effects is provided by the DDK strain of mice. When DDK females are crossed with males from other strains, early embryonic lethality is observed. No such effect is seen in the reciprocal cross (Wakasugi *et al.*, 1967). Nuclear transplantation and cytoplasmic injection experiments demonstrated that the lethality is due to an interaction between DDK cytoplasm and non-DDK nuclei (Babinet *et al.*, 1990), although the mechanism of this effect is still unclear.

In humans, there are indications of possible imprinting effects in several diseases. Huntington's diseases (HD) is due to an autosomal dominant

mutation, leading to neurodegeneration. Paternal inheritance of the mutated gene is linked to a form of the disease characterized by an earlier onset and more severe symptoms (Ridley *et al.*, 1992). However, there is emerging evidence that the process by which the normal gene is converted to the mutated form (the expansion in length of a highly polymorphic CAG repeat in the 5′ region of the gene) occurs only during transmission of the allele through the male germ line (Goldberg *et al.*, 1993; Myers *et al.*, 1993). Since there is a correlation between the length of the repeat and the age of onset of HD (Duyao *et al.*, 1993; Snell *et al.*, 1993; Andrew *et al.*, 1993), a defective paternal HD gene containing a clinically relevant but small CAG repeat may be converted during passage through the male germ line into an HD gene containing a longer CAG repeat, causing an earlier onset of the disease in the offspring of the affected father. Therefore, the parent-of-origin effects seen in HD may be a consequence of differences in the stability of repeated sequences during male and female gametogenesis rather than a somatically stable epigenetic change which distinguishes the maternal and paternal alleles.

Myotonic dystrophy is also due to an autosomal dominant mutation, an expansion of a CTG repeat in the myotonin protein kinase gene. Maternal inheritance of the mutation leads to the rare congenital form of the disease, while paternal inheritance leads to a less severe adult onset form (Howeler *et al.*, 1989); however, expansion of the repeat can occur upon inheritance from either parent (Barcelo *et al.*, 1993), suggesting that other imprinting-like phenomena occur.

In the case of chronic myelogenous leukemia, an abnormality termed the Philadelphia chromosome forms as a result of a reciprocal translocation between chromosomes 9 and 22, leading to fusions between the BCR gene (on chromosome 9) and the ABL gene (on chromosome 22) (reviewed in Daley and Ben-Neriah, 1991; Campbell and Arlinghaus, 1991). One study demonstrated that the paternal chromosome 9 and the maternal chromosome 22 are involved in the translocations in every case in which the parental origins could be determined (Haas *et al.*, 1992), suggesting that BCR and ABL might be imprinted in opposite ways. However, in the mouse, BCR maps to chromosome 10, which does not display any obvious imprinting effects (Beechey and Cattanach, 1993). While the murine *abl* gene does map to a region of chromosome 2 that leads to embryonic death in the case of maternal disomy, homologous recombination experiments have shown that loss of the *abl* gene is not responsible for this lethality (Tybulewicz *et al.*, 1991; Schwartzberg *et al.*, 1991). It is possible that these two genes are imprinted in humans but not mice or that *abl* and *bcr* are in fact imprinted but that the effects of altering the expression of either of these two genes singly through uniparental disomy are subtle.

III. Mechanisms of Imprinting

A. DNA Methylation: An Overview

The nature of the imprint requires that it be an epigenetic event stable enough to persist throughout the lifetime of the organism in most somatic cells, yet be labile enough to be altered in germ cells and in some transformed cells. DNA methylation is considered a likely candidate since methylation patterns are heritable and static under most circumstances but are dynamic during specific developmental processes. A brief review of the process of DNA methylation in mammals follows; the topic has been extensively reviewed (Bestor and Coxon, 1983; Doerfler, 1992; Bird, 1992; Hergersberg, 1991).

1. 5-Methylcytosine in Eukaryotic Cells

The modified nucleotide 5-methylcytosine (5-mC) is found in higher eukaryotic DNA at frequencies ranging from 1 to 2% in *Neurospora crassa* to over 25% in some plant species. Vertebrates contain roughly 4–7% 5-mC, with 60–90% of 5′-CpG-3′ dinucleotides bearing this modification. In mammals, DNA methylation is accomplished by the action of the enzyme DNA (cytosine-5)-methyltransferase (methylase), a 190-kDa protein with homology to bacterial cytosine-specific methylases (Bestor *et al.*, 1988). *In vitro*, the mammalian enzyme has 50-fold higher activity on the sequence 5′-CpG-3′ than CpA or CpT (Hubrich-Kuhner *et al.*, 1989) and shows a strong preference for the hemimethylated DNA that would arise after semiconservative replication (Gruenbaum *et al.*, 1982; Bestor and Ingram, 1983). This latter property ensures the faithful transmittal of the methylated CpG dinucleotide in daughter cells. The importance of DNA methylation in the mouse is underscored by the observation that targeted mutation of the methylase resulted in the death of embryos homozygous for the mutation by midgestation, although embryonic stem cells which were homozygous for the mutation were viable (Li *et al.*, 1992). The strong preference of the enzyme for hemimethylated sites has led to the suggestion that a separate enzyme may be responsible for the *de novo* methylation observed under certain conditions (see the following discussion). Although no additional enzyme has been identified, the persistence of low levels of methylation in mice homozygous for the disrupted methylase gene is consistent with this possibility.

While CpG in bacteria is found at frequencies close to those predicted by random base composition, most eukaryotic genomes show an approximately 80% decrease in the occurrence of CpG (Kricker *et al.*, 1992). This

is presumably due to the unstable nature of 5-mC; oxidative deamination of this modified base leads to the formation of thymidine (C to T transitions are the most frequent mutations in human DNA; Fig. 3) (Coulondre *et al.*, 1978; Bird and Taggart, 1980). Nonetheless, the genomes of higher eukaryotes possess distinct regions which contain CpG at a frequency much higher than that found in the rest of the genome (Bird, 1986). These "CpG islands" are frequently found in association with the promoters and RNA leader sequences of housekeeping genes, although some tissue-specific gene promoters contain such regions. It is thought that CpG islands are maintained because they are only rarely methylated in most, if not all, cells of the animal (Cooper *et al.*, 1983) (see the following discussion). The ability of these CpG islands to escape methylation may be due to their frequent association with constituitively active promoters; the binding of transcription factors may block the access of the methylase to the DNA. In keeping with this hypothesis are observations that the CpG islands of pseudogenes first become methylated and then are depleted of CpG sites, implying a link between transcription of the sequence and lack of CpG island methylation (Bird *et al.*, 1987; Quigley *et al.*, 1989). An alternative hypothesis is that true CpG islands, unlike scattered CpG dinucleotides in the body of eukaryotic genes, are inherently resistant to methylation. Carotti *et al.* (1989) and Bestor *et al.* (1992) have used partially purified mammalian methylase to compare the rate of methylation *in vitro* of known CpG islands and eukaryotic non-island CpG sequences with the rate of methylation of random bacterial sequences with higher G + C content. Their results suggest that true CpG islands are methylated at significantly lower rates *in vitro*. Analysis of the sequence context of the island CpG dinucleotides showed that the CpGs in known islands were significantly more likely to be flanked on both sides by C or G than by A or T, even taking into account the higher occurrence of G and C bases in the islands

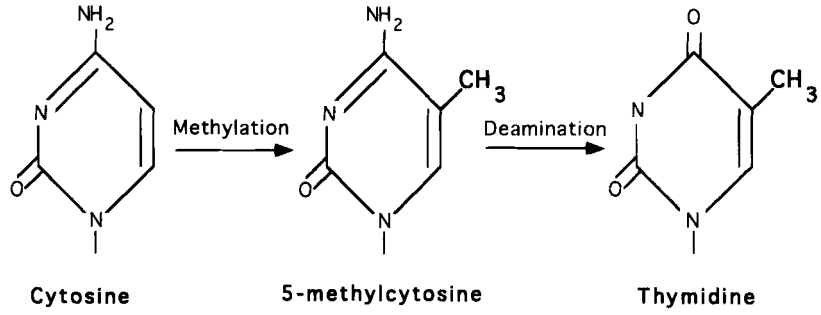

Fig. 3 Methylation of cytosine forms 5-methylcytosine; oxidative deamination of the modified base results in the formation of thymidine, leading to a C to T transistion mutation.

(Bestor *et al.*, 1992). There is also evidence for an active demethylation of inappropriately methylated CpG island sequences in early embryos and embryonic cell lines (Kolsto *et al.*, 1986; Frank *et al.*, 1991) (see the next section).

2. Role of Methylation in Eukaryotes

In general, highly methylated sequences are not transcriptionally active. It has been suggested that methylation functions to prevent the nonspecific interaction of DNA with transcription factors and other essential regulatory DNA-binding proteins; this would have become an acute problem as the size of the genome increased (Bird, 1986). Consistent with this idea, there is a rough correlation between genome size and extent of methylation (Hergersberg, 1991). The nonspecific interaction could be prevented either by the inability of the regulatory/transcription factors to bind methylated DNA or by the action of proteins which specifically bind methylated sequences and block the interactions with other regulatory/transcription factors (see the following discussion).

Although there is an inverse relationship between DNA methylation and transcription, it is not clear whether methylation is the cause or the consequence of transcriptional repression. Methylation *in vitro* of many genes leads to a loss of activity upon transfection into cultured cells; in some cases, repression seems to depend on the density of CpG sites near the promoter (Murray and Grosveld, 1987; Boyes and Bird, 1991), in others, methylation of individual sites is sufficient for repression (Klages *et al.*, 1992). The addition of the methylation inhibitor 5-azacytidine to cultured cells can cause the activation of genes which are normally repressed in these cell lines (Gounari *et al.*, 1987; Sneller and Gunter, 1987; Jones *et al.*, 1990). It should be noted, however, that CpG islands which are unmethylated in all tissues are frequently methylated in permanent cell lines (Antequera *et al.*, 1990); since the genes associated with some of these CpG islands show tissue-specific expression, some other mechanism must be responsible for their repression *in vivo*.

There is evidence that at least some of the postulated repression by methylation is indirect. A viral thymidine kinase gene which had been methylated *in vitro* was show to be transcribed for at least 8 hr in mouse L cells prior to being silenced, suggesting the need for interaction with a cellular component (Buschhausen *et al.*, 1987). Two proteins which preferentially bind methylated DNA, MeCP-1 and MeCP-2, have been identified (Meehan *et al.*, 1989; Boyes and Bird, 1991; Lewis *et al.*, 1992). MeCP-1 binds strongly to regions of DNA which contain at least 12 symmetrically methylated CpG doublets and inhibits transcription of methyl-

ated constructs *in vitro* and apparently *in vivo* (Boyes and Bird, 1991). The more abundant MeCP-2 binds strongly to single methylated CpG doublets and can repress transcription from both methylated and unmethylated templates *in vitro* (Lewis *et al.*, 1992; Meehan *et al.*, 1992).

In contrast, several studies have demonstrated that inactivation can *precede* methylation of specific genes (Gausctsch and Wilson, 1983; Niwa *et al.*, 1983; Lock *et al.*, 1987; Enver *et al.*, 1988). This is most notable in the process of X inactivation in placental mammals. In the embryo proper, inactivation and repression of X-linked genes precedes methylation of the inactive X chromosome by several days; in the extraembryonic lineages, the inactive paternal X does not become as highly methylated as the inactive X in embryonic lineages (Lock *et al.*, 1987). In marsupials, X inactivation and repression of transcription are not accompanied by increased methylation (Kaslow and Migeon, 1987).

An interesting possibility is that DNA methylation may serve as a type of "cellular immune response" (Bestor, 1990; Doerfler, 1992), inactivating viral genomes or transposons that might otherwise perturb normal growth. Studies on individual M-MuLV proviruses in early mouse embryos have demonstrated that viruses are rendered noninfectious and become heavily methylated in preimplantation embryos and embryonal carcinoma cells (Jahner and Jaenisch, 1984, 1985). Drosophila, which lacks detectable 5-mC, has a high frequency of mutations caused by transposon-like elements whereas transposition-induced mutations are rare in mammals. Perhaps DNA methylation serves to inactivate transposable elements in mammals. This function may be a special example of a mechanism which exists to prevent DNA duplications, which would appear as a result of an active transposing element. In the fungus *Neurospora crassa* a process called RIP (repeat-induced point mutation) drives the sequence divergence of repeated elements and duplicated sequences through a series of transition mutations reminiscent of those thought to be caused by the deamination of 5-mC to thymidine (Selker, 1990). Besides the potential for creating new genes by this process, RIP would also prevent gross chromosomal rearrangements due to homologous recombination by decreasing the amount of homology between two elements. The possibility of a RIP-like process functioning in mammals was raised by Kricker *et al.* (1992), whose analysis of numerous eukaryotic genes, repeat sequences, gene families, and pseudogenes reveals a striking bias toward sequence divergence coupled with CpG depletion between blocks of duplicated sequences above a threshold length. Thus, DNA methylation may also play a role in the stabilization of the mammalian genome.

Finally, the possibility that specific methylation patterns may result in the imprinting of both transgenes and endogenous genes must be considered. In order to evaluate this mechanism, the timeline of methylation in

the embryo and the presence of specific methylation differences between maternally and paternally inherited genes will be examined.

B. DNA Methylation Activity Is Regulated during Development

It has generally been assumed that differential marking of maternal and paternal alleles must occur when the two alleles are physically separate; accordingly, modification is usually postulated to occur during postmeiotic germ cell development. However, it has been pointed out that the process could occur after fertilization, prior to pronuclear fusion, when the sperm and egg genomes are still separate (McGowan *et al.*, 1990). A comparison of the extent of methylation of gene families (Howlett and Reik, 1991) and individual genes (Shemer *et al.*, 1991; Kafri *et al.*, 1992) in both gametes and early embryos showed that dynamic changes in methylation occur during germ cell development and embryogenesis, with important implications for the possible role of methylation in imprinting.

The methylation status of individual CpG dinucleotides is commonly assayed by (1) Southern analysis of genomic DNAs which have been digested with isoschizomers of restriction enzymes which are either sensitive or insensitive to the presence of 5-mC in their recognition sites; and (2) similar digestions of genomic DNA followed by PCR with gene-specific primers flanking the restriction sites. Less commonly, genomic footprinting is used, in which normal or modified Maxam-Gilbert sequencing reactions are performed which show the presence or absence of 5-mC. The first two methods only detect 5-mC when it is present in known restriction sites; the third allows the evaluation of all potential sites of 5-mC.

Studies of specific genes have revealed important differences between the methylation patterns of CpG island sequences and non-island CpG doublets. In general, while non-island sequences show variable patterns of methylation in different tissues at different times, CpG islands remain unmethylated (Bird *et al.*, 1985; Bird, 1986; Gardiner-Garden and Frommer, 1987). An important exception to this rule in the mouse is found in the inactive X chromosome of both embryonic and adult tissues, where the CpG islands of repressed genes are heavily methylated (reviewed in Grant and Chapman, 1988; Singer-Sam *et al.*, 1990).

While not all methylated sites in all genes behave identically, genes in sperm show more methylation than in eggs (Howlett and Reik, 1991; Kafri *et al.*, 1992); both types of gametes show lower levels of methylation than do somatic tissues (Gama-Sosa *et al.*, 1983). The early embryo shows lower levels of methylation than do either mature sperm or eggs, with indications of active demethylation during the first several cell divisions.

A new wave of methylation occurs at about the time of implantation and increases at the time of gastrulation in embryonic lineages such that the patterns of methylation found in adult somatic tissues are established at about 6.5 days of gestation (Monk *et al.*, 1987; Monk, 1988). The extraembryonic lineages do not appear to undergo this wave of methylation (Sanford *et al.*, 1985; Monk *et al.*, 1987).

The establishment of the methylation patterns of mature gametes is a gradual process. Both male and female fetal germ cells are unmethylated at embryonic day 12.5–13.5 and new methylation is not detected until day 15.5 (Howlett and Reik, 1991; Kafri *et al.*, 1992). It has been suggested that the ability of the fetal germ cells to avoid the wave of methylation which occurs at the late blastula/early gastrula stage is related to the migration of the fetal germ cell precursors from the epiblast into the yolk sac, where they remain before entering the fetal gonad at day 11–12 (Kafri *et al.*, 1992). A combination of further methylations and new demethylations at specific sites occurs in both the male and female germ line, until the final gametic patterns are achieved postmeiotically during sperm and oocyte maturation. It should be noted that different sites within the same gene can be methylated in sperm alone or in both sperm and oocytes; i.e., differential parental methylation appears to occur at the level of individual sites and not necessarily entire genes (Kafri *et al.*, 1992).

One way in which the overall methylation of the early embryo might decrease is through a passive process. In this case, the hemimethylated sites arising from DNA replication might not become fully methylated, leading to a gradual loss of 5-mC. At least for the L1 repeat family, DNA replication appears to be required for demethylation to proceed between the 8 and 16 cell stages (Howlett and Reik, 1991). This decrease in methylation does not appear to be due to low levels of DNA methyltransferase, as oocytes and preimplantation embryos contain very high levels of the enzyme (Carlson *et al.*, 1992).

On the other hand, there is evidence for an active mechanism of demethylation in the early embryo. When copies of the hamster APRT gene were methylated *in vitro* and injected into fertilized mouse oocytes, analysis of the transgenic mice showed that the CpG island sequences in all cases were specifically demethylated while other non-island CpG dinucleotides remained methylated. New methylation also occurred at sites which had not been methylated *in vitro*. Similar results were obtained when the methylated construct was transfected into three different EC cell lines for 48 hr, but demethylation was not observed when mouse L cells were used. Fusion between L cells carrying a methylated APRT gene and EC cells led to demethylation of the APRT gene's CpG island, implying that demethylation is dominant in these hybrids. No such effect was seen when fibroblast cells were substituted for the EC cells (Frank *et al.*, 1991).

Similar demethylation was seen when the CpG island was unlinked from the rest of the promoter, implying that transcription is not a prerequisite for the demethylation (Razin *et al.*, 1990). Furthermore, *in vitro*-methylated bacterial sequences were also demethylated in EC cells but not in L cells, indicating that the mechanism responsible for recognizing and demethylating CpG islands may be activated by high CpG densities alone, distinct from the recognition requirements of the methyltransferase (Razin *et al.*, 1990) (see section IV,A,2).

Examination of the degree of methylation found in gametes indicates that the maternal and paternal chromosomes show potentially important differences in methylation prior to fertilization. Although demethylation occurs in the early embryo such that the majority (perhaps all) of the parental methylation differences are lost by the blastocyst stage, there is some evidence that even after pronuclear fusion, the maternal and paternal chromosomes are treated differently by the embryo. While sites in specific genes that are found to be methylated in both the oocyte and sperm are demethylated by the 16 cell stage, sites which are methylated in sperm but not oocytes are demethylated more rapidly, by the 8 cell stage (Kafri *et al.*, 1992). As detailed in the APRT gene studies, the early embryo also shows the ability to distinguish between different types of CpG dinucleotides in applying or removing methyl groups. Furthermore, as shown by the studies of methylation in fetal germ cells, the methylation pattern is erased and then restored during gametogenesis, a time when the imprinting of endogenous genes is thought to be erased and then reset (Howlett and Reik, 1991; Kafri *et al.*, 1992). Methylation therefore has the potential to function as a signal of great significance in genomic imprinting.

C. Methylation Status of Imprinted Genes

1. Methylation of Transgenes

In order to consider methylation as a possible mechanism responsible for establishing or maintaining the imprint, it may be useful to distinguish between endogenous genes and transgenes. Although much work has been done on the latter topic, it is by no means certain that the mechanisms involved in producing gamete of origin effects on artificial DNA constructs are also responsible for the imprinted status of endogenous genes. The observation that 10–20% of transgenes may show imprinting effects contrasted with the low number of known imprinted endogenous genes may indicate that fundamentally different processes are at work. Moreover, there is a vast preponderance of maternally affected transgenes whereas there are approximately equal numbers of maternally and paternally transcribed, imprinted endogenous genes.

In principle, transgenes may be subject to imprinting as a result of several different factors:

Transgenes may contain portions of endogenous genes that are imprinted and demonstrate the same imprinted pattern as the endogenous gene. Bartolomei *et al.* (1993) constructed a transgene derived from the *H19* gene containing 4 kb of 5′ flanking DNA, a truncated coding region (to avoid the lethality associated with *H19* overexpression), and 8 kb of 3′ flanking sequences. Maternal-specific expression was observed for at least two out of six lines carrying the transgene (Bartolomei *et al.*, 1993). Similarly, a transgene containing the *Igf1I* promoter and 3′ flanking sequences showed paternal-specific expression in one out of six lines of transgenic mice (Lee *et al.*, 1993)(but see Section IV,C,2).

Transgenes may integrate into genes or chromosomal domains that are normally imprinted. The clearest example of transgene imprinting due to insertion sites is the work of DeLoia and Solter (1990), who identified the mutation Acrodysplasia (*ADP*) in a line of mice containing the integrated transgene pdBPV-MMTneo; other mice containing the same actively expressed transgene in distinct insertion sites did not display this phenotype. The *ADP* line is characterized by deformity of the paws, affecting the small bones. Offspring inheriting the transgene maternally were phenotypically normal; those inheriting the transgene paternally expressed variable degrees of the deformity. No expression of the transgene was detected in limb tissues at the stage of development in which small bone formation first manifested abnormalities, suggesting that *ADP* is due to the insertional inactivation of an imprinted gene rather than a stage-specific effect of transgene expression. (It should be noted that penetrance of the mutation was less than 100% in the latter class of mice, suggesting that the maternal allele of the *ADP* locus might not be completely inactive.) Expression of the transgene in the adult was restricted to those mice displaying the *ADP* mutation, implying that the transgene was also subject to imprinting due to the site of integration.

Only one example has been reported of a transgene that demonstrates imprinting effects regardless of the site of integration (Chaillet *et al.*, 1991). This could be taken as evidence that most imprinted transgenes have integrated into imprinted chromosomal regions. Indeed, the transgene MPA434, which shows parent-of-origin differences in methylation (Sasaki *et al.*, 1989), has been mapped to a known imprinted region of chromosome 11; surprisingly, the intact transgene integration site in this case does not itself demonstrate similar differences in methylation (Sasaki *et al.*, 1991). However, the insertion sites of other imprinted transgenes are in regions of chromosomes which do not seem to be imprinted (Hadchouel *et al.*, 1987; Reik *et al.*, 1990), although it is possible that subtle imprinted effects were not detected in these experiments.

Finally, transgenes may contain sequences which are fortuitously recognized as imprinting signals by the cellular machinery. It has been noted (Sasaki *et al.*, 1991) that all transgenes which demonstrate imprinted characteristics contain prokaryotic sequences, either in the gene itself (e.g., *lacZ, CAT*) or in noncoding portions of the vector (e.g., pBR322) which integrate along with the transgene. Because prokaryotic sequences have not been subjected to the same selection pressures as eukaryotic genes, bacterial DNA differs in both epigenetic modifications and base composition. For example, many bacteria contain restriction modification systems which are designed to degrade foreign but not host cell DNA. Protection of the host is accomplished by the presence of 5-mC in specific sequence combinations; another modified base, N^6-methyldeoxyadenosine, is also used to distinguish between host and foreign DNA. Furthermore, the frequency of the dinucleotide CpG is distinct between prokaryotes and most eukaryotes (Section IV,A,1). The juxtaposition of DNA having either atypical methylation patterns or unusual base composition with a eukaryotic promoter may mark the transgene for unusual regulation or modification that might approximate the behavior of endogenous imprinted genes.

The complexities of transgene methylation are illustrated by the observations that several different transgenes only show imprinting effects on hybrid backgrounds (Sapienza *et al.*, 1987, 1989; McGowan et al., 1989; Reik *et al.*, 1990; Allen *et al.*, 1990). When crossed into inbred strains, these transgenes lose the parent-of-origin methylation effects and become either hyper- or hypomethylated, depending on the strain of mouse used. These transgenes show increased levels of methylation when crossed into BALB/c backgrounds and decreased levels when crossed into DBA or C57BL/6 backgrounds (McGowan *et al.*, 1989; Allen *et al.*, 1990; Reik *et al.*, 1990); a strain-specific modifier (*Ssm-1*) of transgene methylation has been mapped to chromosome 4 (Engler *et al.*, 1991). In at least one case, the ability of the BALB/c background to increase the methylation of a hypomethylated transgene appeared dependent on the sex of the nontransgenic BALB/c parent (Allen *et al.*, 1990). However, further investigation suggested a complex interaction between the strain derivation of the oocyte cytoplasm and the BALB/c genome, which could be derived from either parent (Surani *et al.*, 1990), reminiscent of the interactions of DDK oocytes with foreign sperm (see Section III,B,7).

A possible example of strain-specific imprinting of an endogenous sequence (the maternal-effect lethal *Tme* locus) was detailed by Forejt and Gregorova (1992), who were able to obtain viable offspring of T^{hp} mothers by mating the T^{hp} females with males of three different inbred *Mus m. musculus* strains. The authors postulated the existence of an imprintor gene (*Imp-1*) responsible for the inactivation of the paternal T^{hp} allele, which was inactive when derived from *M. m. musculus*. Interestingly,

Igf1lr was still imprinted in these offspring, which led to the suggestion that although *Igf1lr* is imprinted similarly to T^{me} and maps to the same region of chromosome 17, *Igf1lr* and T^{me} are not identical (Forejt and Gregorova *et al.*, 1992). However, other workers have demonstrated that viable offspring of T^{hp} mothers can also be obtained by crossing the females with males homozygous for a disrupted *Igf1l* gene (Filson *et al.*, 1993). This result, coupled with the lack of success in obtaining transgenic mice which overexpress *Igf1l* (Allen and Reik, 1992), suggests another possibility—namely, that *Igf1lr* is equivalent to T^{me} and that the maternal lethality of T^{me} is due to toxicity of excess *Igf1l* since *Igf1lr* is thought to be involved in the degradation of *Igf1l* (Oka *et al.*, 1985; Haig and Graham, 1991). The ability of the *M. m. musculus* males to rescue the offspring of T^{hp} mothers might be due to either lower levels of expression of the *M. m. musculus Igf1l* gene or lower activity of the *M. m. musculus* IGFII protein with the maternal signaling receptor (Allen and Reik, 1992). *Imp-1* then would equivalent to the *M. m. musculus Igf1l* gene.

Since the behavior of many imprinted transgenes differs from that of most endogenous imprinted genes, the most illuminating examples may be those which behave most like the known genes.

As mentioned previously, the transgene TG.A is only expressed in the myocardium of the offspring of transgenic fathers; imprinting is seen on an inbred background (FVB/N) and the imprinted expression is independent of the insertion site (Swain *et al.*, 1987; Chaillet *et al.*, 1991). TG.A contains the Rous sarcoma virus long terminal repeat and a fusion between the murine Igα heavy chain and c-*myc* genes, as well as pBR322 sequences. The maternally inherited transgene is fully methylated in all adult somatic tissues, while the paternally inherited transgene is only partially methylated.

Analysis of the transgene methylation in day 13.5 fetal germ cells of both sexes showed that the transgene became completely unmethylated. The establishment of adult methylation patterns differed between male and female gametes. By embryonic day 17.5, prior to meiosis, new methylation was detected in male germ cells, although the pattern was distinct from that seen in adult somatic tissues. Further methylation was found in mature sperm; again, this pattern was distinct from the adult pattern. After fertilization, the pattern in mature sperm was lost, as the transgene became fully unmethylated in both the ICM and trophoblast of the day 3.5 blastocyst. The adult pattern was established by day 6.5 in both embryonic and extraembryonic tissues. Thus, for the paternally transmitted gene, changes in methylation mirrored those seen for endogenous, nonimprinted genes, with erasure of methylation in early fetal germ cells, gradual changes in methylation during spermatogenesis, and demethylation in the early embryo followed by reestablishment of adult patterns at the time of

gastrulation. In female germ cells the transgene remained unmethylated until maturation, at which point the transgene assumed its adult pattern. Unexpectedly, the maternally inherited transgene did not undergo demethylation in the early embryo; the adult pattern was present from the earliest stage (Chaillet *et al.*, 1991).

The methylation of a transgene containing the mouse metallothionein-I (*Mt-I*) promoter driving the human transthyretin (TTR) gene, with flanking pUC18 sequences, was also examined during gametogenesis (Sasaki *et al.*, 1991; Ueda *et al.*, 1992). Because expression of the transgene occurred at very low levels it was not possible to detect parent-of-origin differences in expression. As in the case of TG.A, the maternally inherited gene is highly methylated in both the promoter and body of the transgene in all adult somatic tissues; unlike TG.A, the promoter of the paternally inherited transgene is completely unmethylated in the adult. Notably, the maternally inherited *Mt-I*/TTR is also methylated on the CpG island in the transgenic metallothionein-I promoter; the same CpG island in the endogenous metallothionein-I promoter remains unmethylated at all times (Ueda *et al.*, 1992).

The *Mt-I*/TTR transgene promoter was unmethylated in day 14.5 germ cells of both sexes. Methylation of the transgene promoter in female germ cells was only detected in the mature egg, and this pattern corresponded to the adult pattern, in accordance with the findings for TG.A. In male germ cells no methylation of the *Mt-I*/TTR transgene promoter was detected, and this lack of methylation persisted at least up to the blastocyst stage. The methylation state of the maternally inherited transgene in the early embryo was not reported (Ueda *et al.*, 1992).

The major difference between methylation profiles of the two transgenes is the degree of methylation detected in sperm, although this may be related to the fact that adult methylation patterns of the two transgenes are different. Because no specific analysis of CpG islands in the TG.A transgene was performed, it is not known if the maternally inherited allele also showed unusual methylation. It would also be of great interest to determine whether the maternally inherited *Mt-I*/TTR transgene escapes the global demethylation seen in the early embryo. The observations of unusual CpG island methylation and escape from demethylation of the maternally inherited transgenes may be circumstantial evidence that the imprinted patterns detected are a result of silencing the maternal alleles rather than specific activation of the paternal alleles.

2. Methylation Status of Endogenous Imprinted Genes

The methylation patterns of three endogenous imprinted genes have been examined at length: *Igf2* (Sasaki *et al.*, 1992; Brandeis *et al.*, 1993), *Igf2r*

(Stoger *et al.*, 1993; Brandeis *et al.*, 1993), and *H19* (Ferguson-Smith *et al.*, 1993; Zhang *et al.*, 1993; Bartlomei *et al.*, 1993; Brandeis *et al.*, 1993). In each case, there are parent-specific methylation differences, but the nature of those differences varies considerably.

The methylation of *Igf2* was compared in normal embryos and in MatDi7 embryos, which have a paternal deficiency and a maternal duplication for the distal portion of chromosome 7, including the *Igf2* gene. Both the paternally inherited, active allele and the maternally inherited, repressed allele were unmethylated in both the promoter and coding region of the gene. DNase I hypersensitivity studies demonstrated that both alleles were in an indistinguishable open chromatin configuration, and, consistent with this finding, closer examination of the MatDi7 embryos revealed that the two maternal alleles were transcribed at low levels (3–7% of controls). Similar results were obtained with parthenogenetic embryos, which contain only maternally derived DNA (Sasaki *et al.*, 1992). Further investigation showed that a region 3–4 kb upstream of the *Igf2* promoter was found to be more methylated on the paternal chromosome (Sasaki *et al.*, 1992; Brandeis *et al.*, 1993) (Fig. 4).Contrary to expectations, this upstream methylation was detected in both sperm and mature oocytes, thus placing in doubt the role of this region in establishing the imprint. However, while methylation of most of the HpaII sites in this region was lost by the 16–32 cell morula stage, one site remained fully methylated at this stage and during subsequent development (Brandeis *et al.*, 1993). This observation implies either *de novo* methylation of this site on the paternal allele after genome-wide demethylation or paternal allele-specific protection of this HpaII site from the normal wave of demethylation during early embryonic development. Examination of the status of this site at earlier embryonic stages will be required to resolve this question. In this case, the only parent-specific methylation correlates with expression rather than repression of the imprinted gene, but there is no evidence yet that alteration of the methylation status of this region affects *Igf2* expression.

In both mice and humans, the promoter of the paternal, unexpressed *H19* allele is methylated while the promoter of the maternal, expressed allele is undermethylated in adult and mid- to late gestation embryonic tissues (Ferguson-Smith *et al.*, 1993; Zhang *et al.*, 1993; Bartlomei *et al.*, 1993; Brandeis *et al.*, 1993) (Fig. 5). Significantly, a CpG island in the *H19* promoter is methylated on the paternal allele. While some paternal-specific methylated sites are also detected in mature sperm, the CpG island methylation is not, indicating that it is established after fertilization (Ferguson-Smith *et al.*, 1993; Bartlomei *et al.*, 1993; Brandeis *et al.*, 1993). Furthermore, all paternal-specific methylation detected in sperm is erased by the morula stage (Brandeis *et al.*, 1993) and must thus be reestablished

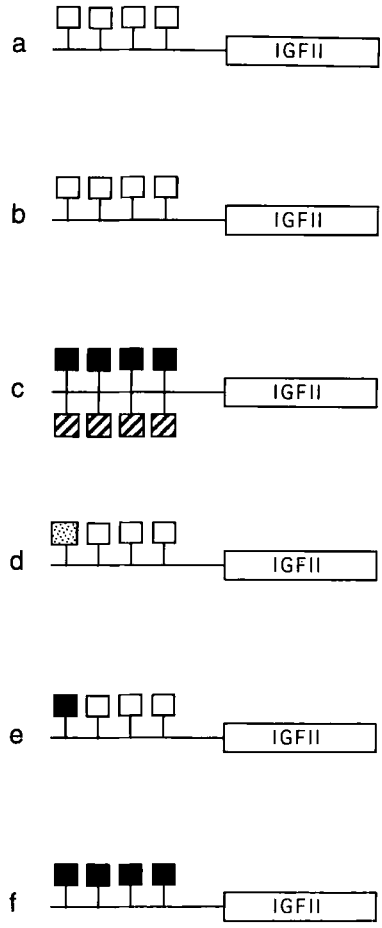

Fig. 4 Changes in methylation of the region 3–4 kb upstream from the *Igf1l* promoter in 13.5-day p.c. primordial germ cells (a), 21.5-day p.c. oogonia and sperm (b), mature sperm and oocytes (c), morulae (d), blastulae (e), and the adult (f). Open boxes, unmethylated sites; stippled box, methylated site, parent-of-origin unknown; solid boxes, methylated sites derived from the paternal allele; hatched box, methylated site derived from the maternal allele. (Adapted from Brandeis *et al.*, 1993.)

prior to day 9 of gestation (Ferguson-Smith *et al.*, 1993). In later embryonic and adult tissues the promoter of the paternal allele is maintained in a closed configuration, while the maternal promoter displays an open chromatin configuration in both expressing and nonexpressing tissues (Ferguson-Smith *et al.*, 1993; Bartlomei *et al.*, 1993). The correlation between imprinted expression and maternal-specific hypomethylation is consistent: a study of the human H19 gene showed that in every case,

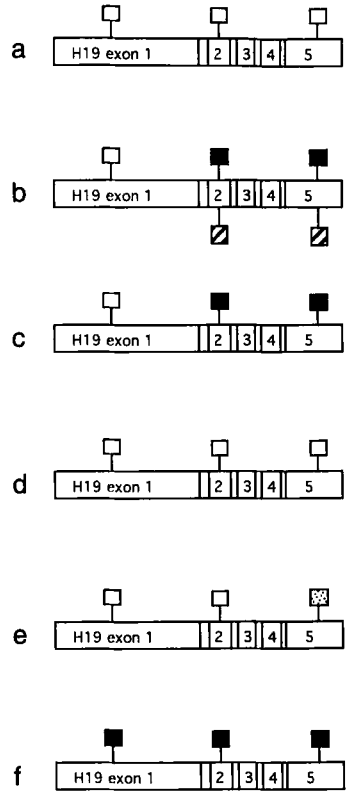

Fig. 5 Changes in methylation of selected sites within the *H19* gene in 13.5-day p.c. primordial germ cells (a), 21.5-day p.c. oogonia and sperm (b), mature sperm (the methylation pattern in mature oocytes has not been reported) (c), morulae (d), blastulae (e), and the adult (f). Open boxes, unmethylated sites; stippled boxes, methylated site, parent-of-origin unknown; hatched boxes, methylated sites derived from the maternal allele; solid boxes, methylated sites derived from the paternal allele. (Adapted from Brandeis *et al.*, 1993.)

the active maternal allele was undermethylated while the inactive paternal allele was methylated. In one individual, the paternal allele was methylated and inactive in all tissues except for the lung, where both alleles were unmethylated and expressed, and in the cerebellum, where the maternal allele was silent and the paternal allele was expressed. In the cerebellum, the paternal allele became unmethylated while the maternal allele was methylated (Zhang *et al.*, 1993).

Because the *H19* gene is both physically linked to *IgfII* and imprinted in the opposite manner, it has been suggested that there is a common regulatory mechanism for the two genes, perhaps involving competition for limiting transcription factors (Bartolomei and Tilghman, 1992; Zemel

et al., 1992; Bartolomei *et al.*, 1993). Two enhancer elements located approximately 5 kb downstream of the *H19* polyadenylation site are required for high level tissue-specific expression of *H19* (Yoo-Warren *et al.*, 1988). While there is no direct evidence that these enhancers also regulate *Igf2* transcription, the two genes show very similar patterns of expression in both the embryo and neonate (Lee *et al.*, 1990; Poirer *et al.*, 1991). No methylation differences between the maternal and paternal enhancers were detected, although the enhancers displayed hypersensitivity to cleavage by EcoRI only in *H19*-expressing tissues (Bartolomei *et al.*, 1993).

The enhancer competition model (Bartolomei *et al.*, 1993) (Fig. 6) suggests that on the paternal chromosome the methylated *H19* gene promoter is unable to interact with the 3′ enhancer element and so remains silent; by default, the *Igf2* promoter is then stimulated by the enhancer. On the maternal chromosome, the unmethylated *H19* promoter is proposed to have a higher affinity for the enhancer-binding factors than does the *Igf2* promoter, resulting in expression of *H19* and repression of *Igf2*. The same authors note that in the choroid plexus and leptomeninges, *H19* is expressed at lower levels than *Igf2*, and suggest that the loss of *Igf2* imprinting seen in these tissues is due to diminished competition of the *H19* promoter for limiting enhancer-binding factors, perhaps due to higher levels of the limited factor in these tissues. This model proposes a relatively passive model for *Igf2* imprinting, and would suggest that while an *H19* transgene containing the *H19* promoter and 3′ enhancer would still demonstrate maternal-specific expression, an *Ifg2* transgene which included

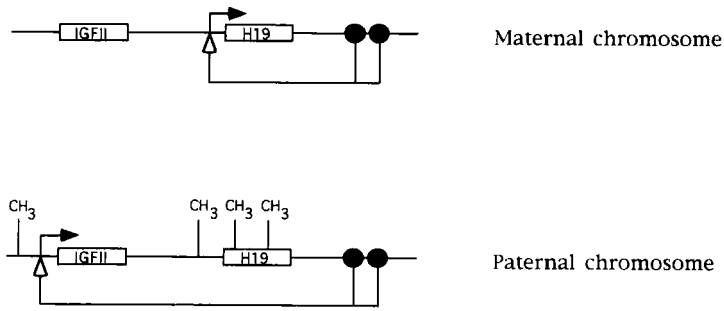

Fig. 6 The enhancer competition model (Bartolomei and Tilghman, 1992). The maternally inherited copies of the linked *Igf2* and *H19* genes are unmethylated, and the two enhancers (solid circles) downstream from the *H19* gene stimulate transcription from the *H19* gene promoter. On the paternally inherited chromosome, methylation of the *H19* gene makes the *H19* promoter unresponsive to the effects of the enhancers, while specific methylation upstream from the paternally inherited *Igf2* gene results in the *Igf2* promoter becoming responsive to the enhancers. (Adapted from Bartolomei *et al.*, 1993.)

the *H19* enhancer but lacked the *H19* promoter would not demonstrate imprinting effects. Transgenes containing the *H19* promoter and enhancers can in fact demonstrate maternal-specific expression (Bartolomei *et al.*, 1993). On the other hand, one of six transgenic mouse lines containing a *lacZ* gene driven by the *IgfII* promoter and 3′ region (*not* including the *H19* promoter or enhancers) showed paternal-specific expression (Lee *et al.*, 1993). However, the high background of other transgenes showing a similar pattern of paternal-specific expression makes it difficult to ascribe the imprinted expression of this transgene to regulatory sequences within the normal IgfII gene. Additionally, Mutter *et al.* (1993) detected transcription of both H19 and IGFII in the same cells in tissue derived from a hydatidiform mole, suggesting that the regulation of the two genes may be more complex than the simplest version of the enhancer competition model would allow.

Two regions of differential methylation were seen in the *IgfIIr* gene, both corresponding to distinct CpG islands (Fig. 7). One island (region 1) near the start site of transcription was found to be methylated on the repressed paternal allele. This methylation was undetectable in sperm and was incomplete at midgestation, only acquiring the final adult pattern at early postnatal stages. The authors propose that the paternal-specific methylation of region 1 is the consequence rather than the cause of repression since the paternal allele is known to be silent by embryonic day 15, before the establishment of this paternal-specific methylation (Stoger *et al.*, 1993). The other CpG island (region 2) is in an unusual location, in an intron 27 kb downstream from the start site. Region 2 is methylated on the expressed maternal allele. A subset of region 2 sites was methylated in oocytes and at all embryonic stages, including the morula and blastocyst, and thus could serve as the imprinting signal (Stoger *et al.*, 1993; Brandeis *et al.*, 1993). At least two region 2 sites are not methylated in oocytes but become methylated prior to the morula stage (Brandeis *et al.*, 1993). Thus, establishment of the normal somatic pattern of region 2 methylation involves both the protection from demethylation of certain sites and the early, specific *de novo* methylation of others.

D. Evidence for the Involvement of Methylation in Imprinting

The best evidence for the role of DNA methylation in some facet of genomic imprinting is that the normal patterns of expression of *IgfII*, *H19*, and *IgfIIr* are altered in mice homozygous for mutation in DNA methyltransferase (Li *et al.*, 1993). Mice homozygous for the disrupted methyltransferase allele MTase^n contain approximately 30% of the normal levels of 5-mC. (The remaining amount of 5-mC may result either from

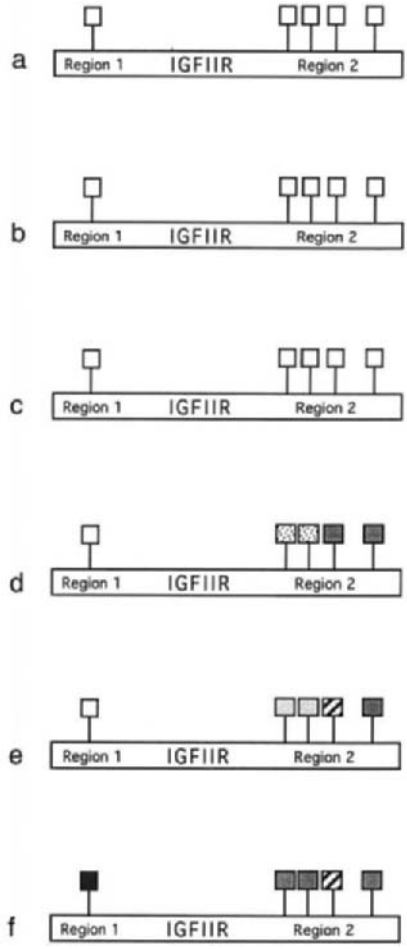

Fig. 7 Changes in methylation of selected sites within regions 1 and 2 of the *IgfIIr* gene in 13.5-day p.c. primordial germ cells (a), 21.5-day p.c. oogonia and sperm (b), mature sperm and oocytes (c), morulae (d), blastulae (e), and the adult (f). The box in region 1 represents multiple sites. Open boxes, unmethylated sites; stippled boxes, methylated sites, parent-of-origin unknown; solid box, methylated site derived from the paternal allele; hatched boxes, methylated sites derived from the maternal allele. (Adapted from Brandeis *et al.*, 1993.)

the activity of an uncharacterized second methylase or the retention of low levels of activity of the mutated allele.) These mutant mice exhibit decreased methylation of the *H19* gene. While normal mice express only the maternal copy of *H19* and the paternal copy of *Igf1l*, MTase^n/MTase^n mice express both the maternal and paternal copies of *H19* at embryonic day 10.5 while *Igf1l* expression is almost undetectable. This result is consistent with the enhancer competition model (Bartolomei *et al.*, 1993) since a demethylated *H19* promoter is predicted to outcompete the *Igf1l* promoter for limited transcription factors.

In contrast, expression of the *Igf1lr* gene was unaffected in MTase^n/MTase^n mice. Interestingly, the decrease in methylation of region 2 in the *Igf1lr* gene in the mutant mice was less pronounced than the decrease seen in the *H19* gene. The authors, speculating that the *Igf1lr* imprint was quantitatively more resistant to diminished DNA methylation than the *H19* and *Igf1l* imprints, examined *Igf1lr* imprinting in mice with a more extensive loss of DNA methylation. Homozygotes for the disrupted methyltransferase allele MTase^s suffer more severe effects upon development than do homozygotes for MTase^n, suggesting that MTase^s may be a complete loss of function mutation. In both MTase^n/MTase^s compound heterozygotes and MTase^s/MTase^s homozygotes, the *Igf1lr* gene was repressed, and in MTase^n/MTase^s compound heterozygotes, region 2 methylation was more significantly decreased than in MTase^n/MTase^n mice. This result is consistent with the proposal of Stoger *et al.* (1993) that the maternal-specific methylation of region 2 in normal mice prevents the binding of a transcriptional repressor.

Less direct evidence for the involvement of methylation in imprinting results from the effects of treating cell lines with agents affecting methylation or chromatin structure. As mentioned previously, MatDi7 embryos contain two copies of the maternally derived *Igf1l* gene; both copies are largely unmethylated and transcribed at low levels (Sasaki et al., 1992). Nonetheless, treatment of cell lines derived from MatDi7 embryos with agents that perturb methylation (5-aza-2′-deoxycytidine) or chromatin configuration (5-bromo-2′-deoxyuridine) led to an increase in the expression of *Igf1l*, although overall levels of *Igf1l* expression were still much lower than in cell lines derived from normal embryos. No increased expression of *Igf1l* was seen in normal embryonic cell lines treated with the same agents (Eversole-Cire *et al.*, 1993). The results in MatDi7 cell lines conflict with those obtained from MTase^n homozygotes, where diminished methylation silenced the *Igf1l* gene. It is known that cell lines undergo methylation events which are not seen in normal tissues (Antequara *et al.*, 1990), and 5-aza-2′-deoxycytidine appears to have effects upon cells which are unrelated to its effects upon methylation (Jones, 1985; Li *et al.*, 1992); either of these factors may explain the discrepancy.

A comparison of some features of the best-characterized imprinted transgenes and endogenous genes is shown in Table I.

Although complete information is not available for every gene, the majority of the imprinted genes (with the exception of *Igf1l*) are characterized by parent-specific methylation of CpG islands. (*Igf1l* may not conform to this pattern because its imprinting may be "passive," due to its proximity to *H19* and its enhancers.) Most of these genes also maintain their methylation patterns during early embryogenesis, at a time when the methylation of other genes is erased. How might these characteristics be relevant to imprinting?

Repression of the inactive allele through promoter CpG island methylation is consistent with the effect of *in vitro* methylation on transfected gene expression. Inhibition of gene expression is thought to result from the inability of transcription factors to bind to methylated recognition sequences. In contrast, the maternal-specific methylation of the *Igf1lr* gene, which correlates with transcriptional activity, might be due to the inability of a repressor to bind to this methylated sequence; the placement of this CpG island might indicate a role in regulation of transcription distinct from those CpG islands typically found near the mRNA start site. As described earlier (Section IV,A,1), the protein MeCP-1 binds specifically to regions of DNA which contain at least 12 fully methylated CpG dinucleotides and is able to repress transcription of constructs containing such regions (Boyes and Bird, 1991). MeCP-1 is a good candidate for a protein involved in the repression of genes imprinted by methylation of CpG islands located near promoters. Alternatively, MeCP-1 could block the binding of a repressor to the downstream CpG island in the *Igf1lr* gene, thus sustaining transcription.

In somatic tissues of postgastrulation embryos, neonates, and adults, the methylation imprint should be stable by virtue of the properties of

Table I Distribution of Methylation in Imprinted Transgenes and Endogenous Genes

Gene	Parent-specific methylation	Parent-specific expression	CpG island methylation	Methylation in early embryo
TG.A	M	P	?	Yes
MT-1/TTR	M	?	Yes	?
Igf1l	P	P	No	Yes
H19	P	M	Yes	No
Igf1lr	M,P[a]	M	Yes	Yes

[a] The paternal-specific methylation of the *Igf1lr* gene is established late in development.

DNA methylase (see Section IV,A,1). In order to reach these stages, the parent-specific methylation must evade not only the global loss of methylation in early embryogenesis, but also the demonstrated ability of the early embryo to demethylate CpG islands specifically. The way in which the imprinted genes escape these processes is not known. Access of the proposed demethylating enzymes to the imprinted genes might be blocked by factors bound to the CpG islands of imprinted genes; alternatively, the imprinted chromosomal regions might be physically compartmentalized in such a way as to prevent access. The intriguing observation has been made that the regions of the paternal chromosomes containing *Igf2, H19, Igf2r,* and *Snrpn* all replicate earlier in the cell cycle than do the same regions on the maternal chromosomes in both mice and humans, in contrast to the near synchronous replication of both alleles of most nonimprinted genes (Kitsberg *et al.*, 1993). The imprinted genes appear to be embedded within discrete chromosomal regions which replicate at early times; these regions also include some closely mapping nonimprinted genes (Barlow *et al.*, 1991; Villar and Pedersen, 1994; Rinchik *et al.*, 1993; Nicholls *et al.*, 1993). The significance of this observation is unclear, but it implies that imprinting may involve large-scale alterations in chromosomes.

Are these unique methylation patterns the primary imprint or a consequence of imprinting? While the correlation between methylation and imprinting is impressive, and inactivation of DNA methyltransferase has profound effects upon the expression of *Igf2, H19,* and *Igf2r* (Li *et al.*, 1993), it should be noted that (1) the maternal allele-specific methylation of the *H19* gene is lost during early embryogenesis and reestablished later, implying that the maternal allele is marked at least transiently by some mechanism other than methylation; and (2) early fetal germ cells appear to be completely unmethylated and therefore lack the parent-specific methylation seen at later stages, implying that something other than pre-existing methylation patterns is recognized by the DNA methylase. It has been demonstrated that the testis contains a DNA methylase mRNA of variant size (Trasler *et al.*, 1992); perhaps there is a testis-specific form of the enzyme with different sequence recognition properties.

The establishment of the specific methylation and the imprint itself should ultimately be dictated by the primary sequence of the DNA, which might contain regions that are inherently more subject to methylation than other regions with similar CpG contents (see Section IV,A,1). The retention of appreciable levels of methylation in region 2 of *Igf2r* in $MTase^n/MTase^n$ homozygote mice (Li *et al.*, 1993) may indicate that this region has either an especially high affinity for DNA methyltransferase or an intrinsic resistance to demethylation; further examination of this sequence is clearly warranted.

While it remains possible that subtle methylation differences remain in fetal germ cells, undetectable by methods which only detect changes that occur at restriction enzyme recognition sites, another interpretation is that methylation is a critical, early event in the establishment of the imprint, but that the alleles are marked in a more fundamental way. This mark could correspond to a sequence which binds one or more ovary- or testis-specific factors and dictates the establishment of an imprint; later, DNA methylase may recognize this pattern and "lock in" the open or closed chromatin configuration of the imprinted gene's promoter.

In summary, DNA methylation and genomic imprinting are intimately associated, although evidence that methylation is the primary imprinting signal remains elusive. More examples of endogenous imprinted genes are clearly desirable. Further examination of the status of imprinted genes in mice homozygous for the DNA methyltransferase gene disruption (Li *et al.*, 1992, 1993) will provide useful information to resolve this problem. Targeted disruption of the MeCP genes may also help elucidate the role of methylation in the regulation of imprinted genes. Other strategies toward this goal are described in the next section.

IV. Experimental Approaches to Identifying Imprinted Genes

Two approaches to identifying new imprinted genes are being pursued. The first approach evaluates genes which map near previously identified imprinted genes or chromosomal regions for parent-specific differences in expression. In this method, the maternal and paternal alleles of candidate genes must be clearly distinguishable. For this reason, interspecific hybrids are often used. In the second, differential screening of cDNA libraries with probes derived from normal and various abnormal embryos is performed.

A. Using Interspecific Hybrids to Identify Imprinted Genes

The ability to distinguish between maternal and paternal alleles is essential for evaluating the status of potentially imprinted genes. Matings between different mouse species are useful since the parental alleles can be distinguished by the presence or absence of DNA sequence polymorphisms in the genes of interest. When the polymorphism is present within the mRNA, the parental source of the transcript can be identified. The 5′ and 3′ nontranslated regions are frequent sites of species-specific differences since

higher degrees of divergence may be tolerated in noncoding regions. For an abundant transcript, allele-specific expression may be identified by RNase protection assays. In the case of a low-abundance mRNA, reverse transcription coupled with PCR (RT/PCR) can be used. Allele-specific expression may be identified by SSCP mutation detection or by restriction enzyme digestion (when the sequence polymorphism results in either the loss or gain of an enzyme recognition site).

Hybrid offspring of *M. musculus* and *M. spretus* have been useful in establishing the imprinted status of *H19* (Bartolomei *et al.*, 1991) and *Snrpn* (Leff *et al.*, 1992), as well as in demonstrating the limits of the affected regions by showing that adjacent genes are not imprinted (Villar and Pedersen, 1994; Nicholls *et al.*, 1993).

The use of interspecific hybrids is a powerful approach for verifying the status of known genes, but the usefulness of this strategy is limited by the need to first identify candidate genes. Differential screening techniques may provide a source of genes for further evaluation.

B. Differential Screening Techniques

The ideal differential screen for imprinted genes would involve a comparison of gene expression between identical tissues or animals, varying only in the presence and absence of genomic imprinting. Unfortunately, no such matched pairs have been identified. An alternate approach is to compare gene expression in normal tissues and comparable tissues showing alterations in imprinting. Parthenogenetic and androgenetic embryos may be used as the source of abnormally imprinted tissues. These experimentally produced embryos contain only maternal or paternal DNA, respectively (see Introduction). Parthenogenotes should be deficient in the expression of imprinted genes expressed only from the paternal alleles; conversely, androgenotes lack the expression of genes expressed only from the maternal alleles.

Potential drawbacks to using parthenogenotes or androgenotes are the amount of effort required in their production (particularly true of androgenotes) and the limited stage of development reached by these abnormal embryos. Although parthenogenotes progress farther than androgenotes, their postimplantation development is highly abnormal. Frequently tissues are missing or highly disorganized (see Introduction). Thus, direct comparison between gene expression in parthenogenotes or androgenotes with normal embryos is complicated by (1) the low amounts of RNA which are obtainable through experimental production of parthenogenotes and androgenotes and (2) the loss of entire classes of tissue-specific genes in the parthenogenotes.

Parthenogenetic cells can, however, form well-organized and advanced extraembryonic tissues when combined with tetraploid (4N) cells derived from normal fertilized embryos (Tarkowski *et al.*, 1977; Nagy *et al.*, 1990). Parthenogenones are produced by the *in vitro* activation of unfertilized mouse eggs, followed by cytochalasin D treatment to allow nuclear division in the absence of cell division. After removal of the cytochalasin D, the now diploid embryos are cultured and then combined with tetraploid embryonic cells to form chimeras which are eventually implanted in foster mothers. The resultant chimeras develop well until the 30–35 somite stage, at which point the chimeras fail. The resultant embryos are equivalent in development to approximately 9.5-day normal embryos. The use of parthenogenetic and 4N cells expressing different GPI isoforms has allowed the demonstration that, in the majority of cases, the embryo proper is derived from the parthenogenetic cells while the extraembryonic tissues are derived from the 4N cells (A. I. Spindle *et al.*, unpublished observations). These advanced, well-organized parthenogenetic embryos can be used as a source of RNA for the production of cDNA. A variation of the "lone linker" technique (Ko *et al.*, 1990) is currently being used to produce large quantities of parthenogenetic embryo cDNA by PCR. This technique involves the batch amplification of all transcribed sequences in the embryo under conditions which retain the differences in relative abundance seen in the starting mRNA population (Brady *et al.*, 1990). These PCR products are used as probes in a differential screen of a cDNA library derived from normal 9.5-day embryos. Recombinant phage which hybridize to the normal embryonic but not parthenogenetic probe are strong candidates for imprinted genes. It is hoped that the identification of more imprinted genes will elucidate not only the mechanism of but also the biological and evolutionary role of genomic imprinting.

V. Summary

This chapter can be summarized by the following main points:

Genomic imprinting results in the functional nonequivalence of the maternal and paternal genomes, thereby preventing the development of viable parthenogenotes and androgenotes in eutherian mammals. Imprinting may have arisen as a result of the specialized evolutionary requirements of the parental genomes or may have been an obligatory step in the development of placentation.

A substantial proportion of transgenes and a smaller number of endogenous genes demonstrate imprinted pattern of expression in mice and humans.

An analysis of DNA methylation in somatic tissues and germ cells during embryonic and postnatal development reveals dynamic changes, particularly during gametogenesis and early embryogenesis. The nature and timing of these changes suggest that DNA methylation may be involved in genomic imprinting.

Imprinted genes display complex methylation patterns. Many aspects of these patterns are consistent with a role for methylation in the imprinted phenotype, although it is currently unclear whether methylation functions in the establishment of imprinting or plays a secondary role in the maintenance of the imprinted pattern of expression.

Studies underway to identify new imprinted genes may help elucidate both the function and mechanism of genomic imprinting.

Acknowledgments

We are grateful to the following for providing us with details of their unpublished work: Timothy Bestor, Michael Brandeis, Rudolf Jaenisch, Shirley Tilghman, Sue Varmuza, and Angela Villar. We thank Liana Hartanto for her excellent administrative support. Joseph D. Gold was supported by National Institutes of Health Research Service Award 5T32 ES07016. Work performed in this laboratory was supported by NIH/NICHD Grant HD26732 and by USDOE Office of Health and Environmental Research Contract DE-AC03-76-SF01012.

References

Allen, N., and Reik, W. (1992). Imprintor or imprinted? *BioEssays* **14,** 857–859.

Allen, N. D., Norris, M. L., and Surani, A. (1990). Epigenetic control of transgene expression and imprinting by genotype-specific modifiers. *Cell* **61,** 853–861.

Andrew, S. E., Goldberg, Y. P., Kremer, B., Telenius, H., Theilmann, J., Adams, S., Starr, E., Squitieri, F., Lin, B., Kalchman, M. A., Graham, R. K., and Hayden, M. R. (1993). The relationship between trinucleotide (CAG) repeat length and clinical features of Huntington's disease. *Nature Genet.* **4,** 398–403.

Antequera, F., Boyes, J., and Bird, A. (1990). High levels of *de novo* methylation and altered chromatin structure at CpG islands in cell lines. *Cell* **62,** 503–514.

Babinet, C., Richoux, V., Guenet, J.-L., and Renard, J.-P. (1990). The DDK inbred strain as a model for the study of interactions between parental genomes and egg cytoplasm in mouse preimplantation development. *Development Suppl.* 81–88.

Barcelo, J. M., Mahadevan, M. S., Tsifilfidis, C., MacKenzie, A. E., and Korneluk, R. G. (1993). Intergenerational stability of the myotonic dystrophy protomutation. *Hum. Mol. Genet.* **2,** 705–709.

Barlow, D. P., Stoeger, R., Herrmann, B. G., Saito, K., and Schweifer, N. (1991). The mouse insulin-like growth factor type-2 receptor is imprinted and closely linked to the *Tme* locus. *Nature* (*London*) **349,** 84–87.

Bartolomei, M. S., and Tilghman, S. M. (1992). Parental imprinting of mouse chromosome 7. *Sem. Dev. Biol.* **3,** 107–117.

Bartolomei, M. S., Webber, A. L., Brunkow, M. E., and Tilghman, S. M. (1993).

Epigenetic mechanisms underlying the imprinting of mouse *H19* gene. *Genes Dev.* **7,** 1663–1673.

Bartolomei, M. S., Zemel, S., and Tilghman, S. M. (1991). Parental imprinting of the mouse H19 gene. *Nature (London)* **351,** 153–155.

Barton, S., Ferguson-Smith, A., Fundele, R., and Surani, M. A. (1991). Influence of paternally imprinted genes on development. *Development* **113,** 679–687.

Barton, S. C., Adams, C. A., Norris, M. L., and Surani, M. A. H. (1985). Development of gynogenetic and parthenogenetic inner cell mass and trophectoderm tissues in reconstituted blastocysts in the mouse. *J. Embryol. Exp. Morphol.* **90,** 267–285.

Barton, S. C., Surani, M. A. H., and Norris, M. L. (1984). Role of paternal and maternal genomes in mouse development. *Nature (London)* **311,** 374–376.

Beatty, R. A. (1967). Parthenogenesis in vertebrates. *In* "Fertilization" (C. B. Mertz and A. Monroy, eds.), Vol. 1, pp. 413–331. Academic Press, New York.

Beechey, C. V., and Cattanach, B. M. (1993). Genetic imprinting map. *Mouse Genome* **91,** 102–104.

Belyaev, D. K., Ruvinsky, A. O., and Borodin, P. M. (1981). Inheritance of alternative states of the fused gene in mice. *J. Hered.* **72,** 107–112.

Bestor, T. H. (1990). DNA methylation: Evolution of a bacterial immune function into a regulator of gene expression and genome structure in higher eukaryotes. *Phil. Trans. R. Soc. Lond. (Biol.)* **326,** 179–187.

Bestor, T. H., and Coxon, A. (1993). The pros and cons of DNA methylation. *Curr. Biol.* **3,** 384–386.

Bestor, T. H., Gundersen, G., Kolsto, A.-B., and Prydz, H. (1992). CpG islands in mammalian gene promoters are inherently resistant to de novo methylation. *GATA* **9,** 48–53.

Bestor, T. H., and Ingram, V. M. (1983). Two DNA methyltransferases from murine erythroleukemia cells: Purification, sequence specificity, and mode of interaction with DNA. *Proc. Natl. Acad. Sci. USA* **80,** 5559–5563.

Bestor, T. H., Laudano, A., Mattaliano, R., and Ingram, V. (1988). Cloning and sequencing of a cDNA encoding DNA methyltransferase of mouse cells. *J. Mol. Biol.* **203,** 971–983.

Bird, A. (1986). CpG-rich islands and the function of DNA methylation. *Nature (London)* **321,** 209–213.

Bird, A. (1992). The essentials of DNA methylation. *Cell* **70,** 5–8.

Bird, A., and Taggart, M. H. (1980). Variable patterns of total DNA and rDNA methylation in animals. *Nucleic Acids Res.* **8,** 1485–1487.

Bird, A., Taggart, M., Frommer, M., Miller, O. J., and Macleod, D. (1985). A fraction of the mouse genome that is derived from islands of nonmethylated, CpG-rich DNA. *Cell* **40,** 91–99.

Bird, A., Taggart, M. H., Nicholls, R., and Higgs, D. R. (1987). Nonmethylated CpG-rich islands at the human α-globin locus: Implications for evoluation of the α-globin pseudogene. *EMBO J.* **6,** 999–1004.

Borsani, G., Tonlorenzi, R., Simmler, M. C., Dandalo, L., Arnaud, D., Capra, V., Grompe, M., Pizzati, A., Muzay, D., Lawrence, C., Willard, H. F., Avner, P., and Ballabio, A. (1991). Characterisation of a murine gene expressed from the inactive X chromosome. *Nature (London)* **351,** 325–329.

Boyes, J., and Bird, A. (1991). DNA methylation inhibits transcription indirectly via a methyl-CpG binding protein. *Cell* **64,** 1123–1134.

Brady, G., Barbara, M., and Iscove, N. N. (1990). Representative in vitro cDNA amplification from individual hemopoietic cells and colonies. *Meth. Mol. Cell. Biol.* **2,** 17–25.

Brandeis, M., Kafri, T., Ariel, M., Chaillet, M. R., McCarrey, J., Razin, A., and Cedar, H. (1993). The ontogeny of allele-specific methylation associated with imprinted genes in the mouse. *EMBO J.* **12,** 3669–3677.

Brannan, C. I., Claire, E., Ingram, R., and Tilghman, S. M. (1990). The product of the H19 gene may function as an RNA. *Mol. Cell. Biol.* **10,** 28–36.

Brissenden, J. E., Ullrich, A., and Franke, U. (1984). Human chromosomal mapping of genes for insulin-like growth factors I and II and epidermal growth factor. *Nature (London)* **310,** 781–784.

Brockdorff, N., Ashworth, A., Kay, G. F., Cooper, P., Smith, S., McCabe, V. M., Norris, D. P., Penny, G. D., Patel, D., and Rastan, S. (1991). Conservation of position and exclusive expression of mouse *Xist* from the inactive X chromosome. *Nature (London)* **351,** 329–331.

Brockdorff, N., Ashworth, A., Kay, G. F., McCabe, V. M., Norris, D. P., Cooper, P. J., Swift, S., and Rastan, S. (1992). The product of the mouse *Xist* gene is a 15 kb in active X-specific transcript containing no ORF and located in the nucleus. *Cell* **71,** 515–526.

Brown, C. J., Ballabio, A., Rupert, J. L., Lafeniere, R. G., Grompe, M., Tonlorenzi, R., and Willard, H. F. (1991). A gene from the region of the human X-inactivation center is expressed exclusively from the inactive X chromosome. *Nature (London)* **349,** 38–44.

Brunkow, M. E., and Tilghman, S. M. (1991). Ectopic expression of the H19 gene in mice causes prenatal lethality. *Genes Dev.* **5,** 1092–1101.

Buschhausen, G., Wittig, B., Graessman, M., and Graessman, H. (1987). Chromatin structure is required to block transcription of the methylated herpes simplex virus thymidine kinase gene. *Proc. Natl. Acad. Sci. USA* **84,** 1177–1181.

Campbell, M. L., and Arlinghaus, R. B. (1991). Current status of the BCR gene and its involvement with human leukemia. *Adv. Cancer Res.* **57,** 227–256.

Carlson, L. L., Page, A. W., and Bestor, T. H. (1992). Properties and localization of DNA methyltransferase in preimplantation mouse embryos: Implications for genomic imprinting. *Genes Dev.* **6,** 2536–2541.

Carroti, D., Palitti, F., Lavia, P., and Strom, R. (1989). *In vitro* methylation of CpG-rich islands. *Nucleic Acids Res.* **17,** 9219–9229.

Cattanach, B. M. (1986). Parental origin effects in mice. *J. Embryol. Exp. Morphol.* **97,** 137–150.

Cattanach, B. M., Barr, J. A., Evans, E. P., Burtenshaw, M., Beechey, C. V., Leff, S. E., Brannan, C. I., Copeland, N. G., Jenkins, N. A., and Jones, J. (1992). A candidate mouse model for Prader-Willi syndrome which shows an absence of Snrpn expression. *Nature Genet.* **2,** 270–274.

Cattanach, B. M., and Beechey, C. V. (1990). Autosomal and X-chromosome imprinting. *Development Suppl.* 63–72.

Chaillet, J. R., Vogt, T. F., Beier, D. R., and Leder, P. (1991). Parental-specific methylation of an imprinted transgene is established during gametogenesis and progressively changes during embryogenesis. *Cell* **66,** 77–83.

Clairmont, K. B., and Czech, M. P. (1989). Chicken and *Xenopus* mannose 6-phosphate receptors fail to bind insulin-like growth factor II. *J. Biol. Chem.* **264,** 16,390–16,392.

Clarke, H. J., Varmuza, S., Prideaux, V. R., and Rossant, J. (1988). The developmental potential of parthenogenetically derived cells in chimeric mouse embryos: Implications for action of imprinted genes. *Development* **104,** 175–182.

Cooper, D. N., Taggart, M. H., and Bird, A. (1983). Unmethylated domains in vertebrate DNA. *Nucleic Acids Res.* **11,** 647–658.

Cooper, D. W. (1993). The evolution of sex determination, sex chromosome dimorphism,

and X-inactivation in therian mammals: A comparison of metatherians (marsupials) and eutherians ("placentals"). *In* "Sex, Genes and Chromosomes" (K. C. Reed and J. A. Marshall Graves, eds.). Harwood Academic Publishers (in press).

Cortese-Hasset, A. L., Misra, D. N., Kunz, H. W., and Gill, T. J., III (1991). The MHC of the rat. *In* "Immunogenetics of the Major Histocompatibility Complex" (R. Srivastava, B. P. Ram, and P. Tyler, eds.), pp. 309–347. VCH Publishers, Inc., New York.

Coulondre, C., Miller, J. H., Farabaugh, P. J., and Gilbert, W. (1978). Molecular basis of base substitution hotspots in *Escherichia coli*. *Nature (London)* **274,** 775–780.

Czech, M. P. (1989). Signal transmission by the insulin-like growth factors. *Cell* **59,** 235–238.

Daley, G. Q., and Ben-Neriah, Y. (1991). Implicating the bcr/abl gene in the pathogenesis of Philadelphia chromosome-positive human leukemia. *Adv. Cancer Res.* **57,** 151–184.

DeChiara, T. M., Robertson, E. J., and Efstradiatis, A. (1991). Parental imprinting of the mouse insulin-like growth factor II gene. *Cell* **64,** 849–859.

DeLoia, A. J., and Solter, D. (1990). A transgene insertional mutation at an imprinted locus in the mouse genome. *Development Suppl.* 73–80.

Doerfler, W. (1992). DNA methylation: Eukaryotic defense against the transcription of foreign genes? *Microbiol Pathol.* **12,** 1–8.

Duyao, M., Ambrose, C., Myers, R., Noveletto, A., Perischetti, F., Frontali, F., Folstein, S., Ross, C., Franz, M., Abbot, M., Gray, J., Conneally, P., Young, A., Penney, J., Hollingsworth, Z., Shoulson, I., Lazzarini, A., Falek, A., Koroshetz, W., Sax, D., Bird, E., Vonsattel, J., Bonilla, E., Alvir, J., Bickham Conde, J., Cha, J.-H., Dure, L., Gomez, F., Ramos, M., Sanchez-Ramos, J., Snodgrass, S., de Young, M., Wexler, N., Mosccowitz, C., Penschaszadeh, G., MacFarlane, H., Anderson, M., Jenkins, B., Srinidhi, J., Gusella, J., and MacDonald, M. (1993). Trinucleotide repeat length instability and age of onset in Huntington's disease. *Nature Genet.* **4,** 387–392.

Engler, P., Haasch, D., Pinkert, C. A., Doglio, L., Glymour, M., Brinster, R., and Storb, U. (1991). A strain-specific modifier on mouse chromosome 4 controls the methylation of independent transgene loci. *Cell* **65,** 939–947.

Enver, T., Zhang, J.-W., Papayannopoulou, T., and Stamatoyannopoulos, G. (1988). DNA methylation: A secondary event in globin gene switching? *Genes Dev.* **2,** 698–706.

Epstein, C. J. (1972). Expression of the mammalian X chromosome before and after fertilization. *Science* **175,** 1467–1468.

Evans, M., Bradley, A., and Robertson, E. (1985). EK cell contribution to chimeric mice: From tissue culture to sperm. *In* "Genetic Manipulation of the Early Mammalian Embryo, Banbury Report 20" (F. Constantini and R. Jaenisch, eds.), pp. 93–102. Cold Spring Harbor Laboratory, Cold Spring Harbor, NY.

Eversole-Cire, P., Ferguson-Smith, A. C., Sasaki, H., Brown, K. D., Cattanach, B. M., Gonzales, F. A., Surani, M. A., and Jones, P. A. (1993). Activation of an imprinted *Igf 2* gene in mouse somatic cell cultures. *Mol. Cell. Biol.* **13,** 4928–4938.

Ferguson-Smith, A. C., Saski, H., Cattanach, B. M., and Surani, M. A. (1993). Parental-origin-specific epigenetic modification of the mouse *H19* gene. *Nature (London)* **362,** 751–755.

Filson, A. J., Louvi, A., Efstratiadis, A., and Robertson, E. J. (1993). Rescue of the T-associated maternal effect in mice carrying null mutations in *Igf-2* and *Igf-2r*, two reciprocally imprinted genes. *Development* **118,** 731–736.

Forejt, J., and Gregorova, S. (1992). Genetic analysis of genomic imprinting: An

imprintor-1 gene controls inactivation of the paternal copy of the mouse Tme locus. *Cell* **70,** 443–450.

Frank, D., Keshet, I., Shani, M., Levine, A., Razin, A., and Cedar, H. (1991). Demethylation of CpG islands in embryonic cells. *Nature (London)* **351,** 239–241.

Fundele, R., Norris, M., Barton, S., Fehlau, M., Howlett, S., Mills, W., and Surani, M. A. (1990). Temporal and spatial selection against parthenogenetic cells during development of fetal chimeras. *Development* **108,** 203–211.

Gama-Sosa, M. A., Midgett, R. M., Slagel, V. A., Githens, S., Kuo, K. C., Gehrke, C., and Ehrlich, M. (1983). Tissue-specific differences in DNA methylation in various mammals. *Biochim. Biophys. Acta* **740,** 212–219.

Gardiner-Garden, M., and Frommer, M. (1987). CpG islands in vertebrate genomes. *J. Mol. Biol.* **196,** 261–282.

Gardner, R. L., and Lyon, M. F. (1971). X-chromosome inactivation studies by injection of a single cell into the mouse blastocyst. *Nature* **231,** 385–386.

Gautsch, J. M., and Wilson, M. C. (1983). Delayed *de novo* methylation in teratocarcinoma cells suggests additional tissue-specific mechanisms for controlling gene expression. *Nature (London)* **301,** 32–37.

Giannoukakis, N., Deal, C., Paquette, J., Goodyer, C. G., and Polychronakos, C. (1993). Parental genomic imprinting of the human IGF2 gene. *Nature Genet.* **4,** 98–101.

Goldberg, Y. P., Kremer, B., Andrew, S. E., Theilmann, J., Graham, R. K., Squitieri, F., Telenius, H., Adam, S., Sajoo, A., Starr, E., Heiberg, A., Wolff, G., and Hayden, M. R. (1993). Molecular analysis of new mutations for Huntington's disease: Intermediate alleles and sex of origin effects. *Nature Genet.* **5,** 174–179.

Goldman, M. A. (1992). The silence of the X. *Nature Genet.* **2,** 169–170.

Gounari, F., Banks, G., Khazaie, K., Jeggo, P., and Holliday, R. (1987). Gene reactivation: A tool for the isolation of mammalian DNA methylation mutants. *Genes Dev.* **1,** 899–912.

Graham, C. F. (1974). The production of parthenogenetic mammalian embryos and their use in biological research. *Biol. Rev.* **49,** 399–422.

Grant, S. G., and Chapman, V. M. (1988). Mechanisms of X-chromosome regulation. *Annu. Rev. Genet.* **22,** 199–233.

Gruenbaum, Y., Cedar, H., and Razin, A. (1982). Substrate and sequence specificity of a eukaryotic DNA methylase. *Nature* **295,** 620–622.

Guthrie, C. (1991). Messenger RNA splicing in yeast: Clues to why the spliceosome is a ribonucleoprotein. *Science* **253,** 157–163.

Haas, O. A., Argyriou-Tirita, A., and Lion, T. (1992). Parental origin of chromosomes involved in the translocation t(9;22). *Nature* **359,** 414–416.

Hadchouel, M., Farza, H., Simon, D., Tiollais, D., and Pourcel, C. (1987). Maternal inhibition of hepatitis B surface antigen expression in transgeneic mice correlates with *de novo* methylation. *Nature (London)* **329,** 454–456.

Haig, D., and Graham, C. (1991). Genomic imprinting and the strange case of the insulin-like growth factor II receptor. *Cell* **64,** 1045–1046.

Hall, J. G. (1990). Genomic imprinting: Review and relevance to human diseases. *J. Hum. Genet.* **46,** 857–873.

Hao, Y., Crenshaw, T., Moulton, T., Newcomb, E., and Tycko, B. (1993). Tumour-suppressor activity of H19 RNA. *Nature (London)* **365,** 764–767.

Harper, M. E., Ullrich, A., and Saunders, G. F. (1981). Localization of the human insulin gene to the distal end of the short arm of chromosome 11. *Proc. Natl. Acad. Sci. USA* **78,** 4458–4460.

Harrison, K. B. (1989). X-chromosome inactivation in the human cytotrophoblast. *Cyt. Cell Genet.* **52,** 37–41.

Henry, I., Bonaiti-Pellie, C., Chehensse, V., Beldjord, C., Schwartz, C., Utermann, G., and Junien, C. (1991). Uniparental paternal disomy in a genetic cancer-predisposing syndrome. *Nature (London)* **351,** 665–667.

Hergersberg, M. (1991). Biological aspects of cytosine methylation in eukaryotic cells. *Experientia* **47,** 1171–1185.

Howeler, C. J., Busch, H. F., Geraedts, J. P., Niermeijer, M. F., and Staal, A. (1989). Anticipation in myotonic dystrophy: Fact or fiction? *Brain* **112,** 779–797.

Howlett, S. K., and Reik, W. (1991). Methylation levels of maternal and paternal genomes during preimplantation development. *Development* **113,** 119–127.

Hubrich-Kuhner, K., Buhk, H.-J., Wagner, H., Kroger, H., and Simon, D. (1989). Non-C-G recognition sequences of DNA cytosine-5-methyltransferase from rat liver. *Biochem. Biophys. Res. Commun.* **160,** 1175–1182.

Jacobs, P. A., Wilson, C., Sprenkle, J. A., Rosenshein, N. B., and Migeon, B. R. (1980). Mechanism of origin of complete hydatidiform moles. *Nature (London)* **286,** 714–716.

Jahner, D., and Jaenisch, R. (1984). DNA methylation in early mammalian development. *In* "DNA Methylation" (A. Razin, H. Cedar, and A. Riggs, eds.), pp. 189–219. Springer-Verlag, Berlin.

Jahner, D., and Jaenisch, R. (1985). Chromosomal position and specific demethylation in enhancer sequences of germ line-transmitted retroviral genomes during mouse development. *Mol. Cell. Biol.* **5,** 2212–2220.

Johnson, D. R. (1974). Hairpin-Tail: A case of post-reductional gene action in the mouse egg? *Genetics* **76,** 795–805.

Jones, P. A. (1985). Altering gene expression with 5-azacytidine. *Cell* **40,** 485–486.

Jones, P., Wolkowicz, M., Rideout, W., Gonzales, F., Marziasz, C., Coetzee, G., and Tapscott, S. (1990). *De novo* methylation of the MyoD1 CpG island during the establishment of immortal cell lines. *Proc. Natl. Acad. Sci. USA* **87,** 6117–6121.

Kafri, T., Ariel, M., Brandeis, M., Shemer, R., Urven, L., McCarrey, J., Cedar, H., and Razin, A. (1992). Developmental pattern of gene-specific DNA methylation in the mouse embryo and early germ lines. *Genes Dev.* **6,** 705–714.

Kanbour-Shakir, A., Kunz, H. W., and Gill, T. J., III (1993). Differential genomic imprinting of major histocompatibility complex class I antigens in the placenta of the rat. *Biol. Reprod.* **48,** 977–986.

Kanbour-Shakir, A., Zhang, X., Rouleau, A., Armstrong, D. T., Kunz, H. W., MacPherson, T. A., and Gill, T. J., III (1990). Gene imprinting and major histocompatibility complex I antigen expression in the rat placenta. *Proc. Natl. Acad. Sci. USA* **87,** 444–448.

Kaslow, D. C., and Migeon, B. R. (1987). DNA methylation stabilizes X chromosome inactivation in eutherians but not marsupials: Evidence for multistep maintenance of mammalian X dosage compensation. *Proc. Natl. Acad. Sci. USA* **84,** 6210–6214.

Kaufman, M. H., Barton, S. C., and Surani, M. A. H. (1977). Normal post-implantation development of mouse parthenogenetic embryos to the forelimb bud stage. *Nature (London)* **265,** 53–55.

Kay, G. F., Penny, G. D., Patel, D., Ashworth, A., Brockdorff, N., and Rastan, S. (1993). Expression of Xist during mouse development suggests a role in the initiation of X chromosome inactivation. *Cell* **72,** 171–182.

Kitsberg, D., Selig, S., Brandeis, M., Simon, I., Keshet, I., Driscoll, D. J., Nicholls, R. D., and Cedar, H. (1993). Allele-specific replication timing of imprinted gene regions. *Nature (London)* **364,** 459–463.

Klages, S., Mollers, B., and Renkawitz, R. (1992). The involvement of demethylation in the myeloid-specific function of the mouse lysozyme downstream enhancer. *Nucleic Acids Res.* **20,** 1925–1932.

Ko, M. S., Ko, S. B., Takahashi, N., Nishiguchi, K., and Abe, K. (1990). Unbiased amplification of a highly complex mixture of DNA fragments by 'lone linkers'-tagged PCR. *Nucleic Acids Res.* **18,** 4293–4294.

Kolsto, A.-B., Kollias, G., Giguere, V., Isobe, K. I., Prydz, H., and Grosveld, F. (1986). The maintenance of methylation-free islands in transgenic mice. *Nucleic Acids Res.* **14,** 9667–9678.

Kramer, J. M., and Erickson, R. P. (1981). Developmental program of PGK-1 and PGK-2 isozymes in spermatogenic cells of the mouse: Specific activities and rates of synthesis. *Dev. Biol.* **87,** 37—45.

Kratzer, P. G., and Gartler, S. M. (1978a). HGPRT activity changes in preimplantation mouse embryos. *Nature* **274,** 503–504.

Kratzer, P. G., and Gartler, S. M. (1978b). Hypoxanthine guanine phosphoribosyl transferase expression in early mouse development. *In* "Genetic Mosaics and Chimeras in Mammals" (L. B. Russell, ed.), pp. 247–260. Plenum, New York.

Kricker, M. C., Drake, J. W., and Radman, M. (1992). Duplication-targeted DNA methylation and mutagenesis in the evolution of eukaryotic chromosomes. *Proc. Natl. Acad. Sci. USA* **89,** 1075–1079.

Lalley, P. A., and Chirgwin, J. M. (1984). Mapping of the mouse insulin genes. *Cytogenet. Cell Genet.* **37,** 515.

Lee, J. E., Pintar, J., and Efstratiadis, A. (1990). Pattern of the insulin-like growth factor II gene expression during early mouse embryogenesis. *Development* **110,** 151–159.

Lee, J. E., Tantravahi, U., Boyle, A. L., and Efstratiadis, A. (1993). Parental imprinting of an *Igf-2* transgene. *Mol. Reprod. Dev.* **35,** 382–390.

Leff, S. E., Brannan, C. I., Reed, M. L., Ozcelik, T., Francke, U., Copeland, N. G., and Jenkins, N. A. (1992). Maternal imprinting of the mouse Snrpn gene and conserved linkage homology with the human Prader-Willi syndrome region. *Nature Genet.* **2,** 259–264.

Lewis, J. D., Meehan, R. R., Henzel, W. J., Maurer-Fogy, I., Jeppesen, P., Klein, F., and Bird, A. (1992). Purification, sequence, and cellular localization of a novel chromosomal protein that binds to methylated DNA. *Cell* **69,** 905–914.

Li, E., Beard, C., and Jaenisch, R. (1993). The role of DNA methylation in genomic imprinting. *Nature (London)* **366,** 362–365.

Li, E., Bestor, T. H., and Jaenisch, R. (1992). Targeted mutation of the DNA methyltransferase gene results in embryonic lethality. *Cell* **69,** 915–926.

Li, S., Klein, E. S., Russo, A. F., Simmons, D. M., and Rosenfeld, M. G. (1989). Isolation of cDNA clones encoding small nuclear ribonucleoparticle-associated proteins with different tissue specificities. *Prod. Natl. Acad. Sci. USA* **86,** 9778–9782.

Lock, L. F., Takagi, N., and Martin, G. R. (1987). Methylation of the Hprt gene on the inactive X occurs after chromosome inactivation. *Cell* **48,** 39–46.

Luhrmann, R., Kastner, B., and Bach, M. (1990). Structure of spliceosomal SnRNPs and their role in pre-mRNA splicing. *Biochim. Biophys. Acta* **1087,** 265–292.

Lyon, M. (1972). X-chromosome inactivation and developmental patterns in mammals. *Biol. Rev.* **47,** 1–35.

Lyon, M., and Glenister, P. H. (1977). Factors affecting the observed number of young resulting from adjacent-2 disjunction in mice carrying a translocation. *Genet. Res.* **29,** 83–92.

Lyon, M. F. (1961). Gene action in the X-chromosome of the mouse (*Mus musculus* L.). *Nature* **190,** 372–373.

Mann, J. R., Gadi, I., Harbison, M. L., Abbondanzo, S. J., and Stewart, C. L. (1990). Androgenetic mouse embryonic stem cells are pluripotent and cause skeletal defects in chimeras: Implications for genetic imprinting. *Cell* **62,** 251–260.

Mann, J. R., and Lovell-Badge, R. H. (1984). Inviability of parthenogenones determined by pronuclei, not egg cytoplasm. *Nature (London)* **310,** 66–67.

Mann, J. R., and Stewart, C. L. (1991). Development to term of mouse androgenetic aggregation chimeras. *Development* **113,** 1325–1333.

Markert, C. L., and Seidel, G. E., Jr. (1981). Parthenogenesis, identical twins and cloning in mammals. *In* "New Technologies in Animal Breeding" (B. G. Brackett, G. E. Seidel, Jr., and S. M. Seidel, eds.), pp. 181–200. Academic Press, New York.

McAllister, G., Amara, S. G., and Lerner, M. R. (1988). Tissue-specific expression and cDNA cloning of a small nuclear ribonucleoprotein-associated polypeptide N. *Proc. Natl. Acad. Sci. USA* **85,** 5296–5300.

McAllister, G., Roby-Shemkovitz, A., Amara, S. G., and Lerner, M. R. (1988). cDNA sequence of the rat U snRNP-associated protein N: Description of a potential Sm epitope. *EMBO J.* **8,** 1177–1181.

McCarrey, J. R., and Dilworth, D. D. (1992). Expression of *Xist* in mouse germ cells correlates with X chromosome inactivation. *Nature Genet.* **2,** 200–203.

McGowan, R., Campbell, R., Peterson, A., and Sapienza, C. (1989). Cellular mosaicism in the methylation and expression of hemizygous loci in the mouse. *Genes Dev.* **3,** 1669–1676.

McGowan, R., Tran, T.-H., Paquette, J., and Sapienza, C. (1990). Transgene methylation imprints are established post-fertilization. *In* "Nucleic Acid Methylation" (G. A. Clawson, D. B. Willis, A. Weissbach, and P. A. Jones, eds.), pp. 367–379. Wiley-Liss, New York.

McGrath, J., and Solter, D. (1983). Nucler transplantation in the mouse embryo by microsurgery and cell fusion. *Science* **220,** 1300–1303.

McGrath, J., and Solter, D. (1984). Completion of mouse embryogenesis requires both maternal and paternal genomes. *Cell* **37,** 179–183.

Meehan, R. R., Lewis, J. D., McKay, S., Kleiner, E. L., and Bird, A. P. (1989). Identification of a mammalian protein that binds specifically to DNA containing methylated CpGs. *Cell* **58,** 499–507.

Meehan, R. R., Lewis, J. D., and Bird, A. P. (1992). Characterization of MeCP2, a vertebrate DNA binding protein with affinity for methylated DNA. *Nucleic Acids Res.* **20,** 5085–5092.

Mohandas, T. K., Passage, M. B., Williams, J. W., Sparkes, R. S., Yen, P. H., and Shapiro, L. J. (1989). X-chromosome inactivation in cultured cells from human chorionic villi. *Somat. Cell Mol. Genet.* **15,** 131–136.

Monk, M. (1988). Genomic imprinting. *Genes Dev.* **2,** 921–925.

Monk, M., Boubelik, M., and Lehnert, S. (1987). Temporal and regional changes in DNA methylation in the embryonic, extraembryonic, and germ cell lineages during mouse embryo development. *Development* **99,** 371–382.

Monk, M., and Harper, M. (1978). X-chromosome activity in preimplantation mouse embryos from XX and XO mothers. *J. Embryol. Exp. Morphol.* **46,** 53–64.

Monk, M., and Harper, M. I. (1979). Sequential X-chromosome inactivation coupled with cellular differentiation in early mouse embryos. *Nature* **281,** 311–313.

Morgan, D. O., Edman, J. C., Standring, D. N., Fried, V. A., Smith, M. C., Roth, R. A., and Rutter, W. J. (1987). Insulin-like growth factor II receptor as a multifunctional binding protein. *Nature (London)* **329,** 301–307.

Mukherjee, A. B. (1976). Cell cycle analysis and X-chromosome inactivation in the developing mouse. *Proc. Natl. Acad. Sci. USA* **73,** 1608–1611.

Murray, E., and Grosveld, F. (1987). Site-specific demethylation in the promoter of human γ-globin gene does not alleviate methylation mediated suppression. *EMBO J.* **6,** 2329–2335.

Mutter, G. L., Stewart, C. L., Chaponot, M. L., and Pomponio, R. J. (1993). Oppositely imprinted genes H19 and insulin-like growth factor 2 are coexpressed in human androgenetic trophoblast. *Am. J. Hum. Genet.* **53,** 1096–1102.

Myers, R. H., MacDonald, M. E., Koroshetz, W. J., Duyao, M. P., Ambrose, C. M., Taylor, S. A. M., Barnes, G., Srinidhi, J., Lin, C. S., Whaley, W. L., Lazzarini, A. M., Schwarz, M., Wolff, G., Bird, E. D., Vonsattel, J.-P. G., and Gusella, J. F. (1993). *De novo* expansion of a $(CAG)_n$ repeat in sporadic Huntington's disease. *Nature Genet.* **5,** 168–173.

Nagy, A., Gocza, E., Diaz, E. M., Prideaux, V. R., Ivanyi, E., Markkula, M., and Rossant, J. (1990). Embryonic stem cells alone are able to support fetal development in the mouse. *Development* **110,** 815–821.

Nagy, A., Sass, M., and Markkula, M. (1989). Systematic non-uniform distribution of parthenogenetic cells in adult mouse chimeras. *Development* **106,** 321–324.

Nicholls, R. D. (1993). Genomic imprinting and uniparental disomy in Angelman and Prader-Willi syndrome: A review. *Am. J. Med. Genet.* **46,** 16–25.

Nicholls, R. D., Gottlieb, W., Russell, L. B., Davda, M., Horsthemke, B., and Rinchik, E. M. (1993). Evaluation of potential models for imprinted and nonimprinted components of human chromosome 15q11-q13 syndromes by fine-structure homology mapping in the mouse. *Proc. Natl. Acad. Sci. USA* **90,** 2050–2054.

Nicholls, R. D., Pai, G. S., Gottlieb, W., and Cantu, E. S. (1992). Parental uniparental disomy in Angelman syndrome. *Ann. Neurol.* **32,** 512–518.

Nishimoto, I. (1993). The IGF-II receptor-system: A G protein-linked mechanism. *Mol. Reprod. Dev.* **35,** 398–407.

Niwa, O. Yokota, Y., Ishida, H., and Suguhara, T. (1983). Independent mechanisms involved in suppression of Moloney leukemia virus genome during differentiation of murine teratocarcinoma cells. *Cell* **32,** 1105–1113.

Ogawa, O., Eccles, M. R., Szeto, J., McNoe, L. A., Yun, K., Maw, M. A., Smith, P. J., and Reeve, A. E. (1993). Relaxation of insulin-like growth factor II gene imprinting implicated in Wilms' tumor. *Nature* (*London*) **362,** 749–751.

Ohlsson, R., Nystrom, A., Pfeifer-Ohlsson, S., Tohonen, V., Hedborg, F., Schofield, P., Flam, F., and Ekstrom T. J. (1993). IGF2 is parentally imprinted during human embryogenesis and in the Beckwith-Wiedemann syndrome. *Nature Genet.* **4,** 94–97.

Oka, Y., Rozek, L. M., and Czech, M. P. (1985). Direct demonstration of rapid insulin-like growth factor II receptor internalization and recycling in rat adipocytes: Insulin stimulates ^{125}I-insulin-like growth factor II degradation by modulating the IGF-II receptor recycling process. *J. Biol. Chem.* **260,** 9435–9442.

Olsen, M. W. (1960). Nine year summary of parthenogenesis in turkeys. *Proc. Soc. Exp. Biol. Med.* **105,** 279–281.

Ozcelik, T., Leff, S., Robinson, W., Donlon, T., Lalande, M., Sanjines, E., Schinzel, A., and Francke, U. (1993). Small nuclear ribonucleoprotein polypeptide N (*SNRPN*), an expressed gene in the Prader-Willi syndrome critical region. *Nature Genet.* **2,** 265–269.

Pachnis, V., Brannan, C. I., and Tilghman, S. M. (1984). Locus unlinked to α-fetoprotein under the control of the murine *raf* and *Rif* genes. *Proc. Natl. Acad. Sci. USA* **81,** 5523–5527.

Pal, N., Wadey, R. B., Buckle, B., Yeomans, E., Pritchard, J., and Cowell, J. K. (1990). Preferential loss of maternal alleles in sporadic Wilms' tumour. *Oncogene* **5,** 1665–1668.

Pedersen, R. A., Sturm, K. S., Rappolee, D. A., and Werb Z. (1993). Effects of imprinting on early development of mouse embryos. *In* "Preimplantation Embryo Development" (B. D. Bavister, ed.), pp. 212–226. Springer-Verlag, New York.

Poirier, F., Chan, C.-T. J., Timmons, P. M., Robertson, E. J., Evans, M. J., and Rigby, P. W. J. (1991). The murine H19 gene is activated during embryonic stem cell differentiation *in vitro* and at the time of implantation in the developing embryo. *Development* **113,** 1105–1114.

Quigley, F., Brinkmann, H., Martin, W. F., and Cerff, R. (1989). Strong functional GC pressure in a light-regulated maize gene encoding subunit GAPA of chloroplast glyceraldehyde-3-phosphate dehydrogenase: Implications for the evolution of GAPA pseudogenes. *J. Mol. Evol.* **29,** 412–421.

Rachmilewitz, J., Gileadi, O., Eldar-Geva, T., Schneider, T., de Groot, N., and Hochberg, A. (1992). Transcription of the H19 gene from differentiating cytotrophoblasts from the human placenta. *Mol. Reprod. Dev.* **32,** 196–202.

Rainier, S., Johnson, L. A., Dobry, C. J., Ping, A., Grundy, P. A., and Feinberg, A. P. (1993). Relaxation of imprinted genes in human cancer. *Nature* (*London*) **362,** 747–749.

Rappolee, D. A., Sturm, K. S., Behrendsten, O., Schultz, G. A., Pedersen, R. A., and Werb, Z. (1992). Insulin-like growth factor II acts through an endogenous growth pathway regulated by imprinting in early mouse embryos. *Genes Dev.* **6,** 939–952.

Razin, A., Frank, D., Lichtenstein, M., Paroush, Z., Bergman, Y., Shani, M., and Cedar, H. (1990). Changing methylation patterns during development. *In* "Nucleic Acid Methylation" (G. A. Clawson, D. B. Willis, A. Weissbach, and P. A. Jones, eds.), pp. 257–274. Wiley-Liss, New York.

Reed, S. C. (1937). The inheritance and expression of fused, a new gene in the house mouse. *Genetics* **22,** 1–13.

Reik, W., Collick, A., Norris, M. L., Barton, S. C., and Surani, M. A. (1987). Genomic imprinting determines methylation of parental alleles in transgenic mice. *Nature* (*London*) **328,** 248–251.

Reik, W., Howlett, S. K., and Surani, M. A. (1990). Imprinting by DNA methylation: From transgene to endogenous gene sequences. *Development Suppl.* 99–106.

Richler, C., Soreq, H., and Wahrman, J. (1992). X inactivation in mammalian testis is correlated with inactive X-specific transcription. *Nature Genet.* **2,** 192–195.

Ridley, R. M., Frith, C. D., and Conneally, P. M. (1992). Non-Mendelian features of the inheritance of Huntington's disease: A possible example of genomic imprinting. *Sem. Dev. Biol.* **3,** 127–137.

Rinchik, E. M., Bultman, S. J., Horsthemke, B., Lee, S. T., Strunk, K. M., Spritz, R. A., Avidano, K. M., Jong, M. T., and Nicholls, R. D. (1993). A gene for the mouse pink-eyed dilution locus and for human type II oculocutaneous albinism. *Nature* (*London*) **361,** 72–76.

Ruvinsky, A. O., and Agulnik, A. I. (1990). Gametic imprinting and the manifestation of the fused gene in the house mouse. *Dev. Genet.* **11,** 263–269.

Ruvinsky, A. O., Agulnik, A. I., Protopopov, A. I., Agulnik, S. I., and Belyaev, D. K. (1988). Effect of the t^{12} haplotype on penetrance and inheritance of the fused and kinky genes in mice. *J. Hered.* **79,** 141–146.

Salido, E. C., Yen, P. H., Mohandas, T. K., and Shapiro, L. J. (1992). Expression of the X-inactivation-associated gene XIST during spermatogenesis. *Nature Genet.* **2,** 196–199.

Sanford, J. P., Chapman, V. R., and Rossant, J. (1985). DNA methylation in extraembryonic lineages of mammals. *Trends. Genet.* **1,** 89–93.

Sapienza, C., Peterson, A. C., Rossant, J., and Balling, R. (1987). Degree of methylation of transgenes is dependent on gamete of origin. *Nature* (*London*) **328,** 251–254.

Sapienza, C., Tran, T.-H., Paquette, J., McGowan, R., and Peterson, A. (1989). A methylation mosaic model for mammalian genome imprinting. *Prog. Nucleic Acids Res. Mol. Biol.* **36,** 145–152.

Sasaki, H., Hamada, T., Ueda, T., Seki, R., Higashinakagawa, T., and Sasaki, Y. (1991). Inherited type of alleleic methylation variations in a mouse chromosome region where an integrated transgene shows methylation imprinting. *Development* **111,** 573–581.

Sasaki, H., Jones, P. A., Chaillet, J. R., Ferguson-Smith, A. C., Barton, S. C., Reik, W., and Surani, A. (1992). Parental imprinting: Potentially active chromatin of the repressed maternal allele of the mouse insulin-like growth factor II (*Igf2*) gene. *Genes Dev.* **6,** 1843–1856.

Sasaki, H., Nakasato, M., Saraiva, M. J. M., Matsuo, H., Kato, Y., and Sasaki, Y. (1989). Activity of a metallothionein-transthyretin fusion gene in transgenic mice: Possible effects of plasmid sequences on tissue-specific expression. *Mol. Biol. Med.* **6,** 345–353.

Schroeder, W. T., Chao, L. Y., Dao, D. D., Strong, L. C., Pathak, S., Riccardi, V., Lewis, W. H., and Saunders, G. F. (1987). Nonrandom loss of maternal chromosome 11 alleles in Wilms tumors. *Am. J. Hum. Genet.* **40,** 413–420.

Schwartzberg, P. L., Stall, A. M., Hardin, J. D., Bowdish, K. S., Humaran, T., Boast, S., Harbison, M. L., Robertson, E. J., and Goff, S. P. (1991). Mice homozygous for the ablm1 mutation show poor viability and depletion of selected B and T cell populations. *Cell* **65,** 1165–1175.

Searle, A. G., and Beechey, C. V. (1990). Genome imprinting phenomena on mouse chromosome 7. *Genet. Res.* **56,** 237–244.

Selker, E. U. (1990). Premeiotic instability of repeated sequences in *Neurospora crassa*. *Annu. Rev. Genet.* **24,** 579–613.

Shemer, R., Kafri, T., O'Connell, A., Eisenberg, S., Breslow, J. L., and Razin, A. (1991). Methylation changes in the apolipoprotein AI gene during embryonic development of the mouse. *Proc. Natl. Acad. Sci. USA* **88,** 11,300–11,304.

Singer-Sam, J., Grant, M., LeBon, J. M., Okuyama, K., Chapman, V., Monk, M., and Riggs, A. D. (1990). Use of *HpaII*-polymerase chain reaction assay to study DNA methylation in the Pgk-1 CpG island of mouse embryos at the time of X-chromosome inactivation. *Mol. Cell. Biol.* **10,** 4987–4989.

Snell, R. G., MacMillan, J. C., Cheadle, J. P., Fenton, I., Lazarou, L. P., Davies, P., MacDonald, M. E., Gusella, J. F., Harper, P. S., and Shaw, D. J. (1993). Relationship between trinucleotide repeat expansion and phenotypic variation in Huntington's disease. *Nature Genet.* **4,** 393–397.

Sneller, M. C., and Gunter, K. C. (1987). DNA methylation alters chromatin structure and regulates Thy-1 expression in EL-4 T cells. *J. Immunol.* **138,** 3505–3512.

Solter, D. (1988). Differential imprinting and expression of maternal and paternal genomes. *Annu. Rev. Genet.* **22,** 127–146.

Stevens, L. C. (1984). Germ cell origin of testicular and ovarian teratomas. *Transplant. Proc.* **16,** 502–504.

Stevens, L. C., Varnum, D. S., and Eicher, E. M. (1977). Viable chimaeras produced from normal and parthenogenetic mouse embryos. *Nature* (*London*) **269,** 515.

Stoger, R., Kubicka, A., Liu, C.-G., Kafri, T., Razin, A., Cedar, H., and Barlow, D. P. (1993). Maternal-specific methylation of the imprinted mouse *Igf2r* locus identifies the expressed locus as carrying the imprinting signal. *Cell* **73,** 61–71.

Sturm, K. S., Flannery, M. L., and Pedersen, R. A. (1994). Abnormal development of embryonic and extraembryonic cell lineages in parthenogenetic mouse embryos. Submitted for publication.

Stylianopoulou, F., Efstratiatis, A., Herbert, J., and Pintar, J. (1988a). Pattern of insulin-like growth factor II gene expression during rat embryogenesis. *Development* **103,** 497–506.

Stylianopoulou, F., Herbert, J., Soares, M. B., and Efstratiatis, A. (1988b). Expression of the insulin-like growth factor II gene in the choroid plexus and the leptomeninges of the adult rat central nervous system. *Proc. Natl. Acad. Sci. USA* **85,** 141–145.

Surani, M. A., Barton, S. C., Howlett, S. K., and Norris, M. L. (1988). Influence of chromosomal determinants on development of androgenetic and parthenogenetic cells. *Development* **103,** 171–178.

Surani, M. A., Kothary, R., Allen, N. D., Singh, P. B., Fundele, R., Ferguson-Smith, A. C., and Barton, S. C. (1990). Genomic imprinting and development in the mouse. *Development Suppl.* 89–98.

Surani, M. A. H. (1986). Evidences and consequences of differences between maternal and paternal genomes during embryogenesis in the mouse. *In* "Experimental Approaches to Mammalian Embryonic Development" (J. Rossant and R. A. Pedersen, eds.), pp. 401–435. Cambridge University Press, New York.

Surani, M. A. H. (1991). Genomic imprinting: Developmental significance and molecular mechanism. *Curr. Opin. Genet. Dev.* **2,** 241–246.

Surani, M. A. H., Barton, S. C., and Kaufman, M. H. (1977). Development to term of chimaeras between diploid parthenogenetic and fertilized embryos. *Nature (London)* **270,** 601–602.

Surani, M. A. H., Barton, S. C., and Norris, M. L. (1984). Development of reconstituted mouse eggs suggests imprinting of the genome during gametogenesis. *Nature (London)* **308,** 548–550.

Surani, M. A. H., Barton, S. C., and Norris, M. L. (1986). Nuclear transplantation in the mouse: Heritable differences between parental genomes after activation of the embryonic genome. *Cell* **45,** 127–136.

Swain, J. L., Stewart, T. A., and Leder, P. (1987). Parental legacy determines methylation and expression of an autosomal transgene: A molecular mechanism for parental imprinting. *Cell* **50,** 719–727.

Szulman, A. E., and Surti, V. (1984). Complete and partial hydatidiform moles: Cytogenetic and morphological aspects. *In* "Human Trophoblast and Neoplasms" (R. A. Patillo and R. O. Hussa, eds.), pp. 135–146. Plenum, New York.

Takagi, N. (1974). Differentiation of X chromosomes in early female mouse embryos. *Exp. Cell Res.* **86,** 127–135.

Takagi, N., Sugawara, O., and Sasaki, M. (1982). Regional and temporal changes in the pattern of X-chromosome replication during the early post-implantation development of the female mouse. *Chromosoma (Berlin)* **85,** 275–286.

Tarkowski, A. K., Witkowska, A., and Opas, J. (1977). Development of cytochalasin B-induced tetraploid and diploid/tetraploid mosaic mouse embryos. *J. Embryol. Exp. Morphol.* **41,** 47–64.

Thomson, J. A., and Solter, D. (1988). The developmental fate of androgenetic, parthenogenetic, and gynogenetic cells in chimeric gastrulating mouse embryos. *Genes Dev.* **2,** 1344–1351.

Thomson, J. A., and Solter, D. (1989). Chimeras between parthenogenetic or androgenetic blastomeres and normal embryos: Allocation to the inner cell mass and trophectoderm. *Dev. Biol.* **131,** 580–583.

Thorey, I., Pedersen, R. A., Linney, E., and Oshima, R. G. (1992). Parent-specific expression of a human keratin 18/β-galactosidase fusion gene in transgenic mice. *Dev. Dynam.* **195,** 100–112.

Trasler, J. M., Alcivar, A. A., Hake, L. E., Bestor, T., and Hecht, N. B. (1992). DNA methyltransferase is developmentally expressed in replicating and non-replicating male germ cells. *Nucleic Acids Res.* **20,** 2541–2545.

Tybulewicz, V. L., Crawford, C. E., Jackson, P. K., Bronson, R. T., and Mulligan,

R. C. (1991). Neonatal lethality and lymphopenia in mice with a homozygous disruption of the c-abl proto-oncogene. *Cell* **65,** 1153–1163.

Ueda, T., Yamazaki, K., Suzuki, R., Fujimoto, H., Sasaki, H., Sasaki, Y., and Higashinakawa, T. (1992). Parental methylation patterns of a transgenic locus in adult somatic tissues are imprinted during gametogenesis. *Development* **116,** 831–839.

Van de Berg, J. L., Johnston, P .G., Cooper, D. W., and Robinson, E. S. (1983). X-chromosome inactivation and evolution in marsupials and other mammals. *In* "Isozymes: Current Topics in Biological and Medical Research," Vol. 9, pp. 201–218.

Varmuza, S. (1992). Teratogenic effects of parthenogenetic cells from LTXBO mice, a strain which develops ovarian tumours at high frequency. *Rouxs Arch. Dev. Biol.* **201,** 142–148.

Varmuza, S., Mann, M., and Rogers, I. (1993). Site of action of imprinted genes revealed by phenotypic analysis of parthenogenetic embryos. *Dev. Genet.* **14,** 239–248.

Villar, A., and Pedersen, R. A. (1994). Spatially restricted imprinting of mouse chromosome 7. *Mol. Reprod. Dev.* **37,** 247–254.

Wakasugi, N., Tomita, T., and Kondo, K. (1967). Differences of fertility in reciprocal crosses between inbred strains of mice DDK, KK and NC. *J. Reprod. Fertil.* **13,** 41–50.

Winking, H., and Silver, L. M. (1984). Characterization of a recombinant mouse t haplotype that expresses a dominant maternal effect. *Genetics* **108,** 1013–1020.

Yoo-Warren, H., Pachnis, V., Ingram, R. S., and Tilghman, S. M. (1988). Two regulatory domains flank the mouse H19 gene. *Mol. Cell. Biol.* **8,** 4707–4715.

Zemel, S., Bartolomei, S. M., and Tilghman, S. M. (1992). Physical linkage to two mammalian imprinted genes, H19 and insulin-like growth factor 2. *Nature Genet.* **2,** 61–65.

Zhang, Y., Shields, T., Crenshawq, T., Hao, Y., Moulton, T., and Tycko, B. (1993). Imprinting of human H19: Allele-specific CpG methylation, loss of the active allele in Wilms tumor, and potential for somatic allele switching. *Am. J. Hum. Genet.* **53,** 113–124.

Zhang, Y., and Tycko, B. (1992). Monoallelic expression of the human H19 gene. *Nature Genet.* **1,** 40–44.

NOTE ADDED IN PROOF. It has recently been shown that the murine insulin 1 and 2 genes are imprinted in the yolk sac (biallelic expression of both genes was detected in embryonic pancreas) (Giddings *et al., Nature Genet.* **6,** 310–313, 1994). Additionally, two groups have identified a new imprinted splicing factor-related gene on mouse chromosome 11 (Hatada *et al., Nucleic Acids Res.* **21,** 5577–5582, 1993; Hayashizaki *et al., Nature Genet.* **6,** 33–40, 1994). In humans, *SNRPN* is imprinted similarly to the murine *SnrpN* gene (Glenn *et al., Human Molec. Genet.* **2,** 2001–2005, 1993); the Wilms' tumor suppressor gene is imprinted in some but not all human placentae (Jinno *et al., Nature Genet.* **6,** 305–309, 1994); and biallelic expression of *IGF2R* has been detected using PCR (Kalscheuer *et al., Nature Genet.* **5,** 74–78, 1993).

8

Mechanisms of Nondisjunction in Mammalian Meiosis

Ursula Eichenlaub-Ritter
Universität Bielefeld, Gentechnologie/Mikrobiologie
33501 Bielefeld, Germany

I. Introduction

Nondisjunction as a disturbance in the segregation of chromosomes was first detected and described by Bridges in 1913 in studies of the sex chromosomes of *Drosophila*. According to the "Glossary of Genetics" (Rieger *et al.*, 1991), the term "nondisjunction," as used today, generally refers to the failure of chromatids or homologous chromosomes to disjoin at anaphase to the spindle poles. Thus, nondisjunction results in the production of daughter cells that are aneuploid, being either hyperploid, with extra chromosomes, or hypoploid, with chromosomes missing. In the extreme, if all chromatids or homologs fail to disjoin, polyploidy results. In a broader sense, genetic nondisjunction comprises all types of abnormal meiotic behavior that induce aneuploidy. This chapter discusses the mechanisms of nondisjunction with regard to the origin of aneuploidy in mammalian germ cells at the molecular, cellular, and tissue level.

The importance of nondisjunction in meiosis versus that in mitosis becomes obvious when considering the consequences of both events. A monosomic or trisomic cell arising during mitosis in a mammalian tissue, particularly if it originates from nondisjunction at a late stage of development preceding terminal differentiation, will usually have limited effects,

Current Topics in Developmental Biology, Vol. 29

involving only the cell itself and its derivatives, whose chances of cell survival and fitness might become restricted because of the unbalanced chromosomal constitution and altered gene expression (Antonarakis *et al.*, 1993). In contrast, aneuploidy arising during meiosis will result in a chromosomally unbalanced embryo after fertilization [reviewed in Bond and Chandley (1983)]. Especially in mammals, a hypoploid or hyperploid condition due to the loss or gain of an autosome leads to a severe disturbance in development, affects the physiological and mental condition, and reduces the life expectancy of the affected individual (e.g., Epstein, 1986; Hook, 1986; Gearhart *et al.*, 1987). Most numerical chromosomal aberrations, particularly monosomies, appear to be incompatible with normal embryonic and fetal development in mammals and will induce abortion (Gropp *et al.*, 1975; Hassold and Jacobs, 1984). Accordingly, about 40% of all spontaneously aborted human embryos and fetuses have chromosomal aberrations, and of these more than 50% carry autosomal trisomies and another 19% exhibit sex chromosome aneuploidies (Hsu, 1992). Of those autosomal trisomies detected by amniocentesis, 30% (for trisomy 21) to 68% (for trisomy 18) cause fetal death within the first and second trimester, and data from chorionic villus sampling have linked even considerably higher percentages of fetal death to chromosomal aberrations, probably because such data include the loss of abnormal embryos at early stages of development (Hook *et al.*, 1988; Hsu, 1992). In humans, trisomy 21 is the most common autosomal aneuploidy in live offspring, and an extra chromosome 13 or 18, or an extra sex chromosome, are also compatible with development to term [reviewed in Hassold and Sherman (1993)]. In the mouse, trisomy of autosome 19, the smallest chromosome, permits longer survival than any other autosomal aneuploidy, but like other numerical chromosomal aberrations, it is associated with congenital malformations and a short lifespan (Epstein, 1985). Since embryos with a severe chromosomal imbalance are unable to develop normally after fertilization, genetic or occupationally induced predisposition to meiotic nondisjunction may result in fetal wastage, reduced fertility, or even total sterility (e.g., Lyon and Meredith, 1966; Gropp and Winking, 1982; Allen *et al.*, 1986; Chandley *et al.*, 1986; Eichenlaub-Ritter and Winking, 1990) [for a review, see also Speed (1990)]. Even a trisomic condition corrected by the loss of one surplus chromosome during early embryogenesis may have adverse effects if it results in uniparental disomy, with two copies of a chromosome from one parent. Depending on whether the respective chromosomes are maternally or paternally imprinted [for a review, see Wilson (1992)], gene expression may be affected, and the individual may suffer from a disorder such as Prader-Willi syndrome despite an apparently "normal" chromosome constitution (Cassidy *et al.*, 1992). Thus, meiotic aneuploidy followed by secondary nondisjunction that is complemented by loss or gain

of a chromosome during early embryogenesis can cause genetic disorders in mammals (Peterson *et al.*, 1992a).

Among all mammals, humans appear to have the highest rate of meiotic nondisjunction. Aneuploidy is estimated to occur in 18–19% of oocytes and in 3–4% of sperm (Martin *et al.*, 1991). In older women, up to 60% of all oocytes may be chromosomally unbalanced (Hassold and Jacobs, 1984), and on the average 1 in 13 conceptions, and possibly more than 1 in 5 may result in a chromosomally defective embryo (Plachot, 1991; Burgoyne *et al.*, 1991). The incidence of aneuploidy in other mammals is much lower, with estimates of less than 2% at conception (Bond and Chandley, 1983). This difference may be related to environmental factors that uniquely affect human health or may reflect differences among species in genetic constitution and pattern of development of germ cells. Distinct predisposing factors and mechanisms of nondisjunction appear to exist as supported by the following observations, (i) the incidence of aneuploidy is sex related, being considerably higher in the oocyte than in the spermatocyte, particularly in humans (Pellestor, 1991b; Martin *et al.*, 1991); (ii) the most important risk factor for nondisjunction in humans and several other mammals is the age of the individual, which appears to significantly affect female meiosis I, but not male meiosis (Bond and Chandley, 1983; Catala *et al.*, 1988; Hassold and Jacobs, 1984; Estop, 1989; Hatch *et al.*, 1990); and (iii) there appear to be chromosome-specific differences in the incidence of nondisjunction (Pellestor, 1991a; Zenzes *et al.*, 1992; Hassold and Sherman, 1993; Kamigushi *et al.*, 1993). Thus, the history and development of a germ cell, the individual genetic constitution, and the importance of a chromosome in cell development all affect the occurrance of nondisjunction. The purpose of this chapter is to give an overview of recent data on the origin of aneuploidy, the factors responsible for disturbances in the development of mammalian germ cells, and ideas about the mechanisms underlying chromosomal nondisjunction in spermatogenesis and oogenesis.

II. Methods of Detecting Nondisjunction in Mammalian Meiosis

The oocytes and spermatocytes of mammals are not easily accessible to studies on the mechanisms of nondisjunction as are, for instance, the spermatocytes of insects (e.g., Steffen *et al.*, 1986; Nicklas *et al.*, 1979; Janicke and LaFountain, 1989; Nicklas and Arana, 1992) or the oocytes of some marine organisms (e.g., Inoue and Sato, 1967; Sluder *et al.*, 1989), which are ideally translucent and can be flattened, contain few clearly recognizable chromosomes, and can be manipulated without adverse ef-

fects. To detect nondisjunction in mammalian meiosis, indirect methods have usually been employed. These methods involve three strategies: (i) cytologic or genetic detection of a preceding meiotic nondisjunction event in embryos, the fetus, or live-born offspring; (ii) cytogenetic analysis of the chromosomal constitution of spermatocytes and sperm; and (iii) cytogenetic analysis of maturing, metaphase II-arrested or parthenogenetically activated oocytes. Investigators have also developed a method for a direct analysis of meiotic nondisjunction, in which spindle formation and chromosomal behavior are examined after fixation and processing of germ cells for anti-tubulin immunofluorescence.

Although much information has been accumulated on nondisjunction in humans (reviewed in Hassold and Jacobs, 1984; Chandley, 1988; Speed, 1990; Burgoyne *et al.*, 1991; Hassold and Sherman, 1993), ethical considerations make it necessary to use animal models for experimental studies. The majority of research has been performed on mice and rats (e.g., Polani and Jagiello, 1976; Brook and Chandley, 1986; Eichenlaub-Ritter *et al.*,1988a; Adler *et al.*,1989; Martin-DeLeon, 1989; Mailhes *et al.*, 1990; de Boer *et al.*, 1991; Nachman, 1992), but there are also studies on other mammals, such as the common shrew, *Sorex araneus* (Mercer *et al.*, 1992); the vole, *Microtus* (Tates *et al.*,1989); the hamster (e.g., Sugawara and Mikamo, 1983; Hummler *et al.*, 1987); and some domestic animals (e.g., Blazak, 1987; Power, 1987; Iwasaki *et al.*, 1989) [for review, see Bond and Chandley (1983) and Speed (1990)].

In experimental animals such as the mouse, the incidence of nondisjunction in male and female meiosis can be assessed earliest in embryos that have been recovered from the ampullae after the first embryonic S-phase, exposed to nocodazole, and then spread (Catala *et al.*, 1988; Martin-DeLeon, 1989; Mailhes *et al.*, 1990; de Boer and van der Hoeven, 1991). Since the formation of the spindle during syngamy has been blocked, condensed chromosomes of paternal and maternal origin generally remain in separate regions of the cytoplasm and can be distinguished by their relative degree of condensation. Thus, in studies of embryos from mature C57B1/6J × CBA/Ca hybrid mice, Catala and colleagues (1988) showed that hyperploidy was low (1.69%) and involved male as often as female pronuclear chromosomes. However, the incidence of nondisjunction appeared to be significantly higher in female meiosis when embryos of immature and aged females were analyzed.

In humans, chorionic villus sampling and amniocentesis are the earliest tests for numerical chromosomal aberrations in the embryo and for nondisjunction during meiosis [reviewed in Milunsky (1992)]. However, in a trisomic condition, it cannot be determined whether the male or the female gamete caused the chromosomally unbalanced state unless the homologous chromosomes exhibit either structural heteromorphisms (e.g., Mik-

kelsen *et al.*, 1980) or DNA polymorphisms at or near centromeres. The availability of highly polymorphic markers for all human chromosomes and centromere-specific polymorphisms for most of them has allowed investigators to trace the origin of extra chromosomes to the maternal or paternal meiosis and to distinguish between errors in chromosome segregation during the first and second meiotic divisions. These data indicate that nondisjunction primarily occurs at female meiosis I (e.g., Antonarakis *et al.*, 1992; Hassold and Sherman, 1993; Peterson *et al.*, 1992b) (Fig. 1). Moreover, use of the polymerase chain reaction in linkage analysis between polymorphisms of centromeric or pericentromeric markers, and such along chromosome arms, as well as those between interstitial and distal markers, has opened up new ways of studying the mechanisms of meiotic nondisjunction with regard to recombination (Hassold *et al.*, 1991; Sherman *et al.*, 1991; Peterson *et al.*, 1992b; Lorda-Sanchez *et al.*, 1992; Tanzi *et al.*, 1992).

A direct analysis of nondisjunction in spermatocytes has been possible in those animal models in which testes can be recovered and cells can be easily separated, fixed, and spread (Evans *et al.*, 1964; Chandley, 1975;

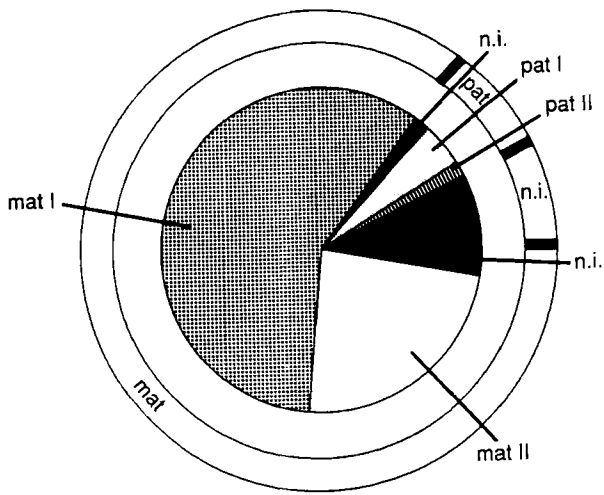

Fig. 1 Parental origin and meiotic stage of nondisjunction in 68 cases of trisomy 21 as determined by DNA polymorphisms (Peterson *et al.*, 1992b). As shown in other studies, the majority of surplus chromosomes appears to be generated by nondisjunction during maternal (mat) meiosis, predominantly during first maturation division (mat I). Only a minority [between 4 and 7%; according to studies by Antonarakis *et al.* (1992) and Sherman *et al.* (1991)] are due to errors in chromosome distribution during paternal meiosis (pat) or during mitosis. pat I/pat II, mat I/mat II, nondisjunction during first or second paternal or maternal meiosis, respectively; n.i., not informative cases for parental origin or division, or mitotic error.

Laurie *et al.*, 1985; Brook and Chandley, 1986; Miller and Adler, 1992). However, human testicular tissue generally becomes available only when patients attend a clinic for infertility (e.g., Chandley *et al.*, 1986). The chromosomal constitution of sperm from apparently normal human males has been determined after interspecific fusion of zona-free hamster eggs with human spermatozoa (Rudak *et al.*, 1978; Martin, 1983), since condensed pronuclear sperm chromosomes become available for cytogenetic analysis 12–14 hr after fusion of the gametes. In the future, this time-consuming method may be replaced by techniques that do not require the presence of condensed chromosomes and in which chromosome-specific probes are directly hybridized to sperm (Guttenbach and Schmid, 1991; Coonen *et al.*,1991; Goldman and Hulten, 1992a,b; Holmes and Martin, 1993). For single copy sequences, each sperm head should contain one signal, whereas no signal or multiple spots indicate nullisomy or polysomy for the respective chromosome (Figs. 2A–2D). For examination of the relationship among homologous pairing (Fig. 2E), chiasma distribution, and nondisjunction, prophase spermatocytes have been surface spread to follow the formation of synaptonemal complexes (e.g., Solari, 1980; Chandley *et al.*, 1986).

The fundamental difference between spermatocytes and oocytes in meiotic maturation is reflected in the methods employed to detect nondisjunction and its mechanisms in the two types of cells. Mammalian oocytes are among the most long-lived cells and they do not continually undergo meiosis in the adult as spermatocytes do. Since oocytes enter meiotic S-phase and the early stages of meiosis in the embryo, fetal ovarian material must be used for oocyte analysis of pairing and synaptonemal complex formation (e.g., Speed and Chandley, 1983; Speed, 1985, 1988). In contrast, the distribution of chiasmata becomes visible only when ovarian oocytes that have been arrested in the dictyate stage of meiosis for months or decades are experimentally released from the antral follicles of adult females and thus become induced to resume meiosis spontaneously (e.g., Henderson and Edwards, 1968; Jagiello *et al.*, 1973; Polani and Jagiello, 1976). In metaphase II-arrested oocytes obtained from spontaneous cycles after ovulation, or after hormonal stimulation, errors in chromosome segregation during first meiosis can be assessed with regard to risk factors (e.g., Tarkowski, 1966; Mailhes *et al.*, 1993; Tease and Fisher, 1991a,b; Eichenlaub-Ritter and Boll, 1989) (Figs. 2F and 2G), whereas second meiotic nondisjunction may become visible in either fertilized eggs prior to syngamy or parthenogenetically activated oocytes (O'Neill and Kaufman, 1989). Most of the data concerning human metaphase II-arrested oocytes were obtained by studying oocytes that failed to develop after *in vitro* fertilization (IVF) (reviewed in Martin *et al.*, 1991; Pellestor, 1991a,b; Plachot, 1991; Zenzes, 1992; Kamiguchi *et al.*, 1993).

Only recently have methods been developed that allow the direct detection of meiotic nondisjunction. Spontaneously maturing oocytes in first meiotic division or oocytes arrested at metaphase II are processed for antitubulin immunofluorescence. Combined with preservation and staining of chromosomes, their behavior can be studied (Eichenlaub-Ritter *et al.*, 1986, 1988a,b; Pickering *et al.*, 1988; Albertini, 1992). Spindle dynamics can also be observed in living cells (Gorbsky *et al.*, 1990). These methods not only reveal the depolymerizing activity of drugs but also the consequences of a brief exposure which might interfere with chromosome distribution during recovery from drug treatment (Eichenlaub-Ritter and Boll, 1989). Thus the relative orientation of chromosomes can be analyzed during prometaphase I and metaphase I (Fig. 3), and the lagging of homologs or failure to disjoin can be recognized (Eichenlaub-Ritter and Winking, 1990). Since the oocytes of some mammals will develop *in vitro* from the dictyate stage to metaphase II, another important parameter in nondisjunction, the progression of cells through the cell cycle, as well as stage-specific alterations in gene expression and protein phosphorylation, can also be analyzed (e.g., Eichenlaub-Ritter, 1989, 1993) [see also Wickramasinghe and Albertini (1993)].

So far, no comparable method is available for studying spermatogenesis. However, immunofluorescence methods are currently being developed for this purpose (Gassner, personal communication), and the successful cultivation of spermatocytes on Sertoli-like feeder cells (Rassoulzadegan *et al.*, 1992) opens up new perspectives for understanding certain aspects of the development of male gametes. Disturbances in cell-cycle progression in spermatogenesis are currently assayed by comparing the fraction of spread cells in different meiotic stages (e.g., Miller and Adler, 1992).

III. Disturbances Predisposing to Nondisjunction

Three main risk factors for meiotic aneuploidy have so far been identified. The most important one is advanced maternal age, which contributes significantly to human fetal wastage [reviewed in Bond and Chandley (1983), Hassold and Chiu (1985), Hook (1986), Warburton (1989), and Gaulden (1992)]. Second, heterozygosity for chromosomal translocations appears to increase the risk for nondisjunction in male and female meiosis [reviewed in Gropp and Winking (1981), Speed (1990), Pellestor (1990), and Martin and Hulten (1993)]. Finally, exposure to physical or chemical genotoxic influences increases errors in chromosome segregation (e.g., Allen *et al.*, 1986; Mailhes *et al.*,1993; Eichenlaub-Ritter and Boll, 1989; Miller and Adler, 1992; Tease, 1992; Sudman *et al.*, 1992).

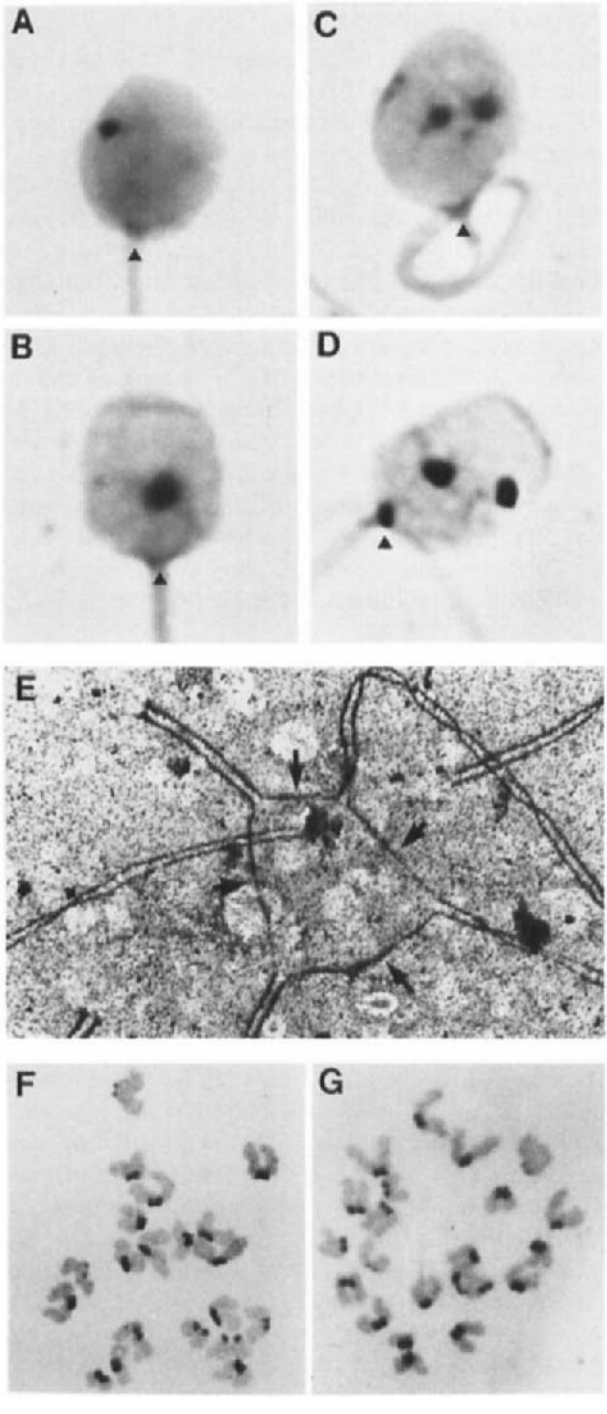
A
C
B
D
E
F
G

Although the association of aneuploidy with these factors has been established, the mechanisms underlying errors in chromosome segregation at the cellular level remain unclear. In the following sections, the possible sites for disturbances and the mechanisms for nondisjunction are discussed in more detail.

A. Chromosomes and Recombination

From studies of lower eukaryotes, particularly yeast, it has been known for some time that mutations affecting the integrity of chromosomes, the organization of chromatin, or chromatid and centromere cohesiveness increase nondisjunction (e.g., Meeks-Wagner and Hartwell, 1986; Rose *et al.*, 1990; Masison and Baker, 1992). In the meiosis of higher eukaryotes, those disturbances which affect the timely resolution of chiasmata at first anaphase and the attachment of chromatids throughout first division are thought to contribute to aneuploidy. In oocytes from the surf clam the activity of topoisomerase II has been tested with regard to chromosome segregation. Surprisingly, the separation of chromosomes during anaphase I was neither delayed nor disturbed when inhibitors for topoisomerase II were applied to cells with condensed chromosomes. This finding indicates that although topoisomerases may be required for decatenation, resolution of interlocked chromosomes during meiotic prophase (Moens and Earnshaw, 1989), and condensation of chromosomes (Wright and Schatten, 1990), the resolution of chiasmata at the transition to anaphase I may not require concurrent activity of topoisomerase II. In contrast, chromosomes failed to separate when spindles assembled in extracts of *Xenopus* eggs were treated with topoisomerase II inhibitors at anaphase II and nondis-

Fig. 2 Methods of detecting nondisjunction and its origin. (A–D) *In situ* hybridization of a biotinylated chromosome 17-specific satellite probe to human sperm nuclei. Euploid sperm nuclei with one hybridization signal (A,B). Aneuploid nuclei with two distinct hybridization signals (C,D), indicating disomy of chromosome 17 as a result of male meiotic nondisjunction. Arrowheads indicate the darker stained basal plate of the sperm nuclei. (Kindly provided by Professor Dr. M. Schmid, Department of Human Genetics, University of Würzburg). (E) Microspread spermatocyte of a patient with an autosomal translocation involving chromosomes 3 and 5 (Guichaoua *et al.*, 1992). Arrows indicate areas of the quadrivalent with asynapsis around the translocation breakpoints, which may affect progression through meiosis, spermatogenic arrest, and susceptibility to nondisjunction. (Courtesy of B. Speed and A. C. Chandley, MRC, Edinburgh.) (F,G) C-banded chromosomes of metaphase II-arrested mouse oocytes after maturation *in vitro*. Euploid complement of a control oocyte (F). Hyperploid oocyte (G) after first meiotic nondisjunction induced by transient exposure of oocytes to the microtubule-depolymerizing drug nocodazole. [From Eichenlaub-Ritter and Boll (1989).]

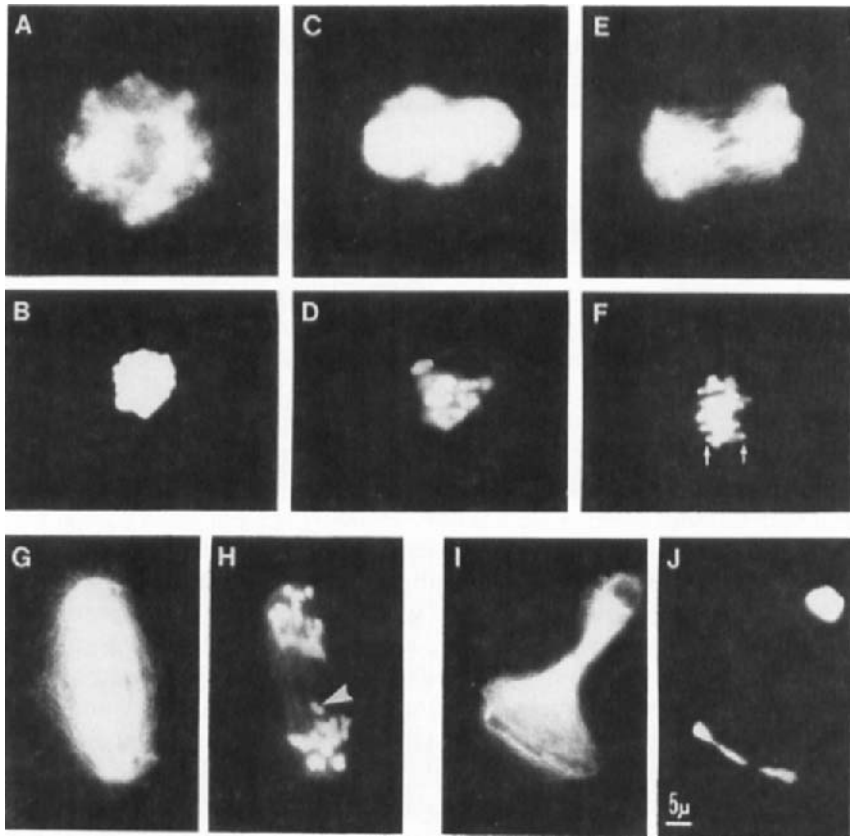

Fig. 3 Spindle formation and chromosomal behavior in maturing mouse oocytes during first meiosis. During prophase I, multiple asters are assembled near condensed chromosomes after germinal vesicle breakdown (A,B). In prometaphase I, a bipolar spindle is formed and bivalents migrate between the poles (C,D). During metaphase I, all bivalents have aligned at the equator of the barrel-shaped spindle, with centromeres of homologs (arrows) oriented toward opposite spindle poles (E,F). Sequential separation of individual bivalents can be observed during anaphase I (G,H); arrowhead points to a late migrating chromosome (H). At telophase I, all chromosomes have reached the spindle poles in the polar body (lower portion) or in the oocyte proper (upper portion), respectively. A,C,E,G,I: anti-tubulin immunofluorescence; B,D,F,H,J: DAPI-stained chromosome of the same cell. [From Eichenlaub-Ritter and Boll (1989).]

junction resulted (Shamu and Murray, 1992). Therefore, disturbances in topoisomerase expression may be responsible for nondisjunction during meiosis, but appear to have particularly severe effects during the second division and mitosis, while first prophase may fail altogether without functional topoisomerase.

Whereas topoisomerase is essential for mitosis and meiosis, a gene product has been identified in *Drosophila* that attaches chromatids at the kinetochores during first division up to anaphase II and appears to be meiosis specific. Mutations in this gene lead to equational nondisjunction, presumably due to the presegregation of chromatids (Kerrebrock *et al.*, 1992). Mutations in another meiotic gene in yeast whose product is involved in synaptonemal complex formation cause total arrest of meiotic progression before M-phase (Sym *et al.*, 1993). These observations imply that synapsis in meiosis of eukaryotes may be monitored by a meiotic quality control, which usually prevents progression into later stages when disturbances occur [reviewed in Hawley and Arbel (1993)]. In mammals, a possibly similar component of synaptonemal complexes has been detected, but its function has not yet been tested (Smith and Benavente, 1992a). With the advent of recombinant gene technology, more genes functionally homologous to those of *Drosophila* and yeast may soon be identified in oogenesis or spermatogenesis of mammals.

Controversy still surrounds the question whether pairing, recombination, and synapsis are essential for proper chromosome distribution during meiosis, and whether the appearance of univalents in first meiosis will necessarily result in random or precocious segregation, or anaphase lagging. In yeast, there is compelling evidence that disturbances in recombination may cause a high incidence of nondisjunction. This effect appears to be due to both precocious sister chromatid separation and nondisjunction of homologs (e.g., Sears *et al.*, 1992). On the other hand, mere recombination is not sufficient to ensure disjunction of alien DNA in yeast, whereas the introduction of a yeast recombinational hot spot, together with crossing over, restores fidelity of chromosome segregation (Ross *et al.*, 1992). Therefore, it has been suggested that only crossovers that occur within a specific region or context are sufficient to ensure disjunction (Hawley and Arbel, 1993).

The evidence from animal models is contradictory. Several studies have demonstrated that the number of univalents and the types of chromosomes that frequently are asynapsed in prometaphase I and metaphase I are not necessarily associated with increased nondisjunction (Polani and Jagiello, 1976; Sugawara and Mikamo, 1983; Wauben-Penris *et al.*, 1983; Liang *et al.*, 1986). However, particularly in humans, there is good evidence that maternal age-related increases in nondisjunction of chromosome 21 at meiosis I are correlated with reduced recombination (Sherman *et al.*,

1991; Tanzi *et al.*, 1992). The meiotic map of chromosome 21 in trisomies resulting from errors in chromosome segregation during female meiosis I shows that culminative recombination becomes significantly reduced from 24 to 99 cM (Hassold and Sherman, 1993) (Fig. 4). Similarly, reduced recombination is implied when extra maternal X chromosomes are found (Lorda-Sanchez *et al.*, 1992; Hassold and Sherman, 1993). However, these observations do not necessarily mean that the absence of a chiasma has resulted in nondisjunction. While the vast majority of nondisjoined chromosomes 21 of maternal origin and those originating from failure in paternal X/Y chromosome separation do not exhibit any crossing-over at all (Hassold *et al.*, 1991; Sherman *et al.*, 1991), the majority (90 and 82%, respectively) of extra chromosomes 16 and of the X of maternal origin have at least one cross-over [reviewed by Hassold and Sherman (1993)]. The trisomic maternal X and chromosome 21 may even have increased recombination at the pericentromeric region (Hassold *et al.*, 1991; Peterson *et al.*, 1992b). Since the genetic map of those extra chromosomes 21 which resulted from nondisjunction during second meiosis is also reduced (Fig. 4), it may not be univalency in meiosis I as such that is the predisposing factor. Rather, an overall altered distribution and frequency of recombination in risk groups may indicate another disturbance, for instance in chromosomal constitution, or in cell-cycle progression during early prophase of germ-cell development, which affects the behavior of individual chromosomes on the spindle. Maternal meiosis I and II nondisjunction with reduced recombination is thus also associated with advanced maternal age, at least for chromosome 21 in man (e.g., Antonarakis *et al.*, 1992), whereas the mitotic (Antonarakis *et al.*, 1993) or infrequent paternal meiotic errors in chromosome segregation do not appear to be age related since they occur mostly at the mean normal reproductive age of 27 years (Antonarakis *et al.*, 1992).

Recombination is not randomly distributed along chromosomes of mammals, but appears to depend on sex (Fisher Lindahl, 1991; Tanzi *et al.*, 1992; Hunt and LeMaire, 1992; McKee and Handel, 1993) and to be enhanced in euchromatic areas of chromatin rich in (CAGG) or CA/GT repeats (Fischer Lindahl, 1991; Pearlman *et al.*, 1992); in consensus sequences for transcription factors, enhancers, and promoters (Fisher Lindahl, 1991); and in chromatin with a particularly open conformation at R-bands (Chandley, 1986) which are associated with hyperacetylated histone H4 (Jeppeson and Turner, 1993). A hotspot in the mouse H-2 locus thus coincides with a DNase I hypersensitive site (Shenkar *et al.*, 1991). It has been suggested that both chromosome organization and recombination are correlated with early replication (Chandley, 1986; McKee and Handel, 1993). In accordance, recombination occurs early during telomere formation in yeast (Pluta and Zakian, 1989), and formation of the synapto-

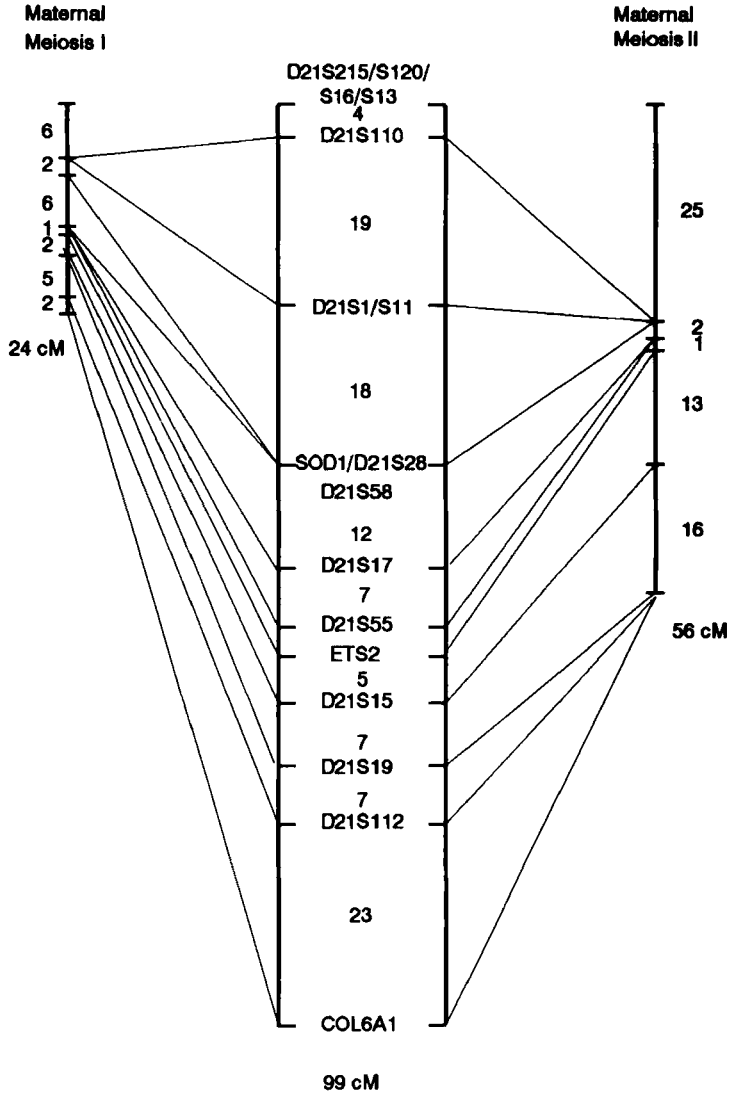

Fig. 4 Genetic linkage map of a normal chromosome 21 from a human female (middle) compared to that of a surplus chromosome 21 of a trisomy due to nondisjunction during first meiotic division (left) or to a second meiotic error (right). Relative genetic distances between loci are given in centimorgans. [Modified from Hassold and Sherman (1993).]

nemal complex is often initiated at telomeres (Speed, 1988; Mohandes *et al.*, 1992). At the same time, genetic exchange appears to be enhanced at meiosis in subtelomeric regions in mammals such as humans and mice (Polani, 1972; Hulten *et al.*, 1990; O'Connell *et al.*, 1987; Tanzi *et al.*, 1992). Moreover, it has been shown that telomeres themselves seem to enhance recombination, at least in male meiosis (Ashley *et al.*, 1993a,b; Ashley and Ward, 1993). The high incidence of chiasmata near telomeres may thus be one mechanism in preventing the occurrence of univalents and nondisjunction in germ cells, particularly in male meiosis. In contrast, delay in S-phase (Polani and Crolla, 1991) or altered chromatin conformation may be responsible for reductions in recombination at telomeres in a cohort of oocytes that can resume meiosis only at increased maternal age and are at high risk for nondisjunction (Tanzi *et al.*, 1992). In addition, polymorphisms at telomeres may upset the process of homologous pairing of certain chromosomes and predispose them to aneuploidy (e.g., chromosome 16 in man) [reviewed by Ledbetter (1992)].

The sex-specific accessibility of chromatin for proteins engaged in transcription (Thomas and Rothstein, 1991), replication (Jeppeson and Turner, 1993), and recombination could generally govern the efficiency and timing of these events in different regions of the chromosome. Disturbances in chromosomal constitution and time of replication may delay the synaptic process preceding recombination and induce gametogenic failure (Mittwoch and Mahadevaiah, 1992). McKee and Handel (1993) propose that in cases of meiotic delay, double-strand breaks at recombination hotspots that appear early in meiotic prophase (Padmore *et al.*, 1991) fail to be repaired efficiently. The delay in homologous pairing may therefore result in a prevalence of damaged DNA. This condition can have two consequences. First, a disturbance in cell-cycle progression or total meiotic arrest may be initiated because a meiotic quality control mechanism senses the DNA damage. In yeast, such a quality control can either delay or prevent meiotic progression beyond the G2-stage (Bishop *et al.*, 1992; Bennett *et al.*, 1993; Resnick, 1993). Second, even if mammalian germ cells escape the initial arrest, since repair would be taking place at a later stage than in normal development, the timing of distal meiotic events could still be affected. For instance, cytoplasmic and nuclear maturation events may become uncoupled or the synchrony in anaphase trigger and chromosome separation may be disturbed. Alterations in the overall rate and distribution of chiasmata may also affect the sequential disjoining of homologs in bivalents at first anaphase, predispose to premature separation (predivision), or cause a delay in resolution of chiasmata (with anaphase lagging). All of these events could induce nondisjunction.

In mitosis, chromosome separation appears to proceed in a well-ordered and rather synchronous fashion (Vig, 1983). From studies on the meiotic

maturation of oocytes evidence for a sequential rather than synchronous segregation of homologs to the spindle poles during first anaphase has been obtained (Eichenlaub-Ritter *et al.*, 1988a) (Figs. 3g and 3h). So far, investigators have not attempted to characterize a sequential order relative to individual chromosomes, and/or the presence and distribution of chiasmata, mainly due to technical difficulties. Anaphase is considerably shorter than other meiotic stages, and only a few of a population of unselected and asynchronously dividing cells will have just initiated this stage. However, evidence for the existence of a defined order in the sequence of chromosome separation in mammalian meiosis has been provided (Hummler and Hansmann, 1985). A technique for inducing metaphase I-arrested mouse oocytes to enter anaphase I has been developed (Soewarto and Eichenlaub-Ritter, 1993). Studies combining this method with *in situ* hybridization with chromosome-specific probes may elucidate correlations between recombination, the order of chromosome segregation, and nondisjunction in mammalian meiosis.

Several of the extrinsic factors that might affect chromosomal integrity and thereby induce aneuploidy have been studied, including radiation and drugs that induce chromosome breaks or chemical modifications of DNA. Although direct effects of radiation on spindles have not been observed, the results of radiation studies imply that, at least for oocytes, the predominant mechanism of malsegregation is based on exchanges between sister chromatids and the presence of dicentric or acentric chromosomes rather than on damage to kinetochores at anaphase (de Boer and van der Hoeven, 1991). Studies examining the relative sensitivity of male and female germ cells to chromosome breakage by ionizing radiation and drugs have not provided unequivocal evidence of a sex-limited mutagenic effect. However, the degree of sensitivity may be linked to sex and the stage of development during exposure (Tease, 1992). Even if the mechanisms underlying the nondisjunction induced by these factors during meiotic division are similar in the two sexes, the relative significance for aneuploidy in offspring may still be different, since spermatogenic cells with damaged chromosomes may be selected against and therefore may be undetectable in the embryo [discussed by Tease (1992)]. The selection against some such cells could be due to disturbances in postmeiotic gene expression (e.g., Erickson, 1993). Oocytes may escape such quality control if the exposure to radiation, drugs, or noxes has occurred fairly close to the time of resumption of meiosis, when cells have already acquired an abundant store of mRNA transcripts.

In general, structural rearrangements and chromosome breaks are much more common in mammalian sperm than oocytes, and their incidence in sperm increases with age of the male (e.g., Martin and Rademaker, 1987; Estop *et al.*, 1991). This difference could reflect an effective repair system

in oocytes, as has been suggested by mutation studies [reviewed in Russell and Russell (1992)]. On the other hand, oocytes appear to be particularly susceptible to the chromosomal aberrations produced by intercalating chemicals, which probably induce unequal exchanges between chromosomes, resulting in the appearance of univalents, ring or chain multivalents, and single chromatids (Sudman *et al.*, 1992). Since these changes are likely to promote nondisjunction, the oocyte may be at greater risk than sperm for chromosomal imbalance induced by drugs such as the cancer chemotherapeutic agent bleomycin (Sudman *et al.*, 1992).

Genetic predisposition to nondisjunction has been shown in many studies to be correlated also with heterozygosity for translocations (e.g., Rickards, 1983; Hansmann *et al.*, 1988; Pellestor, 1990; Speed, 1990; Martin and Hulten, 1993; Nicklas and Arana, 1992). While the segregation behavior of different translocations varies enormously, is unpredictable, and is assumed to be unique for individual chromosomes (Chandley, 1988; Templado *et al.*, 1990; Tease and Fisher, 1991b; Martin and Hulten, 1993), it seems to follow some general rules. Thus, in humans risk rates for unbalanced segregants diagnosed through amniocentesis are inversely related to the size of the reciprocal translocation [reviewed in Hsu (1992)]. However, lower risk of large translocations may also be related to a higher degree of lethality resulting in undetected early embryonic or fetal loss (Hsu, 1992). An effect of the reciprocal translocation on the behavior of other chromosomes, e.g., on numerical chromosomal aberrations and nondisjunction (interchromosomal effect), has so far not been statistically established in man (e.g., Spriggs *et al.*, 1992; Schinzel *et al.*, 1992; Hsu, 1992), but has been implicated in malorientation and aneuploidy under certain conditions in translocation stocks of mice, for example, those which carry large multivalents during meiosis [reviewed by Hansmann *et al.* (1988)]. Occasionally, second meiotic nondisjunction in carriers of reciprocal translocation may contribute to the chromosomally unbalanced state (Masuno *et al.*, 1991), perhaps because of a failure in proper alignment of chromosomes on the spindle (see later and Fig. 6d).

In paracentric inversions, recombination in the inverted segments may give rise to dicentric and acentric chromosomes, both of which appear to be highly unstable during meiosis since they either cannot become attached to the spindle or fail to orient correctly. As in trisomy, the chromosomal duplication/deletion state in the postmeiotic cell will almost certainly result in embryonic failure and early fetal death (Hsu, 1992).

Interestingly, most structural heterozygotes of reciprocal translocations show changes in autosomal chiasma frequency per cell (e.g., Chandley *et al.*, 1986; Goldman and Hulten, 1993a). Studies on meiotic progression have also implied that pairing may be impaired, particularly at translocation breakpoints (Guichaoua *et al.*, 1992; see Fig. 2E), and that the period

from S-phase to diplotene may concomitantly become longer [reviewed by Hansmann *et al.*, (1988) and Van Buul *et al.* (1992)]. Studies using fluorescence *in situ* hybridization (FISH) have for the first time correlated the incidence and distribution of chiasmata with first meiotic segregation patterns (Goldman and Hulten, 1993a,b). Further studies of this type may allow predictions of the behavior of chromosomes with regard to translocation breakpoints in distal or proximal arms of the affected chromosomes, or their location in a G-positive or G-negative region (Ashley, 1990). It may thus become feasible to correlate the presence and localization of a chiasma relative to the breakpoints, the degree of nonhomologous pairing [synaptic adjustment, reviewed by Speed (1990) and Ashley (1990)], and the likelihood that balanced gametes will be produced in the carriers of such heterozygous translocations. Such studies may also reveal why certain heterozygous Robertsonian translocations, in which whole acrocentric chromosomes are translocated at their centromeres, have a high risk for nondisjunction, whereas others become distributed with normal fidelity (Pellestor, 1990). One can speculate that in certain translocations, telomeric sequences may be retained at the translocation breakpoint and may induce unscheduled recombination (Ashley and Ward, 1993; Ashley *et al.*, 1993a). The data available so far suggest that D-D Robertsonian translocations in humans are very stable, whereas translocations involving chromosome 21 are likely to induce nondisjunction (Hsu, 1992). The basis for this disparity is unclear, but it may reflect either steric constraints that favor adjacent orientation of the Rb chromosome and the single chromosome 21 in a trivalent, or synaptic and recombinational failure.

Studies on experimental and wild animals suggest that comparatively newly established Rb translocation events, particularly if exposed to an allopatric genetic background, have a different outcome than evolutionary old ones that have undergone natural selection for many generations (Searle, 1990; Mercer *et al.*, 1992; Wallace *et al.*, 1992). For instance, Searle (1990) did not detect increased nondisjunction in zones of overlap between subpopulations of *Sorex araneus* carrying different Robertsonian translocations. Similarly, Wallace and colleagues (1992) observed only slightly reduced fertility in wild mice heterozygous for a single Robertsonian metacentric. Near-normal fertility may, however, be the result of (i) an increase in the overall number of germ cells and embryos, or (ii) selective loss of abnormal germ cells with pairing failures at pachytene (Wallace *et al.*, 1992) rather than represent prevention of nondisjunction through a compensatory mechanism that controls the correct orientation or positioning of chromosomes at prometaphase and metaphase I of meiosis. In contrast, crosses between wild mice with many different Robertsonian translocations usually produce subfertility or infertility in the heterozy-

gous animals (e.g., Eichenlaub-Ritter and Winking, 1990). This finding, and several similar observations, has led to the assumption that Robertsonian translocation is implicated in speciation due to the high rates of nondisjunction in meiosis (e.g., Baker and Bickham, 1986; Eichenlaub-Ritter and Winking, 1990). Spindles and chromosome orientation in heterozygous carriers of Robertsonian translocations of wild mice in female meiosis have been examined to elucidate the origin of this type of genetic predisposition to nondisjunction at the cellular level. The results of these studies are discussed in the next section.

B. Spindle Apparatus and Cytoskeleton

The segregation of chromosomes during meiosis involves concerted and complex interactions between chromosomes and cytoskeletal components. Whereas spindle formation in mammalian spermatocytes has not yet been directly observed, several immunofluorescent studies have revealed the unique, centriol-free, barrel-shaped spindle apparatus in oocytes (see Fig. 3) and the relative positioning of chromosomes during first and second meiosis (e.g., Eichenlaub-Ritter *et al.*, 1988a,b; Eichenlaub-Ritter and Boll, 1989; Maro *et al.*, 1985; Pickering *et al.*, 1988; Schatten *et al.*, 1985; Van Blerkom and Henry, 1992; Albertini, 1992). The microtubules in oocyte spindles have been demonstrated to turn over rapidly (Gorbsky *et al.*, 1990). In meiosis, as in mitosis, characteristic elements, the kinetochores, have to be assembled at centromeres that may induce polymerization of microtubules, can capture microtubules, and provide sites for attachment of spindle fibers and motor proteins for chromosome congression and anaphase movement [for review, see Earnshaw and Tomkiel (1992), Bloom (1993), and Wadsworth (1993)]. Thus, any disturbance in kinetochore formation and the dynamics of tubulin polymerization might impede chromosome distribution in both sexes. In fact, disorders involving structurally aberrant centromeres, such as in Roberts syndrome, may predispose not only to aneuploidy in somatic tissues but also to reduced fertility, presumably due to nondisjunction and chromosomally unbalanced germ cells (Fitzgerald *et al.*, 1986; Gabarron *et al.*, 1986).

Studies concerning the group of centromere proteins (CENP) have shown that the injection of antibodies against CENP C, a basic protein of M_r 107,000 that is located at the inner plate of trilaminar kinetochores and can bind to DNA, disrupts mitosis in HeLa cells by inhibiting the assembly of kinetochores. When applied at G2-phase, the antibodies impair kinetochore formation, and the resulting fragile kinetochores are pulled apart during anaphase (Earnshaw *et al.*, 1993). Disturbances of chromosome separation and, at the extreme, polyploidy will result. Al-

though all mutations leading to defective kinetochores generally predispose to aneuploidy in mitosis as well as in meiosis, some processes, such as the pronounced reorientation and migration of bivalents back and forth between spindle poles during meiotic prometaphase I or the promotion of microtubule polymerization by chromatin in a meiotic cell, may involve meiosis-specific gene products (Rieder *et al.*, 1993). Thus, antibodies against a centromeric protein of 80 kDa prevent chromosome congression when injected before prometaphase I into mouse oocytes but not when injected at metaphase I or II (Simerly *et al.*, 1990). Injection at prometaphase also induces micronucleus formation and nondisjunction due to lagging and the inability of chromosomes to assemble correctly on the spindle (Simerly *et al.*, 1990). The formation of micronuclei is likewise induced by mutant NuMA-protein, a factor associated with spindle poles during mitotis and the nuclei during interphase (Crompton and Cleveland, 1993). NuMA is also expressed in mammalian oogenesis and may have a function in chromosome condensation and in spindle and pronuclear formation (U. Eichenlaub-Ritter *et al.*, in preparation). Therefore, when the distribution or expression of such proteins fails, bivalents segregate randomly.

Other genes and gene products that are implicated in meiotic nondisjunction have been identified in *Drosophila*. They provide for the ordered segregation of chromosomes that have not undergone recombination (distributive pairing) and are related to the microtubule motor protein kinesin (Knowles and Hawley, 1991). The presence of such proteins in a meiotic cell (only divisions in the oocyte and early embryo appear to depend on these proteins) provides further support to the idea that recombination may not be essential for proper chromosome segregation during first meiosis and that germ cells possess redundant systems ensuring that homologues will be faithfully distributed. The addition of antibodies to a similar protein, Eg5, belonging to the kinesin superfamily or the immunodepletion of this protein also affects spindle formation in meiotic cell extracts of *Xenopus* (Sawin *et al.*, 1992). It may therefore be necessary for maintaining spindle pole integrity and interactions between antiparallel microtubules (Sawin *et al.*, 1992). To date, no meiosis-specific kinesin-related proteins have been identified in mammals, but the existence of multiples of such potential motor proteins in diverse mitotic cells and many species [for reference see Wadsworth (1993)] suggests that they may also be present and functioning in germ cells.

Malfunctioning of spindles is postulated to be a major source of meiotic nondisjunction and has been implicated in chemically induced meiotic aneuploidy in female and male meiosis (e.g., Mailhes and Marchetti, 1993; Miller and Adler, 1992), as well as maternal age-related predisposition to nondisjunction [for reference see Eichenlaub-Ritter *et al.* (1988a), and

Eichenlaub-Ritter and Boll (1989), Albertini (1992), and Gaulden (1992)]. Evidence for the adverse effect of drugs or influences interfering with microtubule polymerization comes from several sources, including studies on the effect on mouse oocytes of colchicine (Tease and Fisher, 1986; Mailhes *et al.*, 1990), nocodazole (Eichenlaub-Ritter and Boll, 1989), vinblastine-sulfate (Russo and Pacchierotti, 1988), benomyl (Mailhes and Aardema, 1992), griseofulvin (Tiveron *et al.*, 1992), ethanol (O'Neill and Kaufman, 1989), and low temperature (Pickering and Johnson, 1987), as well as from observations on postovulatory aged oocytes of humans and mice arrested at metaphase II (Eichenlaub-Ritter *et al.*, 1986, 1988b; Pickering *et al.*, 1988). Although oocytes appear to be more susceptible to the activity of many genotoxic drugs and microtubule-depolymerizing agents (Mailhes *et al.*, 1993) than spermatocytes (Miller and Adler, 1992), some compounds do not appear to affect female nondisjunction significantly (Mailhes *et al.*, 1993). This observation and findings linking the incidence of nondisjunction with time of treatment and dose have made it clear that risk assessment is difficult and that such factors as the biology of the germ cell itself, chemical pharmacokinetics, and mode of action must all be considered for meaningful assessment of the nondisjunctional potential of any agent *in vivo*.

Our own work on oocytes maturing *in vitro* (Eichenlaub-Ritter and Boll, 1989) and studies *in vivo* by several other groups have implied that the influence of genotoxic drugs on spindle structure leads to a delay in meiotic progression (Hummler *et al.*, 1987; Miller and Adler, 1992; Mailhes and Marchetti, 1993) [reviewed by Hansmann *et al.* (1988)]. Such alterations in meiotic progression may be the main reason for the disturbance in chromosome segregation, since most cells exposed to depolymerizing drugs are able to assemble spindles with normal morphology after recovery (Eichenlaub-Ritter and Boll, 1989). However, the effects on timing of meiotic events may be more severe and cannot be reversed (Fig. 5). Janicke and LaFountain (1989) have shown that the meiotic delay after exposure of spermatocytes of the crane fly to any condition or drug inhibiting microtubule polymerization, such as low temperature, colcemid, or nocodazole, may induce premature loosening of centromeric dots that appear to represent kinetochores of sister chromatids. This event, which usually is triggered only at second meiosis, may facilitate the malorientation of sister kinetochores to opposite poles, lagging at anaphase, and nondisjunction. Furthermore, meiotic cells appear to speed up development to adjust to their normal gametogenic schedule after a block in maturation due to microtubule depolymerization (Eichenlaub-Ritter and Boll, 1989; Eichenlaub-Ritter, 1993). This faster development can result in a dramatic shortening of the time available for spindle formation and chromosome orientation before anaphase I, as well as a less stringent

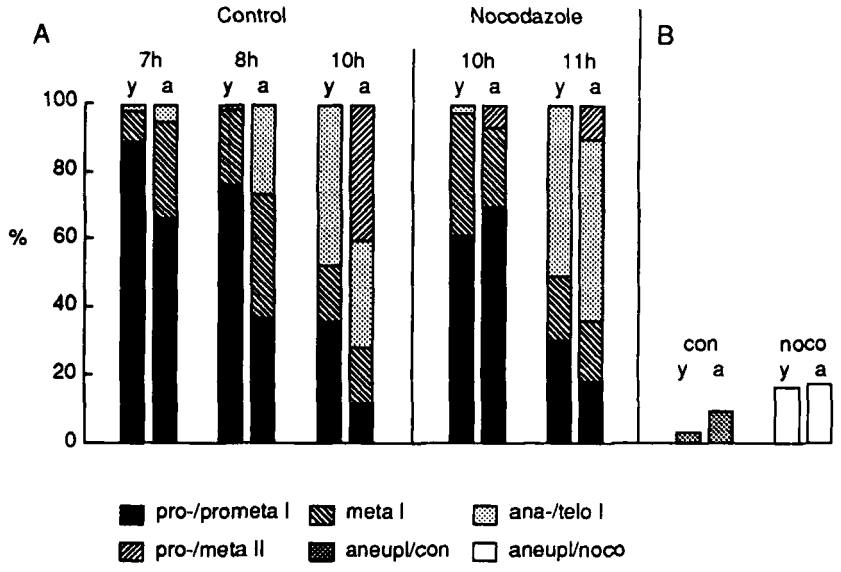

Fig. 5 (A) Kinetics of cell-cycle progression of oocytes from young (y) or aged (a) CBA/Ca mice during spontaneous maturation *in vitro*. (Left) Control: Oocytes from both age groups were processed for indirect immunofluorescence at defined times after resumption of maturation *in vitro*, and the percentage of cells in characteristic meiotic stages as presented in Fig. 3 was determined. There are always more oocytes in advanced stages of meiosis present in the population of cells obtained from aged females. (Middle) Nocodazole: After nocodazole exposure for 1 hr (after 7 hr of culture) and recovery, the percentages of cells in individual stages of meiosis are nearly identical in the cell populations obtained from young and aged mice. As a result, anaphase I is delayed by about 1 hr (after 11 hr instead of 10 hr of culture), and the time available for spindle formation after recovery from microtubule depolymerization and before anaphase I is reduced to about 3 hr. (B) (Right) Aneuploidy (conservatively estimated as 2× hyperploids) in metaphase II-arrested control (con) and nocodazole-exposed (noc) oocytes from young (y) or aged (a) CBA mice. Although nondisjunction increases, the differences in aneuploidy between age groups disappear after nocodazole treatment. [Data from Eichenlaub-Ritter and Boll (1989).]

fidelity of chromosome segregation (Eichenlaub-Ritter and Boll, 1989) (Fig. 5). Thus, depending on the time of exposure, increased nondisjunction may result not only from the reduction in the number of spindle fibers, but also from the uncoupling of events such as prometaphase congression and anaphase trigger, or chiasma resolution and cytokinesis. Therefore, meiotic delay may be a valuable test for a first assessment of the genotoxic potential of a drug (Mailhes and Marchetti, 1993; Miller and Adler, 1992).

The sex-specific differences in the effect of translocations (Gropp *et al.*, 1974) or exposure to spindle poisons (Mailhes *et al.*, 1993; Miller and

Adler, 1992) on nondisjunction in meiosis may partially reflect differences in the rate and distribution of recombination, but may also reside in differences between spindles of spermatocytes and oocytes [discussed in Eichenlaub-Ritter and Winking (1990) and Rieder *et al.* (1993)]. The spermatocyte of mammals possesses, like most other mitotically dividing animal cells, a pair of centrioles that replicate, divide, and become positioned at the center of the pointed spindle poles during meiosis. In contrast, the oocytes of mammals appear to lose their centrioles during early oogenesis, and a large number of microtubule organizing centers (MTOCs) form asters, are recruited by chromosomes, and become located at the poles of the barrel-shaped spindle during meiosis (e.g., Maro *et al.*, 1985; Schatten *et al.*, 1985; Eichenlaub-Ritter *et al.*, 1988a; Eichenlaub-Ritter and Winking, 1990; Pickering *et al.*, 1988; Messinger and Albertini, 1991). It has been suggested that under adverse conditions, particularly when multivalents are present or oocytes are temporarily exposed to depolymerizing drugs, multipolar spindles or several mini-spindles might be formed, resulting in a high risk of nondisjunction. However, it has been shown that mouse oocytes can establish a functional bipolar spindle (Figs. 6a and 6a′) in spite of the presence of a large ring multivalent in a Rb translocation heterozygote (Eichenlaub-Ritter and Winking, 1990). Nevertheless, almost no normal metaphase I stage with chromosomes aligned at the spindle equator was observed. Instead, the physical attachment of chromosomes in the multivalent by chiasmata appeared to stabilize adjacent orientations in which the centromeres of neighboring chromosomes faced to the same spindle pole (Fig. 6b) and remained displaced from the equator (Eichenlaub-Ritter and Winking, 1990). This may be a result of tension forces provided by microtubules attached to kinetochores of other chromosomes in the multivalent that face the opposite pole (Ault and Nicklas, 1989). After observing the position of trivalents in the spindle during the first meiotic metaphase of several insects, Nicklas and Arana (1992) proposed that during evolution, certain orientations of chromosomes in multivalents may become stabilized and may thus ensure alternate orientation of centromeres and correct alignment of chromosomes at the spindle equator. In situations when a relatively new chromosomal rearrangement is present in a heterozygote in mammals and, as a consequence, a multivalent is formed in meiosis, those mechanisms which mediate normal orientation to opposite poles may instead stabilize malorientation and genetic chaos (Nicklas and Arana, 1992). However, no evidence exists that the mammalian oocyte is more susceptible to such a disturbance in chromosome orientation than the spermatocyte. It has been concluded that asymmetric spindles and malorientation of chromosomes (Figs. 6b and 6b′), together with only slight disturbances in cell-cycle progression, and delayed asynchronous migration of homologues to spindle poles at first

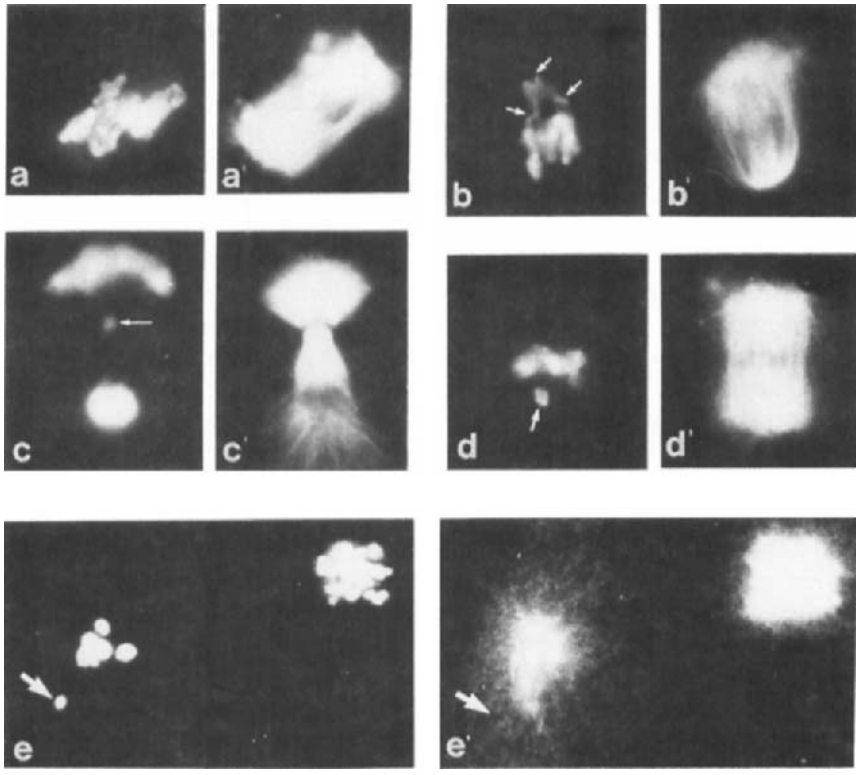

Fig. 6 (a–d) Spindles and chromosomes in oocytes of the CD/Cremona mouse which is heterozygous for 9 Rb translocations with alternating arm homologies. (a,a') A bipolar spindle can be formed during prometaphase I; however, chromosomes in the large ring multivalent do not appear to assemble at the spindle equator at metaphase I (b,b'), but remain maloriented, with centromeres of neighboring homologs facing the same spindle pole (arrows in b). At late telophase (c,c'), lagging of chromosomes is evident (arrow in c). During second metaphase (d,d'), chromosomes are also often displaced from the spindle equator (arrow in d). [From Eichenlaub-Ritter and Winking (1990).] (e,e') Unfertilized human oocyte after IVF with only one polar body, but two sets of chromosomes, some of which appear to be displaced from the remnants of the spindle (arrow). [From Eichenlaub-Ritter *et al.* (1988b).]

anaphase (Figs. 6c and 6c') in the translocation heterozygotes will predispose to aneuploidy since the homologues that separate latest can become trapped in the interpolar space. Secondary nondisjunction may contribute to additional chromosomal abnormalities, because some chromosomes in metaphase II do not become aligned at the spindle equator (Figs. 6d and 6d') and may therefore upset second meiosis (Eichenlaub-Ritter and Winking, 1990).

Several hypotheses on the etiology of maternal age-related increases in aneuploidy have connected nondisjunction to disturbances in the spindle. It has been postulated that spindle formation might be affected by insult to the oocyte's metabolism or to spindle precursors during the long resting period in dictyate stage in the ovary before resumption of maturation, or by alterations in hormonal environment and oxygen supply affecting the pH of the follicular fluid [for review, see Bond and Chandley (1983) and Gaulden (1992)]. In fact, spontaneously ovulated oocytes from aged CBA/Ca mice have shorter metaphase II spindles than oocytes from young mice, and their chromosomes are more often spread around the spindle equator. However, this effect is not strictly dependent on the chronological age of the female, but rather depends on the depletion and physiological age of the ovary (Eichenlaub-Ritter *et al.*, 1986). When oocytes from young and aged mice were obtained at the same day of the natural estrous cycle and observed first meiosis during their spontaneous maturation *in vitro*, no evidence for a disturbance in spindle formation in the aged oocytes was found. Nevertheless, even though culture conditions were the same for oocytes from both age groups, hyperploidy was elevated in oocytes from aged individuals (Eichenlaub-Ritter *et al.*, 1986; Eichenlaub-Ritter and Boll, 1989). This observation, along with comparisons of nocodazole-exposed oocytes from young and aged mice (see Fig. 5), led us to propose that alterations in cell-cycle progression rather than spindle formation per se may be the primary cause for maternal age-related predisposition to nondisjunction (Eichenlaub-Ritter and Boll, 1989). Therefore, differences in the response of oocytes of different age groups to drugs (Tease and Fisher, 1986; Mailhes and Yuan, 1987) may not arise from an altered sensitivity of the spindle, but rather may reflect characteristic changes in cell-cycle progression (see discussion in the next section).

When considering the site of action of genotoxic compounds, one should keep in mind that the microfilamentous cytoskeleton also has an important function in cellular organization of meiotic cells and in the final stages of chromosome segregation. The integrity of the microfilamentous system is especially important for the correct positioning of the spindle at the cell periphery in the large mammalian oocyte. Inhibitors of actin assembly arrest oocytes at metaphase I and, since this block in maturation may eventually be overcome, may result in polyploidy (e.g., Kubiak *et al.*, 1991; Soewarto and Eichenlaub-Ritter, 1993 and unpublished). In the mouse oocyte, the spindle appears to be tightly attached with its long axis perpendicular to the cell cortex by an actin shoulder. In contrast, in the human oocyte only one of the spindle poles is in contact with the cell cortex (Pickering *et al.*, 1988). The labile attachment and the ease with which spindles can be dislodged from the cell periphery in human oocytes

may explain the rather high incidence of "diploid" oocytes with two sets of metaphase II chromosomes (Figs. 6e and 6e′) among oocytes retrieved for IVF (e.g., Eichenlaub-Ritter *et al.*, 1988b). Disturbances in the regulation of actin assembly may therefore be one reason why even when a functional spindle is present in female meiosis there can be a total failure in chromosome disjunction, resulting in polyploidy and reduced fertility. Mitotic cells which express mutant forms of inner centromere proteins (INCENPs) exhibit similar phenotypes, in that newly divided cells rejoin to form a binucleate cell (W. E. Earnshaw, personal communcation). This suggests that INCENPs are also necessary in the process of cytokinesis. Failure of mammalian germ cells to express or target such INCENPs to the appropriate sites may therefore result in phenotypes resembling total nondisjunction (Schmiady *et al.*, 1994).

C. Cell Cycle

The cell cycle in all eukaryotic cells appears to be governed by highly conserved mechanisms and molecules. Central to the regulation of both mitosis and meiosis is the activity of the universal M-phase factor, maturation-promoting factor (MPF), which has two components: a regulatory subunit, cyclin B, and a catalytic subunit, the $p34^{cdc2}$ serin–threonine–kinase [reviewed by Maller (1991)]. Entry into M-phase and meiosis is regulated by a cascade of phosphorylation/dephosphorylation events and feedback controls, which ensure that (i) S-phase has been completed before division starts, and (ii) a spindle is present before anaphase is triggered [reviewed by Nishimoto *et al.* (1992)].

In mammalian meiosis, several studies indicate that for spermatocytes, the time before spindle formation and M-phase represents a selective barrier in which disturbances in meiotic progression, homologous pairing, and DNA damage are checked (e.g., Speed, 1990; Mittwoch and Mahadevaiah, 1992; Burgoyne *et al.*, 1992; Van Buul *et al.*, 1992). Nondisjunction is prevented because aberrant spermatocytes are likely to die [reviewed by Hansmann *et al.* (1988), Speed (1990), and Navarro *et al.* (1990)]. In oocytes, a similar checkpoint appears to exist during meiotic prophase I, before cells enter the diplotene and dictyate stages (Speed, 1988). Another quality control which induces atresia appears to operate before the resumption of meiosis. However, since oocytes inside atretic follicles can resume meiosis and undergo pseudomaturation, the quality control may instead operate by monitoring the physiological conditions in the oocyte and its environment instead of chromosome pairing, recombination, and synapsis. Only if an oocyte fails to respond to the signals from its environment restraining it from meiosis or if deficiencies in its microenvironment,

such as a reduced number or an impaired physiological state of corona cells release the meiotic arrest, apoptosis may be triggered [reviewed by Crisp (1992)]. However, oocytes which lagged behind in the gametogenic schedule during early prophase (Polani and Crolla, 1991) and escaped the initial checkpoint before entering dictyate stage or those which become damaged during the arrest in meiosis during dictyate stage may still be selected in a dominant follicle and resume meiosis. Selection of such oocytes may occure more often when the pool of "fit" cells and follicles has become depleted (Warburton, 1989) and the mechanisms sensing the metabolic state of the follicle have relaxed due to age or when the hormonal status is inadequate to sustain the control mechanisms.

Studies have shown that oocytes from aged females have a different constitution, which could result from both early meiotic inadequacies and changes in microenvironment, and are prone to altered progression through the cell cycle as well as nondisjunction (see Fig. 5) (Eichenlaub-Ritter and Boll, 1989; Eichenlaub-Ritter, 1993). Comparison of the protein phosphorylation patterns in GV-stage oocytes obtained from aged and young CBA/Ca mice revealed that a protein(s) with a M_r or 34K was less abundant in the old age group (Eichenlaub-Ritter, 1993). Since the status of protein phosphorylation and the presence of certain phosphoproteins are important factors governing the activity of microtubule-organizing centers in oocytes (Messinger and Albertini, 1991; Abertini, 1992), this reduction in protein phosphorylation may affect chromosome segregation. The activity of phosphatases has also been implicated in chromatid segregation and aneuploidy in somatic cells (e.g., Ghosh and Paweletz, 1992). Experiments are now in progress to determine whether these proteins might correspond to the catalytic subunit of MPF, the $p34^{cdc2}$ kinase, which is activated by differential dephosphorylation and regulates cell cycle progression (Maller, 1991; Wickramasinghe and Albertini, 1993). In fact, oocytes from aged females have an altered meiotic schedule, since they undergo GVBD later but initiate anaphase I and polar body formation sooner (Fig. 5) than oocytes from young mice (Eichenlaub-Ritter, 1993). Concomitantly, hyperploidy is more prevailent in the oocytes from aged mice (Eichenlaub-Ritter and Boll, 1989). Phenotypically similar alterations in the cell cycle can be induced in oocytes from young mice by transient exposure to a tumor-promoting phorbol ester, phorbol 12,13-dibutyrate, which can activate the calcium-phospholipid-dependent protein kinase and transcription [for reference see Eichenlaub-Ritter (1993)]. This treatment also induces lagging of chromosomes at telophase I and increases nondisjunction to a level comparable to that observed in untreated aged oocytes. Since the tumor promoter does not induce a significant rise in aneuploidy in oocytes from aged females (Table I), it is assumed that it predisposes to aneuploidy in oocytes from young mice by acting on a

Table I First Meiotic Nondisjunction of Mouse Oocytes Matured *in Vitro*

	Incidence of hyperploidy	
	Oocytes from young mice	Oocytes from aged mice
Control	1.5%[a]	5.7%[a]
After phorbol exposure	6.8%[b]	5.1%[b]

[a] From Eichenlaub-Ritter and Boll (1989).
[b] From Eichenlaub-Ritter (1993).

pathway in cell-cycle control converging with the pathway that is already disturbed in untreated oocytes of aged females (Eichenlaub-Ritter, 1993).

Tentative evidence indicates that the tumor promoter does not affect the phosphorylation of the p34 protein(s), but enhances transcription of the *c-mos* proto-oncogene. The product of this oncogene appears to correspond to the cytostatic factor maintaining oocytes at metaphase II until fertilization [for reference, see Kinloch and Wassarman (1993)]. Moreover, the *c-mos* protein binds to tubulin, and ablation of *c-mos* expression has been shown to arrest oocytes at GV-stage. Alterations in *c-mos* levels appear to affect spindle formation and induce disturbances in metaphase congression, failure in correct orientation of bivalents, and anaphase I lagging (I. Hansmann, personal communication). Hence, for both, the alterations in protein phosphorylation observed in aged oocytes and the alterations in expression of *c-mos* in oocytes exposed to the tumor promoter, the role of the affected gene product in cell-cycle regulation is linked to disturbances in meiotic progression and in chromosome distribution. As pointed out earlier, the disturbance with maternal age might reflect a delayed or sped up gametogenetic schedule which affected already early prophase, success of pairing, and genetic exchange in oocytes of the embryo, but might in addition reflect the altered physiological state of the ovary and the depletion of the oocyte pool. The phorbol-induced cell-cycle alterations and nondisjunction in mammalian oocytes and the tumor-promoting activities of phorbols in mitotic systems indicate that there may be common mechanisms underlying age-related aneuploidy and multistage carcinogenesis. The importance of certain tumor-suppressor genes for checkpoints in cell-cycle progression and the correlations between loss of function of these genes, disturbances in the cell cycle, and genetic instability have been recognized (Hartwell, 1992).

Further evidence that alterations in cell-cycle progression are involved in age-related aneuploidy was obtained from experiments in which nocoda-

zole was used to block oocytes in first prometaphase (Eichenlaub-Ritter and Boll, 1989). After the oocytes had recovered from the block, the age-related differences in maturation pattern were abolished concomitantly with those in aneuploidy (see Fig. 5).

These experiments also demonstrate that, at least for meiotic oocyte maturation, the second checkpoint in the cell cycle, before onset of anaphase, is operative, because oocytes without a spindle were arrested with condensed bivalents. Preliminary evidence exists that even a transient depolymerization of spindle microtubules may inhibit the deactivation of MPF (Soewarto and Eichenlaub-Ritter, 1993; B. Maro, personal communication), triggered by cyclin B degradation, and progression into anaphase. The possible consequences of this arrest in prometaphase have already been mentioned earlier. In normal meiosis, this checkpoint appears to ensure that chromosomes all align at the metaphase plate and orient correctly before they separate. However, a severe delay in overall meiotic progression under environmental stress or sped up development in oocytes from aged females may affect the synchrony in the chromosomal and cytoplasmic cycle and thus give rise to nondisjunction. The predivision of chromosomes observed in human oocytes (Angell, 1991) may be the result of the asynchrony in chromosomal and spindle events.

D. Physiological Parameters

Considerations on the contribution of disturbances in spindle formation and cell-cycle progression to meiotic nondisjunction imply that any condition which alters a physiological parameter in the gamete, such as gene expression, protein synthesis, protein phosphorylation, or calcium-homeostasis, has the potential to induce aneuploidy. Thus, elevations in free intracellular calcium in metaphase I-blocked oocytes can trigger first anaphase but can also induce precocious separation of centromeres of homologues (presegregation), which will predispose to second meiotic nondisjunction (Soewarto and Eichenlaub-Ritter, 1993 and unpublished). In second meiosis in mouse oocytes, inhibition of protein synthesis induces anaphase without fertilization, which has unknown consequences for fidelity of chromosome distribution.

It is not within the scope of this chapter to go into details on gene expression during gametogenesis, and readers interested in this topic are referred to reviews by Kinloch and Wasserman (1993) and Erickson (1993). However, the sex-specific developmental schedule should be taken into account when the risk factors and mechanisms of nondisjunction are discussed. The oocytes of mammals are extremely long-lived and fairly large cells. During most of their life span, they are meiotically arrested but

metabolically active (Wickramasinghe and Albertini, 1993), and they must provide many components for early embryonal development [reviewed by Kinloch and Wasserman (1993)]. The degree of maturity of the oocyte, its physiological state, and its competence to resume meiosis may be critical in determining predisposition to nondisjunction since oocytes from prepubertal mice that have been hormonally stimulated to resume meiosis show significantly greater amounts of hyperploidy than those from adult mice (Catala *et al.*, 1988). Immature oocytes arrested at metaphase I after maturation *in vitro* often possess highly aberrant spindles (U. Eichenlaub-Ritter, unpublished). Immaturity may also be a risk factor for meiotic nondisjunction in human oocytes since a plot of aneuploidy with advancing age gives a J-shaped curve, showing elevation in trisomy in offspring of very young as well as aged females (Erickson, 1978) [see also Gaulden (1992)]. Gene expression, in particular of cell-cycle regulating factors and of germ cell specific proteins supporting normal gametogenic development, appears to be very important. The time and extent of removal of imprints during gametogenesis, and new imprinting and *de novo* methylation of DNA, such as occur during oocyte growth (e.g., Ueda *et al.*, 1992), may thus have far-reaching consequences for the physiological state of the oocyte. For example, they may influence the status of chromosome condensation, efficiency of recombination, and gene expression.

For spermatocytes, the removal of imprints and hyperacetylated histone H4 (Jeppeson and Turner, 1993), and also the transcriptional inactivation of the single X chromosome in the sex vesicle, may be important for normal development and chromosome distribution. In the mouse, a meiotic gene product has been characterized that might control the allocyclic behavior of the sex chromosomes (Smith and Benavente, 1992b). Another critical phase in the physiological state of a spermatocyte is the time after meiosis, when postmeiotic gene expression, in particular of certain proto-oncogenes, is required (Erickson, 1993). Some sperm with certain chromosomal aberrations thus appear to be prezygotically selected against (Chayko and Martin-DeLeon, 1992). Since the sex chromosomes are for the most part transcriptionally inactive during meiosis, their nondisjunction, when they occasionally escape the meiotic quality control of pairing failure (see the following discussion), may contribute to the XXY condition in man (e.g., Lorda-Sanchez *et al.*, 1992).

E. Environment and Cell–Cell Interactions

The maturation of oocytes and spermatocytes is tightly regulated by interactions with their supportive cells and the environment. For example, maturation arrest of spermatocytes appears to be associated with abnor-

malities in Sertoli cell junctional connections (Meyer *et al.*, 1992). Atresia of oocytes is also accompanied by a loss of contact by gap junctions between oocyte and follicle cells. To prevent environmental insult leading to cell-cycle, spindle, or chromosome damage, the blood–testis barrier may be of particular importance for the spermatocyte, whereas the zona pellucida, which might represent a barrier to certain compounds or to physical stress, protects the oocyte only after the initial stages of prophase and growth [reviewed by Kinloch and Wassarman (1993)]. For interactions with granulosa and Sertoli cells, respectively, both types of germ cells appear to express the tyrosine kinase receptor *c-kit*. Although meiosis does not appear to depend on its expression either in spermatocytes or in oocytes (Yoshinaga *et al.*, 1991), oocytes and spermatogenic cells in mutant (W/W) mice of the W (white-spotting) locus, which corresponds to *c-kit*, develop more slowly [reviewed by Kinloch and Wassarman (1993)]. Given the possible importance of cell–cell interactions and mitogens for the initiation and timing of meiosis (e.g., Parvinen *et al.*, 1992), particularly in the female (Polani and Crolla, 1991), alterations in the kinetics of development may still affect meiosis and chromosome segregation indirectly. Thus, the ligand of *c-kit* may be part of a checkpoint in cell-cycle progression, since oocytes of juvenile Sl/Sl^{l} infertile females become blocked from further growth in primordial follicles.

It is well known that hormonal environment severely affects the developmental potential, degeneration, and atresia of germ cells. For instance, gonadotrophins may induce nondisjunction in oocytes of certain mammals, and the sensitivity to hormonal stimulation appears to be genetically determined and species specific (e.g., Hansmann *et al.*, 1988; de Boer *et al.*, 1991). It has been suggested that estrogenic compounds may also be involved in predisposition to nondisjunction by interfering with microtubule polymerization (Albertini, 1992). In addition, they may affect the pH of the follicular fluid. When oocytes were cultured at elevated pH, no increases in aneuploidy were found, therefore gonadotrophins may rather affect meiotic rate and nondisjunction indirectly (Eichenlaub-Ritter and Sobek-Klocke, 1993).

IV. Development, and Chromosome- and Sex-Specific Mechanisms of Nondisjunction

Human cytogenetic data imply that nondisjunction does not randomly affect all chromosomes (Fig. 7) and that chromosome-specific rates depend on sex (e.g., Pellestor, 1991b; Kamigushi *et al.*, 1993). Moreover, female meiotic errors but not those in male gametogenesis appear associated with advanced age (e.g., Antonarakis *et al.*, 1992). The patterns of maternal

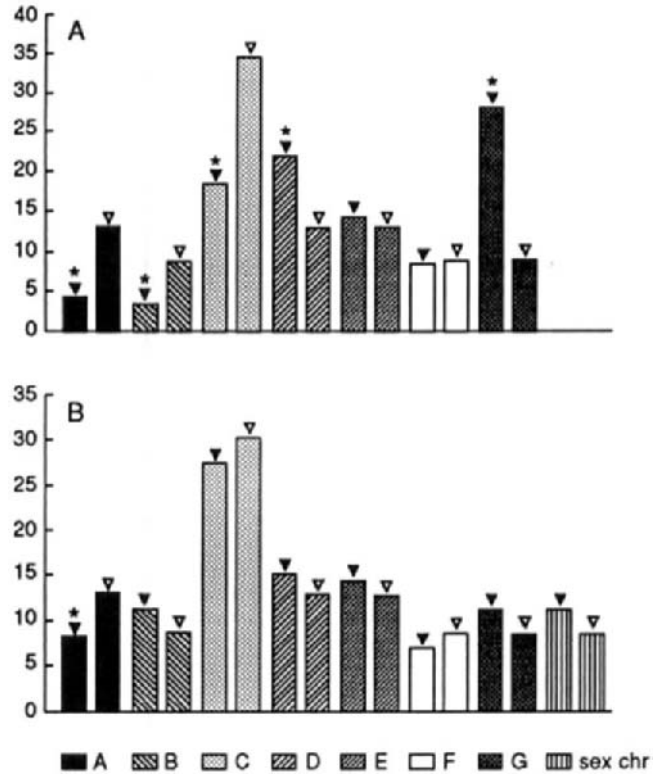

Fig. 7 The distribution of nondisjunction is nonrandom for chromosome groups in human oocytes (A) and sperm (B), and appears to be different in the two sexes. Frequencies of 2× hyperploidy as percentages (closed arrowheads) according to chromosome groups, as determined in several studies, compared to the expected frequencies of aneuploidy, assuming a random distribution of nondisjunction (open arrowheads). For some chromosome groups, the observed percentages of aneuploidy are lower (e.g., A-group), for others higher (e.g., G-group in oocytes), than the expected percentages. Significant differences between the expected and observed percentages are indicated by a star. [Collected data from Pellestor (1991).]

age-related increases in nondisjunction are, in addition, chromosome specific in that they may be rather linear over all ages or may become exponentially elevated from a certain age onward [reviewed by Sherman and Hassold (1993)]. Similarly, recombination frequencies differ among chromosomes and between the sexes (e.g., Tanzi *et al.*, 1992), possibly because of differences in chromatin conformation and gene expression in addition to differences in environment. Differences in gene expression are most evident in the sex chromosomes, since spermatocytes possess a Y chromosome that carries genes essential for spermatogenesis (Burgoyne *et al.*,

1992) and a transcriptionally inactive X chromosome, whereas reactivation of the X chromosome in females prior to meiosis may render both X chromosomes active [for review see Hunt and LeMaire (1992)]. Several studies in mammals as well as nonmammalian species show that the pairing of the X and Y chromosomes in particular is monitored by a meiotic quality control in males, because failure to pair induces spermatogenic impairment (Miklos, 1974; Burgoyne *et al.*, 1992). The pairing and the obligatory crossover of the XY pair in mammals are mediated by the pseudoautosomal region in the male, because the telomeric segments alone are insufficient to support formation of the synaptonemal complex (Mohandas *et al.*, 1992). In female meiosis, the efficiency of pairing and recombination between the two X chromosomes appears to be substantially reduced in the pseudoautosomal region (Hunt and LeMaire, 1992). Therefore, although pairing in the female may occur over the entire length of the X chromosomes, there is no pair of homologues in female meiosis that matches the male pseudoautosomal region in length, relative to efficiency in synapsis and recombination. Thus, the mechanism sensing failures in pairing may also be relaxed in oogenesis. This hypothesis is supported by the observation that the deletion of distal Xp in man arrests meiosis and causes azoospermia (Mohandas *et al.*, 1992). However, females with an XO constitution can still be fertile, although a perinatal wave of atresia reduces oocyte numbers dramatically and shortens the reproductive life span (Lyon and Hawker, 1973).

V. Summary: Current Concepts on Etiology of Nondisjunction in Mammals

Developing germ cells appear to be especially sensitive to any environmental insult or to a chromosomal constitution that induces perturbations in the highly ordered timing of events in meiotic progression. The interactions of germ cells with their supporting tissues may be one of the factors that decides meiotic success rate, since it may influence the kinetics of the initial phases of the cell cycle, particularly the S-phase. A delay in synapsis and recombination may delay pairing and repair of DNA breaks and may trigger meiotic arrest and atresia at the end of the meiotic prophase. However, germ cells that escape this quality control may have increased risks for nondisjunction since the early disturbance in cell-cycle progression may also affect distal meiotic events, for example, by causing the chromosome cycle to become uncoupled from anaphase progression. According to the sequence of separation for individual chromosomes at anaphase I, which may be influenced by the number and position of chiasmata, certain chromosomes are at elevated risk for either segregating prema-

turely or becoming trapped in the spindle at late anaphase and distributed randomly.

In mammalian meiosis, the risk factors for nondisjunction in males and females differ because of sex-dependent differences in the development and history, chromosomal constitution, and environment of the germ cells. The main risk factor for numerical chromosomal aberrations in oogenesis, maternal age, may be multifactorial in that a cohort of oocytes, many of which have disturbed recombination and altered cell cycles, may be left in the ovary of an aged female. The physiological age of the ovary, the limited oocyte pool, altered hormonal status, and a relaxed follicle selection may create a microenvironment that has additional adverse effects on oocyte constitution before actual resumption of meiosis. At the cellular level, the chromosome-specific distribution of chiasmata and alterations in protein phosphorylation and expression of cell-cycle regulating factors influence meiotic progression. Disturbances in these processes may cause asynchrony in chromosome separation and anaphase I, may favor precocious separation of certain bivalents, may hamper resolution of certain chiasmata, such as those near centromeres, and may cause lagging or delayed migration of others. In shortened cell cycles, late-separating chromosomes may be at high risk for becoming trapped in the interpolar space. All of these disturbances can ultimately result in aneuploidy.

In male meiosis, safeguarding mechanisms, particularly those which monitor the timing and extent of pairing of the X/Y gonosomes, may generally reduce the risk of aneuploidy since abnormal cells will die. However, in spermatogenesis, as in oogenesis, the adverse influences of chromosomal rearrangement, telomere polymorphisms, nonhomologous pairing, spindle poisons, or metabolic insult can upset fidelity of chromosome segregation, especially if they affect the coordination of events in cell-cycle progression.

It is of great importance in understanding mammalian nondisjunction to obtain further insights into the mechanisms that govern or may compromise cell-cycle control during meiosis and thus may be a main target for loss of fidelity of chromosome segregation in mammalian germ cells.

Acknowledgments

I gratefully acknowledge the contribution of several colleagues who shared their views, comments, and unpublished observations with me during the preparation of the manuscript for this chapter. The critical reading of the manuscript by Dr. R. Eichenlaub and Dr. A. C. Chandley is gratefully acknowledged. I apologize to all those workers whose papers were not cited, or were cited only through reviews, due to the restricted length of the review. This chapter is dedicated to Professor A. Ruthmann, my former teacher, whose advice, enthusiasm, and interest in my work has greatly supported my scientific efforts. This work was supported by the DFG (SFB 223).

References

Adler, I. D., Johannison, R., and Winking, H. (1989). The influence of the Robertsonian translocation Rb (X.2) 2Ad on anaphase I non-disjunction in mice. *Genet. Res.* **53,** 77–86.

Albertini, D. F. (1992). Cytoplasmic microtubular dynamics and chromatin organization during oogenesis and oocyte maturation. *Mutat. Res.* **296,** 57–68.

Allen, J. W., Liang, J. J., Carrano, V., and Preston, R. J. (1986). Review of the literature on chemically-induced aneuploidy in mammalian male germ cells. *Mutat. Res.* **167,** 123–137.

Angell, R. R. (1991). Predivision in human oocytes at meiosis I: A mechanism for trisomy formation in man. *Hum. Genet.* **86,** 383–387.

Antonarakis, S. E., Peterson, M. B., McInnis, M. G., Adelsberger, P. A., Schinzel, A. A., Binkert, F., Pangalos, C., Raoul, O., Salughterhaupt, S. A., Hafets, M., Cohen, M., Roulsen, D., Schwartz, S., Mikkelsen, M., Tranebjaerg, L., Greenberg, F., Hoar, D. I., Rudd, N. L., Warren, A. C., Metaxotou, C., Bartsocas, C., and Chakravarti, A. (1992). The meiotic stage of nondisjunction in trisomy 21: Determination by using DNA polymorphisms. *Am. J. Hum. Genet.* **50,** 544–550.

Antonarakis, S. E., Avramopoulos, D., Blouin, J.-L., Talbot, C. C., and Schinzel, A. A. (1993). Mitotic errors in somatic cells cause trisomy 21 in about 4.5% of cases and are not associated with advanced maternal age. *Nature Genet.* **3,** 146–150.

Ashley, T. (1990). Prediction of mammalian meiotic synaptic and recombination behavior of inversion heterozygotes based on mitotic breakpoint data and the possible evolutionary consequences. *Genetica* **83,** 1–7.

Ashley, T., Cacheiro, N. L. A., Russell, L. B., and Ward, D. C. (1993a). Molecular characterization of a pericentric inversion in mouse chromosome 8 implicates telomeres as promoters of meiotic recombination. *Chromosoma* **102,** 112–120.

Ashley, T., Ried, T., and Ward, D. C. (1993b). Multicolor fluorescence *in situ* hybridization (FISH) of meiotic and postmeiotic cells from XY_{Sxr} mice detects both nondisjunction and recombination. *Genetics* (in press).

Ashley, T., and Ward, D. C. (1993). A "hot spot" of recombination coincides with an interstitial telomeric sequence in the Armenian hamster. *Cytogenet. Cell Genet.* **62,** 169–171.

Ault, J. G., and Nicklas, R. B. (1989). Tension, microtubule rearrangements, and the proper distribution of chromosomes in mitosis. *Chromosoma* **98,** 33–39.

Baker, R. J., and Bickham, J. W. (1986). Speciation by monobranchial centric fusions. *Proc. Natl. Acad. Sci. USA* **83,** 8245–8248.

Bennett, C. B., Lewis, A. L., Baldwin, K. K., and Resnick, M. A. (1993). Lethality induced by a single site-specific double strand break in a dispensable yeast plasmid. *Proc. Natl. Acad. Sci. USA* **90,** 5615–5617.

Bishop, D. K., Park, D., Xu, L., and Kleckner, N. (1992). DMC1: A meiosis-specific yeast homolog of *E. coli recA* required for recombination, synaptonemal complex formation, and cell cycle progression. *Cell* **69,** 439–456.

Blazak, W. F. (1987). Incidence of aneuploidy in farm animals. *In* "Aneuploidy, Part A: Incidence and Etiology" (B. K. Vig, and A. A. Sandberg, eds.), pp. 103–116. A. R. Liss, New York.

Bloom, K. (1993). The centromere frontier: Kinetochore components, microtubule-based motility, and the CEN-value paradox. *Cell* **73,** 621–624.

Bond, D. J., and Chandley, A. C. (1983). "Aneuploidy." Oxford monographs on medical genetics, No. 11. Oxford University Press, Oxford.

Bridges, C. B. (1913). Nondisjunction of the sex chromosome in Drosophila. *J. Exp. Zool.* **15,** 587–606.

Brook, J. D., and Chandley, A. C. (1986). Testing for the chemical induction of aneuploidy in the male mouse. *Mutat. Res.* **164,** 117–125.

Burgoyne, P. S., Holland, K., and Stephens, R. (1991). Incidence of numerical chromosomal anomalies in human pregnancy estimation from induced and spontaneous abortion data. *Hum. Reprod.* **6,** 555–565.

Burgoyne, P. S., Mahadevaiah, S., Sutcliffe, M. J., and Palmer, S. J. (1992). Fertility in mice requires X-Y pairing and a Y-chromosomal "spermiogenesis" gene mapping to the long arm. *Cell* **71,** 391–398.

Cassidy, S. B., Lai, L. W., Erickson, R. P., Magnuson, L., Thomas, E., Gendron, R., and Herrmann, J. (1992). Trisomy 15 with loss of the paternal 15 as a cause of Prader-Willi syndrome due to maternal disomy. *Am. J. Hum. Genet.* **51,** 701–708.

Catala, V., Estop, A. M., Santalo, J., and Egozue, J. (1988). Sexual immaturity and maternal age: Incidence of aneuploidy and polyploidy in first cleavage mouse embryos. *Cytogenet. Cell Genet.* **48,** 233–237.

Chandley, A. C. (1975). Human meiotic studies. *In* "Modern Trends in Human Genetics" (A. E. H. Emery, ed.), Chap. 2. Butterworth, London.

Chandley, A. C. (1986). A model for effective pairing and recombination at meiosis based on early replication sites (R-bands) along chromosomes. *Hum. Genet.* **72,** 50–57.

Chandley, A. C. (1988). Meiosis in man. *TIG* **4,** 79–84.

Chandley, A. C., McBeath, S., Speed, R. M., Yorsten, L., and Hargreave, T. B. (1987). Pericentric inversion in human chromosome 1 and the risk for male sterility. *J. Med. Genet.* **24,** 325–334.

Chandley, A. C., Speed, R. M., McBeath, S., and Hargreave, T. B. (1986). A human 9;20 reciprocal translocation associated with male infertility. *Cytogenet. Cell Genet.* **41,** 145–153.

Chayko, A. C., and Martin-DeLeon, P. A. (1992). The murine Rb (6.16) translocation: Alterations in the proportion of alternate sperm segregants effecting fertilization *in vitro* and *in vivo*. *Hum. Genet.* **90,** 79–85.

Compton, D. A., and Cleveland, D. W. (1993). NuMA is required for the proper completion of mitosis. *J. Cell Biol.* **120,** 947–957.

Coonen, E., Pieters, M. H., Dumoulin, J. C., Meyer, H., Evers, J. L., Ramaekers, F. C., and Geraedts, J. P. (1991). Nonisotopic *in situ* hybridization as a method for nondisjunction studies in human spermatozoa. *Mol. Reprod. Dev.* **28,** 18–22.

Crisp, T. M. (1992). Organization of the ovarian follicle and events in its biology: Oogenesis, ovulation or atresia. *Mutat. Res.* **296,** 89–106.

de Boer, P., and van der Hoeven, F. A. (1991). Chromosome damage and nondisjunction in normal and mutant female mice irradiated at the diakinesis stage of female meiosis. *Mutat. Res.* **248,** 155–162.

de Boer, P., van der Hoeven, F. A., Wolters, E. M., and Mattheij, J. A. (1991). Embryo loss, blastomere development and chromosome constitution after chorionic gonadotrophin-induced ovulation in mice and rats with regular cycles. *Gynecol. Obstet. Invest.* **32,** 200–205.

Earnshaw, W. C., and Tomkiel, J. E. (1992). Centromere and kinetochore structure. *Curr. Opin. Cell Biol.* **4,** 86–93.

Earnshaw, W. E., Saitoh, J. E., Tomkiel, J. E., Cooke, C. A., Bernat, R. L., Rathrie, H., Maurere, M., and Rothfield, N. F. (1993). Molecular cloning and characterization of human centromeric autoantigen CENP-C: A component of the inner kinetochore plate. *In* "Chromosomes Today" (A. T. Sumner and A. C. Chandley, eds.), Vol. 11, pp. 23–34. Chapman and Hall, London.

Eichenlaub-Ritter, U. (1989). The spindle of mammalian oocytes: Alterations in morphology and progression through meiosis with maternal age. *In* "Molecular and Cytogenetic Studies of Non-disjunction" (T. J. Hassold and C. J. Epstein, eds.), pp. 199–220. A. R. Liss, New York.

Eichenlaub-Ritter, U. (1993). Studies on maternal age-related aneuploidy in mammalian oocytes and cell cycle control. *In* "Chromosomes Today" (A. Sumner and A. C. Chandley, eds.), Vol. 11, pp. 323–226. Chapman and Hall, London.

Eichenlaub-Ritter, U., and Boll, I. (1989). Nocodazole sensitivity, age-related aneuploidy, and alterations in the cell cycle during maturation of mouse oocytes. *Cytogenet. Cell Genet.* **52,** 170–176.

Eichenlaub-Ritter, U., Chandley, A. C., and Gosden, R. G. (1986). Alterations in the microtubular cytoskeleton and increased disorder of chromosome alignment in spontaneously ovulated mouse oocytes aged *in vivo*: An immunofluorescent study. *Chromosoma* **94,** 337–345.

Eichenlaub-Ritter, U., Chandley, A. C., and Gosden, R. G. (1988a). The CBA mouse as a model for maternal age-related increases in aneuploidy in man: Studies on oocyte maturation, spindle formation and chromosome alignment during meiosis. *Chromosoma* **96,** 220–226.

Eichenlaub-Ritter, U., and Sobek-Klocke, I. (1993). Implications of meiotic cell cycle disturbances for meiotic aneuploidy: Studies on a mouse model system. *In* "Chromosome Segregation and Aneuploidy" (B. K. Vig, ed.), pp. 173–182. Springer-Verlag, Heidelberg.

Eichenlaub-Ritter, U., Stahl, A., and Luciani, J. M. (1988b). The microtubular cytoskeleton and chromosomes of unfertilized human oocytes aged *in vitro*. *Hum. Genet.* **80,** 259–264.

Eichenlaub-Ritter, U., and Winking, H. (1990). Nondisjunction, disturbances in spindle structure, and characteristics of chromosome alignment in maturing oocytes of mice heterozygous for Robertsonian translocations. *Cytogenet. Cell Genet.* **54,** 47–54.

Epstein, C. J. (1985). Mouse monosomies and trisomies as experimental systems for studying mammalian aneuploidy. *TIG* **5,** 129–134.

Epstein, C. J. (1986). "The Consequences of Chromosome Imbalance: Principles, Mechanisms, and Models." Cambridge University Press, Cambridge.

Erickson, J. D. (1978). Down syndrome, paternal age, maternal age and birth order. *Ann. Hum. Genet.* **41,** 289–298.

Erickson, R. P. (1993). Molecular genetics of mammalian spermatogenesis. *In* "Genes in Mammalian Reproduction" (R. B. L. Gwatkin, ed.), pp. 1–26. Wiley-Liss, Inc., New York.

Estop, A. (1989). Nondisjunction and maternal age in the mouse. *In* "Molecular and Cytogenetic Studies of Non-disjunction" (T. J. Hassold and C. J. Epstein, eds.), pp. 221–224. A. R. Liss, New York.

Estop, A. M., Cieply, K., Vankirk, V., Munne, S., and Garver, K. (1991). Cytogenetic studies in human sperm. *Hum. Genet.* **87,** 447–451.

Evans, E. P., Breckon, G., and Ford, C. E. (1964). An air-drying method for meiotic preparations from mammalian testes. *Cytogenetics* **3,** 289–294.

Fang, J. S., and Jagiello, G. M. (1991). Unique state of sexual dimorphism of crossing-over in diplotene spermatocytes and oocytes of *Mesocricetus brandti*, a species with neonatal oogenesis. *Biol. Reprod.* **45,** 447–454.

Fischer Lindahl, K. (1991). His and hers recombinational hotspots. *TIG* **7,** 273–276.

Fitzgerald, P. H., Archer, S., and Morris, M. (1986). Evidence for the repeated primary non-disjunction of chromosome 21 as a result of premature centromere division (PCD). *Hum. Genet.* **72,** 58–62.

Gabarron, J., Jimenez, A., and Glover, G. (1986). Premature centromere division dominantly inherited in a subfertile family. *Cytogenet. Cell Genet.* **43,** 69–73.

Gaulden, M. E. (1992). Maternal age effect: The enigma of Down syndrome and other trisomic conditions. *Mutat. Res.* **296,** 69–88.

Gearhart, J. D., Oster-Granite, M. L., Reeves, R. H., and Coyle, J. T. (1987). Developmental consequences of autosomal aneuploidy in mammals. *Dev. Genet.* **8,** 249–265.

Ghosh, S., and Paweletz, N. (1992). Okadaic acid inhibits sister chromatid separation in mammalian cells. *Exp. Cell Res.* **200,** 215–217.

Goldman, A. S. H., and Hulten, M. A. (1993a). Meiotic analysis by FISH of a human male 46,XY, t(15;20) (q11.2,q11.2) translocation heterozygote: Quadrivalent configuration, orientation and first meiotic segregation. *Chromosoma* **102,** 102–111.

Goldman, A. S. H., and Hulten, M. A. (1993b). Analysis of chiasma frequency and first meiotic segregation in a human male reciprocal translocation heterozygote t(1;11)(p36.3;q13.1) using fluorecescence *in situ* hybridization. *Cytogenet. Cell Genet.* **63,** 16–23.

Gorbsky, G. J., Simerly, C., Schatten, G., and Borisy, G. G. (1990). Microtubules in the metaphase-arrested mouse oocyte turn over rapidly. *Proc. Natl. Acad. Sci. USA* **87,** 6049–6053.

Gropp, A., Giers, D., and Kolbus, U. (1974). Trisomy in the fetal backcross progeny of male and female metacentric heterozygotes of the mouse. *Cytogenet. Cell Genet.* **13,** 511–535.

Gropp, A., Kolbus, U., and Giers, D. (1975). Systematic approach to the study of trisomy in the mouse. *Cytogenet. Cell Genet.* **14,** 42–62.

Gropp, A., and Winking, H. (1981). Robertsonian translocations: Cytology, meiosis, segregation patterns and biological consequences of heterozygosity. *Zool. Soc. London Symp.* **47,** 141–181.

Guichaoua, M. R., Speed, R. M., Luciani, J. M., Delafontaine, D., and Chandley, A. C. (1992). Infertility in human males with autosomal translocations. II. Meiotic studies in three reciprocal rearrangements, one showing tertiary monosomy in a 45-chromosome individual and his father. *Cytogenet. Cell Genet.* **60,** 96–101.

Guttenbach, M., and Schmid, M. (1991). Non-isotopic detection of chromosome 1 in human meiosis and demonstration of disomic sperm nuclei. *Hum. Genet.* **87,** 261–265.

Hamers, A. J. H., Meyer, H., Jongbloed, J. E., Van der Hulst, W. J., and Geraedts, J. P. M. (1990). Rate of recombination of chromosomes 21 in parents of children with Down syndrome. *Clin. Genet.* **37,** 463–469.

Hansmann, E., De Boer, P., and Speed, R. M. (1988). Aneuploidy-related delay of meiotic development in the mouse and the Djungarian hamster. *In* "The Cytogenetics of Mammalian Autosomal Rearrangements" (A. Daniel, ed.), Vol. 8, pp. 295–314. A. R. Liss, New York.

Hartwell, L. (1992). Defects in a cell cycle checkpoint may be responsible for the genomic instability of cancer cells. *Cell* **71,** 543–546.

Hassold, T., and Chiu, D. (1985). Maternal age-specific rates of numerical chromosome abnormalities with specific reference to trisomy. *Hum. Genet.* **70,** 11–17.

Hassold, T., and Jacobs, P. A. (1984). Trisomy in man. *Annu. Rev. Genet.* **18,** 69–97.

Hassold, T., and Sherman, S. (1993). The origin of non-disjunction in humans. *In* "Chromosomes Today" (A. Summer and A. C. Chandley, eds.), Vol. 11, pp. 313–322. Chapman and Hall, London.

Hassold, T. J., Sherman, S. L., Pettay, D., Page, D. C., and Jacobs, P. A. (1991). XY chromosome nondisjunction in man is associated with diminished recombination in the pseudoautosomal region. *Am. J. Hum. Genet.* **49,** 253–260.

Hatch, M., Kline, J., Levin, B., Hutzler, M., and Warburton, D. (1990). Paternal age and trisomy among spontaneous abortions. *Hum. Genet.* **85,** 355–361.

Hawley, R. S., and Arbel, T. (1993). Yeast genetics and the fall of the classical view of meiosis. *Cell* **72,** 301–303.

Henderson, S. A., and Edwards, R. G. (1968). Chiasma frequency and maternal age in mammals. *Nature* **218,** 22–28.

Holmes, J. M., and Martin, R. H. (1993). Aneuploidy detection in human sperm nuclei using fluorescence *in situ* hybridization. *Hum. Genet.* **91,** 20–24.

Hook, E. B. (1986). The impact of aneuploidy upon public health: Mortality and morbidity associated with chromosome abnormalities. *In* "Aneuploidy, Etiology and Mechanisms" (V. L. Dellarco, P. E. Voytek, and A. Hollaender, eds.), Vol. 36, pp. 7–33. Plenum, New York.

Hook, E. B., Cross, P. K., Jackson, L., Pergament, E., and Brambati, B. (1988). Maternal age-specific rates of 47,+21 and other cytogenetic abnormalities diagnosed in the first trimester of pregnancy in chorionic villus biopsy specimens: Comparison with rates expected from observations at amniocentesis. *Am. J. Hum. Genet.* **42,** 797–807.

Hsu, L. F. (1992). Prenatal diagnosis of chromosomal abnormalities through amniocentesis. *In* "Genetic Disorders of the Fetus: Diagnosis, Prevention, and Treatment" (A. Milunsky, ed.), 3rd. Ed. pp. 155–210. The Johns Hopkins University Press, Baltimore.

Hulten, M., Lawrie, N. M., and Laurie, D. A. (1990). Chiasma-based genetic maps of chromosome 21. *Am. J. Med. Genet. Suppl.* **7,** 148–154.

Hummler, E., and Hansmann, I. (1985). Preferential nondisjunction of specific bivalents in oocytes from Djungarian hamsters (*Phodopus sungorus*) following colchicine treatment. *Cytogenet. Cell Genet.* **39,** 161–167.

Hummler, E., Theuring, F., and Hansmann, I. (1987). Meiotic non-disjunction in oocytes from aged Djungarian hamsters correlates with an alteration in meiosis rate but not in univalent formation. *Hum. Genet.* **76,** 357–364.

Hunt, P. A., and LeMaire, R. (1992). Sex-chromosome pairing: Evidence that the behavior of the pseudoautosomal region differs during male and female meiosis. *Am. J. Hum. Genet.* **50,** 1162–1170.

Inoue, S., and Sato, H. (1967). Cell motility by labile association of molecules. *J. Gen. Physiol.* **50,** 259–292.

Iwasaki, S., Shioya, Y., Masuda, H., Hanada, A., and Nakara, T. (1989). Incidence of chromosomal abnormalities in early embryos derived from *in vitro* fertilization. *Gamete Res.* **22,** 83–91.

Jagiello, G. M., Ducayen, M. B., Miller, W. A., Lin, J. S., and Fang, J. S. (1973). A cytogenetic analysis of oocytes from *Macaca mulatta* and *Nemestrina* matured *in vitro*. *Humangenetik* **18,** 117–122.

Janicke, M. A., and LaFountain, J. R. (1989). Centromeric dots in crane fly spermatocytes: Meiotic maturation and malorientation. *Chromosoma* **98,** 358–367.

Jeppeson, P., and Turner, B. M. (1993). The inactive X chromosome in female mammals is distinguished by a lack of histone H4 acetylation, a cytogenetic marker for gene expression. *Cell* **74,** 281–289.

Kamiguchi, Y., Rosenbusch, B., Sterzik, K., and Mikamo, K. (1993). Chromosomal analysis of unfertilized human oocytes prepared by a gradual fixation-air drying method. *Hum. Genet.* **90,** 533–541.

Kerrebrock, A. W., Miyazaki, W. Y., Birnby, D., and Orr-Weaver, T. L. (1992). The Drosophila *mei*-S332 gene promotes sister-chromatid cohesion in meiosis following kinetochore differentiation. *Genetics* **130,** 827–841.

Kinloch, R. A., and Wassarman, P. M. (1993). Specific gene expression during oogenesis

in mice. *In* "Genes in Mammalian Reproduction" (R. B. L. Gwatkin, ed.), pp. 27–43. Wiley-Liss, New York.

Knowles, B. A., and Hawley, R. S. (1991). Genetic analysis of microtubule motor proteins in Drosophila: A mutation at the *ncd* locus is a dominant enhancer of *nod*. *Proc. Natl. Acad. Sci. USA* **88,** 7165–7169.

Kubiak, J., Paldi, A., Weber, M., and Maro, B. (1991). Genetically identical parthenogenetically mouse embryos produced by inhibition of the first meiotic cleavage with cytochalasin D. *Development* **11,** 763–769.

Laurie, D. A., Firkett, C. L., and Hulten, M. A. (1985). A direct cytogenetic technique for assessing the rate of first meiotic non-disjunction in the human male by the analysis of cells at metaphase II. *Ann. Hum. Genet.* **49,** 23–29.

Ledbetter, D. H. (1992). Minireview: Cryptic translocation and telomere integrity. *Am. J. Hum. Genet.* **51,** 451–456.

Liang, L. C., Sherron, D. A., and Johnston, D. (1986). Lack of correlation between mutagen-induced chromosomal univalency and aneuploidy in mouse spermatocytes. *Mutat. Res.* **163,** 285–297.

Lorda-Sanchez, I., Binkert, F., Maechler, M., Robinson, W. P., and Schinzel, A. A. (1992). Reduced recombination and paternal age-effect in Klinefelter syndrome. *Hum. Genet.* **89,** 524–530.

Lyon, M. F., and Hawker, S. G. (1973). Reproductive lifespan in irradiated and unirradiated X0 mice. *Genet. Res.* **21,** 185–194.

Lyon, M. F., and Meredith, R. (1966). Autosomal translocations causing male sterility and viable aneuploidy in the mouse. *Cytogenetics* **5,** 335–354.

Mailhes, J. B., and Aardema, M. J. (1992). Benomyl-induced aneuploidy in mouse oocytes. *Mutagenesis* **7,** 303–309.

Mailhes, J. B., Aardema, M. J., and Marchetti, F. (1993). Investigation of aneuploidy induction in mouse oocytes following exposure to vinblastine-sulfate, pyrimethamine, diethylstilbestrol diphosphate, or chloral hyrate. *Environ. Mol. Mutagen.* **22,** 107–114.

Mailhes, J. B., and Marchetti, F. (1993). The relationship between chemically-induced meiotic delay and aneuploidy in mouse oocytes and zygotes. *In* "Chromosome Segregation and Aneuploidy" (B. K. Vig, ed.), pp. 283–296, Springer-Verlag, Heidelberg.

Mailhes, J. B., and Yuan, Z. P. (1987). Differential sensitivity of mouse oocytes to colchicine-induced aneuploidy. *Environ. Mol. Mutagen.* **10,** 183–188.

Mailhes, J. B., Yuan, Z. P., and Aardema, M. J. (1990). Cytogenetic analysis of mouse oocytes and one cell zygotes as a potential assay for heritable germ cell aneuploidy. *Mut. Res.* **242,** 89–100.

Maller, J. L. (1991). Mitotic control. Curr. Opin. Cell Biol. **3,** 269–275.

Maro, B., Howlett, S. K., and Webb, M. (1985). Non-spindle MTOCs in metaphase II-arrested mouse oocytes. *J. Cell Biol.* **101,** 1665–1672.

Martin, R. H. (1983). A detailed method for obtaining preparations of human sperm chromosomes. *Cytogenet. Cell Genet.* **35,** 252–256.

Martin, R. H., and Hulten, M. A. (1993). Chromosome complements in 695 sperm from three men heterozygous for reciprocal translocations and a review of the literature. *Hereditas* **118,** 165–175.

Martin, R. H., Ko, E., and Rademaker, A. (1991). Distribution of aneuploidy in human gametes: Comparison between human sperm and oocytes. *Am. J. Med. Genet.* **39,** 321–331.

Martin, R. H., and Rademaker, A. W. (1987). The effect of age on the frequency of sperm chromosomal abnormalities in normal men. *Am. J. Hum. Genet.* **41,** 484–492.

Martin-DeLeon, P. A. (1989). Analysis of the chromosome complement in outbred mouse sperm fertilizing *in vitro*. *Gamete Res.* **22,** 71–81.

Masison, D. C., and Baker, R. E. (1992). Meiosis in *Saccharomyces cerevisiae* mutants lacking the centromere-binding protein CP1. *Genetics* **131,** 43–53.

Masuno, M., Cholsong, Y., Kuwahara, T., Shimizu, N., Yamaguchi, S., Kawabata, I., Tamaya, T., Morishita, Y., Yoshimi, N., and Orii, T. (1991). Second meiotic nondisjunction of the rearranged chromosome in a familial reciprocal 5/13 translocation. *Am. J. Med. Genet.* **41,** 32–34.

McKee, B. D., and Handel, M. A. (1993). Sex chromosomes, recombination, and chromatin conformation. *Chromosoma* **102,** 71–80.

Meeks-Wagner, D., and Hartwell, L. H. (1986). Normal stoichiometry of histone dimer sets is necessary for high fidelity of mitotic chromosome transmission. *Cell* **44,** 43–52.

Mercer, S. J., Wallace, B. M., and Searle, J. B. (1992). Male common shrews (*Sorex araneus*) with long meiotic chain configurations can be fertile: Implications for chromosomal models of speciation. *Cytogenet. Cell Genet.* **60,** 68–73.

Messinger, S. M., and Albertini, D. F. (1991). Centrosome and microtubule dynamics during meiotic progression in the mouse oocyte. *J. Cell Sci.* **100,** 289–298.

Meyer, J. M., Maetz, J. L., and Rumpler, Y. (1992). Cellular relationship impairment in maturation arrest of human spermatogenesis: An ultrastructural study. *Histopathology* **21,** 25–33.

Mikkelsen, M., Poulsen, H., Grinsted, J., and Lange, A. (1980). Nondisjunction in trisomy 21: Study of chromosomal heteromorphisms in 110 families. *Ann. Hum. Genet.* **44,** 17–28.

Miklos, G. L. G. (1974). Sex-chromosome pairing and male fertility. *Cytogenet. Cell Genet.* **13,** 558–577.

Miller, B. M., and Adler, I. A. (1992). Aneuploidy induction in mouse spermatocytes. *Mutagenesis* **7,** 69–76.

Milunsky, A. (1992). "Genetic Disorders and the Fetus: Diagnosis, Prevention, and Treatment." The Johns Hopkins University Press, Baltimore.

Mittwoch, U., and Mahadevaiah, K. (1992). Unpaired chromosomes at meiosis: Cause or effect of gametogenic insufficiency? *Cytogenet. Cell Genet.* **59,** 274–279.

Moens, P. B., and Earnshaw, W. C. (1989). Anti-topoisomerase II recognizes meiotic chromosome cores. *Chromosoma* **98,** 317–322.

Mohandas, T. K., Speed, R. M., Passage, M. B., Yen, P. H., Chandley, A. C., and Shapiro, L. T. (1992). Role of the pseudoautosomal region in sex-chromosome pairing during male meiosis: Meiotic studies in a man with a deletion of distal Xp. *Am. J. Hum. Genet.* **51,** 526–533.

Nachman, M. W. (1992). Meiotic studies of Robertsonian polymorphisms in the South American marsh rat, *Holichilus brasiliensis*. *Cytogenet. Cell Genet.* **61,** 17–24.

Navarro, J., Templado, C. Benet, J., Lange, R., Rajmil, O., and Egozcue, J. (1990). Sperm chromosome studies in an infertile man with partial, complete asynapsis of meiotic bivalents. *Hum. Reprod.* **5,** 227–229.

Nicklas, R. B., and Arana, P. (1992). Evolution and the meaning of metaphase. *J. Cell Sci.* **102,** 681–690.

Nicklas, R. B., Brinkley, B. R., Pepper, D. A., Kubai, D. A., and Rickards, G. K. (1979). Electron microscopy of spermatocytes previously studied in life: Methods and some observations on micromanipulated chromosomes. *J. Cell Sci.* **35,** 87–104.

Nishimoto, T., Uzawa, S., and Schlegel, R. (1992). Mitotic checkpoints. *Curr. Opin. Cell Biol.* **4,** 174–179.

O'Connell, P., Luthrop, G., Law, M., Lappert, M., Nakamura, Y., Hoff, M., Kumlin, E., Thomas, W., Elsner, T., Ballard, L., Goodman, P., Azen, E., Sadler, J., Cai, G.,

Lalouel, J.-M., and White, R. (1987). A primary genetic linkage map for human chromosome 12. *Genomics* **1,** 93–102.

O'Neill, G. T., and Kaufman, M. H. (1989). Cytogenetic analysis of ethanol-induced parthenogenesis. *J. Exp. Zool.* **249,** 182–192.

Padmore, R., Cao, L., and Kleckner, N. (1991). Temporal comparison of recombination and synaptonemal complex formation during meiosis in *S. cerevisiae*. *Cell* **66,** 1239–1256.

Parvinen, M., Pelto-Huikko, M., Söder, O., Schultz, R., Kaipia, A., Mali, P., Toppari, J., Hakovirta, H., Lönnerberg, P., Ritzen, E. M., Ebendal, T., Olsen, L., Hökfelt, T., and Persson, H. (1992). Expression of β-nerve growth factor and its receptor in rat seminiferous epithelium: Specific function at the onset of meiosis. *J. Cell Biol.* **117,** 629–641.

Pearlman, R. E., Tsao, N., and Moens, P. B. (1992). Synaptonemal complexes from DNase-treated rat pachytene chromosomes contain (GT)n and LINE/SINE sequences. *Genetics* **130,** 865–872.

Pellestor, F. (1990). Analysis of meiotic segregation in a man heterozygous for a 13;15 Robertsonian translocation and a review of the literature. *Hum. Genet.* **85,** 49–54.

Pellestor, F. (1991a). Frequency and distribution of aneuploidy in human female gametes. *Hum. Genet.* **86,** 283–288.

Pellestor, F. (1991b). Differential distribution of aneuploidy in human gametes according to their sex. *Hum. Reprod.* **6,** 1252–1258.

Peterson, M. B., Bartsch, O., Adelsberger, P. A., Mikkelsen, M., Schwinger, E., and Antonarakis, S. E. (1992a). Uniparental isodisomy due to duplication of chromosome 21 occurring in somatic cells monosomic for chromosome 21. *Genomics* **13,** 269–274.

Peterson, M. B., Frantzen, M., Antoniarakis, S. E., Warren, A. C., Van-Broekenhoven, C., Chakravarti, A., Cox, T. K., Lund, C., Olsen, B., Poulsen, H., Sand, A., Tommerup, N., and Mikkelsen, M. (1992b). Comparative study of microsatellite and cytogenetic markers for detecting the origin of the nondisjoined chromosome 21 in Down syndrome. *Am. J. Hum. Genet.* **51,** 516–525.

Pickering, S. J., and Johnson, M. H. (1987). The influence of cooling on the organization of the meiotic spindle of the mouse oocyte. *Hum. Reprod.* **2,** 207–216.

Pickering, S. J., Johnson, M. H., Braude, P. R., and Houliston, E. (1988). Cytoskeletal organization in fresh, aged and spontaneously activated human oocytes. *Hum. Reprod.* **3,** 978–989.

Plachot, M. (1991). Chromosome analysis of oocytes and embryos. *In* "Preimplantation Genetics" (Y. Verlinsky, and A. Kuliev, eds.), pp. 103–127. Plenum, New York.

Pluta, A. F., and Zakian, V. A. (1989). Recombination occurs during telomere formation in yeast. *Nature* **337,** 429–433.

Polani, P. (1972). Centromere localization at meiosis and the position of chiasmata in the male and female mouse. *Chromosoma* **36,** 343–374.

Polani, P. E., and Crolla, J. A. (1991). A test of the production line hypothesis of mammalian oogenesis. *Hum. Genet.* **88,** 64–70.

Polani, P. E., and Jagiello, G. M. (1976). Chiasmata, meiotic univalents and age in relationship to aneuploid imbalance in mice. *Cytogenet. Cell Genet.* **16,** 505–529.

Power, M. M. (1987). Equine half sibs with an unbalanced X;15 translocation or trisomy 28. *Cytogenet. Cell Genet.* **45,** 163–168.

Rassoulzadegan, M., Paquis, M., Bertino, B., and Cuzin, F. (1992). "Long Term Maintenance and Differentiation of Male Germ-Cells in Culture. VII. Workshop on Molecular Genetics of the Mouse," p. 46. Dourdan. [Abstract]

Resnick, M. A. (1993). Sensing DNA damage: A role for chromosome communication in aneuploidy induction. *In* "Chromosome Segregation and Aneuploidy" (B. K. Vig, ed.), pp. 121–132, Springer-Verlag, Heidelberg.

Rickards, G. (1983). Orientation behavior of chromosome multiples of interchange (reciprocal translocation) heterozygotes. *Annu. Rev. Genet.* **17,** 443–498.

Rieder, C. L., Ault, J. G., Eichenlaub-Ritter, U., and Sluder, G. (1993). Morphogenesis of the mitotic and meiotic spindle: Conclusions obtained from one system are not necessarily applicable to the other. *In* "Chromosome Segregation and Aneuploidy" (B. K. Vig, ed.), pp. 183–198, Springer-Verlag, Heidelberg.

Rieger, R., Michaelis, A., and Green, M. M. (1991). "Glossary of Genetics," 5th Ed. Springer, Berlin.

Rose, D., Thomas, W., and Holm, C. (1990). Segregation of recombined chromosomes at meiosis I requires DNA topoisomerase II. *Cell* **60,** 1009–1017.

Ross, L. O., Treco, D., Nicolas, A., Szostak, J. W., and Dawson, D. (1992). Meiotic recombination on artificial chromosomes in yeast. *Genetics* **131,** 541–550.

Rudak, E., Jacobs, P. A., and Yanagimachi, R. (1978). Direct analysis of the chromosome constitution of human spermatozoa. *Nature* **274,** 911–913.

Russell, L. B., and Russell, W. L. (1992). Frequency and nature of specific-locus mutations induced in female mice by radiations and chemicals: A review. *Mutat. Res.* **296,** 107–128.

Russo, A., and Pacchierotti, F. (1988). Meiotic arrest and aneuploidy induced by vinblastine in mouse oocytes. *Mutat. Res.* **202,** 215–221.

Sawin, K. E., LeGuellec, K., Philippe, M., and Mitchison, T. J. (1992). Mitotic spindle organization by a plus-end directed microtubule motor. *Nature* **359,** 540–543.

Schatten, G., Simerly, C., and Schatten, H. (1985). Microtubule configurations during fertilization, mitosis, and early development in the mouse and the requirement for egg microtubule-mediated motility during mammalian fertilization. *Proc. Natl. Acad. Sci. USA* **82,** 4152–4156.

Schinzel, A. A., Adelsberger, P. A., Binkert, F., Basaran, S., and Antonarakis, S. E., (1992). No evidence for a paternal interchromosomal effect from analysis of the origin of nondisjunction in Down syndrome patients with concomitant familial chromosome rearrangements. *Am. J. Hum. Genet.* **50,** 288–293.

Schmiady, H., Soewarto, D., Kentenich, H., and Eichenlaub-Ritter, U. (1994). Consequences of non-extrusion of the first polar body in human oocytes and in mouse oocytes maturing in vitro. Submitted for publication.

Searle, J. B. (1990). A cytogenetical analysis of reproduction in common shrews (*Sorex araneus*) from a karyotypic hybrid zone. *Hereditas* **113,** 121–132.

Sears, D. D., Hegemann, J. H., and Hieter, P. (1992). Meiotic recombination and segregation of human-derived artificial chromosomes in *Saccharomyces cerevisiae*. *Proc. Natl. Acad. Sci. USA* **89,** 5296–5300.

Shamu, C. E., and Murray, A. W. (1992). Sister chromatid separation in frog egg extracts requires DNA topoisomerase II activity during anaphase. *J. Cell Biol.* **117,** 921–934.

Shenkar, R., Shen, M., and Arnheim, N. (1991). DNase I-hypersensitive sites and transcription factor binding motifs within the mouse Eβ meiotic recombination hot spot. *Mol. Cell Biol.* **11,** 1813–1819.

Sherman, S. L., and Hassold, T. (1993). Trisomy in humans: Incidence, origin, and etiology. *Curr. Opin. Genet. Dev.* **3,** 398–403.

Sherman, S. L., Takesu, N., Feeman, S. B., Grantham, M., Phillips, C., Blacksston, R. D., Jacobs, P. A., Cockwell, A. E., Freeman, V., Uchida, I., Mikkelsen, M., Kurnit, D. M., Burakszynska, M., Keats, B. J. B., and Hassold, T. J. (1991). Trisomy 21: Association between reduced recombination and non-disjunction. *Am. J. Hum. Genet.* **49,** 608–620.

Simerly, C., Balczon, R., Brinkley, B. R., and Schatten, G. (1990). Microinjected

kinetochore antibodies interfere with chromosome movement in meiotic mouse oocytes. *J. Cell Biol.* **111,** 1491–1504.

Sluder, G., Miller, F. J., Lewis, K., and Rieder, C. L. (1989). Centrosome inheritance in starfish zygotes: Selective loss of the maternal centrosome after fertilization. *Dev. Biol.* **131,** 567–579.

Smith, A., and Benavente, R. (1992a). Identification of a structural protein component of rat synaptonemal complexes. *Exp. Cell Res.* **198,** 291–297.

Smith, A., and Benavente, R. (1992b). Meiosis-specific protein selectively associated with sex chromosomes of rat pachytene spermatocytes. *Proc. Natl. Acad. Sci. USA* **89,** 6938–6942.

Soewarto, D., and Eichenlaub-Ritter, U. (1993). Regulation of meta- to anaphase transition in meiotic mouse oocytes. *Eur. J. Cell Biol.* **60,** Suppl. 37, 117.

Solari, A. J. (1980). Synaptonemal complexes and associated structures in microspread human spermatocytes. *Chromosoma* **81,** 43–53.

Speed, R. M. (1984). Meiotic configuration in female trisomy 21 fetuses. *Hum. Genet.* **66,** 176–180.

Speed, R. M. (1985). The prophase stages of human foetal oocytes studied by light and electron microscopy. *Hum. Genet.* **69,** 69–75.

Speed, R. M. (1988). The possible role of meiotic pairing anomalies in the atresia of human foetal oocytes. *Hum. Genet.* **78,** 260–266.

Speed, R. M. (1990). Meiosis in mammals. *In* "Advances in Mutagenesis Research" (G. Obe, ed.), Vol. 1, pp. 27–69. Springer, Berlin.

Speed, R. M., and Chandley, A. C. (1983). Meiosis in the fetal mouse ovary. II. Oocyte development and age related aneuploidy. Does a production line exist? *Chromosoma* **88,** 184–189.

Spriggs, E. L., Martin, R. H., and Hulten, M. (1992). Sperm chromosome complements from two human reciprocal translocation heterozygotes. *Hum. Genet.* **88,** 447–452.

Steffen, W., Fuge, H., Dietz, R., Bastmeyer, M., and Muller, G. (1986). Aster free spindle poles in insect spermatocytes: Evidence for chromosome-induced spindle formation. *J. Cell Biol.* **102,** 1679–1687.

Sudman, P. D., Rutledge, J. C., Bishop, J. B., and Generoso, W. M. (1992). Bleomycin: Female-specific dominant lethal effects in mice. *Mutat. Res.* **296,** 143–156.

Sugawara, S., and Mikamo, K. (1983). Absence of correlation between univalent formation and meiotic nondisjunction in the aged female Chinese hamster. *Cytogenet. Cell Genet.* **35,** 34–40.

Sym, M., Engelbrecht, J. A., and Roeder, G. S. (1993). ZIP1 is a synaptonemal complex protein required for meiotic recombination. *Cell* **72,** 365–378.

Tanzi, R. E., Watkins, P. C., Steward, G. D., Wexler, N. S., Gusella, J. F., and Haines, J. L. (1992). A genetic linkage map of human chromosome 21: Analysis of recombination as a function of sex and age. *Am. J. Hum. Genet.* **50,** 551–558.

Tarkowski, A. K. (1966). An air drying method for chromosome preparations from mouse eggs. *Cytogenetics* **5,** 394–400.

Tates, A. D., de Vogel, N., Rotteveel, A. H., Leupe, F., and Davis, J. A. (1989). The response of spermatogonia and spermatocytes of the Northern vole *Microtus oeconomus* to the induction of sex-chromosome nondisjunction, diploidy, and chromosome breakage by X-rays and fast fission neutrons. *Mutat. Res.* **210,** 173–189.

Tease, C. (1992). Radiation- and chemically-induced chromosome aberrations in mouse oocytes: A comparison with effects in males. *Mutat. Res.* **296,** 135–142.

Tease, C., and Fisher, G. (1986). Oocytes from young and old female mice respond differently to colchicine. *Mutat. Res.* **173,** 31–34.

Tease, C., and Fisher, G. (1991a). The influence of maternal age on radiation-induced chromosome aberrations in mouse oocytes. *Mutat. Res.* **262,** 57–62.

Tease, C., and Fisher, G. (1991b). Two new X-autosome Robertsonian translocations in the mouse. I. Meiotic chromosome segregation in male hemizygotes and female heterozygotes. *Genet. Res.* **58,** 115–121.

Templado, C., Navarro, J., Requena, R., Benet, J. Ballesta, F., and Egozcue, J. (1990). Meiotic and sperm chromosome studies in a reciprocal translocation t(1;2) (q32;q36). *Hum. Genet.* **84,** 159–162.

Thomas, B. J., and Rothstein, R. (1991). Sex, maps and imprinting. *Cell* **64,** 1–4.

Tiveron, C., Marchett, F., Bassani, B., and Pacchierotti, F. (1992). Griseofulvin-induced aneuploidy and meiotic delay in female mouse germ cells. I. Cytogenetic analysis of metaphase II oocytes. *Mutat. Res.* **266,** 143–150.

Tomkiel, J., and Earnshaw (1993). Structure of the mammalian centromer. *In* "Chromosome Segregation and Aneuploidy" (B. K. Vig, ed.), pp. 13–29. Springer-Verlag, Heidelberg.

Ueda, T., Yamazaki, K., Suzuki, R., Fujimoto, H., Sasaki, H., Sasaki, Y., and Higashinakagawa, T. (1992). Parental methylation patterns of a transgenic locus in adult somatic tissues are imprinted during gametogenesis. *Dev. Biol.* **116,** 831–839.

Van Blerkom, J., and Henry, G. (1992). Oocyte dysmorphism and aneuploidy in meiotically mature human oocytes after ovarian stimulation. *Hum. Reprod.* **7,** 379–390.

Van Buul, P. P., Seelen, C. M., and Goudzwaard, J. H. (1992). Meiotic delay of mouse spermatocytes carrying x-ray-induced translocations. *Cytogenet. Cell Genet.* **60,** 146–149.

Vig, B. K. (1983). Sequence of centromere separation: Occurrence, possible significance and control. *Cancer Genet. Cytogenet.* **8,** 249–273.

Wadsworth, P. (1993). Mitosis: Spindle assembly and chromosome motion. *Curr. Opin. Cell Biol.* **5,** 123–128.

Wallace, B. M. N., Searle, J. B., and Everett, C. A. (1992). Male meiosis and gametogenesis in wild house mice (*Mus musculus domesticus*) from a chromosomal hybrid zone; a comparison between "simple" Robertsonian heterozygotes and homozygotes. *Cytogenet. Cell Genet.* **61,** 211–220.

Warburton, D. (1989). The effect of maternal age on the frequency of trisomy: Change in meiosis or *in utero* selection? *In* "Molecular and Cytogenetic Studies of Non-disjunction" (T. Hassold, and C. J. Epstein, eds.), pp. 165–181. A. R. Liss, New York.

Wauben-Penris, P. J. J., van der Hoeven, F. A., and de Boeer, P. (1983). Chiasma frequency and nondisjunction in heteromorphic bivalents: Meiotic behavior in T(1;13)70T(1;13)1Wa mice as compared to T(1;13)70T(1;13(1;13)70H mice. *Cytogenet. Cell Genet.* **36,** 547–553.

Wickramasinghe, D., and Albertini, D. F. (1993). Cell cycle control during mammalian oogenesis. *Curr. Top. Dev. Biol.* **28,** 126–153.

Wilson, G. N. (1992). Mutational risks in females: Genomic imprinting and maternal molecules. *Mutat. Res.* **262,** 157–166.

Wright, S. J., and Schatten, G. (1990). Teniposide, a topoisomerase II inhibitor, prevents chromosome condensation and separation but not decondensation in fertilized surf clam (*Spisula solidissima*) oocytes. *Dev. Biol.* **142,** 224–232.

Yoshinaga, K., Nishikawa, S., Ogawa, M., Hayashi, S., Kunisuda, T., Fujimoto, T., and Nishikawa, S. (1991). Role of *c-kit* in mouse spermatogenesis: Identification of spermatogonia as a specific site of *c-kit* expression and function. *Development* **113,** 689–699.

Zenzes, M. T., Wang, P., and Casper, R. F. (1992). Evidence for maternal predisposition to chromosome aneuploidy in multiple oocytes of some *in vitro* fertilization patients. *Fertil. Steril.* **57,** 143–149.

9

Timing of Events during Flower Organogenesis: *Arabidopsis* as a Model System

Elizabeth M. Lord, Wilson Crone, and Jeffrey P. Hill†*
Department of Botany and Plant Sciences
University of California
Riverside, California 92521

I. Introduction

A. Heterochrony and Homeosis in Flower Development

Evolutionary biologists have long recognized that species appear to be derived from one another through changes in the relative timing of events during development. These early timing changes may have profound effects on mature form, even when they can be attributed to mutations in only one or a few heterochronic genes (Raff and Kaufman, 1983). The most thorough studies of such genes are in the nematode *Caenorhabdites elegans*, where there are many cases of heterochronic mutations that

*Present address: Department of Biology, Rensslaer Polytechnic Institute, Troy, New York 12180.
†Present address: Department of Biological Sciences, Idaho State University, Pocatello, Idaho 83209-9984.

Current Topics in Developmental Biology, Vol. 29

cause precocious cessation of cell division in lineages leading to complex organs (Ambros and Horvitz, 1984). The resultant mutant phenotypes often resemble species in natural populations, so heterochrony is considered a likely mode of evolution in this group.

In plants, a number of studies have implicated heterochrony in the evolution of floral form (Lord and Hill, 1987). Guerrant's (1982) work on *Delphinium* species showed how small changes in the timing of differentiation could account for the probable derivation of one floral type from an ancestral form. Studies on cleistogamy, a condition where closed, inbred flowers are borne on the same plant with open and outcrossed flowers, and on species with inbreeding floral forms have established that heterochrony can explain the derivation of the reduced flower in both of these cases (Lord *et al.*, 1989; Hill and Lord, 1990b). Only slight changes in the absolute timing of onset of stamen differentiation and the duration of cell division activity in sporogenous tissue could explain the significant differences in the mature flower forms found in the cleistogamous species *Collomia grandiflora* (Lord *et al.*, 1989).

The only published works on heterochronic genes in plants are those of Poethig (1988) and Bertrand-Garcia and Freeling (1991) on corn. Corn has mutants with a prolonged juvenile phase that can be ascribed to alterations in developmental timing. In yeast, heterochronic mutations have been described in genes that regulate the progression and timing of the cell cycle (Lee and Nurse, 1988). In the WEE+ mutant of yeast, differentiation (i.e., cell division in this single-celled eukaryote) begins precociously in a cell that has not grown to the full wild-type size, so that the resultant cell is smaller than normal, a heterochronic derivative. Therefore, yeast provides a wealth of genetic mutants for the study of heterochronic genes and their products in a simple, unicellular model system.

The terms heterochrony and homeosis are used to describe evolutionary change in processes that govern, respectively, the timing of development and the placement of parts in an organism (Raff and Kaufman, 1983) or a complex organ structure like the flower. Since heterochrony is defined as an alteration in developmental timing, heterochronic genes can be expected to be regulatory in nature and to be involved in controlling the timing and duration of events during ontogeny. The term homeosis describes the spatial transference of one part of an organism's body to a new position where it normally does not occur. Homeotic genes are regulatory as well and are involved in the proper placement of parts in an organism or organ system. A concerted effort to understand their role in development is now the focus of studies on a number of species, including plants. Study of homeotic mutants of *Drosophila melanogaster* has provided most of the information available on the regulation of organogenesis

during embryonic stages. Cloning of the genes whose mutant phenotypes are disruptions of developmental patterns allowed for rapid progress in discovering the means by which these genes direct pattern formation in embryos. Positional information is now known to be programmed by a family of related genes that specify segments in the fly body during embryogenesis (Ingham, 1988). Investigators in several laboratories have taken the same approach to the study of plant development, locating homeotic mutants in flowers that are controlled by single genes. They have found that though these floral genes do not contain the homeobox, they do contain a conserved region, found in a variety of organisms, that codes for another transcription factor (Coen *et al.*, 1990; Sommer *et al.*, 1990; Yanofsky *et al.*, 1990).

The study of heterochrony, which focuses on documenting the timing of events in development, highlights a significant difference between *Drosophila* embryogenesis and flower ontogeny. Segments of the body are determined simultaneously in the fly embryo with homeotic genes providing the necessary positional information at one critical point in time. The flower is analogous to an animal embryo in certain respects: organs are initiated, go through an "embryonic" phase of cell proliferation, and subsequently differentiate to function as organs that later senesce. But plants have an open system of growth, and organs are constantly being produced in an iterative fashion. The identity of floral organs is probably determined, not simultaneously in a floral apex, but sequentially as the apex produces organs acropetally.

Growth and new organ formation occur at the apices in plants and continue throughout the organism's life, so that temporal and spatial considerations in the control of organogenesis are perhaps not as distinct as they are in animal development. Nevertheless, measures of time in studies of development should be incorporated, first, because there is good evidence that alterations in developmental timing have played a role in the evolution of plant form, and second, in order to test models for pattern formation in plants such as those proposed to explain flower organogenesis.

B. Organ Identity Genes in Flower Development

Work on the single gene mutants that disrupt flower form (the so-called homeotic or flower organ identity mutants) has demonstrated the presence of three classes of genes that control the identity of the progression of organs produced in the flower. These classes were discovered by using three classes of organ identity mutants (Haughn and Sommerville, 1988; Schwartz-Sommer *et al.*, 1990; Coen, 1991; Meyerowitz *et al.*, 1991). All

three classes of mutants show a disruption in two adjacent whorls of organs (Fig. 1). The first class of mutants is missing normal sepals and petals, the second is missing normal petals and stamens, and the third kind of mutant is missing normal stamens and carpels. The first whorl, sepals, is controlled by class A genes alone; the second whorl, petals, by classes A and B genes; the third whorl, stamens, by classes B and C genes; and the final whorl, carpels, by class C genes alone. This genetic model of Meyerowitz and colleagues (1991) is a proposal for how "unspecified organ primordia learn their fate." The model also proposes that in the absence of one class of gene, these unspecified organ primordia are transformed into organs normally found in another whorl, thereby leading to the homeotic phenotype. For example, in class A mutants, sepals and petals are replaced by carpels and stamens; in class B, petals and stamens are replaced by sepals and carpels; and in class C, stamens and carpels are replaced by petals and sepals.

1. Spatial and Temporal Models for Specifying Pattern in the Flower

There are two models to explain how the organ identity genes might operate in specifying the pattern of the flower, the spatial model of Holder (1979) and the temporal or sequential model of Wardlaw (1957). Holder (1979) applied Wolpert's (1969) positional information theory to plants in his proposal that the floral apex prepattern might be set up by concentric fields of hormones specifying each whorl of floral organs. He saw the floral apex as segmented like a *Drosophila* embryo, with all of the floral whorls specified simultaneously and then each differentiating independently of the others. He even proposed examining the homeotic mutants known in flowers to test the genetic basis of such a theory. Now, a decade later, genes have been cloned for the flower organ identity mutants (Schwartz-Sommer *et al.*, 1990; Meyerowitz *et al.*, 1991), and they code

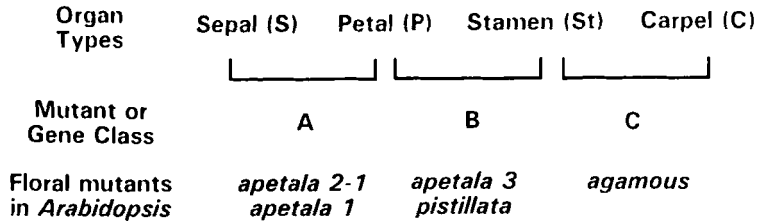

Fig. 1 Genetic model for organ identity gene action in flowers of *Arabidopsis thalliana*. Three gene classes (A–C) govern organ identity in *Arabidopsis*. [Revised from Meyerowitz *et al.* (1991).]

for transcription factors that must, themselves, be turned on by earlier events. Holder's model has been adopted by the groups working on flower organ identity genes (Schwartz-Sommer *et al.*, 1990; Meyerowitz *et al.*, 1991).

Wardlaw's (1957) alternative view of floral morphogenesis relies less on fields of chemicals than it does on initial switches; the initiation of the sepals sets up a sequence of events leading to carpel formation due to a cascade of gene expression. Here, groups of genes are turned on in an irreversible sequence to produce the flower. Hormones are postulated to be the initial trigger, but organs are specified over time, not simultaneously as in Holder's (1979) model. In addition, the organs are not viewed as being independent of each other during their differentiation (Heslop-Harrison, 1964).

An important feature distinguishing these models from each other is the time when genes act in the flower apex, simultaneously and prior to flower organ initiation in the spatial model or sequentially as organs are initiated in the temporal model. To determine which hypothesis is correct, a means of timing the events at the floral apex is necessary. In this chapter, the literature on various means of measuring time in plant development is reviewed and then one such measure is used to document events in flower development in *Arabidopsis thaliana*. The wild-type developmental program is compared to that of three organ identity mutants and one organ-number (meristic) mutant of this species. These data will better describe the alterations in the mutants and, in conjunction with the recently published expression patterns of the three classes of organ identity genes, the validity of the models for control of flower development will be examined.

II. Developmental Indices for Measuring Time in Plants

In general, time has been measured in studies of plant development by either (1) chronological age, or (2) the use of a numerical index (Erickson and Michelini, 1975; Williams, 1975; Silk, 1984; Green *et al.*, 1991). Chronological age (e.g., days after sowing, days to flowering, etc.) is often an unsatisfactory way of measuring time in developmental studies, because it does not account for significant variation in developmental rates among individuals (Lamoreaux *et al.*, 1978), nevertheless, it is the method most commonly used (Lord and Eckard, 1985; Smyth *et al.*, 1990). The development of the dental impression replica technique for viewing growing plant meristems (Hernandez *et al.*, 1991) allows for the timing of early events in floral organogenesis in a single individual with considerable accuracy. A numerical index is a character, such as bud length, that can be measured

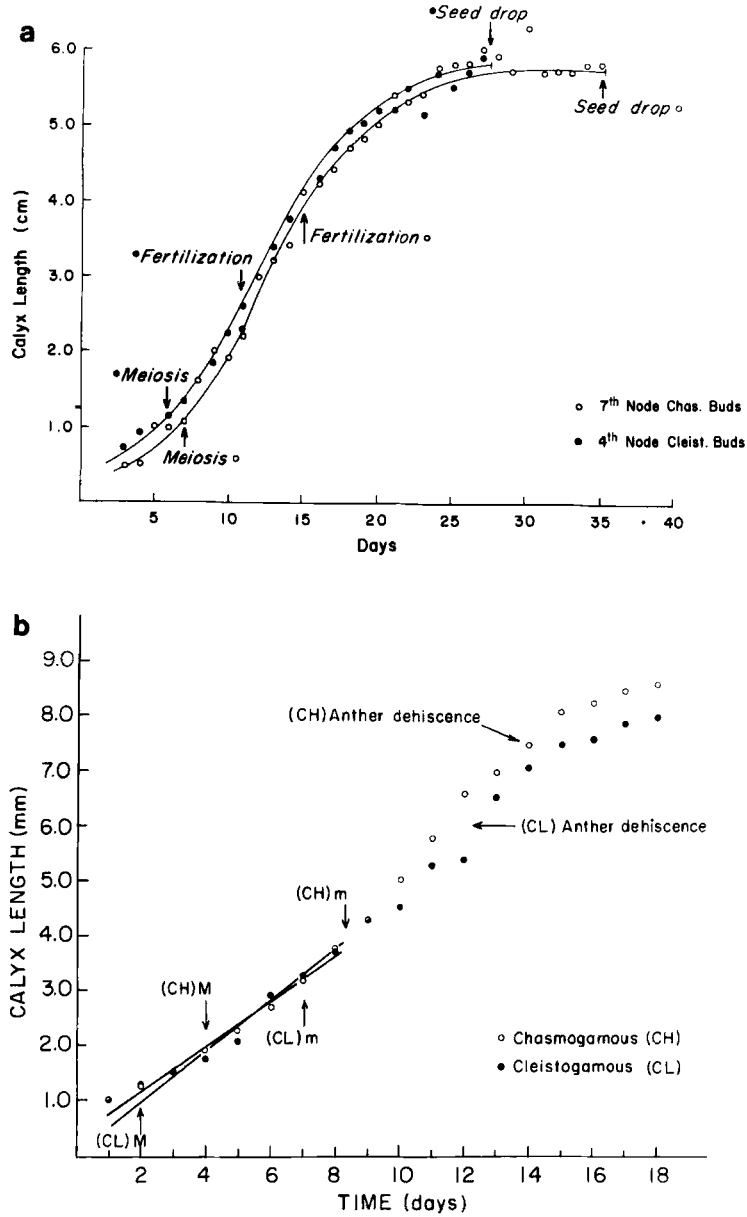

Fig. 2 (a) *Lamium amplexicaule*. Comparative growth curves for node 4 cleistogamous (●) and node 7 chasmogamous (○) flower buds (calyx length) for 35 days. [Reprinted from Lord (1979), with permission.] (b) *Collomia grandiflora*. Comparative growth plots of cleistogamous (CL) (●) and chasmogamous (CH) (○) flowers; bud (calyx) length versus time. M, final stage of meiosis, tetrad formation; m, mitotic division of microspores. [Reprinted from Minter and Lord (1983), with permission.] (c) *Viola odorata*. Lengths of successive leaves plotted logarithmically against time. Each curve represents the mean of five plants grown in chambers under 8- and 16-hr days with identical temperature and light treatments. Growth rates were determined by regression analysis for the linear portion of the curves. [Reprinted from Mayers and Lord (1983), with permission.]

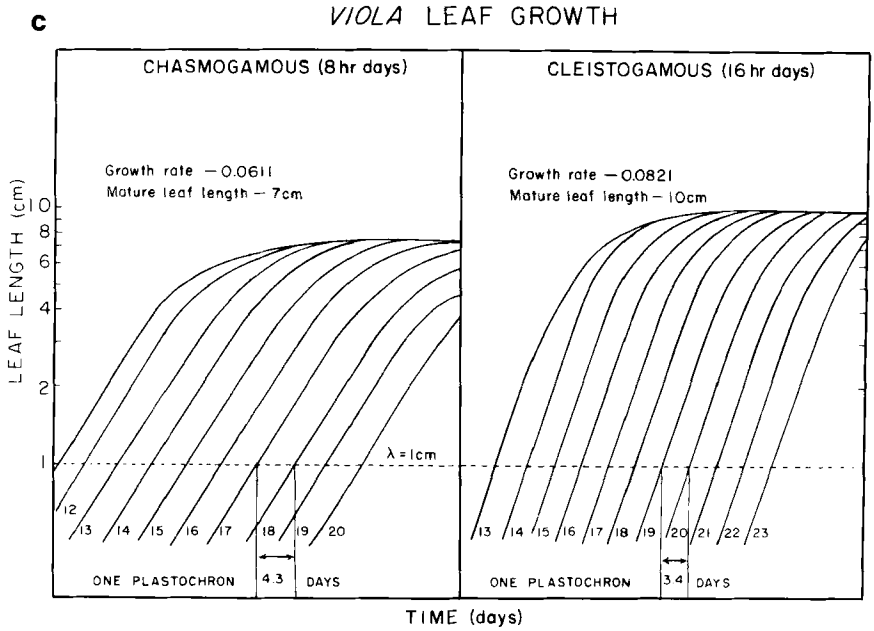

Fig. 2 *Continued*

as an indicator of relative time (Erickson, 1948; Guerrant, 1982; Lord, 1979). If the relationship between the index and time is known (Figs. 2a and 2b), then the character can be used as a standard from which developmental rates of other structures, growing over the same period of time, can be determined. Since young flower buds may be inaccessible for accurate measurements, this method is best used for events after organ initiation, such as meiosis in the anther and ovule (Erickson, 1948). The best method for measuring events during early organogenesis is the plastochron index which can specify the developmental status of a shoot, often with only small error (Erickson and Michelini, 1957). The plastochron is the time interval between the initiation of sequentially produced organs, typically leaves in plants. The plastochron index has been used to stage flower development as well since flowers are produced sequentially in an inflorescence (Sundberg, 1982; Mayers and Lord, 1983; Hill and Lord, 1990a; Hill and Malmberg, 1991; Hill *et al.*, 1992; Crone and Lord, 1993,1994) (Fig. 2c; Table I).

Both methods of measuring time have proven useful for documenting the time spent at various stages of flower development. Only a few studies are available for comparison, but these show a great range in the duration of flower organogenesis from inception to anthesis. *Citrus sinensis*, a tree, is at one extreme (100 days), and *Arabidopsis thaliana*, an annual herb,

Table I Timing of Events in Flower Development

Species	Growth habit	Duration (days) from initiation to anthesis	Duration (days) from flower meristem initiation to carpel initiation	Reference
Arabidopsis thaliana[a]	Herbaceous annual	10[b]	4[b]	Crone and Lord (1994)
Lamium amplexicaule	Herbaceous annual	15	—	Lord (1979)
Collomia grandiflora	Herbaceous annual	15	—	Minter and Lord (1983)
Anagallis arvensis[a]	Herbaceous annual	—	~5	Green *et al.* (1991)
Arenaria uniflora[a]	Herbaceous biennial	28[b]	~5[b]	Hill *et al.* (1992)
Cyclamen persicum	Herbaceous perennial	~280[b]	50[b]	Sundberg (1982)
Viola odorata[a]	Herbaceous perennial	60[b]	—	Mayers and Lord (1983)
Lilium longiflorum[a]	Herbaceous perennial	50	—	Crone and Lord (1991)
Citrus sinensis	Woody perennial	100	—	Lord and Eckard (1985)

[a] Grown under controlled-growth chamber conditions.
[b] Use of plastochron index to measure time.

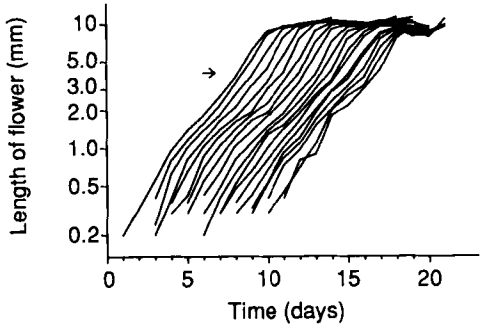

Fig. 3 Inflorescence plastochron determination for *Arabidopsis thaliana*. Flower growth curves for the first 20 nodes in the inflorescence of wild-type plants (N = 63). Measurements for each flower position averaged to form a composite plot. Reference length used for plastochron determination was 5 mm. Arrow indicates the length (~3.5 mm) at which the fertilized gynoecium (silique) becomes the longest part of the flower. [Reprinted from Crone and Lord (1994), with permission.]

Table II Staging and Timing of *Arabidopsis* Wild-Type Flower Development[a]

Stage	Developmental event	Plastochrons	SD	Duration in hours	SD	N^b
1	Flower buttress	1.9	0.3	23	4	9
2	Stalked flower primordium	2.1	1.0	26	12	15
3	Sepal initiation	1.1	0.5	14	6	16
4	Sepal primordial development	0.9	0.6	11	7	17
5	Petal/stamen initiation	0.7	0.5	9	6	18
6	Petal/stamen primordial development and carpel initiation	1.7	1.0	21	12	20
7	Anther archesporial cell initiation and first periclinal division	1.1	0.6	14	8	21
8	Sporogenous cell proliferation in anthers	1.8	0.9	22	12	21
9	Pollen mother cell differentiation and ovule initiation	1.7	0.8	21	11	17
10	Tetrad stage of meiosis, megaspore mother cell differentiation	1.1	0.7	14	9	11
11	Microspore maturation	1.6	0.7	19	9	9
12	Pollen and embryo sac maturation	2.0	0.8	25	10	4
13	Anthesis, self-pollination fertilization	1.8	1.0	22	12	4
14	Zygote and endosperm formation	1.0	0.0	12	0	4
15	Four-cell embryo	1.0	0.0	12	0	4
16	Sixteen-cell embryo (protoderm present)	0.8	0.5	9	6	4
17	Globular stage embryo	1.8	1.0	22	12	4
18	Heart stage embryo	1.5	0.7	19	9	2
19	Torpedo stage embryo	1.5	0.7	19	9	2

[a] Reprinted from Crone and Lord (1994) with permission.
[b] Number of inflorescences studied that contain that stage.

is at the other (10 days) (Crone and Lord, 1994; Fig. 3, Tables I and II). Sundberg (1982) was the first to use the plastochron index to measure the timing of early events in *Cyclamen* flower development. Organization of the flower apex and initiation of the four whorls of flower organs takes about 50 days in *Cyclamen persicum*, versus about 4 days in *Arabidopsis thaliana* (Crone and Lord, 1994). In both *Aradidopsis* and *Cyclamen*, about half of that time is spent in organizing the floral apex before sepal initiation. *Cyclamen* is an unusually slow-growing perennial with a long plastochron, 5.5 days, and *Arabidopsis* is a very fast-growing annual with a short plastochron, 12.4 hr.

Though the plastochron method has been the only means for examining the timing of events during early organogenesis, in *Arabidopsis* there is significant variation in the inflorescence plastochron within and among plants (Crone and Lord, 1994). This variation hampers any attempt to time development precisely. A possible source of the variation in this fast-

growing annual may be the *erecta* mutation in a Landsberg background. *Arabidopsis* is largely self-pollinating, and inbred lines are known to show more phenotypic variation than their outcrossed relatives (Falconer, 1989).

For this reason, small, rapidly growing annuals are not the plants of choice for studying the timing of events early in flower organogenesis. However, since the most interesting genetic and molecular work has been done on such annuals, for the time being these plants will continue to be used to gain a picture of how gene action specifies flower organogenesis.

The fact that floral homeotic genes appear to be highly conserved among angiosperms suggests that studies of the timing of events in flower development using probes for these genes may include larger flowered species that have more prolonged flower organogenesis.

III. *Arabidopsis thaliana:* A Model System for the Study of Flower Development

A. Wild-Type Flower Development

This chapter describes flower development in *Arabidopsis thaliana* wild type, as well as in members of the three classes of organ identity mutants and one meristic (organ number) mutant. Histological and morphological techniques were employed in conjunction with the plastochron index (Fig. 3) to better describe events in terms of time. The first six stages of flower development, when organs are initiating, coincide with those of Smyth *et al.* (1990), whose stages were designed using morphological features (Table II). Subsequent stages are based mainly on histological events, so they do not necessarily coincide with those of Smyth *et al.* (1990).

The *Arabidopsis* flower is typical of the Brassicaceae containing four whorls of organs, four sepals, four petals, six stamens (four long, two short), and a single bicarpelate gynoecium (Figs. 4a–4c). Sepals are the green outer appendages that enclose the floral bud as it grows before anthesis. Petals are the often showy, pigmented organs that expand rapidly at anthesis and are the most noticeable of the flower organs. The stamens are comprised of a stalk (filament) and a terminal anther that contains the male gametophyte, pollen. The gynoecium is composed of carpels that enclose the ovules which, when fertilized, become the seeds. The main axis inflorescence emerges from a rosette of leaves and produces many laterally borne flowers that have dorsiventral symmetry initially due to differences in sepals, the first whorl organs (Fig. 4d). In Figure 4d, floral developmental stages 1–5 are evident at the inflorescence apex. A number of stage 1 flower buttresses can be seen, as well as stage 2 stalked flower

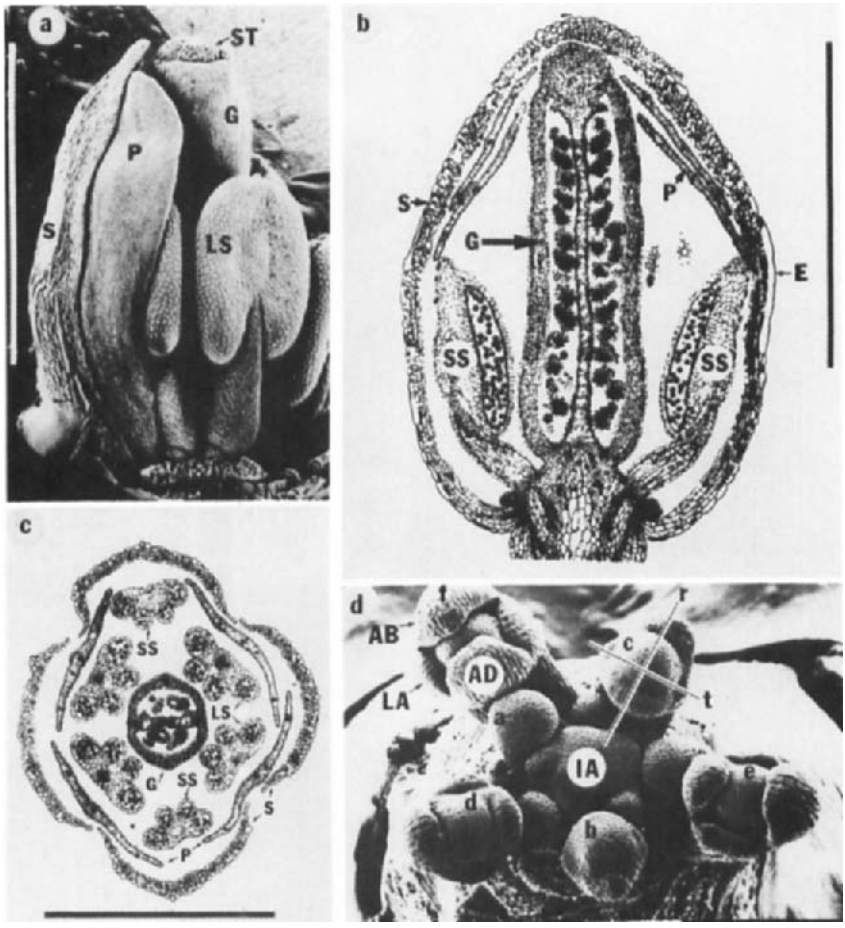

Fig. 4 Histology of wild-type (WT) flowers of *Arabidopsis thaliana*. (a) SEM view of WT flower with three sepals (S) and three petals (P) removed. At anthesis, petals expand beyond the sepals and gynoecium (G), and the long stamen (LS) filaments elongate so that the anthers are next to the stigma (ST). Bar = 1 mm. (b) Longitudinal section of WT flower in the plane of the short stamens (SS). The gynoecium (G) has a central septum characteristic of this family. Sepals (S) have many elongate epidermal cells (E) on their abaxial surface. Bar = 1 mm. (c) Transverse section of WT flower. Four petals (P) are positioned alternate to four sepals (S). Short stamens (SS) are in front of lateral sepals. Bar = 1 mm. (d) SEM view of WT inflorescence apex (IA) with several flowers initiated. Flowers a–f show the morphology of the early phases of flower development. Each flower has a dorsiventral symmetry, with one abaxial (AB) and one adaxial (AD) sepal, and two lateral (LA) sepals. Longitudinal sections are in the radial (r) or tangential (t) plane, or they are oblique. Bar = 0.1 mm. [Reprinted from Hill and Lord (1989), with permission.]

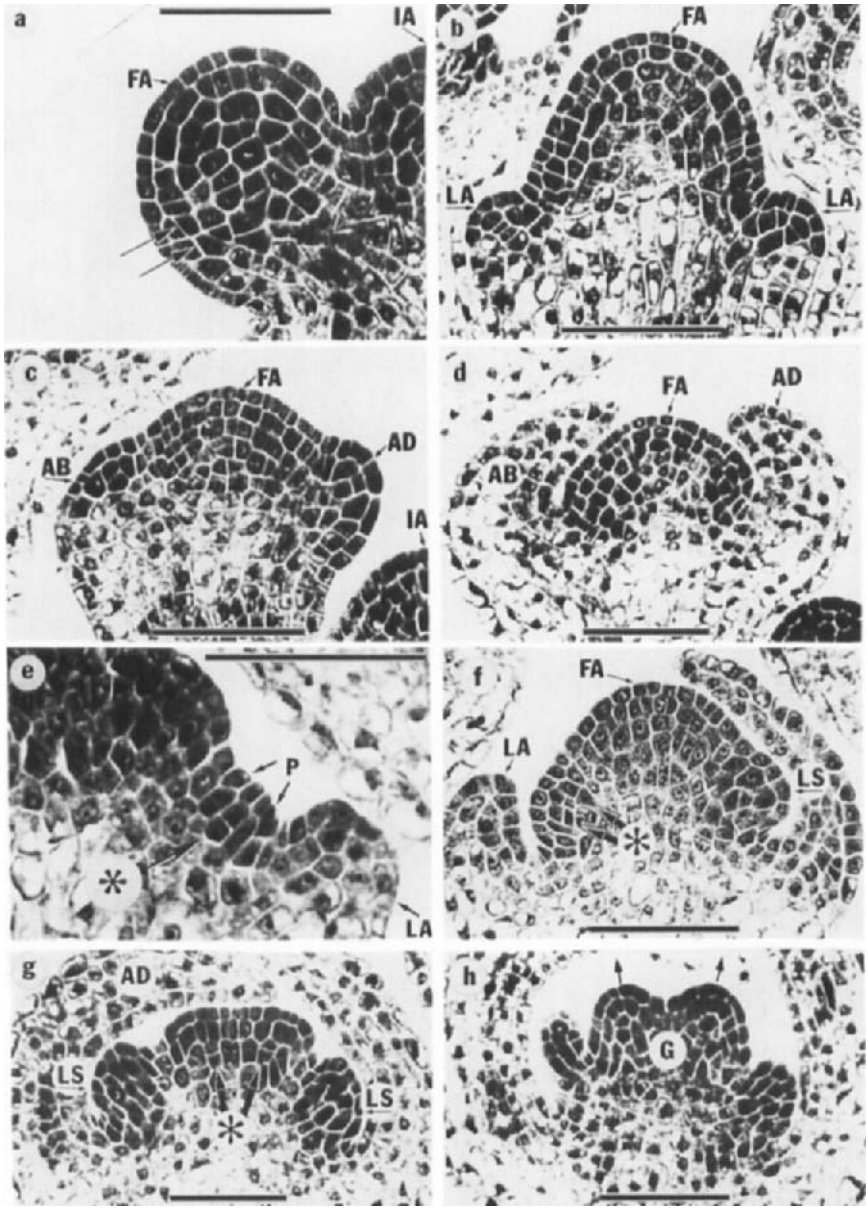

Fig. 5 Sepal, petal, and stamen and gynoecium initiation in wild-type (WT) *Arabidopsis thaliana*. (a) Radial section of abaxial sepal initiation by periclinal divisions in L_2 (arrows). (b) Tangential section of WT flower showing the early development of lateral sepals. (c) Radial section of WT flower at an early stage of abaxial and adaxial sepal development. (d) Radial section of WT flower just before petal and stamen initiation. The abaxial and adaxial sepals nearly cover the floral apex. (e) Petal initiation in a WT flower. The asterisk

primordia (the oldest is labeled a), stages 3 and 4, when sepals develop (labeled b and c), and stage 5, when petals and stamens initiate (labeled f). The interval between these separate flower intiation events, the inflorescence plastochron, is about 12.4 hr (Fig. 3). This interval was used as a means of timing the events in early organogenesis and it was found that stages 1 and 2 last about 2 days, stages 3 and 4 last about 1 day, and stage 5 lasts less than a day, totaling about 4 days from the time the flower meristem forms until carpels initiate (Fig. 11b; Table II). The perennial herb *Cyclamen* takes 50 days to develop to the same point, but in a larger flower (Sundberg, 1982).

A close histological examination of events during these early stages shows that each organ whorl arises in a distinctive manner and as a consequence is readily distinguishable from the other organ types right from inception (Fig. 5). When one quantifies the earliest events in organ initiation—cell expansion and division patterns on the flanks of the flower meristem where the organ arises—one can also ascribe distinct behaviors to each organ type (Fig. 6). The shoot apical meristem in angiosperms is often layered with respect to cell division planes. The outermost layer, L_1, shows typically only anticlinal (perpendicular to the surface) divisions which serve to perpetuate it as a dermal layer. The L_2 layer shows mainly anticlinal divisions until organs are initiated and then periclinal (parallel to the surface) divisions can be seen. The L_3 shows both types of divisions as well as oblique (Sussex, 1989). Sepals initiate as broad primordia with mainly periclinal divisions in the L_2 layer of the apex, with some L_3 cells participating as well (Figs. 5a–5d and 6a). Petals and stamens initiate next, alternate with the sepals and further up the flower apex. These two organ types are also readily distinguishable from one another histologically (Figs. 5e and 5f) and in their cell division patterns (Figs. 6b and 6c). Petals are diminutive organs initially, evident mainly as L_2 cell expansions in an anticlinal plane rather than by many periclinal divisions. Stamens are more massive and show periclinal divisions at initiation in L_2 and L_3 layers of the apex. The last organ to initiate is the gynoecium, arising as a ring

---

indicates a recent periclinal division of an elongate L_2 cell; the L_2 cells on either side of this cell have not yet divided. (f) WT short stamen initiation in front of a lateral sepal by periclinal cell divisions in L_2 (*). The section passes obliquely through a long stamen already initiated on the other side of the meristem. (g) Initiation of a WT gynoecium in L_3 (*). (h) Early development of WT gynoecium. Arrows indicate the two principle regions of apical growth visible in the radial plane. FA, floral apex; IA, inflorescence apex; LA, lateral sepal; AB, abaxial sepal; AD, adaxial sepal; P, petal; LS, long stamem; G, gynoecium. Bar = 50 μm. [Reprinted from Hill and Lord (1989), with permission.]

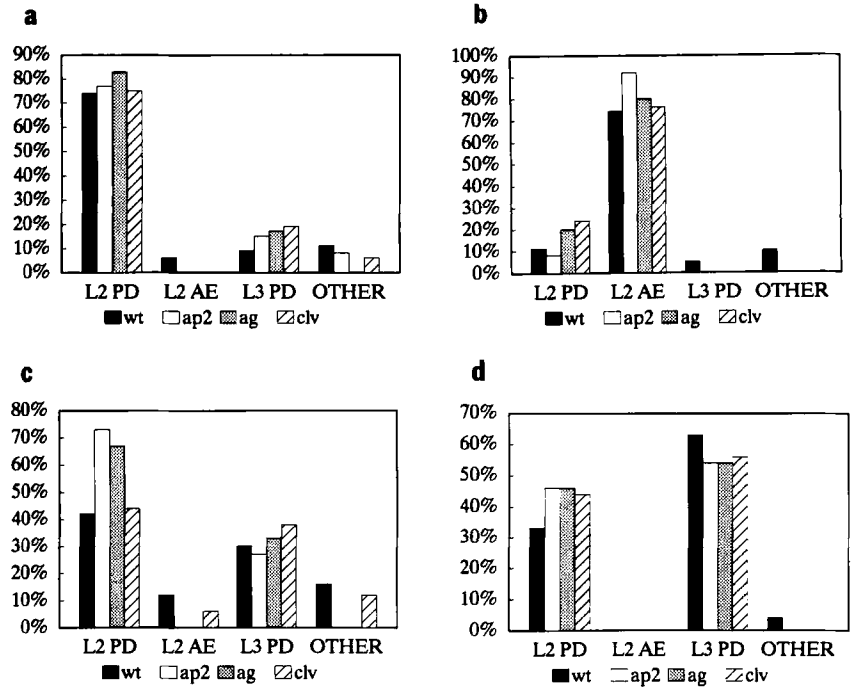

Fig. 6 Cell division patterns at initiation for all floral organs. (a) Initiation patterns for first whorl organs (sepals in wild type). wt, N = 35 flowers; ap2, N = 13; ag, N = 12; clv, N = 16. (b) Initiation patterns for second whorl organs (petals in wild type). wt, N = 19; ap2, N = 12; ag, N = 10; clv, N = 17. (c) Initiation patterns for third whorl organs (stamens in wild type). wt, N = 26; ap2, N = 11; ag, N = 12; clv, N = 16. (d) Initiation patterns for fourth whorl organs (gynoecium in wild type). wt, N = 27; ap2, N = 13; ag, N = 13; clv, N = 16. Number of inflorescences studied: wt, N = 21; ap2, N = 9; ag, N = 9; clv, N = 18. wt, wild type; ap2, *apetala2-1;* ag, *agamous;* clv, *clavata1-1;* L refers to cell layer in meristem; AE, anticlinal elongation; PD, periclinal division; OTHER, other cell division/expansion pattern. [Reprinted from Crone (1992), with permission.]

structure at the apex summit (Figs. 5g and 5h) and showing distinct cell division patterns, predominantly in the L_3 layer but in the L_2 layer as well (Fig. 6d).

B. Initiation Patterns in Organ Identity Mutants

Since the various flower organ types can be distinguished right at inception in the wild type, the prevalent hypothesis that the altered organs in the homeotic or organ identity mutants of *Arabidopsis* were one-for-one organ replacements was tested. If this were indeed the case, then in the *pistillata*

mutant, for example, a Class B type, where petals are replaced by sepals and stamens by carpels, the second whorl organs should initiate as do sepals with predominantly L_2 periclinal divisions, and the third whorl should initiate as do carpels with predominantly L_3 periclinal divisions. To test this idea, allometric analyses were used to describe shape changes in the organs as they grow and conventional histological techniques (i.e., cell number at initiation, in young primordia, and in mature organs when possible) to examine growth in the altered organs of the mutants. To incorporate an element of time, plastochron indices were developed for two of the organ identity mutants, *apetala2-1* and *agamous*, and for one meristic or organ number mutant, *clavata1-1*. The general observation was that organs initiate appropriately to their whorl as defined by the wild type, regardless of the mutant type. Subsequent development of the altered organs was divergent, and they took on features of the organs in adjacent whorls that were differentiating at the same time. Alterations in the timing of events were striking: all mutants had altered inflorescence plastochron durations, with prolongation of specific stages in flower development as well (Crone and Lord, 1993,1994).

The next section describes events in each of the three types of organ identity mutants and then describes the meristic mutant. The organs will be referred to as whorls 1 to 4 instead of their phenotypes in order to avoid confusion, since the altered organs in the mutants are often mosaic in nature.

1. Class A Mutant: *Apetala*

The *apetala2-1* mutant is a class A mutant in which whorls 1 and 2 are altered and are said to be transformed into carpels and stamens from sepals and petals, respectively. Hence, whorl 1 should show the initiation patterns of a carpel and whorl 2 should show those of a stamen if the transformation is complete. In fact, the first whorl organ initiates with L_2 periclinal divisions, much as a sepal does in stage 4, although cell number in the primordium is larger than in a wild-type sepal (Figs. 6a and 7a). Subsequent growth in terms of histology and allometry is sepal-like until stage 7, when the organ develops forked trichomes typical of leaves, along with female reproductive features [stigmatic papillae in flowers produced early in the inflorescence (Fig. 6d) and external ovules on those produced later]. The mature organ is a mosaic of leaf, sepal, and carpel features (Crone and Lord, 1994).

The second whorl organs in *apetala2-1* initiate like petals (not like stamens as the model predicts) with anticlinal elongation in the L_2 layer of the floral apex in stage 5 (Figs. 6b and 7b). This similarity also holds in terms of cell number in primordial stage 6 (Fig. 7c). By stage 8 (Fig.

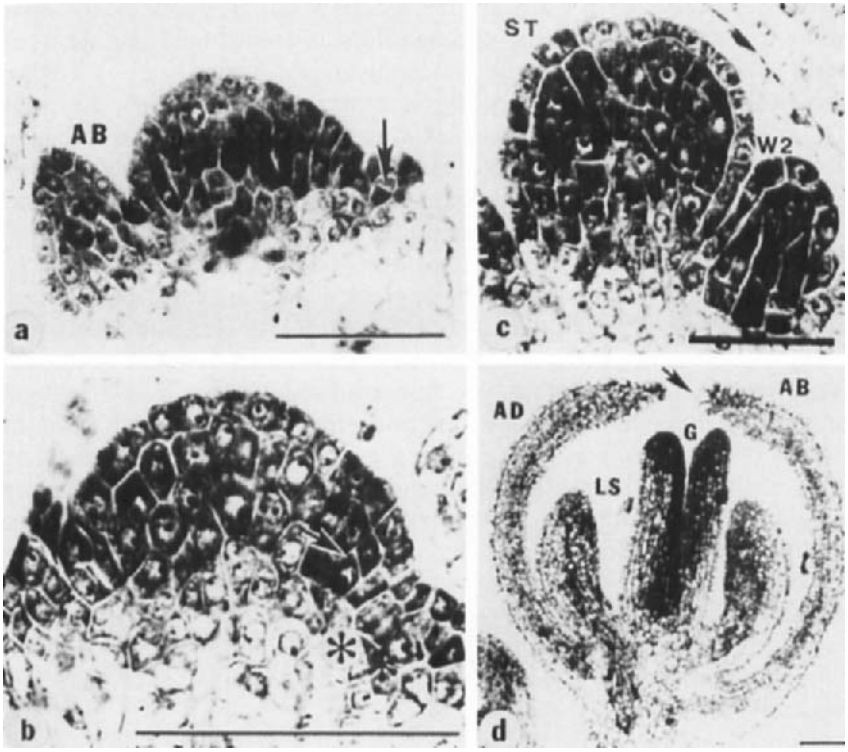

Fig. 7 Floral histology of the *apetala2-1* mutant of *Arabidopsis thaliana*. The patterns of cell division setting up the organs are similar to those of the sepals and petals of the wild type. (a) Radial longitudinal section of a stage 4 flower. Arrow on L_2 periclinal division during initiation of first whorl organ. For a wild-type comparison, see Fig. 5b. (b) Radial longitudinal section of stage 5 *apetala2-1* flower. Arrow points to L_2 periclinal division in initiating stamen primordium, and a star is beneath L_2 anticlinally elongated cells initiating second whorl organ primordium in a petal-like pattern. See Figs. 5e and 5f for wild-type comparisons. (c) Tangential longitudinal section of stage 6 *apetala2-1* flower showing a stamen and a second whorl organ primordium. No distinction can be made between the wild-type petal and the *apetala2-1* second whorl organ until stage 8. (d) Radial longitudinal section of a stage 8 flower. Arrowhead on stigmatic papillae of abaxial first whorl organ. The first and second whorls of the *apetala2-1* flower achieve their altered phenotype during later differentiation and not early initiation processes. AB, abaxial first whorl organ; AD, adaxial first whorl organ; G, gynoecium; ST, stamen; W2, second whorl organ of *apetala2-1*. Bars = 25 μm for c, 50 μm for a, b, d. [Reprinted from Crone and Lord (1994), with permission.]

7d), when the first whorl organ diverges and forms stigmatic tips on the leaf-like organ, the second whorl diverges to form a stamen with sporogenous cell proliferation. This staminoid structure in whorl 2 remains developmentally retarded compared to the third whorl normal stamen, but

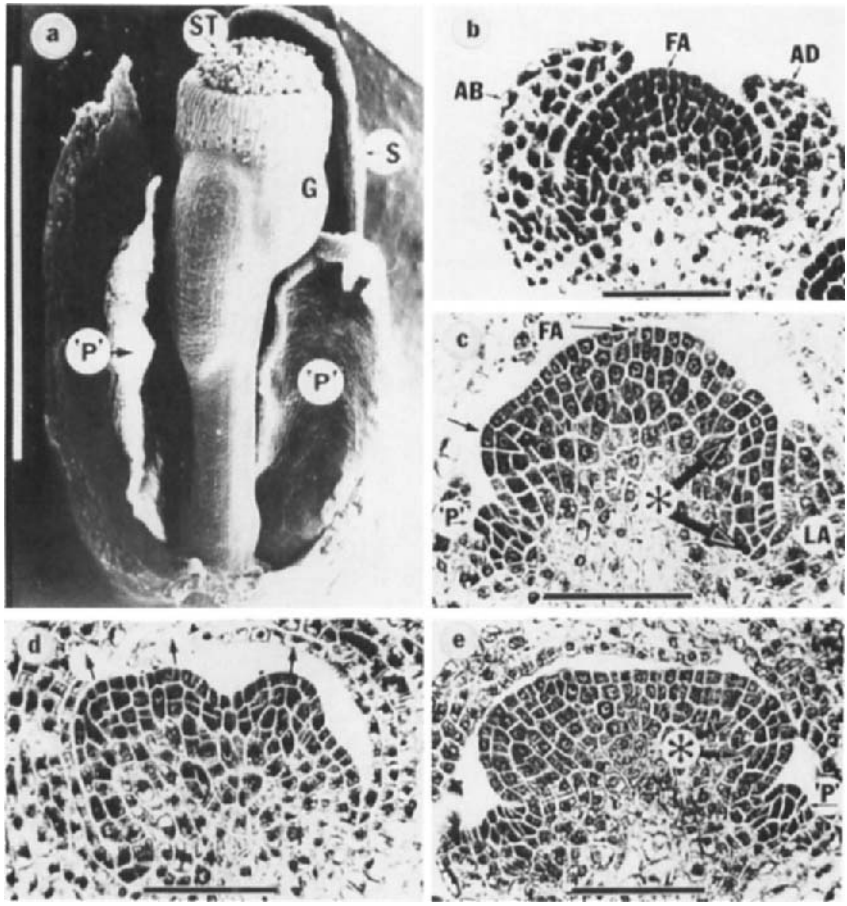

Fig. 8 Floral histology of the pistillata (PI) mutants of *Arabidopsis thaliana*. (a) SEM view of the pistillata flower with two sepals (S) and two "petals" (P) removed. The morphology of the gynoecium (G) is extremely variable in PI flowers. Bar = 1 mm. (b) Radial section of PI flower at the same point in development as the WT flower in Fig. 5d. The structure of WT and PI flowers at this stage is similar. AB, abaxial sepal; AD, adaxial sepal; FA, floral apex. (c) An oblique section of a PI flower near the time of stamen initiation in a WT flower. The floral meristem has an abnormal shape and pattern of cell division initiated by periclinal divisions in L_2 and L_3 distributed along the flanks of the floral meristem and not restricted to the sites of stamen initiation as in the WT (see Fig. 5g). A primordial buttress resembling a stamen primordium is visible (small arrow) above a developing "petal" ('P'). Asterisk shows periclinal divisions. (d) PI flower at a comparable stage with the WT flower in Fig. 5h when the gynoecium is initiating. The regions of apical growth (arrows) no longer conform to the wild-type pattern. (e) Oblique section of a PI flower at the time of gynoecium initiation in the WT flower (see Fig. 5g). There is an excessive number of periclinal divisions (asterisk) along the flanks of the floral meristem. No stamen primordia are evident in this section, but "petal" primordia are comparable to those in the WT flower. Bars = 50 μm for b–e. [Reprinted from Hill and Lord (1989), with permission.]

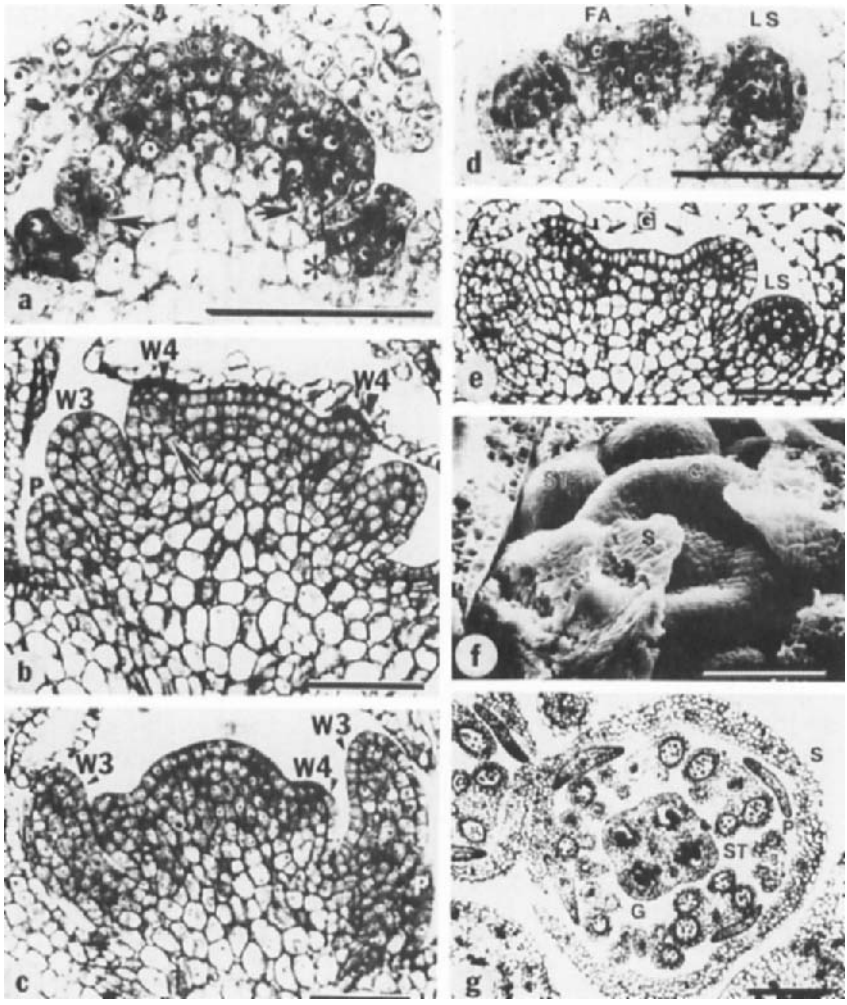

Fig. 9 Floral histology of the *agamous-1* and *clavata1-1* mutants of *Arabidopsis thaliana*. (a–c) Histology of the *agamous-1* flower. As with the *apetala2-1* floral mutation, organs initiate and develop as primordia appropriate to their whorl in *agamous-1* flowers. (a) Tangential longitudinal section of stage 5 *agamous-1* flower. Arrows point to L_2 periclinal divisions in initiating third whorl organ primordia, and an asterisk is beneath L_2 anticlinally elongated cells in initiating petal primordium. (b) Tangential longitudinal section of stage 6 *agamous-1* flower. Arrow points to L_3 periclinal division. The altered third whorl in the *agamous-1* flower initiates with a stamen pattern (a) and develops as a stamen primordium (b). (c) Diagonal longitudinal section of stage 7 *agamous-1* flower. The third whorl organs assume petaloid features in stage 7, when stamens in the wild type are undergoing sexual differentiation with archesporial cell differentiation. The altered fourth whorl organs initiate as do carpels, but on the flanks of the meristem (b), before they rapidly assume sepaloid histology and the floral apex reorganizes (c). P, petal; W3, third whorl organ of *agamous-1*; W4, fourth whorl organ of *agamous-1*. Bars = 50 μm. (d–g) Histology of the *clavata1-1* flower. The *clavata1-1* affects the organ number of all whorls, most notably forming a

eventually matures as a mosaic structure of petal and stamen features with an anther and pollen (Crone and Lord, 1994).

2. Class B Mutant: *Pistillata*

Pistillata is a class B type of organ identity mutant in which whorls 2 and 3 are altered and are said to be transformed into sepals and carpels, from petals and stamens, respectively (Meyerowitz *et al.*, 1991). The *apetala3* mutant shows the same phenotype and is thought to function with *pistillata* to specify petals and stamens (Jack *et al.*, 1993). So, in the mutant, whorl 2 should have sepal initiation features and whorl 3, carpel initiation patterns. In fact, after normal stages 1–4 for the flower apex (Fig. 8b), whorl 2 initiates in stage 5 (Fig. 8c) and develops as a petal until stage 8 (bud L 0.5 mm), when it is ~90μm in length. By this point, it has diverted on a sepal pathway in terms of differential growth and histology, resulting in a mature sepal–petal mosaic organ (Fig. 8a) (Hill and Lord, 1989).

In stage 5, the third whorl in *pistillata* initiates like a stamen (Fig. 8c) (not like a carpel as the model predicts), but very soon thereafter the floral apex becomes aberrant, with random proliferations on its flanks. The gynoecium initiates in stage 6 and seems to merge with the previously initiated stamen primordia to form aberrant carpeloid structures fused to the whorl 4 (often aberrant) gynoecium (Figs. 8a and c–e). So, while *apetala2-1* development is like that of the wild type through stage 6, *pistillata* diverges at about stage 5 due to early disruption in the stamen development, though petals are not visibly disrupted until stage 8 (Hill and Lord, 1989).

3. Class C Mutant: *Agamous*

Agamous is a class C mutant in which whorls 3 and 4 are altered and said to be transformed into petals and sepals from stamens and carpels, respectively (Meyerowitz *et al.*, 1991).

---

four-carpeled gynoecium. The floral apex of both wild-type and *clavata1-1* flowers appears similar before gynoecial initiation (Crone, 1992). (d) Radial longitudinal section of a late stage 5 flower before carpel initiation. This stage lasts longer in the mutant than in the wild type, and this prolongation results in an increase in cell number in the apex before carpel initiation. The carpels in *clavata1-1* initiate on the flanks of the floral apex, in a manner reminiscent of the fourth whorl organs of *agamous-1*. (e) Tangential longitudinal section of a stage 6 flower. (f) Axial view of *clavata1-1* at initiation (approximately). As the flower matures, the four-carpeled *clavata1-1* gynoecium is larger than the two-carpeled wild-type gynoecium. (g) Cross section of a stage 10–11 flower. Note the four carpels and seven (vs. six) stamens. FA, floral apex; G, gynoecium; LS, long (median) stamen; S, sepal; ST, stamen. Bars = 50 μm for d, e, f; 200 μm for h. [Reprinted from Crone and Lord (1993, 1994), with permission.]

Therefore, whorl 3 should initiate as a petal with L_2 anticlinal elongations and whorl 4 as a sepal with primarily L_2 periclinal divisions. In fact, the third whorl in *agamous* initiates in stage 5 (Figs. 6a and 6b) much as the wild-type stamen does (Fig. 9a) in terms of cell division patterns, cell number, and growth rate. The mutant organ develops like a stamen (Fig. 9b) until stage 7, taking on petaloid features when the wild-type stamens would normally be differentiating sporogenous tissue (Fig. 9c).

The four organs of the fourth whorl in *agamous* initiate with cell division patterns much like the wild-type gynoecium; divisions are mainly periclinal in L_3 (and some in L_2), but they are located on the flanks of the meristem, not apically (Fig. 9b). In terms of cell division patterns and cell number, these organs are more carpel-like than sepal-like.

In stage 7, the apex recognizes and takes on the look of a flower apex, initiating sepals in stage 3 wild-type flowers (Fig. 9c). Subsequent development of the whorl 3 organs shows them to be mosaic, with epidermal features of sepals and petals (Crone, 1992). The mutant shows a reiterating pattern of organ initiation, with an open system of growth forming flowers within flowers (Meyerowitz (*et al.*, 1991). With the loss of carpels, the apex loses its determinative quality and continues to cycle through the flowering program.

Using the plastochron to monitor the timing of events in both *apetala2-1* and *agamous* shows that the growth of individual flowers is slowed and the inflorescence plastochron prolonged (Figs. 10a and 10b). Many specific stages of flower development are prolonged in both mutants (Tables III and IV).

The three organ identity mutants in each of the three gene classes controlling flower organogenesis show no alterations in the initial stages of organogenesis. Mutant organs take on features of adjcant or neighboring organs during their differentiation. They are all mosaic organs; in no case was complete one-for-one organ transformations seen. It appears as if the identity genes do not affect initiation patterns, but rather are involved in targeting genes that code for differentiation products after initiation. They are certainly organ identity genes in that respect, but perhaps previously acting genes (those that target the identity genes?) are responsible for the cell expansion and division patterns that characterize the flower apex during stages 3–6, when the organs initiate. This proposal is hard to reconcile with the fact that the organ identity genes are first expressed before the organs whose identity they control are initiated, i.e., class A *apetala1* in stages 1 and 2, class B *apetala3* and class C *agamous* in stages 3 and 4, and class A *apetala2-1* virtually all over the plant (Okamura *et al.*, 1993). Until it is known when and where their respective proteins are produced, what genes turn on the identity genes, and what the identity genes themselves target, the story will remain incomplete.

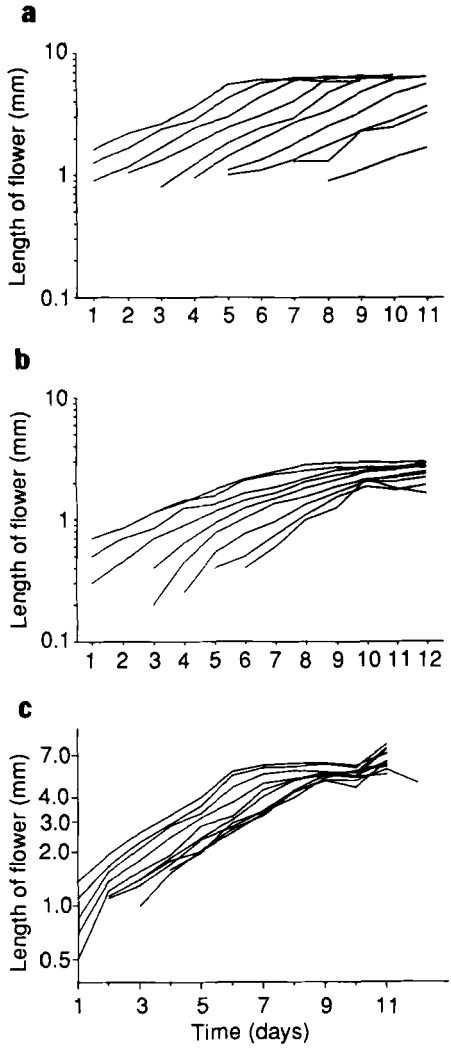

Fig. 10 Inflorescence plastochron determinations for *Arabidopsis thaliana* mutants. (a) Flower growth curves for the first 10 nodes in the *apetala2-1* inflorescence from four plants. Measurements for each flower position were averaged to form a composite plot. Reference length used for plastochron determination was 3 mm. (b) Flower growth curves for the first 9 nodes in the *agamous-1* inflorescences of two plants. Measurements for each flower position were averaged to form a composite plot. Reference length used for plastochron determination was 1 mm. [Reprinted from Crone and Lord (1994), with permission.] (c) Flower growth curves for the *clavata1-1* inflorescence. The composite lines represent the average flower length at each of the first 10 positions of the inflorescences of 10 plants. An index length of 4 mm was used to determine the plastochron. [Reprinted from Crone and Lord (1993), with permission.]

Table III Staging and Timing of *apetala2-1* Flower Development[a]

Stage	Developmental event	Plastochrons	SD	Duration in hours	SD	N^b
1	Flower buttress	1.8[c]	0.7	41[d]	16	9
2	Stalked flower primordium	1.7[c]	0.7	39[d]	16	9
3	First whorl organ initiation	1.8[d]	0.7	41[d]	16	9
4	First whorl organ primordial development	0.7	0.7	15	16	9
5	Second/third whorl organ initiation	1.9[d]	0.6	44[d]	14	9
6	Second/third whorl organ primordial development and carpel initiation	2.1[d]	0.3	49[d]	8	8
7	Anther archesporial cell initiation and first periclinal division	1.0	0.7	23[d]	16	9
8	Sporogenous cell proliferation in anthers, archesporial cell formation in second whorl organs	2.6[d]	0.9	60[d]	21	9
9	Pollen mother cell differentiation and ovule initiation; sporogenous cell formation in second whorl organs	2.0	0.8	47[d]	18	8
10	Tetrad stage of meiosis, megaspore mother cell differentiation; pollen mother cell formation in second whorl organs	0.7[c]	0.5	17	11	7
11	Microspore maturation; tetrad stage of meiosis in second whorl organs	2.3[d]	0.8	54[d]	19	6
12	Pollen and embryo sac maturation; microspore maturation in second whorl organs	1.4[c]	0.5	33	13	5

[a] Reprinted from Crone and Lord (1994) with permission.
[b] Number of sectioned inflorescences studied that contain that stage.
[c] Duration of stage statistically shorter than that of wild type ($p < 0.05$).
[d] Duration of stage statistically longer than that of wild type ($p < 0.05$).

C. Meristic Mutant

The last type of mutant examined is a meristic mutant, *clavata1-1*, which increases the numbers of organs in the whorls, particularly whorl 4, to produce a four-carpeled ovary (Fig. 9g). Development of the flower apex in *clavata1-1* is similar to that of the wild type until stage 5 prior to gynoecium initiation (Fig. 9d). At this point, the apex looks similar to that of the wild type, but stage 5 is prolonged in the mutant (Table V) and this results in an increase in cell number in the apex before carpel initiation (Crone and Lord, 1993). This increase in size is only measurable later, after carpel initiation in stage 7. The carpels initiate on the flanks of the apex in *clavata1-1*, much as whorl 4 initiates in the *agamous* mutant (compare Fig. 9b to Fig. 9e) and unlike the more apical location in the wild type (Fig. 5h). The size of the initiating gynoecium is larger than in the wild type as expected since it is a doubled organ (Figs. 9f and 9g).

Table IV Staging and Timing of *agamous-1* Flower Development[a]

Stage	Developmental event	Plastochrons	SD	Duration in hours	SD	N^b
1	Flower buttress	1.9	0.8	40[c]	16	9
2	Stalked flower primordium	1.3[d]	0.9	28	18	9
3	Sepal initiation	1.2	1.0	26	20	9
4	Sepal primordial development	1.0	0.5	21[c]	11	8
5	Petal/third whorl initiation	1.3[c]	0.5	26[c]	10	8
6	Fourth whorl organ initiation	1.6	1.2	34	25	8
7	Fourth whorl primordial growth	0.9	0.6	18	13	8
	Completion of second flower[e] reiteration (whorls 4–6)	1.3	1.3	26	27	8
	Third flower reiteration (whorls 7–9)	2.5	1.7	53	35	8
	Fourth flower reiteration (whorls 10–12)	2.6	1.1	54	24	7
	Fifth flower reiteration (whorls 13–15)	2.0	1.0	42	21	5
	Sixth flower reiteration (whorls 16–18)	1.0	0.0	21	0	3
	Seventh flower reiteration (whorls 19–21)	1.0	0.0	21	0	1

[a] Reprinted from Crone and Lord (1994) with permission.
[b] Number of sectioned inflorescences studied that contain that stage.
[c] Duration of stage statistically longer than that of wild type ($p < 0.05$).
[d] This and subsequent stages listed are not equivalent to reported stages in wild-type and other mutants.
[e] Duration of stage statistically shorter than that of wild type ($p < 0.05$).

The inflorescence plastochron for *clavata1-1* showed a slower rate of flower growth and a shorter plastochron than the wild type (Fig. 10c). Nonetheless, most stages in flower development were prolonged compared to the wild type (Table V).

IV. Models for Flower Development

Models to explain how the flower meristem becomes determined fall basically into two groups. One suggests that the flower apex is blocked out at one point in time in concentric whorls that correspond with the four whorls of organs; this is referred to as a "spatial model" (Holder, 1979; Schwartz-Sommer *et al.*, 1990; Meyerowitz *et al.*, 1991) (Fig. 11a). The other suggests that the concentric whorls or organs are specified sequentially as the flower apex grows acropetally (Wardlaw, 1957; Heslop-Harrison, 1964). The spatial model predicts that class A, B, and C genes would turn on at one point in time in the flower meristem, before sepal initiation, and that the organs in the four whorls would subsequently differentiate independent of one another. The sequential model predicts

Table V Staging and Timing of *clavata1-1* Flower Development[a]

Stage	Developmental event	Plastochrons	SD	Duration in hours	SD	N^b
1	Flower buttress	2.6[c]	0.7	28	8	10
2	Stalked flower primordium	2.7[c]	0.7	29	7	10
3	Sepal initiation	2.0[c]	0.8	22[c]	9	10
4	Sepal primordial development	1.5[c]	0.8	16	9	10
5	Petal/stamen initiation	2.3[c]	0.7	25[c]	7	10
6	Petal/stamen primordial development and carpel initiation	2.3[c]	0.7	25	7	10
7	Anther archesporial cell initiation and first periclinal division	1.5[c]	0.7	16	8	10
8	Sporogenous cell proliferation in anthers	3.3[c]	0.9	36[c]	10	10
9	Pollen Mother cell differentiation and ovule initiation	2.5[c]	1.0	27	12	10
10	Tetrad stage of meiosis, megaspore mother cell differentiation	1.3	1.1	14	11	9
11	Microspore maturation	4.0[c]	1.9	43[c]	21	9
12	Pollen and embryo sac maturation	1.4	0.8	15	8	7
13	Anthesis, self-pollination	1.7	0.6	18	6	3

[a] Reprinted from Crone and Lord (1993) with permission.
[b] Number of sectioned inflorescences studied that contain that stage.
[c] Duration of stage statistically longer than that of wild type ($p < 0.05$).

that each class of genes would turn on just before the initiation of the whorl they control, i.e., first, class A before sepal and petal initiation; next, class B before petal and stamen initiation; and last, class C before stamen and carpel initiation. Since the gene classes control overlapping sets of organs during their sequential production, this model predicts interactions between adjacent organs as they grow. There are variations on these two themes, such as Irish and Sussex's (1990) model, which is a combination of a sequential and spatial model, with class A genes turned on before class B and C genes, but class A and C genes specifying position in the apex and activating class B genes. In fact, any sequential model has a spatial component to it, but the reverse is not the case.

A. Expression Patterns for the Organ Identity Genes

The expression patterns of the class B and C genes in *Arabidopsis* (*apetala3* and *agamous*) were described first, before the class A genes. The two classes of genes appeared to turn on in late stage 3 or early stage 4

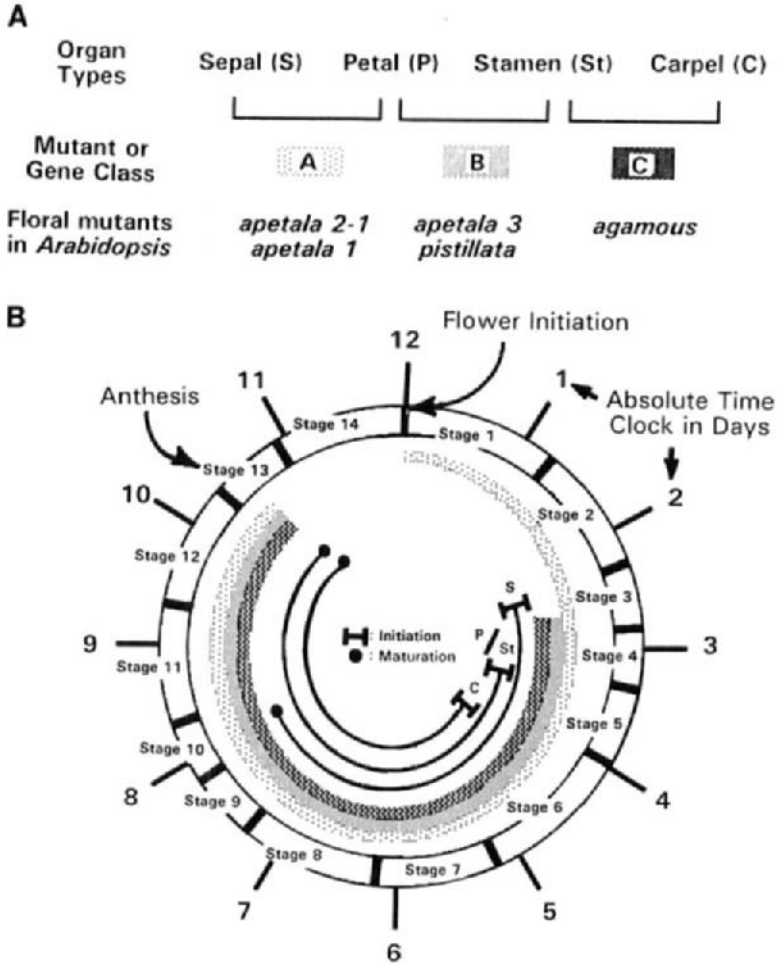

Fig. 11 Model for timing of organogenesis and organ identity gene action in flowers of *Arabidopsis thaliana*. (A) Genetic model for how three gene classes (A–C) govern flower organ identity in *Arabidopsis*. Each gene class controls identity of two adjacent organ types in the flower. The floral mutants show altered organs in the two whorls whose identity is specified by a gene class [revised from Meyerowitz *et al.* (1991)]. (B) A time clock for flower development in *Arabidopsis* based on staging with a plastochron index [data from Crone (1992), which are slightly different from those in Table II because they are from flower positions 1–26 instead of 1–12]. The timing of expression of the three classes of organ identity genes is included based on data from Mandel *et al.* (1992) for *apetala1;* Jack *et al.* (1992) for *apetala3;* and Drews *et al.* (1991) for *agamous*.

after sepal initiation, but before petal/stamen and carpel initiation. This observation was interpreted to "rule out certain types of sequential models" (Jack *et al.*, 1992). But it could also be interpreted as supportive of a sequential model, since neither class B nor class C genes are turned on in the flower meristem in stages 1 and 2 when they should be blocking out the apex with class A genes, as the spatial model predicts. Both petals and stamens arise simultaneously in *Arabidopsis* (Hill and Lord, 1989), and both are specified by a combination of gene classes, A and B for petals and B and C for stamens. In fact, one expects that all three classes of genes would need to be turned on for the initiation of these two organs even if a sequential model were to hold. This raises the difficulty of using the *Arabidopsis* system to test these models. A more typical situation in flowering plants is petal initiation before stamen initiation, and only in such a flower would one expect to see the class B genes (petal- and stamen-controlling) on before class C genes (stamen- and carpel-controlling). So the data on the expression patterns of *apetala3* (class B) and *agamous* (class C) are not as useful for resolving the problem as the data on class A genes. The class A genes, both models predict, would be expressed in the flower meristem in stages 1 and 2, and this is the case. *Apetala2-1* expression is not restricted to these stages though or to flowers, which is unlike the other organ identity genes (Okamura *et al.*, 1993), Data on *apetala1*, a class A gene controlling flower meristem identity as well as sepal and petal identity, have perhaps resolved the matter by showing sequential gene activity in the developing flower meristem as predicted by the sequential model (Mandel *et al.*, 1992). *Apetala1* is first expressed in stages 1 and 2 when flower primordia form. In stages 3 and 4, *apetala1* expression is restricted to the first whorl, as the meristem grows prior to initiation of the petal/stamen whorls. In late stage 3 and stage 4, *apetala3* and *agamous* are first expressed in the growing meristem, higher on the apical dome, above insertion of the sepals. This is presumably in preparation for the next set of organs, petals and stamens, which require class B (*apetala3*) and class C (*agamous*) gene action (Fig. 11b). The class A (*apetala1*) gene remains in the sepals and appears in the newly formed petals; the class B gene (*apetala3*) remains in the petals and stamens; and the class C gene is expressed in the stamens and the carpels when they initiate in stage 6. Since both petals and stamens initiate at once, and necessitate both class B and C gene activity at once, one would expect that *apetala3* and *agamous* would show expression for this event at the same time, even with a sequential model in mind. It is the previous expression of the class A gene *apetala1* alone in stages 1 and 2 that demonstrates the sequential nature of the organ identity gene action in *Arabidopsis*.

Expression patterns for the organ identity genes support the sequential model proposed by Wardlaw (1957) and not the spatial model proposed

by Holder (1979) and are generally accepted by those currently working on the organ identity genes (Jack *et al.*, 1992). To better resolve the exact pattern of the timing of gene activity at the apex during organ specification, flowers whose development is sequential for every organ whorl, as is more typical of angiosperms, and flowers that have a protracted organ initiation schedule rather than an abbreviated one as in *Arabidopsis* should be used (Table I).

B. Altered Whorls in the Organ Identity Mutants Are Not Complete Organ Transformations

When the mutant flowers of *Arabidopsis* were examined, no normal organs, even in the supposedly unaltered whorls, were observed (Crone and Lord, 1994). There were modifications, to some degree, in the form and development of all the organs. The fact that altered whorls bore mosaic organs probably reflects the fact that initiation of all organs followed a basic wild-type plan. Once initiated, the altered organ could take on features of adjacent, more normal whorls, but retained some features of its own whorl, whether cell number in the primordium, differential growth patterns, or even histological features. Each organ whorl may be unspecified as to its ultimate fate at initiation, but some degree of differentiation occurs even at this early stage. The idea of transformation comes from animal studies on homeotic mutants of flies, but even there, the altered organs are mosaics to some degree; in the *antennapedia* mutant of *Drosophila,* the altered organ starts off with a cell number and cell proliferation pattern like that of an antenna, and only after the third instar do the homeotic *antennapedia* organs begin to be leg-like (Postlethwait and Schneiderman, 1971). Schwartz-Sommer *et al.* (1990) recognized the mosaic nature of the altered organs in the mutants of *Antirrhinum majus* and refer to them as sepaloid, and so forth.

In plants, what are often interpreted as transformations or homeotic effects can also be interpreted as heterochronic effects (Hill and Lord, 1989). For example, the LEAFY gene in *Arabidopsis* controls the transition from inflorescence to flower meristem formation (Schultz and Haughn, 1991), much as the FLO gene acts in *Antirrhinum* (Coen *et al.*, 1990). The *leafy* mutant in *Arabidopsis* forms inflorescence meristems where flower meristems should be forming. This can be interpreted as a transformation of the flower meristem into an inflorescence meristem (Weigel *et al.*, 1992), but since the plant normally produces both lateral inflorescence meristems and lateral flower meristems along the main axis of the inflorescence, this sort of mutant can also be interpreted as heterochronic, showing a change in the timing of the switch from lateral inflorescence to lateral floral meristems. Hempel and Feldman (1994) have shown

nicely how knowledge of the relative timing of flower and lateral inflorescence production is essential for interpreting the *leafy* phenotype.

C. A Modification of the Sequential Model

One can look at the organ identity mutant phenotypes as resulting from alterations in developmental timing. The flower apex is programmed to produce a sequence of floral whorls, which form even in the absence of the organ identity genes, but form as leaf-like organs in the proper floral formula or pattern (Meyerowitz *et al.*, 1991). This provides evidence for previously acting genes that control patterning of the organs in the flower (Coen, 1991). Given that initiation patterns of the organs in the organ identity mutants are the same as the wild type, this aspect of early organogenesis is probably under control by these previously acting patterning genes.

When a class of organ identity genes is missing, the timing of differentiation events may become altered (hence, the disrupted plastochrons of the mutants), and the primordia that are initiated may have to rely on neighboring organ differentiation products to complete their development. Hence, the organ is mosaic in nature. The sequential events in organ initiation and development in the flower occur as an overlapping set of programs that obviously are not independent if such mosaic organs can form.

Each of the mutants shows this "nearest-neighbor" effect. In *apetala2-1*, the first whorl organ appears leaf-life, since it is the first organ to initiate in the flower, and the nearest differentiating organ is the cauline leaf on the inflorescence stalk. The addition of ovules on the margins of these "leaves" in the first whorl of *apetala2-1* occurs later in development and can be attributed to differentiation products from carpels which are then present in the *apetala2-1* flower. To propose that carpels can be nearest neighbors to sepals, though, is only conceivable is one considers the flower sequence to occur in a cycle where the progression from sepals to carpels can be reiterated continuously; carpel production typically "uses up" the apex of a flower. It is proposed that once an apex is evoked, a cycle of floral organ whorls turns on that will reiterate if not stopped by carpel production (i.e., in *agamous*, a class C mutant, no carpels are initiated and the cycle can therefore go on to produce flowers inside flowers, an indeterminate floral apex). Green (1989) has noted how like a cycling engine the shoot apex is in the vegetative or inflorescence mode. The flower is a shoot system too, determinate only by virtue of its production of carpels, which may, in some instances, terminate the apex.

The *apetala2-1* second whorl organ initiates as a petal, but is altered to form a stamen-like organ since the nearest normal differentiation product is that of the third whorl stamens. The second whorl in *pistillata* initiates

as a petal, but since the third whorl in this mutant is also altered, the nearest normal organ will be the previous one, the sepal, so that the second whorl organs later assume a sepaloid phenotype. The third whorl organs have as their nearest normal neighbor the carpels, which will initiate shortly after the third whorl organs. The third whorl initiates as a stamen, but then assumes gynoecial characteristics, with periclinal cell division much as occurs in carpels, but here occurring along the flanks of the floral apex (Hill and Lord, 1989).

In *agamous,* the third whorl organs assume, early on, many of the characteristics of the second whorl in terms of slower proliferation of cells and the final petaloid phenotype of the organ. The fourth whorl may utilize the differentiation product of its nearest neighbor, which, if flower development is explained as a reiterating cycle, is the sepal. The other nearest, normally differentiating neighbor is the petal, perhaps explaining the later-developing petaloid margins of the fourth whorl *agamous* organs.

One way to partially test this model would be to examine the triple mutant that lacks any organ identity function (Meyerowitz *et al.,* 1991). These "flowers" have leaf-like organs arranged in the proper floral pattern, all with an appearance similar to that of *apetala2-1* first whorl organ. This model predicts that the whorls in these "flowers" would initiate as normal floral whorls and be diverted into cauline leaves due to the total absence of organ identity gene products. Work on the floral meristem identity genes *leafy* and *apetala-1* demonstrates that the expression of the class B and C genes require their activity (Weigel and Meyerowitz, 1993). Since the *apetala-1* gene plays a dual role in meristem identity and class A function, it appears that a sequence of genes is turned on with flower induction, much as Wardlaw (1957) envisioned. One missing piece of the puzzle is those prepattern genes that establish the flower formula, the feature which makes each flower unique and characteristic of its species. The genetic/molecular approach being taken by many laboratories in the United States and in Europe will no doubt provide an answer in the near future.

References

Ambros, V., and Horvitz, H. R. (1984). Heterochronic mutants of the nematode *Caenorhabdites elegans. Science* **226,** 409–416.

Bertrand-Garcia, R., and Freeling, M. (1991). Hairy-sheath frayed #1-0: A systemic, heterochronic mutant of maize that specifies slow development stage transitions. *Am. J. Bot.* **78,** 747–765.

Coen, E. S. (1991). The role of homeotic genes in flower development and evolution. *Annu. Rev. Plant Physiol. Plant Mol. Biol.* **42,** 241–279.

Coen, E. S., and Meyerowitz, E. M. (1991). The war of the whorls: Genetic interactions controlling flower development. *Nature* **353,** 31–37.

Coen, E. S., Romero, J. M., Doyle, S., Elliott, R., Murphy, G., and Carpenter, R. (1990). *floricaula:* A homeotic gene required for flower development in *Antirrhinum majus*. *Cell* **63,** 1311–1322.

Crone, W. (1992). "Growth Patterns in Floral Organogenesis." Ph.D. Dissertation, University of California, Riverside.

Crone, W., and Lord, E. M. (1991). A kinematic analysis of gynoecial growth in *Lilium longiflorum:* Surface growth patterns in all floral organs are triphasic. *Dev. Biol.* **143,** 408–417.

Crone, W., and Lord, E. M. (1993). Flower development in the organ number mutant *clavata1-1* of *Arabidopsis thaliana* (Brassicaceae). *Am. J. Bot.* **80,** 1419–1426.

Crone, W., and Lord, E. M. (1994). Floral organ initiation and development in wild type *Arabidopsis thaliana* (Brassicaceae) and in the organ identity mutants *apetala2-1* and *agamous1*. *Can. J. Bot.* (in press).

Drews, G. N., Bowman, J. L., and Meyerowitz, E. M. (1991). Negative regulation of the *Arabidopsis* homeotic gene *AGAMOUS* by the *APETALA2* product. *Cell* **65,** 991–1002.

Erickson, R. O. (1948). Cytological and growth correlations in the flower bud and anther of *Lilium longiflorum*. *Am. J. Bot.* **35,** 729–739.

Erickson, R. O., and Michelini, F. J. (1957). The plastochron index. *Am. J. Bot.* **44,** 297–305.

Falconer, D. S. (1989). "Introduction to Quantitative Genetics," 3rd Ed. Longman Scientific and Technical, Essex, England.

Green, P. B. (1989). Shoot morphogenesis, vegetative through floral, from a biophysical perspective. *In* "Plant Reproduction: From Floral Induction to Pollination" (E. M. Lord and G. Bernier, eds.), Vol. 1, pp. 58–75. The American Society of Plant Physiologists Symposium Series.

Green, P. B., Havelange, A., and Bernier, G. (1991). Floral morphogenesis in *Anagallis:* Scanning-electron-micrograph sequences from individual growing meristems before, during, and after the transition to flowering. *Planta* **185,** 502–512.

Guerrant, E. O. (1982). Neotenic evolution of *Delphinium nudicaule* (Ranunculaceae) a humming-bird pollinated larkspur. *Evolution* **36,** 699–712.

Haughn, G. W., and Sommerville, C. R. (1988). Genetic control of morphogenesis in *Arabidopsis*. *Dev. Genet.* **9,** 73–89.

Hempel, F. D., and Feldman, L. J. (1994). Bidirectional inflorescence development in *Arabidopsis thaliana:* Acropetal initiation of flowers and basipetal initiation of paraclades. *Planta* (in press).

Hernandez, L. F., Havelange, A., Bernier, G., and Green, P. B. (1991). Growth behavior of single epidermal cells during flower formation: Sequential scanning electron micrographs provide kinematic patterns for *Anagallis*. *Planta* **185,** 139–147.

Heslop-Harrison, J. (1964). Sex expression in flowering plants. *Brookhaven Symp. Biol.* **16,** 109–125.

Hill, J. P., and Lord, E. M. (1989). Floral development in *Arabidopsis thaliana:* A comparison of the wild type and the homeotic *pistillata* mutant. *Can. J. Bot.* **67,** 2922–2935.

Hill, J. P., and Lord, E. M. (1990a). A method for determining plastochron indices during heteroblastic shoot growth. *Am. J. Bot.* **77,** 1491–1497.

Hill, J. P., and Lord, E. M. (1990b). The role of developmental timing in the evolution of floral form. *In* "Seminars in Developmental Biology" (R. Raff, ed.), pp. 281–287. Saunders, London.

Hill, J. P., Lord, E. M., and Shaw, R. G. (1992). Morphological and growth rate differences among outcrossing and self-pollinating races of *Arenaria uniflora* (Caryophyllaceae). *J. Evol. Biol.* **5,** 559–573.

Hill, J. P., and Malmberg, R. L. (1991). Rates of corolla growth in tobacco determined with the plastochron index. *Planta* **185,** 472–478.

Holder, N. (1979). Positional information and pattern formation in plant morphogenesis and a mechanism for the involvement of plant hormones. *J. Theor. Biol.* **77,** 195–212.

Ingham, P. W. (1988). The molecular genetics of embryonic pattern formation in *Drosophila*. *Nature* **335,** 25–34.

Irish, Y. F., and Sussex, J. M. (1990). Function of the *apetala-1* gene during *Arabidopsis* floral development. *Plant Cell* **2,** 741–753.

Jack, T., Brockman, L. L., and Meyerowitz, E. M. (1992). The homeotic gene *APETALA3* of *Arabidopsis thaliana* encodes a MADS box and is expressed in petals and stamens. *Cell* **68,** 683–697.

Lamoreaux, R. J., Chaney, W. R., and Brown, K. M. (1978). The plastochron index: A review after two decades of use. *Am. J. Bot.* **65,** 586–593.

Lee, M., and Nurse, P. (1988). Cell cycle control genes in fission yeast and mammalian cells. *Trends Genet.* **4,** 287–290.

Lord, E. M. (1979). The development of cleistogamous and chasmogamous flowers in *Lamium amplexicaule* (Labiatae): An example of heteroblastic inflorescence development. *Bot. Gaz.* **140,** 39–50.

Lord, E. M., and Eckard, K. J. (1985). Shoot development in *Citrus sinensis* L. (Washington naval orange). I. Floral and inflorescence ontogeny. *Bot. Gaz.* **146,** 320–326.

Lord, E. M., Eckard, K. J., and Crone, W. (1989). Development of the dimorphic anthers in *Collomia grandiflora:* Evidence for heterochrony in the evolution of the cleistogamous flower anther. *J. Evol. Biol.* **2,** 81–93.

Lord, E. M., and Hill, J. P. (1987). Evidence for heterochrony in the evolution of plant form. *In* "Development as an Evolutionary Process" (R. A. Raff and R C. Raff, eds.), pp. 47–70. A. R. Liss, New York.

Mandel, M. A., Gustafson-Brown, C., Savidge, B., and Yanofsy, M. F. (1992). Molecular characterization of the *Arabidopsis* floral homeotic gene *APETALA1*. *Nature* **360,** 273–377.

Mayers, A. M., and Lord, E. M. (1983). Comparative flower development in the cleistogamous species *Viola odorata*. II. An organographic study. *Am. J. Bot.* **70,** 1556–1563.

Meyerowitz, E. M., Bowman, J. L., Brockman, L. L., Drews, G. N., Jack, T., Sieburth, L. E., and Weigel, D. (1991). A genetic and molecular model for flower development in *Arabidopsis thaliana*. *Development* **112**(Suppl. 1), 157–168.

Minter, T. C., and Lord, E. M. (1983). A comparison of cleistogamous and chasmogamous floral development in *Collomia grandiflora* Dougl. ex. Lindl. (Polemoniaceae). *Am. J. Bot.* **70,** 1499–1508.

Okamura, J. K., den Boer, B. G. W., and Jofuku, K. D. (1993). Regulation of *Arabidopsis* flower development. *Plant Cell* **5,** 1183–1193.

Poethig, R. S. (1988). Heterochronic mutations affecting shoot development in maize. *Genetics* **119,** 959–973.

Postlethwait, J. H., and Schneiderman, H. A. (1971). Pattern formation and determination in the antenna of the homeotic mutant *antennapedia* of *Drosophila melanogaster*. *Dev. Biol.* **25,** 606–640.

Raff, R. A., and Kaufman, T. C. (1983). "Embryos, Genes, and Evolution." Macmillan, New York.

Schultz, E. A., and Haughn, G. W. (1991). *LEAFY*, a homeotic gene that regulates inflorescence development in *Arabidopsis*. *Plant Cell* **3,** 771–781.

Schwartz-Sommer, Z. P., Huijser, W., Nacken, H., Saedler, H., and Sommer, H. (1990). Genetic control of flower development by homeotic genes in *Antirrhinum majus*. *Science* **250,** 831–936.

Silk, W. K. (1984). Quantitative descriptions of development. *Annu. Rev. Plant Physiol.* **35,** 479–518.

Smyth, D. R., Bowman, J. L., and Meyerowitz, E. M. (1990). Early flower development in *Arabidopsis*. *Plant Cell* **2,** 755–767.

Sommer, H., Beltran, J., Huijser, P., Papa, H., Lonnig, W., Saedler, H., and Schwarz-Sommer, Z. (1990). *Deficiens*, a homeotic gene involved in the control of flower morphogenesis in *Antirrhinum majus:* The protein shows homology to transcription factors. *EMBO J.* **9,** 605–613.

Sundberg, M. D. (1982). Floral ontogeny in *Cyclamen persicum* 'F-1 Rosemunde Rose' (Primulaceae). *Am. J. Bot.* **69,** 380–388.

Sussex, I. M. (1989). Developmental programming of the shoot meristem. *Cell* **56,** 225–229.

Wardlaw, C. W. (1957). The floral meristem as a reaction system. *Proc. R. Soc. Edinburgh* **66,** 394–408.

Weigel, D., Alvarez, J., Smyth, D. R., Yanofsky, M. F., and Meyerowitz, E. M. (1992). *LEAFY* controls floral meristem identity in *Arabidopsis*. *Cell* **69,** 843–859.

Weigel, D., and Meyerowitz, E. M. (1993). Activation of floral homeotic genes in *Arabidopsis*. *Science* **261,** 1723–1726.

Williams, R. F. (1975). "The Shoot Apex and Leaf Growth: A Study in Quantitative Biology." Cambridge University Press, Cambridge.

Wolpert, L. (1969). Positional information and the spatial pattern of cellular differentiation. *J. Theor. Biol.* **25,** 1–47.

Yanofsky, M. F., Ma, H., Bowman, J. L., Drews, G. N., Feldman, K. A., and Meyerowitz, E. M. (1990). The protein encoded by the *Arabidopsis* homeotic gene *agomous* resembles transcriptional factors. *Nature* **346,** 35–39.

Index

I

J

K

L

M

N

T

This Page Intentionally Left Blank